Translational Relevance of AIPL1 and NUB1 in Cancer



Ka-Liong TAN

Radcliffe Department of Medicine

Lincoln College

University of Oxford

Trinity 2017

A thesis submitted in fulfilment of the requirements for the degree of
Doctor of Philosophy at the University of Oxford

Abstract

Background: Aryl Hydrocarbon Receptor Interacting Protein-Like 1 (AIPL1) interacts with NUB1 and restricts the entry of NUB1 protein into the nucleus. The interferon-induced NEDD8 ultimate buster (NUB1) protein causes degradation of neddylated and FAT10ylated proteins through the ubiquitin proteasome system. We observed AIPL1 were frequently down-regulated in various cancers compared to normal tissues. The mechanistic roles of AIPL1 and NUB1 protein in cancer cell cycle regulation remain unexplored.

Results: Meta-analysis of cancer databases revealed that expression transcripts of chaperones, including AIPL1, were down-regulated in lung, pancreatic cancer and breast cancer relative to the adjacent normal tissues. Opposite levels of both AIPL1 and NUB1 transcripts were observed in the breast cancer. So it triggers the *in vitro* experiments using breast cancer cells. METABRIC breast cancer clinical cohort highlighted that patients with low NUB1 transcripts had poor survival in the ER-negative subgroup (but not in ER-positive) of breast cancer patients: hazard ratio (HR)=0.66, 95% confidence interval (CI)=0.5-0.87, p=0.003 and triple negative subgroup of breast cancer patients: HR=0.67, 95% CI=0.47-0.96, p=0.028. NUB1 silencing significantly inhibits *in vitro* cell growth in MDA-MB-231 and MCF7 under hypoxia. AIPL1 protein forms multimers in cancer cells. NUB1 protein moved into the nucleus in hypoxia (0.1% O_2 48hrs) with final confluency at 80-90%. p21 (marker of senescence) & p27 (marker of cell cycle arrest) accumulated in NUB1-silent MDA-MB-231 and RCC4 cells. It suggested that low NUB1 nuclear localisation in hypoxia cause cancer cell cycle arrest. In MDA-MB-231 cell, upon hypoxia, neddylation inhibitor (MLN4924) treated and siNUB1 transfected cells showed decreased CUL1 and further accumulated p21 & p27. The evidence suggested lower neddylated CUL1 and reduced NUB1 cooperatively stabilise p21 and p27 as the substrate of CUL1-ubiquitin ligase. The neddylation inhibitor MLN4924 treated and NUB1 knockdown group exhibited more cells in sub-G1 stage as compared to the control group. In connection to higher p21/p27, it is associated with prolonged arrested

cellular aging with depletion. After silencing of NUB1, the increases in cell death of cancer cells upon hypoxia happen through the neddylation-dependent CUL1-p27-p21 and CUL2-VHL axis. We then demonstrated that HIF1α protein could be both neddylated and FAT10ylated upon reoxygenation. In a tissue microarray study of breast cancer, lower cytoplasmic expression (n=57) had worse overall survival than higher cytoplasmic expression (n=57): HR=1.779, 95% CI=1.006-3.346, p=0.048.

Conclusions: AIPL1 and NUB1 proteins exert a role in cell cycle regulation in breast cancer. Low cytoplasmic NUB1 levels are observed in the G_1-S transition of cancer cells. NUB1 depletion causes G_0/G_1 phase arrest due to CUL1 and CUL2 ubiquitin E3 ligase-dependent pathways.

Dedication

To my parents,

Swee-Eng and Min-Ching Tan,

And all of my friends,

Without whom none of my success would be possible.

Acknowledgements

First I would like to thank my parents for their emphasis on learning as a way of life, and my teachers and professors for helping me and maximising my academic potential.

I would like to thank **Academic Staff Training Scheme (ASTS/SLAI)** for the scholarship which allowed me to pursue my doctoral studies at the University of Oxford. I would like to thank my funding department line manager, Prof. Emeritus Dato' Dr. Nik Mohd Nasri Nik Ismail and Professor Dr. Muhammad Shamsir Bin Mohd Aris.

I would also like to thank my DPhil supervisors, Professor Francesco Pezzella and Professor Oreste Acuto for their mentorship and guidance, as well as for their helps in experimental design and techniques.

I would like to pay tribute to my idea donor below for their expert input on my project, and the rest of my colleagues in Oxford for their aid in all other matters.

Tumour Pathology Group
Prof. Francesco Pezzella
Prof. Kevin Gatter
Dr. Jianting Hu
Dr. Russell Leek
Ms. Katherine Freeman
Ms Helen Turley
Mr. Graham Steers

T cell Signaling Group
Prof. Oreste Acuto
Dr. Anna-Lisa Lanz
Dr. Giulia Masi

Hypoxia and Angiogenesis Group
Prof. Adrian Harris
Dr. Christos Zois

Gene Medicine Therapy Group
Prof. Deborah Gill
Mr. Jean-Francois Gelinas

Applied Computational Genomics Group
Dr. Francesca Buffa
Dr. Syed Haider

FACS Facility Team (WIMM)
Kevin Clark
Paul Sopp

High Temperature Superconductivity Group
Prof. Chris Grovenor
Dr. Kexue Li

Centre for Microscopy, Characterisation and Analysis (CMCA), University of Western Australia
Dr. Haibo Jiang



Finally, I would like to acknowledge the Ministry of Education (Malaysia) and NDCLS, RDM for funding this research.

List of figures

Figure 1. 1 Structures of client proteins and the hydrophobic effects..... 5

Figure 1. 2 Roles of chaperones in proteostasis..... 6

Figure 1. 3 Structure of various chaperones..... 9

Figure 1. 4 Details of AIPL1 gene..... 21

Figure 1. 5 The function of AIP and AIPL1. 24

Figure 1. 6 Interaction of AIPL1 and NUB1 proteins.. 27

Figure 1. 7 Structural representation of (A) Ub, NEDD8 and FAT10, and (B) NUB1..... 28

Figure 1. 8 Solution structure of N-terminal ubiquitin-like domain of human NUB1. 30

Figure 1. 9 NEDD8 conjugation pathway and roles of NUB1 on neddylated CUL1..... 33

Figure 1. 10 NEDD8 conjugation and ubiquitination pathway. 34

Figure 1. 11 Domain structure of NUB1L, FAT10 and RPN10. 37

Figure 3. 1 Box and whisker plots of AIPL1 and NUB1 in breast cancer dataset…… 60

Figure 3. 2 Venn diagram of overlapping genes across the NUB1 coexpression networks..62

Figure 3. 3 NUB1 coexpression network profile..... 65

Figure 3. 4 Pairwise association plot of CUL1 and TMEM140 against NUB1 transcripts..66

Figure 3. 5 Survival curves of AIPL1 in different subgroup.. 70

Figure 3. 6 Survival curves of AIPL1 and NUB1 in different subgroup.. 73

Figure 3. 7 Gene expression patterns of AIPL1 and NUB1 based on the intrinsic molecular subtypes status of METABRIC dataset. 76

Figure 3. 8 Survival curves of FAT10 in ER-, Basal and triple negative subgroup……79

Figure 3. 9 Gene expression patterns of NEDD8 and FAT10 based on the intrinsic molecular subtypes status of METABRIC dataset. .....……..81

Figure 3. 10 Gene expression patterns of CUL1 and p21 based on the intrinsic molecular subtypes status of METABRIC dataset. 83

Figure 3. 11 Heatmap showing genes differentially expressed in patients using RNA-Seq data..... 86

Figure 4. 1 Protein expressions……...93

Figure 4. 3 Endogenous transcript expressions in cancer cells…….94

Figure 4. 4 Immunohistochemistry staining of various cancer cells……..98

Figure 4. 5 Oligomerisation of AIPL1 proteins analysed by native PAGE and immunoblotting.. 101

Figure 4. 6 Time course experiment of reoxygenated MDA-MB-231.. 103

Figure 4. 7 Cell cycle analysis in NUB1 knockdown MDA-MB-231.. 105

Figure 4. 8 Cancer cell growth in NUB1 knockdown condition..... 106

Figure 4. 9 Cytoplasmic AIPL1 dimerisation enhances NUB1 shuttling into the nucleus. .. 108

Figure 4. 10 NUB1 silencing enhances neddylation inhibition effects onto p27 (but not p21) protein levels..... 110

Figure 4. 11 Cell cycle profile of MDA-MB-231..... 111

Figure 4. 12 Knockdown of NUB1 and cell cycle analysis.. 112

Figure 5. 1 Ubiquitin E3 ligases and their substrates……114

Figure 5. 2 Schoefeld's first speculation on how VHL regulates p27 and p21.……..116

Figure 5. 3 Cell cycle analysis on the NUB1 knowckdown effect in RCC4plusVHL and RCC4 cells under normoxic and hypoxic conditions.……120

Figure 5. 4 NUB1 knockdown upregulate a. HIF1α and down-regulate b. VHL proteins. .....….122

Figure 5. 5 Cell cycle analysis on the NUB1 knowckdown effect in RCC4 cells under normoxic and hypoxic conditions..……124

Figure 5. 6 Depletion of NUB1 upregulated HIF1α and p27 proteins. 126

Figure 5. 7 NEDD8 and FAT10 signals detected in endogenous HIF1α. 128

Figure 5. 8 Hypothesis pipeline of the chapter 5..... 130

Figure 6. 1 Immunostaining of NUB1 using monoclonal mouse antibody (4H2) (1:20) dilution on RCC4plusVHL cells counterstain with hematoxylin…….....135

Figure 6. 2 NUB1 expression on representative node negative breast cancer tissue microarray spots. 137

Figure 6. 3 Distribution of NUB1 immunohistochemical staining scores in primary breast cancer. …..... 138

Figure 6. 4 Correlation of NUB1 cytoplasmic IPS with nuclear IPS……140

Figure 6. 5 Relationship between ER status and NUB1 localisation.. 141

Figure 6. 6 Relationship between ER and prognosis in breast cancer patients using the log-rank test….. 144

Figure 7. 2 Central dogma of NUB1-mediated cell cycle regulation via p27 and p21..... 155

List of tables

Table 1. 1 Development of the chaperone concept.. 8

Table 1. 3 Classification of A. HSP70 and HSP110 and B. HSP90.. 13

Table 1. 4 List of cochaperones. 14

Table 1. 5 Summary of meta-analysis.. 18

Table 1. 6 Summary of down-regulated AIPL1.. 18

Table 1. 7 Overview of the enzymatic cascade involved in UBLs conjugation. 29

Table 2. 1 Immunostaining Antibodies 46

Table 3. 1 Classification of breast cancer and the key features of the subtypes 133

Table 3. 2 Genes and cancer summary from Oncomine.. 56

Table 3. 3 Summary of A. AIPL1 & B. NUB1 datasets.. 57

Table 3. 4 Summary of NUB1 and CUL1 enriched pathway.. 63

Table 3. 5 Survival curves summary. 74

Table 3. 6 FAT10 Genes and cancer summary from Oncomine.. 80

Table 3. 7 Summary of NUB1 vs. FAT10 and NEDD8 mRNA coefficient, ρ. 81

Table 3. 8 Summary of AIPL1 and NUB1 on CUL1 and p21 mRNA expression. 84

Table 3. 9 HIF1α and downstream target.. 85

Table 4. 1 Summary of AIPL1, NUB1, NEDD8 and FAT10 gene products (protein or transcripts) in all cancer cell line..... 99

Table 6. 1 Clinicopathological variables according to ER status. 139

Table 6. 2 Relationship between high/low NUB1 subcellular localisation and overall survival/ relapse free survival. 143

Table 6. 3 Summary of overall survival analysis based on the mean IPS. 146

List of abbreviations

AIPL1	Aryl hydrocarbon interacting protein like-1
AMPK	AMP-activated protein kinase
ARNT	Aryl hydrocarbon receptor nuclear translocator
ABC	ATP binding cassette
ATG5	Autophagy-related 5
BRAC1	Breast cancer 1
CA	Carbonic anhydrase
cDNA	Complementary DNA
°C	Degrees celcius
COL5A1	Collagen Type V Alpha 1 Chain
ΔΔCT	Delta delta cycle threshold
DLK1	Delta Like Non-Canonical Notch Ligand 1
DNA	Deoxyribonucleic acid
DMSO	Dimethylsulphoxide
ER	Estrogen receptor
ECM	Extracellular matrix
FAS	Fatty acid synthase
FA	Fatty acids
FAT10	HLA-F adjacent transcript 10
FCS	Foetal calf serum
FC	Fold Change
HER2	Human epidermal factor receptor 2
HIF-1	Hypoxia inducible transcription factor 1
HRE	Hypoxia-response elements
IGF	Insulin growth factor
IGF2	Insulin-like growth factor 2
IFNs	Interferons
IL	Interleukins
kDa	kiloDaltons
LDHA	Lactate dehydrogenase-A
L	Litre
LPR	Low density lipoprotein receptor related protein
MMP	Matrix metalloproteinases
mRNA	Messenger RNA (Ribonucleic acid)

µg	Micrograms
µl	Microlitres
µm	Micrometres
µM	Micromolar
ml	Millilitres
mM	Millimolar
M	Molar
mAb	Monoclonal antibodies
MDA5	Melanoma differentiation-associated gene 5
MHC	Major histocompatibility complexes
NEDD8	Neural Precursor Cell Expressed, Developmentally Down-Regulated 8
NF-kB	Nuclear factor-kappaB
NUB1	NEDD8 Ultimate Buster 1
ODDDs	Oxygen dependent degradation domains
%	Percent
PBS	Phosphate-buffered saline
PDGF	Platelet-derived growth factor
PCR	Polymerase chain reaction
pH	Power of hydrogen (in solution)
PHDs	Prolyl hydroxylase
RIG-1	Retinoic acid-inducible gene I
ROS	Reactive oxygen species
RNA	Ribonucleic acid
scr	Scramble control
siRNA	Small interfering RNA
SDS	Sodium dodecyl sulfate
bHLH	Basic helix-loop-helix
TCR	T Cell receptor
TOR	Target of Rapamycin
TGF β	Transforming growth factor β
TNFα	Tumor necrosis factor α
TNFR2	Tumor necrosis factor receptor 2
TAMs	Tumour associated macrophages
VEGF	Vascular endothelial growth factor
VHL	Von Hippel Lindau

Table of content

Abstract I

Dedication III

Acknowledgements IV

List of figures V

List of tables VIII

List of abbreviations X

Table of content XII

Chapter 1 Introduction 1

1.1 Proteostasis (also known as Protein Homoeostasis) 1

1.2 Human Chaperones and Cancer 7

1.2.1 Discovery of Chaperones and historical perspectives 7

1.2.2 Classification of Chaperones 10

1.2.3 Roles of Chaperones and Cochaperones in Cancer 15

1.2 Microarray and chaperones/cochaperones gene-specific meta-analysis 17

1.3 Introduction of AIPL1 protein 19

1.3.1 Interaction of NUB1 and the downstream ubiquitin pathway 25

1.3.2 Background of NUB1 28

1.4 Neddylation and its functions 30

1.5 FAT10ylation and its functions 35

1.6 Ubiquitin Proteasome System 38

1.7 Rationale of study ..... **Error! Bookmark not defined.**

1.8 Objectives of study 42

Chapter 2 Methods and Materials 43

2.1 Cell Line 43

2.2 Cell Culture 43

2.3 Counting Cells 44

2.4 Preparation and Recovery of cell stocks (cryo-preserved cells) 44

2.5 Gene silencing by RNA Interference 45

2.6 Immunostaining of paraffin-embedded tissue sections 45

2.8 Protein Polyacrylamide Gel Electrophoresis (PAGE) 47

2.9 Antibody Incubation 47

2.10 Real-time PCR (qPCR) 48

2.11 Cell cycle analysis using flow cytometry 48

2.12 Presence of disulphide bond with fluoresceine maleimide 48
2.13 Statistical analyses 49
2.14 Buffers and solutions 50
Chapter 3 Systematic Analysis of Gene Expression Alterations and Clinical Outcomes for AIPL1 and NUB1 in Cancer 52
3.1 The rationale of study 52
3.2 Concordant down-regulation of AIPL1 transcripts and upregulated NUB1 level in Oncomine database 54
3.3 NUB1 transcripts consistently coexpressed with CUL1 transcripts in breast cancer 61
3.4 Coexpressions of NUB1 with ATM and FAS signaling pathway 64
3.5 Breast cancer specific analysis using METABRIC database 67
3.5.1 NUB1 transcript expression levels predict the survival probability of ER negative breast cancer patients. 67
3.5.2 No significant difference of AIPL1 and NUB1 transcript levels 75
3.5.3 UBL Pathway analysis: FAT10 which coexpressed with NUB1 could stratify ER-, basal and triple negative subgroup breast cancer patients' survival probability 77
3.5.4 CUL1 related ubiquitin ligase activities and cell cycle regulation 82
3.5.5 Pathway analysis of HIF1A transcription in different breast cancer subtypes 84
3.6 Discussion and Chapter Summary 87
Chapter 4 AIPL1-NUB1 signaling cascade in cell cycle regulation Through CUL1 based E3 ubiquitin SCF-ligase 89
4.1 Rationale of the study 89
4.2 Cell line screening of proteins and their transcript levels 91
4.2.1 Detection of endogenous protein expression in various cancer cell line 91
4.2.2 Quantitative PCR analysis of various cancer cell line 91
4.2.3 Immunohistochemistry staining of various cancer cell line 92
4.3 AIPL1 dimerisation in cancer cells 100
4.4 Changes of NUB1 stability upon reoxygenation 102
4.5 NUB1 silencing caused G_0/G_1 cell cycles arrest 104
4.6 Depletion of NUB1 protein affects cell growth rates 106
4.7 Localisation of AIPL1 and NUB1 proteins in hypoxia and reoxygenation 107
4.8 NUB1 protein regulates cell cycle through neddylation-dependent CUL1 109
4.9 Discussion and Chapter Summary 113
Chapter 5 NUB1 protein destabilise p21 and p27 proteins through VHL-dependent CUL2-based E3 ligase 114

5.1 Rationale of the study 114
5.2 NUB1 protects cells from hypoxia-mediated cell cycle arrest and apoptosis through VHL 118
5.3 Up-regulation of HIF1α and VHL protein levels due to NUB1 knockdown 121
5.4 Cell cycle analysis with NUB1 knockdown status under severe hypoxic conditions. 123
5.5 Stabilisation of p27 and HIF1α by NUB1 depletion are independent of VHL 125
5.6 HIF1α is neddylated and FAT10ylated 127
5.7 Discussion and Chapter Summary 129
Chapter 6 Tissue microarray analysis of NUB1 in primary Breast Cancer shows cytoplasmic localisation is associated with poorer prognosis 131
6.1 Rationale of study 131
6.2 Validation of NUB1 antibody on cancer cells 134
6.3 NUB1 immunohistochemical staining of primary breast tumour tissue 136
6.4 Oestrogen receptor (ER) expression and association with clinicopathological factors 139
6.5 Association of ER status and menopausal status with subcellular localisation of NUB1 140
6.6 Survival analyses 142
6.7 Clinicopathological correlation and analysis 145
6.6 Discussion and Chapter Summary 147
Chapter 7 Discussion 148
7.1 Role of of AIPL1 and NUB1 in cancer 148
7.2 Pathways involved in AIPL1 and NUB1 149
7.3 Hypoxia and reoxygenation stress 152
7.4 Relationship with VHL 155
7.5 Translational perspectives 158
Chapter 8 Concluding Statement 160
Appendix 1 161
List of Awards, Presentations and Publications 162
References 173

Chapter 1

Introduction

1.1 Proteostasis (also known as Protein Homoeostasis)

Proteostasis is defined as ‘a concept that explains the integrated biological pathways within cells that control the synthesis, folding, trafficking and degradation of proteins present within and outside the cell’ (Dobson and Karplus, 1999). It contributes to the cellular protein quality control for the proteins in a single human cell (Hieronymus *et al.*, 2006). The maintenance of proteostasis is attained through a precisely coordinated system that corrects unwanted proteomic changes. The integration of chaperones within the proteostasis network ensures a balanced protein homoeostasis.

Chaperones, also known as heat shock proteins (HSP), are ‘a protein group that directly interacts and folds the client protein to its active conformational state’ (Hartl, 1996). The primary function of these proteins is to govern the folding and refolding mechanism of naive and stress-denatured proteins. They dynamically associate with the exposed hydrophobic surfaces of the unfolded polypeptides, prevent their aggregation and thereby, enhance the folding process. Additionally, chaperones are also involved in protein assembly, translocation and degradation. Hence these proteins are the essential determinants of protein quality control in a cell.

There are some definitions of terms used in the molecular chaperones concept, as detailed below (Ellis, 2013):

“”

Protein folding is the collapse of an extended primary translation product into a stable compact monomer. Monomers possess primary, secondary and tertiary structure. The folding of a protein’s quaternary structure is a part of protein assembly (See next).

Protein assembly is the binding of monomers to one another to produce a functional oligomer. Oligomers possess quaternary structure.

Protein misfolding is the formation of a conformation that cannot reach the native conformation on a biologically relevant timescale.

The term ***‘native’*** refers to the conformation of the purified functional protein. The term ***‘non-native’*** is defined as a conformation that is unable to reach the functional conformation on any timescale.

Protein misassembly is the association of two or more polypeptide chains to form non-functional oligomers. A widely used term to describe protein misassemblies is ‘aggregates’, especially to describe so-called amyloid structures, such as those associated with neurodegenerative diseases. Note that misassembled states are always misfolded, by definition.

Chaperones are a large and diverse group of proteins that share the property of assisting non-covalent folding and unfolding, and the assembly and disassembly, of other macromolecular structures, but are not permanent components of these structures when they are performing their normal biological functions (Ellis, 2006). Chaperone substrates include RNA as well as proteins.

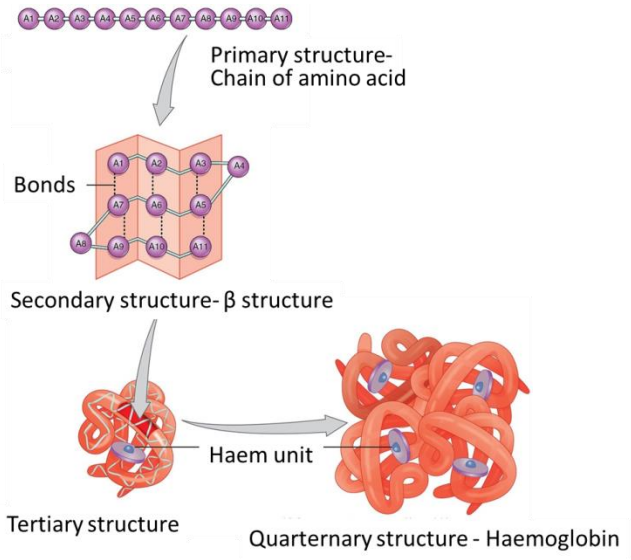
Cochaperones are proteins that modulate chaperone (HSP70 and HSP90) proteins activity. Some cochaperones are also chaperones, e.g. HSP40. Cochaperones modulate the activity of their cognate chaperones in a variety of different ways (Rosser and Cyr, 2007).

HSP and chaperones are not the same. Ellis stated that chaperones present in both stress and unstressed conditions (Ellis, 2013). HSPs are indeed stress proteins. Although chaperones were first recognised as stress-responsive proteins induced mostly by heat shock, other proteotoxic stresses including heavy metals, hypoxia, nutrient deprivation, irradiation, oxidative and toxic stress, infections and exposure to inflammatory cytokines could upregulate their expression too (Lindquist and Craig, 1988; Jaattela, 1999b). However, there are some HSP members that are constitutively expressed. Whilst chaperones and HSPs can constitute overlapping groups of proteins, they are not necessarily identical (Ellis, 1990). The subsequent review assumes that the subset of chaperones discussed is HSPs.

Afinsen's model postulates that for a small globular protein, the native structure is determined only by the protein's amino acid sequence. The primary structure of the protein and its linear amino acid sequence determines its native conformation (Afinsen *et al.*, 1973). The secondary structure involves alpha helices and beta sheets which are stabilised by hydrogen bonds (Pauling *et al.*, 1951). Tertiary structure constitutes a single polypeptide chain formed through hydrophobic interactions, covalent bonding and disulphide bridges between two cysteine residues. Additional interactions of polypeptide chains give rise to quaternary structure formation (Fig 1.1).

The hydrophobic effect is a phenomenon in which the hydrophobic amino acid sequences are buried inside while the more polar amino acids are exposed to the exterior aqueous environment (Figure 1.1) (Dobson and Karplus, 1999). However, active protein-protein interactions tend to expose hydrophobic residues to the exterior environment, risking protein misfolding and aggregation (Zou *et al.*, 2008). To overcome this, chaperones are expressed at high levels in cells after proteotoxic stresses such as exposure to heat shock, heavy metals, alcohols and sodium arsenite (Ritossa, 1962; Ritossa, 1964; Craig, 1985; Calderwood *et al.*, 2010). Chaperones can then permit the folding of client proteins into their functional native states if necessary.

A.



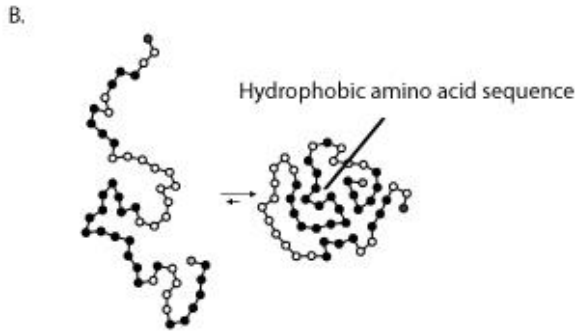


Figure 1. 1 Structures of client proteins (haemoglobin) and the hydrophobic effects. (A) All forms of protein structures are illustrated. (B) Hydrophobic effects is also called Hydrophobic collapse. In the compact fold (on the right), the hydrophobic amino acids (shown as black spheres) collapse toward the centre to become shielded from the aqueous environment (Spolar *et al.*, 1989).

The mechanism of action of chaperones helps to regulate biological proteomes. It is essential to ensure a balanced cellular homoeostasis (Fig 1.2). Protein misfolding and aggregate formation compromise the function of the client proteins. This results in various diseases such as neurodegenerative diseases (e.g. Alzheimer's, Parkinson's disease, and Huntington's disease), cystic fibrosis and cancers (Balch et al., 2008). Many reports support the notion that chaperones are implicated in the pathogenesis of a range of human cancer types. Many of them are in deregulated molecular mechanisms including cell proliferation (Czarnecka *et al.*, 2006; Ghosh *et al.*, 2008), invasiveness (Lemieux *et al.*, 1997), induction of neoangiogenesis (Sanderson *et al.*, 2006), metastasis (Zhao *et al.*, 2007) and the induction of immune tolerance (Calderwood *et al.*, 2005; Cappello *et al.*, 2009).

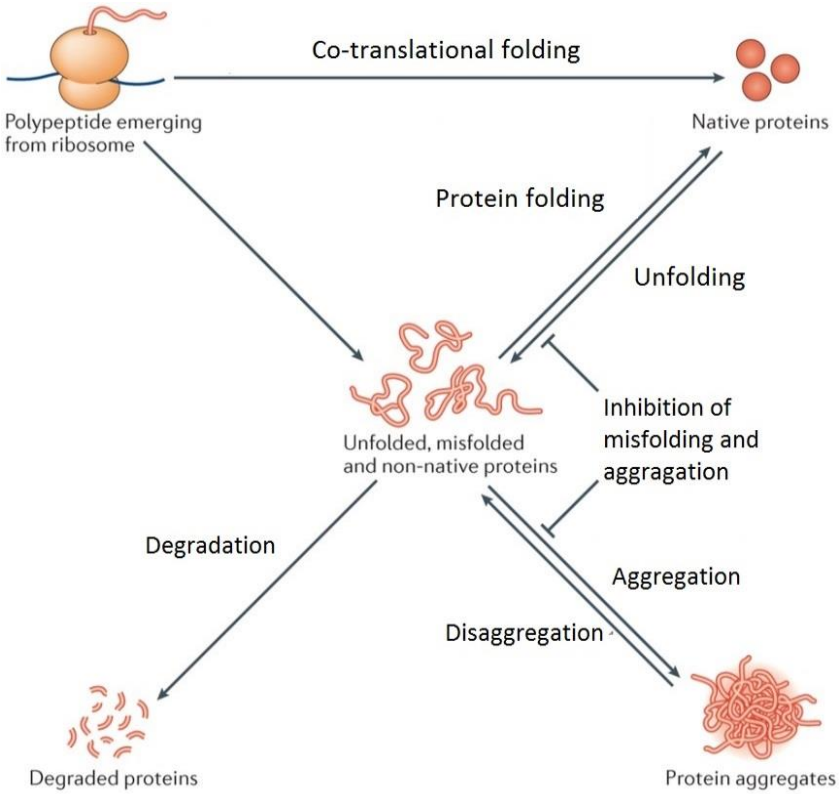


Figure 1. 2 Roles of chaperones in proteostasis. The proteostasis network requires the action of chaperones to fold the client proteins into their native conformations, to prevent misfolding and to reactivate misfolded and aggregated proteins. Chaperones aid in the folding of newly synthesized proteins, the folding of unfolded proteins released from the ribosome and the remodelling of non-native proteins, which are often caused by heat stress and other stress conditions; non-native proteins may be targeted to chaperones associated proteases for degradation; some chaperones could prevent protein misfolding and aggregation; when cells are overwhelmed by stress, non-native proteins might form aggregates; other chaperones can extract and unfold polypeptides from aggregates, thus providing another opportunity for proper folding (Doyle *et al.*, 2013).

1.2 Human Chaperones and Cancer

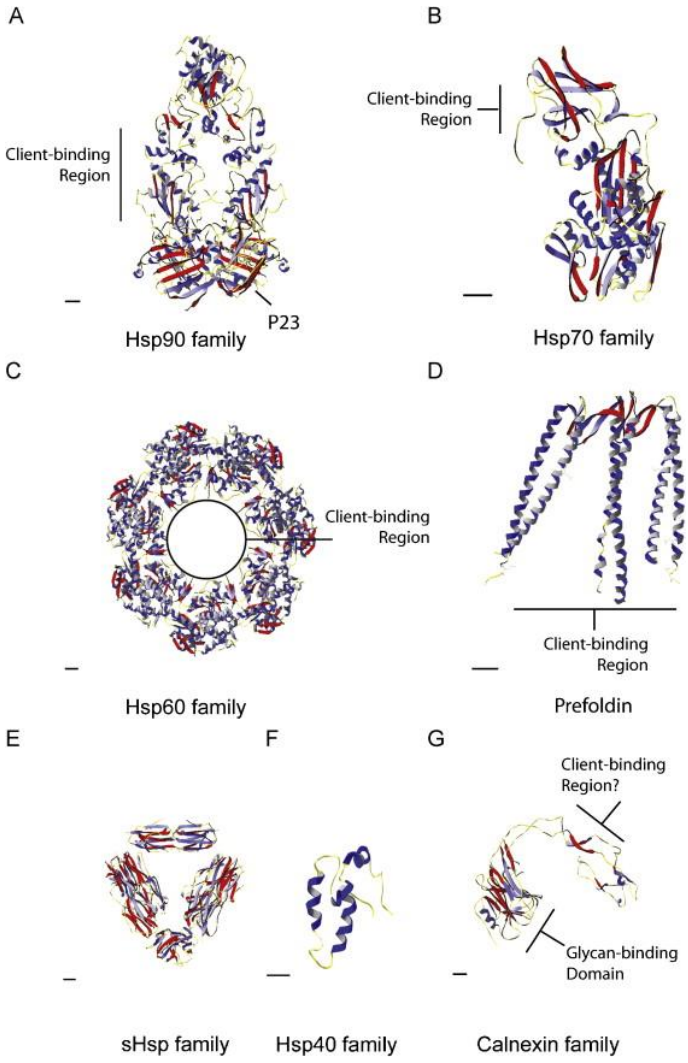
1.2.1 Discovery of Chaperones and historical perspectives

Ferruccio Ritossa first discovered chaperones in a *Drosophila melanogaster* model (Ritossa, 1964). He observed that the salivary gland cells of flies formed chromosomal puffs when they were exposed to higher temperature (Ritossa, 1962). These puffs represented areas with high transcriptional activities in response to heat shock. The transcribed genes and the corresponding proteins were initially named HSPs and then called chaperones (Ellis, 2007; Kampinga *et al.*, 2009). The functions of chaperones onto their respective client proteins were unravelled in the 1980's. The development of the chaperones concept is summarised in table 1.1.

Over the last decades, many HSP90 cochaperones have been discovered and characterised (Pratt and Toft, 1997; Picard, 2002; Wandinger *et al.*, 2008; Li *et al.*, 2012). It is thought that some of the cochaperones facilitate the binding of HSP90 to client proteins and confer specificity to this process (Tai *et al.*, 1993; Johnson *et al.*, 1994; Young *et al.*, 1998; Cox *et al.*, 2007). Others are implicated in regulating the conformational cycle of HSP90 (Chen and Smith, 1998; Chen *et al.*, 1998; Scheufler *et al.*, 2000; Schmid *et al.*, 2012; Li *et al.*, 2013a).

Year	Remarks	Publications
1973	Anfinsen observed that native proteins unfold and lose their biological properties; the proteins can refold into their original functional conformations in the right condition.	(Anfinsen, 1973)
1780	Chloroplast enzyme appears as a large subunit which only forms a smaller subunit when they interact with another protein transiently.	(Barraclough and Ellis, 1980)
1978	The word "molecular chaperones" was used for the first time in the literature by **Ron Laskey** to describe the ability of nucleoplasmin in preventing the aggregation of folded histone proteins with DNA.	(Laskey *et al.*, 1978)
1987	Widespread use of the molecular chaperones noun by **R. John Ellis** in 1987. He described chaperones mediated post-translational protein assembly.	(Ellis, 1987)
1988	It was observed that similar proteins mediated the assembly process in both prokaryotes and eukaryotes.	(Hemmingsen *et al.*, 1988)
1989	The assembly process was confirmed and the ATP-dependent protein folding was demonstrated *in vitro*.	(Goloubinoff *et al.*, 1989)
1993	Earliest recorded discovery of a cochaperone, FKBP59.	(Tai *et al.*, 1993)
1997	HSP90 cochaperones have been discovered and characterised.	(Pratt and Toft, 1997)
2009	Kampinga *et al.* proposed the guideline for the nomenclature of human chaperones.	(Kampinga *et al.*, 2009)

Table 1. 1 Development of the chaperones concept. Important events of chaperones history are summarised. A number of chaperones and their related proteins were found during the 80's and beyond.



	Chaperones	Model	Remark	PDB accession number	Reference
A	HSP90	Yeast	In complex with cochaperone p23 and ATP analogue.	2CG9	(Ali *et al.*, 2006)
B	HSP70	Bovine	Amino acids 1-554 lacking the 10kDa C-terminal domain.	1YUW	(Jiang *et al.*, 2005)
C	HSP60	Bacteria	HSP60 consisting of two stacked homoheptameric rings viewed from above one ring.	1GR1	(Braig *et al.*, 1994)
D	Prefoldin		Hexameric structure prefoldin	1FXK	(Siegert *et al.*, 2000)
E	HSP16.3	*Mycobacterium Tuberculosis*	Dodecameric structure	2BYU	(Kennaway *et al.*, 2005)
F	HSP40		The J-domain of human HSP40 family member	1HDJ	(Qian *et al.*, 1996)
G	Calnexin		Structure of the calnexin luminal domain	1JHN	(Schrag *et al.*, 2001)

Figure 1. 3 Structure of various chaperones. Ribbon diagrams shows the structures and client protein binding sites of the chaperones. α-helices are shown in blue and β-sheets in red. Scale bar represents 10Åm. ATP, Adenosine triphosphate.

1.2.2 Classification of Chaperones

The variety of HSP families has made it necessary to revise the nomenclature. Initially, they were classified according to their molecular mass in kiloDaltons (kDa) (Table 1.2). In 2009, Kampinga *et al.* proposed the guideline for the nomenclature of human chaperones. The chaperones consist of six groups namely HSP110 (HSPH), HSP90 (HSPC), HSP70 (HSPA), HSP40 (J-proteins), and HSPB (small HSP) as well as for the human chaperonin families HSP60/HSP10 (HSPD/E) and chaperonin containing T-Complex Protein (CCT) (Kampinga *et al.*, 2009). This nomenclature is more consistent with the Human Genome Organisation (HUGO) Gene Nomenclature Committee for heat shock genes. Amongst chaperones, the HSP90 and HSP70 groups are the most studied in cancers (Chen *et al.*, 2006). Some of the important structures of chaperones are illustrated (Fig. 1.3).

HSP70s are the most abundant and well characterised HSPs in bacterial and eukaryotic systems. Several types of HSP70s have been reported in all living organisms, and they typically constitute 2-3% of whole cell proteome (Bukau and Horwich, 1998; Mayer *et al.*, 2001).

HSP70s have two conserved domains. The N-terminal Nucleotide binding domain (NBD) and substrate binding domain (SBD) are connected via a linker region. The SBD is a variable helical region which covers the peptide binding cavity and regulates the substrate interaction (Bukau and Horwich, 1998; Mayer *et al.*, 2001). The specificity of HSP70s is largely determined by their partner J-proteins, and together they function as a molecular chaperone machine (Mayer and Bukau, 2005). In organisms, the members of the J-protein family are found in large numbers and often exceed the members of HSP70s. HSP70 is capable of interacting with multiple J-protein partners to exert various physiological functions, thus forming a complex network of chaperones (Mayer *et al.*, 2001; Mayer and Bukau, 2005).

HSP70s and J-proteins are implicated in several essential physiological functions (Hartl and Hayer-Hartl, 2002; Mayer and Bukau, 2005), including prevention of misfolding of newly synthesised polypeptides, protein translocation across biological membranes and degradation processes (Laufen *et al.*, 1999).

HSP90 is a chaperone essential for folding of client proteins, including protein kinases and transcription factors (Csermely *et al.*, 1998), which are involved in the signal transduction process. Typically, HSP90 localised either in the cytoplasm, endoplasmic reticulum or mitochondrial compartments.

The levels of HSP90 are upregulated several fold upon stress induction to protect the conformation of its client proteins (Cowen and Lindquist, 2005). HSP90 contains a conserved N-terminal 'ATP-binding domain' followed by a 'middle region' and C-terminal dimerising domain (Cowen and Lindquist, 2005), which are involved in the binding to different cochaperones and client proteins. They form a constitutive homodimer and in the presence of ATP, adopt a circular structure to stabilise the conformational plasticity of client proteins and assist in the maturation into their native states (Cowen and Lindquist, 2005).

A. HSP70 superfamily: HSPA (HSP70) and HSPH (HSP110) families

	Gene name	Protein name	Old names	Human gene ID
HSPA				
1	*HSPA1A*	HSPA1A	HSP70-1; HSP72; HSPA1	3303
2	*HSPA1B*	HSPA1B	HSP70-2	3304
3	*HSPA1L*	HSPA1L	hum70t; hum70t; HSP-hom	3305
4	*HSPA2*	HSPA2	Heat-shock 70kD protein-2	3306
5	*HSPA5*	HSPA5	BIP; GRP78; MIF2	3309
6	*HSPA6*	HSPA6	Heat shock 70kD protein 6 (HSP70B′)	3310
7	*HSPA7*[a]	HSPA7	Heat shock 70kD protein 7	3311
8	*HSPA8*	HSPA8	HSC70; HSC71; HSP71; HSP73	3312
9	*HSPA9*	HSPA9	GRP75; HSPA9B; MOT; MOT2; PBP74; mot-2	3313
10	*HSPA12A*	HSPA12A	FLJ13874; KIAA0417	259217
11	*HSPA12B*	HSPA12B	RP23-32L15.1; 2700081N06Rik	116835
12	*HSPA13*[b]	HSPA13	Stch	6782
13	*HSPA14*	HSPA14	HSP70-4; HSP70L1; MGC131990	51182
HSPH				
1	*HSPH1*	HSPH1	HSP105	10808
2	*HSPH2*[b]	HSPH2	HSPA4; APG-2; HSP110	3308
3	*HSPH3*[b]	HSPH3	HSPA4L; APG-1	22824
4	*HSPH4*[b]	HSPH4	HYOU1/Grp170; ORP150; HSP12A	10525

[a]Annotated as pseudogene, but possibly a true gene; [b]Under consultation with HGNC and the scientific community; *No information

B. HSP90 (HSPC)

	Protein name	Gene name	Old gene names	Human Gene ID
1	HSPC1	*HSPC1*[a]	***HSP90AA1****; HSPN; LAP2; HSP86; HSPC1; HSPCA; HSP89; HSP90; HSP90A; HSP90N; HSPCAL1; HSPCAL4; FLJ31884*	3320
2	HSPC2	*HSPC2*[a]	***HSP90AA2****; HSPCA; HSPCAL3; HSP90ALPHA;*	3324
3	HSPC3	*HSPC3*[a]	***HSP90AB1****; HSPC2; HSPCB; D6S182; HSP90B; FLJ26984; HSP90-BETA*	3326
4	HSPC4	*HSPC4*[a]	***HSP90B1****;ECGP; GP96; TRA1; GRP94; endoplasmin*	7184
5	HSPC5	*HSPC5*[a]	***TRAP1****; HSP75; HSP90L*	10131

[a]Under consultation with HGNC and the scientific community. GRP-94, G Protein-Coupled Receptor 94; TRAP1, TNF Receptor- Associated Protein 1

Table 1. 2 Classification of A. HSP70 and HSP110 and B. HSP90. The nomenclature of HSP70 and HSP90 protein isoforms are listed. The information is modified from Kampinga *et al.*, 2009 and Chen *et al.*, 2005.

Cochaperones are the proteins that assist in catalysing individual steps in molecular chaperoning as well as in posttranslational modification and intracellular localisation. They work in concert with HSP90 to modulate its conformation and the respective client proteins. Over 20 cochaperones including immunophilins have been shown to regulate the function of the HSP90 protein-folding machinery. Immunophilins consists of FK506 Binding Protein 51/52 (FKBP51/52), Cyclophilin 40 (CYP40) and Aryl Hydrocarbon Receptor Interacting Protein-Like 1 (AIPL1). These cochaperones are thought to provide HSP90 selectivity toward different client proteins. For example, AIPL1 recruits the HSP90 machine in a chaperone heterocomplex that is essential for phosphodiesterase biogenesis and its retinal maturation (Aguila *et al.*, 2014).

Three particular classes of chaperone appear of high significance in cancer, and these include the HSPA, HSPB, and HSPC families (Ciocca *et al.*, 2013). Each HSP class is regulated by an individual cohort of cochaperones and these molecules may be significant factors in cancer and carcinogenesis and potential targets for therapy.

Name	Function	Conserved domain	Role in cancer	Reference
		HSP70		
JDP	Substrate selection	J domain	Supp	(Isomoto *et al.*, 2003)
HSPBP1	Nucleotide exchange	*	Supp	(Souza *et al.*, 2009)
BAG1	Nucleotide exchange	BAG, UBL	Onc	(Aveic *et al.*, 2011)
BAG3	Nucleotide exchange	BAG, WW	Onc	(Stuart *et al.*, 1998)
HOP	Adaptor	TPR	Onc	(Kubota *et al.*, 2010)
		HSP90		
SGT1	Substrate selection	CHORD	*	(Zabka *et al.*, 2008)
p23	ATPase inhibitor	p23	Onc	(Reebye *et al.*, 2012)
AHA1	ATPase inhibitor	AHA1	Onc	(Pearl and Prodromou, 2006)
CDC37	ATPase inhibitor	HSP90 BD	Onc	(Stepanova *et al.*, 2000)
HOP	Adaptor	TPR	Onc	(Walsh *et al.*, 2011)
CYP40	Immunophilin	TPR, PPiase	*	(Schulke *et al.*, 2010)
FKBP1	Immunophilin	TPR, PPiase	Onc	(Denny *et al.*, 2000)
FKBP2	Immunophilin	TPR, PPiase	Onc	(McKeen *et al.*, 2011)
PP5	Protein phosphatase	TPR	*	(Chinkers, 1994)
TTC4	Adaptor, replication	TPR	Supp	(Poetsch *et al.*, 2000)
TTC5	Adaptor, transcription	TPR	*	(Davies *et al.*, 2011)
AIP	Nuclear receptors	TPR	*	(Mazumdar *et al.*, 2001)
AIPL1	Immunophilin, Chaperone and cochaperone	TPR, PPiase	Supp	(Hidalgo-de-Quintana *et al.*, 2008)

Table 1. 3 List of cochaperones. The cochaperones are associated with HSP70 and HSP90 chaperone families. Supp, tumour suppressor; onc, oncogene; JDP, J domain protein; BAG1, Bcl-2-Associated Athanogene 1; BAG1, Bcl-2-associated athanogene 1 and silencer of death domain; UBL, ubiquitin-like domain; WW, tryptophan repeats domain; HOP, Hsp70-Hsp90 Organizing Protein; TPR, Tetratricopeptide repeat-containing domain; SGT1, Suppressor Of G2 Allele Of SKP1; AHA1, activator of Hsp90 ATPase 1; CHORDS, Cysteine- and histidine-rich domains; CDC37, Cell Division Cycle 37; PP5, Protein phosphatase 5; TTC4/5, Tetratricopeptide repeat protein 4/5; AIP, Aryl Hydrocarbon Receptor Interacting Protein; PPIase, Prolyl isomerase.*No information

1.2.3 Roles of Chaperones and Cochaperones in Cancer

Chaperones maintain a balanced proteostasis *via* protein folding, preventing misfolding of proteins and reactivating aggregated proteins. When the cells are challenged by cytotoxic stress, chaperones help client proteins to shift their protein conformations toward ordered, functional forms. However, deregulation of chaperones contributes to pathological conditions including neurodegeneration, cardiovascular diseases and cancers. This deregulation causes more nascent proteins to form and results in the accumulation of toxic aggregates (Voisine *et al.*, 2010). Chaperones are overexpressed in a wide range of human cancers and are implicated in tumour cell proliferation, differentiation, invasion, metastasis and recognition by the immune system (Calderwood, 2013).

The elevated expression of chaperones contributes to oncogenesis (Jaattela, 1999a). Over-expression of HSP72 in Rat-1 fibroblasts generates tumours upon injection into mice (Volloch and Sherman, 1999). In another study, transgenic mice expressing HSP72 developed T-cell lymphoma (Seo *et al.*, 1996). The elevated chaperones levels were associated with malignancy. This phenomenon may be due to the genetic changes associated with tumour progression (Tang *et al.*, 2005). Chaperones have a role in cancer clonal evolution since they provide a selective advantage through proliferation, anti-apoptosis and against other physiological stress (including hypoxia).

Chaperones increase cell survival by overcoming cytotoxic stress (Workman, 2002). Stabilisation of the structural proteins helps in malignant transformation. Kinases (Src and Met tyrosine kinases) and transcription factors (e.g., hypoxia inducible factor, HIF1) allows chaperones to contribute to angiogenesis by promoting endothelial cell proliferation (Workman, 2002).

Chaperones alter the programmed cell death (apoptosis). Chaperones do not fold the mutant (non-functional) forms of tumour suppressors and DNA repair proteins such as p53 and MutS Homolog 2 as the chaperones does not recognise the mutated sequence of the tumour suppressor (Pratt and Toft, 2003; Calderwood *et al.*, 2006; Ekman *et al.*, 2010). However, HSP70 is strongly induced in pancreatic adenocarcinoma cell line its depletion resulted in cancer cell apoptosis (Aghdassi *et al*., 2007). The diminished expression of HSP70 resulted in the apoptosis of pancreatic cancer cells *in vivo* as well as *in vitro* (Phillips *et al.*, 2007). Suppressed HSP110 expression also enhanced apoptosis in cancer cells, but not in normal cells (Hosaka *et al*., 2006).

Malfunctioning chaperones could enhance cancer growth by destabilising tumour suppressive proteins resulted from frequent amino-acid substitution and deletion of amino acid sequence (Miyata *et al.*, 2013). Without functional HSP90, p53 mutant ($p53^{V143A}$) failed to suppress cancer growth for its protein could not be folded into the active form (Blagosklonny *et al.*, 1996). Thus, it is expected that there are many misfolded proteins due to genetic mutations, implicating chaperones in various hallmarks of cancer.

1.2 Microarray and chaperones/cochaperones gene-specific meta-analysis

While chaperones are oncogenic (Jaattela, 1999a), cochaperones can be both oncogenic and tumour suppressive (Table 1.3). Under cellular stresses, the expression levels of HSP increase in tumours as a response to stress to restore the normal protein-folding environment (Ma and Hendershot, 2004: Mosser and Morimoto, 2004; Calderwood et al., 2006). The up-regulation of chaperones during tumour growth reflects an adaptive response to the stress and suggests that HSPs play a significant role in tumour survival in a hypoxic, acidic and nutrient-deprived microenvironment.

Adaikalavan Ramasamy tested the hypothesis on whether down regulation of chaperones which could affect their tumour suppressive client proteins in cancer does indeed occur (Ramasamy*et al*., 2009). He carried out a meta-analysis of chaperones mRNA levels in tumours compared to their corresponding normal tissues from 30 microarray data sets. The analysis focused on genes mapping to Gene Ontology (www.geneontology.org/) with identifier G0:0006457, which refers to the biological process of protein folding. His results demonstrated that the mRNA coding for six chaperones are down-regulated across a large spectrum of tumours. Subsequently, Ramasamy performed an analysis looking at individual data set to investigate which chaperons where down-regulated in some data set but not in others (Ramasamy, Unpublished results) and 13 of these genes where chaperons to well-known and/or putative suppressor genes.

In contrast to normal adjacent tissue, five cochaperone proteins (with number of dataset out of 30 reported by the name of the genes) were down regulated in cancers, *i.e.* PARK7 (6), PIN1 (3), TSC2 (1) and SCG5 (4). Additionally, eight chaperones were reduced in cancer, such as VBP1 (4), TRAP1(4), DNAJA3 (4), PFDN5 (4), HSPB8 (4), HSP90AA1 (3), DNAJC11 (1), DNAJCy7(2). AIPL1, which was down-regulated in four dataset, showed both chaperone and cochaperone functions. A summary of their corresponding client proteins is shown (Table 1.4).

Table 1. 4 Summary of meta-analysis. Chaperones gene transcripts are significantly down-regulated in cancer against the adjacent normal tissue. The known (putative) tumour suppressors regulated by chaperons were listed through the systematic analysis of 30 individual datasets in gene-specific meta-analysis.

Role V	Chaperone genes of interests	Number of studies found to be down-regulated out of 30 microarray studies	Target suppressor	References
Chaperones and cochaperones	AIPL1	4	NUB1	(Akey *et al.*, 2002)
Cochaperones	PARK7	6	p53	(Kato *et al.*, 2013)
	PIN1	3	p53	(Zheng *et al.*, 2002a)
	TSC2	1	TSC1	(Huang and Manning, 2008)
	SCG5	4	PC2	(Waha *et al.*, 2007)
Chaperones	TRAP1	4	Rb1	(Chen *et al.*, 1996)
	VBP1	4	VHL	(Brinke et al. 1997)
	DNAJA3	4	VHL	(Bae *et al.*, 2005)
	PFDN5	4	p73	(Watanabe *et al.*, 2002)
	HSPB8 (HSP22)	4	TAK1	(Li *et al.*, 2007)
	HSP90AA1	3	P53	(Muller *et al.*, 2004)
	DNAJC7	2	RAD1	(Xiang *et al.*, 2001)

Table 1. 5 Summary of down-regulated AIPL1. Microarray studies showing down-regulation of AIPL1 mRNA expression in different cancers. In relative to normal adjacent tissue, there were four microarray studies showing significant reduced level of AIPL1 transcript expression – Basso_B-cell microarray (Log_2 FC=-1.318; *p*-value=<0.001), Dryrskjot_Bladder cancer microarray (Log_2 FC=-1.880; *p*-value=<0.001), Lenburg_renal cancer microarray (Log_2 FC=-0.852; *p*-value=0.019), Ramasamy_colon cancer microarray (Log_2 FC=-1.291; *p*-value=0.010). They were significant with log_2 FC >0.5 or <-0.5. Of all, AIPL1 chaperone signaling is of our interests for there is no correlation to cancer to date.

Dataset	Cancer	Log_2 FC	*p*-Value
Basso *et al. 2005*	B-cells	-1.318	<0.001***
Dryrsjot *et al. 2004*	Bladder	-1.880	<0.001***
Lenburg *et al.*, 2003	Renal	-0.852	0.019*
Ramaswamy *et al.*, 2001	Colon	-1.291	0.010*

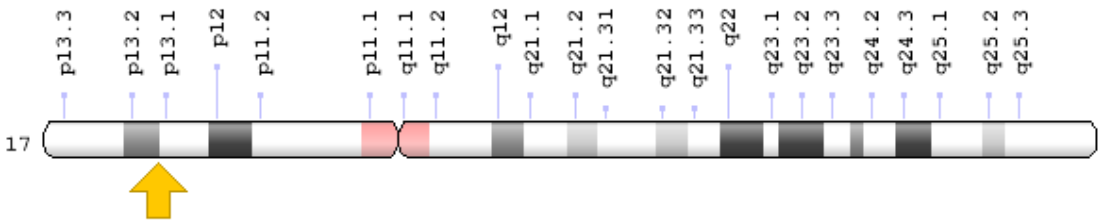
* Significant with *p*-value<0.05; ** Significant with *p*-value<0.005; ***Significant with *p*-value<0.001

1.3 Introduction of AIPL1 protein

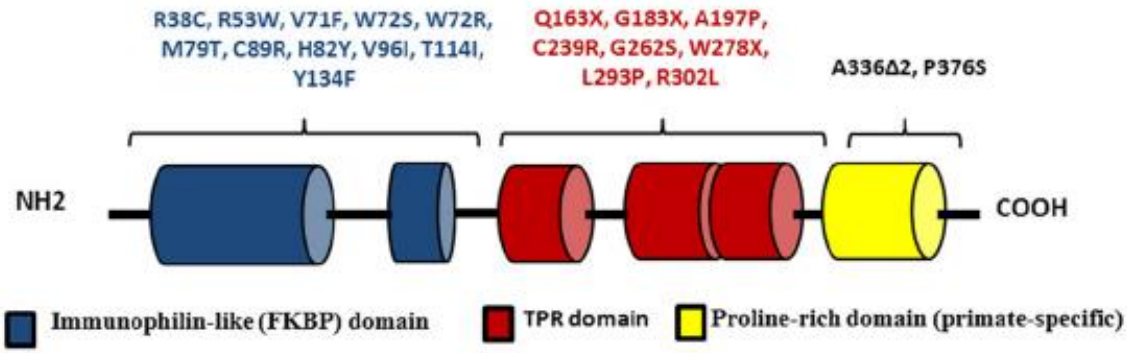
Aryl hydrocarbon receptor-interacting protein-like 1, AIPL1 is a photoreceptor and pineal-expressed gene first described in 2000 (Sohocki *et al.*, 2000). The AIPL1 gene is located on chromosome 17p13.2 (Sohocki *et al.*, 2000)(Figure 1.4a). Functionally, AIPL1 is a chaperone and also a cochaperone. The AIPL1 protein is able to form a chaperone heterocomplex with HSP70 and HSP90 (Hidalgo-de-Quintana *et al.*, 2008).

In the retina and pineal gland, the expression of AIPL1 closely follows the spatial temporal differentiation of rod and cone-receptor in the developing retina (Sohocki *et al.*, 2000). Gene defects in AIPL1 cause heterogeneous set of conditions including Leber's congenital Amaurosis (LCA), retinitis pigmentosa and cone-rod dystrophy (Sohocki *et al.*, 2000). LCA is inherited in an autosomal recessive manner and is characterised by severely impaired vision and blindness at birth (Sohocki *et al.*, 2000). The AIPL1 mRNA transcripts are expressed abundantly in pineal and retinal tissue, and to a much less extent in other tissue.

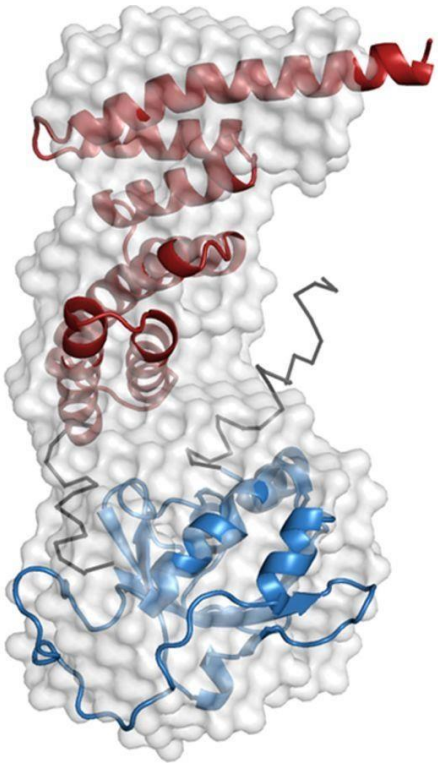
The AIPL1 protein consists of 384 amino acids, with a 44kDa molecular mass. The AIPL1 protein sequence includes three tetratricopeptide repeats (TPR), a 34–amino-acid motif found in proteins with nuclear transport or protein chaperone activity (Ma and Whitlock, 1997). AIPL1 has 49% identity and 69% similarity with the human Aryl hydrocarbon receptor-interacting protein, AIP (Kuzhandaivelu *et al.*, 1996). Figure 1.4b illustrates the topology diagram of AIPL1, AIP and FK506-binding proteins 52 (FKBP52) protein.


p13.3
p13.2
p13.1
p12
p11.2
p11.1
q11.1
q11.2
q12
q21.1
q21.2
q21.31
q21.32
q21.33
q22
q23.1
q23.2
q23.3
q24.2
q24.3
q25.1
q25.2
q25.3
17

A.


R38C, R53W, V71F, W72S, W72R, M79T, C89R, H82Y, V96I, T114I, Y134F
Q163X, G183X, A197P, C239R, G262S, W278X, L293P, R302L
A336Δ2, P376S
NH2
COOH
Immunophilin-like (FKBP) domain
TPR domain
Proline-rich domain (primate-specific)

B.



C.

D.

```
CLUSTAL O(1.2.4) multiple sequence alignment


AIPL1      -MDAALLLNVEGVKKTILHGGTGELPNFITGSRVIFHFRTMKCDEERTVIDDSRQVGQPM
AIP        MADIIARLREDGIQKRVIQEGRGELPDFQDGTKATFHYRTLHSDDEGTVLDDSRARGKPM
             *    *. :*::* ::: * ****:*  *::. **:**::.*:* **:****  *:**

AIPL1      HIIIGNMFKLEVWEILLTSMRVHEVAEFWCDTIHTGVYPILSRSLRQMAQGKDPTEWHVH
AIP        ELIIGKKFKLPVWETIVCTMREGEIAQFLCDIKHVVLYPLVAKSLRNIAVGKDPLEGQRH
           .:***: *** *** :: :**  *:*:* **  *. :**::::***::* **** * : *

AIPL1      TCGLANMFAYHTLGYEDLDELQKEPQPLVFVIELLQVDAPSDYQRETWNLSNHEKMKAVP
AIP        CCGVAQMREHSSLGHADLDALQQNPQPLIFHMEMLKVESPGTYQQDPWAMTDEEKAKAVP
            **:*:*  : :**: *** **::****:* :*:*:*::*. **:: * :::.** ****

AIPL1      VLHGEGNRLFKLGRYEEASSKYQEAIICLRNLQTKEKPWEVQWLKLEKMINTLILNYCQC
AIP        LIHQEGNRLYREGHVKEAAAKYYDAIACLKNLQMKEQPGSPEWIQLDQQITPLLLNYCQC
           ::* *****:: *: :**::** :** **:*** **:* . :*::*:: *. *:******

AIPL1      LLKKEEYYEVLEHTSDILRHHPGIVKAYYVRARAHAEVWNEAEAKADLQKVLELEPSMQK
AIP        KLVVEEYYEVLDHCSSILNKYDDNVKAYFKRGKAHAAVWNAQEAQADFAKVLELDPALAP
            *  *******:* *.**.:: . ****: *.:*** ***  **:**: *****:*::

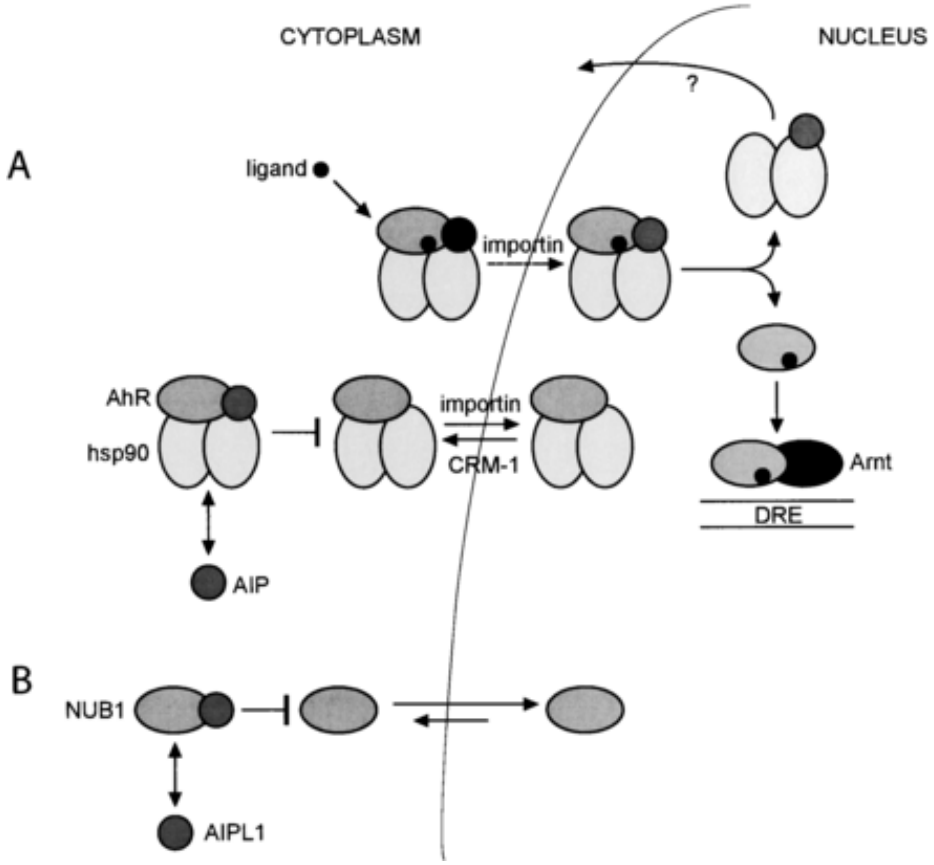
AIPL1      AVRRELRLLENRMAEKQEEERLRCRNMLSQGATQPPAEPPTEPPAQSSTEPPAEPPTAPS
AIP        VVSRELRALEARIRQKDEEDKARFRGIFSH-----------------------------
           .* **** ** *: :*:**:: * *.::*:

AIPL1      AELSAGPPAEPATEPPPSPGHSLQH
AIP        -------------------------
```

Figure 1. 4 Details of AIPL1 gene. (A) Cytogenetic map of chromosome 17 with the cytogenetic location of AIPL1 gene mapped by FISH is indicated alongside the DAPI-banded ideograms at 17p13.2 and genome location at chr17:6393693-6435199. (B) Schematic representation of AIPL1, AIP and FKBP52. The pathological mutations in AIPL1 are shown. The primary structural features are labelled as follows: PP, polyproline-rich sequence; PPIase, peptidyl prolyl isomerase domain. (C) Model of mouse AIPL1 showing homology models of the N-terminal FKBP (blue) and the C-terminal TPR (red) domains with relative orientation. (D) Multiple sequence alignments of AIPL1 and AIP.

The function of AIPL1 is largely unknown. It may function in a similar manner to that of aryl hydrocarbon receptor-interacting protein, AIP (Sohocki *et al.*, 2000; Chapple *et al.*, 2001). AIP and AIPL1 have highly similar primary structures but distinct biological functions. AIP is ubiquitously expressed in almost all tissues, and variants of AIP are associated with familial pituitary adenomas (Ozfirat and Korbonits, 2010; Cazabat *et al.*, 2011). In contrast, AIPL1 is expressed specifically in adult rod photoreceptor cells, where its function is essential but not well understood (Schwartz *et al.*, 2006).

AIPL1 could potentially be involved in the signalling of a nuclear receptor (Fig 1.5). AIP enhances the ligand-induced transcriptional activity of the aryl hydrocarbon receptor, AhR (Ma and Whitlock, 1997; Carver *et al.*, 1998; Meyer *et al.*, 1998; Lees and Whitelaw, 2002; Lees *et al.*, 2003). AIP also stabilises cytoplasmic AhR by preventing the ubiquitination and subsequent degradation of the protein(Meyer and Perdew, 1999; Kazlauskas *et al.*, 2000; LaPres *et al.*, 2000; Meyer *et al.*, 2000; Lees *et al.*, 2003). AIP can inhibit chromosomal maintenance 1 (CRM1)-mediated nucleocytoplasmic shuttling of the AhR and cause its cytoplasmic retention (Petrulis *et al.*, 2000; Petrulis *et al.*, 2003). It is done by altering the conformation of the AhR nuclear localisation signal, thereby hindering interaction with the nuclear import receptor protein, Importin-β (Kazlauskas *et al.*, 2000; Petrulis *et al.*, 2003).


CYTOPLASM
NUCLEUS
?
A
ligand
importin
AhR
hsp90
importin
CRM-1
Arnt
DRE
AIP
B
NUB1
AIPL1

C.

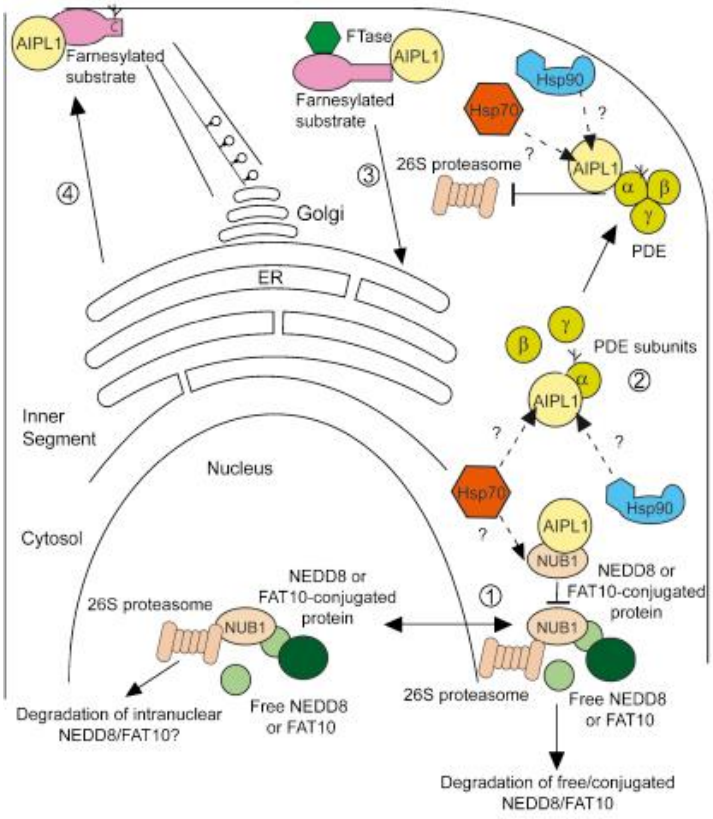


Figure 1. 5 The function of AIP and AIPL1 (**A**) AIP regulates the nuclear translocation and transactivation of the AhR. DRE, dioxin response element. (**B**) Similarly, AIPL1 modulates the nuclear translocation of its client protein, NUB1. (C) roles of AIPL1 in photoreceptors. Schematic representation showing potential roles of AIPL1 within photoreceptors. AIPL1 is able to modulate the nuclear localisation of NUB1, which may affect the NUB1 NEDD8 and FAT10 'busting' activity (1); AIPL1 interacts with and enhances stability of the phosphodiesterase, PDE holoenzyme (2); AIPL1 may enhance transport and stability of farnesylated proteins to the ER (3) or other target membranes (4). AIPL1 is likely to utilize the HSP70 and HSP90 chaperone machinery to execute its cellular functions.

Like other immunophilins, AIPL1 is a chaperone (Li *et al.*, 2013b). The unique pattern of the proline-rich domain of AIPL1 could chaperone specific client proteins. The C-terminal proline-rich region is essentially hydrophilic and greatly influences the chaperone activity (Wayne and Bolon, 2010). The chaperone activity of AIPL1 requires the cooperation between the proline-rich domain and other domains in AIPL1. The linker region connecting the FKBP domain and TPR domain plays an important role in the chaperone activity (Pirkl *et al.*, 2001). Proline-rich regions are common modules mediating protein–protein interactions, especially in proteins involved in signaling transduction pathways (Ruaro *et al.*, 1997). It was found that AIPL1 protein proline-rich domain is a negative regulator of the HSP90 interaction with substrates (Li *et al.*, 2013b).

1.3.1 Interaction of NUB1 and the downstream ubiquitin pathway

AIPL1 is capable of interacting with NUB1 directly in a chaperone-like fashion (van der Spuy and Cheetham, 2004). AIPL1 was found to suppress the aggregation of NUB1 *in vivo* and reduce its nuclear translocation (van der Spuy and Cheetham, 2004). NUB1 recruits the ubiquitin-like protein NEDD8 and its conjugates for proteasomal degradation (Kamitani *et al.*, 2001).

NEDD8 is conjugated specifically to members of the cullin (CUL) family in a manner analogous to ubiquitination (Yeh *et al.*, 2000). The cullins are components of a Skp1, cullin, F-box protein (SCF) ubiquitin E3 ligase composed of SCF and ROC1 (Zheng *et al.*, 2002b). The CUL1 SCF complex catalyses the ubiquitination of inhibitory factor κBα, β-catenin, cyclin D proteins, p27 and p21 (Yu *et al.*, 1998; Hatakeyama *et al.*, 1999; Kitagawa *et al.*, 1999; Suzuki *et al.*, 1999; Morimoto *et al.*, 2000), and NEDD8 conjugation is necessary for the Ubiquitin E3 ligase activity of the CUL1 SCF complex (Podust *et al.*, 2000; Read *et al.*, 2000). The CUL2 and CUL3 SCF complexes target hypoxia-inducible factor-1α (HIF1α) and cyclin E respectively for ubiquitination and proteasomal degradation (Singer *et al.*, 1999; Kamura *et al.*, 2000). Therefore NEDD8–cullin conjugation has been implicated in many important biological events, including cell signalling and cell-cycle regulation.

NUB1 targets NEDD8 and NEDD8 conjugates for proteasomal degradation (Kamitani *et al.*, 2001). Recently, a splicing variant of NUB1 possessing a 14-amino-acid insertion in the C-terminus (NUB1L) was identified (Tanaka *et al.*, 2003). NUB1L has been shown to interact with NEDD8 as well as an additional ubiquitin-like protein FAT10, and to accelerate the proteasomal degradation of these ubiquitin-like proteins (Tanaka *et al.*, 2003; Hipp *et al.*, 2004).

In addition, both NUB1 and NUB1L interact with a ubiquitin precursor UBC1 and mediate the hydrolysis of UBC1 by an unidentified ubiquitin C-terminal hydrolase (UCH) (Tanaka *et al.*, 2003). It has been suggested that the interaction of AIPL1 with NUB1 implicates biological functions related to cell growth and cell cycle regulation. However, the cellular role of AIPL1 with respect to NUB1 still remains to be fully determined.

The expression and localisation of AIPL1 and NUB1 were examined (van der Spuy *et al.*, 2002; van der Spuy *et al.*, 2003). AIPL1 was predominantly cytoplasmic, whereas NUB1 was predominantly nuclear due to a functional nuclear localisation signal near the C-terminus (Kito *et al.*, 2001; van der Spuy *et al.*, 2003). AIPL1 modulates NUB1 nuclear translocation. These results suggest that AIPL1 protein restricts the translocation of NUB1, thereby modulating downstream effects of NUB1 on cell signalling and cell growth.

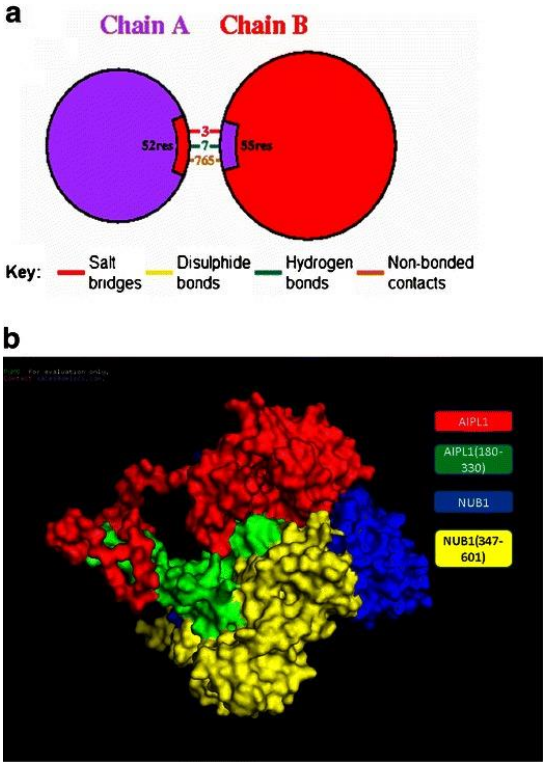


Figure 1. 6 Interaction of AIPL1 and NUB1 proteins. (a) Interaction between AIPL1 and NUB1 from PDBsum server. Chain A represents AIPL1 and chain B indicates NUB1. (b) Docking complex of AIPL1 interaction with NUB1. Illustration of docked complex for AIPL1 and NUB1. The AIPL1 region is represented by *red* and *green*, and the NUB1 region represent for *blue* and *yellow* using PYMOL (Muthukumaran *et al.*, 2012).

1.3.2 Background of NUB1

NUB1 is an interferon (IFN)-inducible protein of 69 kDa, composed of 601 amino acids. It also has a splice variant, NUB1L, which possesses an extra 14 amino acids that encode an additional Ub-associated (UBA) domain (Fig. 1.7). NUB1 proteins can recruit FAT10- and NEDD8-conjugated proteins to the proteasome for degradation and negatively regulate the NEDD8-conjugation system (Kamitani *et al.*, 2001; Kito *et al.*, 2001; Tanaka *et al.*, 2003; Tanji *et al.*, 2005; Groettrup *et al.*, 2008). The NUB1 proteins have been observed in various types of cancer cells, including cervical adenocarcinoma, rectal adenocarcinoma, neuroblastoma, malignant lymphoma and renal cell carcinoma (RCC) (Kito *et al.*, 2001). Upregulated NUB1 expression has been linked to IFNα-induced antimitogenic actions. Additionally, NUB1 has demonstrated anticancer properties in RCC cell line, where it was involved in apoptosis and S-phase transition through its action on p27 and cyclin E (Bornstein *et al.*, 2006; Hosono *et al.*, 2010). Up-regulation of NUB1 effectively inhibits the proliferation of IFNα-resistant RCC cells (Hosono *et al.*, 2010).

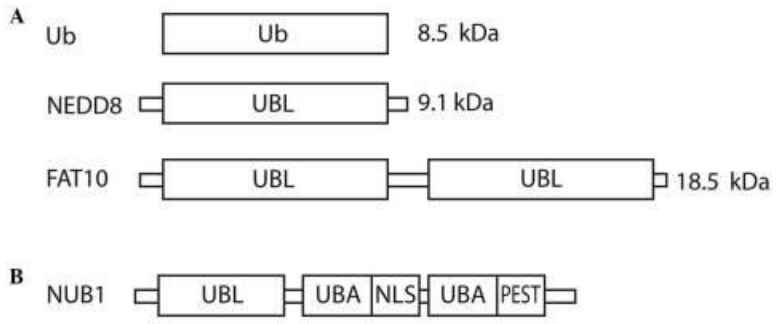


Figure 1. 7 Structural representation of (A) Ub, NEDD8 and FAT10, and (B) NUB1. Ub, ubiquitin; NEDD8, neural precursor cell expressed, developmentally down-regulated 8; FAT10, HLA-F-adjacent transcript 10; NUB1, NEDD8 ultimate buster 1; UBL, ubiquitin-like domain; UBA, ubiquitin-associated; NLS, nuclear localisation signal; PEST, proline-enriched glutamic acid, serine and threonine domain.

NUB1 protein has been reported to play a role in Huntington's disease (Lu *et al.*, 2013) and Congenital Amaurosis (Kanaya *et al.*, 2004). In cancers, the degrading enzyme NUB1 is an attractive candidate for inhibition of $p27^{KIP1}$ and $p21^{CIP1}$ through the regulation of the SCF^{SKP2} ligase activity (Hosono *et al.*, 2010). The upregulated $p21^{CIP1}$ in NUB1-knockdown cancer cells is thought to be promising in directing the cells to senescence. NUB1 protein was reported to be a tumour suppressor as it exerts growth inhibition during its overexpression; upon IFNα treatment, overexpressed NUB1 induced apoptosis in IFNα-resistant A498 cells (Hosono *et al.*, 2010). However, its general lack of enzymatic activities makes NUB1 less suitable for small molecule inhibition (Lu *et al.*, 2013). Thus, the low-molecular-weight proteins FAT10 and NEDD8 could be key to developing novel strategies in anticancer therapy, as they interact with NUB1 (Tanaka *et al.*, 2012).

The UBL enzymatic cascade scheme that results in UBL conjugation and protein degradation involves several distinct steps. Each step requires different classes of enzyme and is shown in table 1.6.

Table 1. 6 Overview of the enzymatic cascade involved in UBLs conjugation.

UBL	**Ub**	**NEDD8**	**FAT10 and Ub**
E1 activating enzymes	UAE	APPBP1-UBA3 heterodimer	UBA6
E2 conjugating Enzymes	UBCs	UBE2M &UBE2F	USE1
E3 ligases	Ub E3 Ligases	NEDD8 E3 Ligases	?
Substrates	1,000s	200s	?

*UBC: Ub conjugating enzymes UBL, ubiquitin-like protein; Ub, ubiquitin; NEDD8, neural precursor cell expressed, developmentally down-regulated 8; FAT10, HLA-F-adjacent transcript 10; UAE, ubiquitin-activating enzymes; APPBP1, amyloid-β precursor protein-binding protein 1; UBA, ubiquitin-like modifier-activating enzyme; UBCs, Ub-conjugating enzymes; UBE2, ubiquitin-conjugating enzymes E2; USE1, UBA6-specific E2 enzyme; N/A, not applicable.

1.4 Neddylation and its functions

Neddylation is a post-translational modification process that conjugates NEDD8 to its target proteins, in a process that is analogous to that observed for ubiquitination. However, the neddylation process uses a distinct E1 and E2 enzyme reaction scheme (Haas *et al.*, 1987; Kamitani *et al.*, 1997; Liu *et al.*, 1999; Ichimura *et al.*, 2000; Bawa-Khalfe and Yeh, 2010) (Table 1.6). Fig1.9 summarises the NEDD8 conjugation and deconjugation steps (Rabut and Peter, 2008; Tanaka *et al.*, 2012). The C-terminal glycine of NEDD8 is adenylated by E1 NEDD8 activating enzymes (NAE), a heterodimer composed of amyloid-β precursor protein binding protein 1 (APPBP1) and ubiquitin-activating enzyme 3 (UBA3). NEDD8 is covalently conjugated to the NAE via a thiolester linkage (Walden *et al.*, 2003). The activated NEDD8 is consecutively transferred to the E2 NEDD8-conjugation enzyme and then to the specific substrates (i.e. cullins) via an isopeptide bond. Some RING finger domain containing proteins including Rbx1/ROC1, MDM2, FBXO11, and c-Cbl, work in an E3 ligase-like fashion for cullin neddylation.

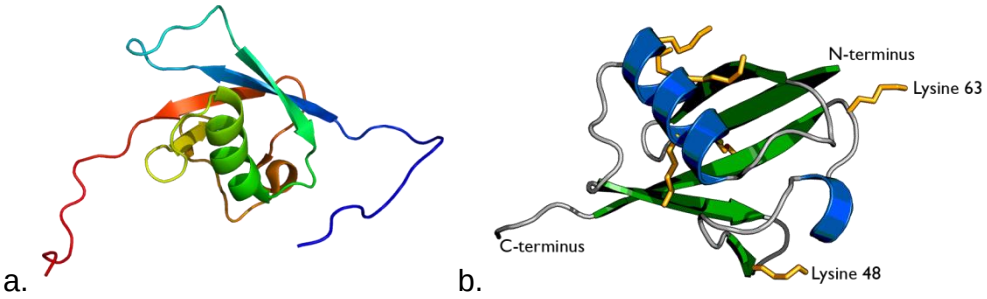


Figure 1. 8 Structure of a) N-terminal ubiquitin-like domain of human NUB1 b) Human ubiquitin.

There are two NEDD8-specific E2 conjugating enzymes, namely UBE2M (also known as UBC12) and UBE2F. These E2 enzymes act to transfer NEDD8 to target protein through E3 enzymes. It was reported that all NEDD8 E3 enzymes can function as ubiquitin E3 enzymes. The predominant NEDD8 E3 ligases are the ring subunits RING-box protein 1 (RBX1) and RBX2 (Kamura *et al.*, 1999; Walden *et al.*, 2003; Huang *et al.*, 2007; Huang *et al.*, 2009; Olsen *et al.*, 2010). Meanwhile, the non-RBX family NEDD8 E3 ligases include c-CBL, RNF111 (ring finger protein 111), MDM2 and inhibitor of apoptosis (Enchev *et al.*, 2015).

Of the numerous NEDD8 substrates, neddylation has been best described in the cullin family (Hjerpe *et al.*, 2012). In this mechanism, NEDD8 from the E2 cysteine active site is transferred onto a lysine residue in the N-terminus of the target proteins (Fig. 1.9) (Saha and Deshaies, 2008). Cullin neddylation is further mediated by defective in cullin neddylation protein 1-like proteins (Enchev *et al.*, 2015). It was reported that RING E3 ligases could neddylate the same substrate on multiple lysine residues (Enchev *et al.*, 2015). However, the interaction between non-RBX RING E3 ligase and E2 enzymes remains to be elucidated.

NEDD8-conjugated substrates are deneddylated by various proteins that include COP9 signalosome (CSN), NEDD8-specific protease 1 (NEDP1/DEN1) and ubiquitin specific peptidase 21 (Lyapina *et al.*, 2001; Schwechheimer *et al.*, 2001; Mendoza *et al.*, 2003; Chan *et al.*, 2008; Rabut and Peter, 2008; Gong *et al.*, 2014). Neddylation may be inhibited by cullin-associated and neddylation-dissociated 1 through its direct binding to cullins (Liu *et al.*, 2002; Goldenberg *et al.*, 2004). NEDD8 and neddylated substrates are recruited by NUB1 for proteasomal degradation (Kamitani *et al.*, 2001; Kito *et al.*, 2001) (Figure 2a). In the G1-S phase transition, Bornstein *et al* demonstrated how neddylated cullin 1 cooperatively activates the SCF^{SKP2} Ub ligase complex, which results in p27 degradation (Fig. 1.9) (Bornstein *et al.*, 2006). Furthermore, previous studies found that cullin neddylation increased the Ub E3 ligase activity of the SCF complex (Fig. 1.10) (Duda *et al.*, 2008; Saha and Deshaies, 2008).

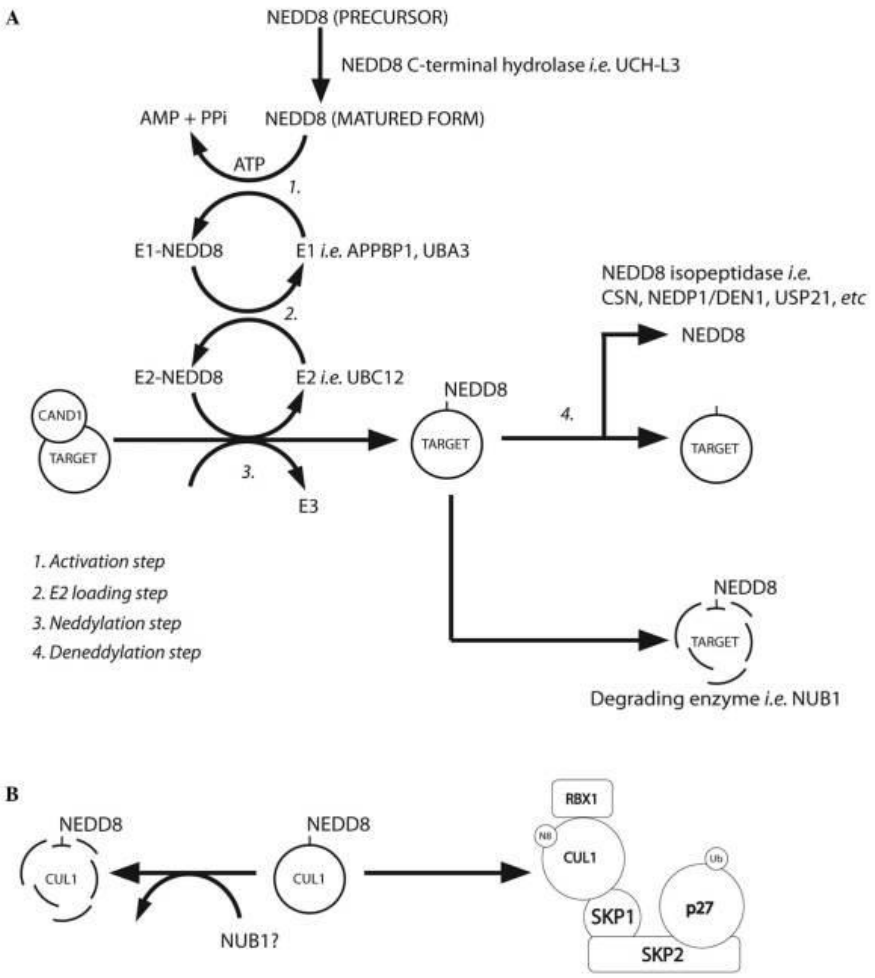


Figure 1. 9 NEDD8 conjugation pathway and roles of NUB1 on neddylated CUL1. (A) Schematic summary of the main steps of the neddylation pathway [modified from Rabut and Peter, 2008 (Rabut and Peter, 2008); Tanaka *et al*, 2012 (Tanaka *et al.*, 2012)]. (B) Neddylated CUL1 locks the SCF complex with phosphorylated p27 and cyclin E [as suggested by Bornstein *et al*, 2006 (Tanaka *et al.*, 2012) and Tanaka *et al*, 2012 (Bornstein *et al.*, 2006)]. CAND1, cullin-associated and neddylation-dissociated 1; AMP, adenosine monophosphate; PPi, anion $P2O7^{4-}$; ATP, adenosine triphosphate; UCH-L3, ubiquitin C-terminal hydrolase isozyme L3; APPBP1, amyloid-β precursor protein binding protein 1; DEN1, deneddylase 1, CSN, COP9 signalosome; NEDP1, NEDD8-specific protease 1; NUB1, NEDD8 ultimate buster 1; USP21, ubiquitin specific peptidase 21, CUL1, cullin 1; SKP1, S-phase kinase-associated protein 1; SKP2, S-phase kinase-associated protein 2; RBX1, ring-box 1, E3 ubiquitin protein ligase; SCF, Skp, cullin, F-box-containing complex.

NEDD8 is negatively down regulated by NEDD8 ultimately buster 1 (NUB1), which links the UBLs to the 26S proteasome for further UPS degradation. Reports described that NUB1 can recruit NEDD8 and NEDD8-conjugated proteins to the proteasome for degradation, and this might modulate the cell cycle profile upon stress (Tanaka *et al.*, 2012). The capability of NEDD8 to activate the ubiquitin E3 ligase-SCF complex (by covalent binding to cullins) adds more complexity to the ubiquitination machinery (Kamitani *et al.*, 1997; Osaka *et al.*, 1998; Wada *et al.*, 1999; Podust *et al.*, 2000; Read *et al.*, 2000; Morimoto *et al.*, 2003). Therefore, validations of NEDD8 targets would be able to identify the genuine NEDD8 substrates.

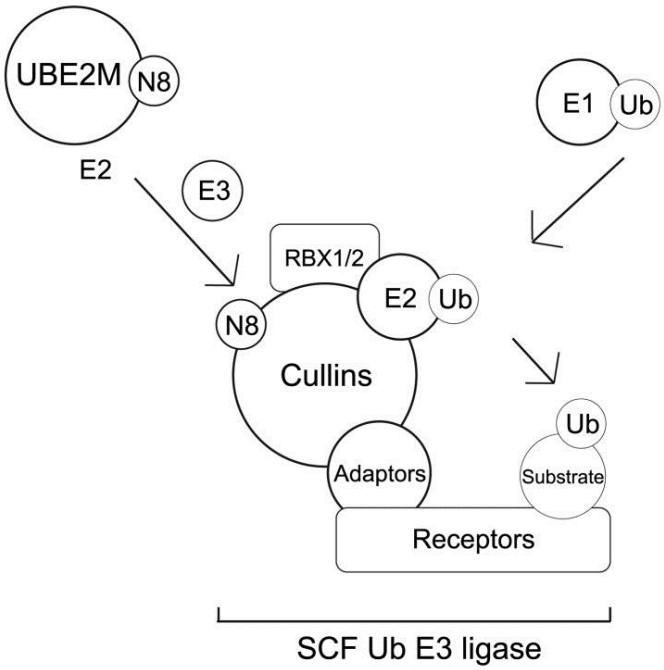


Figure 1. 10 NEDD8 conjugation and ubiquitination pathway through cullin proteins. UBE2M, ubiquitin-conjugating enzyme E2M; RBX1/2, ring-box 1; Ub, ubiquitin; NEDD8, neural precursor cell expressed, developmentally down-regulated 8; SCF, Skp, cullin, F-box-containing complex.

1.5 FAT10ylation and its functions

FAT10 was discovered by Sherman Weisman in 1996 (Qin *et al.*, 2008). Due to the poor solubility of the protein at high concentrations, the structure of FAT10 protein was only recently defined (Theng *et al.*, 2014). The structure of FAT10 consists of two β-grasp fold domains connected by a short linker (Theng *et al.*, 2014). FAT10 protein was found to be expressed predominantly in immune tissue including thymus, lymph nodes and spleen (Michel *et al.*, 2004; Wagenaar-Miller *et al.*, 2004; Tapia *et al.*, 2006). Its expression is stimulated by pro-inflammatory cytokines, namely interferon-γ (IFN-γ) and tumour necrosis factor (TNFα) (Aichem *et al.*, 2012). FAT10 protein is found in mature dendritic cells and it demonstrates oncogenic characteristics. Ectopic expression of FAT10 was observed in malignant tumour transformation and its growth (Gao *et al.*, 2014), and FAT10 is known to be upregulated in several tumour types, for example in liver and colon tumours (Lee *et al.*, 2003; Lukasiak *et al.*, 2008).

FAT10 shares the same E1 and E2 enzymes with the Ub conjugation pathway. The FAT10 E1 enzyme UBA6 can activate both Ub and FAT10 (Chiu *et al.*, 2007; Jin *et al.*, 2007; Pelzer *et al.*, 2007; Groettrup *et al.*, 2008). FAT10's adenylation and transthiolation reactions are kinetically slower than those for Ub. UBA6 protein is thought to be the only FAT10 E1 enzyme in cells, since UBA6 knockdown effectively abolished the formation of FAT10-conjugates *in vitro* (Chiu *et al.*, 2007; Aichem *et al.*, 2010). Similarly, USE1 is the only UBA6-specific E2 enzyme discovered to be involved in FAT10 conjugation, though it also functions in a similar fashion for the conjugation of Ub (Jin *et al.*, 2007). USE1 could only bind to activated Ub from UBA6 but not UBE1 (Jin *et al.*, 2007).

Little is currently known about FAT10 and research to identify possible FAT10 E3 ligases and deconjugating enzymes continue. However, ectopically expressed FAT10 was not observed to degrade over time, suggesting that a group of FAT10-deconjugating enzymes may not exist (Hipp *et al.*, 2005). It is believed that FAT10 is capable of promoting its own proteasomal-dependent degradation without the aid of deconjugation enzymes (Hipp *et al.*, 2005). FAT10-conjugated proteins were found to have a reduced half-life similar to that observed for ubiquitin-conjugated proteins (Kane *et al.*, 2007). Conversely, it was found that FAT10-conjugated p62 accumulated under proteasome inhibition (Aichem *et al.*).

The interferon inducible protein NUB1 interacts with FAT10 non-covalently (Kamitani *et al.*, 2001) and it significantly accelerates the degradation of FAT10 by the proteasome (Kamitani *et al.*, 2001). NUB1 binds to the proteasome subunit S5a (Tanji *et al.*, 2005) NUB1 also bind to FAT10 via its three C-terminal UBA domains (Fig 1.11) (Hipp *et al.*, 2004). NUB1 is also able to interact with the von Willebrand A (VWA) domain of RPN10 (S5a), one of the subunits of the 26S proteasome (Kamitani *et al.*, 2001; Tanji *et al.*, 2005). The degradation of FAT10 is accelerated further by NUB1 splicing variant, NUB1L which can bind both to RPN10 as well as the 19S regulator subunit RPN1 (S2) (Hipp *et al.*, 2004).

The 26S proteasome subunit RPN10 (S5a) is the docking site for FAT10, NUB1L, and polyubiquitin. Lysine 48-linked poly-ubiquitin chains bind to the ubiquitin interaction motifs (UIM) 1 and 2 of RPN10. Meanwhile, FAT10 can target substrate proteins to the proteasome independently of poly-FAT10ylation. FAT10 directly interacts with the VWA domain of RPN10 and no ubiquitination is required (Tanji *et al.*, 2005). The co-expression of NUB1L accelerated the degradation of FAT10 suggesting the favour of proteasomal degradation (Tanji *et al.*, 2005).

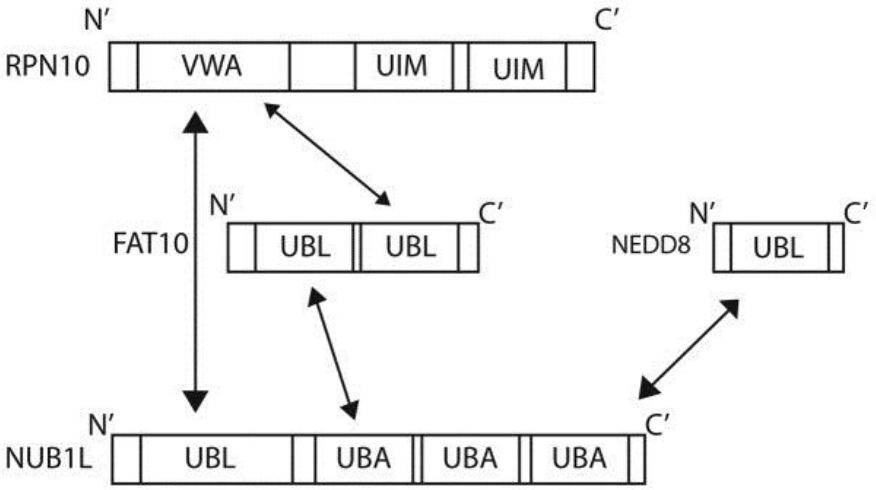


Figure 1. 11 Domain structure of NUB1L, FAT10 and RPN10 and their interacting domains (Kamitani *et al.*, 2001; Hipp *et al.*, 2004; Tanji *et al.*, 2005). RPN10, regulatory particle non-ATPase 10; FAT10, HLA-F-adjacent transcript 10, NUB1L, NEDD8 ultimate buster 1 long isoform; UBL, ubiquitin-like domain; UBA, ubiquitin-associated; UIM, ubiquitin-interacting motif; VWA, von Willebrand A motif.

1.6 Ubiquitin Proteasome System

The UPS is important in regulating protein homeostasis in human cells through programmed degradation. The degradation of regulatory proteins can affect cell-cycle regulation, cell proliferation, intracellular signaling, DNA repair and apoptosis (Ciechanover, 1998; Ciechanover and Schwartz, 1998; Hershko and Ciechanover, 1998; Hershko, 2005). As UPS degradation is a major clearance system associated with proteolysis within the cells, its deregulation can cause the pathogenesis of cancer and other diseases through the inappropriate loss of regulatory proteins or unintentional activation of certain specific signalling cascades. For instance, cancerous cells develop when cell cycle controls break down, leading to unregulated cell proliferation. Cancer cells can also escape from apoptosis induced by several cellular stresses. Hence, an interruption to the normal regulation of the UPS could lead to abnormal cell proliferation.

The 26S proteasome is a protease complex capable of degrading polyubiquitinated proteins. The 26S complex is composed of a barrel-shaped 20S proteasome core with a 19S regulatory particle at either or both of its ends. The 20S proteasome contains the enzymatic active sites, whilst the 19S regulatory particle helps to control access of UBL-conjugated substrates to the core. There are three proteasome active sites within the 20S core, namely the caspase-like (β1), trysin-like (β2) and chymotrypsin-like (β5) domains. These sites use an N-terminal threonine as the catalytic amino-acid residue.

1.7 Rationale of study

The discovery of down-regulated AIPL1 in cancer has promted the interests to identify its role in cancer. Chaperones are thought to contribute to cancer progression, whereas cochaperones could be pleomorphic. Down-regulated chaperones could result in the accumulation of both misfolded and nascent client proteins which are functionally inactive. Though both HSP90 and HSP70 HSPC interact with AIPL1 (in a cochaperone fashion), AIPL1 proteins is able to interact independently with NUB1 in a chaperone-like manner(van der Spuy *et al.*, 2002). AIPL1 also has a role in post-translational modification and regulating intracellular protein trafficking (Berg and Pongratz, 2002).

The AIPL1 signaling pathway was studied for retinal degenerative diseases but no studies were performed to correlate AIPL1 with to cancer metastasis and pathogenesis. The interaction of AIPL1 with NUB1 could serve physiological relevance in cancers. It regulates the ubiquitin proteasome system through FAT10ylation and neddylation. NUB1 is able to recruit FAT10- and NEDD8-conjugated for proteasomal degradation.

The SCF ubiquitin E3 ligases have been shown to be deregulated in various cancers. It results in unlimited cell proliferation and carcinogenesis *via* accumulation of their substrate proteins. As a result, the ubiquitin E3 ligases are gaining attention as a potential target for anticancer therapy.

The search for neddylation targets requires more robust experimental validations. The ectopic overexpression of the UBLs could lead to false positive conjugation of substrates (Enchev *et al.*, 2015). The functional significance of this observation remains unknown. There is a general lack of information on how NUB1 regulates cullin neddylation under homeostatic conditions. It is an open question whether neddylation is functionally distinct from ubiquitination. For example, polyneddylation and polyubiquitination at DNA damage sites or in response to other stress conditions are functionally redundant, and NEDD8 and ubiquitin can be recognized by the same interaction motifs. These two modifications can elicit distinct biological responses. Efforts are clearly needed to identify and characterise NEDD8-interacting domains and proteins.

Unlike such deconjugating enzymes as CSN, NEDP/DEN1 and USP1, NUB1 causes the degradation of both FAT10- and NEDD8-conjugated targets. It therefore appears to be a unique degrading enzyme in cells. Its expression regulates NEDD8- and FAT10-based signalling in response to cellular stresses. However, NUB1 protein and its clinical relevance in UBL' pathways remain to be explored. Hosono *et al.* (2010) found that overexpression of NUB1 inhibits cell growth, and the same study demonstrated lower NUB1 mRNA expression in IFNα-sensitive 4THUR cells (Hosono *et al.*, 2010). The same study highlighted that NUB1 does not get induced in IFNα-resistant cells. The transiently expressed NUB1 sensitise the same cells (Hosono *et al.*, 2010) and induces apoptosis (Hosono *et al.*, 2010). Therefore, there is a potential strategy to kill IFNα-resistant cells by increasing NUB1 activity (Hosono *et al.*, 2010).

FAT10 research is still in an early stage as the biological consequences of FAT10ylation are poorly described. The de-FAT10ylating enzymes are actively pursued as drug targets in the pharmaceutical industry these days knowing that a number of putative FAT10 targets are cancer promoting or inhibitors of apoptosis. Future work should focus on the FAT10 modulated Proteasome System and the mechanism of its cytokine-induced reactions.

Cochaperones are potential targets for cancer therapy in themselves and can be used to assess the likely prognosis of individual malignancies. The key importance of cochaperones for many pathways of protein folding in cancer suggests high promise for the future development of novel pharmaceutical agents. The negative regulation of the Ub, NEDD8 and FAT10-conjugation pathway could impose great potential for cancer suppression. SCF complexes are often deregulated in cancer and could be modulated through manipulation of CUL neddylation. Neddylation and FAT10ylation inhibitors have recently been developed as a novel class of anticancer agent. These compounds are expected to exhibit better specificity for cancer cells and have reduced toxicity. The degrading enzyme (such as CSN and NUB1/NUB1L) is an attractive candidate for inhibition of Ub, NEDD8 and FAT10-ligase activity. They are expected to represent a new strategy in anticancer therapy.

The interplay of these ubiquitin like proteins highlight the roles of both AIPL1 and NUB1. It is essential to understand the mechanisms on how AIPL1 regulates NUB1 and down-regulates the ubiquitin cascade *via* NEDD8 conjugation and the FAT10 pathway. This provides insights into potential cancer therapy that could be used to selectively suppress cancer growth. We are searching for the roles of AIPL1 and its interacting NUB1 partner in cancer. AIPL1 and NUB1 could be potential targets for cancer therapy and be used to assess the prognosis of cancer malignancies.

1.8 Objectives of study

In general, this study aims to describe the specific role of AIPL1 and NUB1 in cancer pathogenesis. The work will focus on the neddylation induced accumulation of p27 and p21 and the corresponding cell cycle regulation.

The specific objectives include

a) To characterise the AIPL1 & NUB1 transcription pattern and the clinico-pathological correlations through bioinformatic analysis.
b) To study how AIPL1 & NUB1 affect p27 and p21 through CUL1-based ubiquitin E3 ligase.
c) To examine the alternative pathway of AIPL1 and NUB1 through CUL2-based ubiquitin E3 ligase.
d) To correlate the NUB1 protein expression to patients' treatment outcome.

Chapter 2

Methods and Materials

2.1 Cell Line

All cancer cell lines were obtained from American Type of Cell Collection (ATCC, Manassas, VA, USA). HCC1806, MCF-7, MDA-MB-231,SKBR3, BT474, ACHN, 786-O, RCC4, RCC4plusVHL and T-47D cells were maintained in DMEM supplemented with 10%(v/v) foetal calf serum (FCS). HCT116 were maintained in McCoy's 5A supplemented with 10%(v/v) FCS. Y79 was cultured in RPMI-1640 with 20%(v/v) FCS. The medium was changed every two to three days. All cell lines were obtained from Cancer Research UK Cell Production Laboratories (Clare Hall, Hertfoshire, UK). All cells were free from mycoplasma contamination. MLN4924 (Pevonedistat®) was purchased from Sigma and was dissolved in dimethyl sulfoxide (DMSO) and stored at −20 °C.

2.2 Cell Culture

Cells were grown in a tissue culture incubator in a humidified atmosphere of 5% CO_2 and 95% filtered atmospheric air, and maintained at a temperature of 37°C, unless otherwise indicated. Cells were passaged by aspirating medium, washing the cells with PBS, and then adding 1x trypsin-EDTA (Invitrogen) until they detached. The trypsin was neutralized by adding equal amount of DMEM supplemented with 10% (v/v) FBS. The cells then were centrifuged for 5 minutes at 1000 rpm to generate a pellet from which the supernatant was aspirated. The pellet was then split 1:10 and reseeded. This process was carried out every 6-7 days. Cells were cultured on sterile, tissue culture grade, non-pyrogenic plasticware (Corning). Cells were treated with MLN4924 (Sigma) at 1µM for 48h.

Hypoxic incubations (0.1% O2, 5% CO2,) were performed using an INVIVO2 400 hypoxic workstation (Pro-Lab Diagnostics). All cells were allowed 6 hours to attach and recover after being plated in final densities before being exposed to hypoxia.

2.3 Counting Cells

Cell counting was performed when a specific number of cells were required for an experiment. Cells were detached, centrifuged, and resuspended, in an appropriate volume of medium. Cells then were counted using the Coulter Particle Counter Z2 (Beckman Coutler) according to maufacturer's instructions. Briefly, 400µL of cell suspension were diluted with 19.6 µL of isoton buffer and a particle count taken in the range of 9-27 µM. The machine was calibrated to calculate the number of cells/mL.

2.4 Preparation and Recovery of cell stocks (cryo-preserved cells)

Only cells in the log phase of growth were used for cryopreservation. Cells were detached as described previously. The cell pellet was then resuspended in freezing medium and divided between rounded bottomed cryo-vials (Corning). Freezing medium was prepared with DMSO, FCS, and culture medium at a ratio of 1:3:6, respectively. Vials were frozen down to 1° C per minute to -80 ° C in an isopropanol-bath freezing container (MrFrosty, Nalgene). Within one week, cell vials were transferred to liquid nitrogen for long term storage. To recover the cells from storage, cryovials were rapidly defrosted to 37°C and transferred to pre-warmed media.

2.5 Gene silencing by RNA Interference

Cells were plated on 6-well dishes at 0.25-1 x 10^6 per dish and left overnight to adhere. siRNA duplexes were transfected into cells at 25pmol using Oligofectamine™ RNAiMAX and then cultured in Optimem™ for 1-3 days (3µL 10µM siRNA, 9µL Oligofectamine™, 150µL Optimem™).

Transfections of siRNA duplexes targeting NUB1 or non-targeting pool were from Dharmacon ON-TARGETplus Human NUB1 siRNA, at a final concentration of 25pmol. The sequences of siRNA used to target NUB1 and control sequence were L-019158-00-0005 and D-001810-10-05 respectively (Dharmacon GE, UK). Reduction in NUB1 protein expression, measured by Western blot analysis, was used to indicate gene silencing.

2.6 Immunostaining of paraffin-embedded tissue sections

Staining of formalin-fixed paraffin-embedded tissues was performed according to the following description. Slides were heated at 120°C for 10 min to melt the wax and help the sections adhere. They were then dewaxed and immersed in Citroclear (HD, Supplies, UK) for 5 min twice and rehydrated in graded Industrial Methylated Spirit solutions (100% twice followed by 50% once for 5min in each) before rinsing in tap water followed by a PBS wash. Antigen retrieval was performed in a decloaking chamber (Biocare Medical, USA) set at 2min, high pressure, in EDTA pH8.0. Then, the cooling slides were placed in PBS.

To minimize non-specific antibody binding, the slides were blocked with 10% normal horse serum (Vector Laboratories, UK). In the next step, primary antibody was applied to the slides and incubated at room temperature for 1 hour. Both antibodies were diluted in RPM1 (Lonza) with 10% bovine serum (Sigma-Aldrich). After 1 hour incubation, the slides were washed three times with PBS, and then they were incubated with the anti-mouse secondary antibody for 50 minutes at room temperature. The slides were then washed with PBS for three times, and DAB was applied to the sections for 5-8 min. The reaction was stopped by washing the slides with tap water. In the final step the slides were counterstained and immersed in heamatoxylin solution (Gill No3) for 20s, rinsed in tap water and mounted with Aquamount. Slides were visualized on a BX51 microscope (Olympus) attached to a DP70 digital camera (Olympus) and images were captured using the DP manager and DP Contoller software (Olympus).

Antibody	Antibody name/catalogue number	Species	Clonality	Source
NUB1	4H2	Mouse	Monoclonal	Novus biologicals
AIPL1	3B4	Mouse	Monoclonal	Novus biologicals
FAT10	4F1	Mouse	Monoclonal	EMD Milipore
NEDD8	Y297	Rabbit	Monoclonal	Abcam
HIF1α	610958	Mouse	Monoclonal	BD Biosciences
HIF2α	Hif2a 237	Mouse	Monoclonal	Ximbio
CA9	M75	Mouse	Monoclonal	Absolute antibody
PARP	D64E10	Rabbit	Monoclonal	Cell signaling technologies
P21	EA10	Mouse	Monoclonal	EMD Milipore
CUL2	51-1800	Rabbit	Polyclonal	Invitrogen
VHL	S2-647	Mouse	Monoclonal	BD Biosciences
P27	D69C12	Rabbit	Monoclonal	Invitrogen
CUL1	71-8700	Rabbit	Polyclonal	Cell signaling technologies

Table 2. 1 Immunostaining Antibodies

2.7 Protein Extraction

Cells were washed in ice cold PBS and lysed in 2 x sample buffer (125mmol/L Tris [pH 6.8], 4% sodium dodecyl sulfate, 0.01% bromophenol blue, 10% β-mercaptoethanol, 10% glycerol).

2.8 Protein Polyacrylamide Gel Electrophoresis (PAGE)

The required volume of 6x SDS-PAGE sample buffer (72mM Tris pH 6.8, 20% glycerol, 4.5 % SDS, 10% β-mercaptoethanol and 0.015% bromophenol blue) was added and samples were heated to 95^{o}C for 10 minutes. Whole cell lysates were resolved by SDS-PAGE followed by electroblotting onto polyvinylidene-difluoride membrane (Millipore).

2.9 Antibody Incubation

Membranes were incubated overnight with an appropriate concentration of primary antibody in PBS containing 5% milk powder and 0.1% Tween-20. Membranes were incubated with Horseradish peroxidase-conjugated anti-rabbit or anti-mouse antibodies (DAKO Inc). Immunoreactivity was detected using CL system (Amersham Biosciences). The following antibodies were used, mouse anti-HIF-1α (BD Transduction Laboratories, USA), mouse anti-NUB1 (Novus biologicals), mouse anti-AIPL1 (Novus biologicals), mouse anti-FAT10 (4F1) (Cell signaling), rabbit anti-NEDD8 (Y297) (Novus Biologicals), mouse anti-HIF2α and (Ximbio) mouse anti-CAIV (Absolute Antibodies). Blots and densitometry analysis was carried out using ImageJ software (Scion Corporation).

2.10 Real-time PCR (qPCR)

Retrotranscription was performed using RetroScript kit (Ambion). All mRNA and β-actin expression was analyzed by PCR using TaqMan Gene Expression Assays (Applied Biosystems). The reaction was performed on a PTC-200 thermal cycler with a Chromo 4 continuous fluorescence detector (Bio-Rad, Hemel Hempstead, UK). The comparative cycle threshold (C_T) method was used to analyse the data by generating relative values of the amount of target cDNA, according to the $2^{-\Delta\Delta CT}$ method using β-actin house-keeping gene as calibrator.

2.11 Cell cycle analysis using flow cytometry

Samples were prepared as described in Sabatinos & Forsburg (Sabatinos and Forsburg, 2009). Briefly, cells were fixed in 1ml 70% ethanol; 300µl of this mixture washed in 3ml 50mM Na citrate, pellets resuspended in 0.5ml 50mM Na citrate containing 0.1mg/ml RNase A (Sigma) and left at room temperature for 2h. A volume of 0.5ml 50mM Na citrate containing 8µg/ml propidium iodide (Sigma) was subsequently added to a final concentration of 4µg/mL. 20,000 single events were analysed for FSC, SSC and DNA content using the Becton Dickinson® LSR II Research Flow Cytometer and the Flow_Jo v.9.2 Software.

2.12 Presence of disulphide bond with fluoresceine maleimide

Free thiols in lysate were blocked in the protein with iodoacetamide and remove the excess. The protein is denatured with SDS or urea. Then divided into 2 samples: leave one oxidised and reduced the other with tris(2-carboxyethyl)phosphine, TCEP. Each sample was reacted with fluorescein maleimide. The samples were run on SDS-PAGE. If there was a disulfide bond in the protein, the TCEP-reduced sample will be fluorescent and the oxidised sample will not be.

2.13 Statistical analyses

Statistical analysis was performed using SPSS 15.0 (Chicago, IL, USA). Data obtained from cell count, colony formation, MIB1 staining, cell cycle and mitochondrial function experiments were analysed by the Student´s t test or the Mann-Whitney U test for parametric and nonparametric variables, respectively. For survival analysis, Kaplan-Meier survival curves and the log rank test were used to analyze differences in RFS (the median was selected as the cut-off value). Multivariate analysis was carried out using the Cox proportional hazards model. Only variables of $P<0.1$ from the univariate analysis were entered in the Cox regression analysis. The proportional hazards assumption was examined by testing interactions between the covariates of the final model and time. A P value less than 0.05 was considered statistically significant.

2.14 Buffers and solutions

The preparation of bufferes and solutions are as detailed below:-

For cell culture:	
PBS	137mM NaCl
	2.7mM KCL
	4.3 mM Na_2HPO_4
	1.4 mM KH_2PO_4
	Ca^{2+} and Mg^{2+} free (pH 7.3)
Trypsin/EDTA 20 mg/ml Trypsin	1 mM ethylenediaminetetraacetic acid (EDTA) in PBS

For protein extraction from monolayer cell cultures:	
Lysis Buffer	10% (v/v) glycerol
	10 mM Tris-HCL pH 6.8
	5mM dithiothreitol (DTT)
	1% (v/v) sodium dodecyl sulphate (SDS)
	6.25 M urea
	1 protease inhibitor tablet (Roche Diagnostics) per 50 ml

For protein analysis:	
1x running buffer	25 mM Tris
	250mM glycine
	0.1% (v/v) SDS
6x sample buffer	72mM Tris-HCL pH 6.8
	20% (v/v) glycerol
	4.5% (v/v) SDS
	10% (v/v) β-mercaptoethanol
	0.015% (v/v) bromophenol blue
Transfer buffer	25mM Tris
	192 mM glycine
	15% (v/v) methanol
TBS	50mM Tris-HCl
	150mM NaCl
	pH 7.4
Stripping buffer	62.5 mM Tris-HCl pH 6.8
	2% (v/v) SDS
	100mM b-mercaptoethanol

For immunohistochemistry:	
Citrate Buffer	10mM citric acid pH 6.0
Tris EDTA buffer	50mM Tris 2mM EDTA pH 9.0
EDTA buffer	1mM EDTA pH 8.0

Chapter 3
Systematic Analysis of Gene Expression Alterations and Clinical Outcomes for AIPL1 and NUB1 in Cancer

3.1 The rationale of study

Combined microarray and clinical databases are a precious resource for scientists to acquire of the possible role of genes and pathways in cancer and look for basic information as far as the possible clinical meaning of specific gene expression signatures in cancer is concerned. This chapter aims to systematically analyse the AIPL1 and NUB1 transcription and identify whether their transcription levels have any prognostic value. I have been exploiting the Oncomine and METABRIC databases. The database could reveal the biological functions and provide the information for the possible underlying mechanism of AIPL1 and NUB1 genes. It improves our understanding of the genes in cancer mechanisms.

Through DNA microarray technology, public databases could address the fundamental physiological research questions in the postgenomic era. These genome-scale methodologies provide a more global perspective. My research question asks in what cancers or cancer subtypes are AIPL1 and NUB1 gene being altered? Do the AIPL1 and NUB1 genes manage to distinguish metastatic cancer from primary disease? Do the AIPL1 or NUB1 genes serve as biomarkers for a particular cancer or cancer subtype? The differential expression pattern implies the potential cancer promoting role or tumour suppressor role in cancer and leads to a reliable hypothesis for cancer research.

Meta-analysis demonstrates the robustness of AIPL1 and NUB1 molecular signatures. This is essential when the hypotheses or molecular signatures derived experimentally are to be validated *in silico*. Besides, large-scale gene-expression profiles for tumours allow the identification of prognostic disease markers or predictors of therapeutic response. Investigators can perform meta-analysis of mRNA expression patterns between datasets to uncover sets of genes important in specific phenotypes or clinical behaviours.

There is a need for acquiring the genetic details in order to speculate the meaningful outline of how AIPL1 and NUB1 proteins may affect cancer physiology. Most of the AIPL1 reports were on retinal degenerative diseases and none in cancers. Therefore the potential role of AIPL1 could be extended to be a part of a signaling pathway in cancer tissues.

The differential expression of AIPL1 facilitates advanced mining of the data in various cancer types. For instance, instead of merely detecting under-expression of AIPL1, it is possible to detect activation of this pathway via differential expression of downstream genes. This will allow for therapeutic targeting of pathways at multiple levels rather than single targets.

The integrative bioinformatics analyses will generate novel hypotheses with respect to cancer progression. The gene alterations and gene signatures of more aggressive cancers identify the possible oncogenic or tumour suppressive nature of gene products in cancers. Further insight into these pathways will be acquired by comparing cancer promoting signatures from cell line and *in vivo* cancer progression models with the expression patterns obtained from tumor specimens. The analyses will demonstrate the significance of AIPL1 and NUB1 in tumor formation of various kinds of cancer and the association of expression level with survival of cancer patient.

The goal is to use bioinformatics methods to analyse the publicly available data in order to outline the potential role of gene products such as AIPL1 and NUB1 and to formulate novel hypotheses speculating on mechanisms of action. The data mining and function prediction is useful to know more about AIPL1 and to generate hypotheses. The global objective is to identify biomarkers that can be used to classify tumours and to determine which treatment is best suited for each type.

It is hypothesized that chaperones could be down-regulated in tumours. This phenomenon represents a new cancer causing mechanism. Following reduced availability of chaperones proteins, the tumour suppressor activity is lost as the normal protein cannot fold properly. To our best knowledge, this is the first systematic analysis addressing the role of AIPL1 in cancer progression.

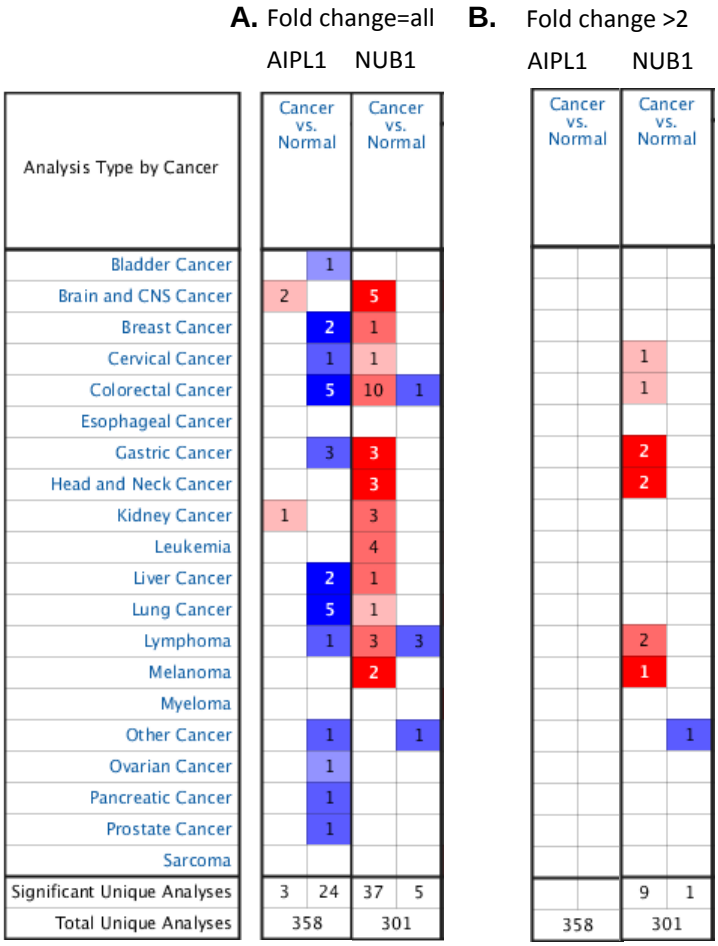
3.2 Concordant down-regulation of AIPL1 transcripts and upregulated NUB1 level in Oncomine database

To elucidate the AIPL1 expression pattern in cancer, the systematic analysis of AIPL1 and NUB1 expression was done using Oncomine database (http://www.oncomine.org). The expression of AIPL1 was compared between tumour and normal tissue in different types of cancers (Table 3.1). The threshold was designed as the following parameters, *p*-value of 0.05 and top gene rank 10%. The AIPL1 expression was higher in cancer than in normal tissue in brain and kidney cancers. On the other hand, cancer AIPL1 expression was lower in bladder, breast, cervical, colorectal, gastric, liver, lung, lymphoma, ovarian, pancreatic and prostate and other cancers (Table 3.1). The AIPL1 mRNA was found significantly and concordantly down-regulated in cancer tissues compared with normal tissues (with number of dataset, 24 vs. 3). These data suggests that AIPL1 plays a tumour suppressive role in cancers. Meanwhile for NUB1 under the same threshold, the transcripts were mostly upregulated in cancers (number of dataset): Brain and CNS

cancer (5), breast cancer (1), cervical (1), colorectal cancer (10), gastric cancer (3), head and neck cancer (3), kidney (3), leukaemia (4), liver cancer (lymphoma (1) and other (1).

The finding showed AIPL1 and NUB1 play opposite roles to each other. Two breast cancer datasets demonstrate the down-regulated AIPL1 and upregulated NUB1 in mRNA transcripts (Fig 3.1).

Table 3. 1 Genes and cancer summary from Oncomine. The table summarised the number of datasets with AIPL1 mRNA under-expression (blue) and NUB1 mRNA over-expression (red) on various cancers in relative normal tissue. The number of dataset was indicated in the box. The threshold was set with the following parameters: *p*-value of 1E-4, gene ranking of top 10% with (A) all $\log_{10}$ fold change and (B) more than 2 $\log_{10}$ fold change. In relative to normal cells, AIPL1 mRNA expressions were lower than 2 $\log_{10}$ fold change in cancers while some NUB1 mRNA expressions (in cervical, colorectal, gastric, head and neck, lymphoma and melanoma cancer) were more than 2 $\log_{10}$ fold change.



A. Fold change=all

Analysis Type by Cancer	AIPL1 Cancer vs. Normal		NUB1 Cancer vs. Normal	
Bladder Cancer		1		
Brain and CNS Cancer	2		5	
Breast Cancer		2	1	
Cervical Cancer		1	1	
Colorectal Cancer		5	10	1
Esophageal Cancer				
Gastric Cancer		3	3	
Head and Neck Cancer			3	
Kidney Cancer	1		3	
Leukemia			4	
Liver Cancer		2	1	
Lung Cancer		5	1	
Lymphoma		1	3	3
Melanoma			2	
Myeloma				
Other Cancer		1		1
Ovarian Cancer		1		
Pancreatic Cancer		1		
Prostate Cancer		1		
Sarcoma				
Significant Unique Analyses	3	24	37	5
Total Unique Analyses	358		301	

B. Fold change >2

AIPL1 Cancer vs. Normal		NUB1 Cancer vs. Normal	
		1	
		1	
		2	
		2	
		2	
		1	
			1
		9	1
358		301	

Table 3. 2 Summary of A. AIPL1 & B. NUB1 datasets. There were 24 dataset with down-regulated AIPL1 and 37 dataset with upregulated NUB1 mRNA expression of cancers (Table 3.3A). The fold changes of AIPL1 and NUB1 were in Log_2 FC. No datasets showing Log_2 FC <-0.5 in AIPL1. It implicates the AIPL1 is not strongly down-regulated.

A.

Publications	Dataset	Sample size	p-value	Log_2 FC
Compagno Lymphoma, Nature, 2009	1. Follicular Lymphoma vs. Normal	38 vs. 10	<0.001	-0.428
Guichard Liver, Nat Genet, 2012	2. Hepatocellular Carcinoma vs. Normal	99 vs. 86	<0.001	-0.119
Kurashina Colon, Cancer Sci, 2008	3. Colon Adenocarcinoma vs. Normal	52 vs. 38	<0.001	-0.136
TCGA Bladder, No Associated Paper, 2013	4. Infiltrating Bladder Urothelial Carcinoma vs. Normal	99 vs. 24	<0.001	-0.166
TCGA Breast 2, No Associated Paper, 2012	5. Invasive Ductal Breast Carcinoma vs. Normal	111 vs. 639	<0.001	-0.233
	6. Invasive Lobular Breast Carcinoma vs. Normal	111 vs. 71	<0.001	-0.209
TCGA Cervix, No Associated Paper, 2012	7. Cervical Squamous Cell Carcinoma vs. Normal	83 vs. 3	<0.001	-0.152
TCGA Colorectal 2, No Associated Paper, 2011	8. Cecum Adenocarcinoma vs. Normal	65 vs. 79	<0.001	-0.233
	9. Colon Adenocarcinoma vs. Normal	212 vs. 79	<0.001	-0.338
	10. Rectal Adenocarcinoma vs. Normal	90 vs. 79	<0.001	-0.370
	11. Rectosigmoid Adenocarcinoma vs. Normal	24 vs. 15	<0.001	-0.399
TCGA Endometrium, No Associated Paper, 2012	12. Endometrial Serous Adenocarcinoma vs. Normal	50 vs. 25	<0.001	-0.307
TCGA Gastric, No Associated Paper, 2013	13. Diffuse Gastric Adenocarcinoma vs. Normal	45 vs. 94	<0.001	-0.134
	14. Gastric Intestinal Type Adenocarcinoma vs. Normal	41 vs. 94	<0.001	-0.178
	15. Gastric Tubular Adenocarcinoma vs. Normal	31 vs. 94	<0.001	-0.156
TCGA Liver, No Associated Paper, 2012	16. Hepatocellular Carcinoma vs. Normal	97 vs. 59	<0.001	-0.338
TCGA Lung 2, No Associated Paper, 2012	17. Lung Adenocarcinoma vs. Normal	261 vs. 390	<0.001	-0.178
	18. Lung Adenocarcinoma, Mixed Subtype vs. Normal	67 vs. 390	<0.001	-0.149
	19. Squamous Cell Lung Carcinoma vs. Normal	348 vs. 390	<0.001	-0.174
TCGA Ovarian 2, No Associated Paper, 2013	20. Ovarian Serous Cystadenocarcinoma vs. Normal	607 vs. 130	<0.001	-0.320
TCGA Pancreas, No Associated Paper, 2013	21. Pancreatic Adenocarcinoma vs. Normal	32 vs. 8	<0.001	-0.115
TCGA Prostate, No Associated Paper, 2012	22. Acinar Prostate Adenocarcinoma vs. Normal	126 bs. 61	<0.001	-0.076
Weiss Lung, Sci Transl Med, 2010	23. Lung Adenocarcinoma vs. Normal	77 vs. 59	<0.001	-0.104
	24. Squamous Cell Lung Carcinoma vs. Normal	155 vs. 59	<0.001	-0.122
Number of upregulated AIPL1 dataset that are above the threshold of significant and log2 FC$\geq$ 0.5 or $\leq$ -0.5				0
Total upregulated AIPL1 dataset				24

B.

Publication	Dataset	Sample size	p-value	Log_2 FC
Andersson Leukemia, Leukemia, 2007	1. B-Cell Acute Lymphoblastic Leukemia vs. Normal	87 vs. 6	<0.001	0.878 [A]
	2. T-Cell Acute Lymphoblastic Leukemia vs. Normal	11 vs. 6	<0.001	0.722 [A]
Beroukhim Brain, Proc Natl Acad Sci U S A, 2007	3. Primary Glioblastoma vs. Normal	107 vs. 33	<0.001	0.252
Brune Lymphoma, J Exp Med, 2008	4. Nodular Lymphocyte Predominant Hodgkin's Lymphoma vs. Normal	5 vs. 5	<0.001	0.789 [A]
Chen Gastric, Mol Biol Cell, 2003	5. Gastric Intestinal Type Adenocarcinoma vs. Normal	67 vs. 28	<0.001	0.681 [A]
DErrico Gastric, Eur J Cancer, 2009	6. Gastric Intestinal Type Adenocarcinoma vs. Normal	4 vs. 31	<0.001	1.128 [A]
	7. Gastric Mixed Adenocarcinoma vs. Normal	26 vs. 31	<0.001	1.068 [A]
Haferlach Leukemia, J Clin Oncol, 2010	8. B-Cell Childhood Acute Lymphoblastic Leukemia vs. Normal	359 vs. 74	<0.001	0.620 [A]
	9. Pro-B Acute Lymphoblastic Leukemia vs. Normal	70 vs. 74	<0.001	0.680 [A]
Hong Colorectal, Clin Exp Metastasis, 2010	10. Colorectal Carcinoma vs. Normal	70 vs. 12	<0.001	1.436 [A]
Kurashina Colon, Cancer Sci, 2008	11. Colon Adenocarcinoma vs. Normal	52 vs. 38	<0.001	0.138
	12. Rectal Adenocarcinoma vs. Normal	38 vs. 38	<0.001	0.152
Lee Brain, Cancer Cell, 2006	13. Glioblastoma vs. Normal	22 vs. 3	<0.001	0.464
Piccaluga Lymphoma, J Clin Invest, 2007	14. Angioimmunoblastic T-Cell Lymphoma vs. Normal	6 vs. 10	<0.001	1.725 [A]
	15. Unspecified Peripheral T-Cell Lymphoma vs. Normal	28 vs. 10	<0.001	1.398 [A]
Pyeon Multi-cancer, Cancer Res, 2007	16. Cervical Cancer vs. Normal	20 vs. 8	<0.001	1.292 [A]
	17. Oral Cavity Carcinoma vs. Normal	4 vs. 9	<0.001	1.098 [A]
	18. Oropharyngeal Carcinoma vs. Normal	6 vs.9	<0.001	1.877 [A]
Richardson Breast 2, Cancer Cell, 2006	19. Ductal Breast Carcinoma vs. Normal	40 vs. 7	<0.001	0.587 [A]
Riker Melanoma, BMC Med Genomics, 2008	20. Cutaneous Melanoma vs. Normal	14 vs. 4	<0.001	2.372 [A]
Skrzypczak Colorectal, PLoS One, 2010	21. Colorectal Carcinoma vs. Normal	36 vs. 24	<0.001	0.971 [A]
	22. Colon Adenoma vs. Normal	5 vs. 10	<0.001	0.567 [A]
	23. Colon Carcinoma Epithelia vs. Normal	5 vs. 10	<0.001	0.999 [A]
TCGA Brain 2, No Associated Paper, 2013	24. Brain Astrocytoma vs. Normal	63 vs. 37	<0.001	0.184
	25. Brain Glioblastoma vs. Normal	58 vs. 37	<0.001	0.407
	26. Oligoastrocytoma vs. Normal	54 vs. 37	<0.001	0.160
TCGA Colorectal 2, No Associated Paper, 2011	27. Cecum Adenocarcinoma vs. Normal	65 vs. 15	<0.001	0.144
	28. Colon Adenocarcinoma vs. Normal	212 vs. 79	<0.001	0.174
	29. Rectal Adenocarcinoma vs. Normal	90 vs. 15	<0.001	0.175
	30. Rectosigmoid Adenocarcinoma vs. Normal	24 vs. 15	<0.001	0.246
TCGA Melanoma, No Associated Paper, 2013	31. Cutaneous Melanoma vs. Normal	58 vs. 312	<0.001	0.275

Publication	Dataset	Sample size	p-value	Log_2 FC
TCGA Renal 2, No Associated Paper, 2011	32. Clear Cell Renal Cell Carcinoma vs. Normal	489 vs. 441	<0.001	0.112
Vasko Thyroid, Proc Natl Acad Sci U S A, 2007	33. Thyroid Gland Papillary Carcinoma vs. Normal	14 vs. 4	<0.001	0.386
Weiss Lung, Sci Transl Med, 2010	34. Lung Adenocarcinoma vs. Normal	77 vs. 59	<0.001	0.103
Wurmbach Liver, Hepatology, 2007	35. Hepatocellular Carcinoma vs. Normal	35 vs. 10	<0.001	0.934 [A]
Yusenko Renal, BMC Cancer, 2009	36. Clear Cell Renal Cell Carcinoma vs. Normal	26 vs. 3	<0.001	0.751 [A]
	37. Papillary Renal Cell Carcinoma vs. Normal	19 vs. 3	<0.001	0.589 [A]
Number of upregulated NUB1 dataset that are above the threshold of significant and log2 FC≥ 0.5 or ≤ -0.5				22
Total upregulated NUB1 dataset				37

[A] Above the threshold with significat p-value<0.05 and log_2 FC≥ 0.5 or ≤ -0.5

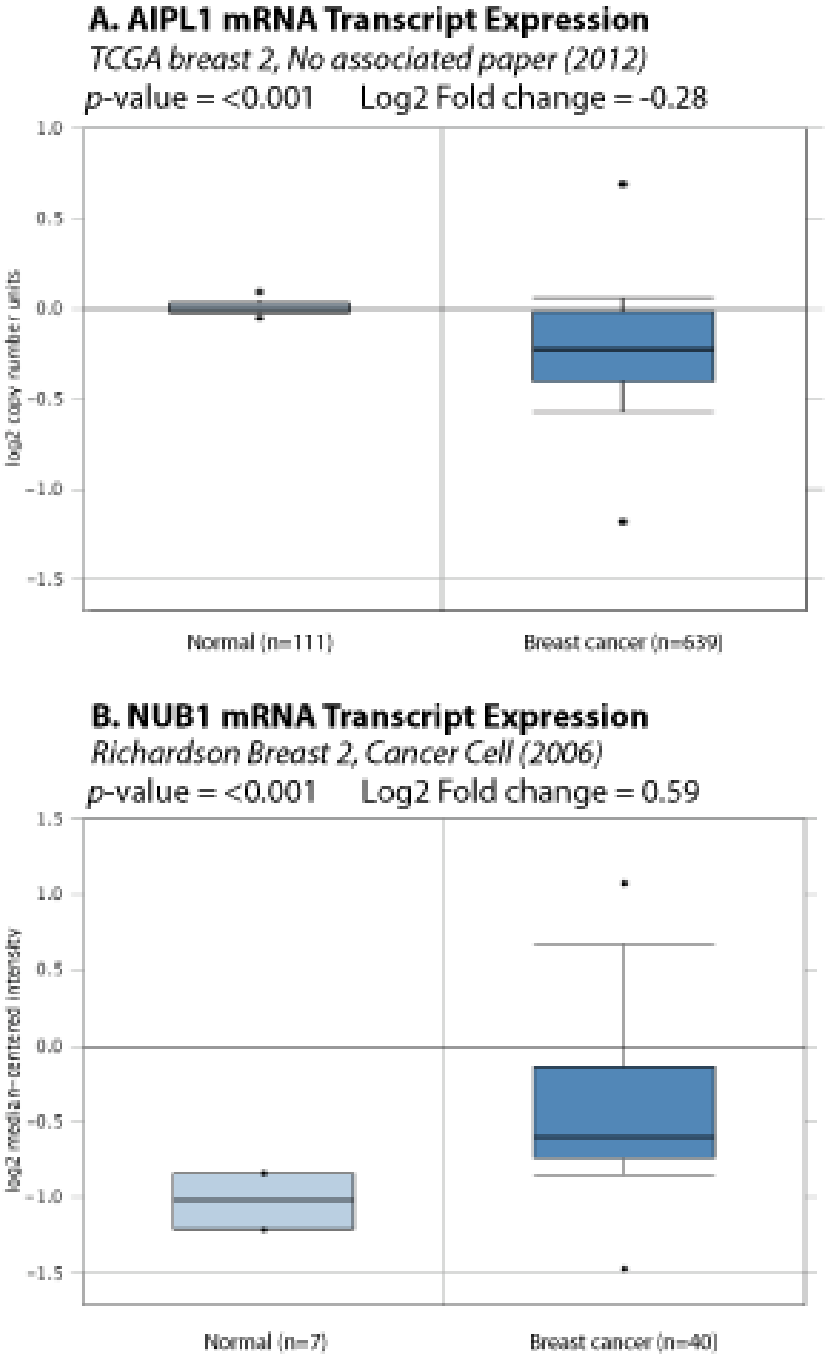


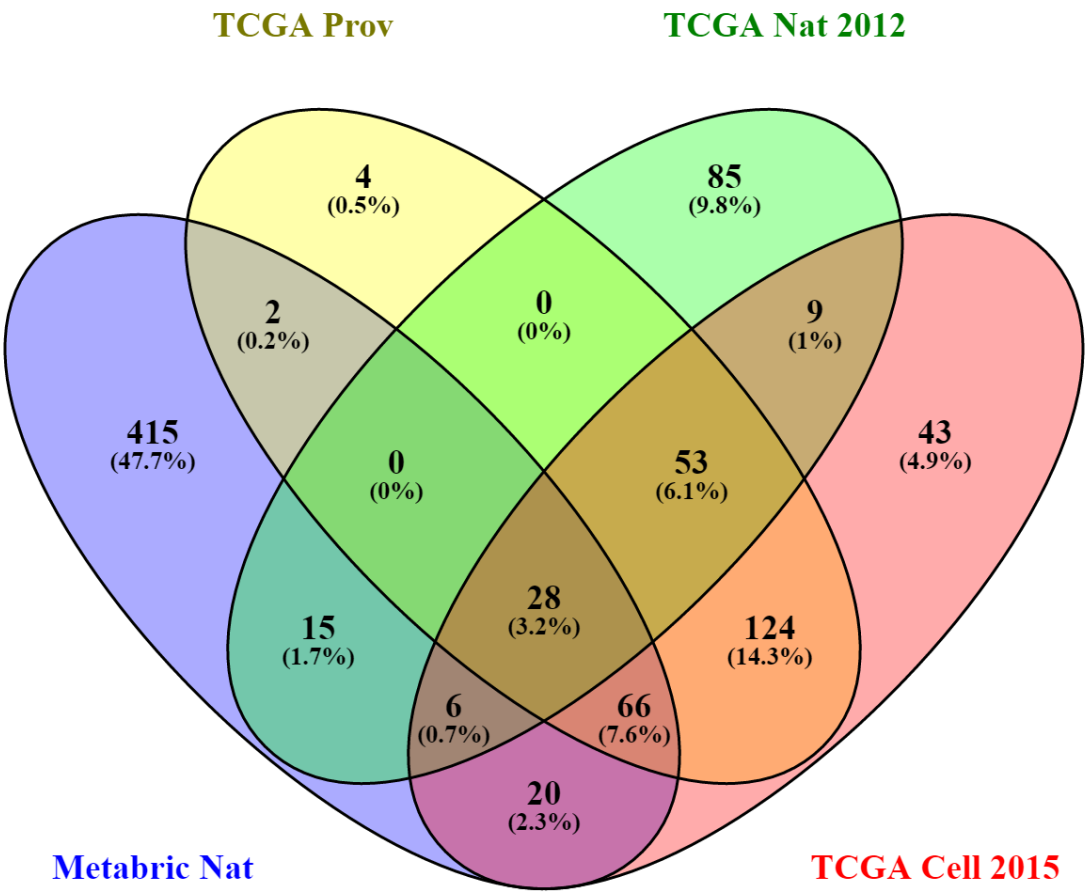
Figure 3. 1 Box and whisker plots of AIPL1 and NUB1 in breast cancer dataset. The box plot comparing specific a. AIPL1 and b. NUB1 mRNA expression in normal (left plot) and cancer tissue (right plot) was derived from Oncomine database. The analysis was shown in breast carcinoma in relative to normal breast. The average signal intensity and average increase (fold change) of the genes are shown as box and whisker plots where the y-axis indicates $\log_2$ fold change.

3.3 NUB1 transcripts consistently coexpressed with CUL1 transcripts in breast cancer

In cBioportal®, the breast invasive carcinoma (TCGA, Cell 2015) and breast invasive carcinoma (TCGA, Provisional) showed AIPL1 coexpressed with Apoptosis Facilitator Bcl-2-Like Protein 14, BCL2L14 gene (Pearson's correlation: 0.92 and 0.86, respectively). We examined the coexpression of genes with the NUB1 transcript among the breast cancer samples from the four datasets on cBioportal – Breast cancer (METABRIC, Nature 2012 & Nat Commun 2016) (N=2509), Breast invasive carcinoma (TCGA, Provisional) (N=1105), Breast invasive carcinoma (TCGA, Nature 2012) (N=825) and Breast invasive carcinoma (TCGA, Cell 2015) (N=817). For each dataset, the genes that satisfy the Spearman correlation $-0.3 \geq \rho \geq 0.3$ are considered as the coexpressed genes for subsequent analysis. Finally, we detected 552, 277, 196 and 349 coexpressing genes in above mentioned datasets, respectively.

To investigate the overlaps among these sets of coexpressing genes, Venn diagram was plotted across all the breast cancer datasets. There was a total of 28 common coexpressing genes, a Venn diagram was shown among all four datasets (Figure 3.2). Overall, there were 28 gene transcripts which coexpressed with NUB1 gene (Appendix 1).

To further investigate the difference between these coexpressed genes and to highlighted the pathway associated with the NUB1 gene, the Reactome® enrichment analysis was applied to search for the enriched biological pathways. Of all 28 genes, 14 of them were enriched in immune system related pathway (Table 3.3). There were several other system related pathways commonly enriched in the up-regulated genes across the physiological environment, including the mitotic cell cycle, haemostasis and metabolism (Table 3.3).



Metabric Nat: Breast cancer (METABRIC, Nature 2012 & Nat Commun 2016) (N=2509), TCGA Prov: Breast invasive carcinoma (TCGA, Provisional) (N=1105), TCGA Nat 2012: Breast invasive carcinoma (TCGA, Nature 2012) (N=825) and TCGA Cell 2015: Breast invasive carcinoma (TCGA, Cell 2015) (N=817).

Figure 3. 2 Venn diagram of overlapping genes across the NUB1 coexpression networks. The difference of CE genes identified in each breast cancer dataset in Oncomine. It highlights the key genes in the weighted coexpression networks. Colour bands represent modules in the network and white regions denote genes outside the modules. There were 28 genes were commonly found to coexpress with NUB1 in all four datasets.

Table 3. 3 Summary of NUB1 and CUL1 enriched pathway. Reactome® analysed 28 NUB1 coexpressing genes. CUL1 transcripts were found in be enriched in various biological pathways.

Pathways	Number of genes involved
Adaptive Immune System	6
TCR signaling	2
Class I MHC mediated antigen processing & presentation	4
Innate Immune System	7
Fc epsilon receptor (FCERI) signaling	2
RIG-I/MDA5 mediated induction of IFN-alpha/beta pathways	2
Cytokine Signaling in Immune system	9
Interferon Signaling	2
Signaling by Interleukins	6
TNFR2 non-canonical NF-kB pathway	3

Abbr. TCR: T cell receptor; MHC: Major histocompatibility complexes; RIG-I: retinoic acid-inducible gene I; MDA5: melanoma differentiation-associated gene 5, TNFR2: Tumor necrosis factor receptor 2; NF-kB: Nuclear factor-kappaB

3.4 Coexpressions of NUB1 with ATM and FAS signaling pathway

Knowing more genes coexpressing with NUB1 could lead to formulating *in vitro* experiments with different stress regimes on cells. To evaluate coexpression of NUB1 transcripts to other related pathways, the multi-scale association explorer in Regulome Explorer® was used to analyse BRCA 03 Feb 2012 (tumour only) dataset. A scale-independent image showed that CUL1 mRNA and Transmembrane Protein 140, TMEM140 mRNA coexpressed with the NUB1 mRNA *in vivo* across a panel of 844 breast cancer samples (Pearson correlation, ρ=0.52 and 0.48, respectively) (Figure 3.4). TMEM140 mRNA is frequently expressed along with fatty acid synthase, FAS gene and ataxia telangiectasia mutated, ATM gene (Fig 3.3). The pool of FAS-centric modules and its coexpressing genes were indicated in the yellow-coloured area.

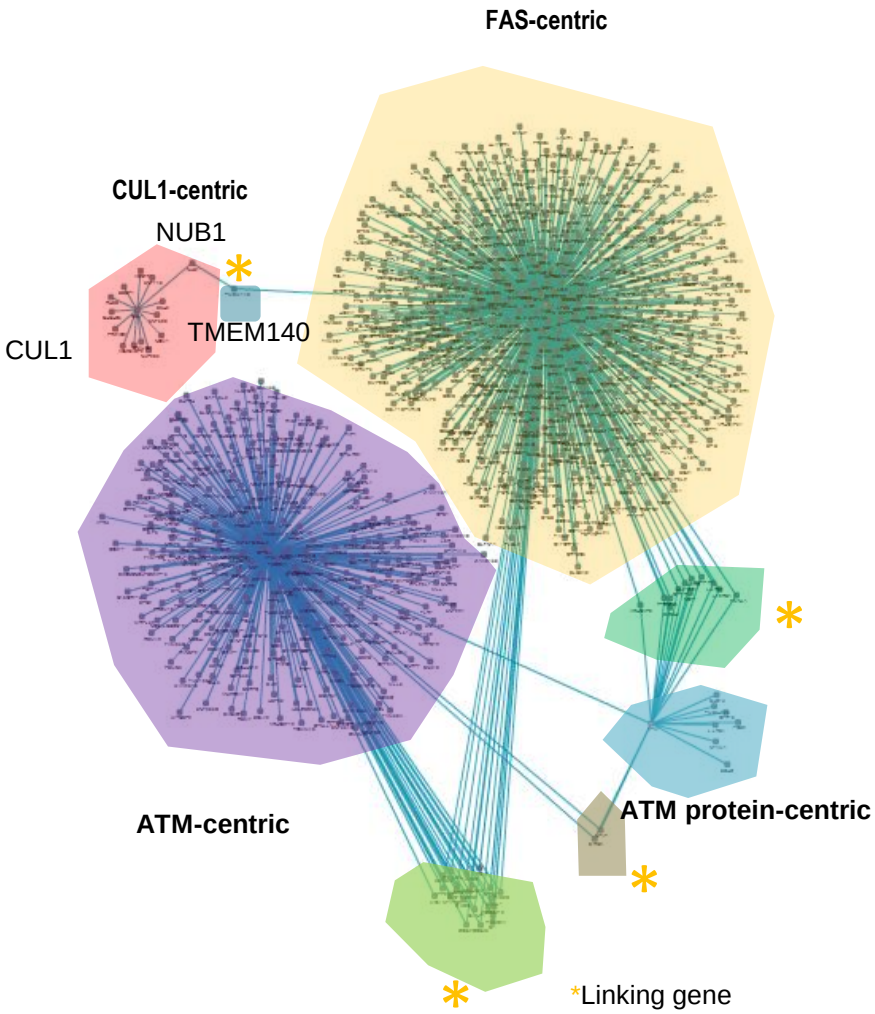


Figure 3. 3 NUB1 coexpression network profile. The network map was derived from Regulome explorer® using BRCA 03 Feb 2012 (tumour only) dataset with a panel of 844 breast cancer samples. The set of feature associations is filtered according to user-specified parameters:- Feature 1 (All association, NUB1 FAS and ATM Label); Feature 2 (Gene expression) and Association (Log_{10} P≥1, max result 1000). Each line corresponds to coexpression. Each dot is a known gene and the coloured modules indicate the pool of genes coexpressing with a single gene.

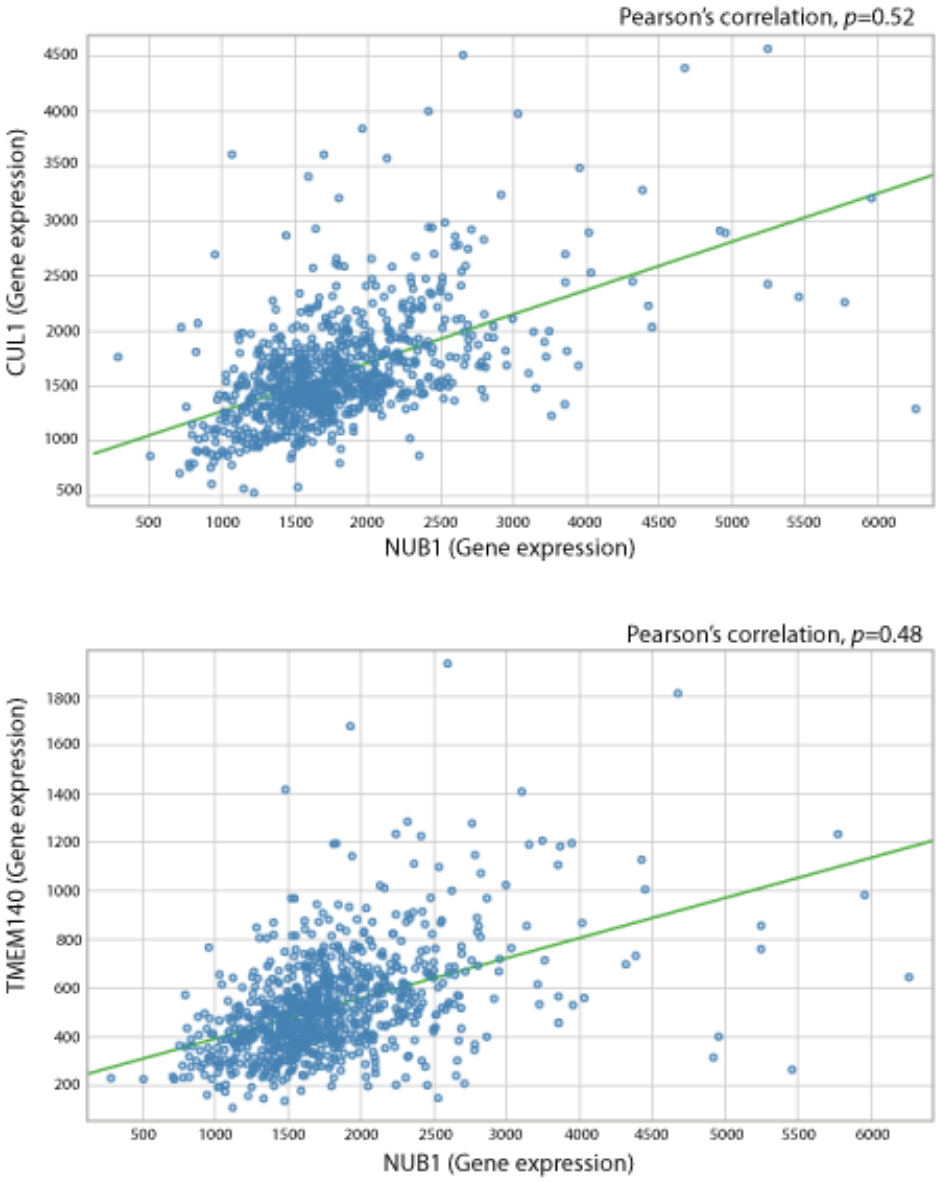


Figure 3. 4 Pairwise association plot of CUL1 and TMEM140 against NUB1 transcripts. The two dimensional association plot of the CUL1 and TMEM140 mRNA transcripts were the only coexpressed genes in this dataset.

3.5 Breast cancer specific analysis using METABRIC database

To validate the findings from cBioportal and Regulome explorer data, we conducted an independent analysis using the METABRIC dataset, containing the 1988 samples. The METABRIC dataset was examined to predict the outcome of breast cancer therapies using molecular features and clinical observations.

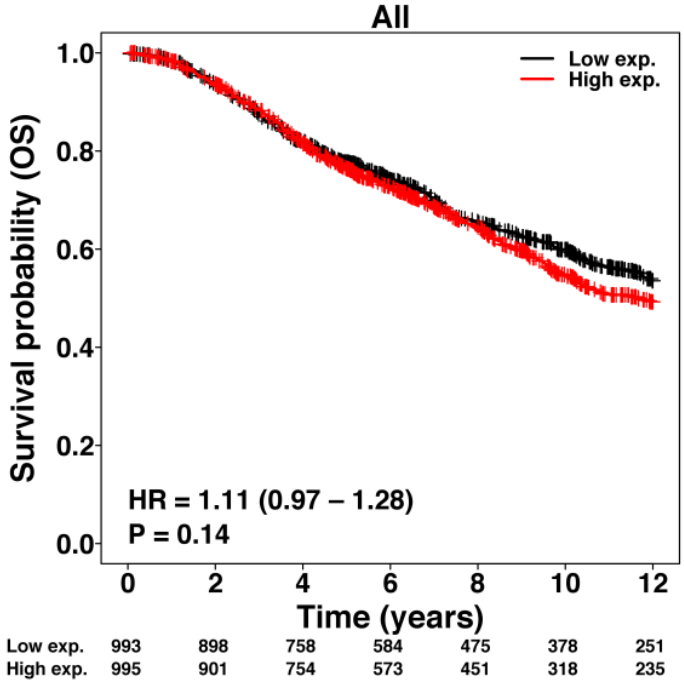
3.5.1 NUB1 transcript expression levels predict the survival probability of ER negative breast cancer patients.

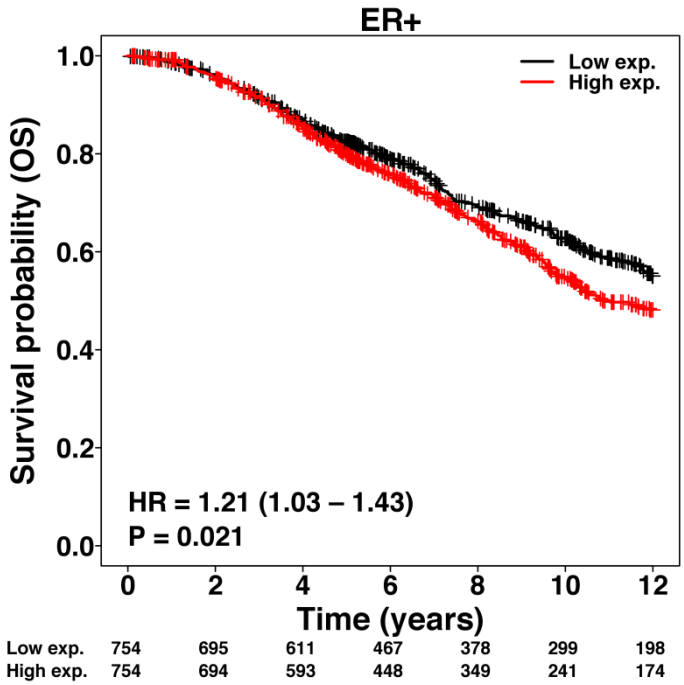
To further elucidate the role of AIPL1 and NUB1 mRNA within breast cancer progression, the prognostic value of AIPL1 and NUB1 gene expression in various breast cancer molecular subtypes was determined according to the parameter of cox p-value<0.05 (Fig. 3.5 and Fig. 3.6). A summary of all hazard ratios across all intrinsic molecular subtypes were shown (Table 3.4).

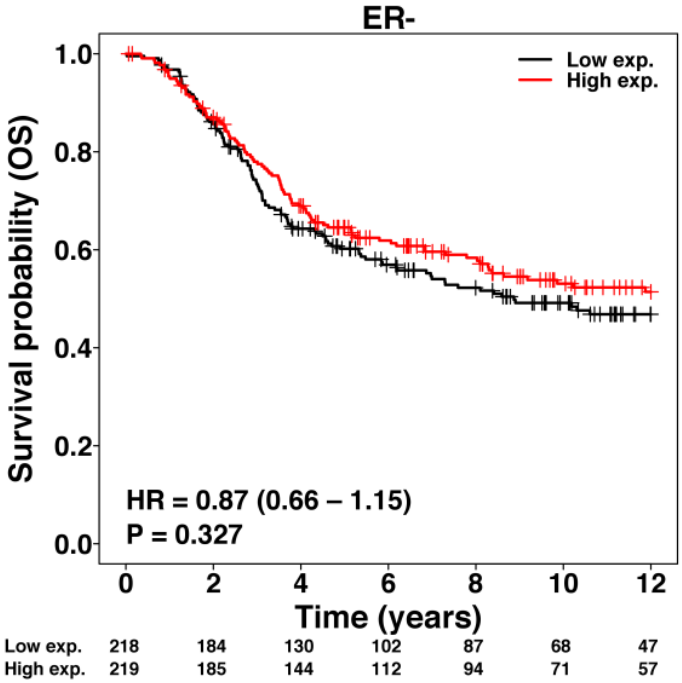
The analysis revealed that AIPL1 was of prognostic value in the subgroup of ER positive patients and, among the ER positive, it was limited to the Lumina B type as the one with higher transcription had a worst outcome over 12 years (Figure 3.5 and Table 3.4).

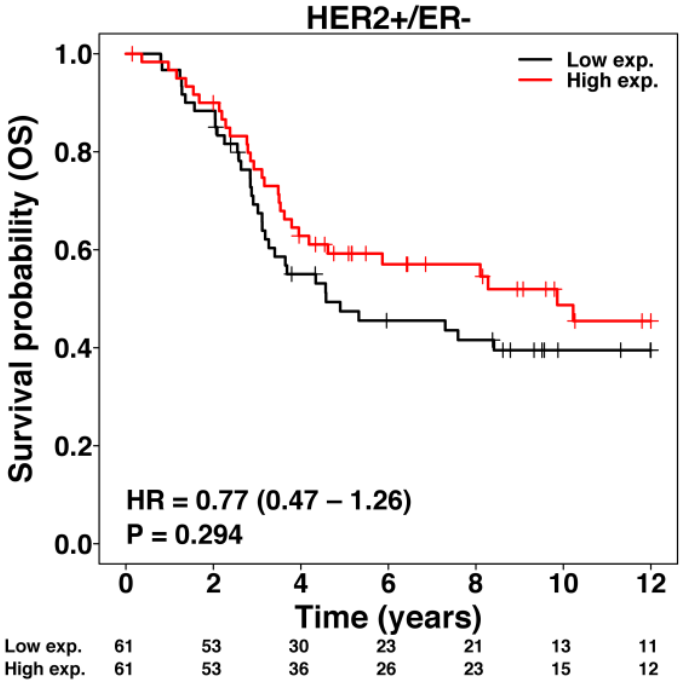
High levels of NUB1 mRNA have been found instead to be associated with better outcome in all the cases, the outcome is even better in NUB1 positive ER negative while NUB1 is of no value in the ER positive. NUB1 high levels of transcript are also associate with goof outcome in the Triple negative tumours and both in the Her2 positive and negative (Figure 3.6 and Table 3.4).

A. Survival probability curve based on AIPL1 transcript expression






ER-
Low exp.
High exp.
Survival probability (OS)
1.0
0.8
0.6
0.4
0.2
0.0
HR = 0.87 (0.66 – 1.15)
P = 0.327
0
2
4
6
8
10
12
Time (years)
Low exp. 218 184 130 102 87 68 47
High exp. 219 185 144 112 94 71 57


HER2+/ER-
Low exp.
High exp.
Survival probability (OS)
1.0
0.8
0.6
0.4
0.2
0.0
HR = 0.77 (0.47 – 1.26)
P = 0.294
0
2
4
6
8
10
12
Time (years)
Low exp. 61 53 30 23 21 13 11
High exp. 61 53 36 26 23 15 12

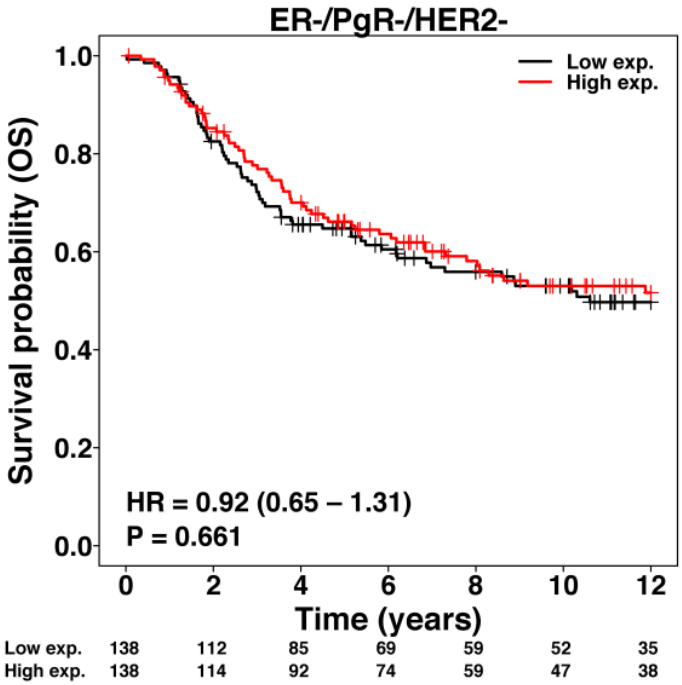
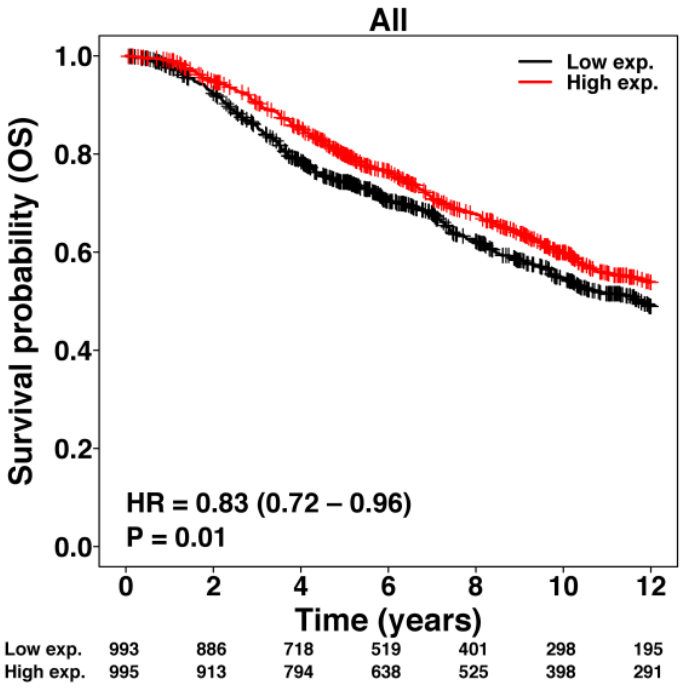
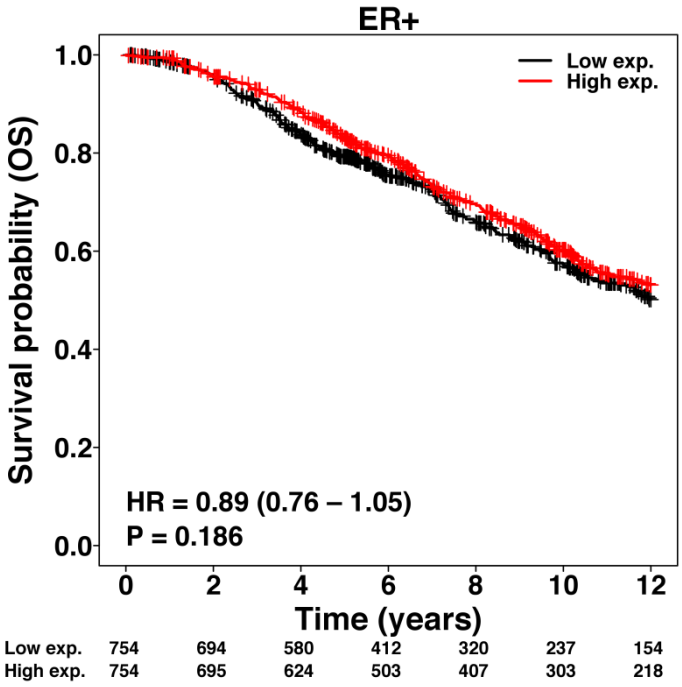
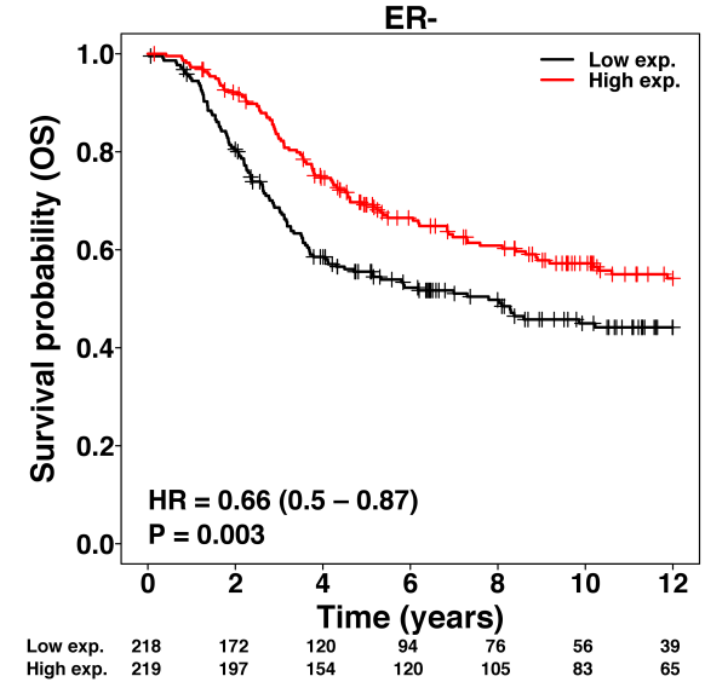


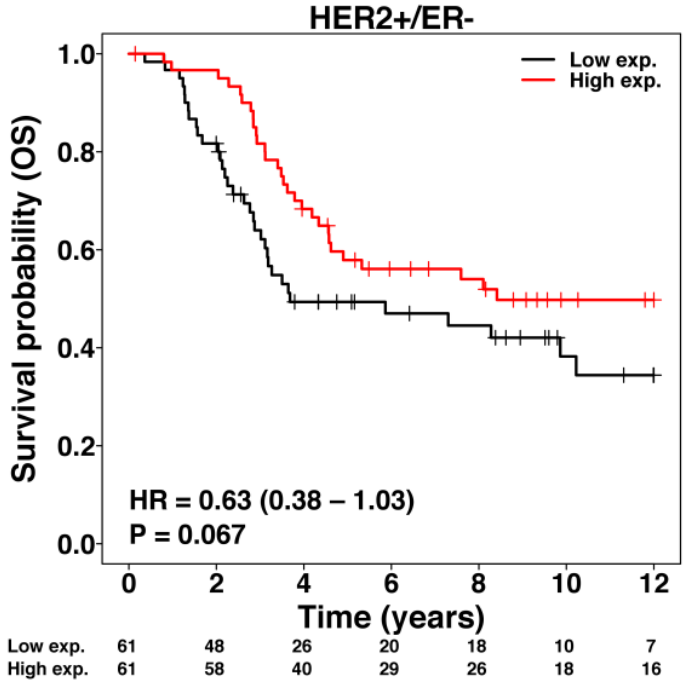
Figure 3. 5 **Survival curves of AIPL1 in different subgroup.** The survival curve comparing the patients with high (red) and low (black) expression in breast cancer was identified as the threshold of cox *p*-value <0.05 from metabric Kaplan Meier database.

B. Survival probability curve based on NUB1 transcript expression






ER-
Low exp.
High exp.
Survival probability (OS)
1.0
0.8
0.6
0.4
0.2
0.0
HR = 0.66 (0.5 – 0.87)
P = 0.003
0
2
4
6
8
10
12
Time (years)
Low exp. 218 172 120 94 76 56 39
High exp. 219 197 154 120 105 83 65


HER2+/ER-
Low exp.
High exp.
Survival probability (OS)
1.0
0.8
0.6
0.4
0.2
0.0
HR = 0.63 (0.38 – 1.03)
P = 0.067
0
2
4
6
8
10
12
Time (years)
Low exp. 61 48 26 20 18 10 7
High exp. 61 58 40 29 26 18 16

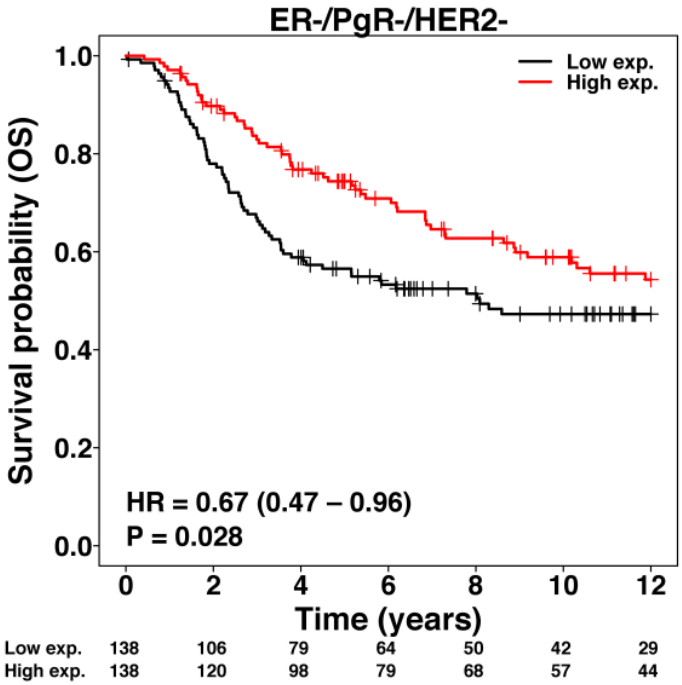


Figure 3. 6 **Survival curves of AIPL1 and NUB1 in different subgroup.** The survival curve comparing the patients with high (red) and low (black) expression in breast cancer was identified as the threshold of cox *p*-value <0.05 from METABRIC Kaplan Meier database.

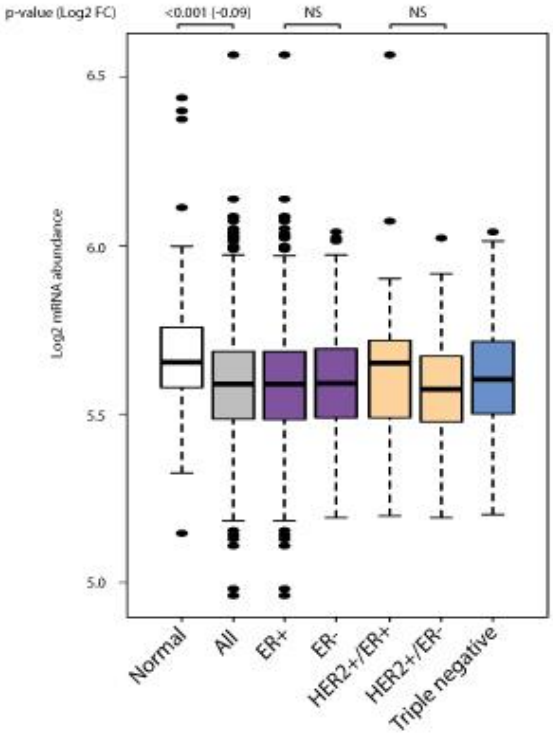
Subtype	AIPL1			NUB1		
	Hazard ratio	95% interval	p-value	Hazard ratio	95% interval	p-value
All	1.11	0.97-1.28	0.140	0.83	0.72-0.96	0.010
Basal	0.99	0.71-1.39	0.974	0.76	0.52-1.01	0.061
ER-	0.87	0.66-1.15	0.327	**0.66**	**0.50-0.87**	**0.003**
ER+	1.21	1.03-1.43	0.021	0.89	0.76-1.05	0.186
HER2	0.79	0.55-1.13	0.192	**0.69**	**0.48-0.99**	**0.047**
HER2-	1.16	1.00-1.36	0.054	0.82	0.70-0.96	0.014
HER2+	0.84	0.59-1.19	0.315	0.86	0.61-1.22	0.396
HER2+/ER-	0.77	0.47-1.26	0.294	**0.63**	**0.38-1.03**	**0.067**
HER2+/ER+	0.84	0.51-1.38	0.492	1.08	0.66-1.78	0.763
Luminal A	1.15	0.89-1.49	0.291	0.84	0.65-1.09	0.192
Luminal B	**1.42**	**1.09-1.85**	**0.009**	1.02	0.78-1.33	0.886
Normal like	0.85	0.52-1.39	0.526	0.83	0.51-1.36	0.456
ER-/PR-/HER2-	0.92	0.65-1.31	0.661	**0.67**	**0.47-0.96**	**0.028**

Table 3. 4 Survival curves summary. The survival curve comparing the patients with high (red) and low (black) expression in breast cancer was identified as the threshold of cox p-value <0.05 from METABRIC Kaplan Meier database. HER2 subgroup is non-luminal *i.e.* HER2 positive but both ER and PR are negative. The statistically significant hazard rations were bolded in various subtypes of breast cancer identified from our analyses.

3.5.2 No significant difference of AIPL1 and NUB1 transcript levels

To examine whether the levels of gene expression of AIPL1 and NUB1 differ between ER+ vs. ER-, HER2+/ER+ vs. HER2+/ER- and triple negative breast cancer, differential transcript expression of genes was determined in the METABRIC dataset. The threshold which we focused on was set at p-value<0.05 and $\log_2$ FC>0.5 or <-0.5. Though there were significant differences of AIPL1 and NUB1 in breast cancer cells and adjacent normal tissue, the fold changes were not varying much ($\log_2$ FC=-0.09; p-value<0.001 and $\log_2$ FC =0.12; p-value<0.001, respectively) (Figure 3.7). There were no significant difference of AIPL1 (p-value not significant) and NUB1 (p-value=0.041; $\log_2$ FC= -0.055) transcripts in ER+ comparing to ER- subgroup. To compare HER2+/ER+ to HER2+/ER- subgroup, both AIPL1 and NUB1 transcripts were not significantly different. Therefore, there were no expression level differences observed in ER+ vs. ER-, HER2+/ER+ vs. HER2+/ER- subgroups.

A. AIPL1 transcript expression



B. NUB1 transcript expression

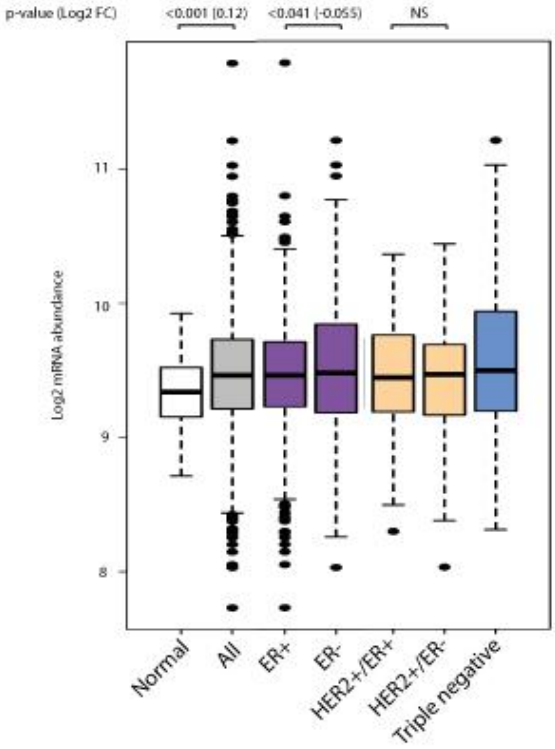


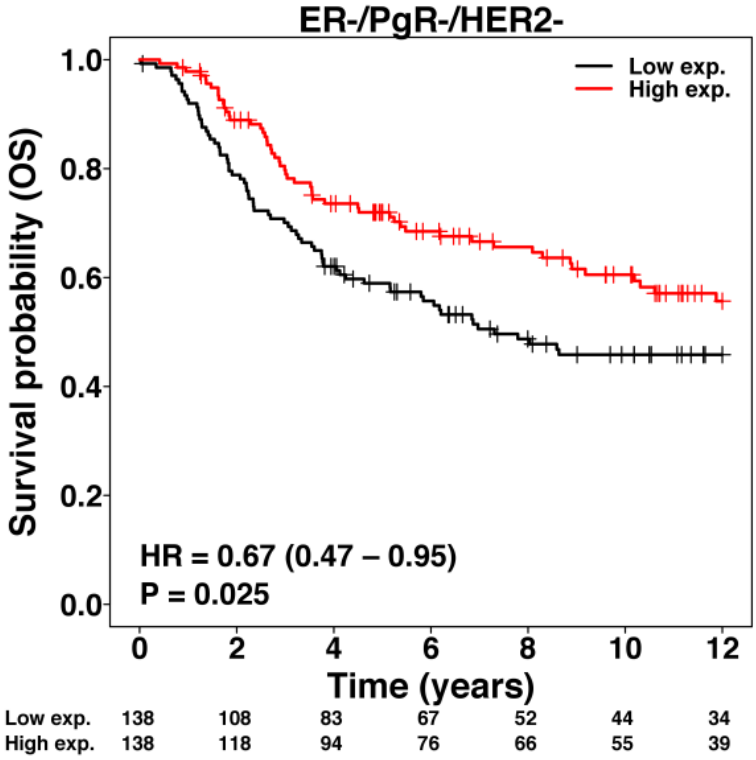
Figure 3. 7 Gene expression patterns of AIPL1 and NUB1 based on the intrinsic molecular subtypes status of METABRIC dataset. Relative transcript abundance of A) AIPL1 and B) NUB1 across the intrinsic subtypes is indicated. The boxes represent the interquartile range (25th and 75th percentiles), and the horizontal line in the box represents the median value. The whiskers show the range of largest and smallest values.

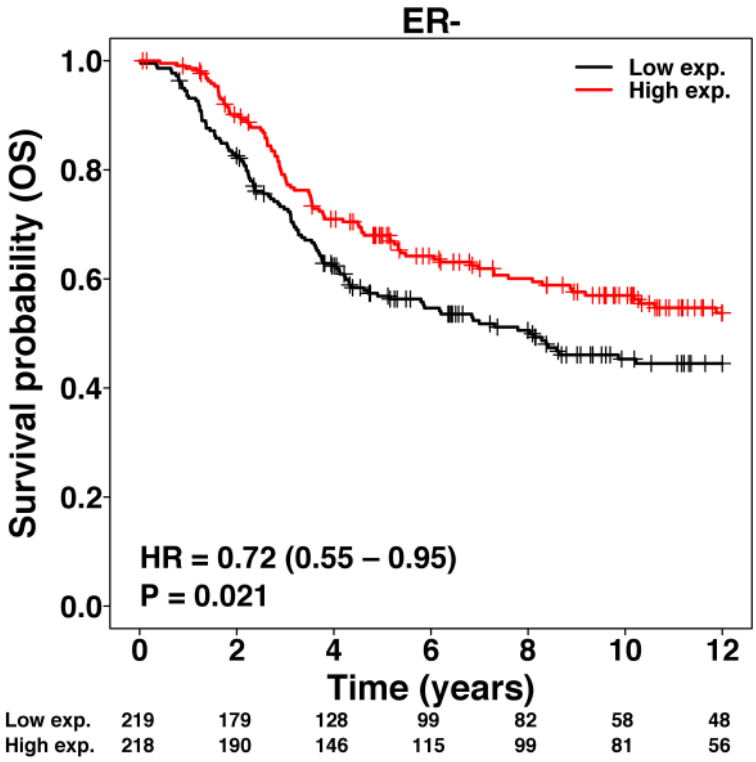
3.5.3 UBL Pathway analysis: FAT10 which coexpressed with NUB1 could stratify ER-, basal and triple negative subgroup breast cancer patients' survival probability

Previous studies showed that NUB1 interacts with both NEDD8 and FAT10 (Kamitani *et al.,* 2001; Groettrup *et al.*, 2008). To examine the clinical significance of NEDD8 and FAT10 mRNA expression in METABRIC, we compared the survival probability curves of their transcripts based on ER status and triple negative subgroups. The hazard ratio threshold of the genes should be < 0.66 or >1 with the *p*-value<0.05 in the subgroups. Only FAT10 (but not NEDD8) transcripts significantly stratify ER- subgroups (hazard ratio=0.65; 95% CI=0.46-0.91, *p*-value=0.011); basal subgroup (hazard ratio=0.72; 95% CI=0.55-0.95, *p*-value=0.021) and triple negative subgroup (Hazard ratio=0.67; 95% CI=0.47-0.95, *p*-value=0.025) (Figure 3.8). High expression of FAT10 mRNA transcripts resulted in better survival among the breast cancer subgroup patients.

To understand the role of FAT10 expression in cancers, the FAT10 gene was reviewed in Oncomine®. In comparison to normal adjacent tissue, the FAT10 gene was highly expressed in cancer tissues (52 vs. 2) (Table 3.5). Same observation was found in METABRIC (Fig. 3.9). Based on this observation, upregulated FAT10 occurs with cancer malignancy.

To investigate whether NUB1 coexpressed with FAT10 in ER-, basal and triple negative subgroups within METABRIC, the Pearson correlation coefficient, ρ was calculated (Table 3.6). The threshold of the ρ should be >0.25 or <-0.25 with *p*-value<0.05. With that, the FAT10 mRNA transcripts showed significant correlation to NUB1 transcripts in ER- (ρ=0.44; p-value<0.001), basal (ρ=0.44; p-value<0.001) and triple negative (ρ=0.42; p-value<0.001). However, no strong correlation of FAT10 to NUB1 in ER+ subgroup was found, suggesting the correlation was only ER- subgroup specific. No correlation was found between NEDD8 and NUB1 expression.


ER-/PgR-/HER2-
Low exp.
High exp.
Survival probability (OS)
1.0
0.8
0.6
0.4
0.2
0.0
HR = 0.67 (0.47 – 0.95)
P = 0.025
0
2
4
6
8
10
12
Time (years)
Low exp. 138 108 83 67 52 44 34
High exp. 138 118 94 76 66 55 39


ER-
Low exp.
High exp.
Survival probability (OS)
1.0
0.8
0.6
0.4
0.2
0.0
HR = 0.72 (0.55 – 0.95)
P = 0.021
0
2
4
6
8
10
12
Time (years)
Low exp. 219 179 128 99 82 58 48
High exp. 218 190 146 115 99 81 56

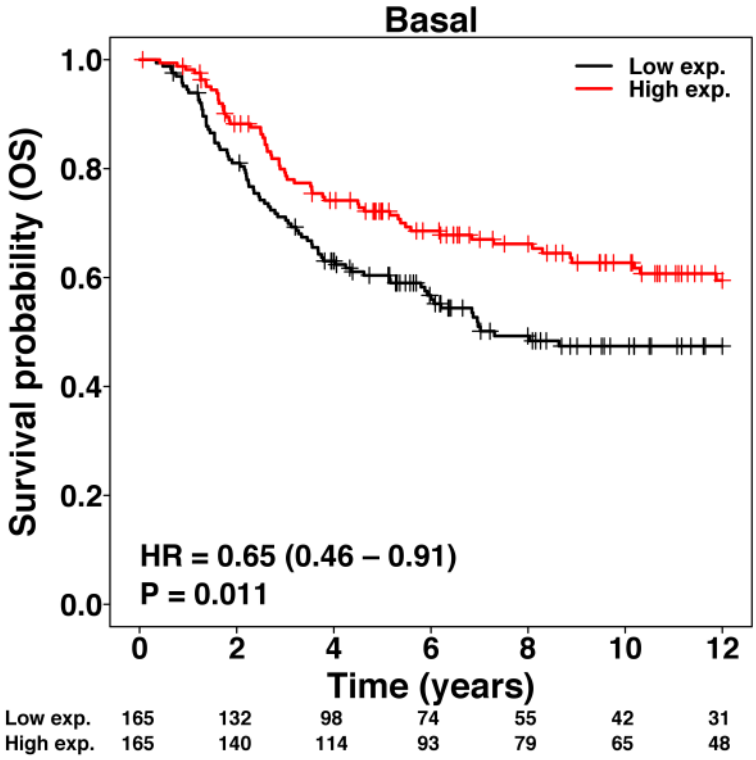


Figure 3. 8 Survival curves of FAT10 in ER-, Basal and triple negative subgroup. The survival curve comparing the patients with high (red) and low (black) expression in breast cancer was identified as the threshold of cox *p*-value <0.05 from metabric Kaplan meier database.

Table 3. 5 FAT10 Genes and cancer summary from Oncomine. The table summarised the number of datasets with FAT10 mRNA under-expression (blue) and over-expression (red) on various cancers in relative normal tissue. The threshold was set with the following parameters: *p*-value of 1E-4, gene ranking of top 10% with (A) all $\log_{10}$ fold change and (B) more than 2 $\log_{10}$ fold change. FAT10 mRNA transcripts are strongly upregulated (>2 $\log_{10}$ fold change) in some cancers (brain cancer, esophageal cancer, lymphoma and other cancer).

	(A)		(B)	
Analysis Type by Cancer	Cancer vs. Normal		Cancer vs. Normal	
Bladder Cancer				
Brain and CNS Cancer	4		1	
Breast Cancer	4			1
Cervical Cancer	2			
Colorectal Cancer	5			
Esophageal Cancer	1		1	
Gastric Cancer	2			
Head and Neck Cancer	2			
Kidney Cancer	3	1		
Leukemia				1
Liver Cancer	7			
Lung Cancer	4			
Lymphoma	8		2	
Melanoma				
Myeloma				
Other Cancer	5		1	
Ovarian Cancer	1			
Pancreatic Cancer	1			
Prostate Cancer				1
Sarcoma		1		
Significant Unique Analyses	49	2	5	3
Total Unique Analyses	394		447	



Cell color is determined by the best gene rank percentile for the analyses within the cell.

NOTE: An analysis may be counted in more than one cancer type.

Table 3. 6 Summary of NUB1 vs. FAT10 and NEDD8 mRNA coefficient, ρ.

	NUB1 mRNA abundance correlation, ρ (*p*-value)					
	Basal	ER+	ER-	HER2+/ER+	HER2+/ER-	Triple negative
FAT10	0.44 <0.001	0.17 <0.001	0.44 <0.001	0.39 <0.001	0.45 <0.001	0.42 <0.001
NEDD8	-0.09 <0.001	-0.13 <0.001	0.04 NS	-0.23 0.013	-0.02 NS	0.03 NS

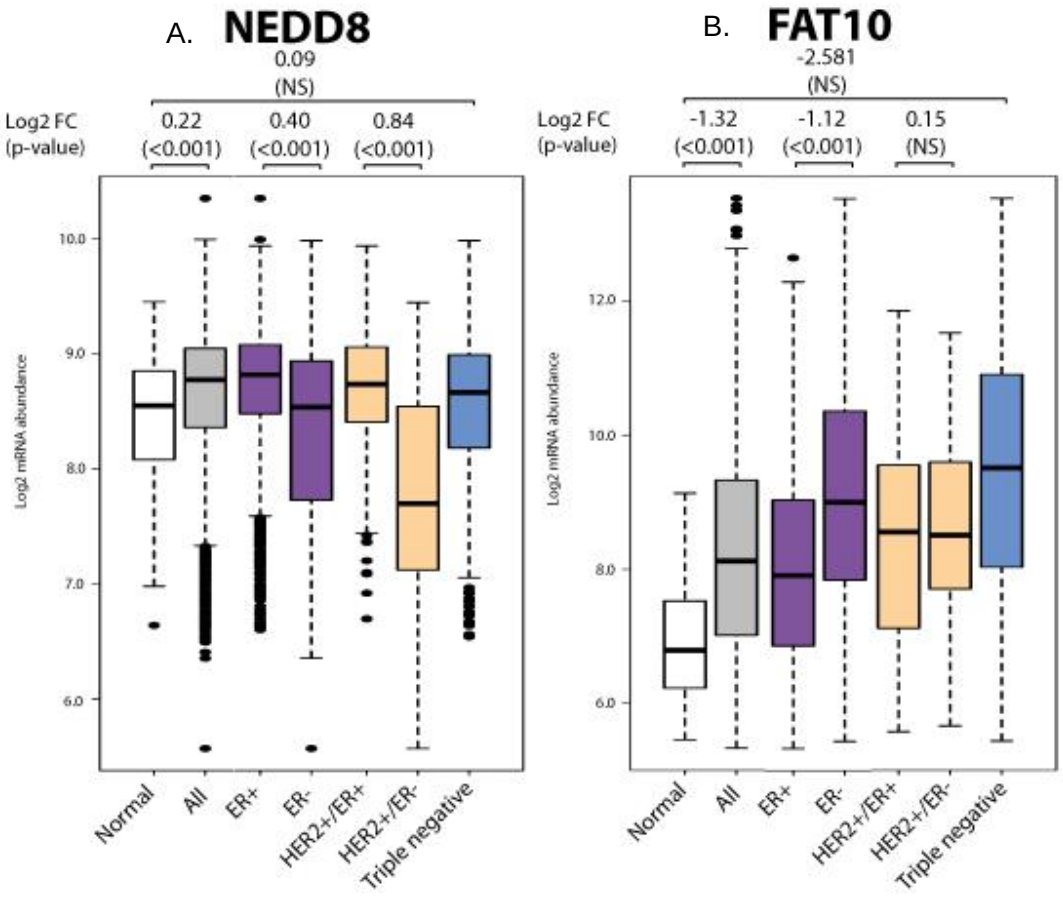


Figure 3. 9 Gene expression patterns of NEDD8 and FAT10 based on the intrinsic molecular subtypes status of METABRIC dataset. Relative transcript abundance of A) NEDD8 and B)FAT10 across the intrinsic subtypes is shown. The boxes represent the interquartile range (25th and 75th percentiles), and the horizontal line in the box represents the median value. The whiskers show the range of largest and smallest values.

3.5.4 CUL1 related ubiquitin ligase activities and cell cycle regulation

To see if CUL1 and p21 expression differs between ER+ vs. ER-, HER2+/ER+ vs. HER2+/ER- and triple negative subtypes of breast cancer, differential transcript expressions of CUL1 genes were determined in METABRIC (Figure 3.10). In comparison to the ER+ subgroup, CUL1 transcripts were expressed higher in the ER- subgroup (log_2 FC= 0.24). HER2+/ER- subgroup expressed 0.13 (log_2) fold change higher CUL1 transcripts than the HER2+/ER+ subgroup. There was a 0.23 (log_2) fold change higher expression of CUL1 transcripts in triple negative breast cancer than normal tissue. And in the ER- and triple negative subgroup, the lower CUL1 transcript level group is 24% (HR= 0.76; 95% CI= 0.58-1.01, *p*-value=0.06) and 27% (HR= 0.73; 95% CI= 0.51-1.04, *p*-value=0.08) more likely to undergo metastasis and die of breast cancer compared to the higher CUL1 expression group, respectively (Appendix 3.3). Unlike AIPL1, NUB1 strongly coexpressed with CUL1 in all the subgroups checked, but there was no co-expression with p21 (Table 3.7). Therefore, CUL1 protein levels, which is directly correlated to NUB1, is a coexpressing factor in NUB1 signaling.

A. B.

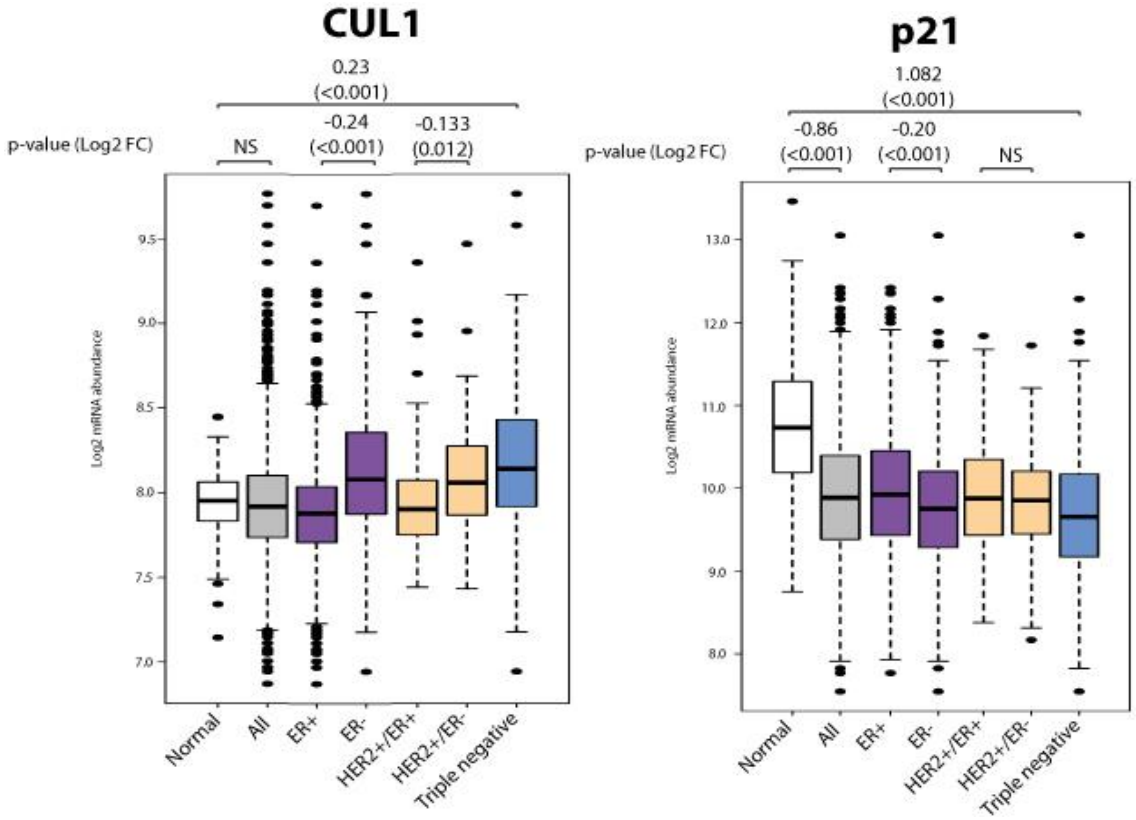


Figure 3. 10 Gene expression patterns of CUL1 and p21 based on the intrinsic molecular subtypes status of METABRIC dataset. Relative transcript abundance of A)CUL1 and B) p21 The boxes represent the interquartile range (25th and 75th percentiles), and the horizontal line in the box represents the median value. The whiskers show the range of largest and smallest values.

Table 3. 7 Summary of AIPL1 and NUB1 on CUL1 and p21 mRNA expression.

Genes		mRNA abundance correlation, ρ (*p*-value)				
		ER+	ER-	HER2+/ER+	HER2+/ER-	Triple negative
CUL1	AIPL1	NS	NS	NS	NS	NS
p21		NS	NS	NS	NS	NS
CUL1	NUB1	0.36 (<0.001)	0.46 (<0.001)	0.43 (<0.001)	0.48 (<0.001)	0.44 (<0.001)
p21		NS	NS	NS	NS	NS

3.5.5 Pathway analysis of HIF1A transcription in different breast cancer subtypes

A potential role of NUB1 signaling is supported by survival probability analysis which identified the poor survival of patients with ER- tumours, for the low NUB1 expression implicate bad prognosis. NUB1 coexpresses with ATM and FAS, both of which are inducible by hypoxia. Therefore, it will be interesting to further explore neddylation of HIF1α and its effect on transcriptional control (Ryu *et al.* 2009). In this case, NUB1 may regulate neddylated HIF1α, we wanted to see if HIF1α downstream targets could be altered by NUB1.

As lower NUB1 transcript levels imposed poorer survival, we studied HIF1α downstream target to NUB1 and related genes with the hope to identify differences in between ER positive and negative patients. The heatmap analysis of the ER-negative subgroup within METABRIC patients showed four HIF1α downstream targets (Table 3.9) including IGF2, DLK1, COL5A1 and ABCB1 were inversely correlated to NUB1 transcripts (Fig. 3.11). It suggests the possibility of the high NUB1 transcript level with low HIF1α mediated transcription activities, and vice versa. Furthermore, AIPL1 transcripts had similar expression with hypoxia signature, a panel of genes which are expressed in hypoxia. Therefore, NUB1 inversely coexpressed to HIF1α downstream target while AIPL1 coexpresses with hypoxia signature at transcriptomic levels.

Table 3. 8 HIF1α and downstream target. These are the genes which are related to hypoxia signature including HIF1α and downstream target of transcriptional activity.

Functional groups of HIF1α downstream targets	Gene
Anti-apoptotic	IGF2
Stem cell properties	DLK1
Metastasis	COL5A1
Therapy resistance	ABCB1

Abbr.: ATP-binding cassette sub-family B member 1 (ABCB1); DLK1: Delta Like Non-Canonical Notch Ligand 1; COL5A1: Collagen Type V Alpha 1 Chain; IGF2: Insulin Like Growth Factor 2

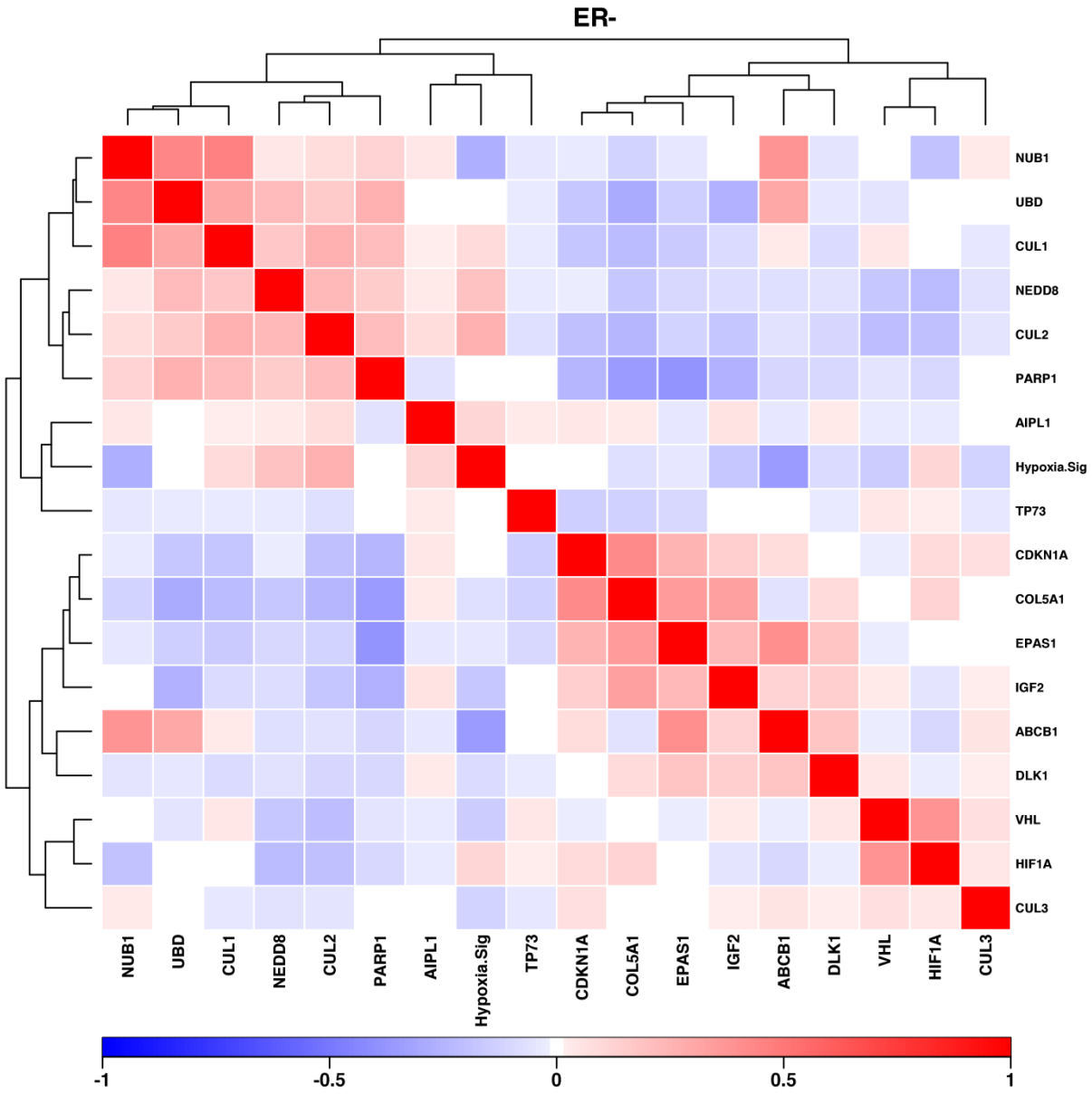


Figure 3. 11 Heatmap showing genes differentially expressed in ER- subgroup patients (n =439), using RNA-Seq data. Each gene is normalized to standard normal distribution with blue indicating lower expression, and red indicating higher expression. HIF1α downstream targets including IGF2, DLK1, COL5A1 and ABCB1 were showing identical expression. To determine the expression profile of NUB1 to HIF1α and its downstream target genes, the correlation coefficients, ρ were compared across all the breast cancer subtypes. The analysis was limited to genes which are related to hypoxia signature including HIF1α and downstream targets of transcriptional activity. NUB1 inversely coexpressed to HIF1α downstream target while AIPL1 coexpresses with hypoxia signature at transcriptomic levels.

3.6 Discussion and Chapter Summary

Meta-analysis approach increases the sensitivity in revealing biomarkers for various cancers. The comparison of mRNA levels between tumours and their corresponding normal tissue demonstrated that AIPL1 mRNA levels are predominantly lower while NUB1 mRNA levels are usually higher in cancers. In Oncomine®, a total of 24 datasets showed down-regulated AIPL1 transcripts and 37 datasets showed up-regulated NUB1 in cancers (Table 3.2). This concordant down-regulated AIPL1 and upregulated NUB1 in cancers may exerts opposite roles in tumourigenesis. This was observed in breast cancers too (Fig. 3.1).

CUL1 was of interest as its mRNA transcripts were found to be frequently coexpressed with NUB1 (Fig. 3.1 and 3.2). Coupled with the finding that NUB1 indirectly coexpressed with FAS and ATM, whose activities are frequently upregulated with hypoxia and reoxygenation, we thought NUB1 may regulate the cancer cell cycle through the ubiquitin ligase activities with varying oxygen tensions. Imposing hypoxia and reoxygenation stress could be a way to study the breast cancer cells *in vitro.*

We found that breast cancer showed the opposite profile of upregulated NUB1 and AIPL1, indicating that this cancer model might be worth studying further. At the protein level, AIPL1 blocks NUB1 entering the nucleus and therefore the differences in expression in expression could cause problems just because the normal chaperone, AIPL1 and client protein, NUB1 are altered. In METABRIC dataset, higher levels of NUB1 mRNA predict better outcome in ER-negative subgroup patients, HER2-positive group, HER2+ with ER-group and triple negative subgroup. It was found that the HIF1α downstream targets had a similar expression profile in the ER-negative breast cancer subgroup as well as an inversed correlation to NUB1 mRNA transcript levels (Fig 3.1).

There are some limitations of the work done this far. Microarray studies revealed the relative mRNAs with less representation to the expression level of the proteins. The number of protein molecules synthesised from mRNA molecule is highly dependent on translation-initiation features of the mRNA sequence. So the *in vitro* study was carried out next to study the protein changes.

Chapter 4

AIPL1-NUB1 signaling cascade in cell cycle regulation Through CUL1 based E3 ubiquitin SCF-ligase

4.1 Rationale of the study

By reviewing chaperones candidates, AIPL1 down-regulation was observed in various cancers. AIPL1 is involved in chaperoning and protein trafficking in retinal tissue (van der Spuy *et al.*, 2002); the role of AIPL1 and its client protein, NUB1 remains unexplored in cancers.

In the previous chapter, it was found that NUB1 protein coexpresses with FAS and ATM proteins, two independent pathways that are involved in the reoxygenation-induced DNA damage pathway (Hammond *et al.*, 2003). We believe hypoxia and reoxygenation could be a way to induce NUB1 activities. Hypoxia occurs in tumour cells growing in suboptimal oxygen concentration (Olcina *et al.*, 2010). This condition is due to tumour progression and a general lack of blood supply (Thomlinson and Gray, 1955). Optimal oxygen tension is crucial for tumour cells to acquire more energy from glucose aerobically. Therefore, proliferating tumour cells need to adapt to the low oxygen pressure.

Clinically, hypoxia is often correlated with an aggressive clinical outcome (Brizel *et al.*, 1996; Le *et al.*, 2004; Erler *et al.*, 2006). Solid tumour under hypoxia often grow within an acidified micro-environment, with increased glycolysis and often drug resistance. Thus, a clinically relevant AIPL1 and NUB1 research aim is to correlate their activities with the hypoxic environment to examine cell death mechanism in cancer cells.

The role of NUB1 in tumour growth has only been investigated in the context of tumor cell death (Hosono *et al.*, 2010) but not with tumour adaptation to hypoxia. Expression of NUB1 could exert anticancer effects in renal cell carcinoma (RCC) cells, by inducing apoptosis via the accumulation of p27 and cyclin E (Tanaka *et al.*, 2013). Prolonged p27 is thought to cause apoptosis. As NUB1 mRNA coexpressed with CUL1 transcript in our

study, it prompted the interest of CUL1 action via the ubiquitin SCF-ligase complexes (as shown below). Therefore, it is worth investigating whether the antiproliferative effect of NUB1 in relationship to hypoxia which is regulated by CUL2.

NUB1 —┤ Neddylated CUL1→Ubquitinated p27 and cyclin E

AIPL1 and NUB1 proteins may take part in many biological processes such as cell proliferation, differentiation, and cell death which depend precisely on the timely synthesis and degradation of key regulatory proteins. The SCF (SKP1-CUL1-F-box protein) E3 ligases are the largest family and are responsible for the turnover of many key regulatory proteins including p21 and p27. Aberrant regulation of SCF E3 ligases is associated with various human diseases, such as cancers, including skin cancer.

In this chapter, we studied how NUB1 regulates the NEDD8 and FAT10 conjugation cascade upon hypoxia and reoxygenation. The chaperoning mechanism of AIPL1 onto NUB1 and the effects on the cancer cell cycle profiles were underlined.

4.2 Cell line screening of proteins and their transcript levels

4.2.1 Detection of endogenous protein expression in various cancer cell line

To characterise the protein expression levels of NUB1, AIPL1, NEDD8 and FAT10 in unstressed cancer cells, 11 different cancer cell line originating from kidney, colon, bone, retina and with six breast cell lines, were analysed. NUB1 protein was found to be abundantly expressed in most cells except U2OS and SKBR3 (Fig 4.1). MDA-MB-231 expresses the most abundant amount of NUB1 protein. All cells form AIPL1 dimer. The role of monomer and dimer of AIPL1 remains to be investigated as these functional aspects of protein were not reported previously. Whilst varying expression levels of AIPL1 monomer were seen, ACHN, U2OS, Y79 and BT474 cells showed higher expression of the monomeric form than the other cell line. NEDD8 proteins were observed in the conjugated CULs, monomers were observed in HCT116, U2OS, HCC1806, and MDA-MB-231 cells. All the FAT10 are in the conjugated form, no free monomers were observed under unstressed condition.

4.2.2 Quantitative PCR analysis of various cancer cell line

To determine relative expression of AIPL1, NUB1, NEDD8 and FAT10 genes between different cell line, we analysed transcript levels by qPCR. Y79 cells were used as a positive control because AIPL1 and NUB1 have been well documented in retinal tissue. Expression was compared to the housekeeping gene, tubulin was used. Very low AIPL1 mRNA transcript levels were observed in all the cancer cells tested, compared to the control Y79 cells (Figure 4.2). In contrast, greater NUB1 transcript levels were observed in all cell line tested as compared to Y79 control cells, with U2OS cells exhibiting the most abundant transcripts. Meanwhile, the highest amount of NEDD8 mRNA transcripts was found in ACHN, MDA-MB-231 and BT474 cells. Abundant amount of FAT10 mRNA was detected in the cells, with the highest amount found in 786-O.

4.2.3 Immunohistochemistry staining of various cancer cell line

To examine protein localisation of AIPL1, NUB1 and NEDD8 in unstressed cancer cells, immunohistochemistry (IHC) staining were performed across the 12 cell line. For AIPL1, the proteins were mostly observed in the cytoplasm and a to a lesser extent, in nucleus. The protein was found the least in ACHN and BT474 cell lines. All cells except U2OS show positive staining for NUB1 protein. NEDD8 proteins could be found abundantly in both the nucleus and the cytoplasm in all cell line tested. FAT10 was found in most cells with the least or no staining in HCT116, T47-D and BT474 (Fig 4.3).

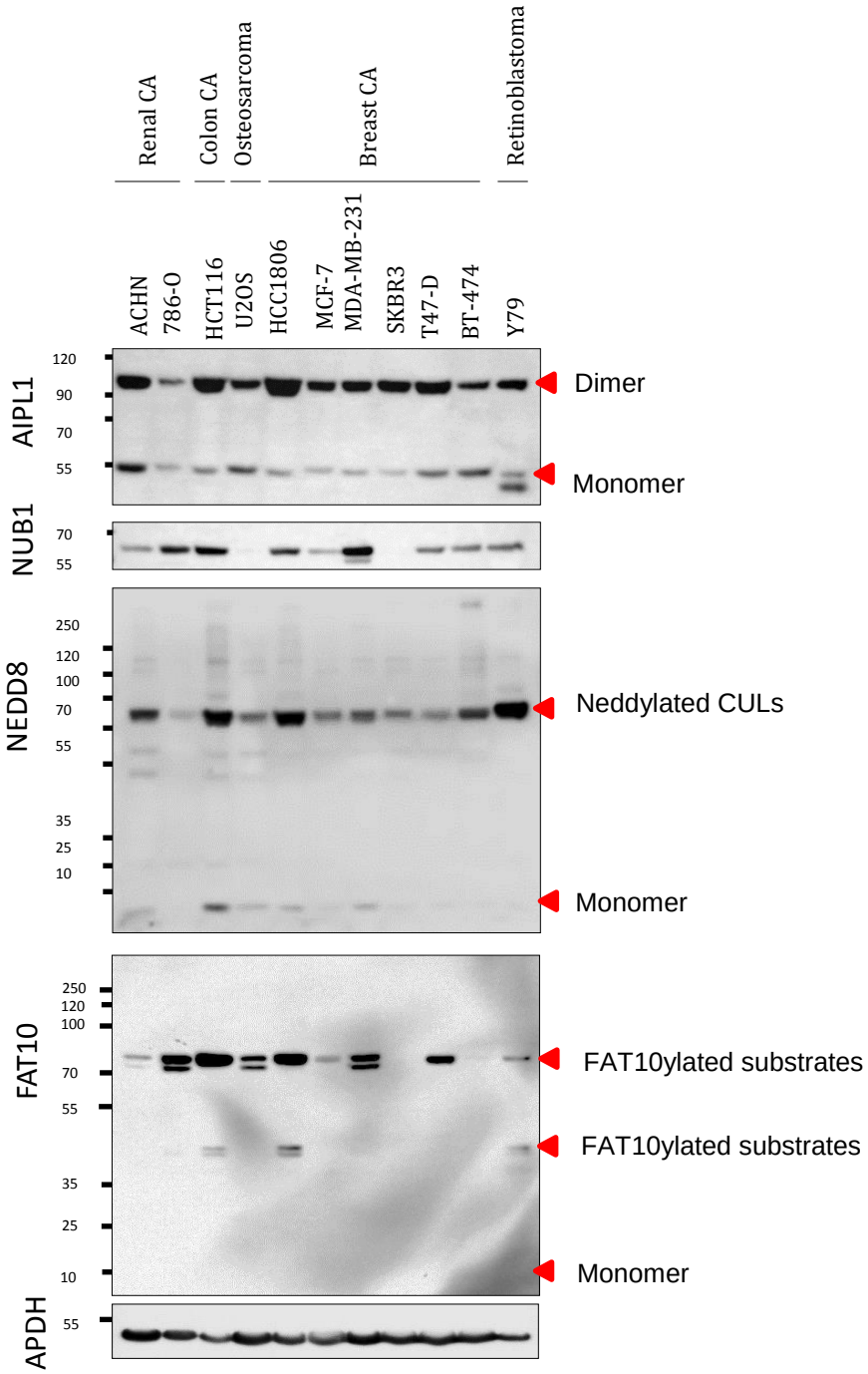


Figure 4. 1 Protein expression patterns. Western blot of neddylated cullins, NUB1, AIPL1 and FAT10 among the cancer cell line derived from varying tissue origins.

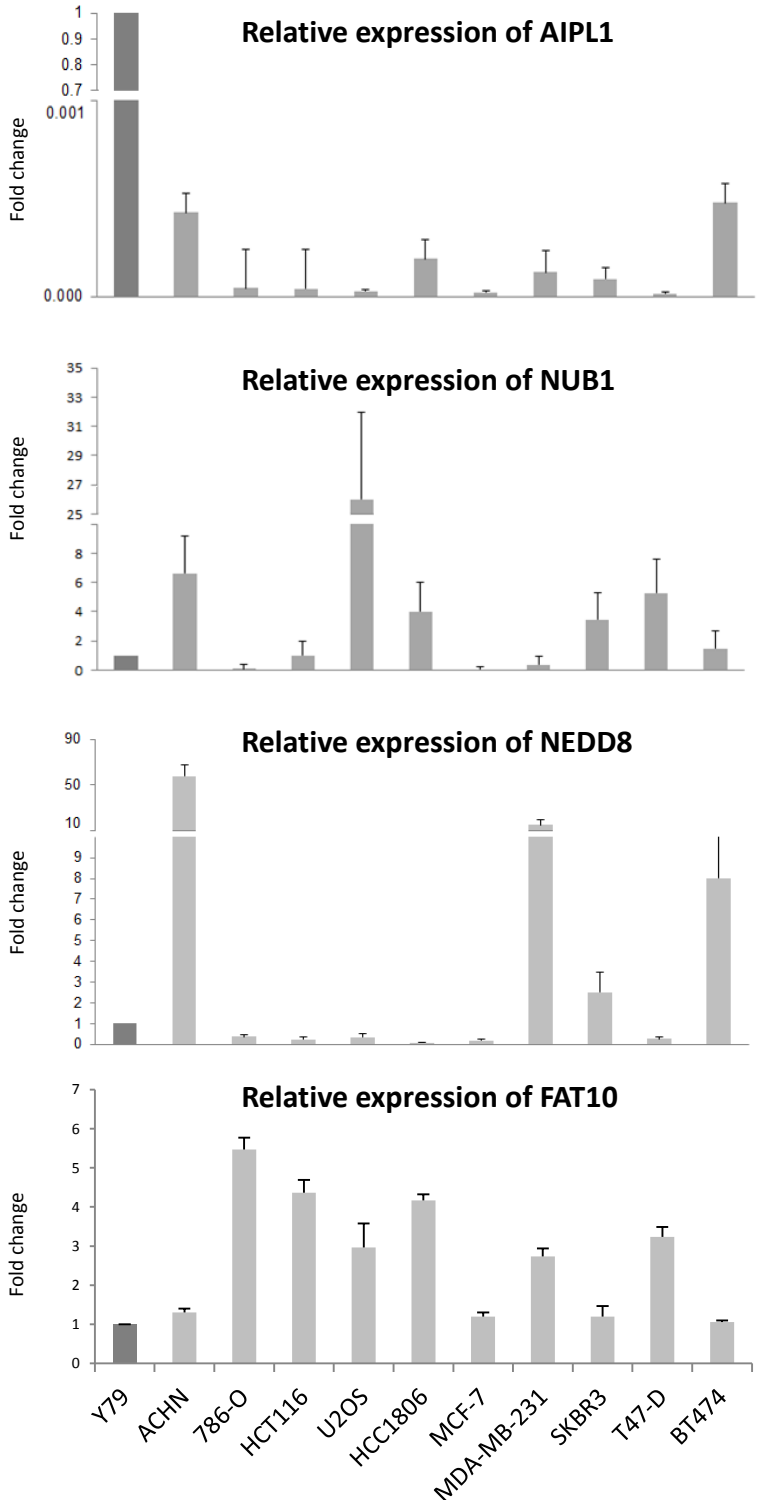
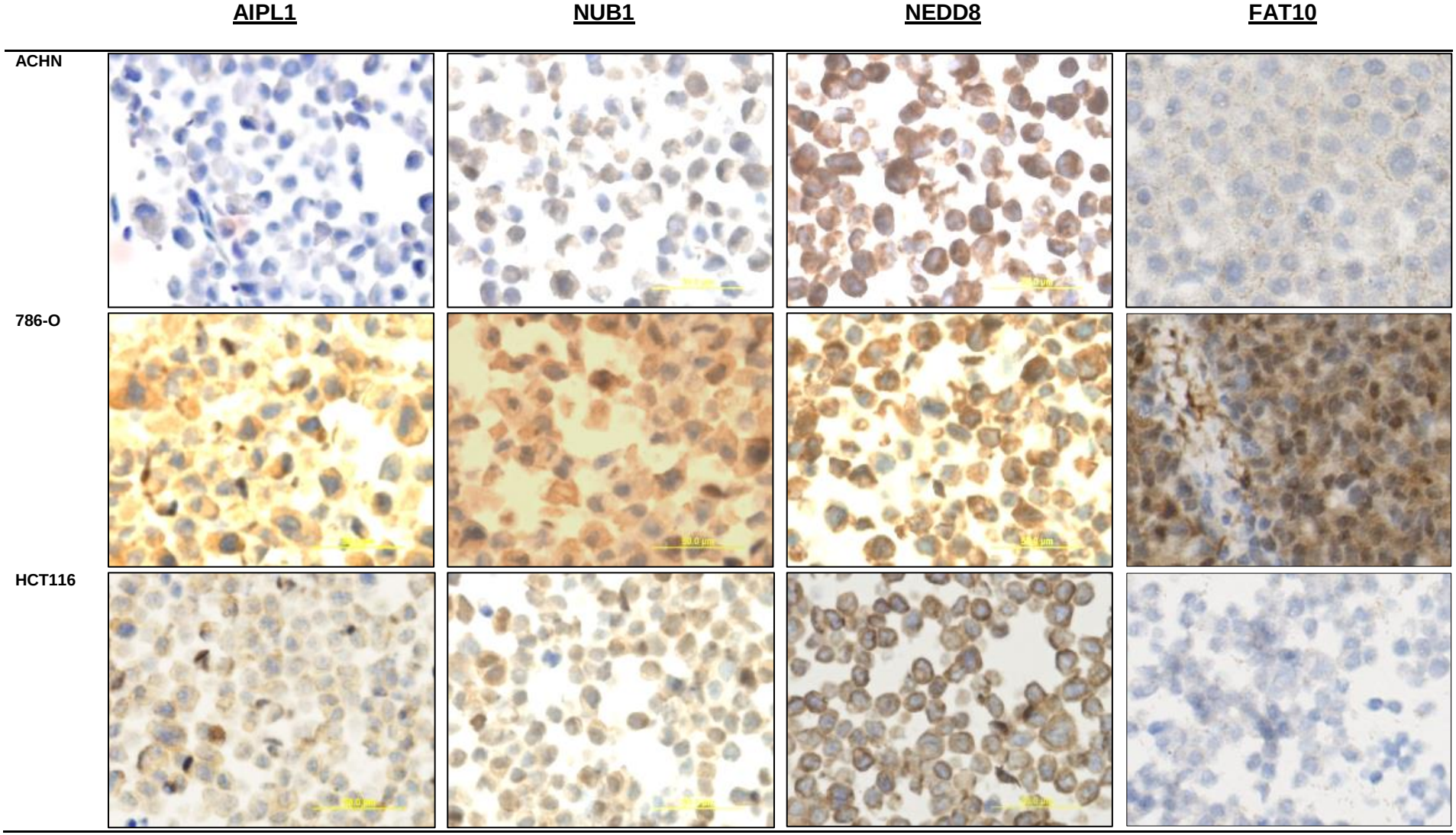
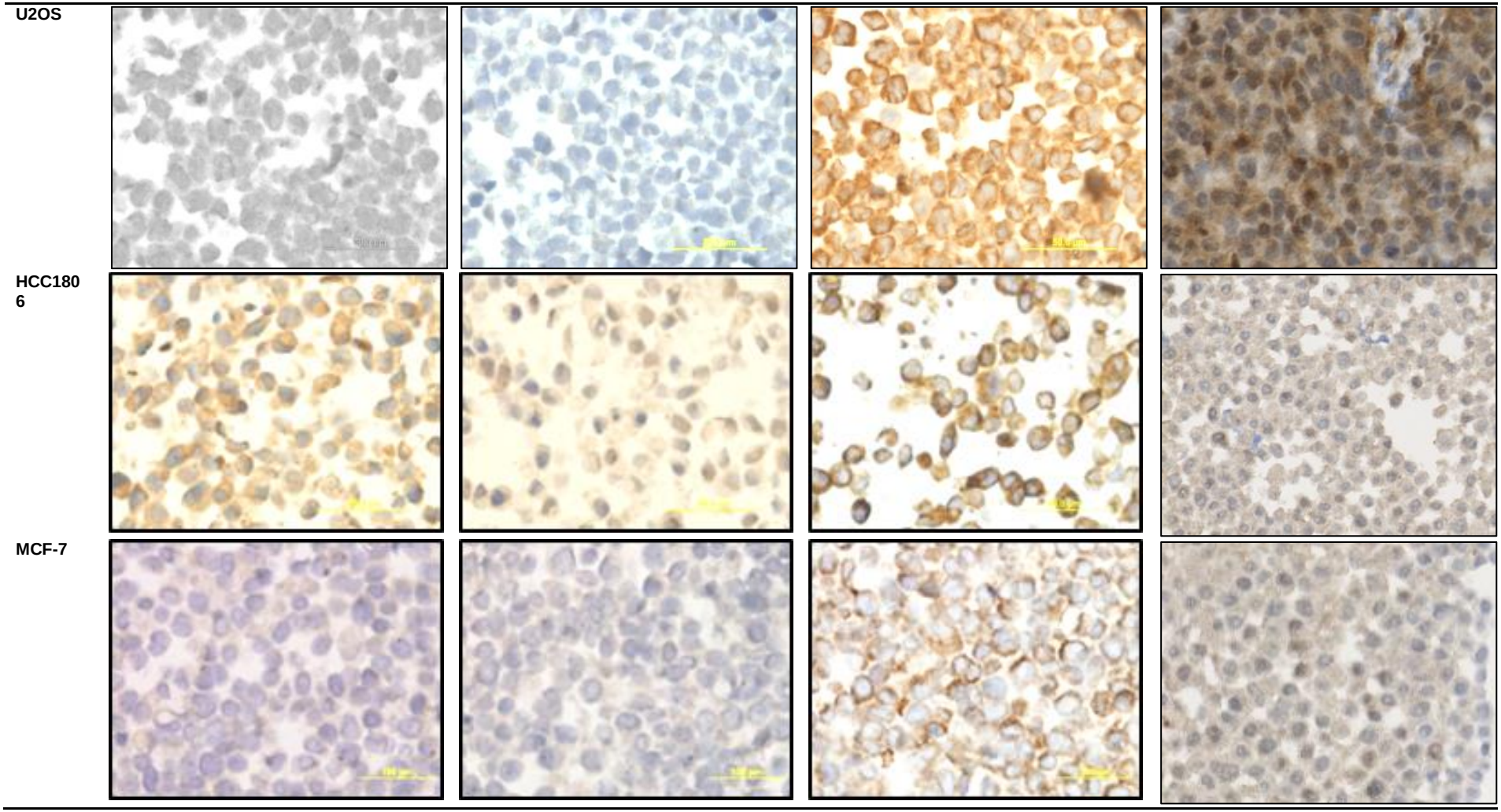
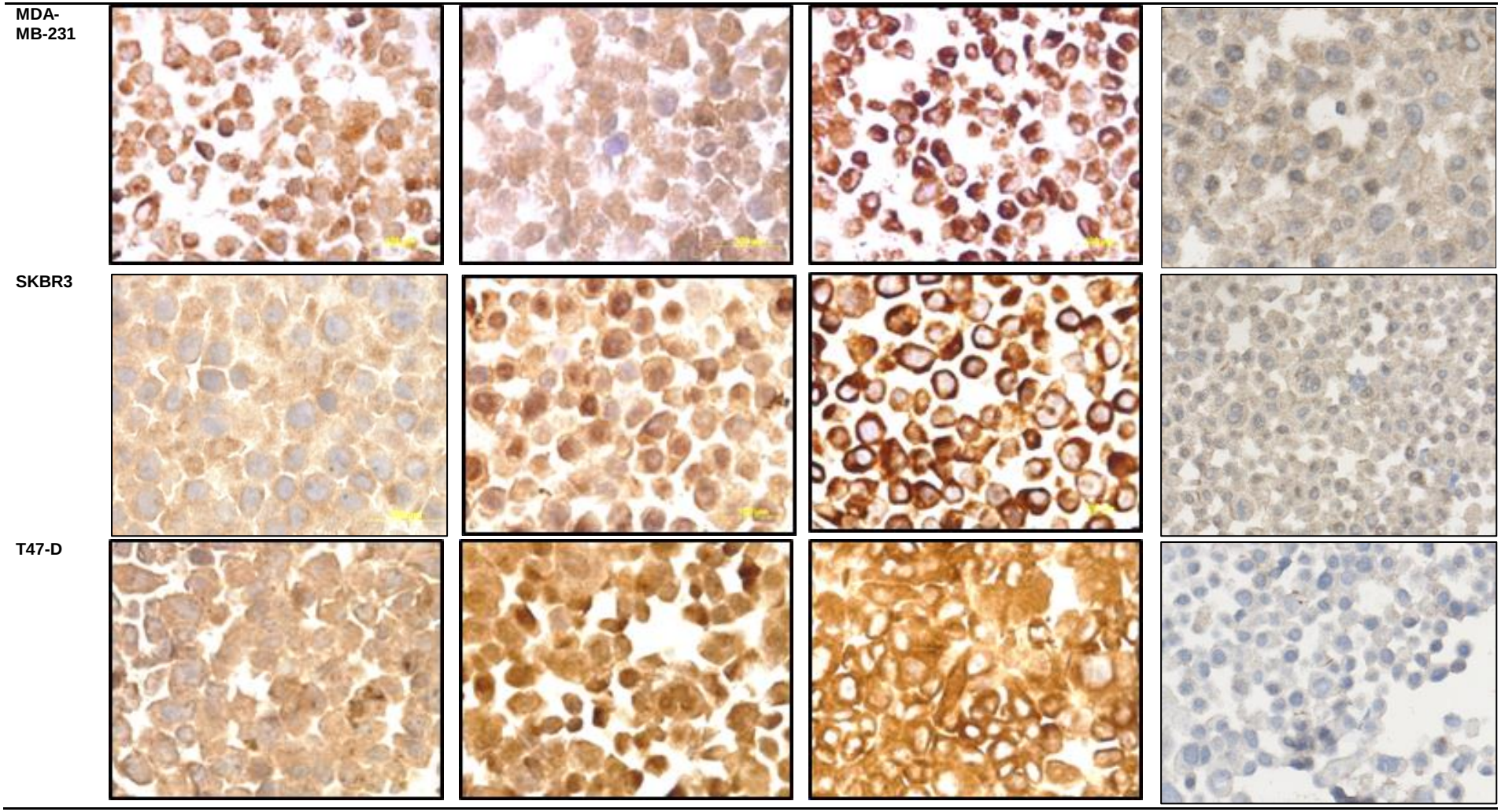


Figure 4. 2 Endogenous transcript expression profile in cancer cells. The relative gene expression levels of AIPL1, NUB1, FAT10 and NEDD8, as determined by qPCR. The results were normalised to β-actin signals. Data shown are means of 3 independent experiments with error bars representing standard deviation. Each bar represents mean ± SEM for each cell lines (n=9).


AIPL1
NUB1
NEDD8
FAT10
ACHN
786-O
HCT116


U2OS
HCC1806
MCF-7


MDA-
MB-231
SKBR3
T47-D

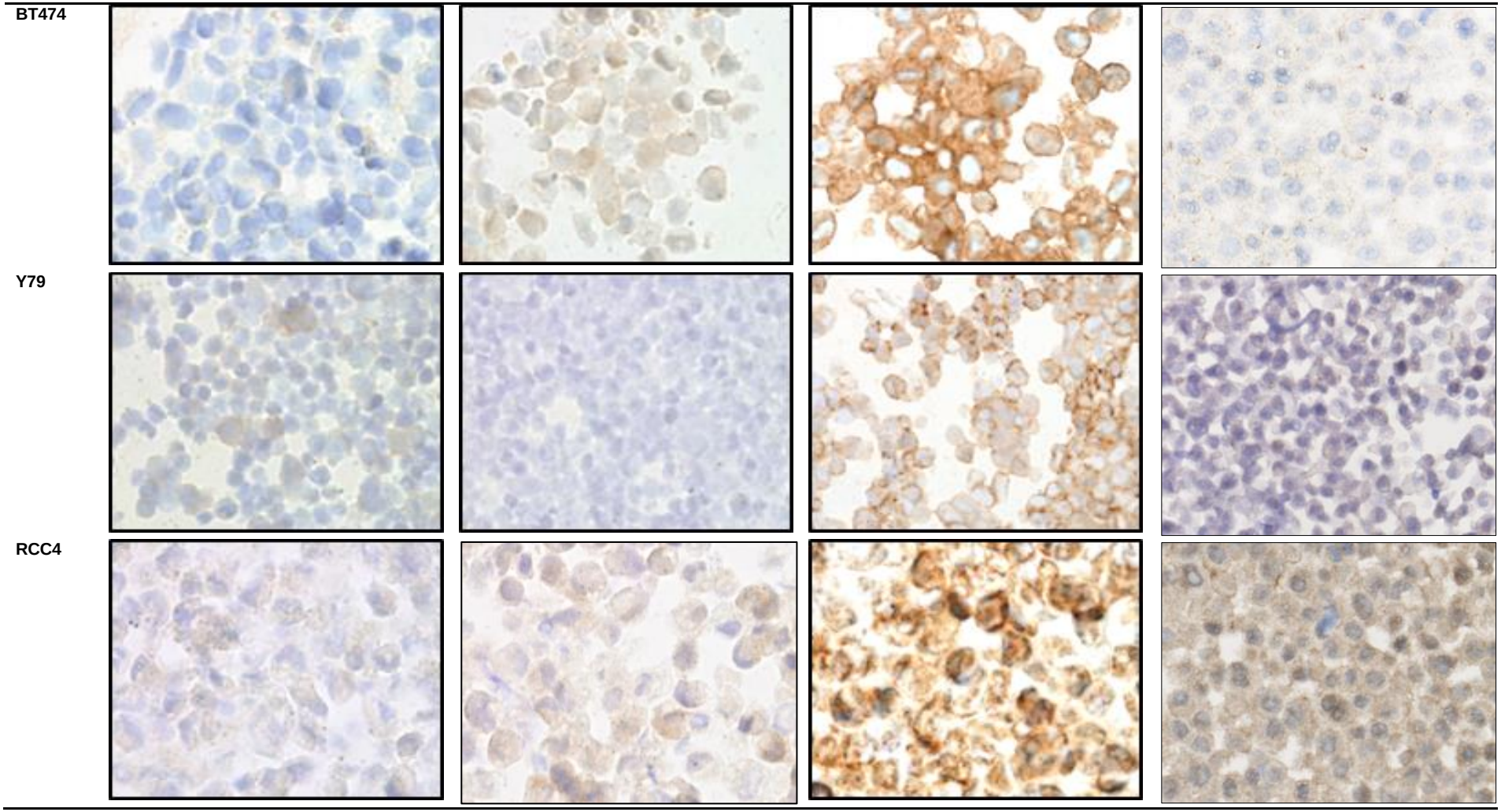


Figure 4. 3 Immunohistochemistry staining of various cancer cells. The representative images of immunohistochemical analysis illustrating AIPL1, NUB1 and NEDD8 protein localisations in various cancer cell line. Brown staining with diaminobenzidine (DAB) indicates immunoreactivity. All magnification of the images are 20X.

Table 4. 1 Summary of AIPL1, NUB1, NEDD8 and FAT10 gene products (protein or transcripts) in all cancer cell line.

Cell line	Proteins*					mRNA				IHC							
	AIPL1		NUB1	^{NEDD8}CULs	FAT10	AIPL1	NUB1	NEDD8	FAT10	AIPL1		NUB1		NEDD8		FAT10	
	Monomer	Dimer								C	N	C	N	C	N	C	N
ACHN	✓	✓	✓	✓	✓	✓	✓	✓	✓	0	0	2+	0	3+	0	0	0
786-O	✓	✓	✓	Low	✓	Low	Low	Low	✓	3+	0	3+	0	3+	0	2+	3+
HCT116	✓	✓	✓	✓	✓	Low	✓	Low	✓	2+	0	2+	0	3+	0	0	0
U2OS	✓	✓	Low	✓	✓	Low	✓	Low	✓	0	0	0	0	3+	0	2+	3+
HCC1806	✓	✓	✓	✓	✓	Low	✓	Low	✓	2+	0	2+	0	3+	0	1+	1+
MCF-7	✓	✓	✓	✓	✓	Low	Low	Low	✓	1	0	0	0	3+	0	1+	0
MDA-MB-231	✓	✓	✓	✓	✓	Low	Low	✓	✓	3+	0	3+	1+	3+	0	1+	0
SKBR3	✓	✓	X	✓	X	Low	✓	✓	✓	3+	1+	3+	2+	3+	0	1+	0
T47D	✓	✓	✓	✓	✓	Low	✓	Low	✓	3+	3+	3+	3+	3+	0	0	0
BT474	✓	✓	✓	✓	Low	Low	✓	✓	✓	0	0	1+	0	2+	0	1+	0
Y79	✓	✓	✓	✓	✓	Low	✓	✓	✓	1+	0	0	0	2+	0	0	0

√ present; X absent, ND: not determined, IHC: Immunohistochemistry, mRNA: messenger RNA, 0, no staining, 1+, mild, 2+, intermdediate; 3+, strong, c, cytoplasm; n, nucleus

4.3 AIPL1 dimerisation in cancer cells

By using a monoclonal mouse anti-AIPL1 antibody (3B4), we observed a band at the right size (41.3kDa), a slightly higher band around 55kDa and a 2-fold larger sized band at 100kDa suggesting a dimerised protein of AIPL1 in Y79 (Fig 4.1). To confirm the oligomer formation, MDA-MB-231 cells were examined *via* native-PAGE analysis. The cells are incubated in reoxygenation as we found AIPL1 protein was upregulated in reoxygenation (Fig. 4.8). No AIPL1 monomer was observed in native conditions (Fig 4.4). Appearance of AIPL1 protein in dimer, trimer and oligomer forms suggests those were the native forms under physiological conditions.

To test the presence of disulfide bonds, we used maleimide fluorescein method. TCEP is a strong reducing agent that separates the cysteine-cysteine disulphide bond apart and prevents the dimer formation. Maleimide fluorescein competitively binds to the exposed cysteine and gives the fluorescein signal. It was observed that the disulfide bonds in the TCEP-reduced sample exhibited stronger fluorescent than the oxidised sample with a visible band and ~55kDa (Fig 4.4). To further confirm the disulphide bonds, the reoxygenated sample of MDA-MB-231 were treated with titrated dithiothreitol (DTT). There were only dimers and monomers were observed. Monomers increased with more DTT concentration. We observed the dimer which is of strong bonds was able to resist DTT reaction. This could be due to the presence of more than two disulphide bonds. Therefore, native and reduced form of the AIPL1 protein verifies the presence of AIPL1 dimer.

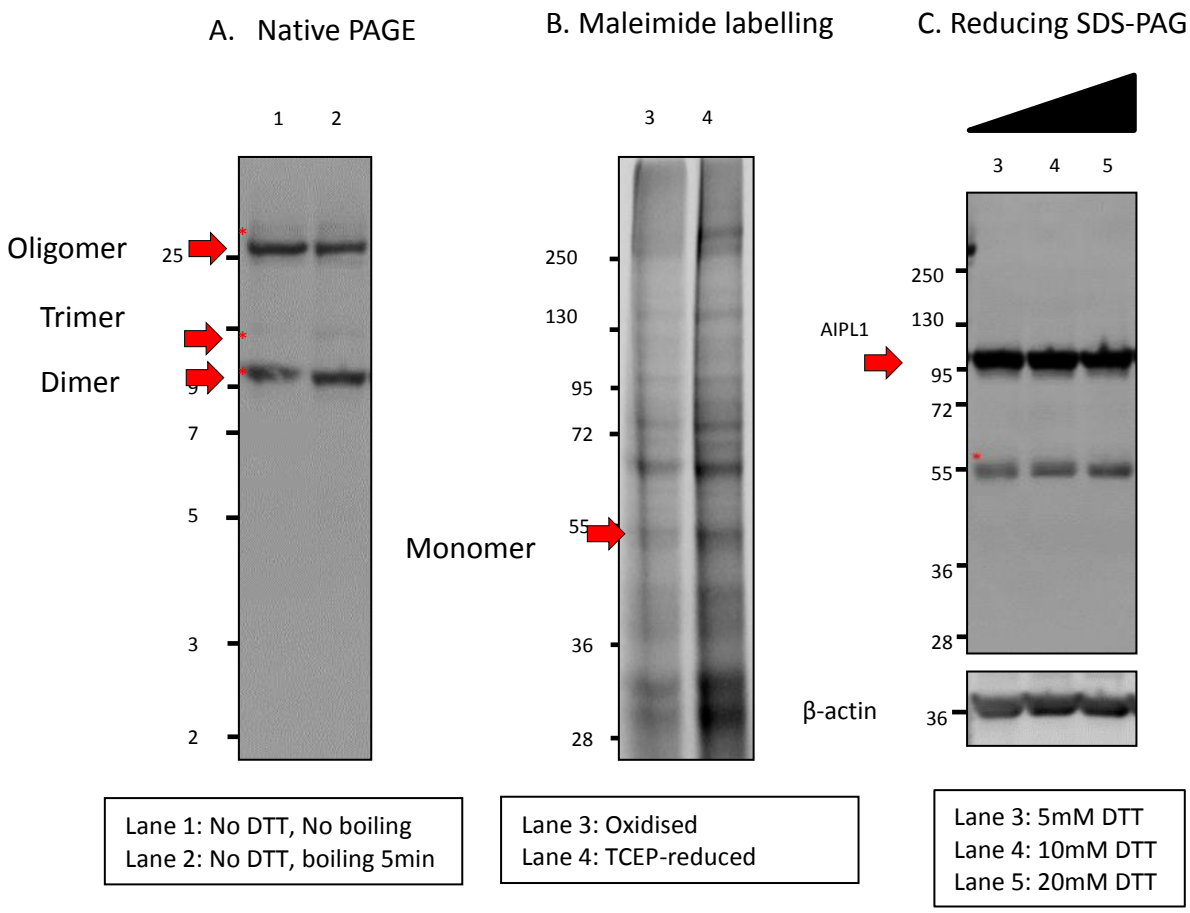


Figure 4. 4 Oligomerisation of AIPL1 proteins analysed by native PAGE and immunoblotting. (A) Native PAGE with and without boiling step. (B) Maleimide labelling with TCEP treatment. We blocked free thiols in the protein with *N*-ethylmaleimide, denature the protein with SDS. Then the denatured protein samples were divided into two- leave one oxidized and reduce the other with TCEP. React each sample with fluorescein maleimide and finally run the samples on SDS-PAGE. Stronger maleimide signal in lane 4 marks the broken disulphine bonds of proteins. (C) Immunoblot with titrated DTT.

4.4 Changes of NUB1 stability upon reoxygenation

To test whether there are changes of proteins under reoxygenation following severe hypoxia (0.1% O_2 for 48h), protein expression levels were examined. MDA-MB-231 cells were studied for it belongs to ER- and triple negative subtypes. Increased neddylated cullins (^{NEDD8}CULs) and NUB1 protein levels were observed in MDA-MB-231 cells as early as 5 minutes of reoxygenation (Fig. 4.5). AIPL1 monomers and dimers did not change over the time points monitored. These data led us to speculate the involvement of both AIPL1 and NUB1 in response to hypoxia and reoxygenation. With the discovery of neddylated HIF1α (Ryu *et al.*, 2011), it is good to examine the role of AIPL1 and NUB1 in regulating NEDD8 conjugations. It could suggest a possible function in the neddylation of proteins in the HIF1α pathway.

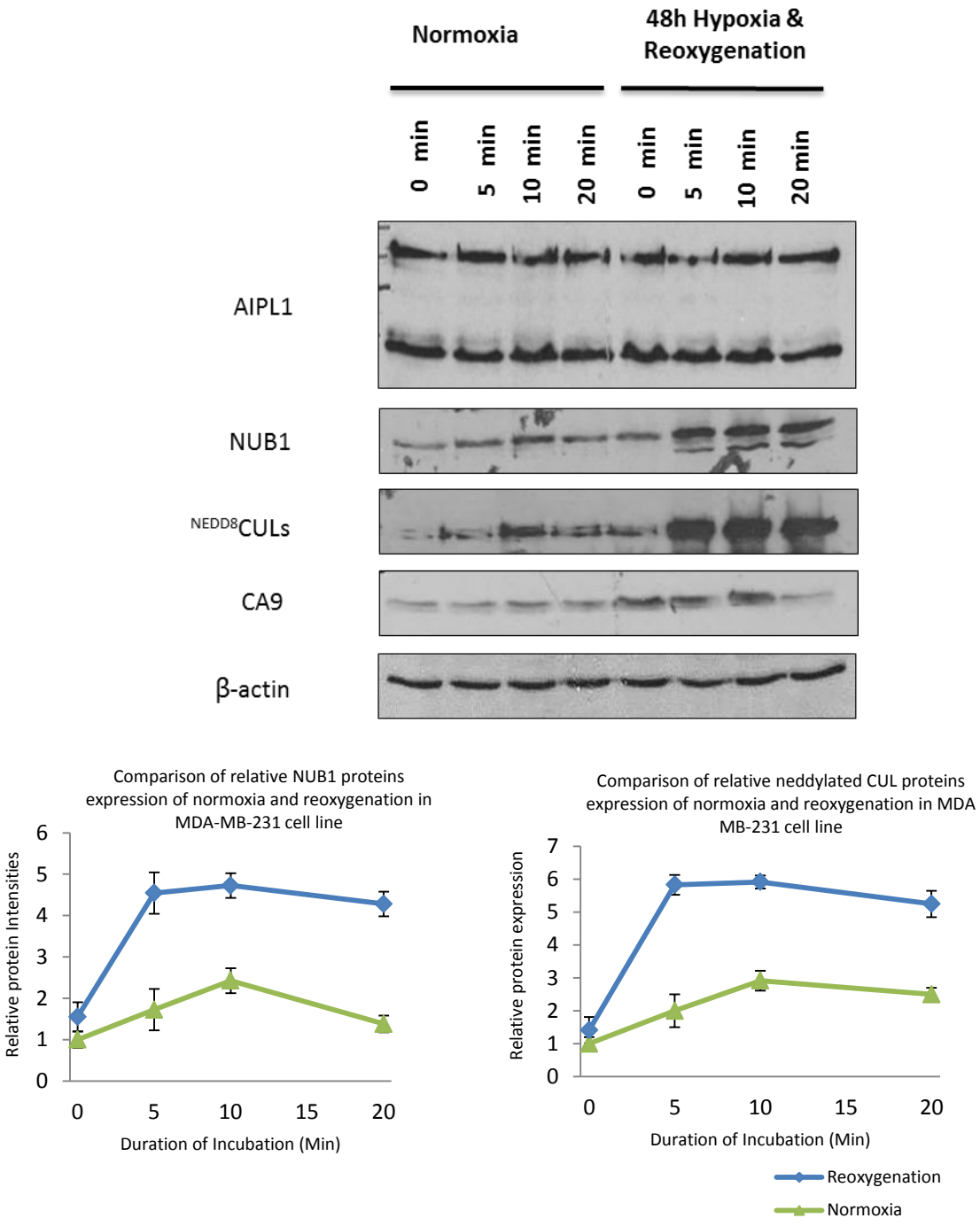


Figure 4. 5 Time course experiment of reoxygenated MDA-MB-231. MDA-MB-231 cells were incubated in hypoxia and reoxygenated. Lysates were collected according to the time point. The levels of proteins were compared to the normoxic cells. Both NUB1 and ^{NEDD8}CULs proteins were significantly different than the normoxic cells. *Abbr* CA9: carbonic anhydrase 9.

4.5 NUB1 silencing caused G_0/G_1 cell cycles arrest

It was found that higher NUB1 protein level triggered cell-cycle alterations through p21/p27 up-regulation and apoptosis (Hosono *et al.*, 2010). To test this, the cell cycle profiles of NUB1 knockdown MDA-MB-231 cells was examined. The cell line was used as it is of ER negative and triple negative subgroup. MDA-MB-231 was transiently transfected with siNUB1 and the cell cycle analysis were perform after 48hr incubation. The experiment demonstrated that NUB1 knockdown lead to a significant reduction in the percentage of cells in the sub-G_1 phase of the cell cycle (Fig 4.5). NUB1 knockdown cells also showed significantly higher level of G_0/G_1 cell population compared with the control (Figure 4.5).

To confirm the G_0/G_1 cell cyle arrest, we observed the up-regulation of two G_0/G_1 cell cycle arrest markers, p21 and p27 proteins in the NUB1 knockdown cells. Therefore, NUB1 protein could promote the G1 to S phase cell cycle transition.

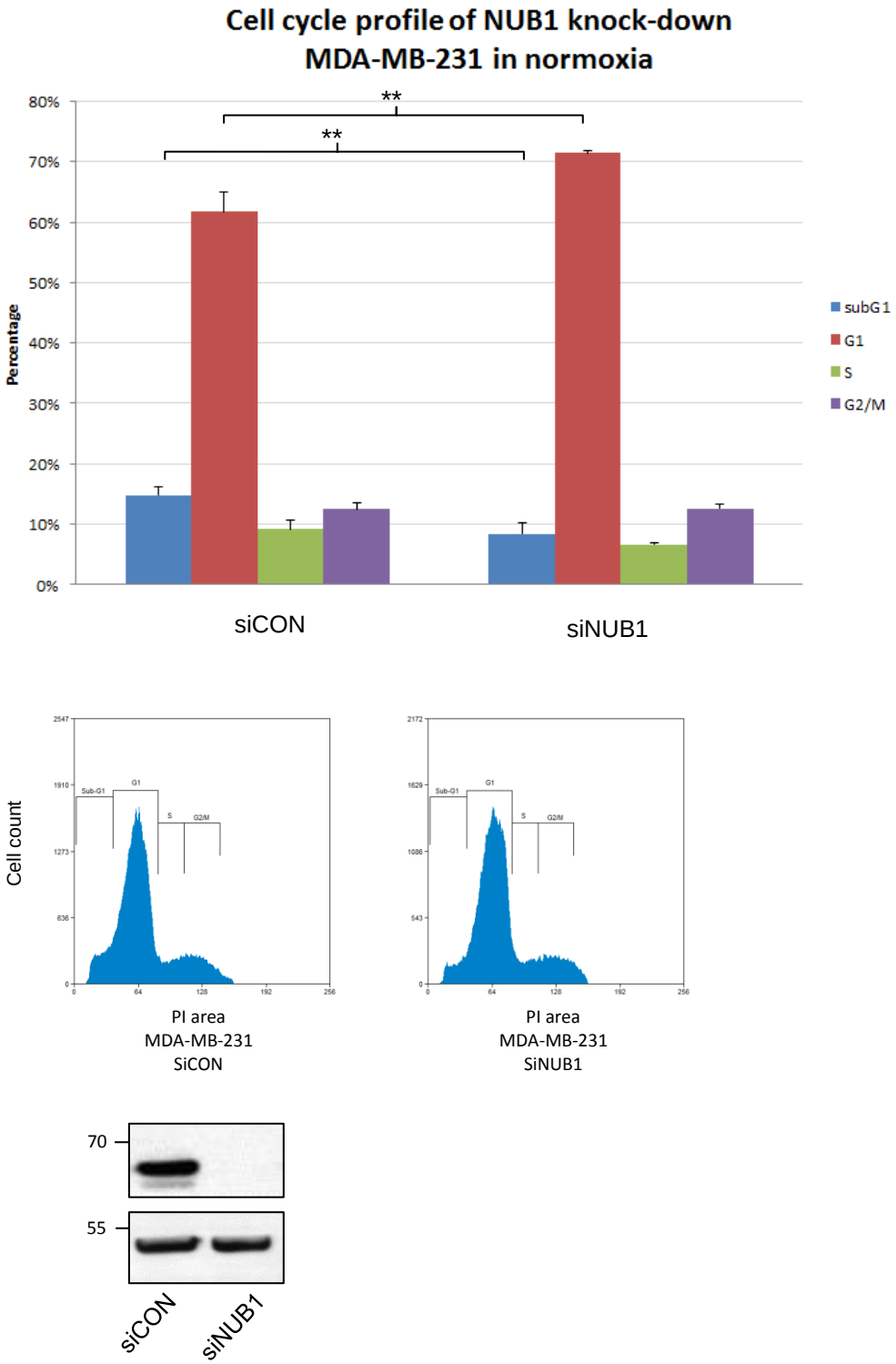


Figure 4. 6 Cell cycle analysis in NUB1 knockdown MDA-MB-231. A. Cell cycle percentage of NUB1 knockdown cells and its control. B. The cell cycle histogram of NUB1 knockdown cells and its control.

4.6 Depletion of NUB1 protein affects cell growth rates

The previous experiment underlined that the NUB1 knockdown causes the G_1 cell cycle arrest, it is important to examine whether NUB1 depletion would alter the growth rate of cancer cells. To evaluate this, the ER- (MDA-MB-231) and ER+ (T-47D) cell lines were used in both normoxia and chronic severe hypoxia (0.1% O_2) for 72hr, respectively. No significant differences were found in normoxia condition (Fig. 4.7). However, in chronic severe hypoxia, NUB1 knock-down in the ER- cell line, MDA-MB-231 showed significant lower viable cell number ($6.2X10^4$/mL vs. $4.1X10^4$/mL, $p<0.001$). So did the ER+ cell line, T-47D under the same hypoxic conditions ($5.7X10^4$/mL vs. $4.7X10^4$/mL, $p=0.01$). This observation implies that loss of NUB1 protein causes greater cell cycle arrest with slower growth rate in chronic severe hypoxia compared to normoxic conditions.

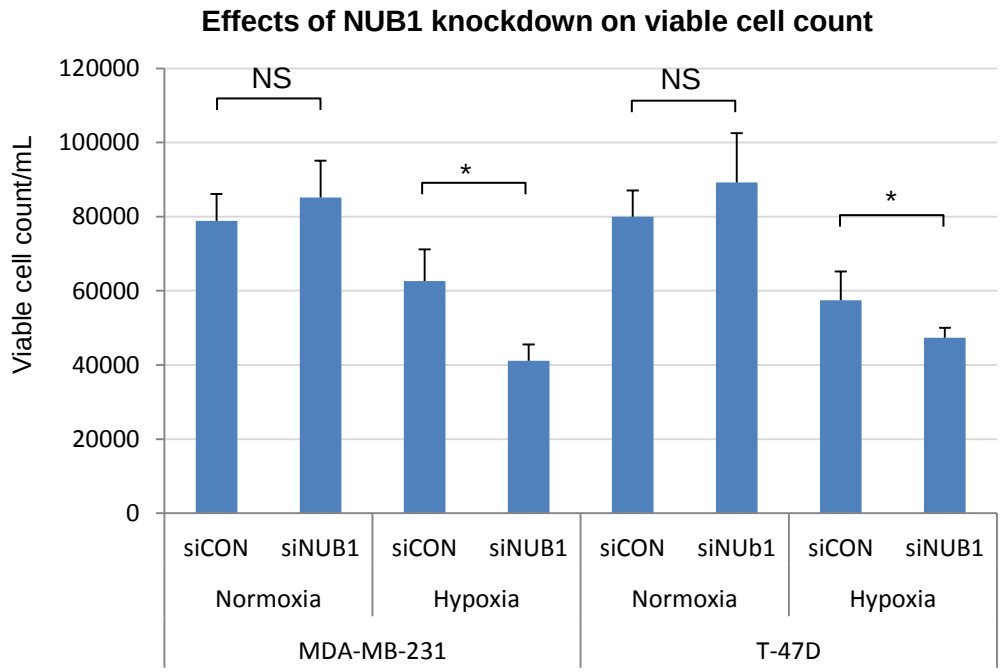


Figure 4. 7 Cancer cell growth in NUB1 knockdown condition. Viable cell number were calculated after siNUB1 transient transfection. Bars, mean+ s.e.m.; n=9; *p<0.05.

4.7 Localisation of AIPL1 and NUB1 proteins in hypoxia and reoxygenation

The subcellular distribution of signaling proteins in proximity to their downstream targets is vital for efficient signal transduction. To examine the distribution of AIPL1 protein and its effect on regulating NUB1 proteins upon hypoxic and reoxygenated conditions, subcellular localisation in MDA-MB-231 was monitored (Fig 4.8).

The AIPL1 protein is predominantly monomerised in normoxia however some dimers present only in the nucleus. In hypoxia and reoxygenation, both monomers and dimers accumulated in the cytoplasm while the nuclear AIPL1 dimers were depleted. We observed more folded nuclear AIPL1 monomers in hypoxia and less in reoxygenation.

NUB1 accumulated in the cytoplasm under normoxia. It migrated to cytoplasm in hypoxia and reoxygenation. After 24 hours of hypoxia, cytoplasmic and nuclear NUB1 levels increased. After 48 hours of hypoxia and after reoxygenation it was progressively accumulated in the nucleus, with little protein in cytoplasm. The phenomenon implies that, in hypoxia and reoxygenation, AIPL1 dimerised in cytoplasm while NUB1 proteins localise into nucleus. We believe dimerised AIPL1 protein is an active forms and it activates and translocates NUB1 into nucleus.

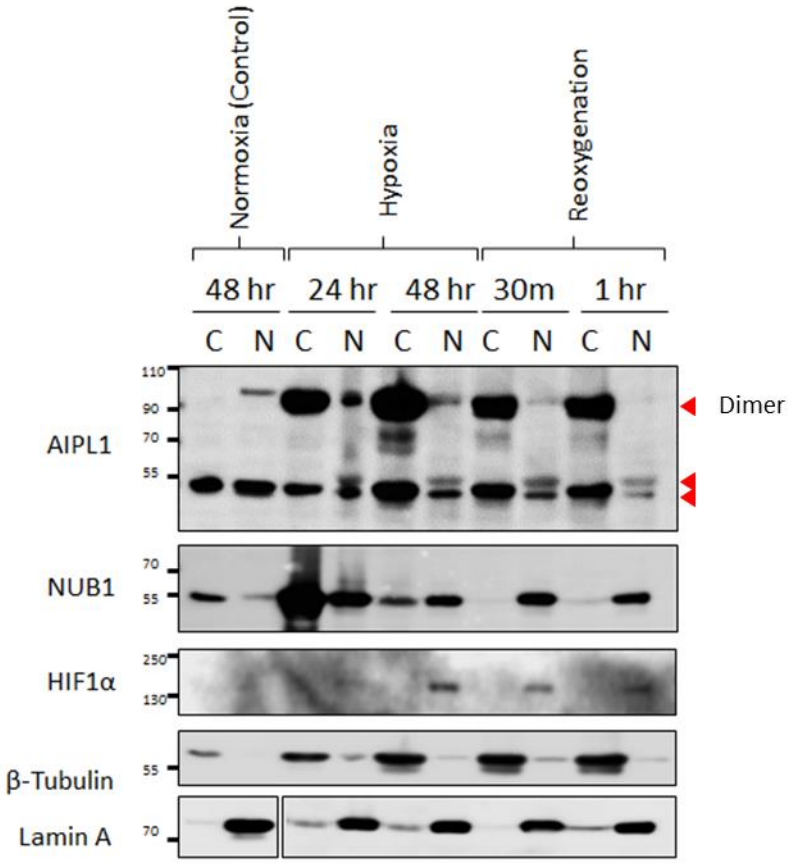


Figure 4. 8 Cytoplasmic AIPL1 dimerisation enhances NUB1 shuttling into the nucleus. Lysates were subjected to subcellular fractionation, cytoplasmic and nuclear fractions were analysed by immunoblotting. β-tubulin and lamin A were used as controls. Endogenous proteins were quantified and values normalised to tubulin or lamin A.

4.8 NUB1 protein regulates cell cycle through neddylation-dependent CUL1

To examine the effects of NUB1 protein in CUL1 neddylation and the overall cell cycle profile of ER- breast cancer cells, the MDA-MB-231 cell line was chosen for immunoblot and cell cycle analysis. p21 and p27 levels were examined to assess the CUL1 activity and its impact upon ubiquitin E3 SCF ligase activity. In normoxia, NUB1 knockdown significantly reduced the neddylated CUL1 levels whilst p27 and p21 were upregulated (p-value=0.02, Fig. 4.9). NUB1 knockdown significantly reduced the free CUL1 (Lane 1 vs. lane 4, Fig 4.9). Neddylation inhibition significantly increases p21 and p27. The precise mechanism for this observation remains to be determined. Two scenarios could be speculated: NUB1 protein regulates CUL1 expression and/or NUB1 protein favourably stabilise CUL1 protein.

For cell cycle analysis, in normoxia and hypoxia, neddylation inhibitor increases accumulation in G_o/G_1 after reoxygenation. The neddylation inhibition also increased the transition from G_0/G_1 to S and G_2/M (Fig. 4.10 and Fig. 4.11). NUB1 knockdown causes accumulation of cells in G_1/G_0 in normoxia and hypoxia but has no effect on reoxygenated cells (Fig. 4.10 and Fig. 4.11).

Under condition of reoxygenation, neddylation inhibition (by MLN4924) slowed down the G1 cell cycle release (Fig. 4.10 and Fig. 4.11). From the result, NUB1 knockdown prolonged G1 arrest (in hypoxia) and caused the down-regulation of neddylated CUL1 protein levels.

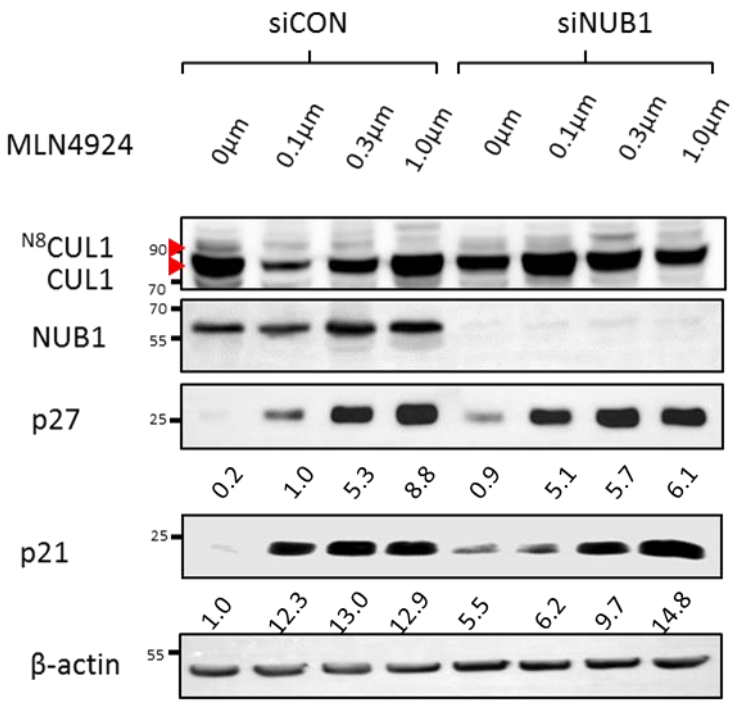


Figure 4. 9 NUB1 silencing enhances neddylation inhibition effects onto p27 (but not p21) protein levels. MDA-MB-231 cell were treated with siRNA and titrated MLN 4924 for 48hr in normoxia. This experiment was performed twice. Densitometry (indicated by numbers beneath the immunoblot) was performed using ImageJ.

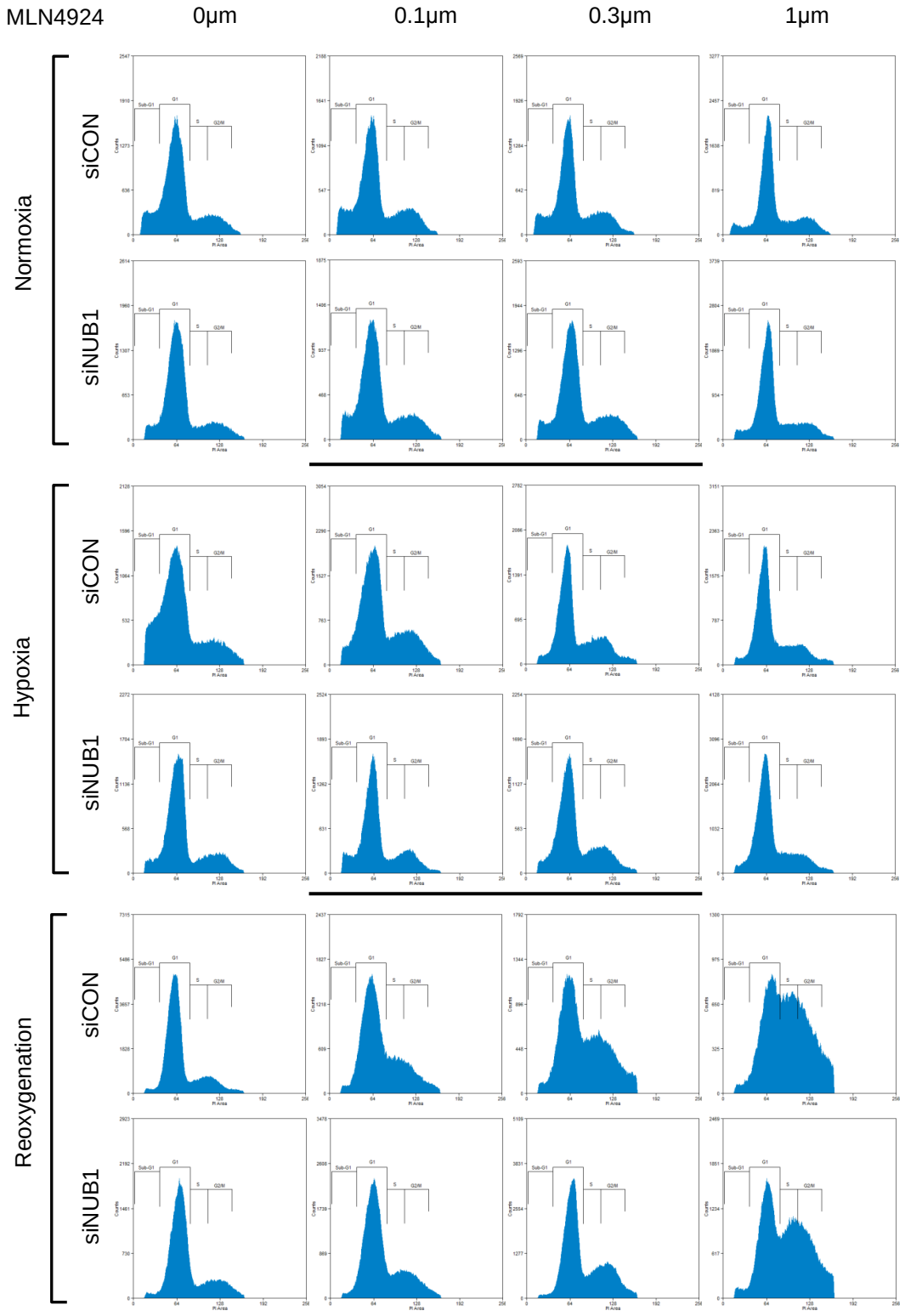


Figure 4. 10 Cell cycle profile of MDA-MB-231. The MDA-MB-231 cells were treated with MLN 4924, a neddylation inhibitor with 24hr in prior. NUB1 gene were transiently knockdown using siRNA and incubated for 48 hours in normoxic and hypoxic environment. For reoxygenation experiment, the cells were further incubated for 12 hours in normoxic environment. Cells were harvested and stained with propidium iodide as proposed. *Abbr*=siCON: control siRNA, siNUB1: NUB1 siRNA.

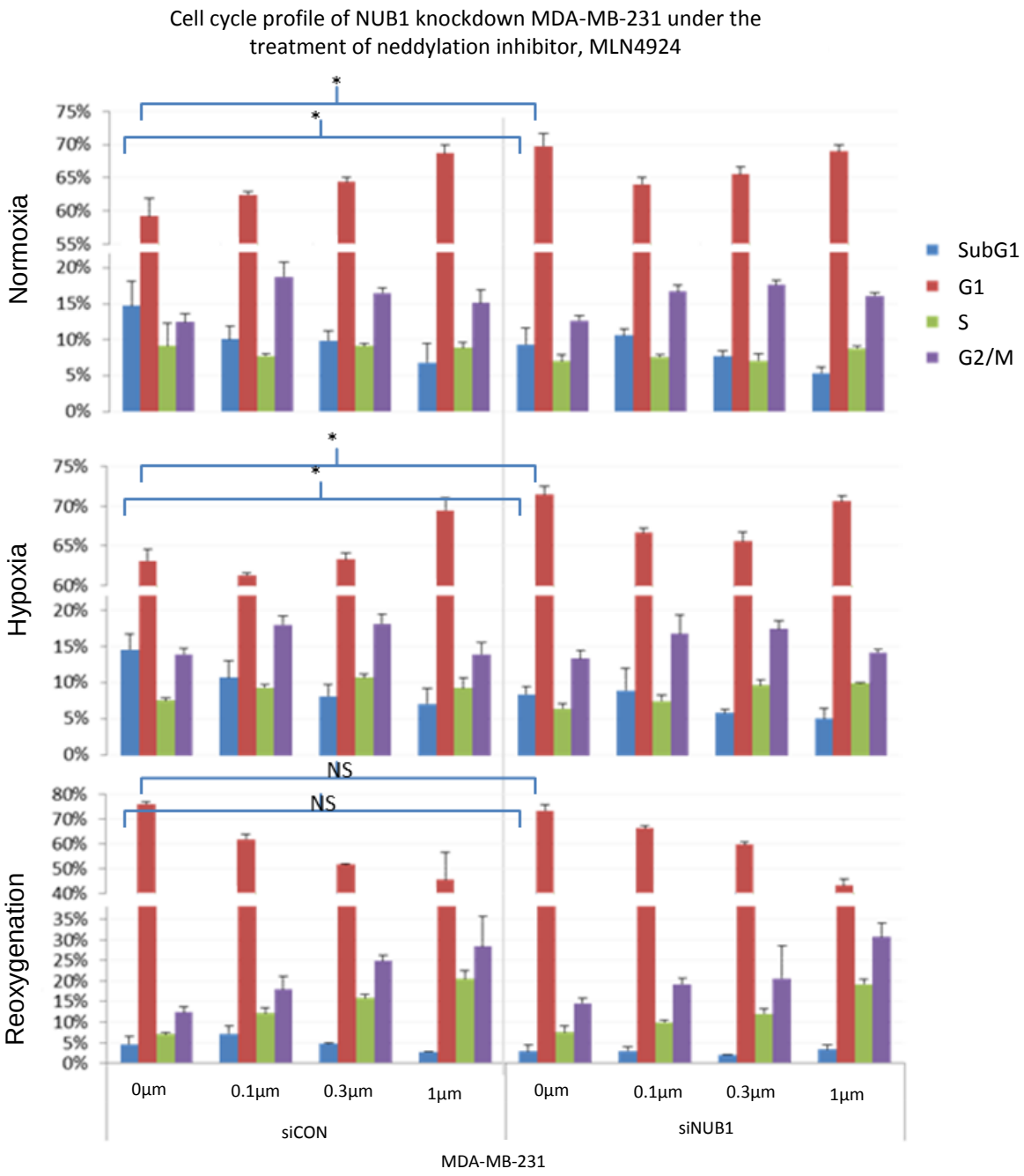


Figure 4. 11 Knockdown of NUB1 and cell cycle analysis. Cell cycle analysis was performed to examine the cell cycle distribution in each group, and quantification. Data represented as mean±s.d; *p<0.05.

4.9 Discussion and Chapter Summary

It was observed that AIPL1 and NUB1 transcripts did not match the protein levels in unstressed condition. This is due to post-transcriptional and/or epigenetic changes which affect the proteins levels. Furthermore, we showed that AIPL1, NUB1 and FAT10 can be located in the cytoplasm and in the nucleus.

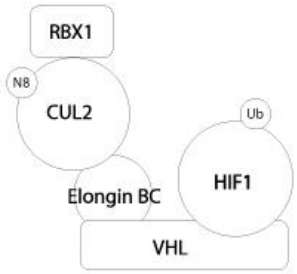
AIPL1 present either as a monomer or dimer, and the proportion between the two forms changes under stresses. Upon hypoxia and reoxygenation, AIPL1 forms dimer and migrated from nucleus to cytoplasm. Reversely, NUB1 localised into the nucleus under the same condition.

In reoxygenation, NUB1 and neddylated CULs were upregulated at protein levels as early as after 5 minutes. They hinted both proteins were responsive to reoxygenation stress. Furthermore, NUB1 knockdown caused MDA-MB-231 cell cycle arrest with lower sub-G1. There was a lack of S-phase transition. The results are consistent with a previous study describing that NUB1 overexpression promotes S-phase transition in A549 renal cells (Hosono *et al.*, 2010). The result also indicated that depleted NUB1 protein increased p27 and p21 through neddylation-dependent CUL1 and subsequent inhibition of ubiquitin-mediated degradation.

Chapter 5
NUB1 protein destabilise p21 and p27 proteins through VHL-dependent CUL2-based E3 ligase

5.1 Rationale of the study

We performed cell cycle analysis on MDA-MB-231 breast cancer cells in last chapter and found that NUB1 silencing decreases the number of cells in subG1, increases the number of cells inn G_0/G_1 and upregulated p27 and p21 in normoxia and hypoxia. Neddylation inhibitor prevents CUL1 neddylation and deactivates the ubiquitin E3 ligase which results in further up-regulation of p27 and p21. This chapter works on the basis that there might be an alternative pathway that confers p21 and p27 up-regulation. A previous study demonstrated that VHL stabilise and increases p21 and p27 levels and protects from apoptosis (Schoenfeld *et al.*, 2000): the authors suggests that one possible mechanism could VHL consumption of NEDD8 and RBX1 proteins which leave them unavailable to facilitate p27 and possibly p21 degradation (Fig 5.2) (Schoenfeld *et al.*, 2000): RBX1 could have this effect trough the CUL2 and Ubiquitin E3 ligases pathway as well. In the ubiquitin E3 ligase, CUL2 assembles with RING protein (RBX1), Elongin B/C proteins as adapter proteins and VHL substrate recognition receptors (Zimmerman *et al.*, 2010; Sarikas *et al.*, 2011).



Scaffold	Adaptor	Receptor	Ring box	Substrates
Cul-1	Skp1	Skp2	Rbx1*	p21, p27, p73, p1 30, Cydin A/ D
Cul-2	Elongin BC	VHL	Rbx1*	HIF1α

Figure 5. 1 Ubiquitin E3 ligases and their substrates. * shared protein as a part of two different complexes.

VHL down-regulates the expression of hypoxia-inducible genes such as vascular endothelial growth factor (VEGF), glucose transporter, GLUT1 and platelet derived growth factor (PDGF) B chain (Iliopoulos *et al.*, 1996), *via* degradation of hypoxia-inducible factor (HIF) alpha subunits (Maxwell *et al.*, 1999; Ohh *et al.*, 2000). The focus of this ongoing study is to examine the activity of NUB1 protein onto the CUL2-based ubiquitin E3 ligase and the cyclin-dependent kinase (CDK) inhibitors, p21 and p27, during hypoxia and reoxygenation. This will provide a rationale on how both AIPL1 and NUB1 work in relation to VHL-mediated cell cycle regulation in cancers, through p21 and p27.

VHL is a known tumor suppressor gene that blocks the development and progression of renal cell carcinogenesis. Individuals with germline mutations in the VHL gene, which lead to its inactivation, are predisposed to VHL disease including renal cell carcinoma (RCC) (Latif *et al.*, 1993; Linehan *et al.*, 1995). Loss of VHL function appears to be an early event in RCC (Lubensky *et al.*, 1996). Furthermore, reintroduction of wild-type VHL expression into VHL-negative renal cells abrogates their cancer causing nature (Iliopoulos *et al.*, 1996; Schoenfeld *et al.*, 1998).

It remains open on how expression of VHL mediates the stabilisation of p27 and p21. VHL protein, which is associated with CUL2-based ubiquitin E3 ligase activities, can block the proteasomal degradation of p21 and p27. VHL protein could sequester ‘sharing’ E3 ligase members such as RBX1 which also facilitate p27 (and perhaps p21) degradation through CUL1-based E3 ligase (Morimoto et al., 2000). Therefore, the stabilisation of these CDK inhibitors may result.

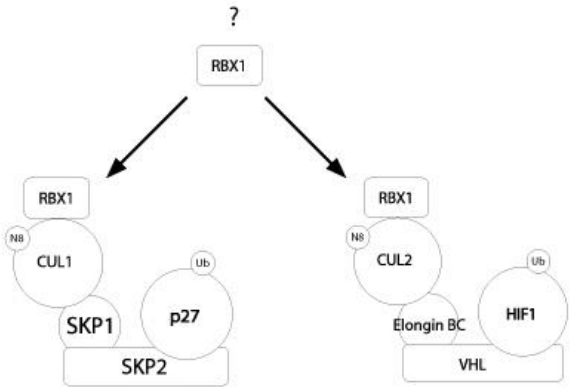


Figure 5. 2 Schoenfeld's first speculation on how VHL regulates p27 and p21.

Secondly, It was also speculated that VHL may increase the half-lives of p21 and p27 mRNAs, perhaps through the degradation of factors that destabilize mRNA, in a manner opposite to HIF1α (Schoenfeld *et al.*, 2000). p21 and p27 stabilisation may therefore occur at the post-transcriptional level. As p21 and p27 cause G_o/G_1 cell cycle arrest, more upregulated p21 and p27 levels in VHL-negative RCC4 might explain why RCC4plusVHL cells differentiate more rapidly.

p21 and p27 belong to the cyclin-dependent kinase (CDK) inhibitors that mediate cell cycle arrest. The roles of the cell cycle inhibitors p21 and p27 are regulated by their cellular localisation. p21 and p27 are tumor suppressors within the nucleus and become oncogenic when localised in the cytoplasm. Therefore, p21 and p27 play a pleomorphic role in cell cycle regulation, its role as an oncogene or a tumour suppressor may be a function of setting.

a. p21 is a tumour suppressor (Katayose *et al.*, 1995; Yang *et al.*, 1995). However, it exerts anti-apoptotic functions when it is localised in the cytoplasm. The binding of p21 to mitogen-activated protein kinase (MAPK) kinase kinase 5 (MAP3K5) in the cytoplasm inhibits the MAPK cascade (Asada *et al.*, 1999; Huang *et al.*, 2003).

Phosphorylation of p21 on T145 by Protein Kinase B (AKT) induces nuclear export of p21 leading to enhanced cell growth (Rossig *et al.*, 2001; Zhou *et al.*, 2001; Li *et al.*, 2002). Cytoplasmic p21 was oncogenic in breast cancer and metastatic *in vivo* (Cheng *et al.*, 2010). Cytoplasmic localisation of p21 is a poor prognostic marker for breast cancer (Winters *et al.*, 2003; Xia *et al.*, 2004), and is involved in mediating resistance to anticancer drugs (Zhang *et al.*, 1995; Ruan *et al.*, 1999; Koster *et al.*, 2010). The cytoplasmic localisation of p21 also resulted in a poor response to tamoxifen (Perez-Tenorio *et al.*, 2006).

b. Cytoplasmic p27 protein is oncogenic as the reduction of cytosolic p27 inhibits cancer cell motility, survival, and tumorigenicity (Wu et al., . T157 phosphorylation by AKT blocks the nuclear import of p27 (Liang *et al.*, 2002; Shin *et al.*, 2002; Viglietto *et al.*, 2002). Whereas S10 phosphorylation induces p27 cytoplasmic localisation and stabilisation (Rodier *et al.*, 2001). The cytoplasmic localisation of p27 is a poor prognostic factor in cancers, including breast (Liang *et al.*, 2002), hepatocellular (Nan *et al.*, 2004), colon (Ogino *et al.*, 2009) and ovarian cancer (Rosen *et al.*, 2005), and Barrett's carcinoma (Singh *et al.*, 1998).

This chapter examines the role of NUB1 in regulating the CUL2-based ubiquitin E3 ligase during hypoxic stress. And the involvement of VHL protein in the cascade with regards to tumour development is examined.

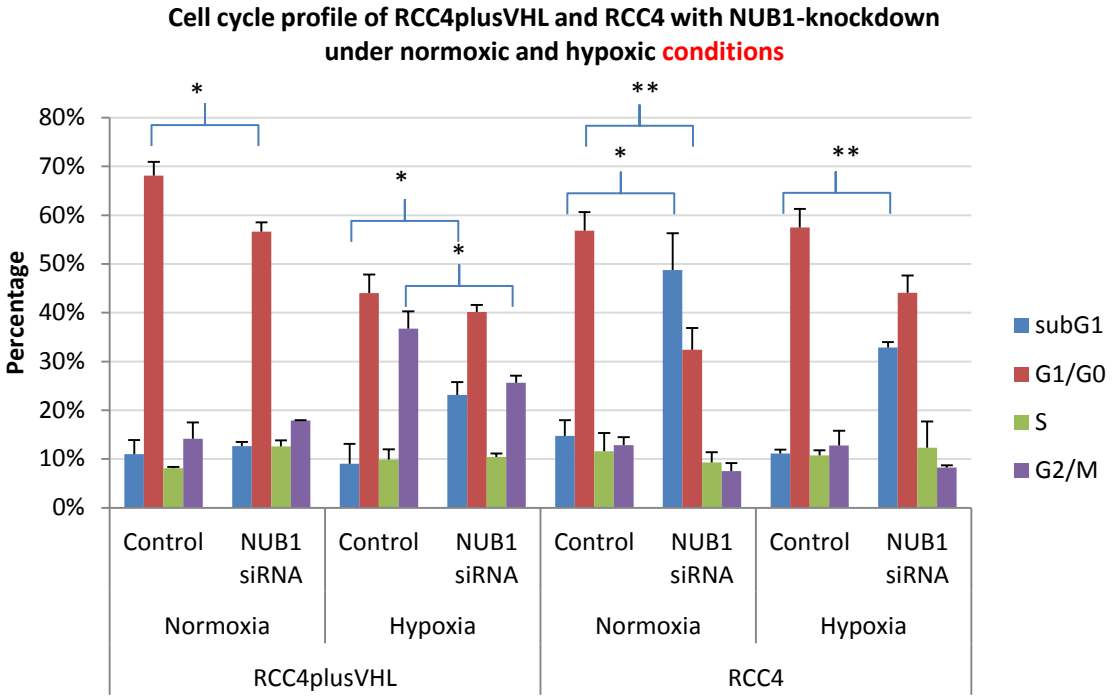
5.2 NUB1 protects cells from hypoxia-mediated cell cycle arrest and apoptosis through VHL

In 2000, Schoenfeld *et al.* found that VHL expression protects UV-treated cells from apoptosis (Schoenfeld *et al.*, 1998). The apoptosis resulted from the perturbation of cell cycle checkpoints in regulating the repair of DNA damage (Schoenfeld *et al.*, 1998). To examine whether chronic severe hypoxia- and reoxygenation-mediated stress exerts the same effect onto these CDK inhibitors (p27 and p21) in renal cancer carcinoma cell line, we explore the effects of NUB1 and VHL protein on the cell cycle regulatory proteins by immunoblot.

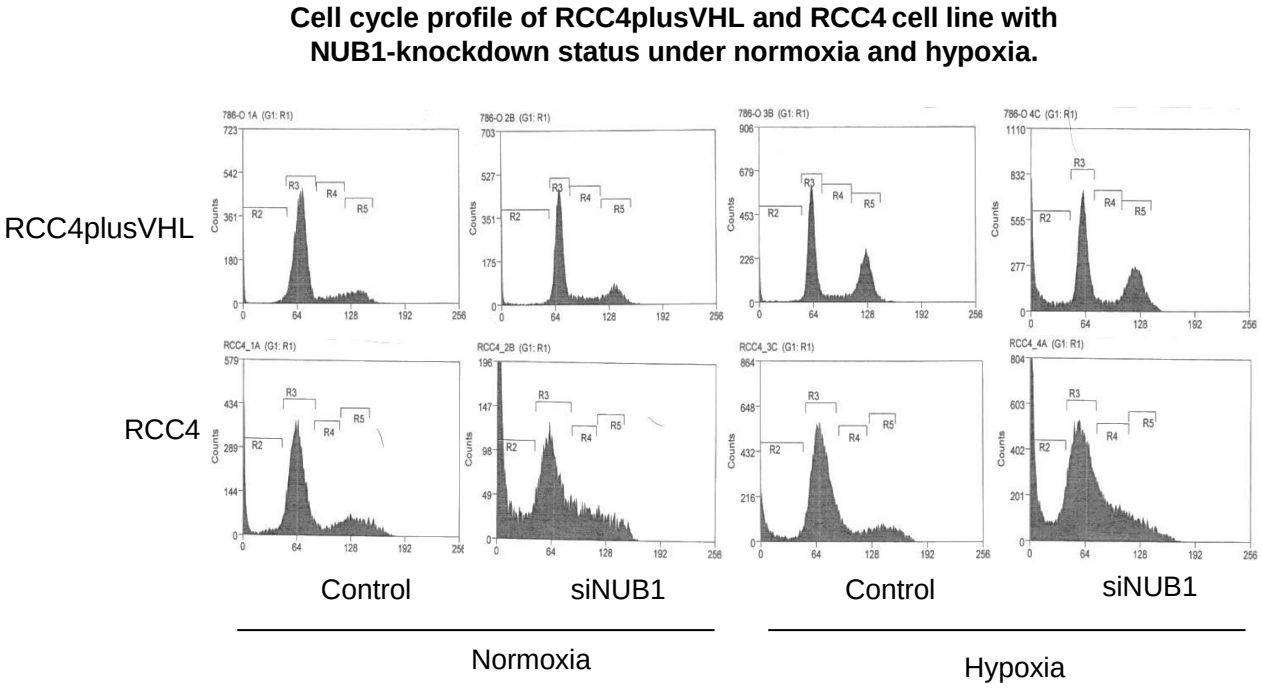
In the RCC4plusVHL cells, NUB1 silencing in hypoxia caused a decrease in G2/M (25.7%±2.5 vs 36.2±3.1; $p<0.001$) and increased sub-G1 (20.2%±0.7 vs. 9.0%±2.16; $p<0.01$) (Fig 5.1a). To differentiate two major type of cell death: apoptotic and necrotic cell death, apoptotic marker, cleaved PARP was observed at hypoxic condition in RCC4plusVHL. Increased sub-G1 with NUB1 knockdown in hypoxia was due to the apoptosis for the presence of cleaved PARP (Fig 5.3). In hypoxia, VHL was reduced (immunoblot) but HIF1α protein was undetected. NUB1 silencing drove the cells toward apoptosis and no apoptosis marker was detected in normoxia. Therefore, NUB1 could protect cells from apoptosis in hypoxia.

In the RCC4 cell cycle, a significantly higher percentage of sub-G1 cells were detected in NUB1 knockdown cells, as compared to non-targeting controls (14.71%±3.21 vs. 48.73%±7.56, $p<0.05$ in normoxia; 11.12%±3.78 vs. 32.89%±2.11, $p<0.05$ in hypoxia). For RCC4plusVHL cells, increased cell death was observed in the hypoxic and NUB1 siRNA treated group. p21 protein in RCCplusVHL remain undetected while increased in NUB1-knockdown in RCC4 cells. This cell cycle analysis underlined a role of NUB1 in protecting cells from cell death under both hypoxia and normoxia. This protective role of NUB1 is independent of VHL.

A.


Cell cycle profile of RCC4plusVHL and RCC4 with NUB1-knockdown under normoxic and hypoxic conditions
Percentage
80%
70%
60%
50%
40%
30%
20%
10%
0%
subG1
G1/G0
S
G2/M
Control
NUB1 siRNA
Normoxia
Hypoxia
RCC4plusVHL
RCC4

B.


Cell cycle profile of RCC4plusVHL and RCC4 cell line with NUB1-knockdown status under normoxia and hypoxia.
RCC4plusVHL
RCC4
Control
siNUB1
Normoxia
Hypoxia

C.

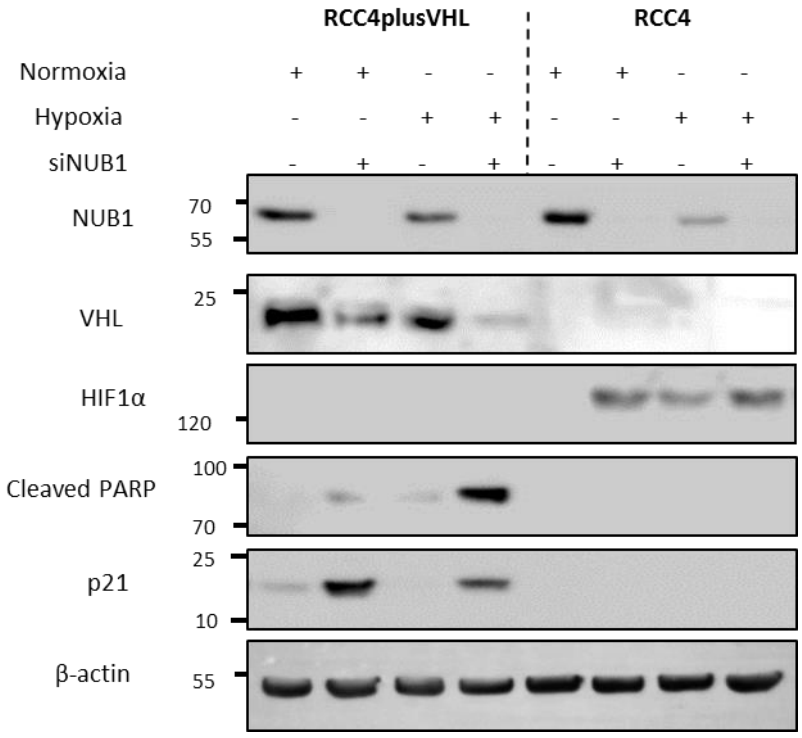
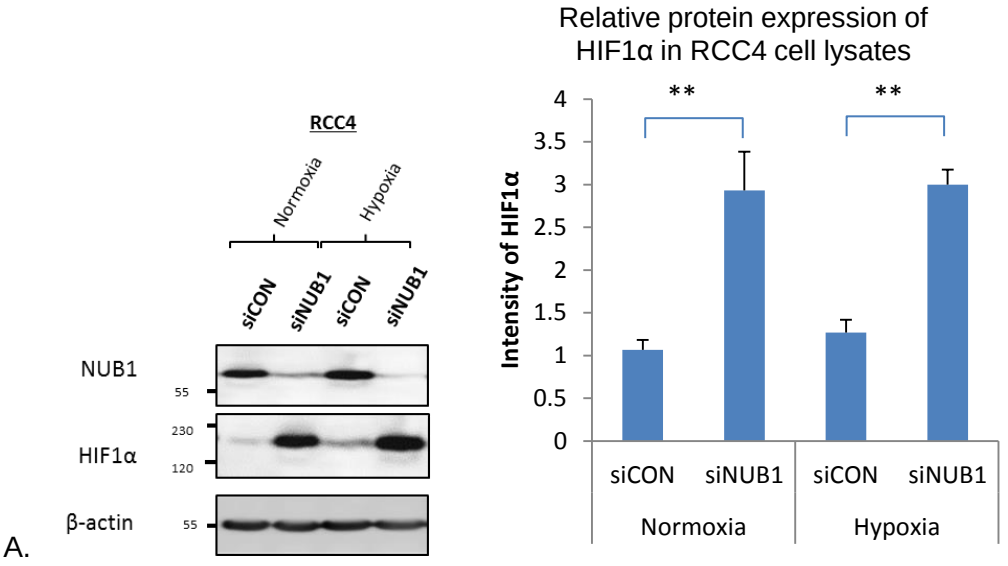


Figure 5. 3 Effect of NUB1 knowckdown on the cell cycle of RCC4plusVHL and control cells under normoxic and hypoxic conditions. Both cell line were transfected with siNUB1 and incubated for 48 hours. A. The cells were harvested and stained with propidium iodide and subjected to FACs analysis. B. Cell cycle profile of each experiment group. Data (A) shown are means of 3 independent experiments with error bars representing standard deviation. C. Immunoblotting of p21 (G1/G0) marker and apoptosis marker, PARP under the different experimental conditons. Each bar represents mean ± SEM for each cell line (n=9). * significant at $p<0.05$; ** significant at $p<0.005$.

5.3 Up-regulation of HIF1α and VHL protein levels due to NUB1 knockdown

CUL2 as part of the ubiquitin E3 ligase regulates ubiquitination and degradation of HIF1α. To test whether NUB1 influences the activity of the CUL2-based complexes, HIF1α and VHL levels were measured in a renal cell carcinoma cell line. The level of HIF1α in normoxia in the NUB1 knockdown RCC4 group was almost 3-fold greater than that found in the control siRNA group (0.73±0.21 vs. 2.1±0.36 fold, P<0.001). The VHL level dropped following NUB1 knockdown in RCC4plusVHL cells (1.06±0.06 vs. 0.32±0.10; p<0.001) (Fig 5.4). Therefore, it was found that stabilised HIF1α in NUB1 knockdown cells is likely due to the down-regulation of VHL and possibly ubiquitin E3 ligase activity.



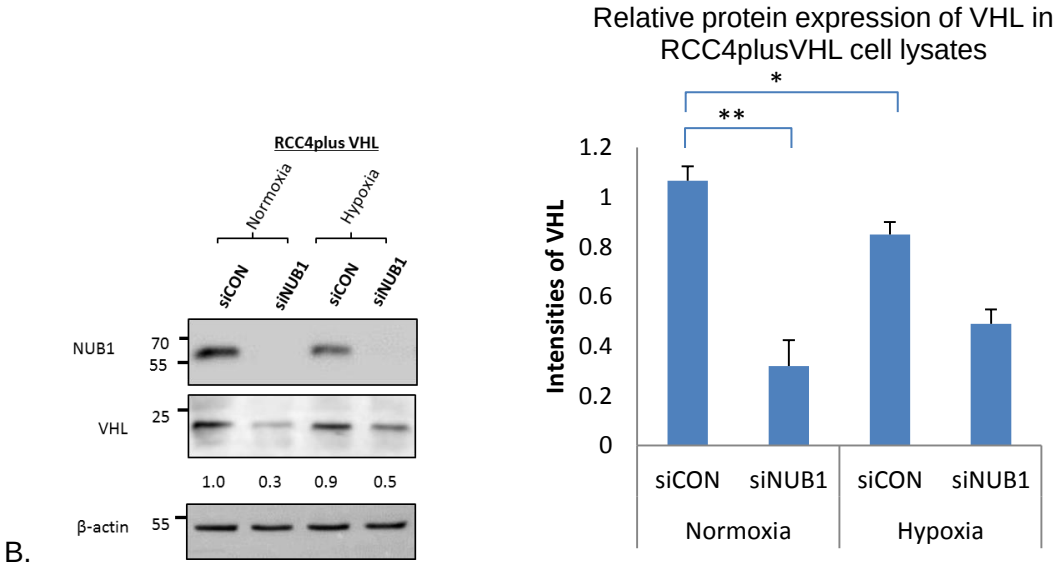


Figure 5. 4 NUB1 knockdown up-regulates HIF1α (A) and down-regulates VHL (B). RCC4plusVHL and RCC4 cells were transfected with 100pmol siRNA as indicated. The amount of HIF-1α was calculated as the difference between siCon and siNUB1 groups. Bars represent the means ± S.D. of 3 independent biological replicates. * significant at $p<0.05$; ** significant at $p<0.005$.

5.4 Cell cycle analysis with NUB1 knockdown status under severe hypoxic conditions.

To examine whether the roles of NUB1 were VHL-dependent, cell cycle profiles of cells exposed to normoxic or hypoxic conditions were examined (Figure 5.5). We use renal cancer cell line, RCC4 in the experiment for they are established cell line with VHL and null-VHL within the cells (Maxwell *et al.*, 1999). Expression of NUB1 was reduced in RCC4 ($VHL^{-/-}$) cells by siRNA, and each treatment was performed in triplicate. In RCC4 cells, a greater percentage of sub-G1 cells were detected in NUB1 siRNA treated samples under hypoxia, as compared to non-targeting controls. Increased cell death was observed in the hypoxic and NUB1 siRNA treated group, suggesting a role for NUB1 in protecting cells from hypoxia induced replication stress. HIF1α was upregulated in NUB1 knockdown cells. This cell cycle analysis has highlighted a potential role for the NUB1 in protecting cells undergoing cell death responses under severe hypoxic conditions.

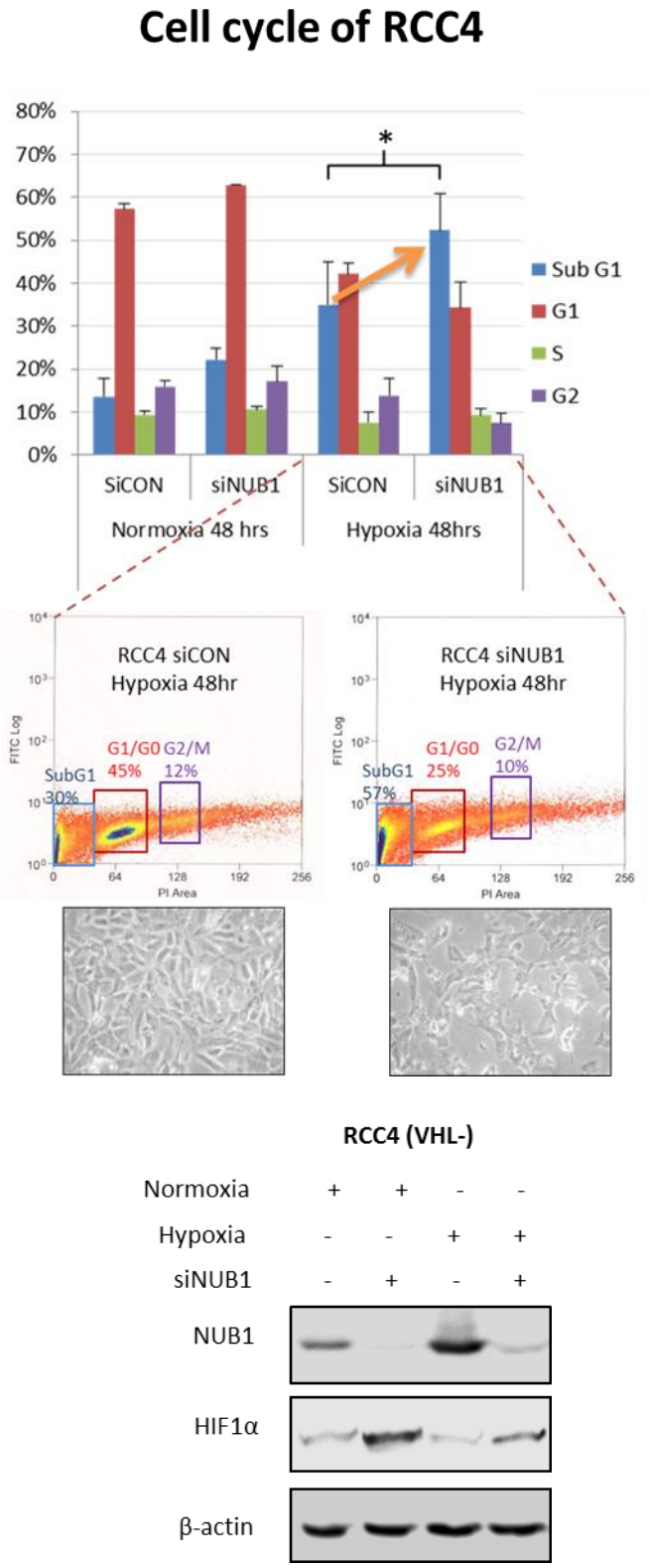


Figure 5. 5 Cell cycle analysis on the NUB1 knowckdown effect in RCC4 cells under normoxic and hypoxic conditions. Cell line were transfected with siNUB1 and incubated for 48 hours. NUB1 knockdown of hypoxic RCC4 showed significant cell death compared to the control. HIF1α was up-regulated in NUB1 knockdown cells. Data shown are means of 3 independent experiments with error bars representing standard deviation. * significant at $p<0.05$; ** significant at $p<0.005$.

5.5 Stabilisation of p27 and HIF1α by NUB1 depletion are independent of VHL

To test Schoenfeld's speculation whether VHL could sequester both RBX1 and SKP1, resulting in reduced engagement of these proteins in CUL1 based degradation complexes, thereby stabilising p21 and p27 (Schoenfeld *et al.*, 2000), we examined both CUL1-based and CUL2-based ubiquitin E3 ligases in RCC4plusVHL and RCC4 cells (Fig. 5.6). It was found that depleted NUB1 upregulates p27 and p21 proteins in RCC4 cells and RCC4plusVHL cells. The cell cycle arrest is NUB1- and VHL-dependent. The amount of p27 was greater in VHL-null cells in normoxia. These data hinted that VHL could occupy the RBX1 which facilitate p27 degradation.

To characterise CUL2 neddylation in the context of NUB1, we examined a representative protein, HIF1α, to test CUL2 activity in normoxia, hypoxia and reoxygenation. We observed that NUB1 knockdown stabilised p27 and p21 protein in both cell line and only HIF1α in RCC4. The result hinted that p27 and p21 stabilisation through NUB1 depletion is independent of RBX1 factor as per suggested by Schoefeld's idea.

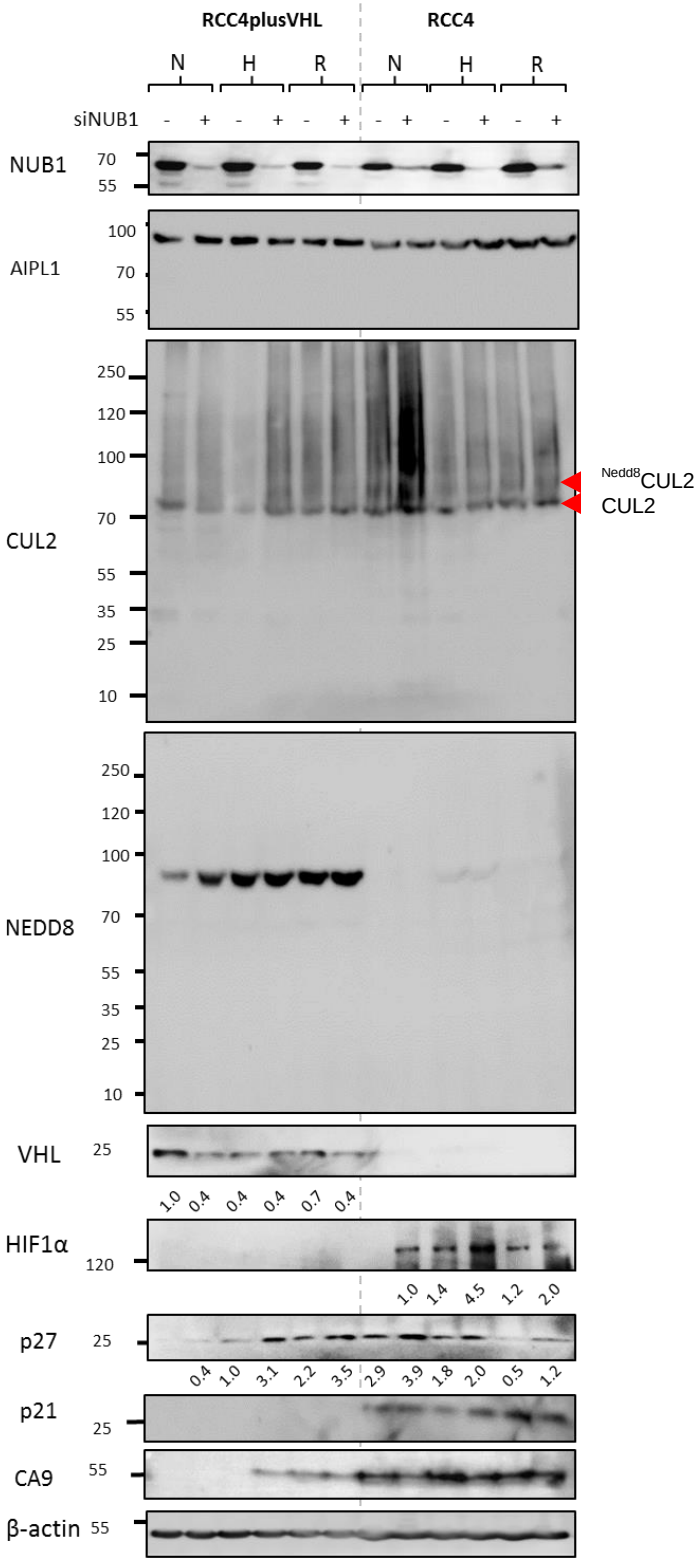


Figure 5. 6 Depletion of NUB1 upregulated HIF1α and p27 proteins. The lysates from RCC4plusVHL and RCC4 cells were transfected with siNUB1 and underwent normoxia, hypoxia for 48 hr and reoxygenated 24 hours. The cell lysates were analysed by Western blotting using antibodies, and by the densitometric analysis. N=normoxia, H: hypoxia, R: reoxygenation. Densitometry was quantified using ImageJ and the figure indicated the relative densities to a band equal to 1.0.

5.6 HIF1α is neddylated and FAT10ylated

We observed up-regulation of HIF1α even when VHL is absent and during NUB1.siRNA treatment. It was thought that HIF1α is stabilised through non-ubiquitin regulated mechanism. To determine whether HIF1α is neddylated, endogenous HIF1α was immunoprecipitated from MDA-MB-231 cell lysate. We checked HIF-1α expression and activity in MDA-MB-231 cells incubated in hypoxia for 48 hours and 1-hr reoxygenation. Endogenous HIF1α was immunoprecipitated from 500μg MDA-MB-231 cell lysate. We found HIF1α was both neddylated and FAT10ylated (Fig 5.7).

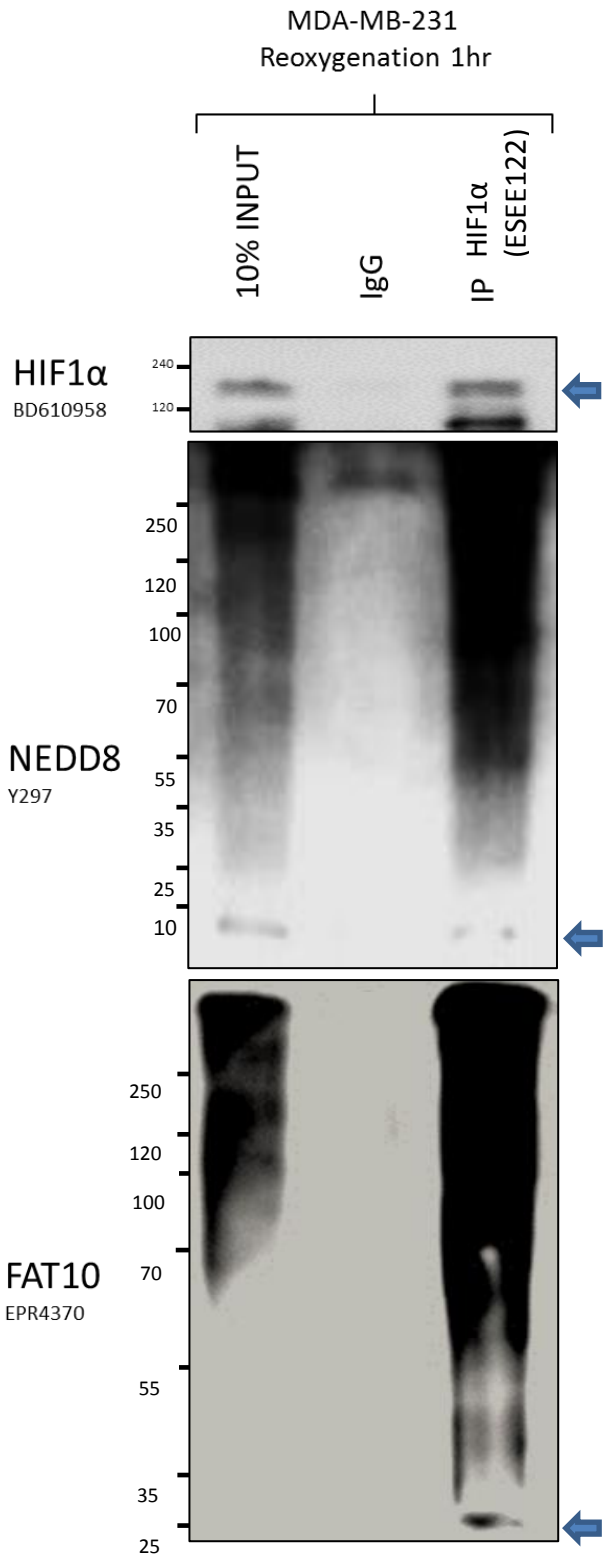


Figure 5. 7 NEDD8 and FAT10 signals detected in endogenous HIF1α. Cells lysate from MDA-MB-231 cells were immunoprecipitated with control IgG or HIF1α antibodies, and subsequently immunoblotted with the indicated antibodies. Input levels of HIF1α protein are as shown.

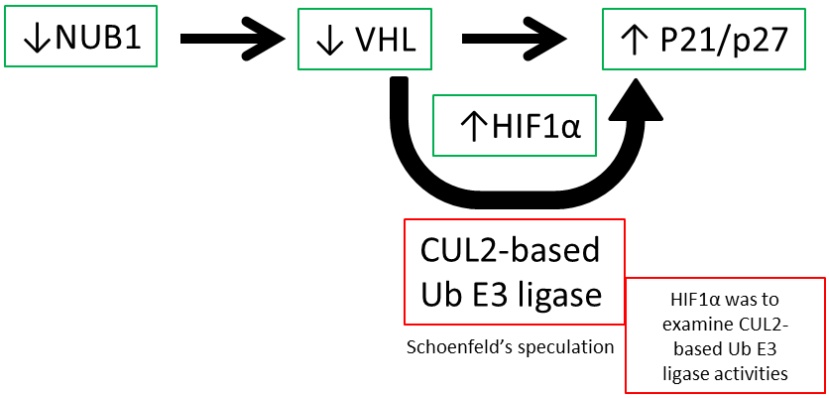
5.7 Discussion and Chapter Summary

As we examine the effect of VHL on RCC4 cells, NUB1 was found to protect RCC4 renal cell carcinoma cells from apoptosis in the presence of VHL especially in chronic severe hypoxia. In absence of VHL, NUB1 is still protecting cells from death through non-apoptotic pathways, as no cleaved-PARP was detected when cell death occurs in absence of NUB1. In the presence of VHL, NUB1 knockdown increased the number of cells in G_0/G_1 in hypoxia. While in absence of VHL, NUB1 silencing caused increase in G_0/G_1 fraction both in hypoxia and normoxia.

It was found that depleted NUB1 down-regulated VHL. In null-VHL RCC4, upregulated HIF1α, p21 and p27 were observed in the same condition. VHL caused a subset of neddylated CUL2 to degrade and increased the levels of total NEDD8. In RCC4plusVHL, the stabilisation of HIF1α did not happen, but p27 and p21 did under hypoxia. In RCC4-null cells, the other mechanism of NUB1 regulating p27/p21 levels remains open.

NUB1 caused a subset of neddylated CUL2 to degrade whilst the other neddylated CUL2-based ubiquitin E3 ligase remain in complex with RBX1. We worked on the hypothesis that CUL2-based ubiquitin E3 ligase competitively bind to RBX1, resulting in less engagement of CUL1-based ubiquitin E3 ligases. This could therefore lead to increased p27 and p21 degradation.

A)



B)

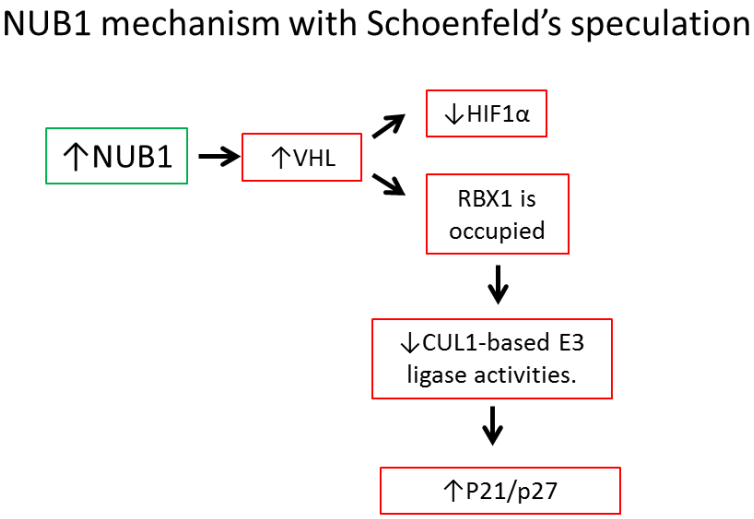


Figure 5. 8 Hypothesis pipeline of the chapter 5. A) The flow chart which explains our observations on reduced VHL would cause stabilisation of HIF1α, p21 and p27. Our finding of depleted NUB1 caused the decreased VHL and upregulated HIF1α. B) NUB1 and VHL may act in the same pathway, VHL caused down-regulation of HIF1α and up-regulation of p21 and p27.

Chapter 6
Tissue microarray analysis of NUB1 in primary Breast Cancer shows cytoplasmic localisation is associated with poorer prognosis

6.1 Rationale of study

The previous chapters have examined the expression and localisation of AIPL1 and NUB1 in ER- subtype breast cancer cell lines. In hypoxia, AIPL1 was found to be predominantly dimerised in the cytoplasm, whereas NUB1 remained mainly in the nucleus. Previous studies have shown that a nuclear localisation signal (NLS) near the C terminus of NUB1 responsible for this nuclear localisation (Kito *et al.*, 2001; van der Spuy *et al.*, 2002; van der Spuy *et al.*, 2003). AIPL1 was found to negatively regulate the nuclear translocation of NUB1.

Subcellular localisation is essential for NUB1 protein to regulate the cell cycle (Kito *et al.*, 2001). The regulation of NUB1 protein trafficking relies on the information that is encoded within its NLS. Subcellular localisation of NUB1 determines the access of proteins to interacting partners and the FAT10 and NEDD8 post-translational modification machinery and enables the conjugated proteins to be modified by the UPS. Generally, aberrantly localised proteins have been linked to human diseases as diverse as Alzheimer's disease, kidney stones and cancer. It is therefore myrationale to examine the mechanisms that regulate subcellular protein localisation implicated in the pathogenesis of human cancer. So we employed immunohistochemistry techniques to compare the subcellular localisation of NUB1 in patients' breast cancer tissue.

Tissue microarray (TMA) is a technique that allows for the immunophenotypical characterisation of hundreds of samples simultaneously (Kononen *et al.*, 1998). More than 1000 different tissue samples can be combined on a single microscope slide to be simultaneously characterised by *in situ* analysis. However, this depends on the needle diameter of the microarray device (Takikita *et al.*, 2007). Virtually all research involving *in situ* tissue studies can be carried out on a TMA format.

In TMA, the specimens with clinical data make the technique a very powerful validation tool to complement the results obtained from the genomic data. The technology reduces the laborious, time-consuming, and expensive conventional immunophenotypical characterisations on single slides. It also diminishes the technical experimental variability in biomarker identification, allowing the analysis of a large number of samples at the same time. TMAs have been constructed from paraffin-embedded tissue cell line or cell blocks representative of the conventional tumour specimens. The breast cancer TMAs has high concordance for common biomarkers as well as reproducible prognostic associations (Kononen *et al.*, 1998). Expression of the TMAs could correspond to the whole section. The protein expression can be analysed retrospectively with the benefit of long-term follow up information.

Besides, the effect of subcellular localisation of NUB1 protein in benign and malignant human cancer has been poorly studied. NUB1 and its splicing variant, NUB1L are found in multiple tissues. Their distributions in cancer cells have been mapped by qPCR techniques, and western blots. However, the expression level of NUB1 has not yet been compared in its relation to cancer progression.

To further elucidate the role of NUB1 in breast cancers, NUB1 expression patterns were correlated with survival outcome and clinico-pathological parameters in a large cohort of primary breast tissues. This study performed immunohistochemistry (IHC) on approximately 125 human primary breast tissues to determine the subcellular localisation of NUB1 in breast cancer and to provide information for future studies on cancer biology.

Classification of breast cancer

There are two main molecular classifications of breast cancer which are of prognostic value. The oldest classify the tumour into Oestrogen Receptor (ER) positive or negative groups. The most update further subdivides these two groups into a total of five subtypes. The ER positive, one within the two groups classification, and the Luminal A within the active group have the best outcome. The joint triple negative (Basal-like and Normal breast like) has the worst outcome within the five groups classification.

Subtypes	Features
Luminal A	ER and PgR positive but Her2 negative; Low proliferation index
Lumina B	ER positive, Her-2 positive, PgR positive or negative; ER positive, Her-2 negative, PgR negative; High proliferation index
Her-2 non luminal	Her-2 positive but ER and PgR (Progesteron Receptor) negative
Basal-like (triple negative)	ER, PgR and Her2 negative; Positive for CK5 and EGFR
Normal breast-like (triple negative)	ER, PgR and Her2 negative; Negative for CK5 and EGFR

Table 3. 9 Classification of breast cancer and the key features of the subtypes (Yersal and Barutca, 2014).

6.2 Validation of NUB1 antibody on cancer cells

Clinical implementation of NUB1 as a biomarker depends on the reliable and validated detection method for the NUB1 protein. As the NUB1 antibody (clone 4H2) was not reported in any previous publication, immunohistochemical validation was performed to examine its binding to the antigen in breast cancer tissue specimens. Two independent pathologist-based evaluations approved the representative staining patterns for antibody in the specimens.

A clear difference of NUB1 immunostaining was observed between the endogenous NUB1 of RCC4plusVHL cells (Fig 6.1) and their corresponding NUB1-knockdown cells. There was no staining in the negative control. To have a technical negative control that helps to avoid false positive, saline was used to replace primary antibody. In another sample, CD34 primary antibody was used as a positive control to make sure the staining protocol was performed correctly.

To ensure the NUB1 protein retains the antigenicity in archival tissues, we stained on aged tonsils. The tonsil was also used as a multi-tissue control block that showed a subset of cells were stained with NUB1 antibody. Although the number of sample in this validation remained small, no systematic loss of antigenicity was observed.

The validation of the antibody for use in western blotting was achieved in a similar way. Targeting the NUB1 by siRNA resulted in the loss of an immunoreactive band at approximately 79 kDa. No other bands were seen on the western blot. Therefore, the 4H2 clone NUB1 antibody is specific towards NUB1 proteins.

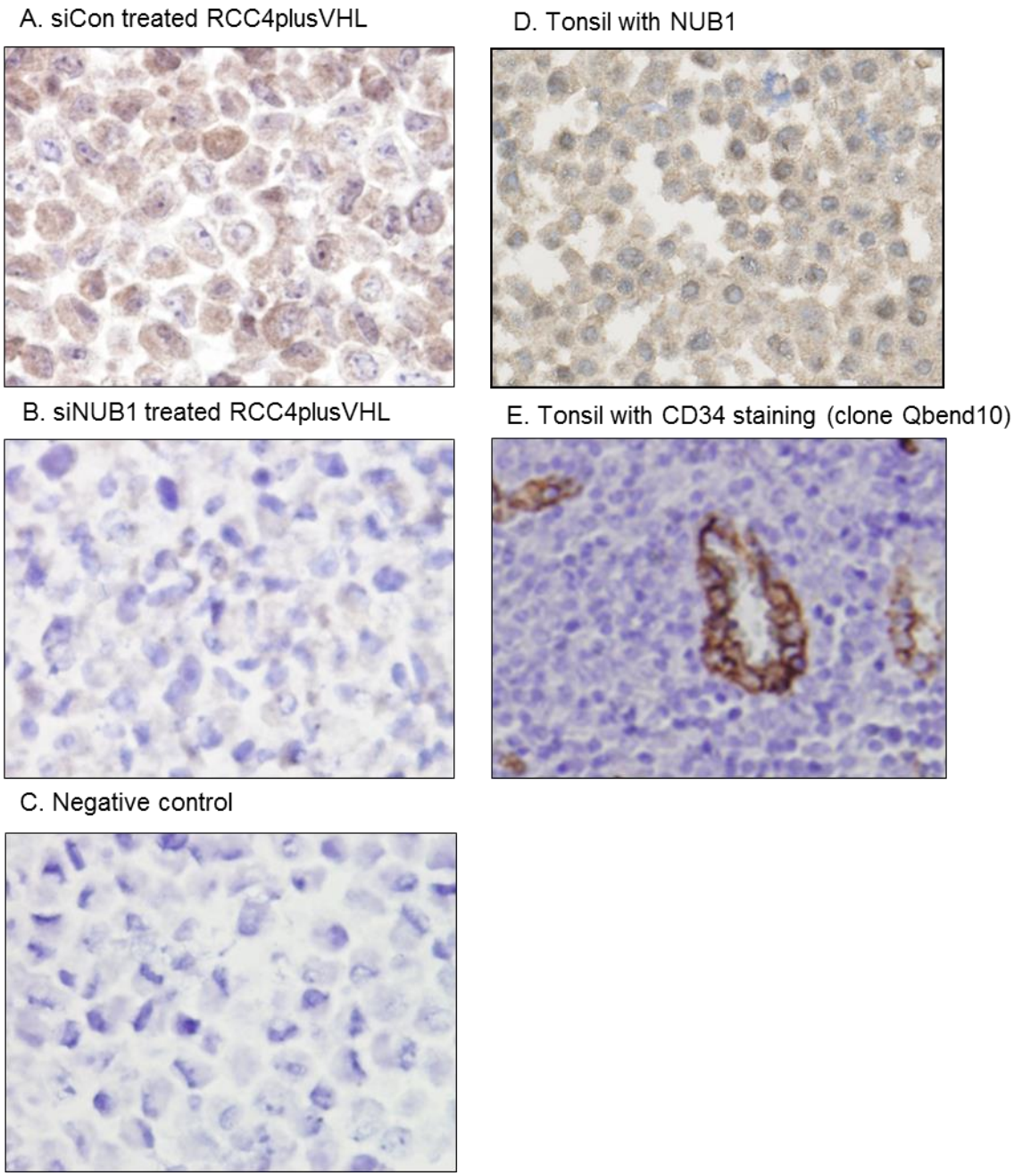


Figure 6. 1 Immunostaining of NUB1 using monoclonal mouse antibody (4H2) (1:20) dilution on RCC4plusVHL cells counterstain with hematoxylin. NUB1 was visualised with DAB (Brown), 40X magnification. A. Endogenous NUB1 treated with siCON. B. RCC4plusVHL treated with siNUB1. C. PBS in replacement of primary antibody was used as technical negative control. D. Tonsil E. Tonsil with CD34 staining serves a positive control. All images were at the magnificantion of 20X.

6.3 NUB1 immunohistochemical staining of primary breast tumour tissue

To have the high-throughput analysis of breast cancer tissue specimens stained for biological markers, we performed TMA on NUB1 staining. Of the 152 primary breast cancer tumours on the tissue microarray, 125 tumour cores (80%) were interpretable for NUB1 staining, all of which had associated survival information. Uninterpretable spots were caused by either loss of tissue on the tissue microarray or no tumour cells in the spot. The immunohistochemical staining of the breast cancer tissue microarray with NUB1 showed cytoplasmic (Fig. 6.2) and/or nuclear localisation. In comparison to ER- (Fig. 6.3), similar distribution pattern but with more 3+ score of NUB1 in ER+ subgroup patients. There were highest frequency of 1+ cytoplasmic staining in ER negative patients whereas highest frequency of 2+ cytoplasmic staining in ER positive subgroup. There were 100 tumours (80%) that were positive for NUB1 cytoplasmic staining and 66 tumours (23.1%) positive for NUB1 nuclear staining. A subset of 99 tumours was positive for both NUB1 cytoplasmic staining and NUB1 nuclear staining (80%).

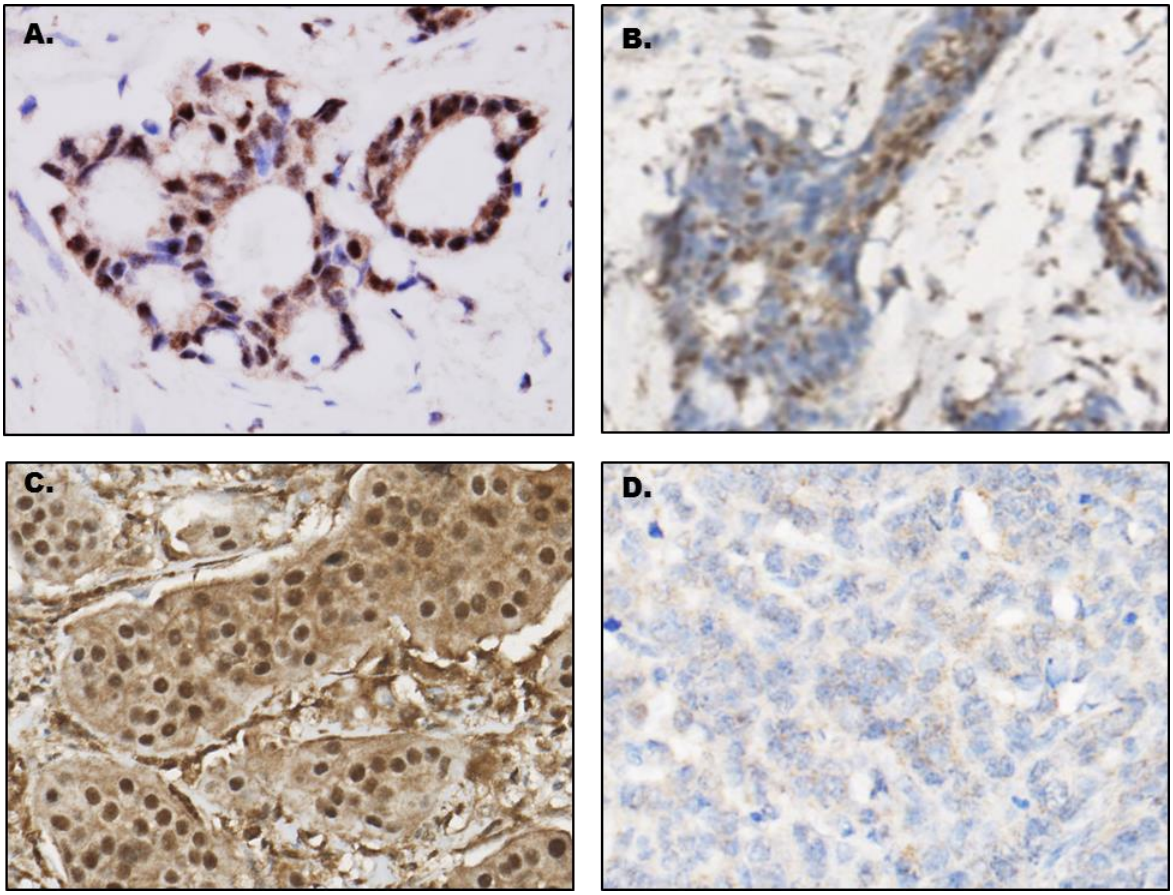


Figure 6. 2 NUB1 expression on representative node negative breast cancer tissue microarray spots. A, normal mammary tissue with glandular cells. B. Heterogenous NUB1 with some mixed cytoplasmic and nuclear staining; C. homogenous strong nuclear NUB1 staining with less cytoplasmic staining; C, Negative NUB1 staining. Figures are at ×100 magnification.

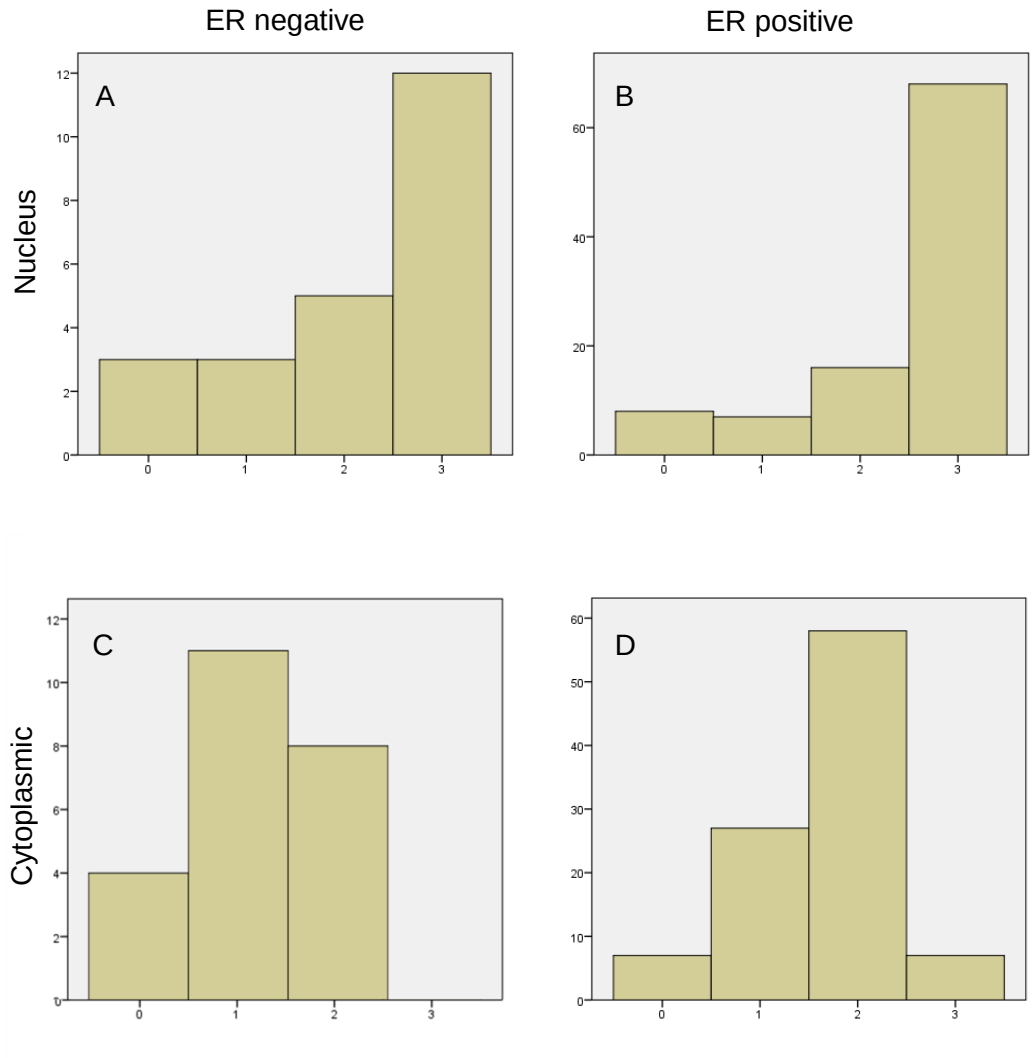


Figure 6. 3 Distribution of NUB1 immunohistochemical staining scores in primary breast cancer. A, NUB1 nuclear staining scores in ER- subgroup; B, NUB1 nuclear staining scores in ER+ subgroup C, NUB1 cytoplasmic staining scores in ER- subgroup; D, NUB1 cytoplasmic staining scores in ER+ subgroup.

6.4 Oestrogen receptor (ER) expression and association with clinicopathological factors

We obtained clinical data and breast cancer characterisation of ER and HER2 staining are from the collaborator, Professor Adrian Harris. ER immunoreactivity was evaluable in 122 (96.1%) cases, and scored positively in 99 (78%) cases (Fig. 6.1) using intensity scores of 2+ and 3+ as indication of ER protein overexpression. Tumours with ER intensity scores of 0 or 1+ were assessed as negative. ER expression was analysed in relation to clinicopathologic criteria (Table 6.1), with a significant association of ER negativity with positive node status (p = 0.009), ER-negative with highest histological grade tumours (p = 0.0001) and ER negative with larger tumour size (p=0.008).

	ER-negative	ER-positive	*p*-value	Overall
Total	23	99		122
c-erbB2 receptor status				
Negative	6	50	0.092	56
Postive	7	17		24
Node status				
Negative	9	16	0.009*	23
Positive	58	38		96
Histologic grade				
Grade I	0	18	0.0001****	18
Grade II	2	50		52
Grade III	15	17		32
Age				
< 50 years	7	19	0.236	28
≥ 50 years	16	80		39
Median (range)	53 (26–90)	59 (34–83)		58 (26–90)
Tumour size				
≤ 2 cm	4	47	0.008**	51
> 2 cm	19	52		71
Median (range)	3.7 (0–8.0)	2.36 (0–7.3)		2.5 (0–8.0)

Table 6. 1 Clinicopathological variables according to ER status. Grade I patients showed significantly more frequent to the rest of the grades in ER positive patients.Positive nodal status was found significantly in ER negative patients. Significantly more patients at > 50 years old were found in ER positive.

6.5 Association of ER status and menopausal status with subcellular localisation of NUB1

To correlate the subcellular distribution to the clinicopathological factors from the patients, we analyse the data statistically. NUB1 expression measured as an IPS was categorised in the nucleus and in the cytoplasm in breast cancer. There was a strong correlation of nuclear NUB1 IPS to the cytoplasmic NUB1 IPS (r=0.76 (0.67-0.83) (Fig. 6.4). Cytoplasmic NUB1 was significantly higher in ER-positive tumours with a mean IPS of 138 (95% CI, 121-155), compared with a mean IPS of 86 (53-120) in ER-negative breast cancers (*P* = 0.017*) (Fig. 6.5). Nuclear NUB1 staining in both ER status groups did not show a significant difference.

These results highlighted that ER-positive tumours showed an increase in both cytoplasmic and nuclear NUB1. The amount of cytoplasmic NUB1 levels is significantly higher in ER-positive compared to ER-negative. This suggests that the link between cytoplasmic NUB1 and ER- positivity.

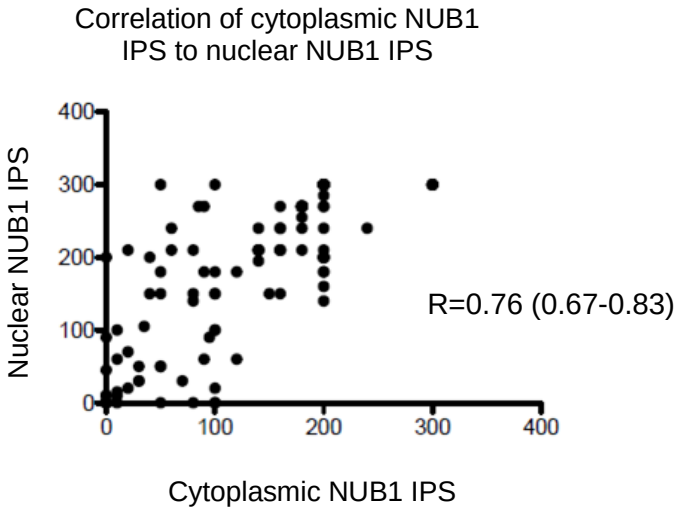


Figure 6. 4 Correlation of NUB1 cytoplasmic IPS with nuclear IPS, r=0.76 (0.67-0.83)

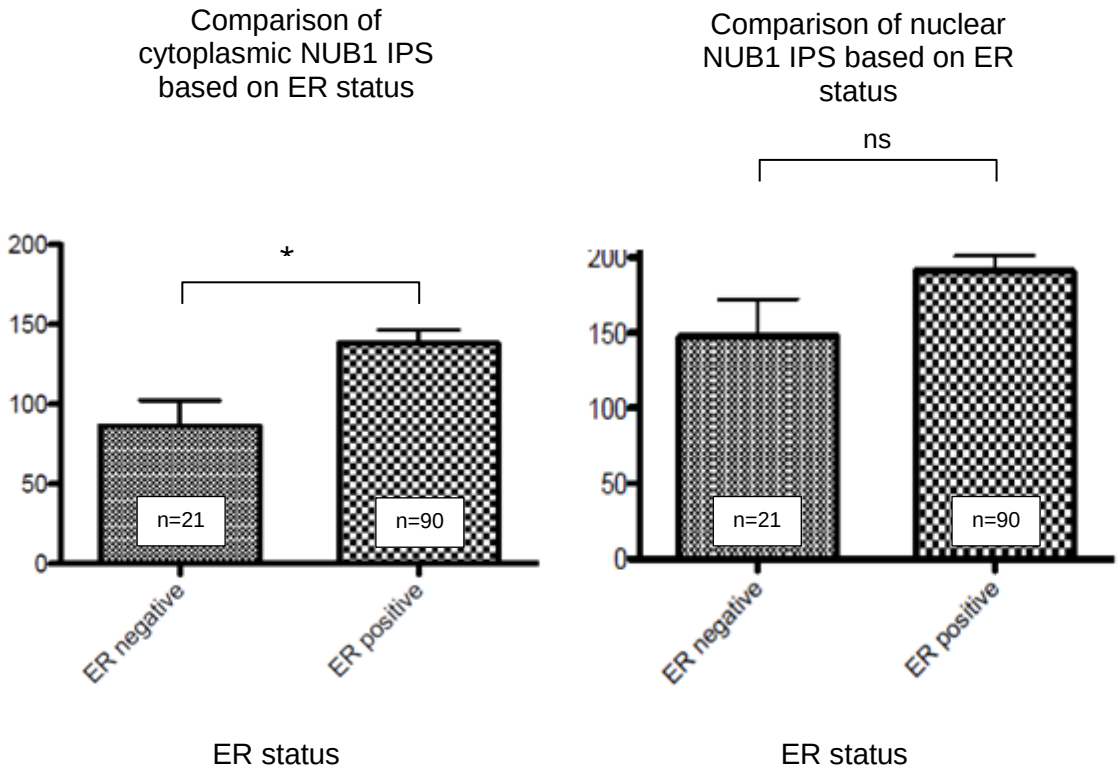


Figure 6. 5 Relationship between ER status and NUB1 localisation. Bar charts according to ER status and the subcellular localisation of NUB1 measured as an IPS. (a)Distribution of cytoplasmic NUB1 IPS and medians according to ER-negative and ER-positive breast cancers, with patient numbers shown. (b) Nuclear NUB1 IPS and medians according to ER status, and numbers of patients. *P* values indicate significance.

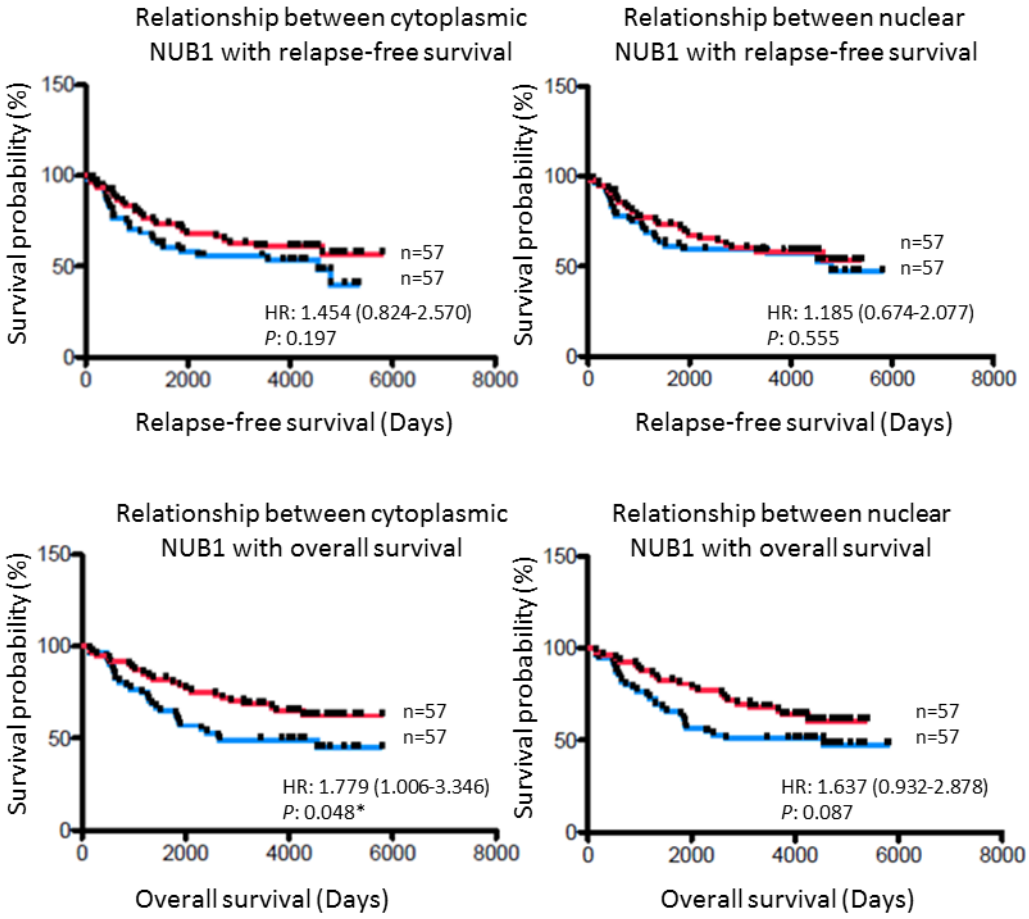
6.6 Survival analyses

The expression of NUB1 evaluated by immunohistochemical staining was correlated with overall survival of the patients with 16-year follow-up times. To determine whether NUB1 expression level is correlated with outcome, Kaplan-Meier survival curves were generated based on the subcellular localisation.

There was no significant difference in overall survival for nuclear NUB1 staining or for ER-negative subgroup (Table 6.3). However, significant survival differences were seen with NUB1 cytoplasmic staining.110 of 128 tumours positive for NUB1 nuclear staining were also positive for NUB1 cytoplasmic staining (88%). It was found that lower NUB1 cytoplasmic staining was significantly correlated with the poorer outcome with 16 years overall survival (p=0.0478; HR=1.779, 95% CI (1.006-3.146) but not with relapse free survival (p=0.1965; HR=1.454, 95% CI, 0.8238-2.568). No significant correlation between nuclear NUB1 staining was seen at 16 years of RFS (p = 0.5545, HR 1.185; 95% CI=0.6755-2.077)) and OS (p= 0.0866, HR=1.637, 95%CI= 0.9315-2.878) respectively.

In the ER status multivariant analysis, lower NUB1 and ER-negative patients showed significantly poorer survival HR=1.854 (0.954-2.124); p: 0.0041 (Fig 6.6). Our result indicated that depleted of both NUB1 and ER would cause significantly poorer survival in the breast cancer patients.

Table 6. 2 Relationship between high/low NUB1 subcellular localisation and overallsurvival/relapse free survival.



	Number of Patients	*Cytoplasmic*			*Nucleus*		
		Hazard ratio	95% confidence interval	*p*	Hazard ratio	95% confidence interval	*p*
Relapse-free survival	114	1.454	0.824-2.570	0.197	1.185	0.674-2.077	0.555
Overall survival	114	1.779	1.006-3.146	0.048*	1.637	0.932-2.878	0.087

Hazard ratios, confidence intervals and P values are given for the results of the univariate analyses. For univariate analyses, the hazard ratio is given for nuclear and cytoplasmic NUB1 in intensity percentage score (IPS), along with the 95% confidence interval. Patients with ductal, lobular or 'mixed' cancer were included where the marker data was available. *Relationship reached significance (P < 0.05). p<0.0001****

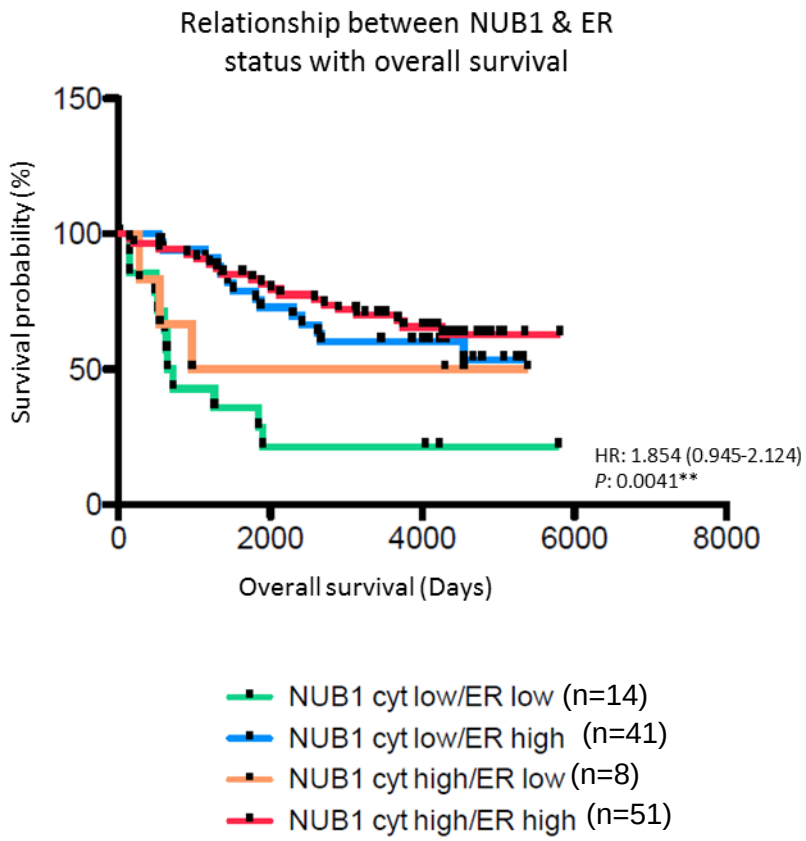


Figure 6. 6 Relationship between ER and prognosis in breast cancer patients using the log-rank test. Overall survival curves according to ER and NUB1 status, classified as negative or positive (b) Relapse-free survival curves according to HER-2 expression. Significant P values are indicated in bold.

6.7 Clinicopathological correlation and analysis

To describe an objective summary and correlation of clinical findings with gross and microscopic findings and with the results of studies performed on the breast cancer tissues, we looked at the clinic pathological characteristics in its relation to IPS (Table 6.3). Significantly lower cytoplasmic IPS was found in the ER-negative subgroup patients as well as pre-menopausal patients. Nuclear NUB1 score was found to be significantly lower in HER2+ and pre-menopausal samples.

Table 6. 3 Summary of overall survival analysis based on the mean IPS.

Variable	Events	Cytoplasmic			nuclear		
		Mean IPS	95% confidence interval	*P*	Mean IPS	95% confidence interval	*P*
Age, yr	116		-0.011, -0.26	0.079[a]		-0.12, 0.25	0.065[a]
Size, cm							
≤2	72	124	105-143		190	157-222	
>2	41	139	114-164	0.371	177	152-201	0.534
Lymph nodes							
Uninvolved	59	137	117-157		190	164-216	
Involved	54	115	92-138	0.172	164	134-194	0.195
Grade							
1	15	143	104-183		206	146-265	
2	51	133	111-155	Ns	180	152-208	ns
3	33	103	74-133	Ns	113	113-189	ns
Histology							
Ductal	94	122	104-183		172	150-194	
Lobular	14	133	111-155	Ns	222	179-265	ns
Other	8	103	74-133	Ns	186	98-274	ns
ER							
Negative	**21**	**86**	**53-120**		147	95-200	
Positive	**90**	**138**	**121-155**	**0.017***	191	170-211	0.166
HER2							
Negative	**52**	132	109-156		**189**	**160-219**	
Positive	**21**	104	64-144	0.300	**138**	**90-187**	**0.043***
Menopausal status							
Pre	**25**	**95**	**58-132**		**138**	**160-183**	
Post	**91**	**135**	**119-151**	**0.022***	**190**	**169-211**	**0.043***
EGFR							
negative	42	130	105-155		183	150-215	
positive	44	145	125-166	0.437	216	192-240	0.143

*Significant p-value, [a] Pearson correlation analysis

6.6 Discussion and Chapter Summary

Tissue microarray provides translational value of the AIPL1 and NUB1 in the breast cancer patients. We first validated a commercialised NUB1 antibody (clone 4H2) in immunoblots and immunohistochemistry.

Normal breast tissue was found positive with NUB1 antibody in the nucleus (Fig. 6.2). The signal was weaker in the cytoplasm. Cancer cells showed varying degree of staining in either nucleus and/or cytoplasm (Fig. 6.2). ER-negative breast cancer cells confer to the presence of nodes and bigger tumour size (Table 6.1). Nuclear NUB1 IPS has strong correlation to cytoplasmic NUB1 IPS (Fig. 6.4). In the survival analyses, the result revealed that depleted of both NUB1 and ER proteins have significantly lower survival rate. This was in full agreement with the mRNA data.

The localisation of AIPL1 and NUB1 could be and indicator of the role exerted onto cancer cells. p21 and p27 protein functions are dependent on their subcellular localisation. We were planning to utilise multiplexed ion beam imaging (MIBI) techniques to compare a panel of in situ proteins expression of high and low cytoplasmic NUB1 protein among ER-negative subgroup primary tumour. The optimised method was showed in Appendix 2.

Chapter 7

Discussion

7.1 Role of of AIPL1 and NUB1 in cancer

In Oncomine®, down-regulated AIPL1 mRNA levels have been demonstrated to associate with cancer growth in several types of cancers. This observation of down-regulated AIPL1 confirmed the meta-analysis on 30 microarrays done by Ramasamy in 2009. Meta-analysis of combined transcriptomic microarray datasets is a powerful method to greatly increase the sensitivity in revealing biomarkers for disease and, potentially, with better specificity with bigger series. In order to identify new biomarkers for (breast) cancer based on survival, we performed meta-analysis which led us to AIPL1 as our candidate of choice.

AIPL1 is required for complex protein folding but the role of AIPL1 has not been studied in any cancer. From the bioinformatics analysis of cancer databases, the AIPL1 fold change was not strongly decreased, marked by less than 0.5 $\log_2$FC difference in between cancer and normal tissue. The opposite role of AIPL1 (down-regulated in cancer) and NUB1 (upregulated) is suggested in causing normal cells to turn into cancer. In a retinal model, AIPL1 protein negatively regulates NUB1 protein trafficking across the nuclear membrane (van der Spuy *et al.*, 2002). Meanwhile, NUB1 showed stronger up-regulation potentials as the $\log_2$FC was frequently more than 0.5 in cancer tissues compared to the normal tissue.

7.2 Pathways involved in AIPL1 and NUB1

Data mining supports the importance of AIPL1 and NUB1 in cancer and give some clues about the possible pathway involved. The Oncomine® evidences support the findings that AIPL1 functions as a tumour suppressor gene in cancer. However, in the present study, NUB1 disagrees with previous work that suggests NUB1 was acting as a tumour suppressor (Hosono *et al.*, 2010). Hosono *et al.* demonstrated that expression levels of cyclin E, p27 and p21 were increased in A498 cells with overexpression of NUB1 as compared to cells expressing an empty vector control (Hosono *et al.*, 2010). However, this thesis presents on *in vitro* study in which we observed the up-regulation of p27 and p21 with NUB1 knockdown in MDA-MB-231, RCC4 and 786-O cells. We believe overexpression of NUB1 does not reflect its physiological state, since NUB1 was aggregated into cytoplasmic inclusion bodies and localised poorly to the nucleus (Tanji *et al.*, 2006).

We analysed NUB1 mRNA coexpression of four dataset from breast cancer samples and identified 28 genes of interests. CUL1 was frequently observed in the search, highlighting the robustness of the observed pattern. This bioinformatics approach provides the *in vivo* system-level understanding of the behaviours of AIPL1 and NUB1 in cancer. Furthermore, both NUB1 and CUL1 were enriched in common biological processes including TCR signaling, signaling by interferon, interleukin *etc.* This is in agreement with the fact that NUB1 is known to be involved in the immunity pathway and is inducible by interferon β (Hosono *et al.*, 2010).

The prognostic role of the mRNA levels further supported the hypothesis that both of the gene products are relevant to cancer. METABRIC data on survival curves showed lower NUB1 mRNA levels corresponded to poorer overall survival in ER-negative and triple negative subgroup patients. The subgroups are considered an aggressive disease and are often associated with poor survival. Our results have shed new light on the intrinsic

heterogeneity within this ER-negative and triple negative subtype and strengthen the importance of genomic studies within tumour subpopulations. The selection of gene expression subtypes for a single cancer is challenging in the clinics (Chen *et al.*, 2012). In clinical practice, the staining of a tumour biopsy for NUB1 may be useful for cancer prognosis assessment and/or for disease progression monitoring.

NUB1 is known to act as the degrading enzyme of NEDD8 and FAT10 and their conjugates. In comparison to NEDD8, FAT10 showed more cancer promoting capabilities in cancers especially in lymphoma, lung cancer, liver and brain cancer via the Oncomine® database. NUB1 recruits both NEDD8 and FAT10 and their conjugates for further proteasomal degradation. In comparison to the ER+/HER2+ patients subgroup, NEDD8 was found to be significantly lower in the ER-/HER2+ subgroup. In the METABRIC dataset, low FAT10 expression significantly stratifies patients in ER-, triple negative and basal subgroups (Fig 3.8). Moreover, FAT10 mRNA is upregulated in all subgroups, suggesting it could be a good anti-cancer target.

In vitro, we reported the presence of folded and unfolded AIPL1 monomer as well as the dimer forms (Fig 4.1). Most of the tested unstressed cancer cell line showed unfolded monomer while the positive control, Y79, exhibited both folded protein and unfolded forms of AIPL1 (Fig 4.1). This intriguing observation leads to the question of whether the folded could be a more active form of AIPL1. For instance, the chaperones protein, calreticulin interacts better in its folded form than its native form with certain peptides (Kim *et al.*, 2013). In a similar fashion, the folded AIPL1 protein would result in a higher affinity for its client proteins and peptides. In neutral pH, Histone-like nucleoid structuring-dependent expression A (HdeA) is a folded, but chaperones-inactive dimer in the native state (Hori *et al.*, 1999). HdeA adopts different conformations when bound to different substrates (Salon *et al.*, 2007).

7.3 Hypoxia and reoxygenation stress

AIPL1 and NUB1 responded to hypoxia and reoxygenation. In reoxygenated conditions, the AIPL1 proteins existed in dimer, trimer and multimer forms (Fig 4.4). The oligomers break down into dimer and monomers as the lysates were treated with reducing agent, DTT. This phenomenon suggests there is more than one type of cysteine-cysteine disulphide bond in between AIPL1 molecules. However, it is too premature at this early stage to infer the different forms of AIPL1 (folded and unfolded). These examples mark the dynamicity of AIPL1 protein to translocate NUB1 into the nucleus, giving us a true physiological picture.

Varying expression levels of NUB1 were observed among the unstressed cancer cell line panels, with the lowest expression observed in U2OS and SKBR3 cells. This observation is in concordance with Hosono *et al., 2002.* Examining the global neddylation in cells indicated varying degrees of neddylated CULs and some NEDD8 monomers in cell lines such as HCT116, U2OS, HCC1806 and MDA-MB-231. Meanwhile, when examining global Fat10-ylation, most of the FAT10-conjugated proteins remain unknown and FAT10 monomer was not found in unstressed cells. Very low levels of AIPL1 mRNA transcripts were observed in the cells, which did not match the abundance of its protein, suggesting the proteins are stable with a long half-life. It is also speculated that AIPL1 mRNA could be induced under stress condition including hypoxia and reoxygenation.

In the reoxygenation of MDA-MB-231 cells, NUB1 and neddylated CUL proteins were upregulated in a timely manner. NUB1 levels were responsive to hypoxia and reoxygenation as hypothesised, since NUB1 mRNA coexpressed with FAS and ATM, two proteins from signaling pathway which are frequently upregulated upon reoxygenation (Olcina *et al.*, 2010).

Through pathway analysis, both NUB1 and CUL1 are enriched in the cell cycle regulation pathway. In 2012, Hosono *et al.* demonstrated that overexpressed NUB1 causes up-regulation of p21 and p27 in renal cell carcinoma (RCC4) cells. In contrast, we observed that reducing NUB1 levels by transient expression of siRNA causes G_0/G_1 cell cycle arrest in MDA-MB-231 (Fig. 4.6) cells, confirmed with three independent biological replicates. We did not perform overexpression experiment for NUB1, since it forms aggregates in cells which are functionally redundant (van der Spuy and Cheetham, 2004). HSP70 and ubiquitin were recruited to these inclusions, suggesting that they may be targeted for proteasomal degradation (van der Spuy and Cheetham, 2004), and AIPL1 was able to suppress the formation of the inclusion bodies(van der Spuy and Cheetham, 2004).

Although there were no significant changes under normoxic conditions, both MDA-MB-231 (ER-) and T-47D (ER+) cells significantly grew slower after NUB1 knockdown in hypoxia. We speculated the altered subcellular distribution of NUB1 protein in hypoxia to the nucleus could determine the cell fate decision making of cancer cells (van der Spuy and Cheetham, 2004). In our study, NUB1 is essential to regulate the cell cycle during limited oxygen supply; its depletion abrogates the G_1 to S phase transition and dampens the growth rate of cancer cells (Fig 4.7).

In the subcellular fractionation experiment (Fig 4.8), AIPL1 migrated into the cytoplasm and formed multimers upon hypoxia and reoxygenation. We observed an interesting interplay. The unfolded AIPL1 monomer was retained in the nucleus whereas the folded AIPL1 protein was observed in the cytoplasm. Folded AIPL1 might suggest its active chaperoning of NUB1 then cause the NUB1 translocation into the nucleus. Opposite to that of AIPL1, NUB1 protein migrated into the nucleus upon hypoxia and reoxygenation in a timely manner. These opposite phenomena mark the oxygen sensing capability of NUB1 and AIPL1 affecting the shuttling of the proteins across the nuclear membrane.

To date, there is no information on how NUB1 regulates neddylated CULs. CULs are the only established neddylation substrates describe this far because overexpression of NEDD8 results in unphysiological false positives that require re-evaluation (Enchev *et al.*, 2015). Neddylated CUL1 was known to be more strongly engaged in the ubiquitin E3 ligase, which causes the degradation of p21 and p27 (Wu *et al.*, 2000). NUB1 depletion reduced the neddylated CUL1 (Fig 7.2). This was thought to be caused by NUB1 knockdown down-regulating the NEDD8 levels (Hosono *et al.*, 2010). NUB1 silencing upregulated the p27 and p21 protein levels in cells. This is in concordance with treatment of cells with the small molecule MLN4724, a neddylation inhibitor, which upregulated p21 and p27 further. This observation is in concordance with a previous study that the demonstrated upregulated p21 and p27 levels in the cells with reduced neddylated CUL1 levels (Wu *et al.*, 2015).

Free CUL1 proteins could act as a reservoir, that when neddylated can engage with the ubiquitin E3 ligase enhancing the degradation of p27 and p21. In the presence of NUB1, we observed the accumulation of the p21 and p27 proteins upon treatment of cells with an increasing concentration of neddylation inhibitor. This correlated with the delay in G1 cell cycle arrest. NUB1 silencing abolished the titrating effect of neddylation inhibitor and caused the accumulation of p27. We observed CUL1 level was down-regulated with titrated MLN4924, without siNUB1. We observed the accumulation of p27 when the cells were treated with neddylation inhibitor and NUB1 knockdown. Based on these, we speculated that NUB1 might cause the degradation of neddylated CUL1.

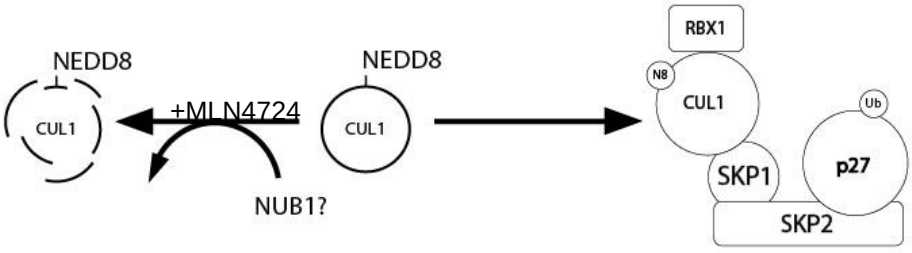


Figure 7. 1 Central dogma of NUB1-mediated cell cycle regulation via p27 and p21. Neddylated CUL1 locks the SCF complex with phosphrylated p27 and cyclin E as suggested by Bornstein et al., 2006 and Tanaka et al., 2012. NUB1 recruits neddylated CUL1 for proteasomal degradation.

7.4 Relationship with VHL

In RCC4plusVHL cells, NUB1 knockdown caused the down-regulation of VHL. Similar findings were also observed when we tried different siRNA sequences (Data not shown). This ruled out any off target effects. We observed more p21 (in normoxia) and more apoptotic cell death (in hypoxia) under NUB1 siRNA treatment as compared to the control condition. NUB1 is essential to foster cell cycle progression in hypoxia, and it also protects cells from cell cycle arrest/ entering senescence. Meanwhile in VHL-null RCC4 cells, NUB1 knockdown caused cell death in normoxic and hypoxic condition, suggesting a necrotic cell death was occurring as there is no cleaved-PARP and no G_o/G_1 cell cycle arrest markers observed. VHL is therefore important for orchestrating the cell fate decision (apoptotic or necrotic) upon NUB1 depletion. In the depleted NUB1 condition, the presence of VHL drives the cells towards apoptosis, while the absence of VHL drives the cells towards non-apoptotic cell death (significant percentage portion of cell death). The number of dead cells were significantly increased in hypoxic cells, suggesting a contribution of NUB1 migrating to the nucleus in hypoxia. We also observed that null-VHL RCC4 cells further upregulated HIF1α, especially in both normoxia and hypoxia in a VHL-independent manner.

NUB1 was examined in the Schoenfeld's idea (Fig 5.2) on how VHL upregulates p21 and p27 using RCC4 and RCC4plusVHL cells. According to Schoenfeld, VHL, a member protein of CUL2-based ubiquitin E3 ligase, is hypothesised to competitively occupy RBX1 and indirectly deactivates CUL1-based ubiquitin E3 ligase. As a result, the p21 and p27 proteins were stabilised within the cells. Therefore, HIF1α levels were examined to assess as the activity of CUL2-based ubiquitin E3 ligase.

In RCC4plusVHL cells, there was low HIF1α levels but upregulated p27, as detected by immunoblot signifying CUL2-based ubiquitin E3 ligase was more active than the CUL1-based one. NUB1 knockdown further stabilised p27 levels. In VHL-null RCC4 cells, increased p21 and p27 levels were observed, hinting that RBX1 is not bound to CUL1 based ubiquitin E3 ligase upon stress. HIF1α levels were stabilised further with NUB1 silencing.

When examining CUL2 protein levels we observed a possible polyubiquitination with multiple higher molecular weight forms. Although there is no report of polyubiquitinated CUL2, CUL1 polyubiquitination was reported *in vivo* and alters the ability of CUL1 to bind to S5a without affecting the stability of CUL1 (Bloom *et al.*, 2006). CUL1 ubiquitination promotes binding to the proteasome, but not degradation (Bloom *et al.*, 2006). In normoxia, NUB1 knockdown increase the polyubiquitination of CUL2 (Bloom *et al.*, 2006), though the functional consequences of this polyubiquitination remain unexplored.

In an attempt to unravel how HIF1α is stabilised in a VHL-independent manner, we examine whether HIF1α is a neddylation and FAT10ylation substrate. HIF-1α was identified to be covalently modified by NEDD8 and FAT10 (Fig. 5.7). Endogenous neddylated HIF1α is a reliable detection compared to transient NEDD8 overexpression. Neddylated HIF1α was reported previously (Ryu *et al.*, 2011). In this study, NEDD8 stabilised HIF-1α even in normoxia and further increased its level in hypoxia. Neddylated HIF1α was observed in VHL-null cell line (Ryu *et al.*, 2011).

The mechanism of how HIF1α degraded by VHL and CUL2 is long standing. The oxygen-dependent degradation of HIF-1α is initiated by the hydroxylation of proline 402 and 564. VHL targets the hydroxylated HIF1α and recruits ElonginB/C, CUL2, and RBX1, which forms the CUL2-based ubiquitin E3 ligase complex to ubiquitinate HIF-1α (Ivan *et al.*, 2001). VHL and CUL2 have been identified to be covalently conjugated by NEDD8. Neddylated VHL preferentially interacts with fibronectin (Russell and Ohh, 2008) and negatively regulate the ubiquitination of HIF1α. On the contrary, CUL2 is neddylated after its recruitment by VHL, and the neddylated CUL2 facilitates the polyubiquitination of HIF1α (Liakopoulos *et al.*, 1999; Sufan and Ohh, 2006; Miyauchi *et al.*, 2008). The net effect of neddylation on HIF-1α stability is obscure. Nonetheless, Ohh et al. suggested that the neddylation process is required for the ubiquitination and subsequent degradation of HIF1α (Ohh *et al.*, 2002). The effects of NEDD8 on HIF1α are linked with VHL-mediated HIF-1α ubiquitination. HIF1α expression and activity were both still regulated by NEDD8 in VHL-defective cells. Therefore, the direct neddylation of HIF1α may overcome the HIF1α-destructive effect of neddylated CUL2. The reciprocal regulations of HIF1α by neddylation remain to be investigated.

To our knowledge, this is the first study investigating the impact of NUB1 in breast cancer patients. NUB1 antibody (Clone 4H2) is an internally validated commercial antibody for both immunoblot and immunohistochemistry. We found a prognostic value of both nuclear and cytoplasmic NUB1 expression in breast cancer. A high expression of cytoplasmic NUB1 tended to be correlated to a better overall survival (Table 6.2). Low expression of NUB1 had a poorer overall survival (but not relapse-free survival) caused by metastasis-induced death. NUB1 mRNA transcript was found to be elevated in several cancers via bioinformatics analysis. Although high NUB1 expression was associated in cancer formation, the distant metastatic clone should be of a very different clone than which a cancer forms. It can be explained by tumour evolution (Fig. 7.1).

The nuclear import of NUB1 is dependent on the AIPL1 protein trafficking machinery (van der Spuy *et al.*, 2002). This report managed to associate NUB1 with initial tumourigenesis and cancer progression. We also explored the role of NUB1 entry to the cancer cell nucleus and reduced the tumour suppressor p21 and p27 levels.

7.5 Translational perspectives

High NUB1 protein expression can be a good prognostic marker to poor overall survival which further stratifies the patient survival in ER-negative patient's subgroup upon tumour initiation and progression. Reduced NUB1 levels may result in reduced nuclear availability to overcome different assaults including hypoxia, DNA damage repair and driver mutations which may potentially cause a failure of the DNA damage signaling cascade and consequently less activation of the downstream apoptotic cell death pathway. Due to the lack of cell death pathway activation, the tumor may continue to proliferate, resulting in distant metastasis.

Alteration of NUB1-mediated tumor-suppressor functions of the p21 and p27 proteins by decreased NUB1-expression could explain this tumour progression. Low NUB1 levels have been demonstrated to upregulate p21 and p27 proteins with tumor-suppressive as well as cancer promoting properties. The roles of p21 and p27 are explained in chaper 6.1, and their functions are localisation dependent . Implementing NUB1 immunostaining for ER-negative subtyped patients could inform the clinical specialists about the prognosis of patients.

The evidences suggested that NUB1 is cancer causing because of its inhibitory effect on apoptosis. However, we found its expression associated with better outcome. For instance, the BCL2 noted as oncogene, acts in the similar way (Pezzella *et al.*, 1993). While some very aggressive tumour, e.g. Burkitt's lymphma, *etc*. which are characterised by BCL2 negativity, showed high levels of apoptosis with high proliferation. It is plausible that both NUB1 and BCL2 are oncogenic but are associated with less aggressive cancer pathways. This suggests that NUB1 positive and negative tumours are different in their biologies.

Targeting strategies for NUB1 have been of interest for treatment of Huntington's disease (Lu *et al.*, 2013). Unfortunately, NUB1 may not be a druggable target for it does not have a receptor or enzymatic function that can be targeted by small molecule inhibitor. Moreover, its major function is achieved *via* interaction with other proteins.

One potential approach to elevate NUB1 expression is through IFNβ (Tanji *et al.*, 2005), a US Food and Drug Administration-approved drug for treating multiple sclerosis (Meyer *et al.*, 2012). Combinational IFNβ treatment in the *in vivo* animal models is a good concept of potential NUB1 therapy.

A potential therapeutics strategy to enhance NUB1 functions could work on the adaptor function of NUB1 and synergise its interaction with neddylated CULs in the pathway. This could be achieved by low-molecular-weight-compound screening using bioluminescence resonance energy transfer technology (Boute *et al.*, 2002). This technology successfully applied to identify Tau–Fyn SH3 interaction inhibitors for Alzheimer's disease (Cochran *et al.*, 2014).

Chapter 8

Concluding Statement

The aim of this study was to evaluate the prognostic influence of NUB1 expression in breast cancer of different stages surveying relapse free survival and overall-survival.

The combination of low nuclear and low cytoplasmic expression was significantly associated with an adverse prognosis in breast cancer, ER-negative cohorts. Interestingly, in the overall survival and tumor specific-survival analysis both the low nuclear/low cytoplasmic NUB1 tended to have an adverse prognosis. This leads to the possible assumption that rather the alteration per se irrespective of the direction of alteration may be relevant in distant metastasis. It remains open if any aberration in NUB1 expression may contribute to resistance.

Data from my work show that they are, as NUB1, which is regulated by AIPL1, affects cell cycle and apoptosis regulation trough NEDD8 and Cullin 1, p21 and p27. Data support the hypothesis that by down regulating p21 and p72, NUB1 has an cancer promoting effect mostly by protecting form apoptosis. In breast cancer NUB1 is associated with a group of less aggressive tumours, in a fashion similar to Bcl2, the prototype of cancer promoting by inhibition of apoptosis.

These results demonstrate that the cytoplasmic and nuclear localisations of proteins might be underestimated. NUB1-expression may be a prognostic marker in breast cancer. In multivariate analysis of prognostic clinicopathologic parameters only NUB1 was an independent significant predictive variable concerning overall survival. Further studies will be needed to estimate whether NUB1 expression is useful as a supplement to conventional clinicopathologic risk factors.

Appendix 1

28 common elements in "Metabric Nat", "TCGA Prov", "TCGA Nat 2012" and "TCGA Cell 2015":

1.	ACAP1,
2.	APOBEC3G,
3.	APOBEC3H,
4.	ARHGAP30,
5.	ARHGAP9,
6.	BTN3A1,
7.	CD4
8.	CORO1A
9.	CUL1
10.	HLA-F
11.	IL10RA
12.	IRF1
13.	MAP4K1
14.	MKRN1
15.	NLRC5
16.	PARP12
17.	PARP14
18.	PRF1
19.	PTPN7
20.	RAC2
21.	SAMD3
22.	SASH3
23.	SEMA4D
24.	SLA2
25.	TAP1
26.	TMEM140
27.	TNFRSF1B
28.	UBASH3A

List of Awards, Presentations and Publications

1. Poster presentation at FASEB SRC on ubiquitin and cellular regulation with poster presentation (June 12-17 2016) in United States.
2. Poster presentation and travel award at 24th Congress of the European Association for cancer research (July 9-11 2016) in Manchester, UK
3. Oral presentation and bursary award for Summer School (24-28 October 2016) in Albufeira, Portugal
4. Paper entitled 'Inhibition of NEDD8- and FAT10-ligase activities through degrading enzyme NUB1- A potential anticancer approach' in Oncology Letter. IF=1.5.

Inhibition of NEDD8 and FAT10 ligase activities through the degrading enzyme NEDD8 ultimate buster 1: A potential anticancer approach (Review)

KA-LIONG TAN[1,2] and FRANCESCO PEZZELLA[1]

[1]Nuffield Division of Clinical Laboratory Sciences, Radcliffe Department of Medicine, John Radcliffe Hospital, Headington, Oxford OX3 9DU, United Kingdom; [2]Faculty of Medicine & Health Sciences, Universiti Sains Islam Malaysia, Kuala Lumpur 55100, Malaysia

Received January 28, 2016; Accepted August 9, 2016

DOI: 10.3892/ol.2016.5232

Abstract. The capabilities of tumour cells to survive through deregulated cell cycles and evade apoptosis are hallmarks of cancer. The ubiquitin-like proteins (UBL) proteasome system is important in regulating cell cycles via signaling proteins. Deregulation of the proteasomal system can lead to uncontrolled cell proliferation. The Skp, Cullin, F-box containing complex (SCF complex) is the predominant E3 ubiquitin ligase, and has diverse substrates. The ubiquitin ligase activity of the SCF complexes requires the conjugation of neural precursor cell expressed, developmentally down-regulated 8 (NEDD8) to cullin proteins. A tumour suppressor and degrading enzyme named NEDD8 ultimate buster 1 (NUB1) is able to recruit HLA-F-adjacent transcript 10 (FAT10)- and NEDD8-conjugated proteins for proteasomal degradation. Ubiquitination is associated with neddylation and FAT10ylation. Although validating the targets of UBLs, including ubiquitin, NEDD8 and FAT10, is challenging, understanding the biological significance of such substrates is an exciting research prospect. This present review discusses the interplay of these UBLs, as well as highlighting their inhibition through NUB1. Knowledge of the mechanisms by which NUB1 is able to downregulate the ubiquitin cascade via NEDD8 conjugation and the FAT10 pathway is essential. This will provide insights into potential cancer therapy that could be used to selectively suppress cancer growth.

Correspondence to: Mr. Ka-Liong Tan or Professor Francesco Pezzella, Nuffield Division of Clinical Laboratory Sciences, Radcliffe Department of Medicine, John Radcliffe Hospital, Headley Way, Headington, Oxford OX3 9DU, United Kingdom
E-mail: ka.tan@lincoln.ox.ac.uk
E-mail: francesco.pezzella@ndcls.ox.ac.uk

Key words: NEDD8, NUB1, FAT10, E3 ubiquitin ligases, cullins, proteasomal degradation, ubiquitin-like proteins

Contents

1. Overview of ubiquitin-proteasome system (UPS) and ubiquitin-like proteins (UBL) pathway as a therapeutic target
2. The NEDD8-conjugation (neddylation) pathway and the effect of neddylation on transcription factors
3. The FAT10-conjugation (FAT10ylation) pathway and its function
4. NEDD8 and FAT10 pathway perspectives
5. Conclusion

1. Overview of ubiquitin-proteasome system (UPS) and ubiquitin-like proteins (UBL) pathway as a therapeutic target

The UPS is important in regulating protein homeostasis in human cells through programmed degradation. The degradation of regulatory proteins can affect cell-cycle regulation, cell proliferation, intracellular signaling, DNA repair and apoptosis (1-4). As UPS degradation is a major clearance system associated with proteolysis within the cells, its deregulation can cause the pathogenesis of cancer and other diseases through the inappropriate loss of regulatory proteins or unintentional activation of certain specific signalling cascades. For instance, cancerous cells develop when cell-cycle controls break down, leading to unregulated cell proliferation. Cancer cells can also evade apoptosis induced by a number of different cellular stresses. Hence, an interruption to the normal regulation of the UPS could lead to abnormal cell proliferation.

The 26S proteasome is a protease complex capable of degrading polyubiquitinated proteins. The 26S complex is composed of a barrel-shaped 20S proteasome core with a 19S regulatory particle at either or both of its ends. The 20S proteasome contains the enzymatic active sites, whilst the 19S regulatory particle helps to control access of ubiquitin-like protein (UBL)-conjugated substrates to the core. There are three proteasome active sites within the 20S core, namely the caspase-like (β1), trypsin-like (β2) and chymotrypsin-like (β5) domains. These sites use an N-terminal threonine as the catalytic amino-acid residue (5,6).

Table I. First- and second-generation proteasome inhibitors.

Drug	Company	Status
First generation		
Bortezomib	Millennium Pharmaceuticals, Inc. (Cambridge, MA, USA)	FDA-approved for multiple myeloma and relapsed mantle cell lymphoma
Second generation		
Carfilzomib (Kyprolis)	Onyx Pharmaceuticals, Inc. (San Francisco, CA, USA)	FDA-approved for multiple myeloma
Oprozomib (ONX0912)	Onyx Pharmaceuticals, Inc. (San Francisco, CA, USA)	Phase I
Ixazomib citrate (MLN9708)	Millennium Pharmaceuticals, Inc. (Cambridge, MA, USA)	Phase I/II
Marizomib (NPI-0052)	Nereus Pharmaceuticals (San Diego, CA, USA)	Phase I
Delanzomib (CEP-18770)	Cephalon, Inc. (Frazer, PA, USA)	Phase I
Calpeptin (IPSI-001)	Lanospharma Laboratories Co., Ltd. (Chongqing, China)	Phase I
ONX0914	Onyx Pharmaceuticals (San Francisco, CA, USA)	Phase I

FDA, Food and Drug Administration.

Ubiquitin (Ub) and UBLs share certain common structural elements, such as a three-dimensional structure called the Ub or β-grasp fold (7). The UBLs are a group of proteins encompassing neural precursor cell expressed, developmentally down-regulated 8 (NEDD8), small ubiquitin-like modifier 1/2/3, interferon-stimulated gene 15 (ISG15), HLA-F-adjacent transcript 10 (FAT10), autophagy-related protein (ATG)8 and ATG12, which conjugate to their targets in a manner similar to that of ubiquitination (8). Ub is a highly conserved protein of 76 amino acids that are able to attach to other proteins in a reversible fashion. There are three vital structural domains within Ub: i) the β-grasp fold, commonly found in all UBLs; ii) a C-terminal tail; and iii) seven lysine residues that correspond to polyubiquitin-linked chains (6). NEDD8 has distinctive functions in cells due to its structural differences, which mediate specialised interactions with target proteins compared with Ub. The crystal structure of NEDD8 is analogous to that of Ub, with the exception of two surface regions (9,10). NEDD8 was initially discovered in fetal mouse brain (11) and can be found predominantly in adult tissues (11-13). NEDD8 and the neddylation pathway enzymes are overexpressed in human cancers (13-15). FAT10 is a 165-amino acid protein that comprises two Ub-like domains with 29% identity and 36% homology to Ub at its N and C-termini, respectively (16). The protein is known to be involved in apoptosis, immune responses and cancer (16-18). Fig. 1A shows the domain structure of Ub, NEDD8 and FAT10.

The roles of UPS and UBL conjugation pathways in normal cell function and in disease has prompted the search for inhibitors that are able to selectively disrupt pathway function. Proteasome inhibitors have been synthesised to halt the function of the proteasomal activities. As mentioned, the proteasome has three active sites (β1, β2 and β5), which utilise N-terminal threonine as the catalytic amino acid residue (7). All UPS inhibitors were developed to covalently modify this threonine residue in order to block the enzyme's kinetics. The therapeutic value of UPS inhibition has been demonstrated with the proteasome inhibitor bortezomib (Velcade®; Millennium Pharmaceuticals, Inc., Cambridge, MA, USA). Bortezomib is used in the treatment of patients suffering from multiple myeloma (19,20) and mantle cell lymphoma (21).

As the first clinical proteasome inhibitor to target the UPS, bortezomib was approved in 2003. Several second-generation proteasome inhibitors are currently in development, such as carfilzomib, oprozomib, ixazomib citrate, marizomib and delanzomib. In comparison with UPS inhibition, blocking of UBL pathways may provide a more specific effect by targeting the substrate proteins. UPS inhibition is a common step in blocking the degradation of a broader range of substrates. For instance, inhibition of E1-activating enzymes may be achieved through covalent inactivation (e.g. PYR-41) (22) and adduct formation (e.g. MLN4924) (23). Blocked E2 interactions offer a more selective inhibition (e.g. synthetic peptide UBC12N26). Recent research has frequently focussed on targeting deubiquitinating enzymes (DUBs), as this class of proteins are capable of reversing the action of the Ub conjugation cascade. Table I summarises the current clinical development of second-generation proteasome inhibitors, and Table II lists the E1/2/3 inhibitors. Furthermore, a NEDD8-activating enzyme (NAE) inhibitor, MLN4924, which targets the NEDD8 pathway, appears to be a potentially important anticancer strategy (24). The development of DUB inhibitors is more recent compared with that of the proteasome and E1/2/3 inhibitors. To the best of our knowledge, no DUB inhibitors have entered clinical trials.

NEDD8 ultimate buster 1 (NUB1), a NEDD8- and FAT10-degrading enzyme, and approaches to anticancer therapy. NUB1 is an interferon (IFN)-inducible protein of 69 kDa, composed of 601 amino acids. It also has a splice variant, NUB1L, which possesses an extra 14 amino acids that encode an additional Ub-associated (UBA) domain (Fig. 1B). NUB1 proteins can recruit FAT10- and NEDD8-conjugated proteins to the proteasome for degradation and negatively

Table II. A summary of small molecule inhibitors targeting E1s, E2s and E3s.

Drug	Target	Company	Status
PYR-41	E1	Millennium Pharmaceuticals, Inc. (Cambridge, MA, USA)	N/A
MLN4924	E1	Millennium Pharmaceuticals, Inc. (Cambridge, MA, USA)	Phase II
CC0651	E2	N/A	N/A
NSC697923	E2	N/A	N/A
Nutlin	E3	Roche Products Limited (Pharmaceuticals) (Welwyn Garden City, UK)	Phase I
MI-773	E3	Sanofi S.A. (Gentilly, France)	Phase I
CGM097	E3	Novartis International AG (Basel, Switzerland)	Phase I

N/A, not applicable.

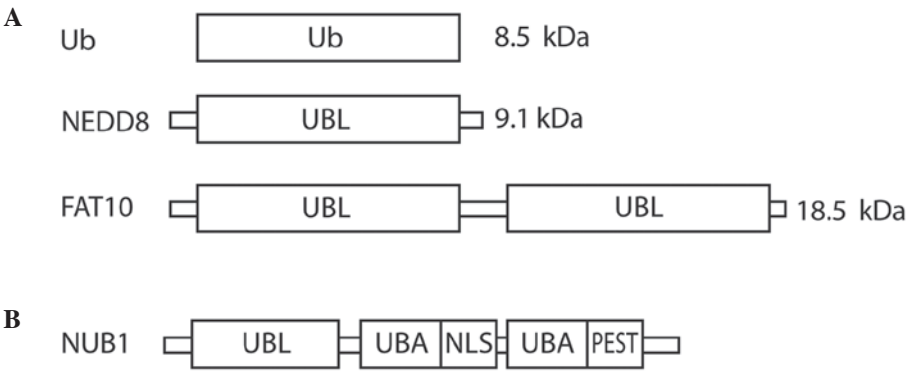


Figure 1. Structural representation of (A) Ub, NEDD8 and FAT10, and (B) NUB1. Ub, ubiquitin; NEDD8, neural precursor cell expressed, developmentally down-regulated 8; FAT10, HLA-F-adjacent transcript 10; NUB1, NEDD8 ultimate buster 1; UBL, ubiquitin-like domain; UBA, ubiquitin-associated; NLS, nuclear localisation signal; PEST, proline-enriched glutamic acid, serine and threonine domain.

regulate the NEDD8-conjugation system (25-29). The NUB1 proteins have been observed in various types of cancer cells, including cervical adenocarcinoma, rectal adenocarcinoma, neuroblastoma, malignant lymphoma and renal cell carcinoma (RCC) (26). Upregulated NUB1 expression has been linked to IFNα-induced antimitogenic actions. Additionally, NUB1 has demonstrated anticancer properties in RCC cell lines, where it was involved in apoptosis and S-phase transition through its action on p27 and cyclin E (30,31). Upregulation of NUB1 effectively inhibits the proliferation of IFNα-resistant RCC cells (31).

NUB1 protein has been reported to play a role in Huntington's disease (32) and congenital amaurosis (33). In cancers, NUB1 is an attractive candidate for inhibition of $p27^{KIP1}$ and $p21^{CIP1}$ via the regulation of the Skp, Cullin, F-box-containing $(SCF)^{SKP2}$ ligase activity (31). The upregulated $p21^{CIP1}$ in NUB1-knockdown cancer cells is thought to be promising in directing the cells to senescence. NUB1 protein was reported to be a tumour suppressor as it exerts growth inhibition during its overexpression; upon IFNα treatment, overexpressed NUB1 induced apoptosis in IFNα-resistant A498 cells (31). However, its general lack of enzymatic activities makes NUB1 less suitable for small molecule inhibition (32). Thus, the low-molecular-weight proteins FAT10 and NEDD8 could be key to developing novel strategies in anticancer therapy, as they interact with NUB1 (34). The current review focuses on the relevance of NUB1 protein in NEDD8 and FAT10 conjugation in cancers, and the potential for targeting it as a novel therapeutic approach.

2. The NEDD8-conjugation (neddylation) pathway and the effect of neddylation on transcription factors

The UBL enzymatic cascade scheme that results in UBL conjugation and protein degradation involves several distinct steps. Each step requires different classes of enzyme, as shown in Table III.

Neddylation is a post-translational modification process that conjugates NEDD8 to its target proteins, in a process that is analogous to that observed for ubiquitination. However, the neddylation process uses a distinct E1 and E2 enzyme reaction scheme (5,8,11,35,36) (Table III). Fig. 2A summarises the NEDD8 conjugation and deconjugation steps (34,37). The C-terminal glycine of NEDD8 is adenylated by an E1 NEDD8-activating enzyme (NAE), a heterodimer composed of amyloid-β precursor protein-binding protein 1 (APPBP1) and Ub-like modifier-activating enzyme (UBA) 3. NEDD8 is covalently conjugated to the NAE via a thiolester linkage (38). The activated NEDD8 is consecutively transferred to the E2 NEDD8-conjugation enzyme and then to the specific substrates (i.e. cullin proteins) via an isopeptide bond (39). The RING-box protein (RBX) 1/ROC1, mouse double minute 2 homolog (MDM2), F-box protein 11 and c-Cbl proteins are neddylated in the same way (39).

There are two NEDD8-specific E2-conjugating enzymes, namely ubiquitin conjugating enzyme E2 (UBE2)M (also known as UBC12) and UBE2F. These E2 enzymes act to

Table III. Overview of the enzymatic cascade involved in UBL conjugation.

UBL	Ub	NEDD8	FAT10 and Ub
E1-activating enzymes	UAE	APPBP1-UBA3 heterodimer	UBA6
E2-conjugating enzymes	UBCs	UBE2M and UBE2F	USE1
E3 ligases	Ub E3 ligases	NEDD8 E3 Ligases	N/A
Substrates	1,000s	200s	N/A

UBL, ubiquitin-like protein; Ub, ubiquitin; NEDD8, neural precursor cell expressed, developmentally down-regulated 8; FAT10, HLA-F-adjacent transcript 10; UAE, ubiquitin-activating enzymes; APPBP1, amyloid-β precursor protein-binding protein 1; UBA, ubiquitin-like modifier-activating enzyme; UBCs, Ub-conjugating enzymes; UBE2, ubiquitin-conjugating enzymes E2; USE1, UBA6-specific E2 enzyme; N/A, not applicable.

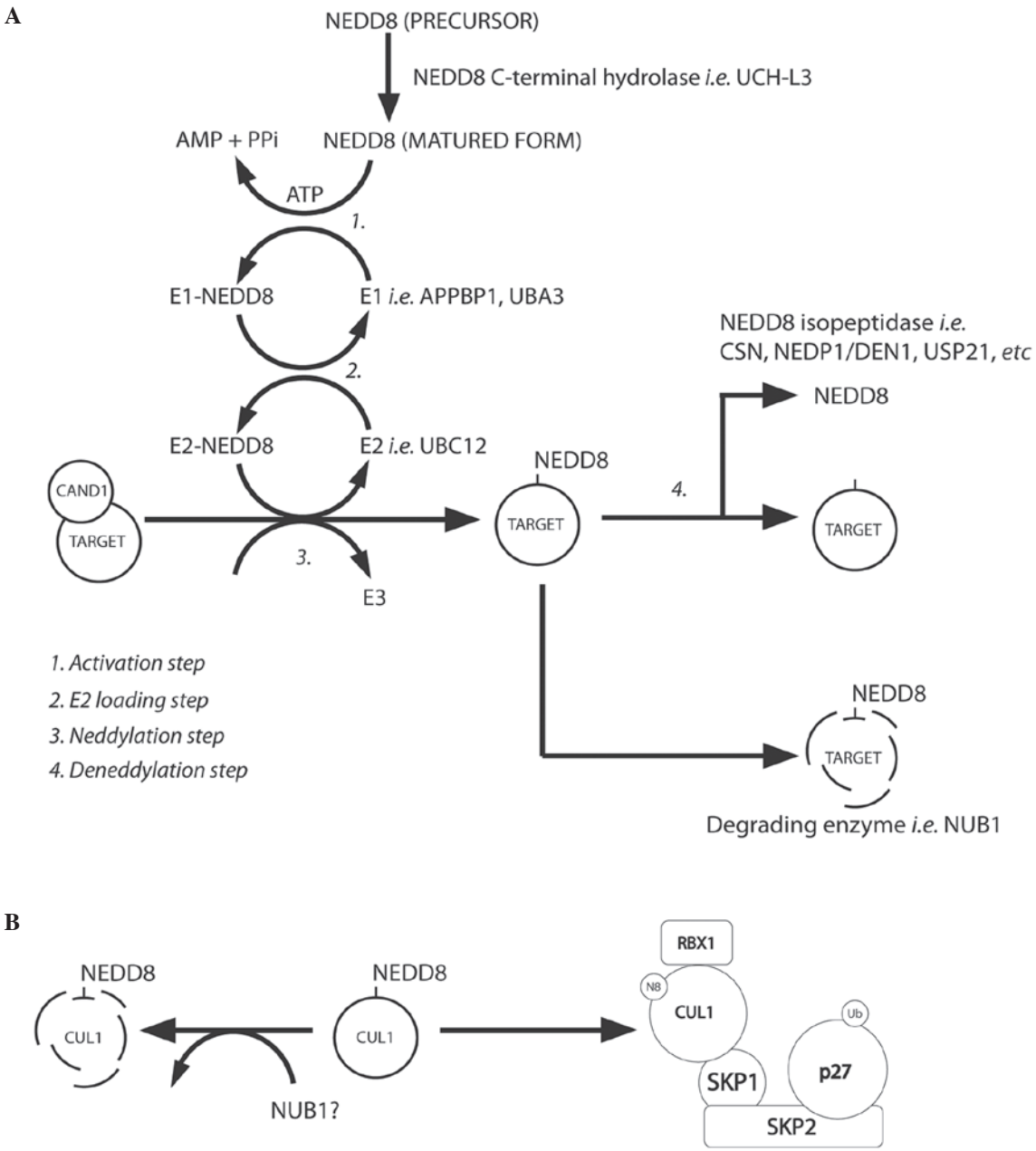


Figure 2. (A) NEDD8 conjugation pathway. Schematic summary of the main steps of the neddylation pathway [modified from Rabut and Peter, 2008 (37); Tanaka *et al*, 2012 (34)]. (B) Neddylated CUL1 locks the SCF complex with phosphorylated p27 and cyclin E [as suggested by Bornstein *et al*, 2006 (30) and Tanaka *et al*, 2012 (34)]. CAND1, cullin-associated and neddylation-dissociated 1; AMP, adenosine monophosphate; PPi, anion $P2O7^{4-}$; ATP, adenosine triphosphate; UCH-L3, ubiquitin C-terminal hydrolase isozyme L3; APPBP1, amyloid-β precursor protein binding protein 1; DEN1, deneddylase 1, CSN, COP9 signalosome; NEDP1, NEDD8-specific protease 1; NUB1, NEDD8 ultimate buster 1; USP21, ubiquitin specific peptidase 21, CUL1, cullin 1; SKP1, S-phase kinase-associated protein 1; SKP2, S-phase kinase-associated protein 2; RBX1, ring-box 1, E3 ubiquitin protein ligase; SCF, Skp, cullin, F-box-containing complex.

transfer NEDD8 to its target protein through E3 enzymes. It has been reported that all NEDD8 E3 enzymes can function as Ub E3 enzymes. The predominant NEDD8 E3 ligases are the RING subunits RBX1 and RBX2 (38,40-43). Meanwhile, the non-RBX family NEDD8 E3 ligases include c-CBL, ring finger protein 111, MDM2 and inhibitor of apoptosis 1 (44).

Of the numerous NEDD8 substrates, neddylation has been best described in the cullin family (45). In this mechanism, NEDD8 from the E2 cysteine active site is transferred onto a lysine residue in the N-terminus of the target proteins (Fig. 2A) (46). Cullin neddylation is further mediated by defective in cullin neddylation protein 1-like proteins (44). It was reported that RING E3 ligases could neddylate the same substrate on multiple lysine residues (44). However, the interaction between non-RBX RING E3 ligase and E2 enzymes remains to be elucidated.

NEDD8-conjugated substrates are deneddylated by various proteins that include COP9 signalosome (CSN), NEDD8-specific protease 1 (NEDP1/DEN1) and ubiquitin specific peptidase 21 (37,47-51). Neddylation may be inhibited by cullin-associated and neddylation-dissociated 1 through its direct binding to cullins (52,53). NEDD8 and neddylated substrates are recruited by NUB1 for proteasomal degradation (25,26) (Fig. 2A). In the G1-S-phase transition, Bornstein *et al* (30) demonstrated how neddylated cullin 1 cooperatively activates the SCF^{SKP2} Ub ligase complex, which results in p27 degradation (Fig. 2B). Furthermore, previous studies found that cullin neddylation increased the Ub E3 ligase activity of the SCF complex (Fig. 3) (46,54).

NEDD8 is negatively regulated by NUB1, which links the UBLs to the 26S proteasome for further UPS degradation. Reports have described that NUB1 is able to recruit NEDD8 and NEDD8-conjugated proteins to the proteasome for degradation, and this may modulate the cell-cycle profile in response to stresses (34). The capability of NEDD8 to activate the Ub E3 ligase-SCF complex (by covalent binding to cullins) adds further complexity to the ubiquitination machinery (11,55-59). Therefore, validation of NEDD8 targets would allow identification of genuine NEDD8 substrates.

Challenges in identifying physiological neddylation targets. Hjerpe *et al* (45) demonstrated that NEDD8 and Ub cascades are independent of one another during normal cellular homeostasis. NEDD8 conjugation onto Ub substrates through the Ub cascade has a spurious role in normal physiological conditions. The single amino acid change in the C-terminus of NEDD8 compared to Ub, from Arg72 to Ala72, confers the specificity between these two UBLs (44). This ensures that the correct UBL is passed to the appropriate E2 enzyme, E3 enzyme and the substrate respectively (Table III). However, when NEDD8 is in excess, the NEDD8 E1 enzyme UBA1 can activate NEDD8, which is then transthiolated to Ub E2 enzymes. This phenomenon results in the neddylation of Ub-specific substrates (10,45). NEDD8 can form NEDD8 chains or mixed Ub-NEDD8 chains (39,60). An increase of NEDD8 over Ub, as a result of cellular stresses, cellular diversity or pathological conditions, could exert different effects on neddylated substrates (44). This raises concerns, since the majority of research performed to date to identify neddylated substrates in cells relies on the overexpression of NEDD8; as this would cause an imbalance between cellular NEDD8 and Ub levels, it could result in the aberrant neddylation of proteins via the Ub pathway (45).

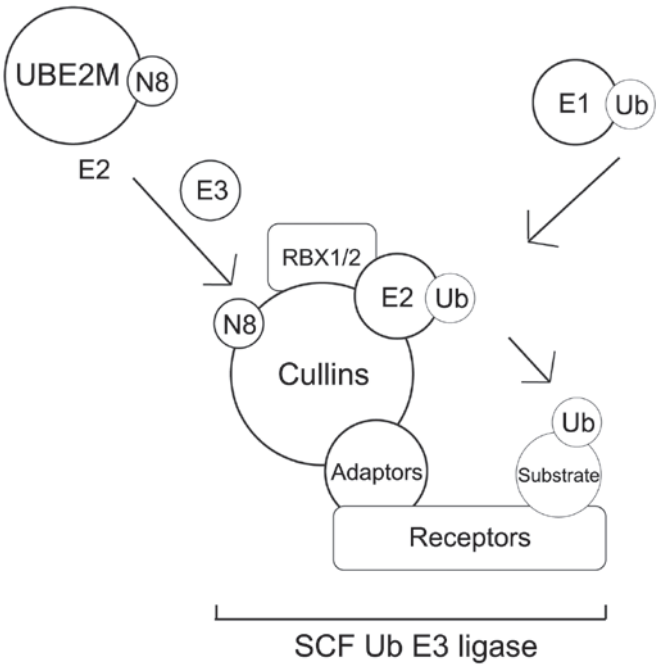


Figure 3. NEDD8 conjugation and ubiquitination pathway through cullin proteins. UBE2M, ubiquitin-conjugating enzyme E2M; RBX1/2, ring-box 1; Ub, ubiquitin; NEDD8, neural precursor cell expressed, developmentally down-regulated 8; SCF, Skp, cullin, F-box-containing complex.

Enchev *et al* (44) therefore revised and proposed a set of criteria to define the search for physiological neddylation targets: A neddylation substrate must demonstrate the covalent attachment of NEDD8 through the carboxyl-terminal glycine to the lysine residue of the substrates; and the neddylation must be detected under homeostatic conditions under endogenous NEDD8 levels and substrate expression. The NAE inhibitor MLN4924 should be incorporated into the study, as it blocks cullin neddylation but not ubiquitination (44). It remains optional to examine the possible NEDD8 E2 and E3 enzymes (44,45). It is also advisable to look at the regulation and biological consequences of neddylation (44). In endogenous protein experiments, immunoprecipitation with specific antibodies is a recommended approach (44). Genome editing techniques, such as a CRISPR/cas9 approach, may be used to introduce affinity-tagged versions of a particular gene product (44). The NEDD8 substrate should also be confirmed using mass spectrometry, using LysC protease as the cleavage enzyme, as it can discriminate between Ub, NEDD8 and ISG15 conjugates (61). Mass spectrometry can also be used to determine the site of the neddylated Lys residue, and the type of NEDD8 chains that are formed. The neddylated Lys residue needs further study if it is also targeted by Ub. The relative abundance of Ub, NEDD8 and FAT10 must be examined for its physiological relevance (44). A mutant form of the substrate that can no longer be neddylated must also be included to serve as a negative experimental control (44).

Overexpression of NEDD8 and the aberrant activation of the neddylation pathway and cullin-RING Ub ligase (CRL) activity can drive the progression of cancers (4,13), inflammatory and autoimmune diseases (7). Mainstream research

focuses on the effects of CRL inhibition, neddylation and deneddylation. The small-molecule NAE inhibitor MLN4924 is undergoing clinical trials. MLN4924 is an analog of adenosine monophosphate that competitively binds to the enzymatic pocket of NAE. This small molecule therefore inhibits neddylation and CRL activity. MLN4924 treatment causes DNA replication by stabilising chromatin licensing and DNA replication factor 1, a DNA replication licensing factor and CRL substrate. MLN4924-treated cells accumulate DNA damage due to DNA repair failure, leading to apoptosis (62) or senescence (19). Neddylation is able to inhibit the transcriptional activity of the tumour suppressors p53 and p73, and to stabilise Hu-antigen R (63), cell division cycle 6 and hypoxia-inducible factors (64). One of the important outcomes of MLN4924 treatment is that it causes the cancer cells to undergo apoptosis and senescence (44).

Transcriptional regulation via the neddylation of transcription factors. Several studies have suggested that neddylation of transcription factors can lead to the suppression of their transcriptional activity (44,65).

E2F transcription factor 1 (E2F1). Neddylation of E2Fs reduces their transcriptional activity (66,67). E2F1 was shown to be neddylated in the DNA-binding domain and its protein levels reduced following neddylation (67). DEN1 deneddylates E2Fs and consequently activates E2F-mediated transcription. DNA damage promotes the expression of DEN1, which subsequently deneddylates E2F and causes its stabilisation (68). Neddylation specifically regulates a subset of E2F target genes; for example, E2F1 deneddylation upon DNA damage triggers the transcription of proapoptotic factors (66).

p53 and p73. p53 acts by inhibiting cell cycle progression or triggering senescence or apoptosis (33). It is inhibited by the RING-domain E3 ligase MDM2, which targets ubiquitinated p53 for degradation. MDM2 is able to neddylate p53 and inhibit its transcriptional activity (33). The neddylated p53 is further recruited by NUB1, leading to its inactivation (69). p73 that is neddylated by MDM2 undergoes cytoplasmic relocalisation and downregulation of transcriptional activity (70). In addition, the Ub E3 ligase SKP1-CUL1-F-box protein 11 (SCF^{Fbox11}) may neddylate p73 and downregulate its transcriptional activities (71).

Nuclear factor κB (NF-κB). When extracellular signaling is absent, NF-κB is distributed in the cytoplasm and inhibited by inhibitor of NF-κB (IκB) family members. Upon stimulation by proinflammatory cytokines [such as tumour necrosis factor (TNF)], IκB kinases (IKKs) -α, -β and -γ phosphorylate IκB, which is then ubiquitylated and targeted for degradation by $SCF^{\beta TrCP}$. Under the same conditions, IKKγ was reported to be neddylated and degraded by the proteasome, which reduces NF-κB activation and inhibits NF-κB activity in gastrointestinal neoplasia (72). Therefore, neddylated IKKγ may exert a tumour suppressor function.

Amyloid precursor protein intracellular domain (AICD). Amyloid precursor protein is cleaved by secretase to become amyloid-β peptide and AICD. AICD is a component of a transcription factor complex with amyloid-β (A4) precursor protein-binding family B member 1 (FE65) and TAT-interactive protein 60 (73). Neddylated AICD blocks its interaction with FE65 and prevents the formation of the transcription factor complex, thereby reducing its transcriptional activity (2,74). Thus, neddylated AICD inhibits the transcription of downstream targets.

3. The FAT10-conjugation (FAT10ylation) pathway and its function

FAT10 was discovered by Sherman Weissman in 1996 (5). Due to the poor solubility of the protein at high concentrations, the structure of FAT10 protein was only recently defined (75). FAT10 consists of two β-grasp fold domains connected by a short linker (75). FAT10 protein was found to be expressed predominantly in immune tissue, including the thymus, lymph nodes and spleen (76-78). Its expression is stimulated by proinflammatory cytokines, namely IFNγ and TNFα (79). FAT10 protein is found in mature dendritic cells and it demonstrates oncogenic characteristics; ectopic expression of FAT10 causes malignant transformation and promotes tumour growth (80), and it is known to be upregulated in several tumour types, including liver and colon tumours (18,81).

FAT10 shares the same E1 and E2 enzymes with the Ub conjugation pathway. The FAT10 E1 enzyme UBA6 is able to activate Ub and FAT10 (29,82-84). The adenylation and transthiolation reactions of FAT10 are kinetically slower than those for Ub. UBA6 protein is thought to be the only FAT10 E1 enzyme in cells, since UBA6 knockdown can effectively abolish the formation of FAT10-conjugates *in vitro* (84,85). Similarly, UBA6-specific E2 enzyme (USE1) is the only UBA6-specific E2 enzyme discovered to be involved in FAT10 conjugation, although it also functions in a similar fashion to the conjugation of Ub (83). USE1 may only bind to activated Ub from UBA6, not UBE1 (83).

Little is currently known about FAT10, and research to identify possible FAT10 E3 ligases and deconjugating enzymes is ongoing. One study demonstrated that ectopically expressed FAT10 was not degraded over time, suggesting the possibility that a group of FAT10-deconjugating enzymes may not exist (86). It is believed that FAT10 is capable of promoting its own proteasomal-dependent degradation without the aid of deconjugating enzymes (86). FAT10-conjugated proteins were found to have a reduced half-life, similar to that observed for Ub-conjugated proteins (21). Conversely, it was demonstrated that FAT10-conjugated p62 accumulated under proteasome inhibition (79).

The interferon-inducible protein NUB1 interacts with FAT10 non-covalently (25), and significantly accelerates the degradation of FAT10 by the proteasome (25). NUB1 binds to the proteasome subunit S5a (28), and also to FAT10 via its three C-terminal UBA domains (Fig. 4) (87). NUB1 is also able to interact with the von Willebrand A (VWA) domain of RPN10 (S5a), one of the subunits of the 26S proteasome (25,28). The degradation of FAT10 is accelerated further by NUB1 splicing variant, NUB1L, which is able to bind to regulatory particle non-ATPase (RPN)10 in addition to the 19S regulator subunit, RPN1 (S2) (87).

The 26S proteasome subunit Rpn10 (S5a) is the docking site for FAT10, NUB1L and polyubiquitin. Ub interaction motifs 1 and 2 of Rpn10 are bound by lysine 48-linked polyubiquitin

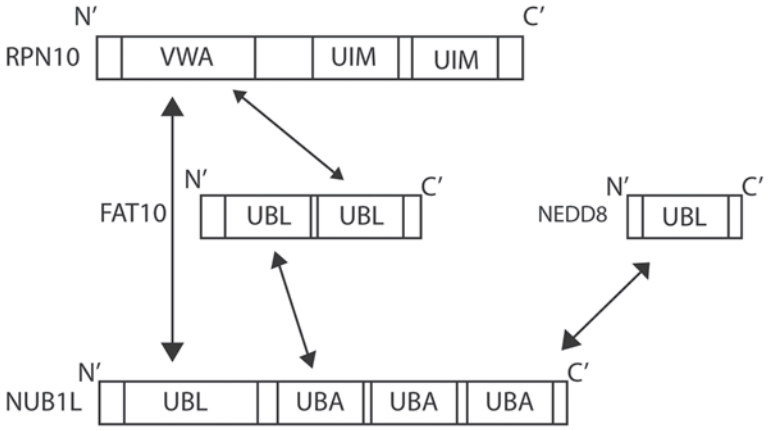


Figure 4. Domain structure of NUB1L, FAT10 and RPN10 and their interacting domains [Hipp *et al* (87); Kamitani *et al* (25); Tanji *et al* (28)]. RPN10, regulatory particle non-ATPase 10; FAT10, HLA-F-adjacent transcript 10, NUB1L, NEDD8 ultimate buster 1 long isoform; UBL, ubiquitin-like domain; UBA, ubiquitin-associated; UIM, ubiquitin-interacting motif; VWA, von Willebrand A motif.

chains. FAT10 is able to target substrate proteins to the proteasome independently of poly-FAT10ylation. FAT10 interacts directly with the VWA domain of RPN10, and no ubiquitination is required (28). The co-expression of NUB1L has been shown to accelerate the degradation of FAT10, suggesting a preference for proteasomal degradation (28).

Substrates of FAT10 conjugation. The biological function of FAT10 remains poorly understood. FAT10 overexpression has been demonstrated to induce apoptosis in mouse fibroblasts (67), HeLa cells (68) and renal tubular epithelial cells (70). FAT10 is synergistically induced by IFNγ and TNF-α, which leads to the induction of apoptosis (25). Several FAT10-interacting proteins have been identified, and are summarised in the following paragraphs.

The inflammatory mediator leucine-rich repeat Fli-I-interacting protein 2 (LRRFIP2) is covalently modified by FAT10 (6). LRRFIP2 positively regulates the activity of NF-κB in the inflammatory response mediated by toll-like receptor (TLR)4 (6). FAT10ylation of LRRFIP2 hinders its recruitment to the plasma membrane, which results in the inhibition of lipopolysaccharides (LPS)/TLR4-mediated NF-κB activation (6). This consequently leads to the reduced expression of NF-κB-responsive genes, including apoptosis inhibitors (6). Overexpression of FAT10 can induce apoptosis, causing $FAT10^{NULL}$ mice to be hypersensitive to LPS challenge due to NF-κB inhibition (33). However, FAT10 was observed to protect leukocytes in the spleen, thymus and bone marrow from apoptosis in a mouse model (33). In another study, the colon cancer cell line HCT116 was protected from TNF-α-induced apoptosis in the presence of FAT10 (88). The induction of apoptosis by FAT10 is therefore cell type-specific; however, the mechanisms involved remain unknown.

Mitotic arrest-deficient 2 (MAD2), a spindle assembly checkpoint protein, binds to FAT10 protein non-covalently (33). In prometaphase, overexpressed FAT10 in HCT116 cells was found to reduce the localisation of MAD2 at the kinetochore (88,89). Ren *et al* (88) reported that TNF-α-induced upregulation of FAT10 also delocalised MAD2 from kinetochores in a similar way and accelerated cell mitosis. The mis-segregation of chromosomes was shown to be abolished when FAT10 levels were reduced by siRNA (89). Hence, FAT10 is considered to cause mis-segregation of chromosomes during cell division (88,89).

FAT10 has been found to be highly expressed in colorectal, ovarian, hepatocellular and uterine carcinomas, suggesting that FAT10 expression may promote oncogenesis (89). A study found that 72% of hepatocellular carcinoma and 53% of colon carcinoma tissues overexpressing FAT10 also expressed the IFNγ/TNF-α-dependent immunoproteasome subunit low molecular mass protein 2 (90), suggesting that the pro-inflammatory cytokine response may be responsible for FAT10 overexpression in carcinoma tissues.

Autophagy adaptor p62 or sequestosome-1 protein can regulate aggresome formation, which protects cells from aggregation-prone protein-induced toxicity (79). FAT10ylated p62 tends to be proteasomally degraded (79). A previous study revealed that FAT10 expression induced by pro-inflammatory cytokines leads to a decrease in endogenous p62 (79). FAT10 was found to be transported by histone deacetlyase 6 along microtubules into aggresomes, causing p62 degradation (79). Under pathological conditions, p62 is localised in aggresomes along with the aggregated proteins found in neuronal diseases, including Alzheimers (91). The impact of FAT10 on P62-induced pathogenesis remains unresolved. However, there is no evidence that FAT10ylated p62 has a role in autophagic pathways (91).

4. NEDD8 and FAT10 pathway perspectives

The SCF Ub E3 ligases have been shown to be deregulated in various cancers; this results in unlimited cell proliferation and carcinogenesis via accumulation of their substrate proteins (34). Consequently, the E3 ligases are the subject of research into potential strategies for anticancer therapy (34). It is believed that the NEDD8-Ub-SCF complexes and the NEDD8-FAT10-degrading enzyme NUB1 are potential candidates for therapy (Fig. 2B) (34).

The search for neddylation targets requires further experimental validation. The conventional ectopic overexpression of UBLs is thought to lead to false positive conjugation of substrates (45). However, genome editing techniques, such as CRISPR-Cas9 technology, could overcome this, as it permits the neddylated substrates to be examined endogenously (44).

In addition to NEDD8 and Ub chain formation, proteomic studies have reported phosphorylation, acetylation and succinylation sites on NEDD8. The functional significance of this observation remains unknown. There is a general lack of information on non-cullin protein neddylation under homeostatic conditions. Furthermore, the physiological relevance of several reported NEDD8 substrates, including p62/sequestosome, remains unknown. Whether neddylation is functionally distinct from ubiquitination is a question that remains unresolved. For example, polyneddylation and polyubiquitination at DNA damage sites or in response to other stress conditions are functionally redundant, and NEDD8 and Ub may be recognised by the same interaction motifs. However, in certain circumstances, such as the neddylation or ubiquitination of TGFβRII, these two modifications can elicit distinct biological responses. Efforts are clearly needed to identify and characterise NEDD8-interacting domains and proteins.

NUB1 proteins cause the degradation of FAT10- and NEDD8-conjugated targets. Their expression regulates NEDD8- and FAT10-based signalling in response to cellular stresses (34,45). However, the structural mechanisms of NUB1 protein and its clinical relevance in UBL pathways remain to be explored. Hosono *et al* (31) found that overexpression of NUB1 inhibits cell growth, and the same study demonstrated lower NUB1 mRNA expression in IFNα-sensitive 4THUR cells. The same study highlighted that NUB1 is not induced in IFNα-resistant cells, although transiently expressed NUB1 sensitised the same cells and induced apoptosis (31). Therefore, killing IFNα-resistant cells by increasing NUB1 activity is a potential strategy (31).

FAT10 research is still in an early stage and the biological consequences of FAT10ylation are poorly described. De-FAT10ylating enzymes are under active investigation as drug targets in the pharmaceutical industry at present, based on the fact that a number of putative FAT10 targets are oncogenes or inhibitors of apoptosis. Future works should focus on the FAT10-modulated proteasome system and mechanisms of cytokine-induced reactions.

5. Conclusion

Experimental studies have demonstrated that negative regulation of the Ub, NEDD8 and FAT10-conjugation pathways have great potential in the context of cancer suppression. SCF complexes are often deregulated in cancer and could be modulated through manipulation of cullin neddylation. Neddylation and FAT10ylation inhibitors have recently been developed as a novel class of anticancer agent. These compounds are expected to exhibit better specificity for cancer cells and have reduced toxicity. Degrading enzymes, such as CSN and NUB1/NUB1L, are attractive candidates for the inhibition of Ub, NEDD8 and FAT10-ligase activities (34). These are expected to provide new strategies in anticancer therapy.

Acknowledgements

Mr. Ka-Liong Tan is financially supported by the Academic Staff Training Scheme (SLAI scheme), Ministry of Education, Malaysia.

References

1. Ciechanover A: The ubiquitin-proteasome pathway: On protein death and cell life. EMBO J 17: 7151-7160, 1998.
2. Ciechanover A and Schwartz AL: The ubiquitin-proteasome pathway: The complexity and myriad functions of proteins death. Proc Natl Acad Sci USA 95: 2727-2730, 1998.
3. Hershko A: The ubiquitin system for protein degradation and some of its roles in the control of the cell division cycle. Cell Death Differ 12: 1191-1197, 2005.
4. Hershko A and Ciechanover A: The ubiquitin system. Annu Rev Biochem 67: 425-479, 1998.
5. Liu YC, Pan J, Zhang C, Fan W, Collinge M, Bender JR and Weissman SM: A MHC-encoded ubiquitin-like protein (FAT10) binds noncovalently to the spindle assembly checkpoint protein MAD2. Proc Natl Acad Sci USA 96: 4313-4318, 1999.
6. Gunawardena HP, Huang Y, Kenjale R, Wang H, Xie L and Chen X: Unambiguous characterization of site-specific phosphorylation of leucine-rich repeat Fli-I-interacting protein 2 (LRRFIP2) in Toll-like receptor 4 (TLR4)-mediated signaling. J Biol Chem 286: 10897-10910, 2011.
7. Hochstrasser M: Origin and function of ubiquitin-like proteins. Nature 458: 422-429, 2009.
8. Bawa-Khalfe T and Yeh ET: SUMO losing balance: SUMO proteases disrupt SUMO homeostasis to facilitate cancer development and progression. Genes Cancer 1: 748-752, 2010.
9. Rao-Naik C, delaCruz W, Laplaza JM, Tan S, Callis J and Fisher AJ: The rub family of ubiquitin-like proteins. Crystal structure of Arabidopsis rub1 and expression of multiple rubs in Arabidopsis. J Biol Chem 273: 34976-34982, 1998.
10. Whitby FG, Xia G, Pickart CM and Hill CP: Crystal structure of the human ubiquitin-like protein NEDD8 and interactions with ubiquitin pathway enzymes. J Biol Chem 273: 34983-34991, 1998.
11. Kamitani T, Kito K, Nguyen HP and Yeh ET: Characterization of NEDD8, a developmentally down-regulated ubiquitin-like protein. J Biol Chem 272: 28557-28562, 1997.
12. Kim DY, Kwon E, Hartley PD, Crosby DC, Mann S, Krogan NJ and Gross JD: CBFβ stabilizes HIV Vif to counteract APOBEC3 at the expense of RUNX1 target gene expression. Mol Cell 49: 632-644, 2013.
13. Hori T, Osaka F, Chiba T, Miyamoto C, Okabayashi K, Shimbara N, Kato S and Tanaka K: Covalent modification of all members of human cullin family proteins by NEDD8. Oncogene 18: 6829-6834, 1999.
14. Salon C, Brambilla E, Brambilla C, Lantuejoul S, Gazzeri S and Eymin B: Altered pattern of Cul-1 protein expression and neddylation in human lung tumours: Relationships with CAND1 and cyclin E protein levels. J Pathol 213: 303-310, 2007.
15. Chairatvit K and Ngamkitidechakul C: Control of cell proliferation via elevated NEDD8 conjugation in oral squamous cell carcinoma. Mol Cell Biochem 306: 163-169, 2007.
16. Raasi S, Schmidtke G and Groettrup M: The ubiquitin-like protein FAT10 forms covalent conjugates and induces apoptosis. J Biol Chem 276: 35334-35343, 2001.
17. Fan W, Cai W, Parimoo S, Schwarz DC, Lennon GG and Weissman SM: Identification of seven new human MHC class I region genes around the HLA-F locus. Immunogenetics 44: 97-103, 1996.
18. Lee CG, Ren J, Cheong IS, Ban KH, Ooi LL, Yong Tan S, Kan A, Nuchprayoon I, Jin R, Lee KH, *et al*: Expression of the FAT10 gene is highly upregulated in hepatocellular carcinoma and other gastrointestinal and gynecological cancers. Oncogene 22: 2592-2603, 2003.
19. Soucy TA, Dick LR, Smith PG, Milhollen MA and Brownell JE: The NEDD8 conjugation pathway and its relevance in cancer biology and therapy. Genes Cancer 1: 708-716, 2010.
20. Richardson PG, Sonneveld P, Schuster MW, Irwin D, Stadtmauer EA, Facon T, Harousseau JL, Ben-Yehuda D, Lonial S, Goldschmidt H, *et al*: Bortezomib or high-dose dexamethasone for relapsed multiple myeloma. N Engl J Med 352: 2487-2498, 2005.
21. San Miguel JF, Schlag R, Khuageva NK, Dimopoulos MA, Shpilberg O, Kropff M, Spicka I, Petrucci MT, Palumbo A, Samoilova OS, *et al*: Bortezomib plus melphalan and prednisone for initial treatment of multiple myeloma. N Engl J Med 359: 906-917, 2008.
22. Kane RC, Dagher R, Farrell A, Ko CW, Sridhara R, Justice R and Pazdur R: Bortezomib for the treatment of mantle cell lymphoma. Clin Cancer Res 13: 5291-5294, 2007.

23. Yang Y, Kitagaki J, Dai RM, Tsai YC, Lorick KL, Ludwig RL, Pierre SA, Jensen JP, Davydov IV, Oberoi P, *et al*: Inhibitors of ubiquitin-activating enzyme (E1), a new class of potential cancer therapeutics. Cancer Res 67: 9472-9481, 2007.
24. Zhao Y, Xiong X, Jia L and Sun Y: Targeting Cullin-RING ligases by MLN4924 induces autophagy via modulating the HIF1-REDD1-TSC1-mTORC1-DEPTOR axis. Cell Death Dis 3: e386, 2012.
25. Kamitani T, Kito K, Fukuda-Kamitani T and Yeh ET: Targeting of NEDD8 and its conjugates for proteasomal degradation by NUB1. J Biol Chem 276: 46655-46660, 2001.
26. Kito K, Yeh ET and Kamitani T: NUB1, a NEDD8-interacting protein, is induced by interferon and down-regulates the NEDD8 expression. J Biol Chem 276: 20603-20609, 2001.
27. Tanaka T, Kawashima H, Yeh ET and Kamitani T: Regulation of the NEDD8 conjugation system by a splicing variant, NUB1L. J Biol Chem 278: 32905-32913, 2003.
28. Tanji K, Tanaka T and Kamitani T: Interaction of NUB1 with the proteasome subunit S5a. Biochem Biophys Res Commun 337: 116-120, 2005.
29. Groettrup M, Pelzer C, Schmidtke G and Hofmann K: Activating the ubiquitin family: UBA6 challenges the field. Trends Biochem Sci 33: 230-237, 2008.
30. Bornstein G, Ganoth D and Hershko A: Regulation of neddylation and deneddylation of cullin1 in SCFSkp2 ubiquitin ligase by F-box protein and substrate. Proc Natl Acad Sci USA 103: 11515-11520, 2006.
31. Hosono T, Tanaka T, Tanji K, Nakatani T and Kamitani T: NUB1, an interferon-inducible protein, mediates anti-proliferative actions and apoptosis in renal cell carcinoma cells through cell-cycle regulation. Br J Cancer 102: 873-882, 2010.
32. Lu B, Al-Ramahi I, Valencia A, Wang Q, Berenshteyn F, Yang H, Gallego-Flores T, Ichcho S, Lacoste A, Hild M, *et al*: Identification of NUB1 as a suppressor of mutant Huntington toxicity via enhanced protein clearance. Nat Neurosci 16: 562-570, 2013.
33. Kanaya K, Sohocki MM and Kamitani T: Abolished interaction of NUB1 with mutant AIPL1 involved in Leber congenital amaurosis. Biochem Biophys Res Commun 317: 768-773, 2004.
34. Tanaka T, Nakatani T and Kamitani T: Inhibition of NEDD8-conjugation pathway by novel molecules: Potential approaches to anticancer therapy. Mol Oncol 6: 267-275, 2012.
35. Haas AL, Ahrens P, Bright PM and Ankel H: Interferon induces a 15-kilodalton protein exhibiting marked homology to ubiquitin. J Biol Chem 262: 11315-11323, 1987.
36. Ichimura Y, Kirisako T, Takao T, Satomi Y, Shimonishi Y, Ishihara N, Mizushima N, Tanida I, Kominami E, Ohsumi M, *et al*: A ubiquitin-like system mediates protein lipidation. Nature 408: 488-492, 2000.
37. Rabut G and Peter M: Function and regulation of protein neddylation. 'Protein modifications: Beyond the usual suspects' review series. EMBO Rep 9: 969-976, 2008.
38. Walden H, Podgorski MS, Huang DT, Miller DW, Howard RJ, Minor DL Jr, Holton JM and Schulman BA: The structure of the APPBP1-UBA3-NEDD8-ATP complex reveals the basis for selective ubiquitin-like protein activation by an E1. Mol Cell 12: 1427-1437, 2003.
39. Leidecker O, Matic I, Mahata B, Pion E and Xirodimas DP: The ubiquitin E1 enzyme Ube1 mediates NEDD8 activation under diverse stress conditions. Cell cycle 11: 1142-1150, 2012.
40. Olsen SK, Capili AD, Lu X, Tan DS and Lima CD: Active site remodelling accompanies thioester bond formation in the SUMO E1. Nature 463: 906-912, 2010.
41. Huang DT, Hunt HW, Zhuang M, Ohi MD, Holton JM and Schulman BA: Basis for a ubiquitin-like protein thioester switch toggling E1-E2 affinity. Nature 445: 394-398, 2007.
42. Huang DT, Ayrault O, Hunt HW, Taherbhoy AM, Duda DM, Scott DC, Borg LA, Neale G, Murray PJ, Roussel MF and Schulman BA: E2-RING expansion of the NEDD8 cascade confers specificity to cullin modification. Mol Cell 33: 483-495, 2009.
43. Kamura T, Conrad MN, Yan Q, Conaway RC and Conaway JW: The Rbx1 subunit of SCF and VHL E3 ubiquitin ligase activates Rub1 modification of cullins Cdc53 and Cul2. Genes Dev 13: 2928-2933, 1999.
44. Enchev RI, Schulman BA and Peter M: Protein neddylation: Beyond cullin-RING ligases. Nat Rev Mol Cell Biol 16: 30-44, 2015.
45. Hjerpe R, Thomas Y, Chen J, Zemla A, Curran S, Shpiro N, Dick LR and Kurz T: Changes in the ratio of free NEDD8 to ubiquitin triggers NEDDylation by ubiquitin enzymes. Biochem J 441: 927-936, 2012.
46. Saha A and Deshaies RJ: Multimodal activation of the ubiquitin ligase SCF by Nedd8 conjugation. Mol Cell 32: 21-31, 2008.
47. Chan Y, Yoon J, Wu JT, Kim HJ, Pan KT, Yim J and Chien CT: DEN1 deneddylates non-cullin proteins in vivo. J Cell Sci 121: 3218-3223, 2008.
48. Gong N, Li XY, Xiao Q and Wang YX: Identification of a novel spinal dorsal horn astroglial D-amino acid oxidase-hydrogen peroxide pathway involved in morphine antinociceptive tolerance. Anesthesiology 120: 962-975, 2014.
49. Lyapina S, Cope G, Shevchenko A, Serino G, Tsuge T, Zhou C, Wolf DA, Wei N, Shevchenko A and Deshaies RJ: Promotion of NEDD-CUL1 conjugate cleavage by COP9 signalosome. Science 292: 1382-1385, 2001.
50. Mendoza HM, Shen LN, Botting C, Lewis A, Chen J, Ink B and Hay RT: NEDP1, a highly conserved cysteine protease that deNEDDylates Cullins. J Biol Chem 278: 25637-25643, 2003.
51. Schwechheimer C, Serino G, Callis J, Crosby WL, Lyapina S, Deshaies RJ, Gray WM, Estelle M and Deng XW: Interactions of the COP9 signalosome with the E3 ubiquitin ligase SCFTIRI in mediating auxin response. Science 292: 1379-1382, 2001.
52. Goldenberg SJ, Cascio TC, Shumway SD, Garbutt KC, Liu J, Xiong Y and Zheng N: Structure of the Cand1-Cul1-Roc1 complex reveals regulatory mechanisms for the assembly of the multisubunit cullin-dependent ubiquitin ligases. Cell 119: 517-528, 2004.
53. Liu J, Furukawa M, Matsumoto T and Xiong Y: NEDD8 modification of CUL1 dissociates p120 (CAND1), an inhibitor of CUL1-SKP1 binding and SCF ligases. Mol Cell 10: 1511-1518, 2002.
54. Duda DM, Borg LA, Scott DC, Hunt HW, Hammel M and Schulman BA: Structural insights into NEDD8 activation of cullin-RING ligases: Conformational control of conjugation. Cell 134: 995-1006, 2008.
55. Morimoto M, Nishida T, Nagayama Y and Yasuda H: Nedd8-modification of Cul1 is promoted by Roc1 as a Nedd8-E3 ligase and regulates its stability. Biochem Biophys Res Commun 301: 392-398, 2003.
56. Osaka F, Kawasaki H, Aida N, Saeki M, Chiba T, Kawashima S, Tanaka K and Kato S: A new NEDD8-ligating system for cullin-4A. Genes Dev 12: 2263-2268, 1998.
57. Podust VN, Brownell JE, Gladysheva TB, Luo RS, Wang C, Coggins MB, Pierce JW, Lightcap ES and Chau V: A Nedd8 conjugation pathway is essential for proteolytic targeting of p27Kip1 by ubiquitination. Proc Natl Acad Sci USA 97: 4579-4584, 2000.
58. Read MA, Brownell JE, Gladysheva TB, Hottelet M, Parent LA, Coggins MB, Pierce JW, Podust VN, Luo RS, Chau V and Palombella VJ: Nedd8 modification of cul-1 activates SCF (beta (TrCP))-dependent ubiquitination of IkappaBalpha. Mol Cell Biol 20: 2326-2333, 2000.
59. Wada H, Yeh ET and Kamitani T: Identification of NEDD8-conjugation site in human cullin-2. Biochem Biophys Res Commun 257: 100-105, 1999.
60. Kim W, Bennett EJ, Huttlin EL, Guo A, Li J, Possemato A, Sowa ME, Rad R, Rush J, Comb MJ, *et al*: Systematic and quantitative assessment of the ubiquitin-modified proteome. Mol Cell 44: 325-340, 2011.
61. Jeram SM, Srikumar T, Zhang XD, Anne Eisenhauer H, Rogers R, Pedrioli PG, Matunis M and Raught B: An improved SUMmOn-based methodology for the identification of ubiquitin and ubiquitin-like protein conjugation sites identifies novel ubiquitin-like protein chain linkages. Proteomics 10: 254-265, 2010.
62. van der Veen AG and Ploegh HL: Ubiquitin-like proteins. Annu Rev Biochem 81: 323-357, 2012.
63. McLarnon A: Cancer: Mdm2-regulated stabilization of HuR by neddylation in HCC and colon cancer-a possible target for therapy. Nat Rev Gastroenterol Hepatol 9: 4, 2011.
64. Ryu JH, Li SH, Park HS, Park JW, Lee B and Chun YS: Hypoxia-inducible factor alpha subunit stabilization by NEDD8 conjugation is reactive oxygen species-dependent. J Biol Chem 286: 6963-6970, 2011.
65. Freiberg RA, Hammond EM, Dorie MJ, Welford SM and Giaccia AJ: DNA damage during reoxygenation elicits a Chk2-dependent checkpoint response. Mol Cell Biol 26: 1598-1609, 2006.
66. Ma T, Chen Y, Zhang F, Yang CY, Wang S and Yu X: RNF111-dependent neddylation activates DNA damage-induced ubiquitination. Mol Cell 49: 897-907, 2013.
67. Le Moan N, Houslay DM, Christian F, Houslay MD and Akassoglou K: Oxygen-dependent cleavage of the p75 neurotrophin receptor triggers stabilization of HIF-1α. Mol Cell 44: 476-490, 2011.

68. Pawlus MR, Wang L and Hu CJ: STAT3 and HIF1α cooperatively activate HIF1 target genes in MDA-MB-231 and RCC4 cells. Oncogene 33: 1670-1679, 2014.
69. Choo YS, Vogler G, Wang D, Kalvakuri S, Iliuk A, Tao WA, Bodmer R and Zhang Z: Regulation of parkin and PINK1 by neddylation. Hum Mol Genet 21: 2514-2523, 2012.
70. Kandala S, Kim IM and Su H: Neddylation and deneddylation in cardiac biology. Am J Cardiovasc Dis 4: 140-158, 2014.
71. Abida WM, Nikolaev A, Zhao W, Zhang W and Gu W: FBXO11 promotes the Neddylation of p53 and inhibits its transcriptional activity. J Biol Chem 282: 1797-1804, 2007.
72. Noguchi K, Okumura F, Takahashi N, Kataoka A, Kamiyama T, Todo S and Hatakeyama S: TRIM40 promotes neddylation of IKKγ and is downregulated in gastrointestinal cancers. Carcinogenesis 32: 995-1004, 2011.
73. Cao X and Sudhof TC: A transcriptionally [correction of transcriptively] active complex of APP with Fe65 and histone acetyltransferase Tip60. Science 293: 115-120, 2001.
74. Lee MR, Lee D, Shin SK, Kim YH and Choi CY: Inhibition of APP intracellular domain (AICD) transcriptional activity via covalent conjugation with Nedd8. Biochem Biophys Res Commun 366: 976-981, 2008.
75. Theng SS, Wang W, Mah WC, Chan C, Zhuo J, Gao Y, Qin H, Lim L, Chong SS, Song J and Lee CG: Disruption of FAT10-MAD2 binding inhibits tumor progression. Proc Natl Acad Sci USA 111: E5282-E5291, 2014.
76. Michel L, Diaz-Rodriguez E, Narayan G, Hernando E, Murty VV and Benezra R: Complete loss of the tumor suppressor MAD2 causes premature cyclin B degradation and mitotic failure in human somatic cells. Proc Natl Acad Sci USA 101: 4459-4464, 2004.
77. Tapia C, Kutzner H, Mentzel T, Savic S, Baumhoer D and Glatz K: Two mitosis-specific antibodies, MPM-2 and phospho-histone H3 (Ser28), allow rapid and precise determination of mitotic activity. Am J Surg Pathol 30: 83-89, 2006.
78. Wagenaar-Miller RA, Gorden L and Matrisian LM: Matrix metalloproteinases in colorectal cancer: Is it worth talking about? Cancer Metastasis Rev 23: 119-135, 2004.
79. Aichem A, Kalveram B, Spinnenhirn V, Kluge K, Catone N, Johansen T and Groettrup M: The proteomic analysis of endogenous FAT10 substrates identifies p62/SQSTM1 as a substrate of FAT10ylation. J Cell Sci 125: 4576-4585, 2012.
80. Gao Y, Theng SS, Zhuo J, Teo WB, Ren J and Lee CG: FAT10, an ubiquitin-like protein, confers malignant properties in non-tumorigenic and tumorigenic cells. Carcinogenesis 35: 923-934, 2014.
81. Lukasiak S, Schiller C, Oehlschlaeger P, Schmidtke G, Krause P, Legler DF, Autschbach F, Schirmacher P, Breuhahn K and Groettrup M: Proinflammatory cytokines cause FAT10 upregulation in cancers of liver and colon. Oncogene 27: 6068-6074, 2008.
82. Pelzer C, Kassner I, Matentzoglu K, Singh RK, Wollscheid HP, Scheffner M, Schmidtke G and Groettrup M: UBE1L2, a novel E1 enzyme specific for ubiquitin. J Biol Chem 282: 23010-23014, 2007.
83. Jin J, Li X, Gygi SP and Harper JW: Dual E1 activation systems for ubiquitin differentially regulate E2 enzyme charging. Nature 447: 1135-1138, 2007.
84. Chiu YH, Sun Q and Chen ZJ: E1-L2 activates both ubiquitin and FAT10. Mol Cell 27: 1014-1023, 2007.
85. Aichem A, Pelzer C, Lukasiak S, Kalveram B, Sheppard PW, Rani N, Schmidtke G and Groettrup M: USE1 is a bispecific conjugating enzyme for ubiquitin and FAT10, which FAT10ylates itself in cis. Nat Commun 1: 13, 2010.
86. Hipp MS, Kalveram B, Raasi S, Groettrup M and Schmidtke G: FAT10, a ubiquitin-independent signal for proteasomal degradation. Mol Cell Biol 25: 3483-3491, 2005.
87. Hipp MS, Raasi S, Groettrup M and Schmidtke G: NEDD8 ultimate buster-1L interacts with the ubiquitin-like protein FAT10 and accelerates its degradation. J Biol Chem 279: 16503-16510, 2004.
88. Ren J, Kan A, Leong SH, Ooi LL, Jeang KT, Chong SS, Kon OL and Lee CG: FAT10 plays a role in the regulation of chromosomal stability. J Biol Chem 281: 11413-11421, 2006.
89. Merbl Y, Refour P, Patel H, Springer M and Kirschner MW: Profiling of ubiquitin-like modifications reveals features of mitotic control. Cell 152: 1160-1172, 2013.
90. Gong P, Canaan A, Wang B, Leventhal J, Snyder A, Nair V, Cohen CD, Kretzler M, D'Agati V, Weissman S and Ross MJ: The ubiquitin-like protein FAT10 mediates NF-kappaB activation. J Am Soc Nephrol 21: 316-326, 2010.
91. Bjorkoy G, Lamark T, Brech A, Outzen H, Perander M, Overvatn A, Stenmark H and Johansen T: p62/SQSTM1 forms protein aggregates degraded by autophagy and has a protective effect on huntingtin-induced cell death. J Cell Biol 171: 603-614, 2005.

Translational Relevance of AIPL1 and NUB1 in Cancer



Ka-Liong TAN

Radcliffe Department of Medicine

Lincoln College

University of Oxford

Trinity 2017

A thesis submitted in fulfilment of the requirements for the degree of
Doctor of Philosophy at the University of Oxford

Abstract

Background: Aryl Hydrocarbon Receptor Interacting Protein-Like 1 (AIPL1) interacts with NUB1 and restricts the entry of NUB1 protein into the nucleus. The interferon-induced NEDD8 ultimate buster (NUB1) protein causes degradation of neddylated and FAT10ylated proteins through the ubiquitin proteasome system. We observed AIPL1 were frequently down-regulated in various cancers compared to normal tissues. The mechanistic roles of AIPL1 and NUB1 protein in cancer cell cycle regulation remain unexplored.

Results: Meta-analysis of cancer databases revealed that expression transcripts of chaperones, including AIPL1, were down-regulated in lung, pancreatic cancer and breast cancer relative to the adjacent normal tissues. Opposite levels of both AIPL1 and NUB1 transcripts were observed in the breast cancer. So it triggers the *in vitro* experiments using breast cancer cells. METABRIC breast cancer clinical cohort highlighted that patients with low NUB1 transcripts had poor survival in the ER-negative subgroup (but not in ER-positive) of breast cancer patients: hazard ratio (HR)=0.66, 95% confidence interval (CI)=0.5-0.87, p=0.003 and triple negative subgroup of breast cancer patients: HR=0.67, 95% CI=0.47-0.96, p=0.028. NUB1 silencing significantly inhibits *in vitro* cell growth in MDA-MB-231 and MCF7 under hypoxia. AIPL1 protein forms multimers in cancer cells. NUB1 protein moved into the nucleus in hypoxia (0.1% O_2 48hrs) with final confluency at 80-90%. p21 (marker of senescence) & p27 (marker of cell cycle arrest) accumulated in NUB1-silent MDA-MB-231 and RCC4 cells. It suggested that low NUB1 nuclear localisation in hypoxia cause cancer cell cycle arrest. In MDA-MB-231 cell, upon hypoxia, neddylation inhibitor (MLN4924) treated and siNUB1 transfected cells showed decreased CUL1 and further accumulated p21 & p27. The evidence suggested lower neddylated CUL1 and reduced NUB1 cooperatively stabilise p21 and p27 as the substrate of CUL1-ubiquitin ligase. The neddylation inhibitor MLN4924 treated and NUB1 knockdown group exhibited more cells in sub-G1 stage as compared to the control group. In connection to higher p21/p27, it is associated with prolonged arrested

cellular aging with depletion. After silencing of NUB1, the increases in cell death of cancer cells upon hypoxia happen through the neddylation-dependent CUL1-p27-p21 and CUL2-VHL axis. We then demonstrated that HIF1α protein could be both neddylated and FAT10ylated upon reoxygenation. In a tissue microarray study of breast cancer, lower cytoplasmic expression (n=57) had worse overall survival than higher cytoplasmic expression (n=57): HR=1.779, 95% CI=1.006-3.346, p=0.048.

Conclusions: AIPL1 and NUB1 proteins exert a role in cell cycle regulation in breast cancer. Low cytoplasmic NUB1 levels are observed in the G_1-S transition of cancer cells. NUB1 depletion causes G_0/G_1 phase arrest due to CUL1 and CUL2 ubiquitin E3 ligase-dependent pathways.

Dedication

To my parents,

Swee-Eng and Min-Ching Tan,

And all of my friends,

Without whom none of my success would be possible.

Acknowledgements

First I would like to thank my parents for their emphasis on learning as a way of life, and my teachers and professors for helping me and maximising my academic potential.

I would like to thank **Academic Staff Training Scheme (ASTS/SLAI)** for the scholarship which allowed me to pursue my doctoral studies at the University of Oxford. I would like to thank my funding department line manager, Prof. Emeritus Dato' Dr. Nik Mohd Nasri Nik Ismail and Professor Dr. Muhammad Shamsir Bin Mohd Aris.

I would also like to thank my DPhil supervisors, Professor Francesco Pezzella and Professor Oreste Acuto for their mentorship and guidance, as well as for their helps in experimental design and techniques.

I would like to pay tribute to my idea donor below for their expert input on my project, and the rest of my colleagues in Oxford for their aid in all other matters.

Tumour Pathology Group
Prof. Francesco Pezzella
Prof. Kevin Gatter
Dr. Jianting Hu
Dr. Russell Leek
Ms. Katherine Freeman
Ms Helen Turley
Mr. Graham Steers

T cell Signaling Group
Prof. Oreste Acuto
Dr. Anna-Lisa Lanz
Dr. Giulia Masi

Hypoxia and Angiogenesis Group
Prof. Adrian Harris
Dr. Christos Zois

Gene Medicine Therapy Group
Prof. Deborah Gill
Mr. Jean-Francois Gelinas

Applied Computational Genomics Group
Dr. Francesca Buffa
Dr. Syed Haider

FACS Facility Team (WIMM)
Kevin Clark
Paul Sopp

High Temperature Superconductivity Group
Prof. Chris Grovenor
Dr. Kexue Li

Centre for Microscopy, Characterisation and Analysis (CMCA), University of Western Australia
Dr. Haibo Jiang



Finally, I would like to acknowledge the Ministry of Education (Malaysia) and NDCLS, RDM for funding this research.

List of figures

Figure 1. 1 Structures of client proteins and the hydrophobic effects..... 5

Figure 1. 2 Roles of chaperones in proteostasis..... 6

Figure 1. 3 Structure of various chaperones..... 9

Figure 1. 4 Details of AIPL1 gene..... 21

Figure 1. 5 The function of AIP and AIPL1. 24

Figure 1. 6 Interaction of AIPL1 and NUB1 proteins.. 27

Figure 1. 7 Structural representation of (A) Ub, NEDD8 and FAT10, and (B) NUB1..... 28

Figure 1. 8 Solution structure of N-terminal ubiquitin-like domain of human NUB1. 30

Figure 1. 9 NEDD8 conjugation pathway and roles of NUB1 on neddylated CUL1..... 33

Figure 1. 10 NEDD8 conjugation and ubiquitination pathway. 34

Figure 1. 11 Domain structure of NUB1L, FAT10 and RPN10. 37

Figure 3. 1 Box and whisker plots of AIPL1 and NUB1 in breast cancer dataset…… 60

Figure 3. 2 Venn diagram of overlapping genes across the NUB1 coexpression networks..62

Figure 3. 3 NUB1 coexpression network profile..... 65

Figure 3. 4 Pairwise association plot of CUL1 and TMEM140 against NUB1 transcripts..66

Figure 3. 5 Survival curves of AIPL1 in different subgroup.. 70

Figure 3. 6 Survival curves of AIPL1 and NUB1 in different subgroup.. 73

Figure 3. 7 Gene expression patterns of AIPL1 and NUB1 based on the intrinsic molecular subtypes status of METABRIC dataset. 76

Figure 3. 8 Survival curves of FAT10 in ER-, Basal and triple negative subgroup……79

Figure 3. 9 Gene expression patterns of NEDD8 and FAT10 based on the intrinsic molecular subtypes status of METABRIC dataset. .....……..81

Figure 3. 10 Gene expression patterns of CUL1 and p21 based on the intrinsic molecular subtypes status of METABRIC dataset. 83

Figure 3. 11 Heatmap showing genes differentially expressed in patients using RNA-Seq data..... 86

Figure 4. 1 Protein expressions……...93

Figure 4. 3 Endogenous transcript expressions in cancer cells…….94

Figure 4. 4 Immunohistochemistry staining of various cancer cells……..98

Figure 4. 5 Oligomerisation of AIPL1 proteins analysed by native PAGE and immunoblotting.. 101

Figure 4. 6 Time course experiment of reoxygenated MDA-MB-231.. 103

Figure 4. 7 Cell cycle analysis in NUB1 knockdown MDA-MB-231.. 105

Figure 4. 8 Cancer cell growth in NUB1 knockdown condition..... 106

Figure 4. 9 Cytoplasmic AIPL1 dimerisation enhances NUB1 shuttling into the nucleus. .. 108

Figure 4. 10 NUB1 silencing enhances neddylation inhibition effects onto p27 (but not p21) protein levels..... 110

Figure 4. 11 Cell cycle profile of MDA-MB-231..... 111

Figure 4. 12 Knockdown of NUB1 and cell cycle analysis.. 112

Figure 5. 1 Ubiquitin E3 ligases and their substrates……114

Figure 5. 2 Schoefeld's first speculation on how VHL regulates p27 and p21.……..116

Figure 5. 3 Cell cycle analysis on the NUB1 knowckdown effect in RCC4plusVHL and RCC4 cells under normoxic and hypoxic conditions.……120

Figure 5. 4 NUB1 knockdown upregulate a. HIF1α and down-regulate b. VHL proteins. .....….122

Figure 5. 5 Cell cycle analysis on the NUB1 knowckdown effect in RCC4 cells under normoxic and hypoxic conditions..……124

Figure 5. 6 Depletion of NUB1 upregulated HIF1α and p27 proteins. 126

Figure 5. 7 NEDD8 and FAT10 signals detected in endogenous HIF1α. 128

Figure 5. 8 Hypothesis pipeline of the chapter 5..... 130

Figure 6. 1 Immunostaining of NUB1 using monoclonal mouse antibody (4H2) (1:20) dilution on RCC4plusVHL cells counterstain with hematoxylin…….....135

Figure 6. 2 NUB1 expression on representative node negative breast cancer tissue microarray spots. 137

Figure 6. 3 Distribution of NUB1 immunohistochemical staining scores in primary breast cancer. …..... 138

Figure 6. 4 Correlation of NUB1 cytoplasmic IPS with nuclear IPS……140

Figure 6. 5 Relationship between ER status and NUB1 localisation.. 141

Figure 6. 6 Relationship between ER and prognosis in breast cancer patients using the log-rank test….. 144

Figure 7. 2 Central dogma of NUB1-mediated cell cycle regulation via p27 and p21..... 155

List of tables

Table 1. 1 Development of the chaperone concept.. 8

Table 1. 3 Classification of A. HSP70 and HSP110 and B. HSP90.. 13

Table 1. 4 List of cochaperones. 14

Table 1. 5 Summary of meta-analysis.. 18

Table 1. 6 Summary of down-regulated AIPL1.. 18

Table 1. 7 Overview of the enzymatic cascade involved in UBLs conjugation. 29

Table 2. 1 Immunostaining Antibodies 46

Table 3. 1 Classification of breast cancer and the key features of the subtypes 133

Table 3. 2 Genes and cancer summary from Oncomine.. 56

Table 3. 3 Summary of A. AIPL1 & B. NUB1 datasets.. 57

Table 3. 4 Summary of NUB1 and CUL1 enriched pathway.. 63

Table 3. 5 Survival curves summary. 74

Table 3. 6 FAT10 Genes and cancer summary from Oncomine.. 80

Table 3. 7 Summary of NUB1 vs. FAT10 and NEDD8 mRNA coefficient, ρ. 81

Table 3. 8 Summary of AIPL1 and NUB1 on CUL1 and p21 mRNA expression. 84

Table 3. 9 HIF1α and downstream target.. 85

Table 4. 1 Summary of AIPL1, NUB1, NEDD8 and FAT10 gene products (protein or transcripts) in all cancer cell line..... 99

Table 6. 1 Clinicopathological variables according to ER status. 139

Table 6. 2 Relationship between high/low NUB1 subcellular localisation and overall survival/ relapse free survival. 143

Table 6. 3 Summary of overall survival analysis based on the mean IPS. 146

List of abbreviations

AIPL1	Aryl hydrocarbon interacting protein like-1
AMPK	AMP-activated protein kinase
ARNT	Aryl hydrocarbon receptor nuclear translocator
ABC	ATP binding cassette
ATG5	Autophagy-related 5
BRAC1	Breast cancer 1
CA	Carbonic anhydrase
cDNA	Complementary DNA
°C	Degrees celcius
COL5A1	Collagen Type V Alpha 1 Chain
ΔΔCT	Delta delta cycle threshold
DLK1	Delta Like Non-Canonical Notch Ligand 1
DNA	Deoxyribonucleic acid
DMSO	Dimethylsulphoxide
ER	Estrogen receptor
ECM	Extracellular matrix
FAS	Fatty acid synthase
FA	Fatty acids
FAT10	HLA-F adjacent transcript 10
FCS	Foetal calf serum
FC	Fold Change
HER2	Human epidermal factor receptor 2
HIF-1	Hypoxia inducible transcription factor 1
HRE	Hypoxia-response elements
IGF	Insulin growth factor
IGF2	Insulin-like growth factor 2
IFNs	Interferons
IL	Interleukins
kDa	kiloDaltons
LDHA	Lactate dehydrogenase-A
L	Litre
LPR	Low density lipoprotein receptor related protein
MMP	Matrix metalloproteinases
mRNA	Messenger RNA (Ribonucleic acid)

µg	Micrograms
µl	Microlitres
µm	Micrometres
µM	Micromolar
ml	Millilitres
mM	Millimolar
M	Molar
mAb	Monoclonal antibodies
MDA5	Melanoma differentiation-associated gene 5
MHC	Major histocompatibility complexes
NEDD8	Neural Precursor Cell Expressed, Developmentally Down-Regulated 8
NF-kB	Nuclear factor-kappaB
NUB1	NEDD8 Ultimate Buster 1
ODDDs	Oxygen dependent degradation domains
%	Percent
PBS	Phosphate-buffered saline
PDGF	Platelet-derived growth factor
PCR	Polymerase chain reaction
pH	Power of hydrogen (in solution)
PHDs	Prolyl hydroxylase
RIG-1	Retinoic acid-inducible gene I
ROS	Reactive oxygen species
RNA	Ribonucleic acid
scr	Scramble control
siRNA	Small interfering RNA
SDS	Sodium dodecyl sulfate
bHLH	Basic helix-loop-helix
TCR	T Cell receptor
TOR	Target of Rapamycin
TGF β	Transforming growth factor β
TNFα	Tumor necrosis factor α
TNFR2	Tumor necrosis factor receptor 2
TAMs	Tumour associated macrophages
VEGF	Vascular endothelial growth factor
VHL	Von Hippel Lindau

Table of content

Abstract I

Dedication III

Acknowledgements IV

List of figures V

List of tables VIII

List of abbreviations X

Table of content XII

Chapter 1 Introduction 1

1.1 Proteostasis (also known as Protein Homoeostasis) 1

1.2 Human Chaperones and Cancer 7

1.2.1 Discovery of Chaperones and historical perspectives 7

1.2.2 Classification of Chaperones 10

1.2.3 Roles of Chaperones and Cochaperones in Cancer 15

1.2 Microarray and chaperones/cochaperones gene-specific meta-analysis 17

1.3 Introduction of AIPL1 protein 19

1.3.1 Interaction of NUB1 and the downstream ubiquitin pathway 25

1.3.2 Background of NUB1 28

1.4 Neddylation and its functions 30

1.5 FAT10ylation and its functions 35

1.6 Ubiquitin Proteasome System 38

1.7 Rationale of study ..... **Error! Bookmark not defined.**

1.8 Objectives of study 42

Chapter 2 Methods and Materials 43

2.1 Cell Line 43

2.2 Cell Culture 43

2.3 Counting Cells 44

2.4 Preparation and Recovery of cell stocks (cryo-preserved cells) 44

2.5 Gene silencing by RNA Interference 45

2.6 Immunostaining of paraffin-embedded tissue sections 45

2.8 Protein Polyacrylamide Gel Electrophoresis (PAGE) 47

2.9 Antibody Incubation 47

2.10 Real-time PCR (qPCR) 48

2.11 Cell cycle analysis using flow cytometry 48

2.12 Presence of disulphide bond with fluoresceine maleimide 48
2.13 Statistical analyses 49
2.14 Buffers and solutions 50
Chapter 3 Systematic Analysis of Gene Expression Alterations and Clinical Outcomes for AIPL1 and NUB1 in Cancer 52
3.1 The rationale of study 52
3.2 Concordant down-regulation of AIPL1 transcripts and upregulated NUB1 level in Oncomine database 54
3.3 NUB1 transcripts consistently coexpressed with CUL1 transcripts in breast cancer 61
3.4 Coexpressions of NUB1 with ATM and FAS signaling pathway 64
3.5 Breast cancer specific analysis using METABRIC database 67
3.5.1 NUB1 transcript expression levels predict the survival probability of ER negative breast cancer patients. 67
3.5.2 No significant difference of AIPL1 and NUB1 transcript levels 75
3.5.3 UBL Pathway analysis: FAT10 which coexpressed with NUB1 could stratify ER-, basal and triple negative subgroup breast cancer patients' survival probability 77
3.5.4 CUL1 related ubiquitin ligase activities and cell cycle regulation 82
3.5.5 Pathway analysis of HIF1A transcription in different breast cancer subtypes 84
3.6 Discussion and Chapter Summary 87
Chapter 4 AIPL1-NUB1 signaling cascade in cell cycle regulation Through CUL1 based E3 ubiquitin SCF-ligase 89
4.1 Rationale of the study 89
4.2 Cell line screening of proteins and their transcript levels 91
4.2.1 Detection of endogenous protein expression in various cancer cell line 91
4.2.2 Quantitative PCR analysis of various cancer cell line 91
4.2.3 Immunohistochemistry staining of various cancer cell line 92
4.3 AIPL1 dimerisation in cancer cells 100
4.4 Changes of NUB1 stability upon reoxygenation 102
4.5 NUB1 silencing caused G_0/G_1 cell cycles arrest 104
4.6 Depletion of NUB1 protein affects cell growth rates 106
4.7 Localisation of AIPL1 and NUB1 proteins in hypoxia and reoxygenation 107
4.8 NUB1 protein regulates cell cycle through neddylation-dependent CUL1 109
4.9 Discussion and Chapter Summary 113
Chapter 5 NUB1 protein destabilise p21 and p27 proteins through VHL-dependent CUL2-based E3 ligase 114

5.1 Rationale of the study 114
5.2 NUB1 protects cells from hypoxia-mediated cell cycle arrest and apoptosis through VHL 118
5.3 Up-regulation of HIF1α and VHL protein levels due to NUB1 knockdown 121
5.4 Cell cycle analysis with NUB1 knockdown status under severe hypoxic conditions. 123
5.5 Stabilisation of p27 and HIF1α by NUB1 depletion are independent of VHL 125
5.6 HIF1α is neddylated and FAT10ylated 127
5.7 Discussion and Chapter Summary 129
Chapter 6 Tissue microarray analysis of NUB1 in primary Breast Cancer shows cytoplasmic localisation is associated with poorer prognosis 131
6.1 Rationale of study 131
6.2 Validation of NUB1 antibody on cancer cells 134
6.3 NUB1 immunohistochemical staining of primary breast tumour tissue 136
6.4 Oestrogen receptor (ER) expression and association with clinicopathological factors 139
6.5 Association of ER status and menopausal status with subcellular localisation of NUB1 140
6.6 Survival analyses 142
6.7 Clinicopathological correlation and analysis 145
6.6 Discussion and Chapter Summary 147
Chapter 7 Discussion 148
7.1 Role of of AIPL1 and NUB1 in cancer 148
7.2 Pathways involved in AIPL1 and NUB1 149
7.3 Hypoxia and reoxygenation stress 152
7.4 Relationship with VHL 155
7.5 Translational perspectives 158
Chapter 8 Concluding Statement 160
Appendix 1 161
List of Awards, Presentations and Publications 162
References 173

Chapter 1

Introduction

1.1 Proteostasis (also known as Protein Homoeostasis)

Proteostasis is defined as ‘a concept that explains the integrated biological pathways within cells that control the synthesis, folding, trafficking and degradation of proteins present within and outside the cell’ (Dobson and Karplus, 1999). It contributes to the cellular protein quality control for the proteins in a single human cell (Hieronymus *et al.*, 2006). The maintenance of proteostasis is attained through a precisely coordinated system that corrects unwanted proteomic changes. The integration of chaperones within the proteostasis network ensures a balanced protein homoeostasis.

Chaperones, also known as heat shock proteins (HSP), are ‘a protein group that directly interacts and folds the client protein to its active conformational state’ (Hartl, 1996). The primary function of these proteins is to govern the folding and refolding mechanism of naive and stress-denatured proteins. They dynamically associate with the exposed hydrophobic surfaces of the unfolded polypeptides, prevent their aggregation and thereby, enhance the folding process. Additionally, chaperones are also involved in protein assembly, translocation and degradation. Hence these proteins are the essential determinants of protein quality control in a cell.

There are some definitions of terms used in the molecular chaperones concept, as detailed below (Ellis, 2013):

“”

Protein folding is the collapse of an extended primary translation product into a stable compact monomer. Monomers possess primary, secondary and tertiary structure. The folding of a protein’s quaternary structure is a part of protein assembly (See next).

Protein assembly is the binding of monomers to one another to produce a functional oligomer. Oligomers possess quaternary structure.

Protein misfolding is the formation of a conformation that cannot reach the native conformation on a biologically relevant timescale.

The term ***‘native’*** refers to the conformation of the purified functional protein. The term ***‘non-native’*** is defined as a conformation that is unable to reach the functional conformation on any timescale.

Protein misassembly is the association of two or more polypeptide chains to form non-functional oligomers. A widely used term to describe protein misassemblies is ‘aggregates’, especially to describe so-called amyloid structures, such as those associated with neurodegenerative diseases. Note that misassembled states are always misfolded, by definition.

Chaperones are a large and diverse group of proteins that share the property of assisting non-covalent folding and unfolding, and the assembly and disassembly, of other macromolecular structures, but are not permanent components of these structures when they are performing their normal biological functions (Ellis, 2006). Chaperone substrates include RNA as well as proteins.

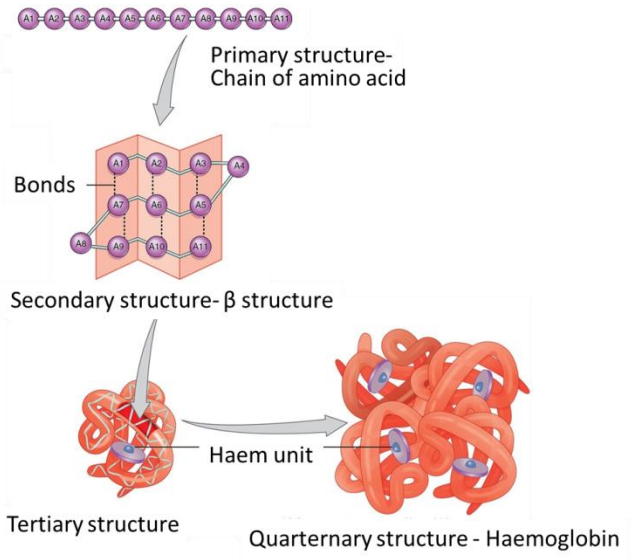
Cochaperones are proteins that modulate chaperone (HSP70 and HSP90) proteins activity. Some cochaperones are also chaperones, e.g. HSP40. Cochaperones modulate the activity of their cognate chaperones in a variety of different ways (Rosser and Cyr, 2007).

HSP and chaperones are not the same. Ellis stated that chaperones present in both stress and unstressed conditions (Ellis, 2013). HSPs are indeed stress proteins. Although chaperones were first recognised as stress-responsive proteins induced mostly by heat shock, other proteotoxic stresses including heavy metals, hypoxia, nutrient deprivation, irradiation, oxidative and toxic stress, infections and exposure to inflammatory cytokines could upregulate their expression too (Lindquist and Craig, 1988; Jaattela, 1999b). However, there are some HSP members that are constitutively expressed. Whilst chaperones and HSPs can constitute overlapping groups of proteins, they are not necessarily identical (Ellis, 1990). The subsequent review assumes that the subset of chaperones discussed is HSPs.

Afinsen's model postulates that for a small globular protein, the native structure is determined only by the protein's amino acid sequence. The primary structure of the protein and its linear amino acid sequence determines its native conformation (Afinsen *et al.*, 1973). The secondary structure involves alpha helices and beta sheets which are stabilised by hydrogen bonds (Pauling *et al.*, 1951). Tertiary structure constitutes a single polypeptide chain formed through hydrophobic interactions, covalent bonding and disulphide bridges between two cysteine residues. Additional interactions of polypeptide chains give rise to quaternary structure formation (Fig 1.1).

The hydrophobic effect is a phenomenon in which the hydrophobic amino acid sequences are buried inside while the more polar amino acids are exposed to the exterior aqueous environment (Figure 1.1) (Dobson and Karplus, 1999). However, active protein-protein interactions tend to expose hydrophobic residues to the exterior environment, risking protein misfolding and aggregation (Zou *et al.*, 2008). To overcome this, chaperones are expressed at high levels in cells after proteotoxic stresses such as exposure to heat shock, heavy metals, alcohols and sodium arsenite (Ritossa, 1962; Ritossa, 1964; Craig, 1985; Calderwood *et al.*, 2010). Chaperones can then permit the folding of client proteins into their functional native states if necessary.

A.



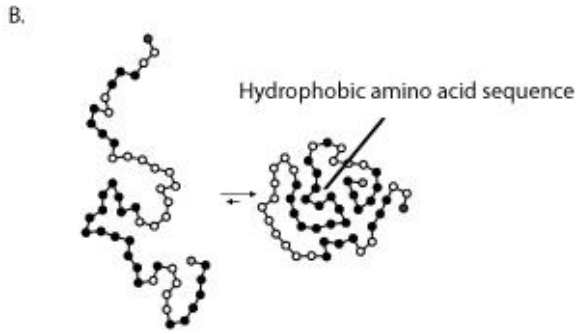


Figure 1. 1 Structures of client proteins (haemoglobin) and the hydrophobic effects. (A) All forms of protein structures are illustrated. (B) Hydrophobic effects is also called Hydrophobic collapse. In the compact fold (on the right), the hydrophobic amino acids (shown as black spheres) collapse toward the centre to become shielded from the aqueous environment (Spolar *et al.*, 1989).

The mechanism of action of chaperones helps to regulate biological proteomes. It is essential to ensure a balanced cellular homoeostasis (Fig 1.2). Protein misfolding and aggregate formation compromise the function of the client proteins. This results in various diseases such as neurodegenerative diseases (e.g. Alzheimer's, Parkinson's disease, and Huntington's disease), cystic fibrosis and cancers (Balch et al., 2008). Many reports support the notion that chaperones are implicated in the pathogenesis of a range of human cancer types. Many of them are in deregulated molecular mechanisms including cell proliferation (Czarnecka *et al.*, 2006; Ghosh *et al.*, 2008), invasiveness (Lemieux *et al.*, 1997), induction of neoangiogenesis (Sanderson *et al.*, 2006), metastasis (Zhao *et al.*, 2007) and the induction of immune tolerance (Calderwood *et al.*, 2005; Cappello *et al.*, 2009).

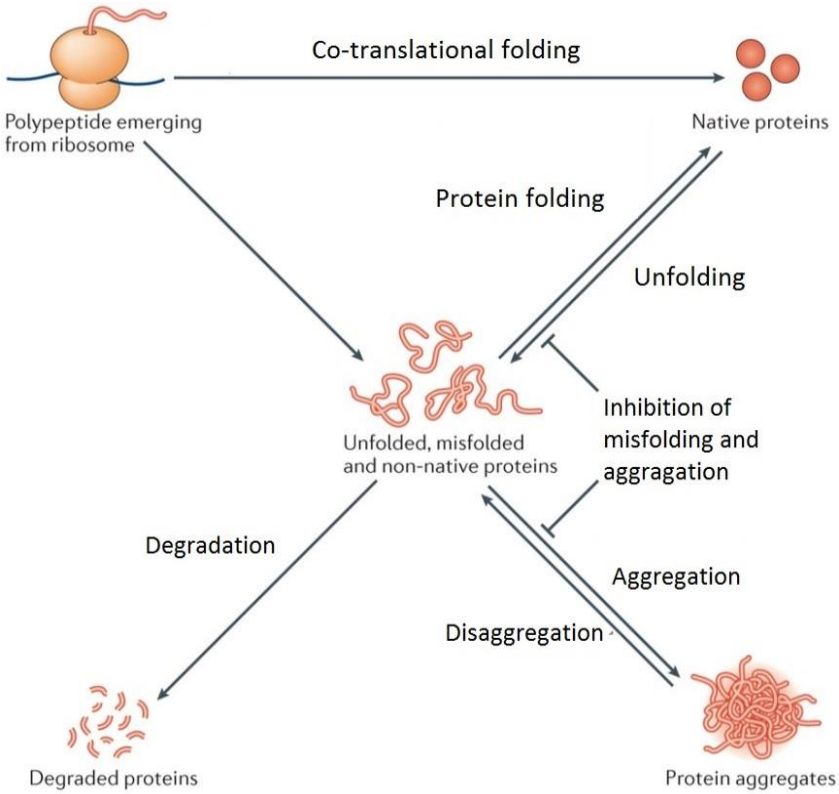


Figure 1. 2 Roles of chaperones in proteostasis. The proteostasis network requires the action of chaperones to fold the client proteins into their native conformations, to prevent misfolding and to reactivate misfolded and aggregated proteins. Chaperones aid in the folding of newly synthesized proteins, the folding of unfolded proteins released from the ribosome and the remodelling of non-native proteins, which are often caused by heat stress and other stress conditions; non-native proteins may be targeted to chaperones associated proteases for degradation; some chaperones could prevent protein misfolding and aggregation; when cells are overwhelmed by stress, non-native proteins might form aggregates; other chaperones can extract and unfold polypeptides from aggregates, thus providing another opportunity for proper folding (Doyle *et al.*, 2013).

1.2 Human Chaperones and Cancer

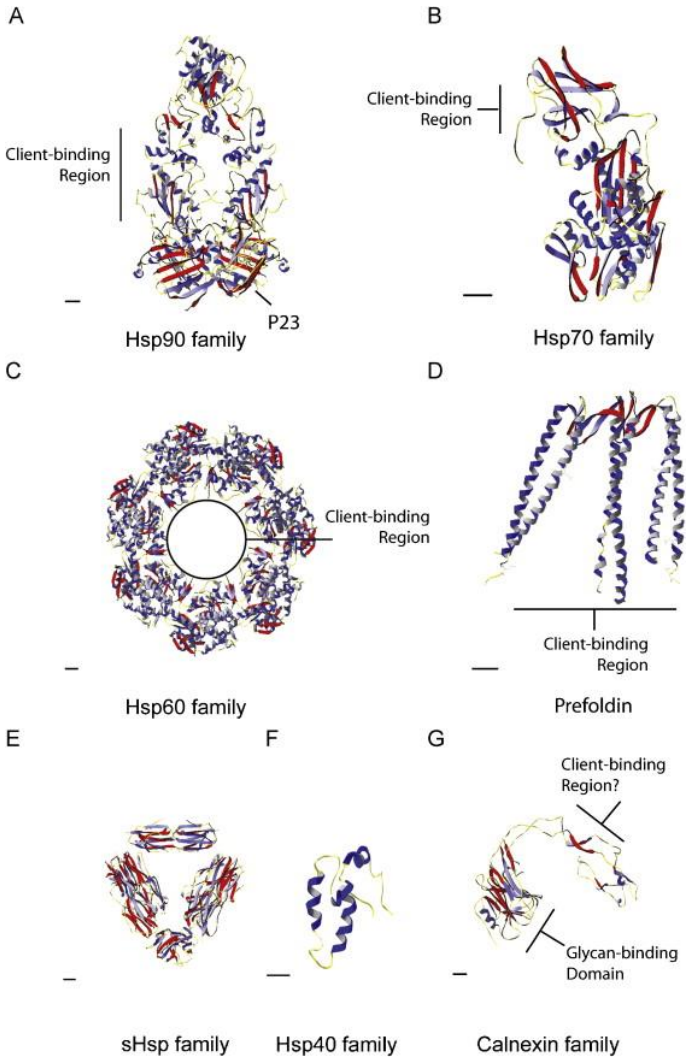
1.2.1 Discovery of Chaperones and historical perspectives

Ferruccio Ritossa first discovered chaperones in a *Drosophila melanogaster* model (Ritossa, 1964). He observed that the salivary gland cells of flies formed chromosomal puffs when they were exposed to higher temperature (Ritossa, 1962). These puffs represented areas with high transcriptional activities in response to heat shock. The transcribed genes and the corresponding proteins were initially named HSPs and then called chaperones (Ellis, 2007; Kampinga *et al.*, 2009). The functions of chaperones onto their respective client proteins were unravelled in the 1980's. The development of the chaperones concept is summarised in table 1.1.

Over the last decades, many HSP90 cochaperones have been discovered and characterised (Pratt and Toft, 1997; Picard, 2002; Wandinger *et al.*, 2008; Li *et al.*, 2012). It is thought that some of the cochaperones facilitate the binding of HSP90 to client proteins and confer specificity to this process (Tai *et al.*, 1993; Johnson *et al.*, 1994; Young *et al.*, 1998; Cox *et al.*, 2007). Others are implicated in regulating the conformational cycle of HSP90 (Chen and Smith, 1998; Chen *et al.*, 1998; Scheufler *et al.*, 2000; Schmid *et al.*, 2012; Li *et al.*, 2013a).

Year	Remarks	Publications
1973	Anfinsen observed that native proteins unfold and lose their biological properties; the proteins can refold into their original functional conformations in the right condition.	(Anfinsen, 1973)
1780	Chloroplast enzyme appears as a large subunit which only forms a smaller subunit when they interact with another protein transiently.	(Barraclough and Ellis, 1980)
1978	The word "molecular chaperones" was used for the first time in the literature by **Ron Laskey** to describe the ability of nucleoplasmin in preventing the aggregation of folded histone proteins with DNA.	(Laskey *et al.*, 1978)
1987	Widespread use of the molecular chaperones noun by **R. John Ellis** in 1987. He described chaperones mediated post-translational protein assembly.	(Ellis, 1987)
1988	It was observed that similar proteins mediated the assembly process in both prokaryotes and eukaryotes.	(Hemmingsen *et al.*, 1988)
1989	The assembly process was confirmed and the ATP-dependent protein folding was demonstrated *in vitro*.	(Goloubinoff *et al.*, 1989)
1993	Earliest recorded discovery of a cochaperone, FKBP59.	(Tai *et al.*, 1993)
1997	HSP90 cochaperones have been discovered and characterised.	(Pratt and Toft, 1997)
2009	Kampinga *et al.* proposed the guideline for the nomenclature of human chaperones.	(Kampinga *et al.*, 2009)

Table 1. 1 Development of the chaperones concept. Important events of chaperones history are summarised. A number of chaperones and their related proteins were found during the 80's and beyond.



	Chaperones	Model	Remark	PDB accession number	Reference
A	HSP90	Yeast	In complex with cochaperone p23 and ATP analogue.	2CG9	(Ali *et al.*, 2006)
B	HSP70	Bovine	Amino acids 1-554 lacking the 10kDa C-terminal domain.	1YUW	(Jiang *et al.*, 2005)
C	HSP60	Bacteria	HSP60 consisting of two stacked homoheptameric rings viewed from above one ring.	1GR1	(Braig *et al.*, 1994)
D	Prefoldin		Hexameric structure prefoldin	1FXK	(Siegert *et al.*, 2000)
E	HSP16.3	*Mycobacterium Tuberculosis*	Dodecameric structure	2BYU	(Kennaway *et al.*, 2005)
F	HSP40		The J-domain of human HSP40 family member	1HDJ	(Qian *et al.*, 1996)
G	Calnexin		Structure of the calnexin luminal domain	1JHN	(Schrag *et al.*, 2001)

Figure 1. 3 Structure of various chaperones. Ribbon diagrams shows the structures and client protein binding sites of the chaperones. α-helices are shown in blue and β-sheets in red. Scale bar represents 10Åm. ATP, Adenosine triphosphate.

1.2.2 Classification of Chaperones

The variety of HSP families has made it necessary to revise the nomenclature. Initially, they were classified according to their molecular mass in kiloDaltons (kDa) (Table 1.2). In 2009, Kampinga *et al.* proposed the guideline for the nomenclature of human chaperones. The chaperones consist of six groups namely HSP110 (HSPH), HSP90 (HSPC), HSP70 (HSPA), HSP40 (J-proteins), and HSPB (small HSP) as well as for the human chaperonin families HSP60/HSP10 (HSPD/E) and chaperonin containing T-Complex Protein (CCT) (Kampinga *et al.*, 2009). This nomenclature is more consistent with the Human Genome Organisation (HUGO) Gene Nomenclature Committee for heat shock genes. Amongst chaperones, the HSP90 and HSP70 groups are the most studied in cancers (Chen *et al.*, 2006). Some of the important structures of chaperones are illustrated (Fig. 1.3).

HSP70s are the most abundant and well characterised HSPs in bacterial and eukaryotic systems. Several types of HSP70s have been reported in all living organisms, and they typically constitute 2-3% of whole cell proteome (Bukau and Horwich, 1998; Mayer *et al.*, 2001).

HSP70s have two conserved domains. The N-terminal Nucleotide binding domain (NBD) and substrate binding domain (SBD) are connected via a linker region. The SBD is a variable helical region which covers the peptide binding cavity and regulates the substrate interaction (Bukau and Horwich, 1998; Mayer *et al.*, 2001). The specificity of HSP70s is largely determined by their partner J-proteins, and together they function as a molecular chaperone machine (Mayer and Bukau, 2005). In organisms, the members of the J-protein family are found in large numbers and often exceed the members of HSP70s. HSP70 is capable of interacting with multiple J-protein partners to exert various physiological functions, thus forming a complex network of chaperones (Mayer *et al.*, 2001; Mayer and Bukau, 2005).

HSP70s and J-proteins are implicated in several essential physiological functions (Hartl and Hayer-Hartl, 2002; Mayer and Bukau, 2005), including prevention of misfolding of newly synthesised polypeptides, protein translocation across biological membranes and degradation processes (Laufen *et al.*, 1999).

HSP90 is a chaperone essential for folding of client proteins, including protein kinases and transcription factors (Csermely *et al.*, 1998), which are involved in the signal transduction process. Typically, HSP90 localised either in the cytoplasm, endoplasmic reticulum or mitochondrial compartments.

The levels of HSP90 are upregulated several fold upon stress induction to protect the conformation of its client proteins (Cowen and Lindquist, 2005). HSP90 contains a conserved N-terminal 'ATP-binding domain' followed by a 'middle region' and C-terminal dimerising domain (Cowen and Lindquist, 2005), which are involved in the binding to different cochaperones and client proteins. They form a constitutive homodimer and in the presence of ATP, adopt a circular structure to stabilise the conformational plasticity of client proteins and assist in the maturation into their native states (Cowen and Lindquist, 2005).

A. HSP70 superfamily: HSPA (HSP70) and HSPH (HSP110) families

	Gene name	Protein name	Old names	Human gene ID
HSPA				
1	*HSPA1A*	HSPA1A	HSP70-1; HSP72; HSPA1	3303
2	*HSPA1B*	HSPA1B	HSP70-2	3304
3	*HSPA1L*	HSPA1L	hum70t; hum70t; HSP-hom	3305
4	*HSPA2*	HSPA2	Heat-shock 70kD protein-2	3306
5	*HSPA5*	HSPA5	BIP; GRP78; MIF2	3309
6	*HSPA6*	HSPA6	Heat shock 70kD protein 6 (HSP70B′)	3310
7	*HSPA7*[a]	HSPA7	Heat shock 70kD protein 7	3311
8	*HSPA8*	HSPA8	HSC70; HSC71; HSP71; HSP73	3312
9	*HSPA9*	HSPA9	GRP75; HSPA9B; MOT; MOT2; PBP74; mot-2	3313
10	*HSPA12A*	HSPA12A	FLJ13874; KIAA0417	259217
11	*HSPA12B*	HSPA12B	RP23-32L15.1; 2700081N06Rik	116835
12	*HSPA13*[b]	HSPA13	Stch	6782
13	*HSPA14*	HSPA14	HSP70-4; HSP70L1; MGC131990	51182
HSPH				
1	*HSPH1*	HSPH1	HSP105	10808
2	*HSPH2*[b]	HSPH2	HSPA4; APG-2; HSP110	3308
3	*HSPH3*[b]	HSPH3	HSPA4L; APG-1	22824
4	*HSPH4*[b]	HSPH4	HYOU1/Grp170; ORP150; HSP12A	10525

[a]Annotated as pseudogene, but possibly a true gene; [b]Under consultation with HGNC and the scientific community; *No information

B. HSP90 (HSPC)

	Protein name	Gene name	Old gene names	Human Gene ID
1	HSPC1	*HSPC1*[a]	***HSP90AA1****; HSPN; LAP2; HSP86; HSPC1; HSPCA; HSP89; HSP90; HSP90A; HSP90N; HSPCAL1; HSPCAL4; FLJ31884*	3320
2	HSPC2	*HSPC2*[a]	***HSP90AA2****; HSPCA; HSPCAL3; HSP90ALPHA;*	3324
3	HSPC3	*HSPC3*[a]	***HSP90AB1****; HSPC2; HSPCB; D6S182; HSP90B; FLJ26984; HSP90-BETA*	3326
4	HSPC4	*HSPC4*[a]	***HSP90B1****;ECGP; GP96; TRA1; GRP94; endoplasmin*	7184
5	HSPC5	*HSPC5*[a]	***TRAP1****; HSP75; HSP90L*	10131

[a]Under consultation with HGNC and the scientific community. GRP-94, G Protein-Coupled Receptor 94; TRAP1, TNF Receptor- Associated Protein 1

Table 1. 2 Classification of A. HSP70 and HSP110 and B. HSP90. The nomenclature of HSP70 and HSP90 protein isoforms are listed. The information is modified from Kampinga *et al.*, 2009 and Chen *et al.*, 2005.

Cochaperones are the proteins that assist in catalysing individual steps in molecular chaperoning as well as in posttranslational modification and intracellular localisation. They work in concert with HSP90 to modulate its conformation and the respective client proteins. Over 20 cochaperones including immunophilins have been shown to regulate the function of the HSP90 protein-folding machinery. Immunophilins consists of FK506 Binding Protein 51/52 (FKBP51/52), Cyclophilin 40 (CYP40) and Aryl Hydrocarbon Receptor Interacting Protein-Like 1 (AIPL1). These cochaperones are thought to provide HSP90 selectivity toward different client proteins. For example, AIPL1 recruits the HSP90 machine in a chaperone heterocomplex that is essential for phosphodiesterase biogenesis and its retinal maturation (Aguila *et al.*, 2014).

Three particular classes of chaperone appear of high significance in cancer, and these include the HSPA, HSPB, and HSPC families (Ciocca *et al.*, 2013). Each HSP class is regulated by an individual cohort of cochaperones and these molecules may be significant factors in cancer and carcinogenesis and potential targets for therapy.

Name	Function	Conserved domain	Role in cancer	Reference
		HSP70		
JDP	Substrate selection	J domain	Supp	(Isomoto *et al.*, 2003)
HSPBP1	Nucleotide exchange	*	Supp	(Souza *et al.*, 2009)
BAG1	Nucleotide exchange	BAG, UBL	Onc	(Aveic *et al.*, 2011)
BAG3	Nucleotide exchange	BAG, WW	Onc	(Stuart *et al.*, 1998)
HOP	Adaptor	TPR	Onc	(Kubota *et al.*, 2010)
		HSP90		
SGT1	Substrate selection	CHORD	*	(Zabka *et al.*, 2008)
p23	ATPase inhibitor	p23	Onc	(Reebye *et al.*, 2012)
AHA1	ATPase inhibitor	AHA1	Onc	(Pearl and Prodromou, 2006)
CDC37	ATPase inhibitor	HSP90 BD	Onc	(Stepanova *et al.*, 2000)
HOP	Adaptor	TPR	Onc	(Walsh *et al.*, 2011)
CYP40	Immunophilin	TPR, PPiase	*	(Schulke *et al.*, 2010)
FKBP1	Immunophilin	TPR, PPiase	Onc	(Denny *et al.*, 2000)
FKBP2	Immunophilin	TPR, PPiase	Onc	(McKeen *et al.*, 2011)
PP5	Protein phosphatase	TPR	*	(Chinkers, 1994)
TTC4	Adaptor, replication	TPR	Supp	(Poetsch *et al.*, 2000)
TTC5	Adaptor, transcription	TPR	*	(Davies *et al.*, 2011)
AIP	Nuclear receptors	TPR	*	(Mazumdar *et al.*, 2001)
AIPL1	Immunophilin, Chaperone and cochaperone	TPR, PPiase	Supp	(Hidalgo-de-Quintana *et al.*, 2008)

Table 1. 3 List of cochaperones. The cochaperones are associated with HSP70 and HSP90 chaperone families. Supp, tumour suppressor; onc, oncogene; JDP, J domain protein; BAG1, Bcl-2-Associated Athanogene 1; BAG1, Bcl-2-associated athanogene 1 and silencer of death domain; UBL, ubiquitin-like domain; WW, tryptophan repeats domain; HOP, Hsp70-Hsp90 Organizing Protein; TPR, Tetratricopeptide repeat-containing domain; SGT1, Suppressor Of G2 Allele Of SKP1; AHA1, activator of Hsp90 ATPase 1; CHORDS, Cysteine- and histidine-rich domains; CDC37, Cell Division Cycle 37; PP5, Protein phosphatase 5; TTC4/5, Tetratricopeptide repeat protein 4/5; AIP, Aryl Hydrocarbon Receptor Interacting Protein; PPIase, Prolyl isomerase.*No information

1.2.3 Roles of Chaperones and Cochaperones in Cancer

Chaperones maintain a balanced proteostasis *via* protein folding, preventing misfolding of proteins and reactivating aggregated proteins. When the cells are challenged by cytotoxic stress, chaperones help client proteins to shift their protein conformations toward ordered, functional forms. However, deregulation of chaperones contributes to pathological conditions including neurodegeneration, cardiovascular diseases and cancers. This deregulation causes more nascent proteins to form and results in the accumulation of toxic aggregates (Voisine *et al.*, 2010). Chaperones are overexpressed in a wide range of human cancers and are implicated in tumour cell proliferation, differentiation, invasion, metastasis and recognition by the immune system (Calderwood, 2013).

The elevated expression of chaperones contributes to oncogenesis (Jaattela, 1999a). Over-expression of HSP72 in Rat-1 fibroblasts generates tumours upon injection into mice (Volloch and Sherman, 1999). In another study, transgenic mice expressing HSP72 developed T-cell lymphoma (Seo *et al.*, 1996). The elevated chaperones levels were associated with malignancy. This phenomenon may be due to the genetic changes associated with tumour progression (Tang *et al.*, 2005). Chaperones have a role in cancer clonal evolution since they provide a selective advantage through proliferation, anti-apoptosis and against other physiological stress (including hypoxia).

Chaperones increase cell survival by overcoming cytotoxic stress (Workman, 2002). Stabilisation of the structural proteins helps in malignant transformation. Kinases (Src and Met tyrosine kinases) and transcription factors (e.g., hypoxia inducible factor, HIF1) allows chaperones to contribute to angiogenesis by promoting endothelial cell proliferation (Workman, 2002).

Chaperones alter the programmed cell death (apoptosis). Chaperones do not fold the mutant (non-functional) forms of tumour suppressors and DNA repair proteins such as p53 and MutS Homolog 2 as the chaperones does not recognise the mutated sequence of the tumour suppressor (Pratt and Toft, 2003; Calderwood *et al.*, 2006; Ekman *et al.*, 2010). However, HSP70 is strongly induced in pancreatic adenocarcinoma cell line its depletion resulted in cancer cell apoptosis (Aghdassi *et al*., 2007). The diminished expression of HSP70 resulted in the apoptosis of pancreatic cancer cells *in vivo* as well as *in vitro* (Phillips *et al.*, 2007). Suppressed HSP110 expression also enhanced apoptosis in cancer cells, but not in normal cells (Hosaka *et al*., 2006).

Malfunctioning chaperones could enhance cancer growth by destabilising tumour suppressive proteins resulted from frequent amino-acid substitution and deletion of amino acid sequence (Miyata *et al.*, 2013). Without functional HSP90, p53 mutant ($p53^{V143A}$) failed to suppress cancer growth for its protein could not be folded into the active form (Blagosklonny *et al.*, 1996). Thus, it is expected that there are many misfolded proteins due to genetic mutations, implicating chaperones in various hallmarks of cancer.

1.2 Microarray and chaperones/cochaperones gene-specific meta-analysis

While chaperones are oncogenic (Jaattela, 1999a), cochaperones can be both oncogenic and tumour suppressive (Table 1.3). Under cellular stresses, the expression levels of HSP increase in tumours as a response to stress to restore the normal protein-folding environment (Ma and Hendershot, 2004: Mosser and Morimoto, 2004; Calderwood et al., 2006). The up-regulation of chaperones during tumour growth reflects an adaptive response to the stress and suggests that HSPs play a significant role in tumour survival in a hypoxic, acidic and nutrient-deprived microenvironment.

Adaikalavan Ramasamy tested the hypothesis on whether down regulation of chaperones which could affect their tumour suppressive client proteins in cancer does indeed occur (Ramasamy*et al*., 2009). He carried out a meta-analysis of chaperones mRNA levels in tumours compared to their corresponding normal tissues from 30 microarray data sets. The analysis focused on genes mapping to Gene Ontology (www.geneontology.org/) with identifier G0:0006457, which refers to the biological process of protein folding. His results demonstrated that the mRNA coding for six chaperones are down-regulated across a large spectrum of tumours. Subsequently, Ramasamy performed an analysis looking at individual data set to investigate which chaperons where down-regulated in some data set but not in others (Ramasamy, Unpublished results) and 13 of these genes where chaperons to well-known and/or putative suppressor genes.

In contrast to normal adjacent tissue, five cochaperone proteins (with number of dataset out of 30 reported by the name of the genes) were down regulated in cancers, *i.e.* PARK7 (6), PIN1 (3), TSC2 (1) and SCG5 (4). Additionally, eight chaperones were reduced in cancer, such as VBP1 (4), TRAP1(4), DNAJA3 (4), PFDN5 (4), HSPB8 (4), HSP90AA1 (3), DNAJC11 (1), DNAJCy7(2). AIPL1, which was down-regulated in four dataset, showed both chaperone and cochaperone functions. A summary of their corresponding client proteins is shown (Table 1.4).

Table 1. 4 Summary of meta-analysis. Chaperones gene transcripts are significantly down-regulated in cancer against the adjacent normal tissue. The known (putative) tumour suppressors regulated by chaperons were listed through the systematic analysis of 30 individual datasets in gene-specific meta-analysis.

Role V	Chaperone genes of interests	Number of studies found to be down-regulated out of 30 microarray studies	Target suppressor	References
Chaperones and cochaperones	AIPL1	4	NUB1	(Akey *et al.*, 2002)
Cochaperones	PARK7	6	p53	(Kato *et al.*, 2013)
	PIN1	3	p53	(Zheng *et al.*, 2002a)
	TSC2	1	TSC1	(Huang and Manning, 2008)
	SCG5	4	PC2	(Waha *et al.*, 2007)
Chaperones	TRAP1	4	Rb1	(Chen *et al.*, 1996)
	VBP1	4	VHL	(Brinke et al. 1997)
	DNAJA3	4	VHL	(Bae *et al.*, 2005)
	PFDN5	4	p73	(Watanabe *et al.*, 2002)
	HSPB8 (HSP22)	4	TAK1	(Li *et al.*, 2007)
	HSP90AA1	3	P53	(Muller *et al.*, 2004)
	DNAJC7	2	RAD1	(Xiang *et al.*, 2001)

Table 1. 5 Summary of down-regulated AIPL1. Microarray studies showing down-regulation of AIPL1 mRNA expression in different cancers. In relative to normal adjacent tissue, there were four microarray studies showing significant reduced level of AIPL1 transcript expression – Basso_B-cell microarray (Log_2 FC=-1.318; *p*-value=<0.001), Dryrskjot_Bladder cancer microarray (Log_2 FC=-1.880; *p*-value=<0.001), Lenburg_renal cancer microarray (Log_2 FC=-0.852; *p*-value=0.019), Ramasamy_colon cancer microarray (Log_2 FC=-1.291; *p*-value=0.010). They were significant with log_2 FC >0.5 or <-0.5. Of all, AIPL1 chaperone signaling is of our interests for there is no correlation to cancer to date.

Dataset	Cancer	Log_2 FC	*p*-Value
Basso *et al. 2005*	B-cells	-1.318	<0.001***
Dryrsjot *et al. 2004*	Bladder	-1.880	<0.001***
Lenburg *et al.*, 2003	Renal	-0.852	0.019*
Ramaswamy *et al.*, 2001	Colon	-1.291	0.010*

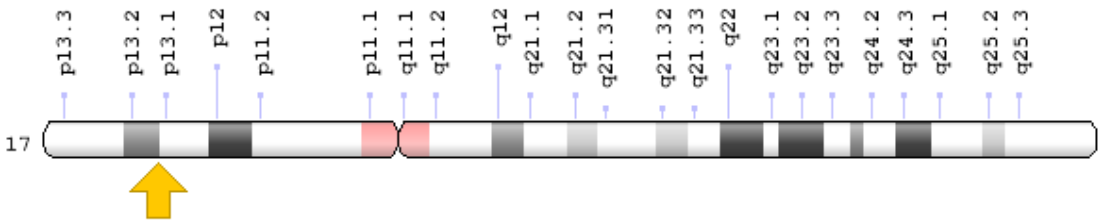
* Significant with *p*-value<0.05; ** Significant with *p*-value<0.005; ***Significant with *p*-value<0.001

1.3 Introduction of AIPL1 protein

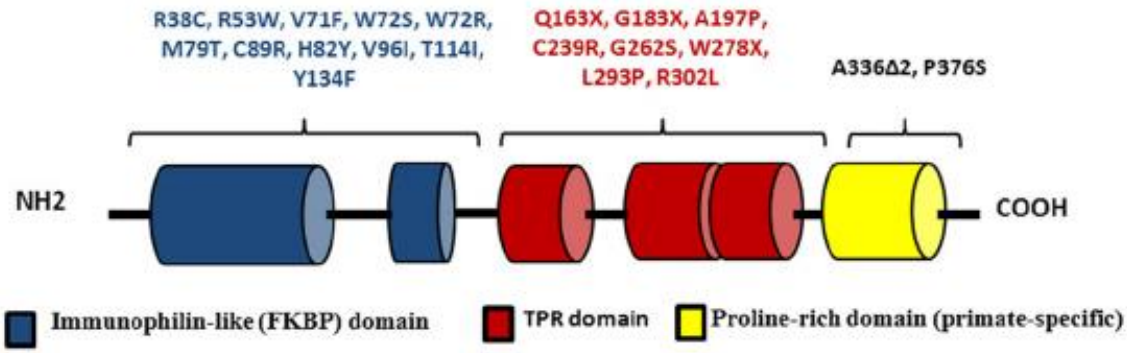
Aryl hydrocarbon receptor-interacting protein-like 1, AIPL1 is a photoreceptor and pineal-expressed gene first described in 2000 (Sohocki *et al.*, 2000). The AIPL1 gene is located on chromosome 17p13.2 (Sohocki *et al.*, 2000)(Figure 1.4a). Functionally, AIPL1 is a chaperone and also a cochaperone. The AIPL1 protein is able to form a chaperone heterocomplex with HSP70 and HSP90 (Hidalgo-de-Quintana *et al.*, 2008).

In the retina and pineal gland, the expression of AIPL1 closely follows the spatial temporal differentiation of rod and cone-receptor in the developing retina (Sohocki *et al.*, 2000). Gene defects in AIPL1 cause heterogeneous set of conditions including Leber's congenital Amaurosis (LCA), retinitis pigmentosa and cone-rod dystrophy (Sohocki *et al.*, 2000). LCA is inherited in an autosomal recessive manner and is characterised by severely impaired vision and blindness at birth (Sohocki *et al.*, 2000). The AIPL1 mRNA transcripts are expressed abundantly in pineal and retinal tissue, and to a much less extent in other tissue.

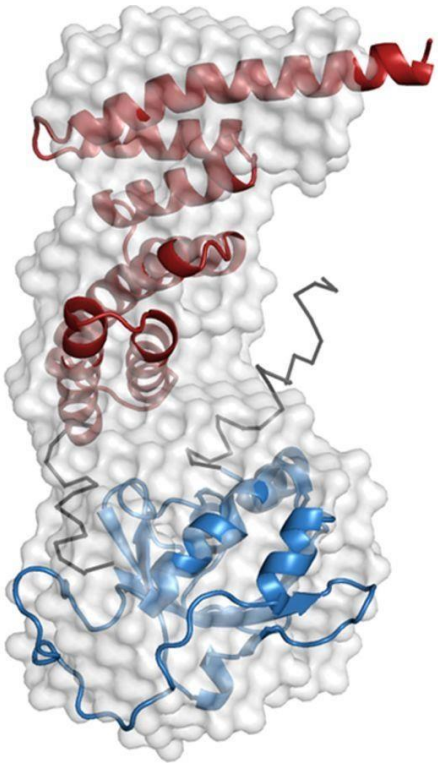
The AIPL1 protein consists of 384 amino acids, with a 44kDa molecular mass. The AIPL1 protein sequence includes three tetratricopeptide repeats (TPR), a 34–amino-acid motif found in proteins with nuclear transport or protein chaperone activity (Ma and Whitlock, 1997). AIPL1 has 49% identity and 69% similarity with the human Aryl hydrocarbon receptor-interacting protein, AIP (Kuzhandaivelu *et al.*, 1996). Figure 1.4b illustrates the topology diagram of AIPL1, AIP and FK506-binding proteins 52 (FKBP52) protein.


p13.3
p13.2
p13.1
p12
p11.2
p11.1
q11.1
q11.2
q12
q21.1
q21.2
q21.31
q21.32
q21.33
q22
q23.1
q23.2
q23.3
q24.2
q24.3
q25.1
q25.2
q25.3
17

A.


R38C, R53W, V71F, W72S, W72R, M79T, C89R, H82Y, V96I, T114I, Y134F
Q163X, G183X, A197P, C239R, G262S, W278X, L293P, R302L
A336Δ2, P376S
NH2
COOH
Immunophilin-like (FKBP) domain
TPR domain
Proline-rich domain (primate-specific)

B.



C.

D.

```
CLUSTAL O(1.2.4) multiple sequence alignment


AIPL1      -MDAALLLNVEGVKKTILHGGTGELPNFITGSRVIFHFRTMKCDEERTVIDDSRQVGQPM
AIP        MADIIARLREDGIQKRVIQEGRGELPDFQDGTKATFHYRTLHSDDEGTVLDDSRARGKPM
             *    *. :*::* ::: * ****:*  *::. **:**::.*:* **:****  *:**

AIPL1      HIIIGNMFKLEVWEILLTSMRVHEVAEFWCDTIHTGVYPILSRSLRQMAQGKDPTEWHVH
AIP        ELIIGKKFKLPVWETIVCTMREGEIAQFLCDIKHVVLYPLVAKSLRNIAVGKDPLEGQRH
           .:***: *** *** :: :**  *:*:* **  *. :**::::***::* **** * : *

AIPL1      TCGLANMFAYHTLGYEDLDELQKEPQPLVFVIELLQVDAPSDYQRETWNLSNHEKMKAVP
AIP        CCGVAQMREHSSLGHADLDALQQNPQPLIFHMEMLKVESPGTYQQDPWAMTDEEKAKAVP
            **:*:*  : :**: *** **::****:* :*:*:*::*. **:: * :::.** ****

AIPL1      VLHGEGNRLFKLGRYEEASSKYQEAIICLRNLQTKEKPWEVQWLKLEKMINTLILNYCQC
AIP        LIHQEGNRLYREGHVKEAAAKYYDAIACLKNLQMKEQPGSPEWIQLDQQITPLLLNYCQC
           ::* *****:: *: :**::** :** **:*** **:* . :*::*:: *. *:******

AIPL1      LLKKEEYYEVLEHTSDILRHHPGIVKAYYVRARAHAEVWNEAEAKADLQKVLELEPSMQK
AIP        KLVVEEYYEVLDHCSSILNKYDDNVKAYFKRGKAHAAVWNAQEAQADFAKVLELDPALAP
            *  *******:* *.**.:: . ****: *.:*** ***  **:**: *****:*::

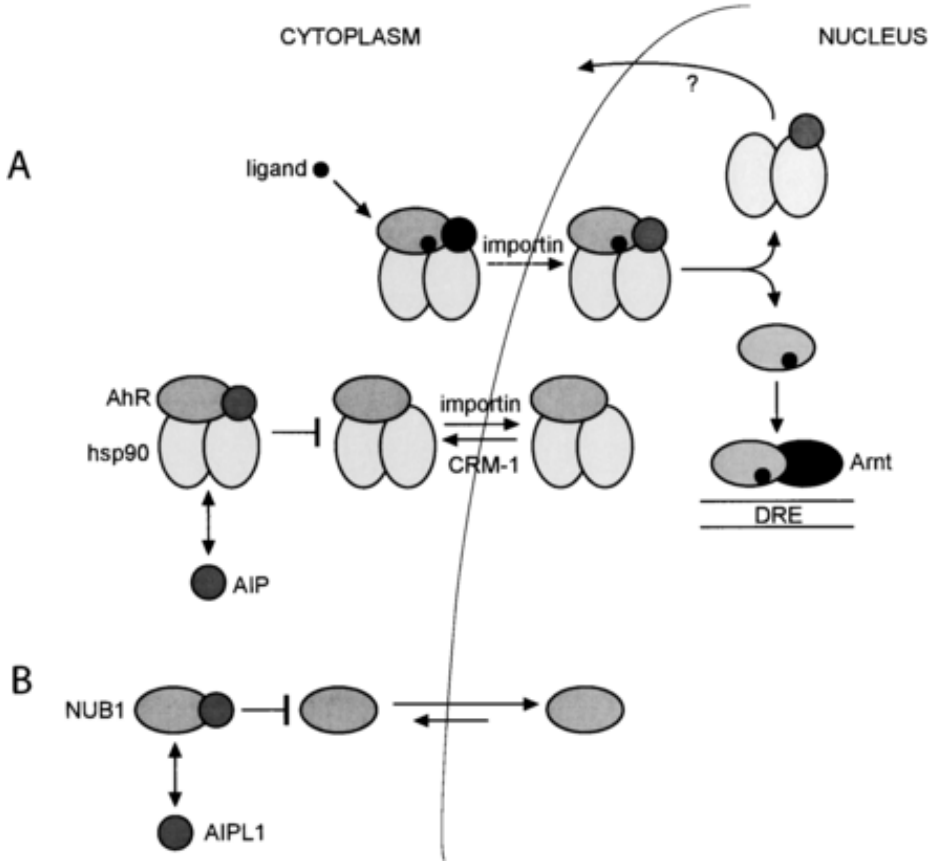
AIPL1      AVRRELRLLENRMAEKQEEERLRCRNMLSQGATQPPAEPPTEPPAQSSTEPPAEPPTAPS
AIP        VVSRELRALEARIRQKDEEDKARFRGIFSH-----------------------------
           .* **** ** *: :*:**:: * *.::*:

AIPL1      AELSAGPPAEPATEPPPSPGHSLQH
AIP        -------------------------
```

Figure 1. 4 Details of AIPL1 gene. (A) Cytogenetic map of chromosome 17 with the cytogenetic location of AIPL1 gene mapped by FISH is indicated alongside the DAPI-banded ideograms at 17p13.2 and genome location at chr17:6393693-6435199. (B) Schematic representation of AIPL1, AIP and FKBP52. The pathological mutations in AIPL1 are shown. The primary structural features are labelled as follows: PP, polyproline-rich sequence; PPIase, peptidyl prolyl isomerase domain. (C) Model of mouse AIPL1 showing homology models of the N-terminal FKBP (blue) and the C-terminal TPR (red) domains with relative orientation. (D) Multiple sequence alignments of AIPL1 and AIP.

The function of AIPL1 is largely unknown. It may function in a similar manner to that of aryl hydrocarbon receptor-interacting protein, AIP (Sohocki *et al.*, 2000; Chapple *et al.*, 2001). AIP and AIPL1 have highly similar primary structures but distinct biological functions. AIP is ubiquitously expressed in almost all tissues, and variants of AIP are associated with familial pituitary adenomas (Ozfirat and Korbonits, 2010; Cazabat *et al.*, 2011). In contrast, AIPL1 is expressed specifically in adult rod photoreceptor cells, where its function is essential but not well understood (Schwartz *et al.*, 2006).

AIPL1 could potentially be involved in the signalling of a nuclear receptor (Fig 1.5). AIP enhances the ligand-induced transcriptional activity of the aryl hydrocarbon receptor, AhR (Ma and Whitlock, 1997; Carver *et al.*, 1998; Meyer *et al.*, 1998; Lees and Whitelaw, 2002; Lees *et al.*, 2003). AIP also stabilises cytoplasmic AhR by preventing the ubiquitination and subsequent degradation of the protein(Meyer and Perdew, 1999; Kazlauskas *et al.*, 2000; LaPres *et al.*, 2000; Meyer *et al.*, 2000; Lees *et al.*, 2003). AIP can inhibit chromosomal maintenance 1 (CRM1)-mediated nucleocytoplasmic shuttling of the AhR and cause its cytoplasmic retention (Petrulis *et al.*, 2000; Petrulis *et al.*, 2003). It is done by altering the conformation of the AhR nuclear localisation signal, thereby hindering interaction with the nuclear import receptor protein, Importin-β (Kazlauskas *et al.*, 2000; Petrulis *et al.*, 2003).


CYTOPLASM
NUCLEUS
?
A
ligand
importin
AhR
hsp90
importin
CRM-1
Arnt
DRE
AIP
B
NUB1
AIPL1

C.

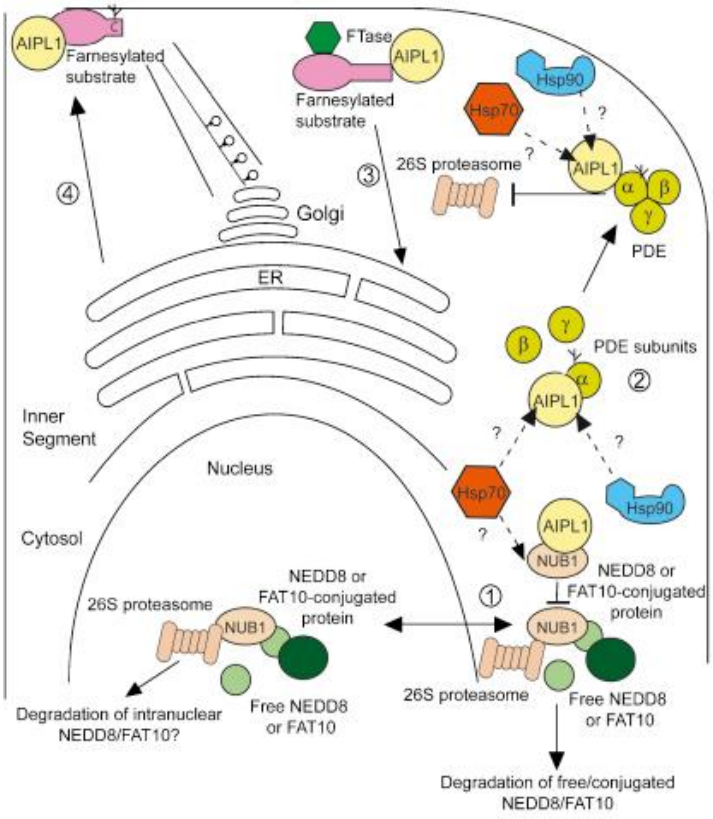


Figure 1. 5 The function of AIP and AIPL1 (**A**) AIP regulates the nuclear translocation and transactivation of the AhR. DRE, dioxin response element. (**B**) Similarly, AIPL1 modulates the nuclear translocation of its client protein, NUB1. (C) roles of AIPL1 in photoreceptors. Schematic representation showing potential roles of AIPL1 within photoreceptors. AIPL1 is able to modulate the nuclear localisation of NUB1, which may affect the NUB1 NEDD8 and FAT10 'busting' activity (1); AIPL1 interacts with and enhances stability of the phosphodiesterase, PDE holoenzyme (2); AIPL1 may enhance transport and stability of farnesylated proteins to the ER (3) or other target membranes (4). AIPL1 is likely to utilize the HSP70 and HSP90 chaperone machinery to execute its cellular functions.

Like other immunophilins, AIPL1 is a chaperone (Li *et al.*, 2013b). The unique pattern of the proline-rich domain of AIPL1 could chaperone specific client proteins. The C-terminal proline-rich region is essentially hydrophilic and greatly influences the chaperone activity (Wayne and Bolon, 2010). The chaperone activity of AIPL1 requires the cooperation between the proline-rich domain and other domains in AIPL1. The linker region connecting the FKBP domain and TPR domain plays an important role in the chaperone activity (Pirkl *et al.*, 2001). Proline-rich regions are common modules mediating protein–protein interactions, especially in proteins involved in signaling transduction pathways (Ruaro *et al.*, 1997). It was found that AIPL1 protein proline-rich domain is a negative regulator of the HSP90 interaction with substrates (Li *et al.*, 2013b).

1.3.1 Interaction of NUB1 and the downstream ubiquitin pathway

AIPL1 is capable of interacting with NUB1 directly in a chaperone-like fashion (van der Spuy and Cheetham, 2004). AIPL1 was found to suppress the aggregation of NUB1 *in vivo* and reduce its nuclear translocation (van der Spuy and Cheetham, 2004). NUB1 recruits the ubiquitin-like protein NEDD8 and its conjugates for proteasomal degradation (Kamitani *et al.*, 2001).

NEDD8 is conjugated specifically to members of the cullin (CUL) family in a manner analogous to ubiquitination (Yeh *et al.*, 2000). The cullins are components of a Skp1, cullin, F-box protein (SCF) ubiquitin E3 ligase composed of SCF and ROC1 (Zheng *et al.*, 2002b). The CUL1 SCF complex catalyses the ubiquitination of inhibitory factor κBα, β-catenin, cyclin D proteins, p27 and p21 (Yu *et al.*, 1998; Hatakeyama *et al.*, 1999; Kitagawa *et al.*, 1999; Suzuki *et al.*, 1999; Morimoto *et al.*, 2000), and NEDD8 conjugation is necessary for the Ubiquitin E3 ligase activity of the CUL1 SCF complex (Podust *et al.*, 2000; Read *et al.*, 2000). The CUL2 and CUL3 SCF complexes target hypoxia-inducible factor-1α (HIF1α) and cyclin E respectively for ubiquitination and proteasomal degradation (Singer *et al.*, 1999; Kamura *et al.*, 2000). Therefore NEDD8–cullin conjugation has been implicated in many important biological events, including cell signalling and cell-cycle regulation.

NUB1 targets NEDD8 and NEDD8 conjugates for proteasomal degradation (Kamitani *et al.*, 2001). Recently, a splicing variant of NUB1 possessing a 14-amino-acid insertion in the C-terminus (NUB1L) was identified (Tanaka *et al.*, 2003). NUB1L has been shown to interact with NEDD8 as well as an additional ubiquitin-like protein FAT10, and to accelerate the proteasomal degradation of these ubiquitin-like proteins (Tanaka *et al.*, 2003; Hipp *et al.*, 2004).

In addition, both NUB1 and NUB1L interact with a ubiquitin precursor UBC1 and mediate the hydrolysis of UBC1 by an unidentified ubiquitin C-terminal hydrolase (UCH) (Tanaka *et al.*, 2003). It has been suggested that the interaction of AIPL1 with NUB1 implicates biological functions related to cell growth and cell cycle regulation. However, the cellular role of AIPL1 with respect to NUB1 still remains to be fully determined.

The expression and localisation of AIPL1 and NUB1 were examined (van der Spuy *et al.*, 2002; van der Spuy *et al.*, 2003). AIPL1 was predominantly cytoplasmic, whereas NUB1 was predominantly nuclear due to a functional nuclear localisation signal near the C-terminus (Kito *et al.*, 2001; van der Spuy *et al.*, 2003). AIPL1 modulates NUB1 nuclear translocation. These results suggest that AIPL1 protein restricts the translocation of NUB1, thereby modulating downstream effects of NUB1 on cell signalling and cell growth.

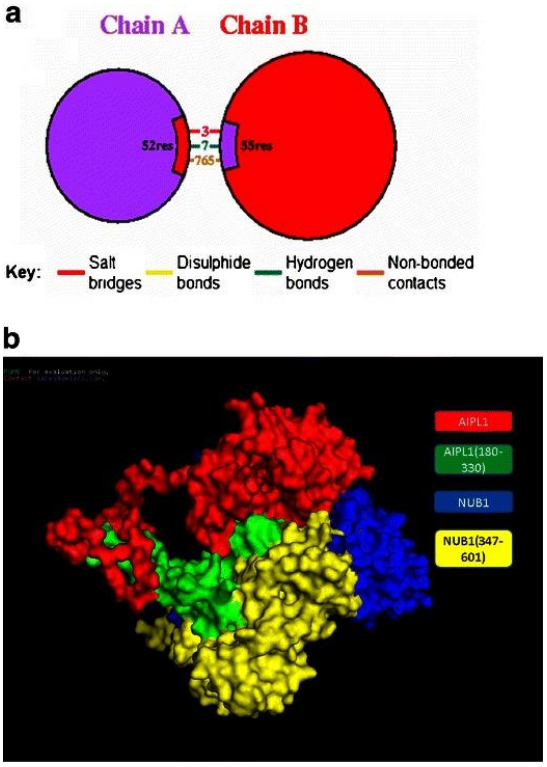


Figure 1. 6 Interaction of AIPL1 and NUB1 proteins. (a) Interaction between AIPL1 and NUB1 from PDBsum server. Chain A represents AIPL1 and chain B indicates NUB1. (b) Docking complex of AIPL1 interaction with NUB1. Illustration of docked complex for AIPL1 and NUB1. The AIPL1 region is represented by *red* and *green*, and the NUB1 region represent for *blue* and *yellow* using PYMOL (Muthukumaran *et al.*, 2012).

1.3.2 Background of NUB1

NUB1 is an interferon (IFN)-inducible protein of 69 kDa, composed of 601 amino acids. It also has a splice variant, NUB1L, which possesses an extra 14 amino acids that encode an additional Ub-associated (UBA) domain (Fig. 1.7). NUB1 proteins can recruit FAT10- and NEDD8-conjugated proteins to the proteasome for degradation and negatively regulate the NEDD8-conjugation system (Kamitani *et al.*, 2001; Kito *et al.*, 2001; Tanaka *et al.*, 2003; Tanji *et al.*, 2005; Groettrup *et al.*, 2008). The NUB1 proteins have been observed in various types of cancer cells, including cervical adenocarcinoma, rectal adenocarcinoma, neuroblastoma, malignant lymphoma and renal cell carcinoma (RCC) (Kito *et al.*, 2001). Upregulated NUB1 expression has been linked to IFNα-induced antimitogenic actions. Additionally, NUB1 has demonstrated anticancer properties in RCC cell line, where it was involved in apoptosis and S-phase transition through its action on p27 and cyclin E (Bornstein *et al.*, 2006; Hosono *et al.*, 2010). Up-regulation of NUB1 effectively inhibits the proliferation of IFNα-resistant RCC cells (Hosono *et al.*, 2010).

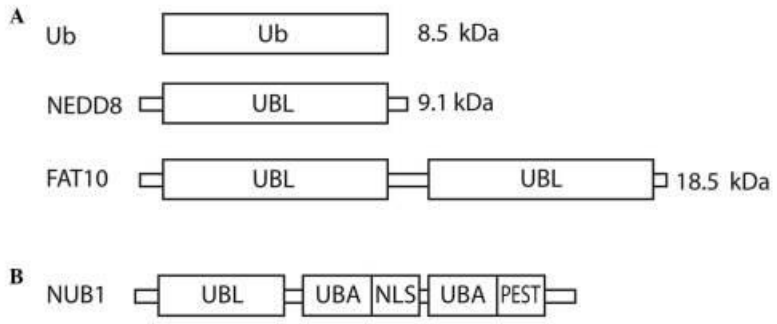


Figure 1. 7 Structural representation of (A) Ub, NEDD8 and FAT10, and (B) NUB1. Ub, ubiquitin; NEDD8, neural precursor cell expressed, developmentally down-regulated 8; FAT10, HLA-F-adjacent transcript 10; NUB1, NEDD8 ultimate buster 1; UBL, ubiquitin-like domain; UBA, ubiquitin-associated; NLS, nuclear localisation signal; PEST, proline-enriched glutamic acid, serine and threonine domain.

NUB1 protein has been reported to play a role in Huntington's disease (Lu *et al.*, 2013) and Congenital Amaurosis (Kanaya *et al.*, 2004). In cancers, the degrading enzyme NUB1 is an attractive candidate for inhibition of $p27^{KIP1}$ and $p21^{CIP1}$ through the regulation of the SCF^{SKP2} ligase activity (Hosono *et al.*, 2010). The upregulated $p21^{CIP1}$ in NUB1-knockdown cancer cells is thought to be promising in directing the cells to senescence. NUB1 protein was reported to be a tumour suppressor as it exerts growth inhibition during its overexpression; upon IFNα treatment, overexpressed NUB1 induced apoptosis in IFNα-resistant A498 cells (Hosono *et al.*, 2010). However, its general lack of enzymatic activities makes NUB1 less suitable for small molecule inhibition (Lu *et al.*, 2013). Thus, the low-molecular-weight proteins FAT10 and NEDD8 could be key to developing novel strategies in anticancer therapy, as they interact with NUB1 (Tanaka *et al.*, 2012).

The UBL enzymatic cascade scheme that results in UBL conjugation and protein degradation involves several distinct steps. Each step requires different classes of enzyme and is shown in table 1.6.

Table 1. 6 Overview of the enzymatic cascade involved in UBLs conjugation.

UBL	**Ub**	**NEDD8**	**FAT10 and Ub**
E1 activating enzymes	UAE	APPBP1-UBA3 heterodimer	UBA6
E2 conjugating Enzymes	UBCs	UBE2M &UBE2F	USE1
E3 ligases	Ub E3 Ligases	NEDD8 E3 Ligases	?
Substrates	1,000s	200s	?

*UBC: Ub conjugating enzymes UBL, ubiquitin-like protein; Ub, ubiquitin; NEDD8, neural precursor cell expressed, developmentally down-regulated 8; FAT10, HLA-F-adjacent transcript 10; UAE, ubiquitin-activating enzymes; APPBP1, amyloid-β precursor protein-binding protein 1; UBA, ubiquitin-like modifier-activating enzyme; UBCs, Ub-conjugating enzymes; UBE2, ubiquitin-conjugating enzymes E2; USE1, UBA6-specific E2 enzyme; N/A, not applicable.

1.4 Neddylation and its functions

Neddylation is a post-translational modification process that conjugates NEDD8 to its target proteins, in a process that is analogous to that observed for ubiquitination. However, the neddylation process uses a distinct E1 and E2 enzyme reaction scheme (Haas *et al.*, 1987; Kamitani *et al.*, 1997; Liu *et al.*, 1999; Ichimura *et al.*, 2000; Bawa-Khalfe and Yeh, 2010) (Table 1.6). Fig1.9 summarises the NEDD8 conjugation and deconjugation steps (Rabut and Peter, 2008; Tanaka *et al.*, 2012). The C-terminal glycine of NEDD8 is adenylated by E1 NEDD8 activating enzymes (NAE), a heterodimer composed of amyloid-β precursor protein binding protein 1 (APPBP1) and ubiquitin-activating enzyme 3 (UBA3). NEDD8 is covalently conjugated to the NAE via a thiolester linkage (Walden *et al.*, 2003). The activated NEDD8 is consecutively transferred to the E2 NEDD8-conjugation enzyme and then to the specific substrates (i.e. cullins) via an isopeptide bond. Some RING finger domain containing proteins including Rbx1/ROC1, MDM2, FBXO11, and c-Cbl, work in an E3 ligase-like fashion for cullin neddylation.

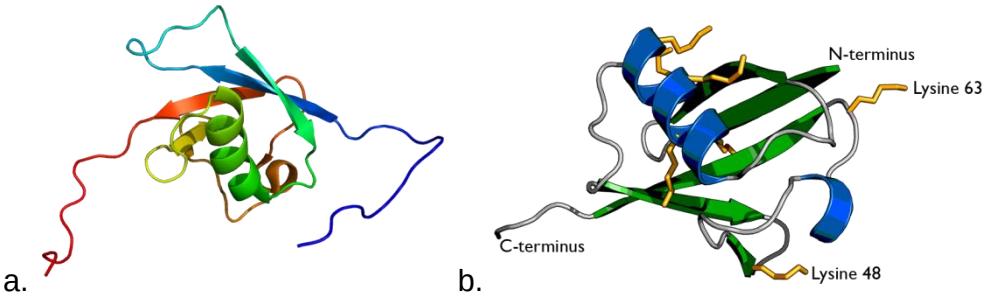


Figure 1. 8 Structure of a) N-terminal ubiquitin-like domain of human NUB1 b) Human ubiquitin.

There are two NEDD8-specific E2 conjugating enzymes, namely UBE2M (also known as UBC12) and UBE2F. These E2 enzymes act to transfer NEDD8 to target protein through E3 enzymes. It was reported that all NEDD8 E3 enzymes can function as ubiquitin E3 enzymes. The predominant NEDD8 E3 ligases are the ring subunits RING-box protein 1 (RBX1) and RBX2 (Kamura *et al.*, 1999; Walden *et al.*, 2003; Huang *et al.*, 2007; Huang *et al.*, 2009; Olsen *et al.*, 2010). Meanwhile, the non-RBX family NEDD8 E3 ligases include c-CBL, RNF111 (ring finger protein 111), MDM2 and inhibitor of apoptosis (Enchev *et al.*, 2015).

Of the numerous NEDD8 substrates, neddylation has been best described in the cullin family (Hjerpe *et al.*, 2012). In this mechanism, NEDD8 from the E2 cysteine active site is transferred onto a lysine residue in the N-terminus of the target proteins (Fig. 1.9) (Saha and Deshaies, 2008). Cullin neddylation is further mediated by defective in cullin neddylation protein 1-like proteins (Enchev *et al.*, 2015). It was reported that RING E3 ligases could neddylate the same substrate on multiple lysine residues (Enchev *et al.*, 2015). However, the interaction between non-RBX RING E3 ligase and E2 enzymes remains to be elucidated.

NEDD8-conjugated substrates are deneddylated by various proteins that include COP9 signalosome (CSN), NEDD8-specific protease 1 (NEDP1/DEN1) and ubiquitin specific peptidase 21 (Lyapina *et al.*, 2001; Schwechheimer *et al.*, 2001; Mendoza *et al.*, 2003; Chan *et al.*, 2008; Rabut and Peter, 2008; Gong *et al.*, 2014). Neddylation may be inhibited by cullin-associated and neddylation-dissociated 1 through its direct binding to cullins (Liu *et al.*, 2002; Goldenberg *et al.*, 2004). NEDD8 and neddylated substrates are recruited by NUB1 for proteasomal degradation (Kamitani *et al.*, 2001; Kito *et al.*, 2001) (Figure 2a). In the G1-S phase transition, Bornstein *et al* demonstrated how neddylated cullin 1 cooperatively activates the SCF^{SKP2} Ub ligase complex, which results in p27 degradation (Fig. 1.9) (Bornstein *et al.*, 2006). Furthermore, previous studies found that cullin neddylation increased the Ub E3 ligase activity of the SCF complex (Fig. 1.10) (Duda *et al.*, 2008; Saha and Deshaies, 2008).

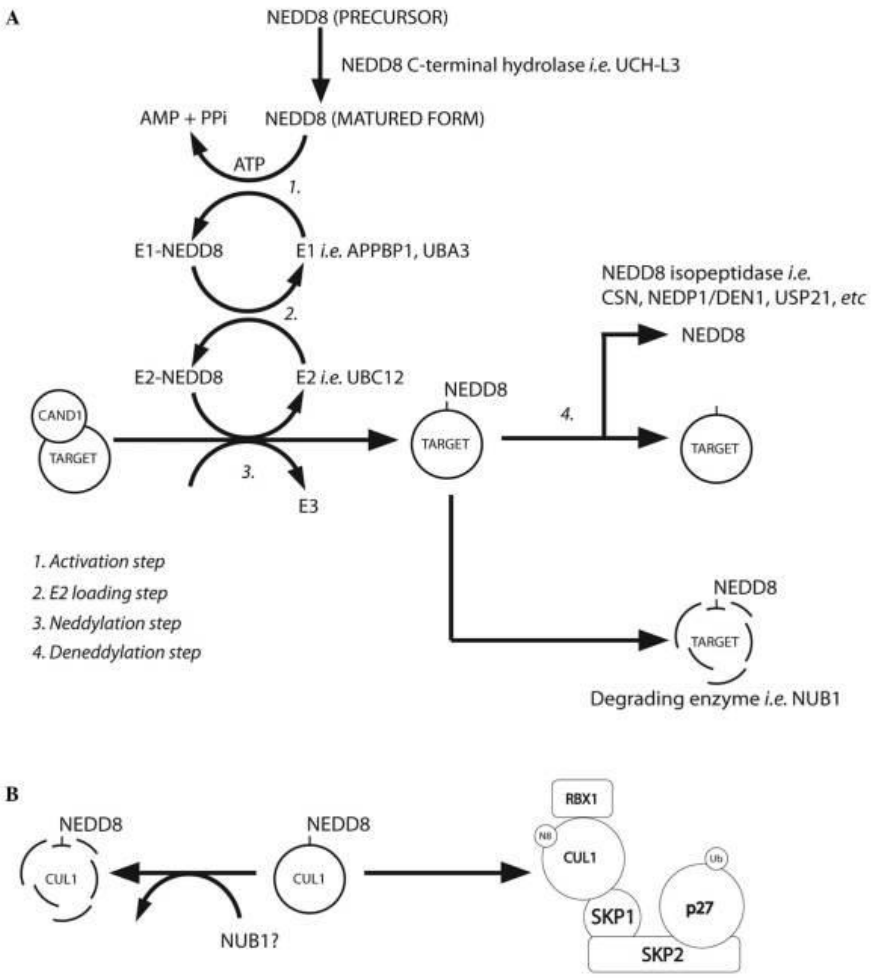


Figure 1. 9 NEDD8 conjugation pathway and roles of NUB1 on neddylated CUL1. (A) Schematic summary of the main steps of the neddylation pathway [modified from Rabut and Peter, 2008 (Rabut and Peter, 2008); Tanaka *et al*, 2012 (Tanaka *et al.*, 2012)]. (B) Neddylated CUL1 locks the SCF complex with phosphorylated p27 and cyclin E [as suggested by Bornstein *et al*, 2006 (Tanaka *et al.*, 2012) and Tanaka *et al*, 2012 (Bornstein *et al.*, 2006)]. CAND1, cullin-associated and neddylation-dissociated 1; AMP, adenosine monophosphate; PPi, anion $P2O7^{4-}$; ATP, adenosine triphosphate; UCH-L3, ubiquitin C-terminal hydrolase isozyme L3; APPBP1, amyloid-β precursor protein binding protein 1; DEN1, deneddylase 1, CSN, COP9 signalosome; NEDP1, NEDD8-specific protease 1; NUB1, NEDD8 ultimate buster 1; USP21, ubiquitin specific peptidase 21, CUL1, cullin 1; SKP1, S-phase kinase-associated protein 1; SKP2, S-phase kinase-associated protein 2; RBX1, ring-box 1, E3 ubiquitin protein ligase; SCF, Skp, cullin, F-box-containing complex.

NEDD8 is negatively down regulated by NEDD8 ultimately buster 1 (NUB1), which links the UBLs to the 26S proteasome for further UPS degradation. Reports described that NUB1 can recruit NEDD8 and NEDD8-conjugated proteins to the proteasome for degradation, and this might modulate the cell cycle profile upon stress (Tanaka *et al.*, 2012). The capability of NEDD8 to activate the ubiquitin E3 ligase-SCF complex (by covalent binding to cullins) adds more complexity to the ubiquitination machinery (Kamitani *et al.*, 1997; Osaka *et al.*, 1998; Wada *et al.*, 1999; Podust *et al.*, 2000; Read *et al.*, 2000; Morimoto *et al.*, 2003). Therefore, validations of NEDD8 targets would be able to identify the genuine NEDD8 substrates.

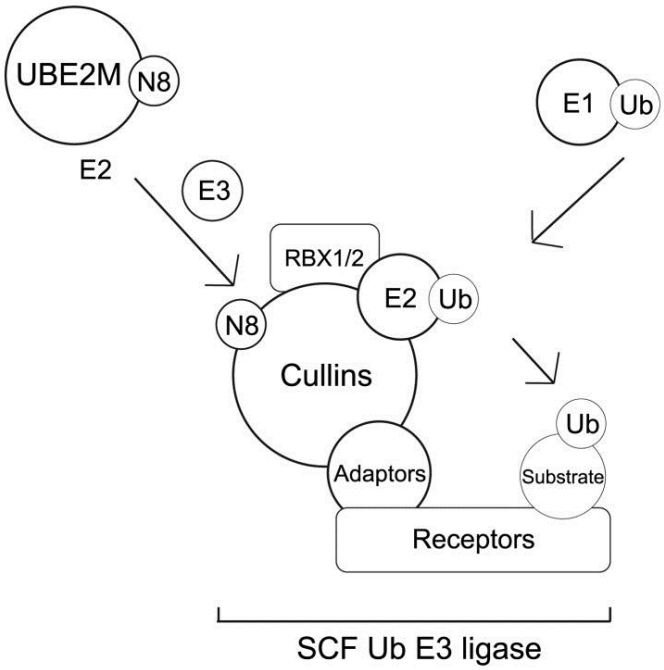


Figure 1. 10 NEDD8 conjugation and ubiquitination pathway through cullin proteins. UBE2M, ubiquitin-conjugating enzyme E2M; RBX1/2, ring-box 1; Ub, ubiquitin; NEDD8, neural precursor cell expressed, developmentally down-regulated 8; SCF, Skp, cullin, F-box-containing complex.

1.5 FAT10ylation and its functions

FAT10 was discovered by Sherman Weisman in 1996 (Qin *et al.*, 2008). Due to the poor solubility of the protein at high concentrations, the structure of FAT10 protein was only recently defined (Theng *et al.*, 2014). The structure of FAT10 consists of two β-grasp fold domains connected by a short linker (Theng *et al.*, 2014). FAT10 protein was found to be expressed predominantly in immune tissue including thymus, lymph nodes and spleen (Michel *et al.*, 2004; Wagenaar-Miller *et al.*, 2004; Tapia *et al.*, 2006). Its expression is stimulated by pro-inflammatory cytokines, namely interferon-γ (IFN-γ) and tumour necrosis factor (TNFα) (Aichem *et al.*, 2012). FAT10 protein is found in mature dendritic cells and it demonstrates oncogenic characteristics. Ectopic expression of FAT10 was observed in malignant tumour transformation and its growth (Gao *et al.*, 2014), and FAT10 is known to be upregulated in several tumour types, for example in liver and colon tumours (Lee *et al.*, 2003; Lukasiak *et al.*, 2008).

FAT10 shares the same E1 and E2 enzymes with the Ub conjugation pathway. The FAT10 E1 enzyme UBA6 can activate both Ub and FAT10 (Chiu *et al.*, 2007; Jin *et al.*, 2007; Pelzer *et al.*, 2007; Groettrup *et al.*, 2008). FAT10's adenylation and transthiolation reactions are kinetically slower than those for Ub. UBA6 protein is thought to be the only FAT10 E1 enzyme in cells, since UBA6 knockdown effectively abolished the formation of FAT10-conjugates *in vitro* (Chiu *et al.*, 2007; Aichem *et al.*, 2010). Similarly, USE1 is the only UBA6-specific E2 enzyme discovered to be involved in FAT10 conjugation, though it also functions in a similar fashion for the conjugation of Ub (Jin *et al.*, 2007). USE1 could only bind to activated Ub from UBA6 but not UBE1 (Jin *et al.*, 2007).

Little is currently known about FAT10 and research to identify possible FAT10 E3 ligases and deconjugating enzymes continue. However, ectopically expressed FAT10 was not observed to degrade over time, suggesting that a group of FAT10-deconjugating enzymes may not exist (Hipp *et al.*, 2005). It is believed that FAT10 is capable of promoting its own proteasomal-dependent degradation without the aid of deconjugation enzymes (Hipp *et al.*, 2005). FAT10-conjugated proteins were found to have a reduced half-life similar to that observed for ubiquitin-conjugated proteins (Kane *et al.*, 2007). Conversely, it was found that FAT10-conjugated p62 accumulated under proteasome inhibition (Aichem *et al.*).

The interferon inducible protein NUB1 interacts with FAT10 non-covalently (Kamitani *et al.*, 2001) and it significantly accelerates the degradation of FAT10 by the proteasome (Kamitani *et al.*, 2001). NUB1 binds to the proteasome subunit S5a (Tanji *et al.*, 2005) NUB1 also bind to FAT10 via its three C-terminal UBA domains (Fig 1.11) (Hipp *et al.*, 2004). NUB1 is also able to interact with the von Willebrand A (VWA) domain of RPN10 (S5a), one of the subunits of the 26S proteasome (Kamitani *et al.*, 2001; Tanji *et al.*, 2005). The degradation of FAT10 is accelerated further by NUB1 splicing variant, NUB1L which can bind both to RPN10 as well as the 19S regulator subunit RPN1 (S2) (Hipp *et al.*, 2004).

The 26S proteasome subunit RPN10 (S5a) is the docking site for FAT10, NUB1L, and polyubiquitin. Lysine 48-linked poly-ubiquitin chains bind to the ubiquitin interaction motifs (UIM) 1 and 2 of RPN10. Meanwhile, FAT10 can target substrate proteins to the proteasome independently of poly-FAT10ylation. FAT10 directly interacts with the VWA domain of RPN10 and no ubiquitination is required (Tanji *et al.*, 2005). The co-expression of NUB1L accelerated the degradation of FAT10 suggesting the favour of proteasomal degradation (Tanji *et al.*, 2005).

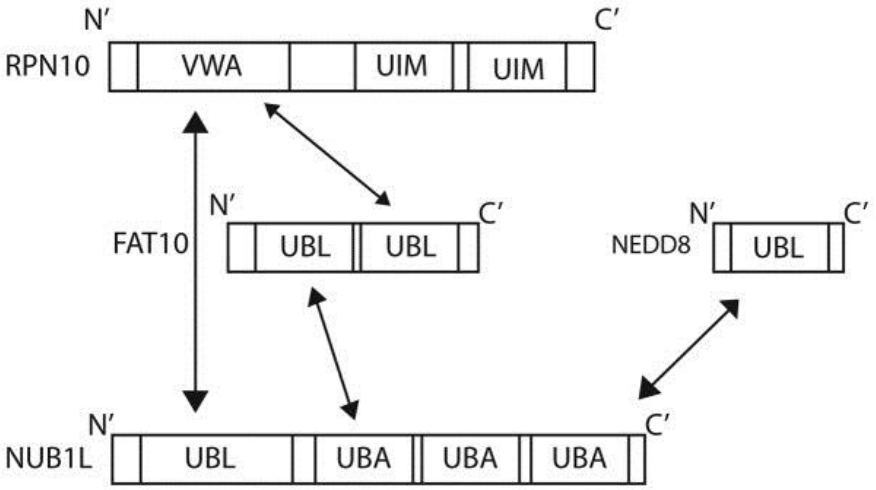


Figure 1. 11 Domain structure of NUB1L, FAT10 and RPN10 and their interacting domains (Kamitani *et al.*, 2001; Hipp *et al.*, 2004; Tanji *et al.*, 2005). RPN10, regulatory particle non-ATPase 10; FAT10, HLA-F-adjacent transcript 10, NUB1L, NEDD8 ultimate buster 1 long isoform; UBL, ubiquitin-like domain; UBA, ubiquitin-associated; UIM, ubiquitin-interacting motif; VWA, von Willebrand A motif.

1.6 Ubiquitin Proteasome System

The UPS is important in regulating protein homeostasis in human cells through programmed degradation. The degradation of regulatory proteins can affect cell-cycle regulation, cell proliferation, intracellular signaling, DNA repair and apoptosis (Ciechanover, 1998; Ciechanover and Schwartz, 1998; Hershko and Ciechanover, 1998; Hershko, 2005). As UPS degradation is a major clearance system associated with proteolysis within the cells, its deregulation can cause the pathogenesis of cancer and other diseases through the inappropriate loss of regulatory proteins or unintentional activation of certain specific signalling cascades. For instance, cancerous cells develop when cell cycle controls break down, leading to unregulated cell proliferation. Cancer cells can also escape from apoptosis induced by several cellular stresses. Hence, an interruption to the normal regulation of the UPS could lead to abnormal cell proliferation.

The 26S proteasome is a protease complex capable of degrading polyubiquitinated proteins. The 26S complex is composed of a barrel-shaped 20S proteasome core with a 19S regulatory particle at either or both of its ends. The 20S proteasome contains the enzymatic active sites, whilst the 19S regulatory particle helps to control access of UBL-conjugated substrates to the core. There are three proteasome active sites within the 20S core, namely the caspase-like (β1), trysin-like (β2) and chymotrypsin-like (β5) domains. These sites use an N-terminal threonine as the catalytic amino-acid residue.

1.7 Rationale of study

The discovery of down-regulated AIPL1 in cancer has promted the interests to identify its role in cancer. Chaperones are thought to contribute to cancer progression, whereas cochaperones could be pleomorphic. Down-regulated chaperones could result in the accumulation of both misfolded and nascent client proteins which are functionally inactive. Though both HSP90 and HSP70 HSPC interact with AIPL1 (in a cochaperone fashion), AIPL1 proteins is able to interact independently with NUB1 in a chaperone-like manner(van der Spuy *et al.*, 2002). AIPL1 also has a role in post-translational modification and regulating intracellular protein trafficking (Berg and Pongratz, 2002).

The AIPL1 signaling pathway was studied for retinal degenerative diseases but no studies were performed to correlate AIPL1 with to cancer metastasis and pathogenesis. The interaction of AIPL1 with NUB1 could serve physiological relevance in cancers. It regulates the ubiquitin proteasome system through FAT10ylation and neddylation. NUB1 is able to recruit FAT10- and NEDD8-conjugated for proteasomal degradation.

The SCF ubiquitin E3 ligases have been shown to be deregulated in various cancers. It results in unlimited cell proliferation and carcinogenesis *via* accumulation of their substrate proteins. As a result, the ubiquitin E3 ligases are gaining attention as a potential target for anticancer therapy.

The search for neddylation targets requires more robust experimental validations. The ectopic overexpression of the UBLs could lead to false positive conjugation of substrates (Enchev *et al.*, 2015). The functional significance of this observation remains unknown. There is a general lack of information on how NUB1 regulates cullin neddylation under homeostatic conditions. It is an open question whether neddylation is functionally distinct from ubiquitination. For example, polyneddylation and polyubiquitination at DNA damage sites or in response to other stress conditions are functionally redundant, and NEDD8 and ubiquitin can be recognized by the same interaction motifs. These two modifications can elicit distinct biological responses. Efforts are clearly needed to identify and characterise NEDD8-interacting domains and proteins.

Unlike such deconjugating enzymes as CSN, NEDP/DEN1 and USP1, NUB1 causes the degradation of both FAT10- and NEDD8-conjugated targets. It therefore appears to be a unique degrading enzyme in cells. Its expression regulates NEDD8- and FAT10-based signalling in response to cellular stresses. However, NUB1 protein and its clinical relevance in UBL' pathways remain to be explored. Hosono *et al.* (2010) found that overexpression of NUB1 inhibits cell growth, and the same study demonstrated lower NUB1 mRNA expression in IFNα-sensitive 4THUR cells (Hosono *et al.*, 2010). The same study highlighted that NUB1 does not get induced in IFNα-resistant cells. The transiently expressed NUB1 sensitise the same cells (Hosono *et al.*, 2010) and induces apoptosis (Hosono *et al.*, 2010). Therefore, there is a potential strategy to kill IFNα-resistant cells by increasing NUB1 activity (Hosono *et al.*, 2010).

FAT10 research is still in an early stage as the biological consequences of FAT10ylation are poorly described. The de-FAT10ylating enzymes are actively pursued as drug targets in the pharmaceutical industry these days knowing that a number of putative FAT10 targets are cancer promoting or inhibitors of apoptosis. Future work should focus on the FAT10 modulated Proteasome System and the mechanism of its cytokine-induced reactions.

Cochaperones are potential targets for cancer therapy in themselves and can be used to assess the likely prognosis of individual malignancies. The key importance of cochaperones for many pathways of protein folding in cancer suggests high promise for the future development of novel pharmaceutical agents. The negative regulation of the Ub, NEDD8 and FAT10-conjugation pathway could impose great potential for cancer suppression. SCF complexes are often deregulated in cancer and could be modulated through manipulation of CUL neddylation. Neddylation and FAT10ylation inhibitors have recently been developed as a novel class of anticancer agent. These compounds are expected to exhibit better specificity for cancer cells and have reduced toxicity. The degrading enzyme (such as CSN and NUB1/NUB1L) is an attractive candidate for inhibition of Ub, NEDD8 and FAT10-ligase activity. They are expected to represent a new strategy in anticancer therapy.

The interplay of these ubiquitin like proteins highlight the roles of both AIPL1 and NUB1. It is essential to understand the mechanisms on how AIPL1 regulates NUB1 and down-regulates the ubiquitin cascade *via* NEDD8 conjugation and the FAT10 pathway. This provides insights into potential cancer therapy that could be used to selectively suppress cancer growth. We are searching for the roles of AIPL1 and its interacting NUB1 partner in cancer. AIPL1 and NUB1 could be potential targets for cancer therapy and be used to assess the prognosis of cancer malignancies.

1.8 Objectives of study

In general, this study aims to describe the specific role of AIPL1 and NUB1 in cancer pathogenesis. The work will focus on the neddylation induced accumulation of p27 and p21 and the corresponding cell cycle regulation.

The specific objectives include

a) To characterise the AIPL1 & NUB1 transcription pattern and the clinico-pathological correlations through bioinformatic analysis.
b) To study how AIPL1 & NUB1 affect p27 and p21 through CUL1-based ubiquitin E3 ligase.
c) To examine the alternative pathway of AIPL1 and NUB1 through CUL2-based ubiquitin E3 ligase.
d) To correlate the NUB1 protein expression to patients' treatment outcome.

Chapter 2

Methods and Materials

2.1 Cell Line

All cancer cell lines were obtained from American Type of Cell Collection (ATCC, Manassas, VA, USA). HCC1806, MCF-7, MDA-MB-231,SKBR3, BT474, ACHN, 786-O, RCC4, RCC4plusVHL and T-47D cells were maintained in DMEM supplemented with 10%(v/v) foetal calf serum (FCS). HCT116 were maintained in McCoy's 5A supplemented with 10%(v/v) FCS. Y79 was cultured in RPMI-1640 with 20%(v/v) FCS. The medium was changed every two to three days. All cell lines were obtained from Cancer Research UK Cell Production Laboratories (Clare Hall, Hertfoshire, UK). All cells were free from mycoplasma contamination. MLN4924 (Pevonedistat®) was purchased from Sigma and was dissolved in dimethyl sulfoxide (DMSO) and stored at −20 °C.

2.2 Cell Culture

Cells were grown in a tissue culture incubator in a humidified atmosphere of 5% CO_2 and 95% filtered atmospheric air, and maintained at a temperature of 37°C, unless otherwise indicated. Cells were passaged by aspirating medium, washing the cells with PBS, and then adding 1x trypsin-EDTA (Invitrogen) until they detached. The trypsin was neutralized by adding equal amount of DMEM supplemented with 10% (v/v) FBS. The cells then were centrifuged for 5 minutes at 1000 rpm to generate a pellet from which the supernatant was aspirated. The pellet was then split 1:10 and reseeded. This process was carried out every 6-7 days. Cells were cultured on sterile, tissue culture grade, non-pyrogenic plasticware (Corning). Cells were treated with MLN4924 (Sigma) at 1µM for 48h.

Hypoxic incubations (0.1% O2, 5% CO2,) were performed using an INVIVO2 400 hypoxic workstation (Pro-Lab Diagnostics). All cells were allowed 6 hours to attach and recover after being plated in final densities before being exposed to hypoxia.

2.3 Counting Cells

Cell counting was performed when a specific number of cells were required for an experiment. Cells were detached, centrifuged, and resuspended, in an appropriate volume of medium. Cells then were counted using the Coulter Particle Counter Z2 (Beckman Coutler) according to maufacturer's instructions. Briefly, 400µL of cell suspension were diluted with 19.6 µL of isoton buffer and a particle count taken in the range of 9-27 µM. The machine was calibrated to calculate the number of cells/mL.

2.4 Preparation and Recovery of cell stocks (cryo-preserved cells)

Only cells in the log phase of growth were used for cryopreservation. Cells were detached as described previously. The cell pellet was then resuspended in freezing medium and divided between rounded bottomed cryo-vials (Corning). Freezing medium was prepared with DMSO, FCS, and culture medium at a ratio of 1:3:6, respectively. Vials were frozen down to 1° C per minute to -80 ° C in an isopropanol-bath freezing container (MrFrosty, Nalgene). Within one week, cell vials were transferred to liquid nitrogen for long term storage. To recover the cells from storage, cryovials were rapidly defrosted to 37°C and transferred to pre-warmed media.

2.5 Gene silencing by RNA Interference

Cells were plated on 6-well dishes at 0.25-1 x 10^6 per dish and left overnight to adhere. siRNA duplexes were transfected into cells at 25pmol using Oligofectamine™ RNAiMAX and then cultured in Optimem™ for 1-3 days (3µL 10µM siRNA, 9µL Oligofectamine™, 150µL Optimem™).

Transfections of siRNA duplexes targeting NUB1 or non-targeting pool were from Dharmacon ON-TARGETplus Human NUB1 siRNA, at a final concentration of 25pmol. The sequences of siRNA used to target NUB1 and control sequence were L-019158-00-0005 and D-001810-10-05 respectively (Dharmacon GE, UK). Reduction in NUB1 protein expression, measured by Western blot analysis, was used to indicate gene silencing.

2.6 Immunostaining of paraffin-embedded tissue sections

Staining of formalin-fixed paraffin-embedded tissues was performed according to the following description. Slides were heated at 120°C for 10 min to melt the wax and help the sections adhere. They were then dewaxed and immersed in Citroclear (HD, Supplies, UK) for 5 min twice and rehydrated in graded Industrial Methylated Spirit solutions (100% twice followed by 50% once for 5min in each) before rinsing in tap water followed by a PBS wash. Antigen retrieval was performed in a decloaking chamber (Biocare Medical, USA) set at 2min, high pressure, in EDTA pH8.0. Then, the cooling slides were placed in PBS.

To minimize non-specific antibody binding, the slides were blocked with 10% normal horse serum (Vector Laboratories, UK). In the next step, primary antibody was applied to the slides and incubated at room temperature for 1 hour. Both antibodies were diluted in RPM1 (Lonza) with 10% bovine serum (Sigma-Aldrich). After 1 hour incubation, the slides were washed three times with PBS, and then they were incubated with the anti-mouse secondary antibody for 50 minutes at room temperature. The slides were then washed with PBS for three times, and DAB was applied to the sections for 5-8 min. The reaction was stopped by washing the slides with tap water. In the final step the slides were counterstained and immersed in heamatoxylin solution (Gill No3) for 20s, rinsed in tap water and mounted with Aquamount. Slides were visualized on a BX51 microscope (Olympus) attached to a DP70 digital camera (Olympus) and images were captured using the DP manager and DP Contoller software (Olympus).

Antibody	Antibody name/catalogue number	Species	Clonality	Source
NUB1	4H2	Mouse	Monoclonal	Novus biologicals
AIPL1	3B4	Mouse	Monoclonal	Novus biologicals
FAT10	4F1	Mouse	Monoclonal	EMD Milipore
NEDD8	Y297	Rabbit	Monoclonal	Abcam
HIF1α	610958	Mouse	Monoclonal	BD Biosciences
HIF2α	Hif2a 237	Mouse	Monoclonal	Ximbio
CA9	M75	Mouse	Monoclonal	Absolute antibody
PARP	D64E10	Rabbit	Monoclonal	Cell signaling technologies
P21	EA10	Mouse	Monoclonal	EMD Milipore
CUL2	51-1800	Rabbit	Polyclonal	Invitrogen
VHL	S2-647	Mouse	Monoclonal	BD Biosciences
P27	D69C12	Rabbit	Monoclonal	Invitrogen
CUL1	71-8700	Rabbit	Polyclonal	Cell signaling technologies

Table 2. 1 Immunostaining Antibodies

2.7 Protein Extraction

Cells were washed in ice cold PBS and lysed in 2 x sample buffer (125mmol/L Tris [pH 6.8], 4% sodium dodecyl sulfate, 0.01% bromophenol blue, 10% β-mercaptoethanol, 10% glycerol).

2.8 Protein Polyacrylamide Gel Electrophoresis (PAGE)

The required volume of 6x SDS-PAGE sample buffer (72mM Tris pH 6.8, 20% glycerol, 4.5 % SDS, 10% β-mercaptoethanol and 0.015% bromophenol blue) was added and samples were heated to 95^{o}C for 10 minutes. Whole cell lysates were resolved by SDS-PAGE followed by electroblotting onto polyvinylidene-difluoride membrane (Millipore).

2.9 Antibody Incubation

Membranes were incubated overnight with an appropriate concentration of primary antibody in PBS containing 5% milk powder and 0.1% Tween-20. Membranes were incubated with Horseradish peroxidase-conjugated anti-rabbit or anti-mouse antibodies (DAKO Inc). Immunoreactivity was detected using CL system (Amersham Biosciences). The following antibodies were used, mouse anti-HIF-1α (BD Transduction Laboratories, USA), mouse anti-NUB1 (Novus biologicals), mouse anti-AIPL1 (Novus biologicals), mouse anti-FAT10 (4F1) (Cell signaling), rabbit anti-NEDD8 (Y297) (Novus Biologicals), mouse anti-HIF2α and (Ximbio) mouse anti-CAIV (Absolute Antibodies). Blots and densitometry analysis was carried out using ImageJ software (Scion Corporation).

2.10 Real-time PCR (qPCR)

Retrotranscription was performed using RetroScript kit (Ambion). All mRNA and β-actin expression was analyzed by PCR using TaqMan Gene Expression Assays (Applied Biosystems). The reaction was performed on a PTC-200 thermal cycler with a Chromo 4 continuous fluorescence detector (Bio-Rad, Hemel Hempstead, UK). The comparative cycle threshold (C_T) method was used to analyse the data by generating relative values of the amount of target cDNA, according to the $2^{-\Delta\Delta CT}$ method using β-actin house-keeping gene as calibrator.

2.11 Cell cycle analysis using flow cytometry

Samples were prepared as described in Sabatinos & Forsburg (Sabatinos and Forsburg, 2009). Briefly, cells were fixed in 1ml 70% ethanol; 300µl of this mixture washed in 3ml 50mM Na citrate, pellets resuspended in 0.5ml 50mM Na citrate containing 0.1mg/ml RNase A (Sigma) and left at room temperature for 2h. A volume of 0.5ml 50mM Na citrate containing 8µg/ml propidium iodide (Sigma) was subsequently added to a final concentration of 4µg/mL. 20,000 single events were analysed for FSC, SSC and DNA content using the Becton Dickinson® LSR II Research Flow Cytometer and the Flow_Jo v.9.2 Software.

2.12 Presence of disulphide bond with fluoresceine maleimide

Free thiols in lysate were blocked in the protein with iodoacetamide and remove the excess. The protein is denatured with SDS or urea. Then divided into 2 samples: leave one oxidised and reduced the other with tris(2-carboxyethyl)phosphine, TCEP. Each sample was reacted with fluorescein maleimide. The samples were run on SDS-PAGE. If there was a disulfide bond in the protein, the TCEP-reduced sample will be fluorescent and the oxidised sample will not be.

2.13 Statistical analyses

Statistical analysis was performed using SPSS 15.0 (Chicago, IL, USA). Data obtained from cell count, colony formation, MIB1 staining, cell cycle and mitochondrial function experiments were analysed by the Student´s t test or the Mann-Whitney U test for parametric and nonparametric variables, respectively. For survival analysis, Kaplan-Meier survival curves and the log rank test were used to analyze differences in RFS (the median was selected as the cut-off value). Multivariate analysis was carried out using the Cox proportional hazards model. Only variables of $P<0.1$ from the univariate analysis were entered in the Cox regression analysis. The proportional hazards assumption was examined by testing interactions between the covariates of the final model and time. A P value less than 0.05 was considered statistically significant.

2.14 Buffers and solutions

The preparation of bufferes and solutions are as detailed below:-

For cell culture:	
PBS	137mM NaCl
	2.7mM KCL
	4.3 mM Na_2HPO_4
	1.4 mM KH_2PO_4
	Ca^{2+} and Mg^{2+} free (pH 7.3)
Trypsin/EDTA 20 mg/ml Trypsin	1 mM ethylenediaminetetraacetic acid (EDTA) in PBS

For protein extraction from monolayer cell cultures:	
Lysis Buffer	10% (v/v) glycerol
	10 mM Tris-HCL pH 6.8
	5mM dithiothreitol (DTT)
	1% (v/v) sodium dodecyl sulphate (SDS)
	6.25 M urea
	1 protease inhibitor tablet (Roche Diagnostics) per 50 ml

For protein analysis:	
1x running buffer	25 mM Tris
	250mM glycine
	0.1% (v/v) SDS
6x sample buffer	72mM Tris-HCL pH 6.8
	20% (v/v) glycerol
	4.5% (v/v) SDS
	10% (v/v) β-mercaptoethanol
	0.015% (v/v) bromophenol blue
Transfer buffer	25mM Tris
	192 mM glycine
	15% (v/v) methanol
TBS	50mM Tris-HCl
	150mM NaCl
	pH 7.4
Stripping buffer	62.5 mM Tris-HCl pH 6.8
	2% (v/v) SDS
	100mM b-mercaptoethanol

For immunohistochemistry:	
Citrate Buffer	10mM citric acid pH 6.0
Tris EDTA buffer	50mM Tris 2mM EDTA pH 9.0
EDTA buffer	1mM EDTA pH 8.0

Chapter 3
Systematic Analysis of Gene Expression Alterations and Clinical Outcomes for AIPL1 and NUB1 in Cancer

3.1 The rationale of study

Combined microarray and clinical databases are a precious resource for scientists to acquire of the possible role of genes and pathways in cancer and look for basic information as far as the possible clinical meaning of specific gene expression signatures in cancer is concerned. This chapter aims to systematically analyse the AIPL1 and NUB1 transcription and identify whether their transcription levels have any prognostic value. I have been exploiting the Oncomine and METABRIC databases. The database could reveal the biological functions and provide the information for the possible underlying mechanism of AIPL1 and NUB1 genes. It improves our understanding of the genes in cancer mechanisms.

Through DNA microarray technology, public databases could address the fundamental physiological research questions in the postgenomic era. These genome-scale methodologies provide a more global perspective. My research question asks in what cancers or cancer subtypes are AIPL1 and NUB1 gene being altered? Do the AIPL1 and NUB1 genes manage to distinguish metastatic cancer from primary disease? Do the AIPL1 or NUB1 genes serve as biomarkers for a particular cancer or cancer subtype? The differential expression pattern implies the potential cancer promoting role or tumour suppressor role in cancer and leads to a reliable hypothesis for cancer research.

Meta-analysis demonstrates the robustness of AIPL1 and NUB1 molecular signatures. This is essential when the hypotheses or molecular signatures derived experimentally are to be validated *in silico*. Besides, large-scale gene-expression profiles for tumours allow the identification of prognostic disease markers or predictors of therapeutic response. Investigators can perform meta-analysis of mRNA expression patterns between datasets to uncover sets of genes important in specific phenotypes or clinical behaviours.

There is a need for acquiring the genetic details in order to speculate the meaningful outline of how AIPL1 and NUB1 proteins may affect cancer physiology. Most of the AIPL1 reports were on retinal degenerative diseases and none in cancers. Therefore the potential role of AIPL1 could be extended to be a part of a signaling pathway in cancer tissues.

The differential expression of AIPL1 facilitates advanced mining of the data in various cancer types. For instance, instead of merely detecting under-expression of AIPL1, it is possible to detect activation of this pathway via differential expression of downstream genes. This will allow for therapeutic targeting of pathways at multiple levels rather than single targets.

The integrative bioinformatics analyses will generate novel hypotheses with respect to cancer progression. The gene alterations and gene signatures of more aggressive cancers identify the possible oncogenic or tumour suppressive nature of gene products in cancers. Further insight into these pathways will be acquired by comparing cancer promoting signatures from cell line and *in vivo* cancer progression models with the expression patterns obtained from tumor specimens. The analyses will demonstrate the significance of AIPL1 and NUB1 in tumor formation of various kinds of cancer and the association of expression level with survival of cancer patient.

The goal is to use bioinformatics methods to analyse the publicly available data in order to outline the potential role of gene products such as AIPL1 and NUB1 and to formulate novel hypotheses speculating on mechanisms of action. The data mining and function prediction is useful to know more about AIPL1 and to generate hypotheses. The global objective is to identify biomarkers that can be used to classify tumours and to determine which treatment is best suited for each type.

It is hypothesized that chaperones could be down-regulated in tumours. This phenomenon represents a new cancer causing mechanism. Following reduced availability of chaperones proteins, the tumour suppressor activity is lost as the normal protein cannot fold properly. To our best knowledge, this is the first systematic analysis addressing the role of AIPL1 in cancer progression.

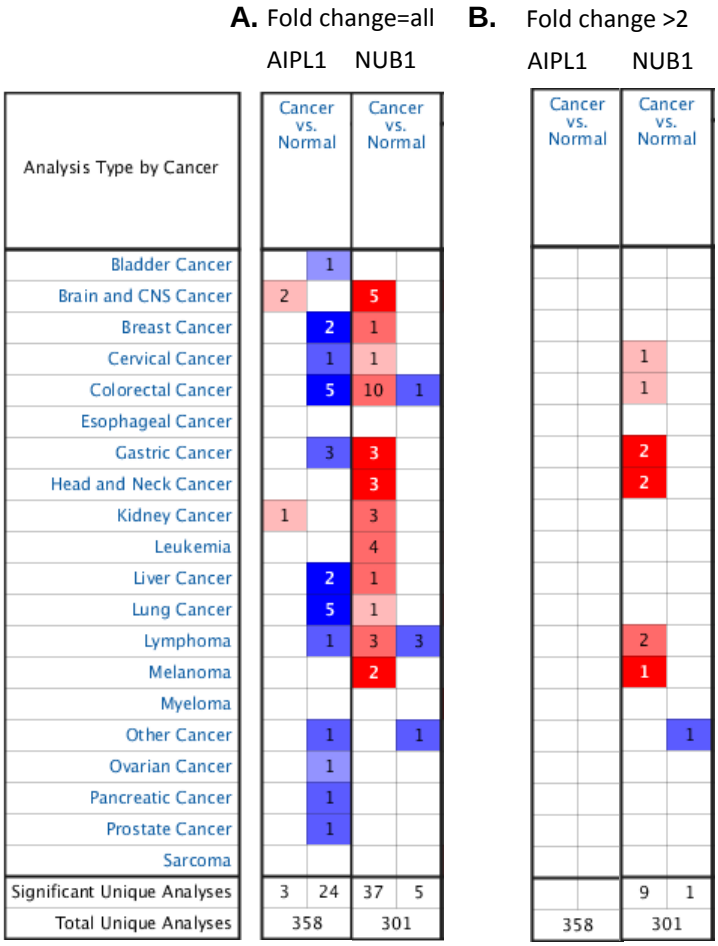
3.2 Concordant down-regulation of AIPL1 transcripts and upregulated NUB1 level in Oncomine database

To elucidate the AIPL1 expression pattern in cancer, the systematic analysis of AIPL1 and NUB1 expression was done using Oncomine database (http://www.oncomine.org). The expression of AIPL1 was compared between tumour and normal tissue in different types of cancers (Table 3.1). The threshold was designed as the following parameters, *p*-value of 0.05 and top gene rank 10%. The AIPL1 expression was higher in cancer than in normal tissue in brain and kidney cancers. On the other hand, cancer AIPL1 expression was lower in bladder, breast, cervical, colorectal, gastric, liver, lung, lymphoma, ovarian, pancreatic and prostate and other cancers (Table 3.1). The AIPL1 mRNA was found significantly and concordantly down-regulated in cancer tissues compared with normal tissues (with number of dataset, 24 vs. 3). These data suggests that AIPL1 plays a tumour suppressive role in cancers. Meanwhile for NUB1 under the same threshold, the transcripts were mostly upregulated in cancers (number of dataset): Brain and CNS

cancer (5), breast cancer (1), cervical (1), colorectal cancer (10), gastric cancer (3), head and neck cancer (3), kidney (3), leukaemia (4), liver cancer (lymphoma (1) and other (1).

The finding showed AIPL1 and NUB1 play opposite roles to each other. Two breast cancer datasets demonstrate the down-regulated AIPL1 and upregulated NUB1 in mRNA transcripts (Fig 3.1).

Table 3. 1 Genes and cancer summary from Oncomine. The table summarised the number of datasets with AIPL1 mRNA under-expression (blue) and NUB1 mRNA over-expression (red) on various cancers in relative normal tissue. The number of dataset was indicated in the box. The threshold was set with the following parameters: *p*-value of 1E-4, gene ranking of top 10% with (A) all $\log_{10}$ fold change and (B) more than 2 $\log_{10}$ fold change. In relative to normal cells, AIPL1 mRNA expressions were lower than 2 $\log_{10}$ fold change in cancers while some NUB1 mRNA expressions (in cervical, colorectal, gastric, head and neck, lymphoma and melanoma cancer) were more than 2 $\log_{10}$ fold change.



A. Fold change=all

Analysis Type by Cancer	AIPL1 Cancer vs. Normal		NUB1 Cancer vs. Normal	
Bladder Cancer		1		
Brain and CNS Cancer	2		5	
Breast Cancer		2	1	
Cervical Cancer		1	1	
Colorectal Cancer		5	10	1
Esophageal Cancer				
Gastric Cancer		3	3	
Head and Neck Cancer			3	
Kidney Cancer	1		3	
Leukemia			4	
Liver Cancer		2	1	
Lung Cancer		5	1	
Lymphoma		1	3	3
Melanoma			2	
Myeloma				
Other Cancer		1		1
Ovarian Cancer		1		
Pancreatic Cancer		1		
Prostate Cancer		1		
Sarcoma				
Significant Unique Analyses	3	24	37	5
Total Unique Analyses	358		301	

B. Fold change >2

AIPL1 Cancer vs. Normal		NUB1 Cancer vs. Normal	
		1	
		1	
		2	
		2	
		2	
		1	
			1
		9	1
358		301	

Table 3. 2 Summary of A. AIPL1 & B. NUB1 datasets. There were 24 dataset with down-regulated AIPL1 and 37 dataset with upregulated NUB1 mRNA expression of cancers (Table 3.3A). The fold changes of AIPL1 and NUB1 were in Log_2 FC. No datasets showing Log_2 FC <-0.5 in AIPL1. It implicates the AIPL1 is not strongly down-regulated.

A.

Publications	Dataset	Sample size	p-value	Log_2 FC
Compagno Lymphoma, Nature, 2009	1. Follicular Lymphoma vs. Normal	38 vs. 10	<0.001	-0.428
Guichard Liver, Nat Genet, 2012	2. Hepatocellular Carcinoma vs. Normal	99 vs. 86	<0.001	-0.119
Kurashina Colon, Cancer Sci, 2008	3. Colon Adenocarcinoma vs. Normal	52 vs. 38	<0.001	-0.136
TCGA Bladder, No Associated Paper, 2013	4. Infiltrating Bladder Urothelial Carcinoma vs. Normal	99 vs. 24	<0.001	-0.166
TCGA Breast 2, No Associated Paper, 2012	5. Invasive Ductal Breast Carcinoma vs. Normal	111 vs. 639	<0.001	-0.233
	6. Invasive Lobular Breast Carcinoma vs. Normal	111 vs. 71	<0.001	-0.209
TCGA Cervix, No Associated Paper, 2012	7. Cervical Squamous Cell Carcinoma vs. Normal	83 vs. 3	<0.001	-0.152
TCGA Colorectal 2, No Associated Paper, 2011	8. Cecum Adenocarcinoma vs. Normal	65 vs. 79	<0.001	-0.233
	9. Colon Adenocarcinoma vs. Normal	212 vs. 79	<0.001	-0.338
	10. Rectal Adenocarcinoma vs. Normal	90 vs. 79	<0.001	-0.370
	11. Rectosigmoid Adenocarcinoma vs. Normal	24 vs. 15	<0.001	-0.399
TCGA Endometrium, No Associated Paper, 2012	12. Endometrial Serous Adenocarcinoma vs. Normal	50 vs. 25	<0.001	-0.307
TCGA Gastric, No Associated Paper, 2013	13. Diffuse Gastric Adenocarcinoma vs. Normal	45 vs. 94	<0.001	-0.134
	14. Gastric Intestinal Type Adenocarcinoma vs. Normal	41 vs. 94	<0.001	-0.178
	15. Gastric Tubular Adenocarcinoma vs. Normal	31 vs. 94	<0.001	-0.156
TCGA Liver, No Associated Paper, 2012	16. Hepatocellular Carcinoma vs. Normal	97 vs. 59	<0.001	-0.338
TCGA Lung 2, No Associated Paper, 2012	17. Lung Adenocarcinoma vs. Normal	261 vs. 390	<0.001	-0.178
	18. Lung Adenocarcinoma, Mixed Subtype vs. Normal	67 vs. 390	<0.001	-0.149
	19. Squamous Cell Lung Carcinoma vs. Normal	348 vs. 390	<0.001	-0.174
TCGA Ovarian 2, No Associated Paper, 2013	20. Ovarian Serous Cystadenocarcinoma vs. Normal	607 vs. 130	<0.001	-0.320
TCGA Pancreas, No Associated Paper, 2013	21. Pancreatic Adenocarcinoma vs. Normal	32 vs. 8	<0.001	-0.115
TCGA Prostate, No Associated Paper, 2012	22. Acinar Prostate Adenocarcinoma vs. Normal	126 bs. 61	<0.001	-0.076
Weiss Lung, Sci Transl Med, 2010	23. Lung Adenocarcinoma vs. Normal	77 vs. 59	<0.001	-0.104
	24. Squamous Cell Lung Carcinoma vs. Normal	155 vs. 59	<0.001	-0.122
Number of upregulated AIPL1 dataset that are above the threshold of significant and log2 FC$\geq$ 0.5 or $\leq$ -0.5				0
Total upregulated AIPL1 dataset				24

B.

Publication	Dataset	Sample size	p-value	Log_2 FC
Andersson Leukemia, Leukemia, 2007	1. B-Cell Acute Lymphoblastic Leukemia vs. Normal	87 vs. 6	<0.001	0.878 [A]
	2. T-Cell Acute Lymphoblastic Leukemia vs. Normal	11 vs. 6	<0.001	0.722 [A]
Beroukhim Brain, Proc Natl Acad Sci U S A, 2007	3. Primary Glioblastoma vs. Normal	107 vs. 33	<0.001	0.252
Brune Lymphoma, J Exp Med, 2008	4. Nodular Lymphocyte Predominant Hodgkin's Lymphoma vs. Normal	5 vs. 5	<0.001	0.789 [A]
Chen Gastric, Mol Biol Cell, 2003	5. Gastric Intestinal Type Adenocarcinoma vs. Normal	67 vs. 28	<0.001	0.681 [A]
DErrico Gastric, Eur J Cancer, 2009	6. Gastric Intestinal Type Adenocarcinoma vs. Normal	4 vs. 31	<0.001	1.128 [A]
	7. Gastric Mixed Adenocarcinoma vs. Normal	26 vs. 31	<0.001	1.068 [A]
Haferlach Leukemia, J Clin Oncol, 2010	8. B-Cell Childhood Acute Lymphoblastic Leukemia vs. Normal	359 vs. 74	<0.001	0.620 [A]
	9. Pro-B Acute Lymphoblastic Leukemia vs. Normal	70 vs. 74	<0.001	0.680 [A]
Hong Colorectal, Clin Exp Metastasis, 2010	10. Colorectal Carcinoma vs. Normal	70 vs. 12	<0.001	1.436 [A]
Kurashina Colon, Cancer Sci, 2008	11. Colon Adenocarcinoma vs. Normal	52 vs. 38	<0.001	0.138
	12. Rectal Adenocarcinoma vs. Normal	38 vs. 38	<0.001	0.152
Lee Brain, Cancer Cell, 2006	13. Glioblastoma vs. Normal	22 vs. 3	<0.001	0.464
Piccaluga Lymphoma, J Clin Invest, 2007	14. Angioimmunoblastic T-Cell Lymphoma vs. Normal	6 vs. 10	<0.001	1.725 [A]
	15. Unspecified Peripheral T-Cell Lymphoma vs. Normal	28 vs. 10	<0.001	1.398 [A]
Pyeon Multi-cancer, Cancer Res, 2007	16. Cervical Cancer vs. Normal	20 vs. 8	<0.001	1.292 [A]
	17. Oral Cavity Carcinoma vs. Normal	4 vs. 9	<0.001	1.098 [A]
	18. Oropharyngeal Carcinoma vs. Normal	6 vs.9	<0.001	1.877 [A]
Richardson Breast 2, Cancer Cell, 2006	19. Ductal Breast Carcinoma vs. Normal	40 vs. 7	<0.001	0.587 [A]
Riker Melanoma, BMC Med Genomics, 2008	20. Cutaneous Melanoma vs. Normal	14 vs. 4	<0.001	2.372 [A]
Skrzypczak Colorectal, PLoS One, 2010	21. Colorectal Carcinoma vs. Normal	36 vs. 24	<0.001	0.971 [A]
	22. Colon Adenoma vs. Normal	5 vs. 10	<0.001	0.567 [A]
	23. Colon Carcinoma Epithelia vs. Normal	5 vs. 10	<0.001	0.999 [A]
TCGA Brain 2, No Associated Paper, 2013	24. Brain Astrocytoma vs. Normal	63 vs. 37	<0.001	0.184
	25. Brain Glioblastoma vs. Normal	58 vs. 37	<0.001	0.407
	26. Oligoastrocytoma vs. Normal	54 vs. 37	<0.001	0.160
TCGA Colorectal 2, No Associated Paper, 2011	27. Cecum Adenocarcinoma vs. Normal	65 vs. 15	<0.001	0.144
	28. Colon Adenocarcinoma vs. Normal	212 vs. 79	<0.001	0.174
	29. Rectal Adenocarcinoma vs. Normal	90 vs. 15	<0.001	0.175
	30. Rectosigmoid Adenocarcinoma vs. Normal	24 vs. 15	<0.001	0.246
TCGA Melanoma, No Associated Paper, 2013	31. Cutaneous Melanoma vs. Normal	58 vs. 312	<0.001	0.275

Publication	Dataset	Sample size	p-value	Log_2 FC
TCGA Renal 2, No Associated Paper, 2011	32. Clear Cell Renal Cell Carcinoma vs. Normal	489 vs. 441	<0.001	0.112
Vasko Thyroid, Proc Natl Acad Sci U S A, 2007	33. Thyroid Gland Papillary Carcinoma vs. Normal	14 vs. 4	<0.001	0.386
Weiss Lung, Sci Transl Med, 2010	34. Lung Adenocarcinoma vs. Normal	77 vs. 59	<0.001	0.103
Wurmbach Liver, Hepatology, 2007	35. Hepatocellular Carcinoma vs. Normal	35 vs. 10	<0.001	0.934 [A]
Yusenko Renal, BMC Cancer, 2009	36. Clear Cell Renal Cell Carcinoma vs. Normal	26 vs. 3	<0.001	0.751 [A]
	37. Papillary Renal Cell Carcinoma vs. Normal	19 vs. 3	<0.001	0.589 [A]
Number of upregulated NUB1 dataset that are above the threshold of significant and log2 FC≥ 0.5 or ≤ -0.5				22
Total upregulated NUB1 dataset				37

[A] Above the threshold with significat p-value<0.05 and log_2 FC≥ 0.5 or ≤ -0.5

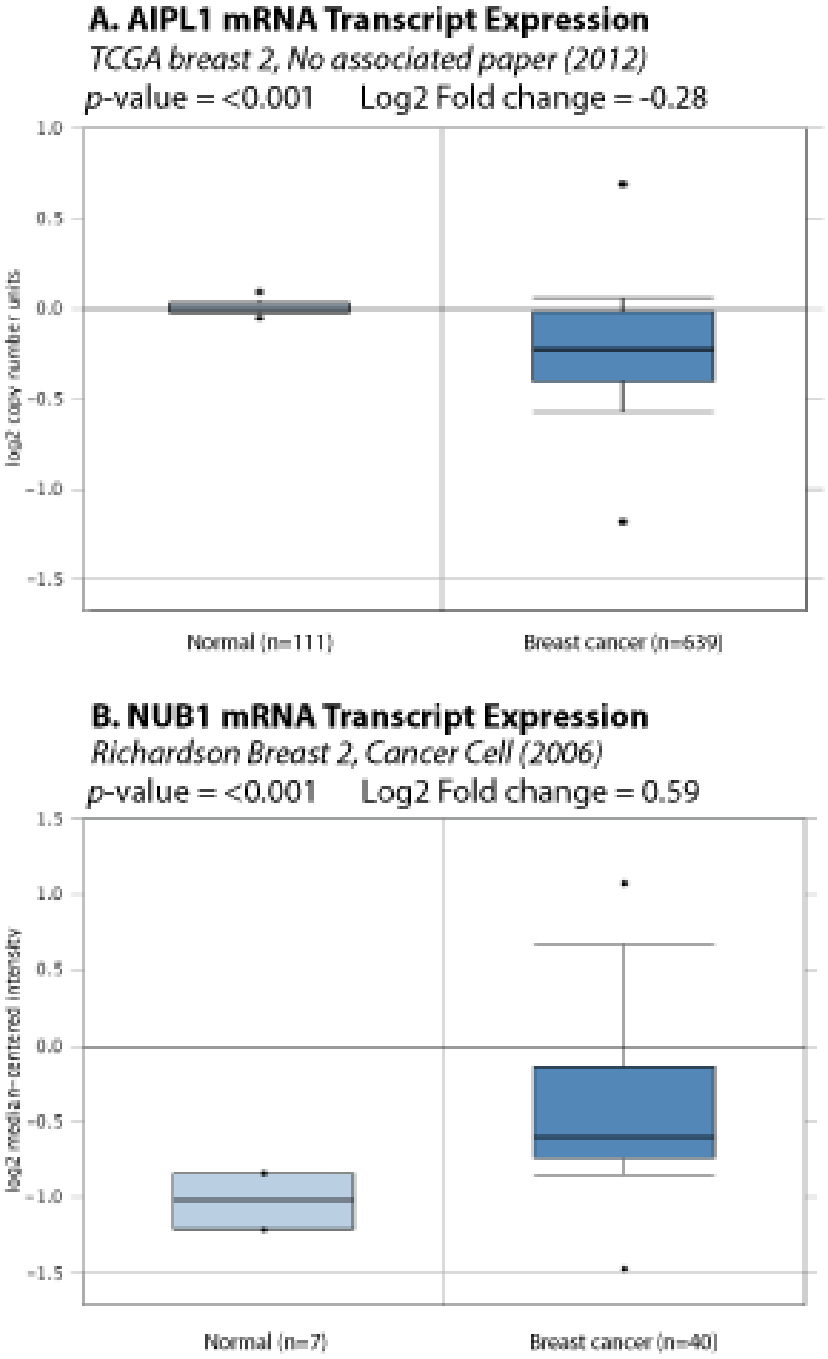


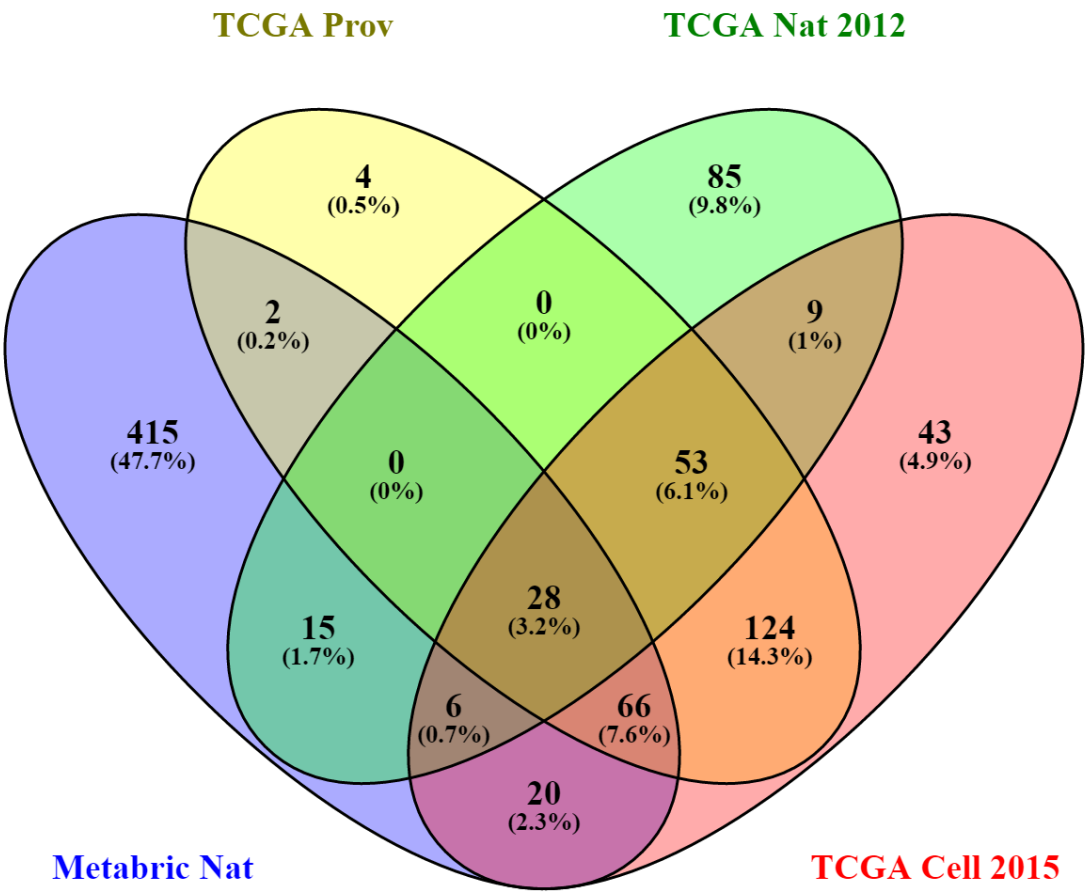
Figure 3. 1 Box and whisker plots of AIPL1 and NUB1 in breast cancer dataset. The box plot comparing specific a. AIPL1 and b. NUB1 mRNA expression in normal (left plot) and cancer tissue (right plot) was derived from Oncomine database. The analysis was shown in breast carcinoma in relative to normal breast. The average signal intensity and average increase (fold change) of the genes are shown as box and whisker plots where the y-axis indicates $\log_2$ fold change.

3.3 NUB1 transcripts consistently coexpressed with CUL1 transcripts in breast cancer

In cBioportal®, the breast invasive carcinoma (TCGA, Cell 2015) and breast invasive carcinoma (TCGA, Provisional) showed AIPL1 coexpressed with Apoptosis Facilitator Bcl-2-Like Protein 14, BCL2L14 gene (Pearson's correlation: 0.92 and 0.86, respectively). We examined the coexpression of genes with the NUB1 transcript among the breast cancer samples from the four datasets on cBioportal – Breast cancer (METABRIC, Nature 2012 & Nat Commun 2016) (N=2509), Breast invasive carcinoma (TCGA, Provisional) (N=1105), Breast invasive carcinoma (TCGA, Nature 2012) (N=825) and Breast invasive carcinoma (TCGA, Cell 2015) (N=817). For each dataset, the genes that satisfy the Spearman correlation $-0.3 \geq \rho \geq 0.3$ are considered as the coexpressed genes for subsequent analysis. Finally, we detected 552, 277, 196 and 349 coexpressing genes in above mentioned datasets, respectively.

To investigate the overlaps among these sets of coexpressing genes, Venn diagram was plotted across all the breast cancer datasets. There was a total of 28 common coexpressing genes, a Venn diagram was shown among all four datasets (Figure 3.2). Overall, there were 28 gene transcripts which coexpressed with NUB1 gene (Appendix 1).

To further investigate the difference between these coexpressed genes and to highlighted the pathway associated with the NUB1 gene, the Reactome® enrichment analysis was applied to search for the enriched biological pathways. Of all 28 genes, 14 of them were enriched in immune system related pathway (Table 3.3). There were several other system related pathways commonly enriched in the up-regulated genes across the physiological environment, including the mitotic cell cycle, haemostasis and metabolism (Table 3.3).



Metabric Nat: Breast cancer (METABRIC, Nature 2012 & Nat Commun 2016) (N=2509), TCGA Prov: Breast invasive carcinoma (TCGA, Provisional) (N=1105), TCGA Nat 2012: Breast invasive carcinoma (TCGA, Nature 2012) (N=825) and TCGA Cell 2015: Breast invasive carcinoma (TCGA, Cell 2015) (N=817).

Figure 3. 2 Venn diagram of overlapping genes across the NUB1 coexpression networks. The difference of CE genes identified in each breast cancer dataset in Oncomine. It highlights the key genes in the weighted coexpression networks. Colour bands represent modules in the network and white regions denote genes outside the modules. There were 28 genes were commonly found to coexpress with NUB1 in all four datasets.

Table 3. 3 Summary of NUB1 and CUL1 enriched pathway. Reactome® analysed 28 NUB1 coexpressing genes. CUL1 transcripts were found in be enriched in various biological pathways.

Pathways	Number of genes involved
Adaptive Immune System	6
TCR signaling	2
Class I MHC mediated antigen processing & presentation	4
Innate Immune System	7
Fc epsilon receptor (FCERI) signaling	2
RIG-I/MDA5 mediated induction of IFN-alpha/beta pathways	2
Cytokine Signaling in Immune system	9
Interferon Signaling	2
Signaling by Interleukins	6
TNFR2 non-canonical NF-kB pathway	3

Abbr. TCR: T cell receptor; MHC: Major histocompatibility complexes; RIG-I: retinoic acid-inducible gene I; MDA5: melanoma differentiation-associated gene 5, TNFR2: Tumor necrosis factor receptor 2; NF-kB: Nuclear factor-kappaB

3.4 Coexpressions of NUB1 with ATM and FAS signaling pathway

Knowing more genes coexpressing with NUB1 could lead to formulating *in vitro* experiments with different stress regimes on cells. To evaluate coexpression of NUB1 transcripts to other related pathways, the multi-scale association explorer in Regulome Explorer® was used to analyse BRCA 03 Feb 2012 (tumour only) dataset. A scale-independent image showed that CUL1 mRNA and Transmembrane Protein 140, TMEM140 mRNA coexpressed with the NUB1 mRNA *in vivo* across a panel of 844 breast cancer samples (Pearson correlation, ρ=0.52 and 0.48, respectively) (Figure 3.4). TMEM140 mRNA is frequently expressed along with fatty acid synthase, FAS gene and ataxia telangiectasia mutated, ATM gene (Fig 3.3). The pool of FAS-centric modules and its coexpressing genes were indicated in the yellow-coloured area.

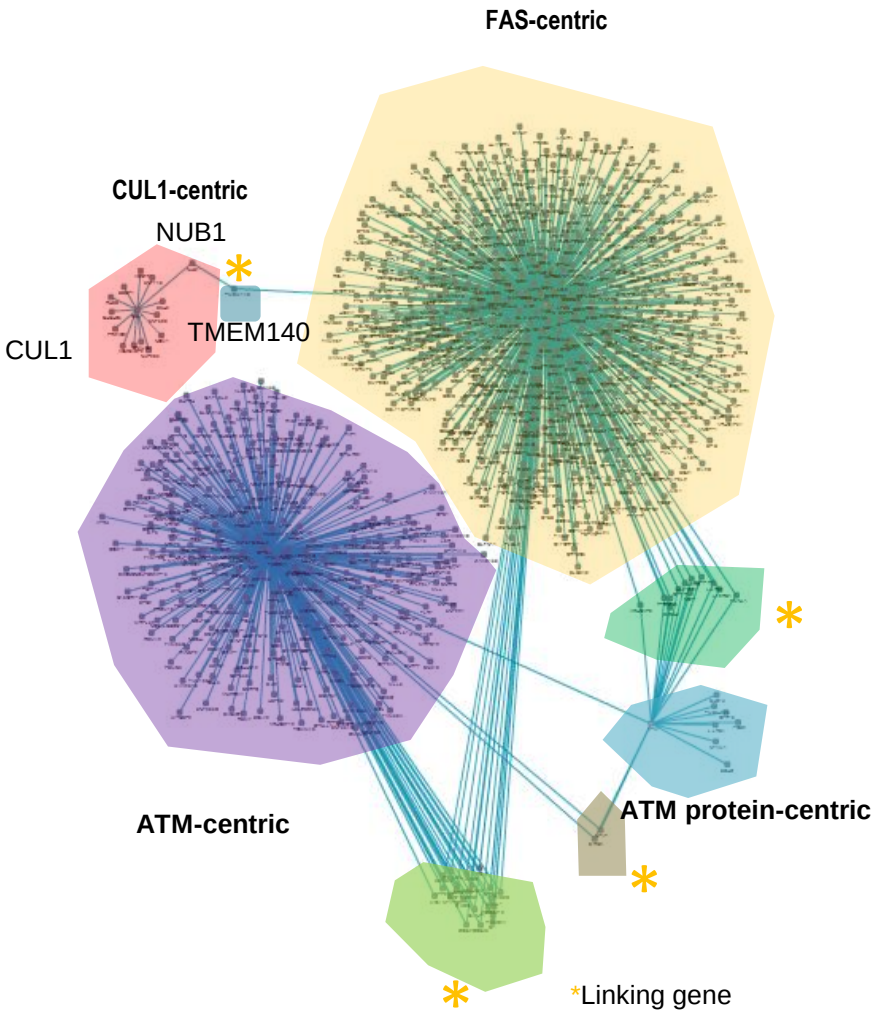


Figure 3. 3 NUB1 coexpression network profile. The network map was derived from Regulome explorer® using BRCA 03 Feb 2012 (tumour only) dataset with a panel of 844 breast cancer samples. The set of feature associations is filtered according to user-specified parameters:- Feature 1 (All association, NUB1 FAS and ATM Label); Feature 2 (Gene expression) and Association (Log_{10} P≥1, max result 1000). Each line corresponds to coexpression. Each dot is a known gene and the coloured modules indicate the pool of genes coexpressing with a single gene.

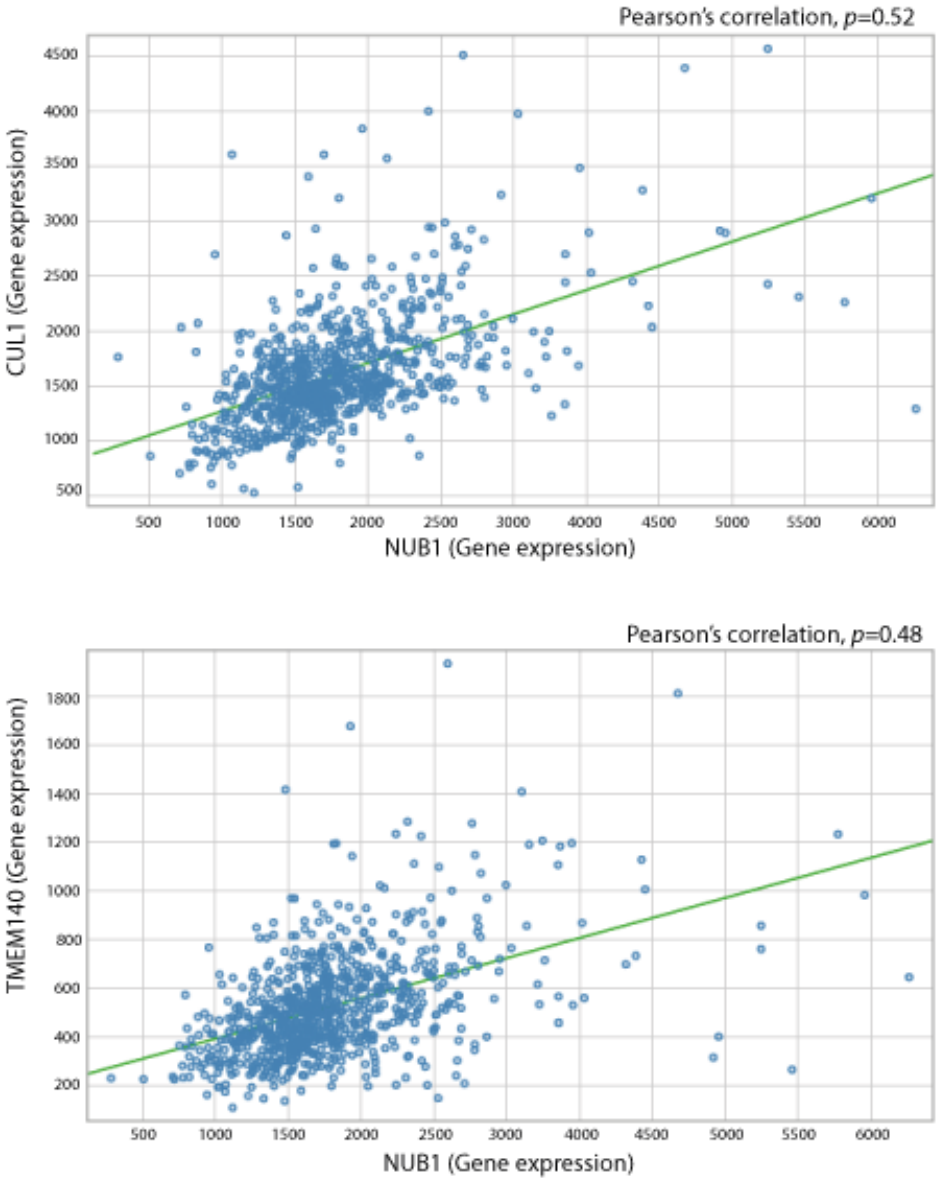


Figure 3. 4 Pairwise association plot of CUL1 and TMEM140 against NUB1 transcripts. The two dimensional association plot of the CUL1 and TMEM140 mRNA transcripts were the only coexpressed genes in this dataset.

3.5 Breast cancer specific analysis using METABRIC database

To validate the findings from cBioportal and Regulome explorer data, we conducted an independent analysis using the METABRIC dataset, containing the 1988 samples. The METABRIC dataset was examined to predict the outcome of breast cancer therapies using molecular features and clinical observations.

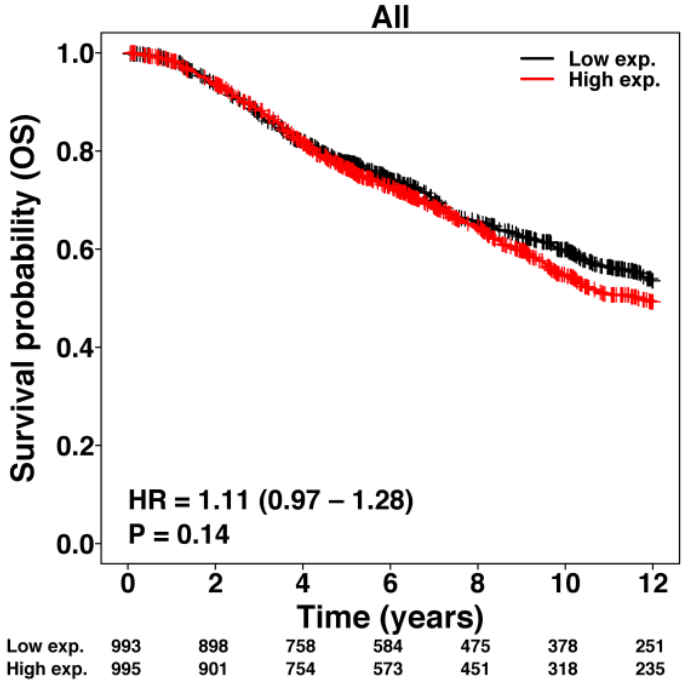
3.5.1 NUB1 transcript expression levels predict the survival probability of ER negative breast cancer patients.

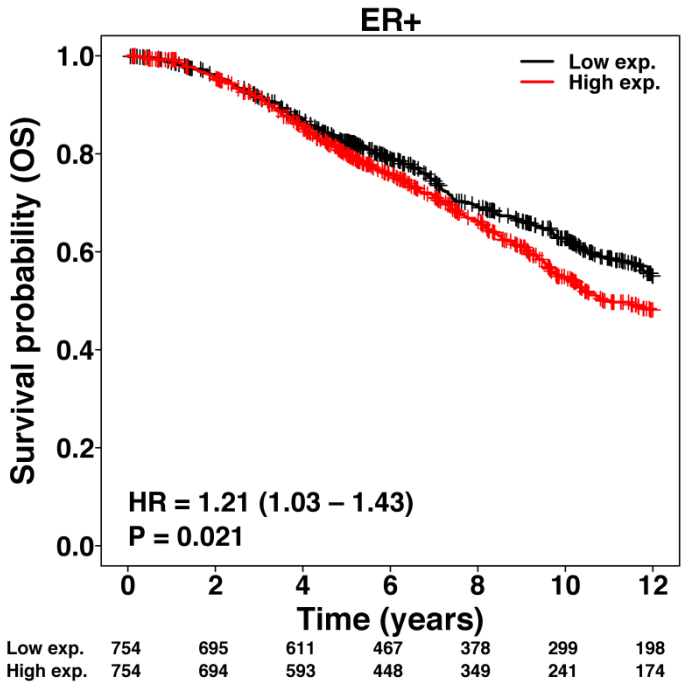
To further elucidate the role of AIPL1 and NUB1 mRNA within breast cancer progression, the prognostic value of AIPL1 and NUB1 gene expression in various breast cancer molecular subtypes was determined according to the parameter of cox p-value<0.05 (Fig. 3.5 and Fig. 3.6). A summary of all hazard ratios across all intrinsic molecular subtypes were shown (Table 3.4).

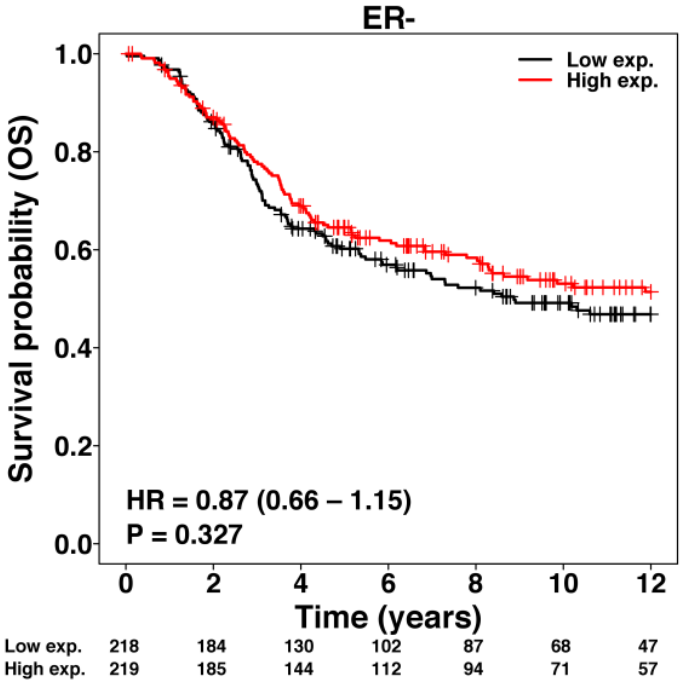
The analysis revealed that AIPL1 was of prognostic value in the subgroup of ER positive patients and, among the ER positive, it was limited to the Lumina B type as the one with higher transcription had a worst outcome over 12 years (Figure 3.5 and Table 3.4).

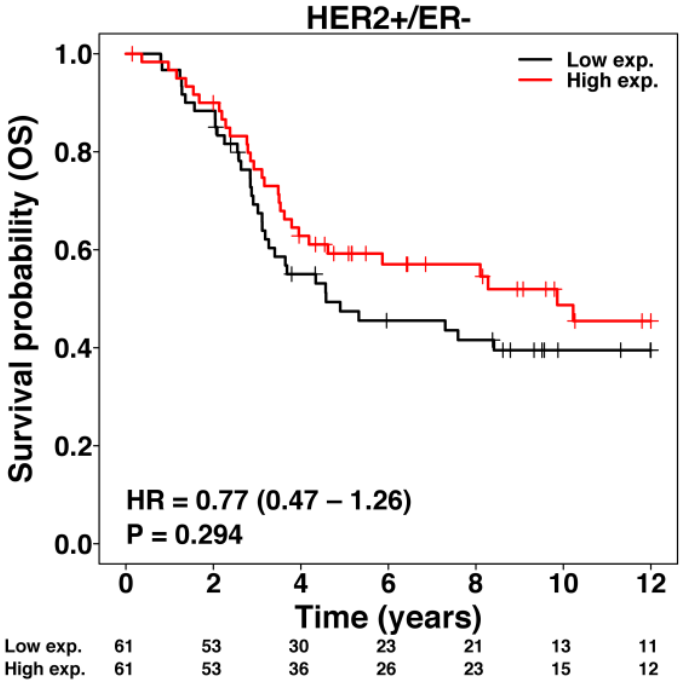
High levels of NUB1 mRNA have been found instead to be associated with better outcome in all the cases, the outcome is even better in NUB1 positive ER negative while NUB1 is of no value in the ER positive. NUB1 high levels of transcript are also associate with goof outcome in the Triple negative tumours and both in the Her2 positive and negative (Figure 3.6 and Table 3.4).

A. Survival probability curve based on AIPL1 transcript expression






ER-
Low exp.
High exp.
Survival probability (OS)
1.0
0.8
0.6
0.4
0.2
0.0
HR = 0.87 (0.66 – 1.15)
P = 0.327
0
2
4
6
8
10
12
Time (years)
Low exp. 218 184 130 102 87 68 47
High exp. 219 185 144 112 94 71 57


HER2+/ER-
Low exp.
High exp.
Survival probability (OS)
1.0
0.8
0.6
0.4
0.2
0.0
HR = 0.77 (0.47 – 1.26)
P = 0.294
0
2
4
6
8
10
12
Time (years)
Low exp. 61 53 30 23 21 13 11
High exp. 61 53 36 26 23 15 12

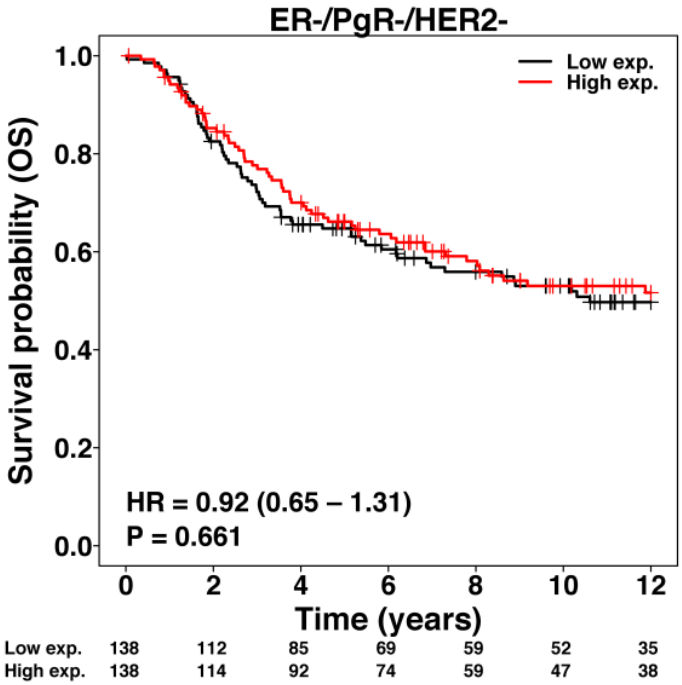
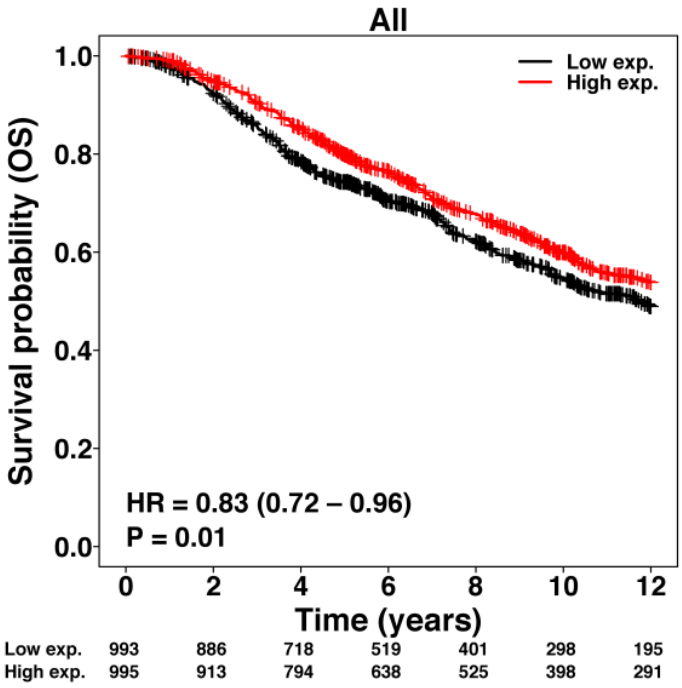
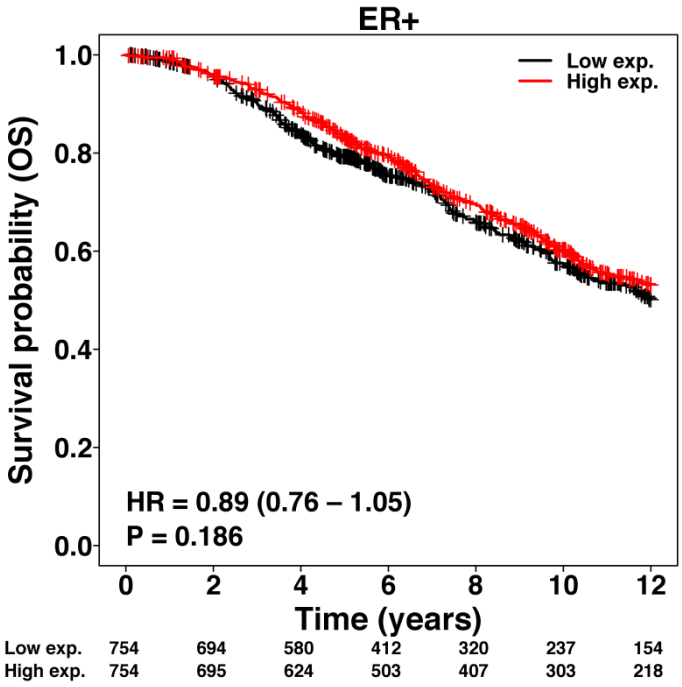
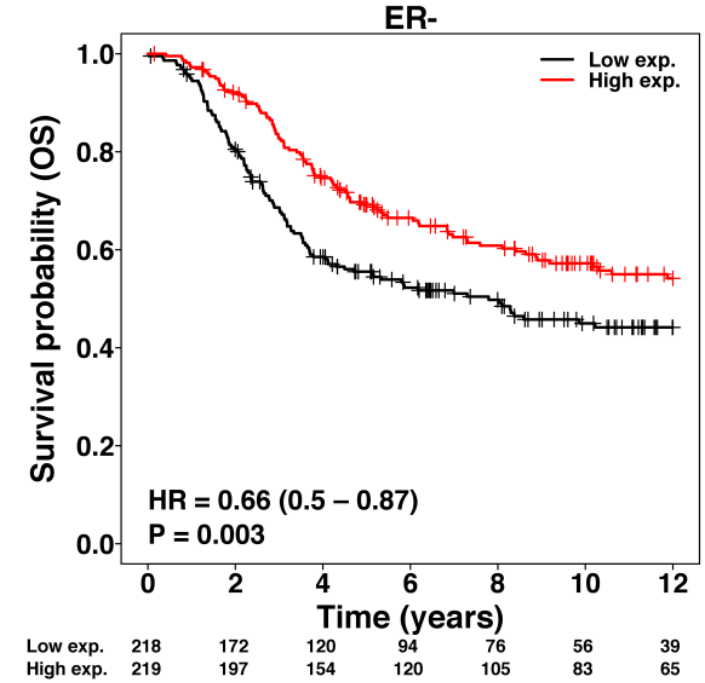


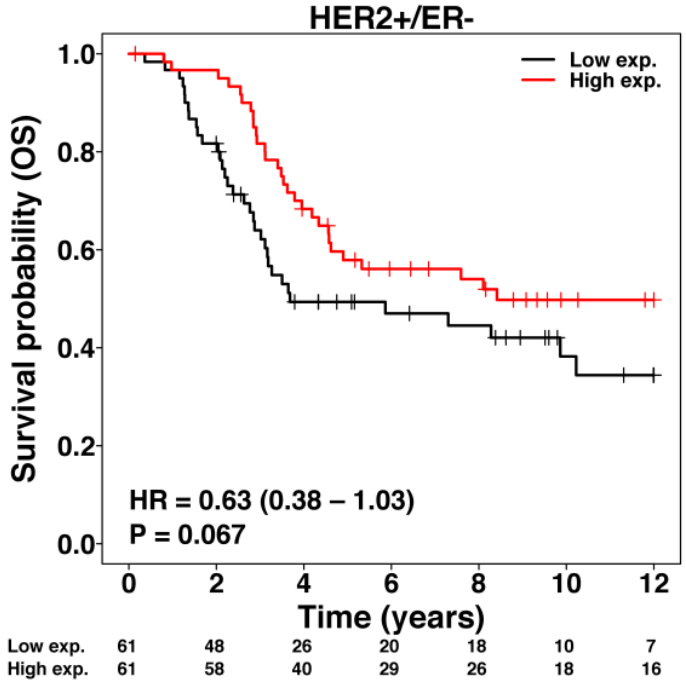
Figure 3. 5 **Survival curves of AIPL1 in different subgroup.** The survival curve comparing the patients with high (red) and low (black) expression in breast cancer was identified as the threshold of cox *p*-value <0.05 from metabric Kaplan Meier database.

B. Survival probability curve based on NUB1 transcript expression






ER-
Low exp.
High exp.
Survival probability (OS)
1.0
0.8
0.6
0.4
0.2
0.0
HR = 0.66 (0.5 – 0.87)
P = 0.003
0
2
4
6
8
10
12
Time (years)
Low exp. 218 172 120 94 76 56 39
High exp. 219 197 154 120 105 83 65


HER2+/ER-
Low exp.
High exp.
Survival probability (OS)
1.0
0.8
0.6
0.4
0.2
0.0
HR = 0.63 (0.38 – 1.03)
P = 0.067
0
2
4
6
8
10
12
Time (years)
Low exp. 61 48 26 20 18 10 7
High exp. 61 58 40 29 26 18 16

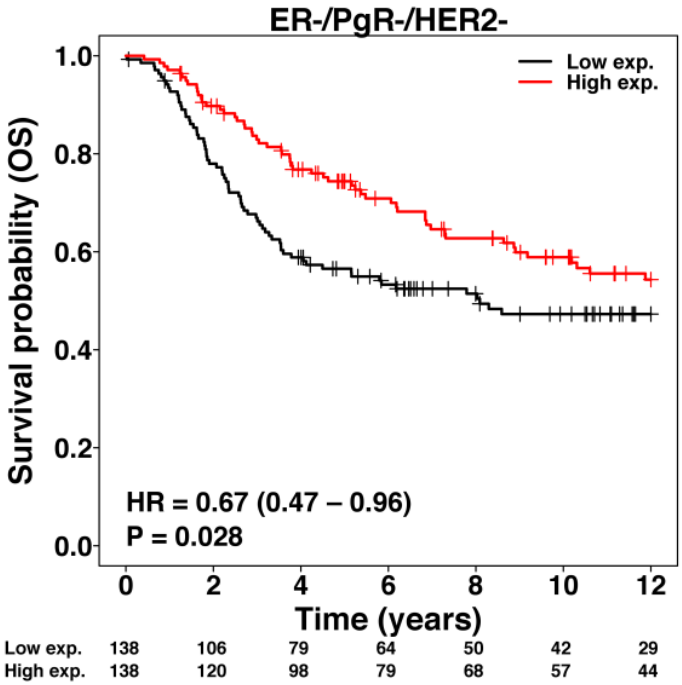


Figure 3. 6 **Survival curves of AIPL1 and NUB1 in different subgroup.** The survival curve comparing the patients with high (red) and low (black) expression in breast cancer was identified as the threshold of cox *p*-value <0.05 from METABRIC Kaplan Meier database.

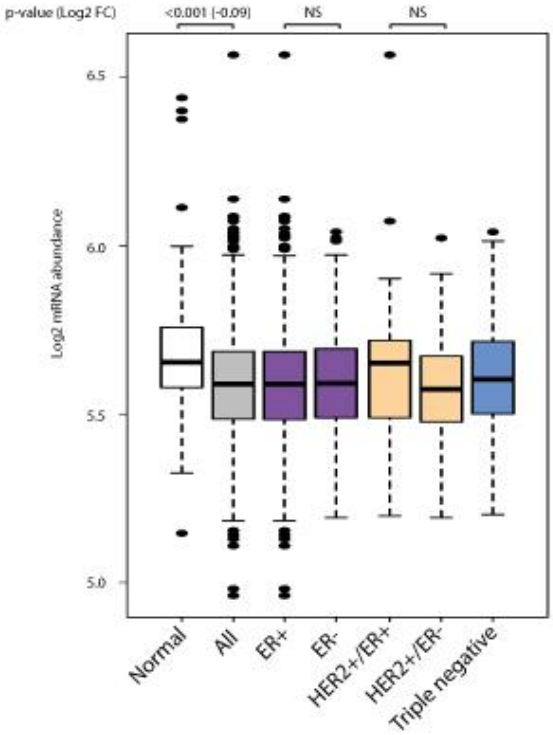
Subtype	AIPL1			NUB1		
	Hazard ratio	95% interval	p-value	Hazard ratio	95% interval	p-value
All	1.11	0.97-1.28	0.140	0.83	0.72-0.96	0.010
Basal	0.99	0.71-1.39	0.974	0.76	0.52-1.01	0.061
ER-	0.87	0.66-1.15	0.327	**0.66**	**0.50-0.87**	**0.003**
ER+	1.21	1.03-1.43	0.021	0.89	0.76-1.05	0.186
HER2	0.79	0.55-1.13	0.192	**0.69**	**0.48-0.99**	**0.047**
HER2-	1.16	1.00-1.36	0.054	0.82	0.70-0.96	0.014
HER2+	0.84	0.59-1.19	0.315	0.86	0.61-1.22	0.396
HER2+/ER-	0.77	0.47-1.26	0.294	**0.63**	**0.38-1.03**	**0.067**
HER2+/ER+	0.84	0.51-1.38	0.492	1.08	0.66-1.78	0.763
Luminal A	1.15	0.89-1.49	0.291	0.84	0.65-1.09	0.192
Luminal B	**1.42**	**1.09-1.85**	**0.009**	1.02	0.78-1.33	0.886
Normal like	0.85	0.52-1.39	0.526	0.83	0.51-1.36	0.456
ER-/PR-/HER2-	0.92	0.65-1.31	0.661	**0.67**	**0.47-0.96**	**0.028**

Table 3. 4 Survival curves summary. The survival curve comparing the patients with high (red) and low (black) expression in breast cancer was identified as the threshold of cox p-value <0.05 from METABRIC Kaplan Meier database. HER2 subgroup is non-luminal *i.e.* HER2 positive but both ER and PR are negative. The statistically significant hazard rations were bolded in various subtypes of breast cancer identified from our analyses.

3.5.2 No significant difference of AIPL1 and NUB1 transcript levels

To examine whether the levels of gene expression of AIPL1 and NUB1 differ between ER+ vs. ER-, HER2+/ER+ vs. HER2+/ER- and triple negative breast cancer, differential transcript expression of genes was determined in the METABRIC dataset. The threshold which we focused on was set at p-value<0.05 and $\log_2$ FC>0.5 or <-0.5. Though there were significant differences of AIPL1 and NUB1 in breast cancer cells and adjacent normal tissue, the fold changes were not varying much ($\log_2$ FC=-0.09; p-value<0.001 and $\log_2$ FC =0.12; p-value<0.001, respectively) (Figure 3.7). There were no significant difference of AIPL1 (p-value not significant) and NUB1 (p-value=0.041; $\log_2$ FC= -0.055) transcripts in ER+ comparing to ER- subgroup. To compare HER2+/ER+ to HER2+/ER- subgroup, both AIPL1 and NUB1 transcripts were not significantly different. Therefore, there were no expression level differences observed in ER+ vs. ER-, HER2+/ER+ vs. HER2+/ER- subgroups.

A. AIPL1 transcript expression



B. NUB1 transcript expression

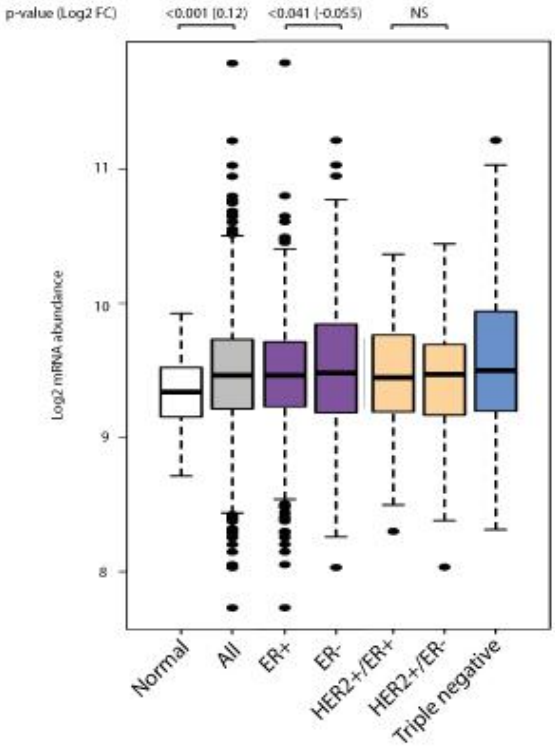


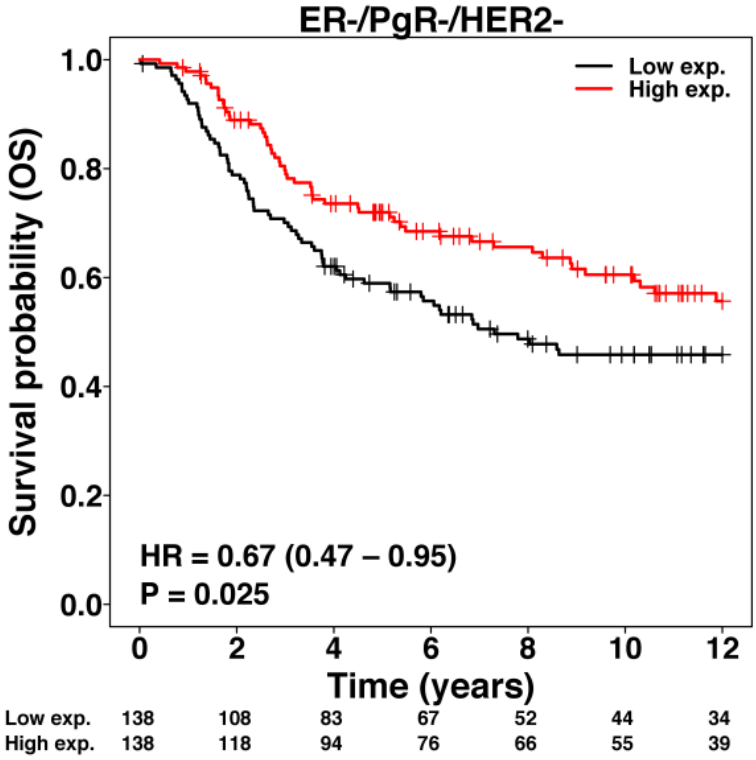
Figure 3. 7 Gene expression patterns of AIPL1 and NUB1 based on the intrinsic molecular subtypes status of METABRIC dataset. Relative transcript abundance of A) AIPL1 and B) NUB1 across the intrinsic subtypes is indicated. The boxes represent the interquartile range (25th and 75th percentiles), and the horizontal line in the box represents the median value. The whiskers show the range of largest and smallest values.

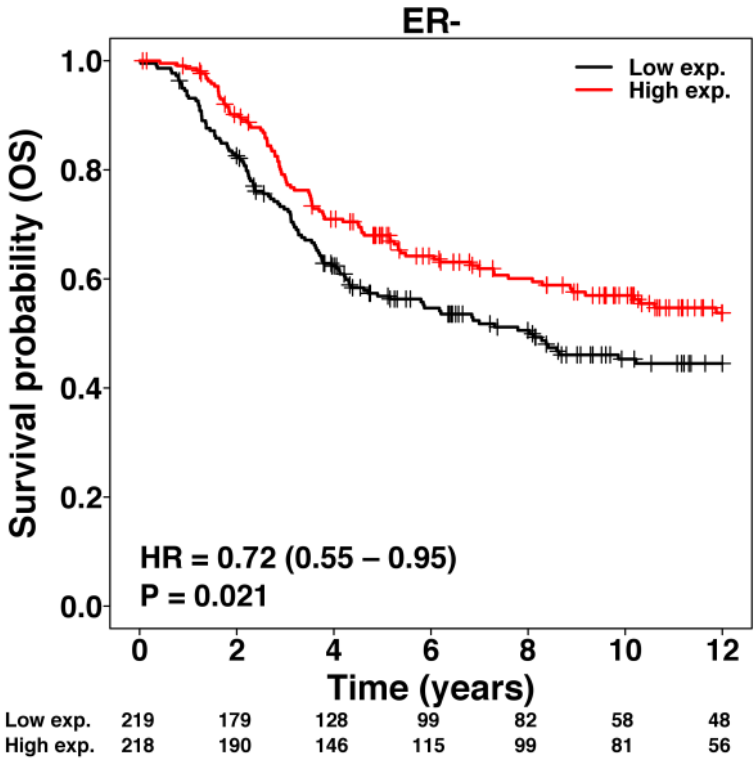
3.5.3 UBL Pathway analysis: FAT10 which coexpressed with NUB1 could stratify ER-, basal and triple negative subgroup breast cancer patients' survival probability

Previous studies showed that NUB1 interacts with both NEDD8 and FAT10 (Kamitani *et al.,* 2001; Groettrup *et al.*, 2008). To examine the clinical significance of NEDD8 and FAT10 mRNA expression in METABRIC, we compared the survival probability curves of their transcripts based on ER status and triple negative subgroups. The hazard ratio threshold of the genes should be < 0.66 or >1 with the *p*-value<0.05 in the subgroups. Only FAT10 (but not NEDD8) transcripts significantly stratify ER- subgroups (hazard ratio=0.65; 95% CI=0.46-0.91, *p*-value=0.011); basal subgroup (hazard ratio=0.72; 95% CI=0.55-0.95, *p*-value=0.021) and triple negative subgroup (Hazard ratio=0.67; 95% CI=0.47-0.95, *p*-value=0.025) (Figure 3.8). High expression of FAT10 mRNA transcripts resulted in better survival among the breast cancer subgroup patients.

To understand the role of FAT10 expression in cancers, the FAT10 gene was reviewed in Oncomine®. In comparison to normal adjacent tissue, the FAT10 gene was highly expressed in cancer tissues (52 vs. 2) (Table 3.5). Same observation was found in METABRIC (Fig. 3.9). Based on this observation, upregulated FAT10 occurs with cancer malignancy.

To investigate whether NUB1 coexpressed with FAT10 in ER-, basal and triple negative subgroups within METABRIC, the Pearson correlation coefficient, ρ was calculated (Table 3.6). The threshold of the ρ should be >0.25 or <-0.25 with *p*-value<0.05. With that, the FAT10 mRNA transcripts showed significant correlation to NUB1 transcripts in ER- (ρ=0.44; p-value<0.001), basal (ρ=0.44; p-value<0.001) and triple negative (ρ=0.42; p-value<0.001). However, no strong correlation of FAT10 to NUB1 in ER+ subgroup was found, suggesting the correlation was only ER- subgroup specific. No correlation was found between NEDD8 and NUB1 expression.


ER-/PgR-/HER2-
Low exp.
High exp.
Survival probability (OS)
1.0
0.8
0.6
0.4
0.2
0.0
HR = 0.67 (0.47 – 0.95)
P = 0.025
0
2
4
6
8
10
12
Time (years)
Low exp. 138 108 83 67 52 44 34
High exp. 138 118 94 76 66 55 39


ER-
Low exp.
High exp.
Survival probability (OS)
1.0
0.8
0.6
0.4
0.2
0.0
HR = 0.72 (0.55 – 0.95)
P = 0.021
0
2
4
6
8
10
12
Time (years)
Low exp. 219 179 128 99 82 58 48
High exp. 218 190 146 115 99 81 56

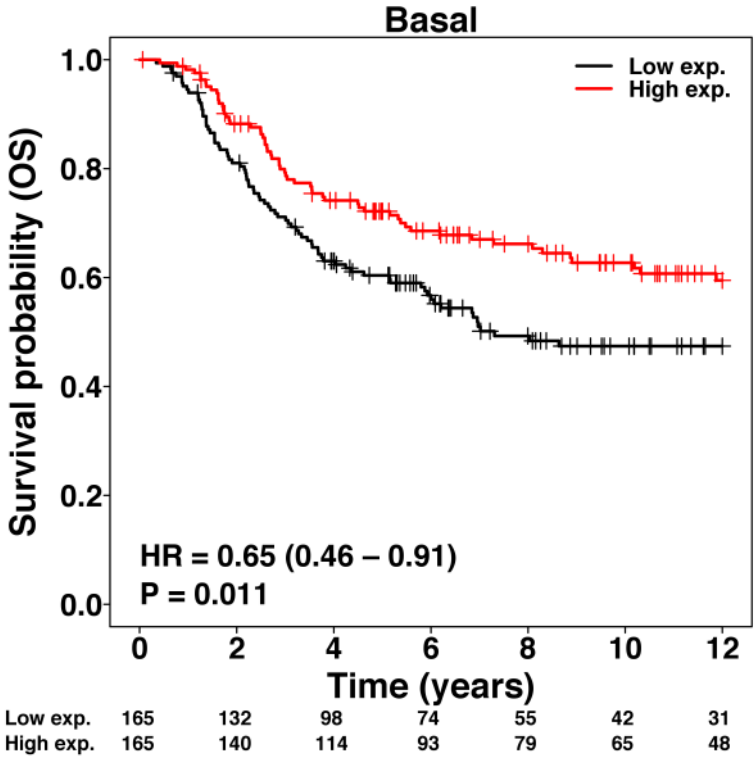


Figure 3. 8 Survival curves of FAT10 in ER-, Basal and triple negative subgroup. The survival curve comparing the patients with high (red) and low (black) expression in breast cancer was identified as the threshold of cox *p*-value <0.05 from metabric Kaplan meier database.

Table 3. 5 FAT10 Genes and cancer summary from Oncomine. The table summarised the number of datasets with FAT10 mRNA under-expression (blue) and over-expression (red) on various cancers in relative normal tissue. The threshold was set with the following parameters: *p*-value of 1E-4, gene ranking of top 10% with (A) all $\log_{10}$ fold change and (B) more than 2 $\log_{10}$ fold change. FAT10 mRNA transcripts are strongly upregulated (>2 $\log_{10}$ fold change) in some cancers (brain cancer, esophageal cancer, lymphoma and other cancer).

	(A)		(B)	
Analysis Type by Cancer	Cancer vs. Normal		Cancer vs. Normal	
Bladder Cancer				
Brain and CNS Cancer	4		1	
Breast Cancer	4			1
Cervical Cancer	2			
Colorectal Cancer	5			
Esophageal Cancer	1		1	
Gastric Cancer	2			
Head and Neck Cancer	2			
Kidney Cancer	3	1		
Leukemia				1
Liver Cancer	7			
Lung Cancer	4			
Lymphoma	8		2	
Melanoma				
Myeloma				
Other Cancer	5		1	
Ovarian Cancer	1			
Pancreatic Cancer	1			
Prostate Cancer				1
Sarcoma		1		
Significant Unique Analyses	49	2	5	3
Total Unique Analyses	394		447	



Cell color is determined by the best gene rank percentile for the analyses within the cell.

NOTE: An analysis may be counted in more than one cancer type.

Table 3. 6 Summary of NUB1 vs. FAT10 and NEDD8 mRNA coefficient, ρ.

	NUB1 mRNA abundance correlation, ρ (*p*-value)					
	Basal	ER+	ER-	HER2+/ER+	HER2+/ER-	Triple negative
FAT10	0.44 <0.001	0.17 <0.001	0.44 <0.001	0.39 <0.001	0.45 <0.001	0.42 <0.001
NEDD8	-0.09 <0.001	-0.13 <0.001	0.04 NS	-0.23 0.013	-0.02 NS	0.03 NS

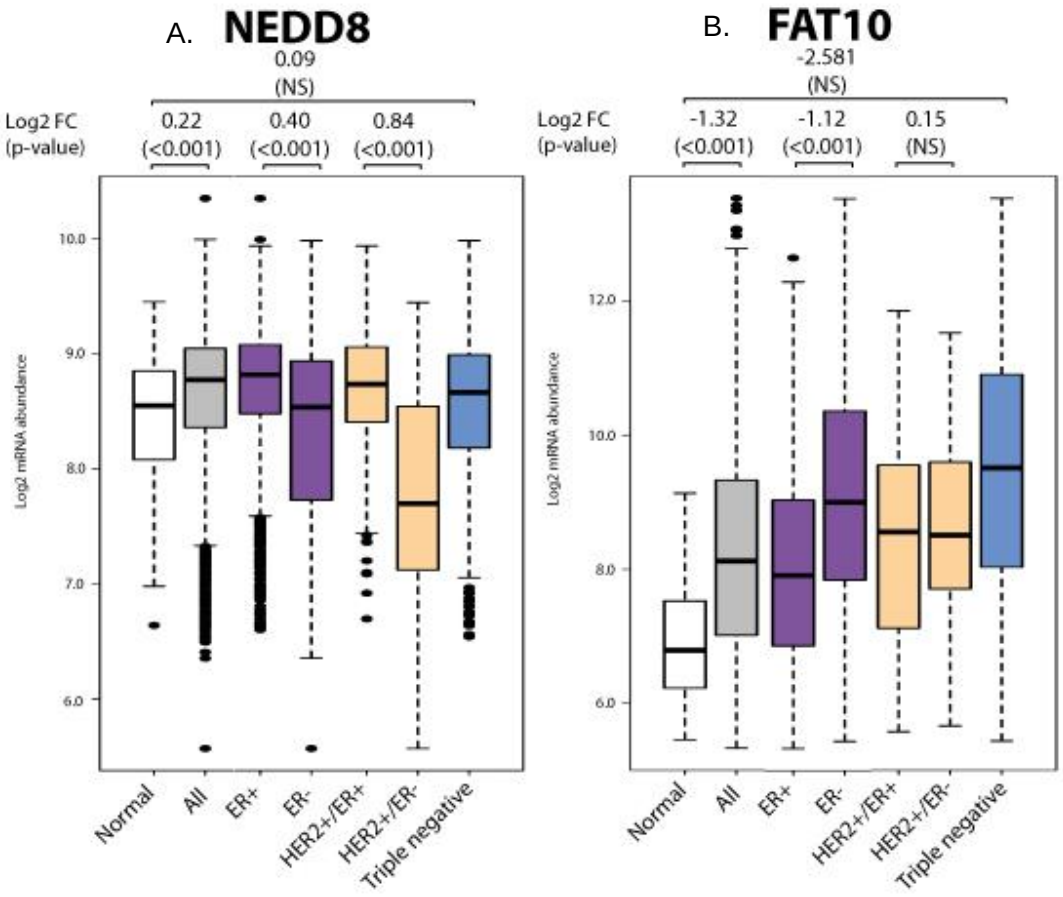


Figure 3. 9 Gene expression patterns of NEDD8 and FAT10 based on the intrinsic molecular subtypes status of METABRIC dataset. Relative transcript abundance of A) NEDD8 and B)FAT10 across the intrinsic subtypes is shown. The boxes represent the interquartile range (25th and 75th percentiles), and the horizontal line in the box represents the median value. The whiskers show the range of largest and smallest values.

3.5.4 CUL1 related ubiquitin ligase activities and cell cycle regulation

To see if CUL1 and p21 expression differs between ER+ vs. ER-, HER2+/ER+ vs. HER2+/ER- and triple negative subtypes of breast cancer, differential transcript expressions of CUL1 genes were determined in METABRIC (Figure 3.10). In comparison to the ER+ subgroup, CUL1 transcripts were expressed higher in the ER- subgroup (log_2 FC= 0.24). HER2+/ER- subgroup expressed 0.13 (log_2) fold change higher CUL1 transcripts than the HER2+/ER+ subgroup. There was a 0.23 (log_2) fold change higher expression of CUL1 transcripts in triple negative breast cancer than normal tissue. And in the ER- and triple negative subgroup, the lower CUL1 transcript level group is 24% (HR= 0.76; 95% CI= 0.58-1.01, *p*-value=0.06) and 27% (HR= 0.73; 95% CI= 0.51-1.04, *p*-value=0.08) more likely to undergo metastasis and die of breast cancer compared to the higher CUL1 expression group, respectively (Appendix 3.3). Unlike AIPL1, NUB1 strongly coexpressed with CUL1 in all the subgroups checked, but there was no co-expression with p21 (Table 3.7). Therefore, CUL1 protein levels, which is directly correlated to NUB1, is a coexpressing factor in NUB1 signaling.

A. B.

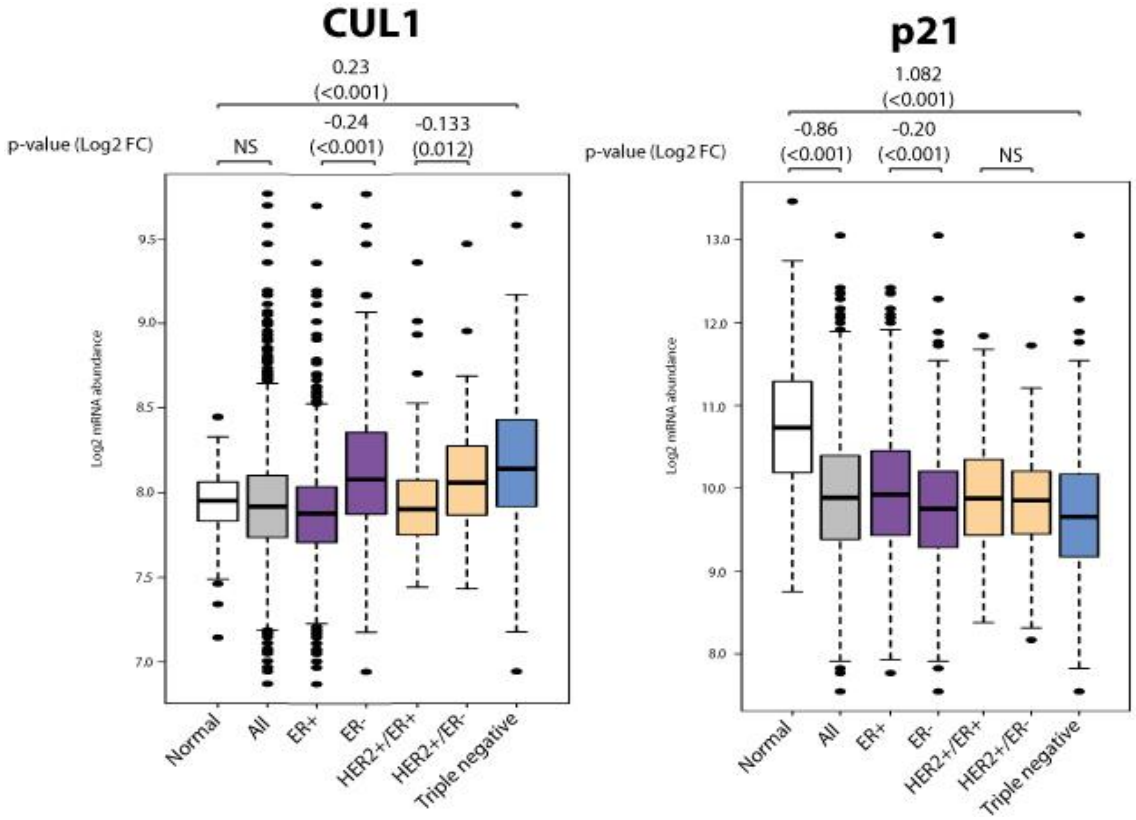


Figure 3. 10 Gene expression patterns of CUL1 and p21 based on the intrinsic molecular subtypes status of METABRIC dataset. Relative transcript abundance of A)CUL1 and B) p21 The boxes represent the interquartile range (25th and 75th percentiles), and the horizontal line in the box represents the median value. The whiskers show the range of largest and smallest values.

Table 3. 7 Summary of AIPL1 and NUB1 on CUL1 and p21 mRNA expression.

Genes		mRNA abundance correlation, ρ (*p*-value)				
		ER+	ER-	HER2+/ER+	HER2+/ER-	Triple negative
CUL1	AIPL1	NS	NS	NS	NS	NS
p21		NS	NS	NS	NS	NS
CUL1	NUB1	0.36 (<0.001)	0.46 (<0.001)	0.43 (<0.001)	0.48 (<0.001)	0.44 (<0.001)
p21		NS	NS	NS	NS	NS

3.5.5 Pathway analysis of HIF1A transcription in different breast cancer subtypes

A potential role of NUB1 signaling is supported by survival probability analysis which identified the poor survival of patients with ER- tumours, for the low NUB1 expression implicate bad prognosis. NUB1 coexpresses with ATM and FAS, both of which are inducible by hypoxia. Therefore, it will be interesting to further explore neddylation of HIF1α and its effect on transcriptional control (Ryu *et al.* 2009). In this case, NUB1 may regulate neddylated HIF1α, we wanted to see if HIF1α downstream targets could be altered by NUB1.

As lower NUB1 transcript levels imposed poorer survival, we studied HIF1α downstream target to NUB1 and related genes with the hope to identify differences in between ER positive and negative patients. The heatmap analysis of the ER-negative subgroup within METABRIC patients showed four HIF1α downstream targets (Table 3.9) including IGF2, DLK1, COL5A1 and ABCB1 were inversely correlated to NUB1 transcripts (Fig. 3.11). It suggests the possibility of the high NUB1 transcript level with low HIF1α mediated transcription activities, and vice versa. Furthermore, AIPL1 transcripts had similar expression with hypoxia signature, a panel of genes which are expressed in hypoxia. Therefore, NUB1 inversely coexpressed to HIF1α downstream target while AIPL1 coexpresses with hypoxia signature at transcriptomic levels.

Table 3. 8 HIF1α and downstream target. These are the genes which are related to hypoxia signature including HIF1α and downstream target of transcriptional activity.

Functional groups of HIF1α downstream targets	Gene
Anti-apoptotic	IGF2
Stem cell properties	DLK1
Metastasis	COL5A1
Therapy resistance	ABCB1

Abbr.: ATP-binding cassette sub-family B member 1 (ABCB1); DLK1: Delta Like Non-Canonical Notch Ligand 1; COL5A1: Collagen Type V Alpha 1 Chain; IGF2: Insulin Like Growth Factor 2

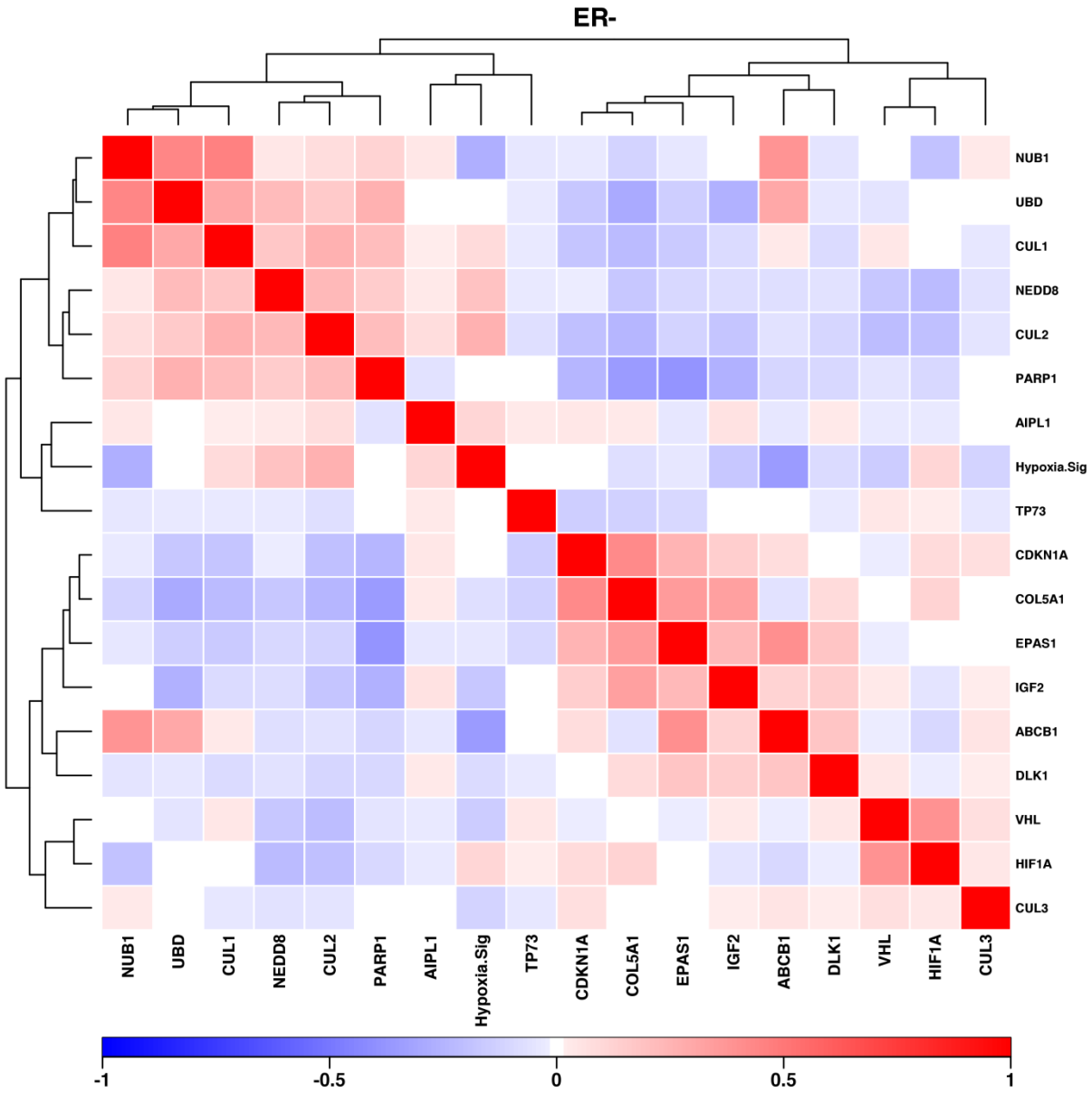


Figure 3. 11 Heatmap showing genes differentially expressed in ER- subgroup patients (n =439), using RNA-Seq data. Each gene is normalized to standard normal distribution with blue indicating lower expression, and red indicating higher expression. HIF1α downstream targets including IGF2, DLK1, COL5A1 and ABCB1 were showing identical expression. To determine the expression profile of NUB1 to HIF1α and its downstream target genes, the correlation coefficients, ρ were compared across all the breast cancer subtypes. The analysis was limited to genes which are related to hypoxia signature including HIF1α and downstream targets of transcriptional activity. NUB1 inversely coexpressed to HIF1α downstream target while AIPL1 coexpresses with hypoxia signature at transcriptomic levels.

3.6 Discussion and Chapter Summary

Meta-analysis approach increases the sensitivity in revealing biomarkers for various cancers. The comparison of mRNA levels between tumours and their corresponding normal tissue demonstrated that AIPL1 mRNA levels are predominantly lower while NUB1 mRNA levels are usually higher in cancers. In Oncomine®, a total of 24 datasets showed down-regulated AIPL1 transcripts and 37 datasets showed up-regulated NUB1 in cancers (Table 3.2). This concordant down-regulated AIPL1 and upregulated NUB1 in cancers may exerts opposite roles in tumourigenesis. This was observed in breast cancers too (Fig. 3.1).

CUL1 was of interest as its mRNA transcripts were found to be frequently coexpressed with NUB1 (Fig. 3.1 and 3.2). Coupled with the finding that NUB1 indirectly coexpressed with FAS and ATM, whose activities are frequently upregulated with hypoxia and reoxygenation, we thought NUB1 may regulate the cancer cell cycle through the ubiquitin ligase activities with varying oxygen tensions. Imposing hypoxia and reoxygenation stress could be a way to study the breast cancer cells *in vitro.*

We found that breast cancer showed the opposite profile of upregulated NUB1 and AIPL1, indicating that this cancer model might be worth studying further. At the protein level, AIPL1 blocks NUB1 entering the nucleus and therefore the differences in expression in expression could cause problems just because the normal chaperone, AIPL1 and client protein, NUB1 are altered. In METABRIC dataset, higher levels of NUB1 mRNA predict better outcome in ER-negative subgroup patients, HER2-positive group, HER2+ with ER-group and triple negative subgroup. It was found that the HIF1α downstream targets had a similar expression profile in the ER-negative breast cancer subgroup as well as an inversed correlation to NUB1 mRNA transcript levels (Fig 3.1).

There are some limitations of the work done this far. Microarray studies revealed the relative mRNAs with less representation to the expression level of the proteins. The number of protein molecules synthesised from mRNA molecule is highly dependent on translation-initiation features of the mRNA sequence. So the *in vitro* study was carried out next to study the protein changes.

Chapter 4

AIPL1-NUB1 signaling cascade in cell cycle regulation Through CUL1 based E3 ubiquitin SCF-ligase

4.1 Rationale of the study

By reviewing chaperones candidates, AIPL1 down-regulation was observed in various cancers. AIPL1 is involved in chaperoning and protein trafficking in retinal tissue (van der Spuy *et al.*, 2002); the role of AIPL1 and its client protein, NUB1 remains unexplored in cancers.

In the previous chapter, it was found that NUB1 protein coexpresses with FAS and ATM proteins, two independent pathways that are involved in the reoxygenation-induced DNA damage pathway (Hammond *et al.*, 2003). We believe hypoxia and reoxygenation could be a way to induce NUB1 activities. Hypoxia occurs in tumour cells growing in suboptimal oxygen concentration (Olcina *et al.*, 2010). This condition is due to tumour progression and a general lack of blood supply (Thomlinson and Gray, 1955). Optimal oxygen tension is crucial for tumour cells to acquire more energy from glucose aerobically. Therefore, proliferating tumour cells need to adapt to the low oxygen pressure.

Clinically, hypoxia is often correlated with an aggressive clinical outcome (Brizel *et al.*, 1996; Le *et al.*, 2004; Erler *et al.*, 2006). Solid tumour under hypoxia often grow within an acidified micro-environment, with increased glycolysis and often drug resistance. Thus, a clinically relevant AIPL1 and NUB1 research aim is to correlate their activities with the hypoxic environment to examine cell death mechanism in cancer cells.

The role of NUB1 in tumour growth has only been investigated in the context of tumor cell death (Hosono *et al.*, 2010) but not with tumour adaptation to hypoxia. Expression of NUB1 could exert anticancer effects in renal cell carcinoma (RCC) cells, by inducing apoptosis via the accumulation of p27 and cyclin E (Tanaka *et al.*, 2013). Prolonged p27 is thought to cause apoptosis. As NUB1 mRNA coexpressed with CUL1 transcript in our

study, it prompted the interest of CUL1 action via the ubiquitin SCF-ligase complexes (as shown below). Therefore, it is worth investigating whether the antiproliferative effect of NUB1 in relationship to hypoxia which is regulated by CUL2.

NUB1 —┤ Neddylated CUL1→Ubquitinated p27 and cyclin E

AIPL1 and NUB1 proteins may take part in many biological processes such as cell proliferation, differentiation, and cell death which depend precisely on the timely synthesis and degradation of key regulatory proteins. The SCF (SKP1-CUL1-F-box protein) E3 ligases are the largest family and are responsible for the turnover of many key regulatory proteins including p21 and p27. Aberrant regulation of SCF E3 ligases is associated with various human diseases, such as cancers, including skin cancer.

In this chapter, we studied how NUB1 regulates the NEDD8 and FAT10 conjugation cascade upon hypoxia and reoxygenation. The chaperoning mechanism of AIPL1 onto NUB1 and the effects on the cancer cell cycle profiles were underlined.

4.2 Cell line screening of proteins and their transcript levels

4.2.1 Detection of endogenous protein expression in various cancer cell line

To characterise the protein expression levels of NUB1, AIPL1, NEDD8 and FAT10 in unstressed cancer cells, 11 different cancer cell line originating from kidney, colon, bone, retina and with six breast cell lines, were analysed. NUB1 protein was found to be abundantly expressed in most cells except U2OS and SKBR3 (Fig 4.1). MDA-MB-231 expresses the most abundant amount of NUB1 protein. All cells form AIPL1 dimer. The role of monomer and dimer of AIPL1 remains to be investigated as these functional aspects of protein were not reported previously. Whilst varying expression levels of AIPL1 monomer were seen, ACHN, U2OS, Y79 and BT474 cells showed higher expression of the monomeric form than the other cell line. NEDD8 proteins were observed in the conjugated CULs, monomers were observed in HCT116, U2OS, HCC1806, and MDA-MB-231 cells. All the FAT10 are in the conjugated form, no free monomers were observed under unstressed condition.

4.2.2 Quantitative PCR analysis of various cancer cell line

To determine relative expression of AIPL1, NUB1, NEDD8 and FAT10 genes between different cell line, we analysed transcript levels by qPCR. Y79 cells were used as a positive control because AIPL1 and NUB1 have been well documented in retinal tissue. Expression was compared to the housekeeping gene, tubulin was used. Very low AIPL1 mRNA transcript levels were observed in all the cancer cells tested, compared to the control Y79 cells (Figure 4.2). In contrast, greater NUB1 transcript levels were observed in all cell line tested as compared to Y79 control cells, with U2OS cells exhibiting the most abundant transcripts. Meanwhile, the highest amount of NEDD8 mRNA transcripts was found in ACHN, MDA-MB-231 and BT474 cells. Abundant amount of FAT10 mRNA was detected in the cells, with the highest amount found in 786-O.

4.2.3 Immunohistochemistry staining of various cancer cell line

To examine protein localisation of AIPL1, NUB1 and NEDD8 in unstressed cancer cells, immunohistochemistry (IHC) staining were performed across the 12 cell line. For AIPL1, the proteins were mostly observed in the cytoplasm and a to a lesser extent, in nucleus. The protein was found the least in ACHN and BT474 cell lines. All cells except U2OS show positive staining for NUB1 protein. NEDD8 proteins could be found abundantly in both the nucleus and the cytoplasm in all cell line tested. FAT10 was found in most cells with the least or no staining in HCT116, T47-D and BT474 (Fig 4.3).

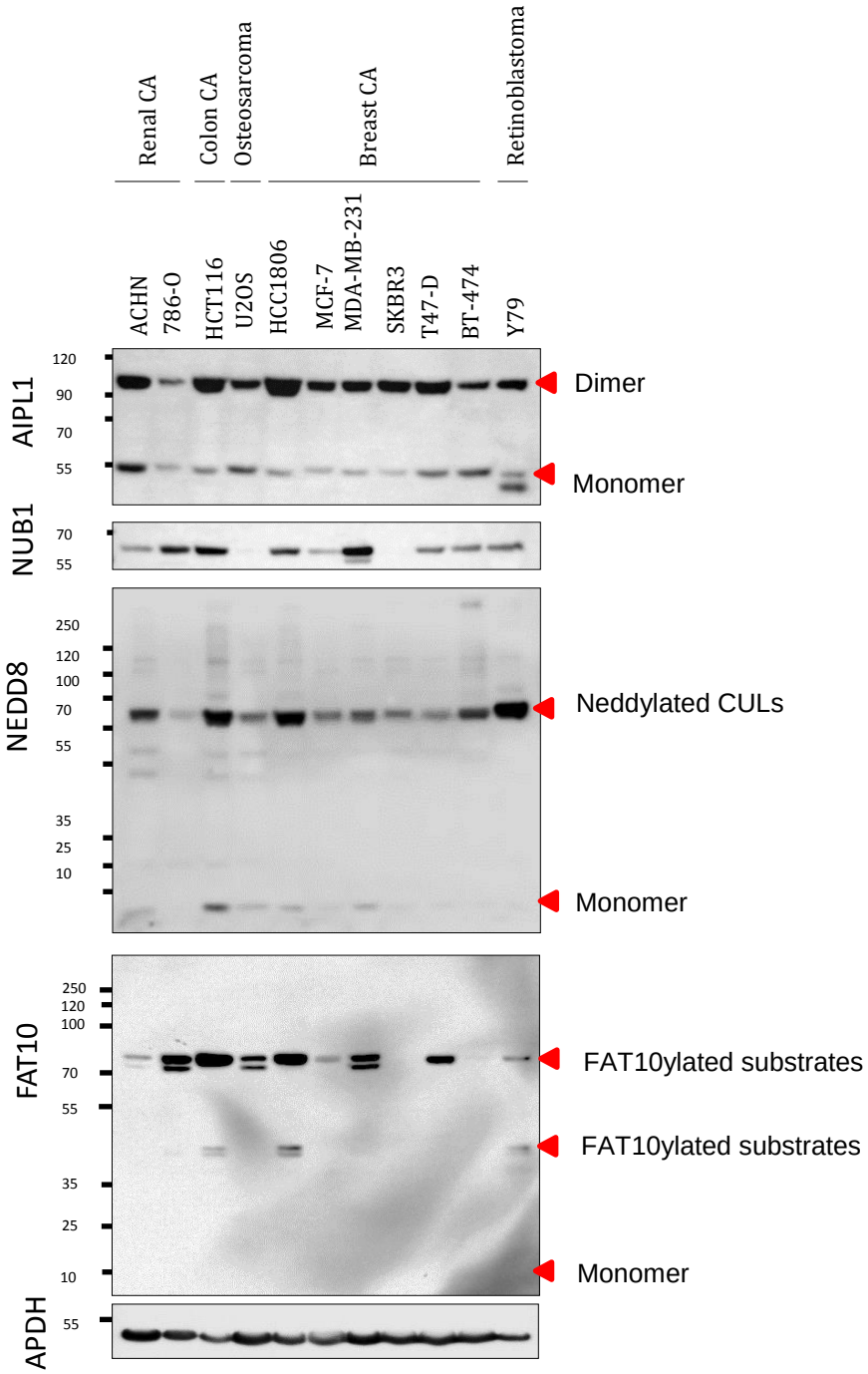


Figure 4. 1 Protein expression patterns. Western blot of neddylated cullins, NUB1, AIPL1 and FAT10 among the cancer cell line derived from varying tissue origins.

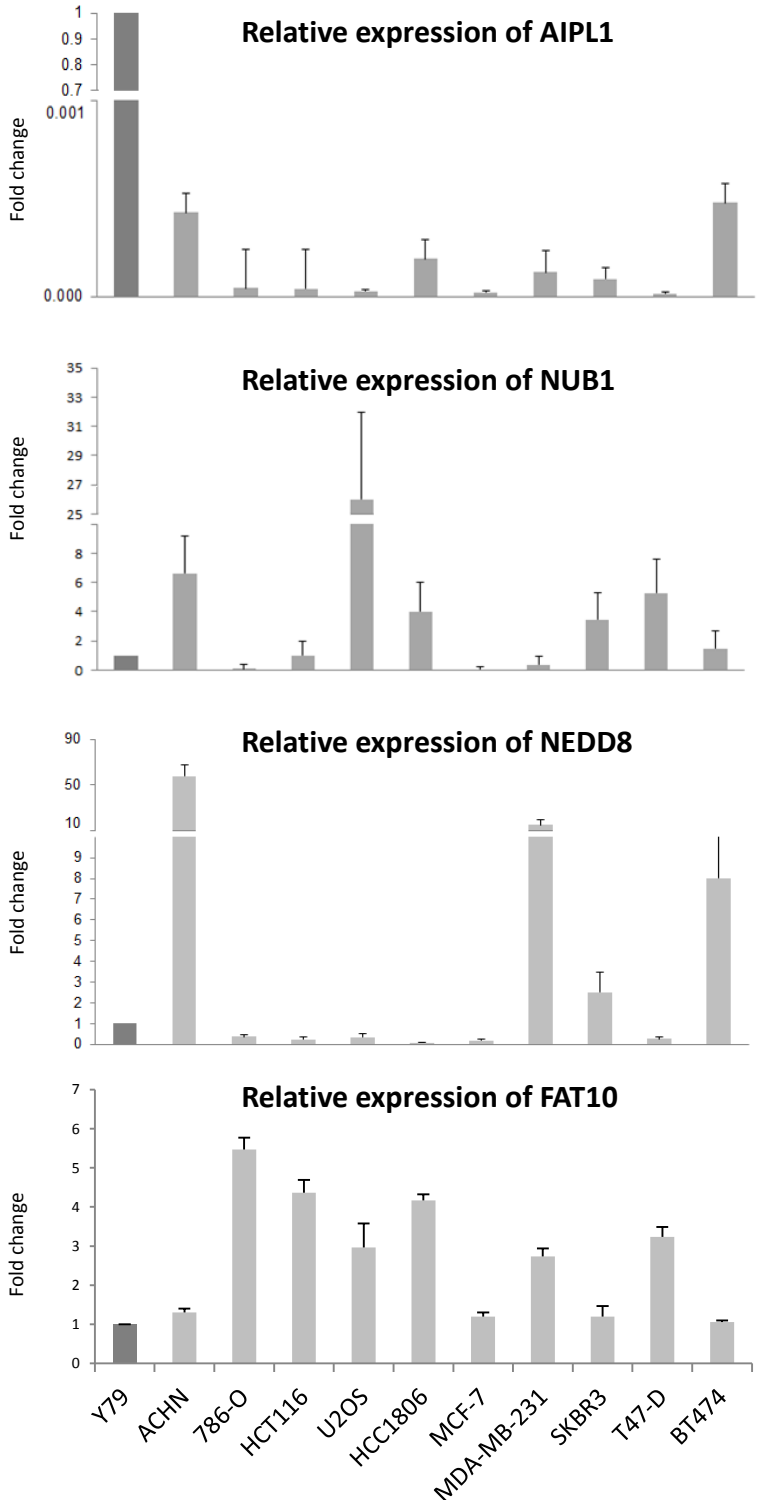
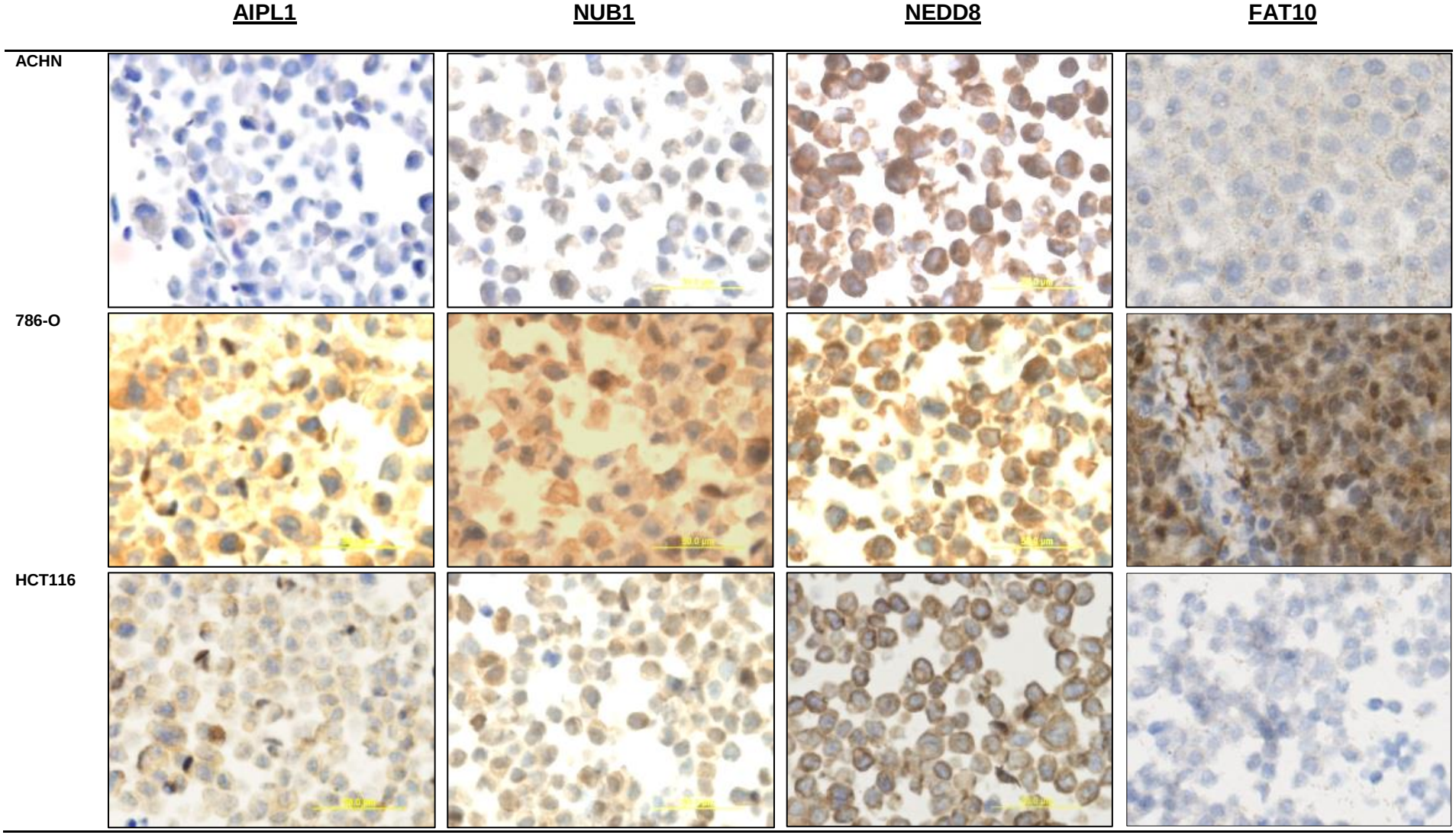
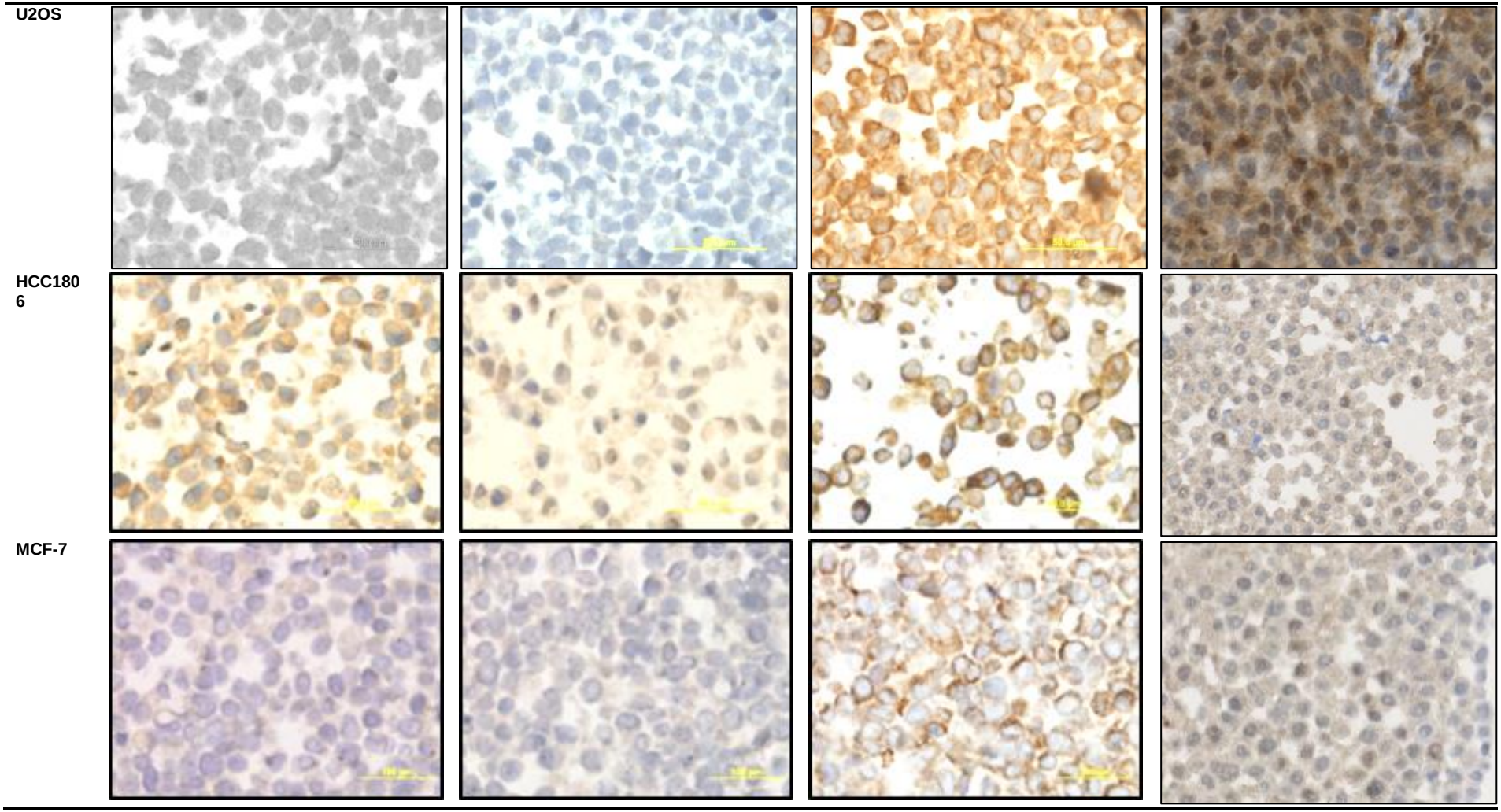
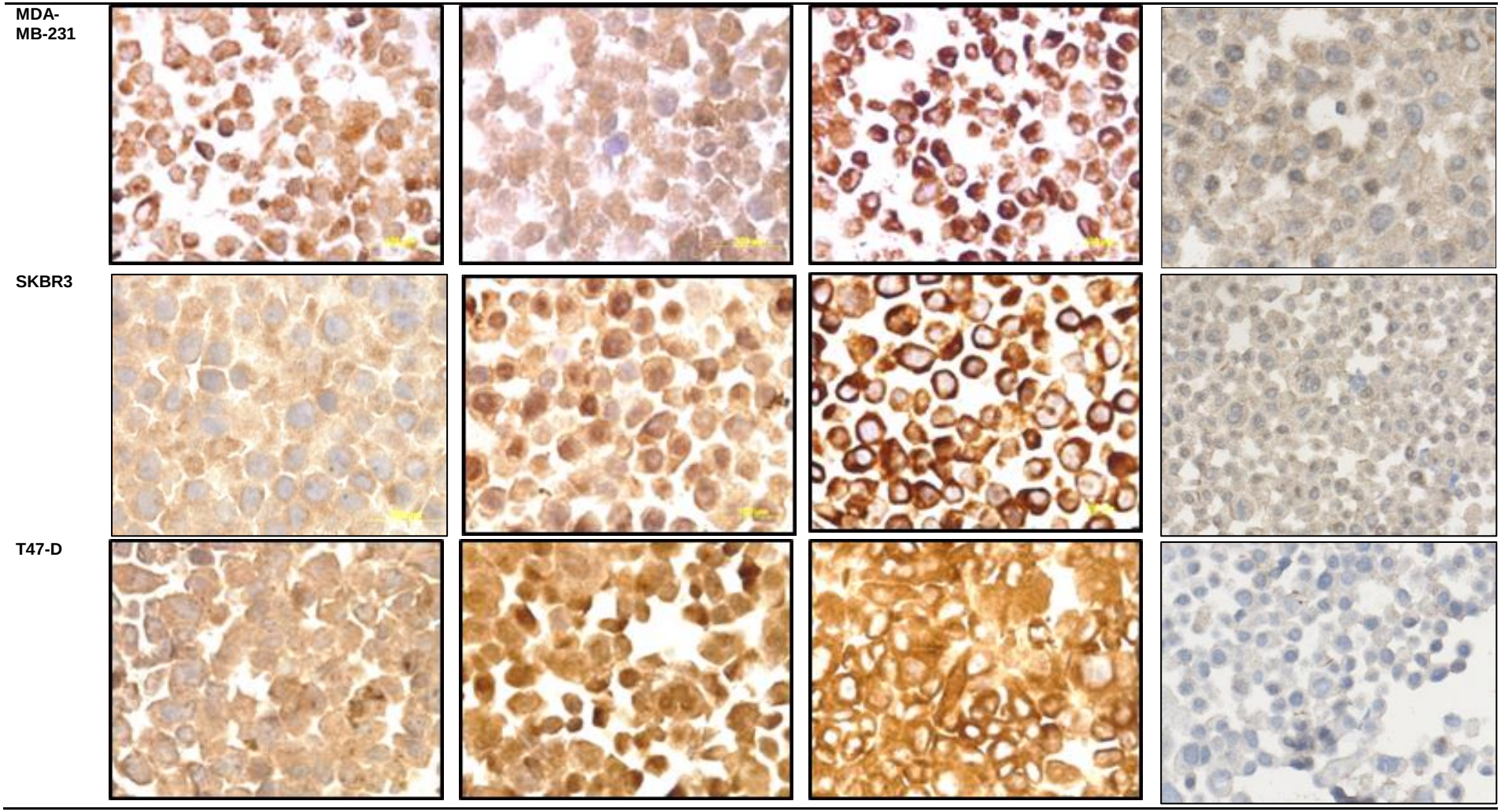


Figure 4. 2 Endogenous transcript expression profile in cancer cells. The relative gene expression levels of AIPL1, NUB1, FAT10 and NEDD8, as determined by qPCR. The results were normalised to β-actin signals. Data shown are means of 3 independent experiments with error bars representing standard deviation. Each bar represents mean ± SEM for each cell lines (n=9).


AIPL1
NUB1
NEDD8
FAT10
ACHN
786-O
HCT116


U2OS
HCC1806
MCF-7


MDA-
MB-231
SKBR3
T47-D

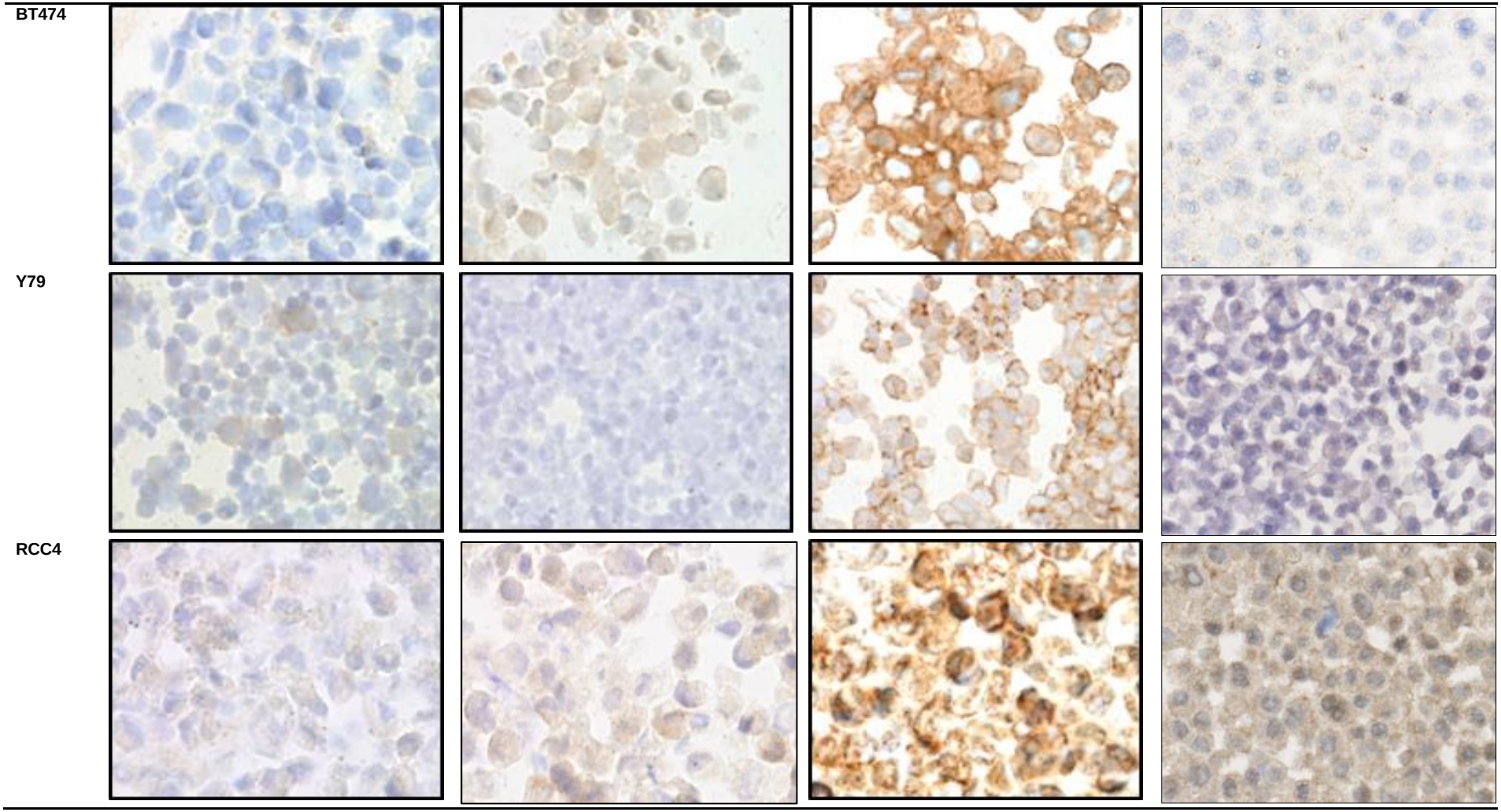


Figure 4. 3 Immunohistochemistry staining of various cancer cells. The representative images of immunohistochemical analysis illustrating AIPL1, NUB1 and NEDD8 protein localisations in various cancer cell line. Brown staining with diaminobenzidine (DAB) indicates immunoreactivity. All magnification of the images are 20X.

Table 4. 1 Summary of AIPL1, NUB1, NEDD8 and FAT10 gene products (protein or transcripts) in all cancer cell line.

Cell line	Proteins*					mRNA				IHC							
	AIPL1		NUB1	^{NEDD8}CULs	FAT10	AIPL1	NUB1	NEDD8	FAT10	AIPL1		NUB1		NEDD8		FAT10	
	Monomer	Dimer								C	N	C	N	C	N	C	N
ACHN	✓	✓	✓	✓	✓	✓	✓	✓	✓	0	0	2+	0	3+	0	0	0
786-O	✓	✓	✓	Low	✓	Low	Low	Low	✓	3+	0	3+	0	3+	0	2+	3+
HCT116	✓	✓	✓	✓	✓	Low	✓	Low	✓	2+	0	2+	0	3+	0	0	0
U2OS	✓	✓	Low	✓	✓	Low	✓	Low	✓	0	0	0	0	3+	0	2+	3+
HCC1806	✓	✓	✓	✓	✓	Low	✓	Low	✓	2+	0	2+	0	3+	0	1+	1+
MCF-7	✓	✓	✓	✓	✓	Low	Low	Low	✓	1	0	0	0	3+	0	1+	0
MDA-MB-231	✓	✓	✓	✓	✓	Low	Low	✓	✓	3+	0	3+	1+	3+	0	1+	0
SKBR3	✓	✓	X	✓	X	Low	✓	✓	✓	3+	1+	3+	2+	3+	0	1+	0
T47D	✓	✓	✓	✓	✓	Low	✓	Low	✓	3+	3+	3+	3+	3+	0	0	0
BT474	✓	✓	✓	✓	Low	Low	✓	✓	✓	0	0	1+	0	2+	0	1+	0
Y79	✓	✓	✓	✓	✓	Low	✓	✓	✓	1+	0	0	0	2+	0	0	0

√ present; X absent, ND: not determined, IHC: Immunohistochemistry, mRNA: messenger RNA, 0, no staining, 1+, mild, 2+, intermdediate; 3+, strong, c, cytoplasm; n, nucleus

4.3 AIPL1 dimerisation in cancer cells

By using a monoclonal mouse anti-AIPL1 antibody (3B4), we observed a band at the right size (41.3kDa), a slightly higher band around 55kDa and a 2-fold larger sized band at 100kDa suggesting a dimerised protein of AIPL1 in Y79 (Fig 4.1). To confirm the oligomer formation, MDA-MB-231 cells were examined *via* native-PAGE analysis. The cells are incubated in reoxygenation as we found AIPL1 protein was upregulated in reoxygenation (Fig. 4.8). No AIPL1 monomer was observed in native conditions (Fig 4.4). Appearance of AIPL1 protein in dimer, trimer and oligomer forms suggests those were the native forms under physiological conditions.

To test the presence of disulfide bonds, we used maleimide fluorescein method. TCEP is a strong reducing agent that separates the cysteine-cysteine disulphide bond apart and prevents the dimer formation. Maleimide fluorescein competitively binds to the exposed cysteine and gives the fluorescein signal. It was observed that the disulfide bonds in the TCEP-reduced sample exhibited stronger fluorescent than the oxidised sample with a visible band and ~55kDa (Fig 4.4). To further confirm the disulphide bonds, the reoxygenated sample of MDA-MB-231 were treated with titrated dithiothreitol (DTT). There were only dimers and monomers were observed. Monomers increased with more DTT concentration. We observed the dimer which is of strong bonds was able to resist DTT reaction. This could be due to the presence of more than two disulphide bonds. Therefore, native and reduced form of the AIPL1 protein verifies the presence of AIPL1 dimer.

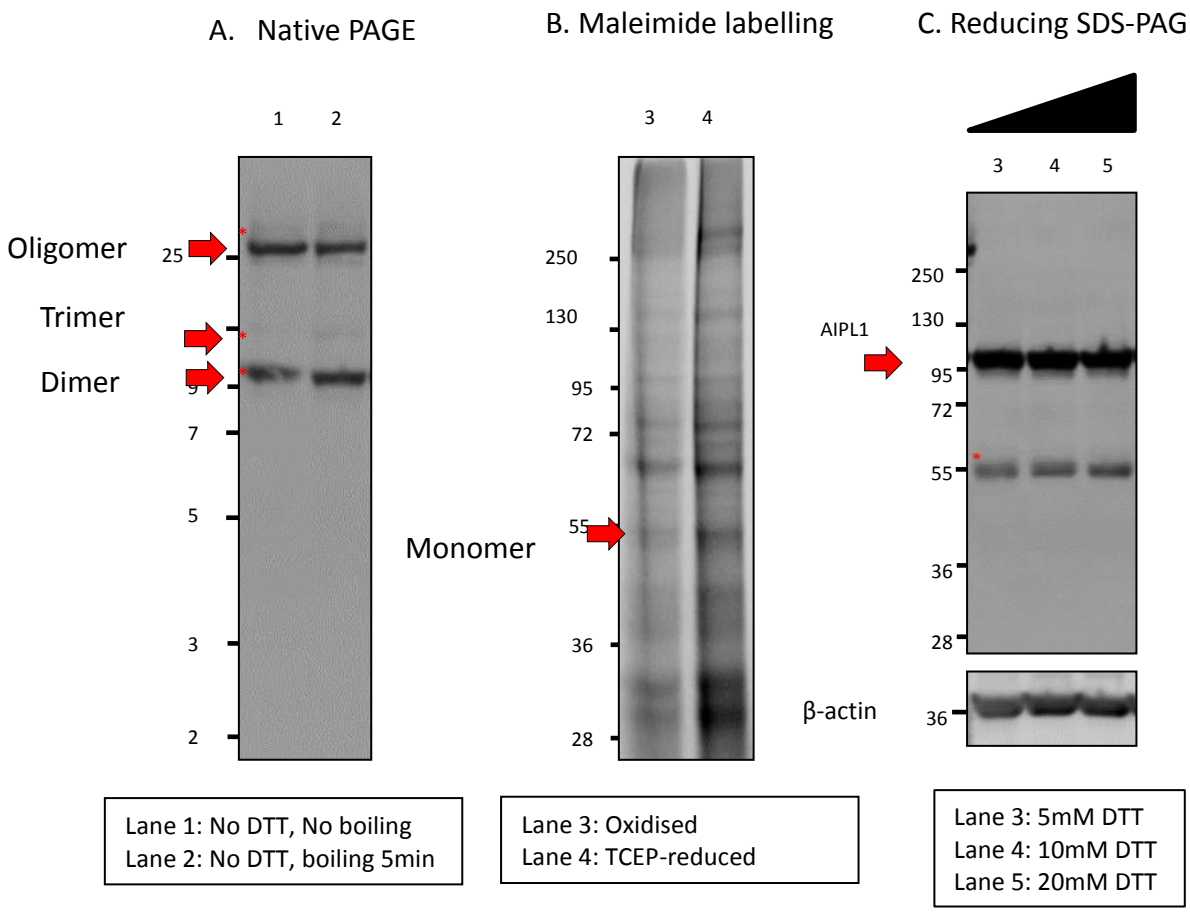


Figure 4. 4 Oligomerisation of AIPL1 proteins analysed by native PAGE and immunoblotting. (A) Native PAGE with and without boiling step. (B) Maleimide labelling with TCEP treatment. We blocked free thiols in the protein with *N*-ethylmaleimide, denature the protein with SDS. Then the denatured protein samples were divided into two- leave one oxidized and reduce the other with TCEP. React each sample with fluorescein maleimide and finally run the samples on SDS-PAGE. Stronger maleimide signal in lane 4 marks the broken disulphine bonds of proteins. (C) Immunoblot with titrated DTT.

4.4 Changes of NUB1 stability upon reoxygenation

To test whether there are changes of proteins under reoxygenation following severe hypoxia (0.1% O_2 for 48h), protein expression levels were examined. MDA-MB-231 cells were studied for it belongs to ER- and triple negative subtypes. Increased neddylated cullins (^{NEDD8}CULs) and NUB1 protein levels were observed in MDA-MB-231 cells as early as 5 minutes of reoxygenation (Fig. 4.5). AIPL1 monomers and dimers did not change over the time points monitored. These data led us to speculate the involvement of both AIPL1 and NUB1 in response to hypoxia and reoxygenation. With the discovery of neddylated HIF1α (Ryu *et al.*, 2011), it is good to examine the role of AIPL1 and NUB1 in regulating NEDD8 conjugations. It could suggest a possible function in the neddylation of proteins in the HIF1α pathway.

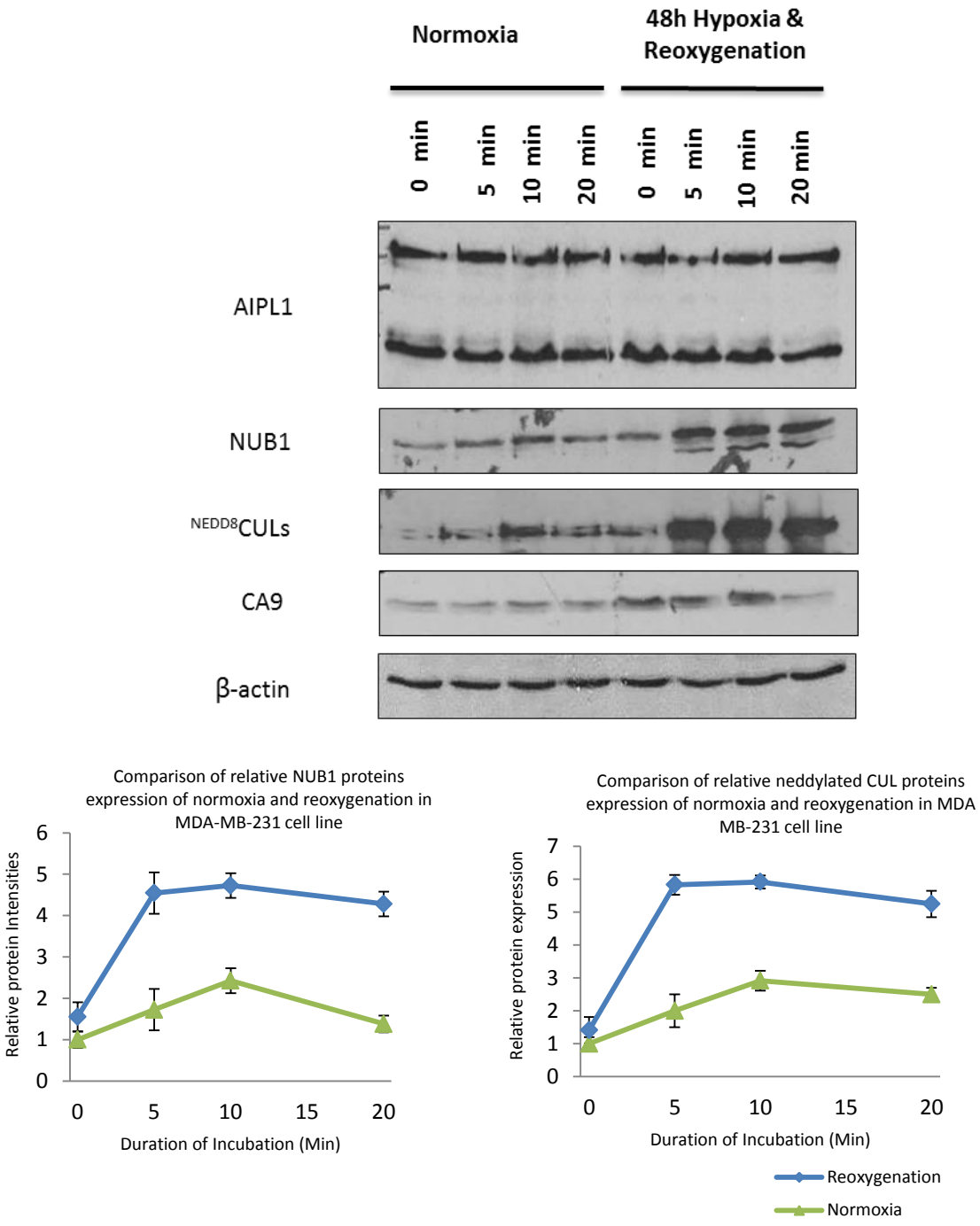


Figure 4. 5 Time course experiment of reoxygenated MDA-MB-231. MDA-MB-231 cells were incubated in hypoxia and reoxygenated. Lysates were collected according to the time point. The levels of proteins were compared to the normoxic cells. Both NUB1 and ^{NEDD8}CULs proteins were significantly different than the normoxic cells. *Abbr* CA9: carbonic anhydrase 9.

4.5 NUB1 silencing caused G_0/G_1 cell cycles arrest

It was found that higher NUB1 protein level triggered cell-cycle alterations through p21/p27 up-regulation and apoptosis (Hosono *et al.*, 2010). To test this, the cell cycle profiles of NUB1 knockdown MDA-MB-231 cells was examined. The cell line was used as it is of ER negative and triple negative subgroup. MDA-MB-231 was transiently transfected with siNUB1 and the cell cycle analysis were perform after 48hr incubation. The experiment demonstrated that NUB1 knockdown lead to a significant reduction in the percentage of cells in the sub-G_1 phase of the cell cycle (Fig 4.5). NUB1 knockdown cells also showed significantly higher level of G_0/G_1 cell population compared with the control (Figure 4.5).

To confirm the G_0/G_1 cell cyle arrest, we observed the up-regulation of two G_0/G_1 cell cycle arrest markers, p21 and p27 proteins in the NUB1 knockdown cells. Therefore, NUB1 protein could promote the G1 to S phase cell cycle transition.

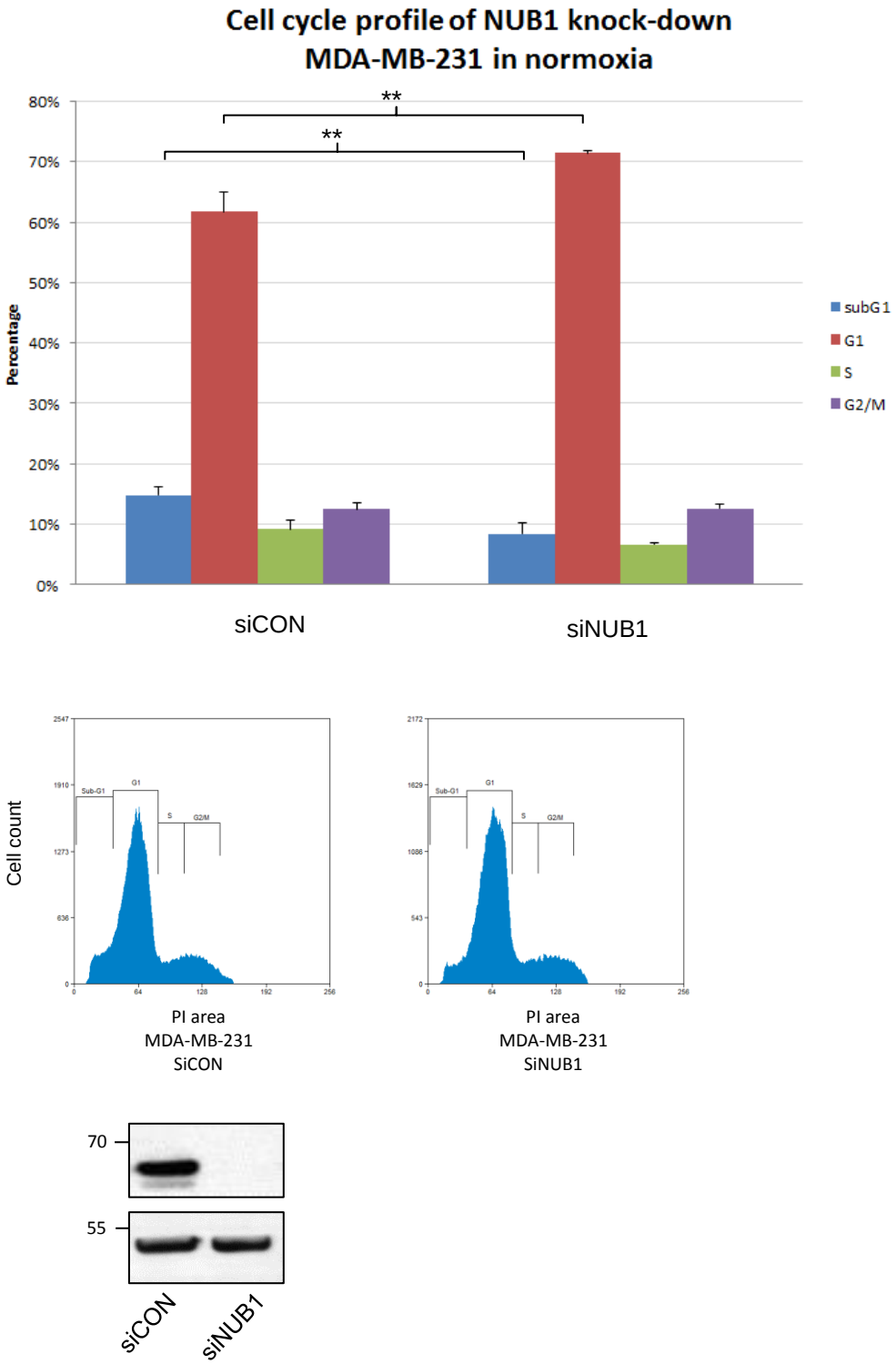


Figure 4. 6 Cell cycle analysis in NUB1 knockdown MDA-MB-231. A. Cell cycle percentage of NUB1 knockdown cells and its control. B. The cell cycle histogram of NUB1 knockdown cells and its control.

4.6 Depletion of NUB1 protein affects cell growth rates

The previous experiment underlined that the NUB1 knockdown causes the G_1 cell cycle arrest, it is important to examine whether NUB1 depletion would alter the growth rate of cancer cells. To evaluate this, the ER- (MDA-MB-231) and ER+ (T-47D) cell lines were used in both normoxia and chronic severe hypoxia (0.1% O_2) for 72hr, respectively. No significant differences were found in normoxia condition (Fig. 4.7). However, in chronic severe hypoxia, NUB1 knock-down in the ER- cell line, MDA-MB-231 showed significant lower viable cell number ($6.2X10^4$/mL vs. $4.1X10^4$/mL, $p<0.001$). So did the ER+ cell line, T-47D under the same hypoxic conditions ($5.7X10^4$/mL vs. $4.7X10^4$/mL, $p=0.01$). This observation implies that loss of NUB1 protein causes greater cell cycle arrest with slower growth rate in chronic severe hypoxia compared to normoxic conditions.

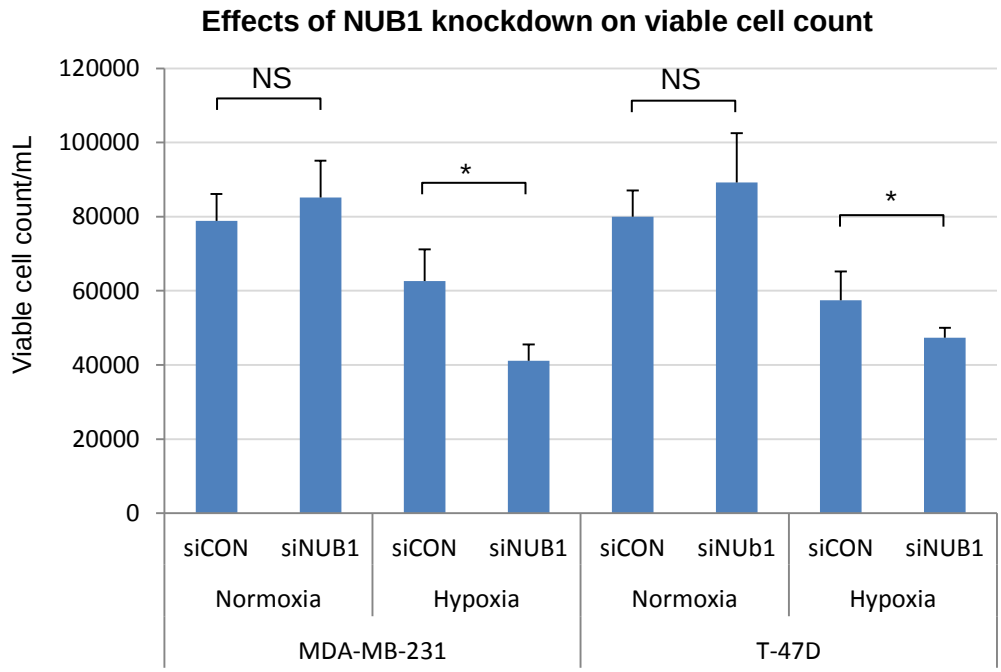


Figure 4. 7 Cancer cell growth in NUB1 knockdown condition. Viable cell number were calculated after siNUB1 transient transfection. Bars, mean+ s.e.m.; n=9; *p<0.05.

4.7 Localisation of AIPL1 and NUB1 proteins in hypoxia and reoxygenation

The subcellular distribution of signaling proteins in proximity to their downstream targets is vital for efficient signal transduction. To examine the distribution of AIPL1 protein and its effect on regulating NUB1 proteins upon hypoxic and reoxygenated conditions, subcellular localisation in MDA-MB-231 was monitored (Fig 4.8).

The AIPL1 protein is predominantly monomerised in normoxia however some dimers present only in the nucleus. In hypoxia and reoxygenation, both monomers and dimers accumulated in the cytoplasm while the nuclear AIPL1 dimers were depleted. We observed more folded nuclear AIPL1 monomers in hypoxia and less in reoxygenation.

NUB1 accumulated in the cytoplasm under normoxia. It migrated to cytoplasm in hypoxia and reoxygenation. After 24 hours of hypoxia, cytoplasmic and nuclear NUB1 levels increased. After 48 hours of hypoxia and after reoxygenation it was progressively accumulated in the nucleus, with little protein in cytoplasm. The phenomenon implies that, in hypoxia and reoxygenation, AIPL1 dimerised in cytoplasm while NUB1 proteins localise into nucleus. We believe dimerised AIPL1 protein is an active forms and it activates and translocates NUB1 into nucleus.

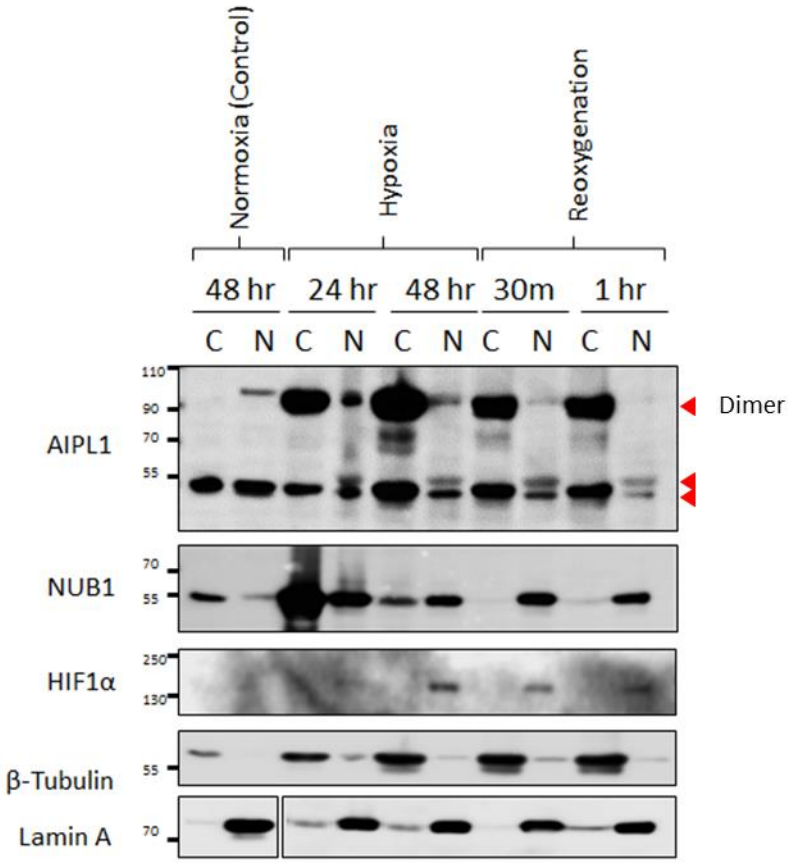


Figure 4. 8 Cytoplasmic AIPL1 dimerisation enhances NUB1 shuttling into the nucleus. Lysates were subjected to subcellular fractionation, cytoplasmic and nuclear fractions were analysed by immunoblotting. β-tubulin and lamin A were used as controls. Endogenous proteins were quantified and values normalised to tubulin or lamin A.

4.8 NUB1 protein regulates cell cycle through neddylation-dependent CUL1

To examine the effects of NUB1 protein in CUL1 neddylation and the overall cell cycle profile of ER- breast cancer cells, the MDA-MB-231 cell line was chosen for immunoblot and cell cycle analysis. p21 and p27 levels were examined to assess the CUL1 activity and its impact upon ubiquitin E3 SCF ligase activity. In normoxia, NUB1 knockdown significantly reduced the neddylated CUL1 levels whilst p27 and p21 were upregulated (p-value=0.02, Fig. 4.9). NUB1 knockdown significantly reduced the free CUL1 (Lane 1 vs. lane 4, Fig 4.9). Neddylation inhibition significantly increases p21 and p27. The precise mechanism for this observation remains to be determined. Two scenarios could be speculated: NUB1 protein regulates CUL1 expression and/or NUB1 protein favourably stabilise CUL1 protein.

For cell cycle analysis, in normoxia and hypoxia, neddylation inhibitor increases accumulation in G_o/G_1 after reoxygenation. The neddylation inhibition also increased the transition from G_0/G_1 to S and G_2/M (Fig. 4.10 and Fig. 4.11). NUB1 knockdown causes accumulation of cells in G_1/G_0 in normoxia and hypoxia but has no effect on reoxygenated cells (Fig. 4.10 and Fig. 4.11).

Under condition of reoxygenation, neddylation inhibition (by MLN4924) slowed down the G1 cell cycle release (Fig. 4.10 and Fig. 4.11). From the result, NUB1 knockdown prolonged G1 arrest (in hypoxia) and caused the down-regulation of neddylated CUL1 protein levels.

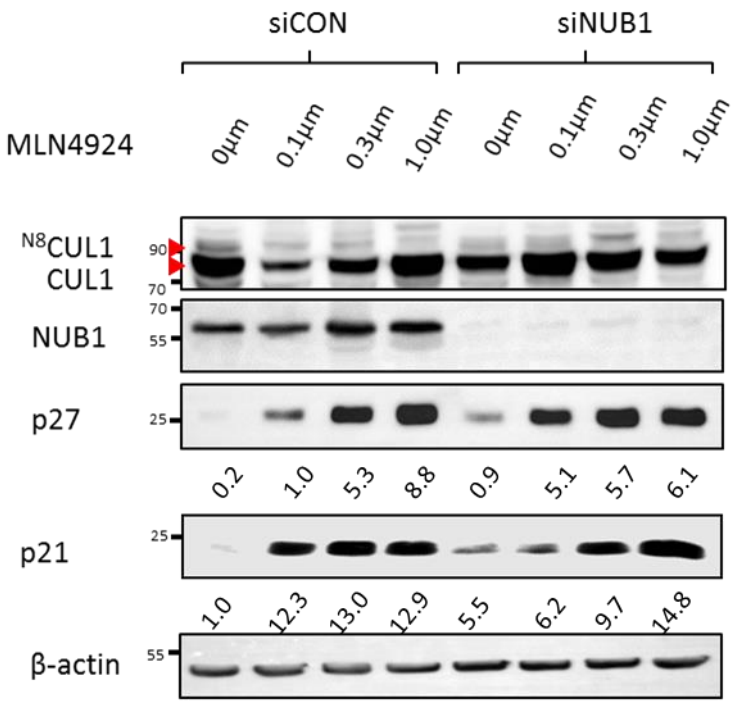


Figure 4. 9 NUB1 silencing enhances neddylation inhibition effects onto p27 (but not p21) protein levels. MDA-MB-231 cell were treated with siRNA and titrated MLN 4924 for 48hr in normoxia. This experiment was performed twice. Densitometry (indicated by numbers beneath the immunoblot) was performed using ImageJ.

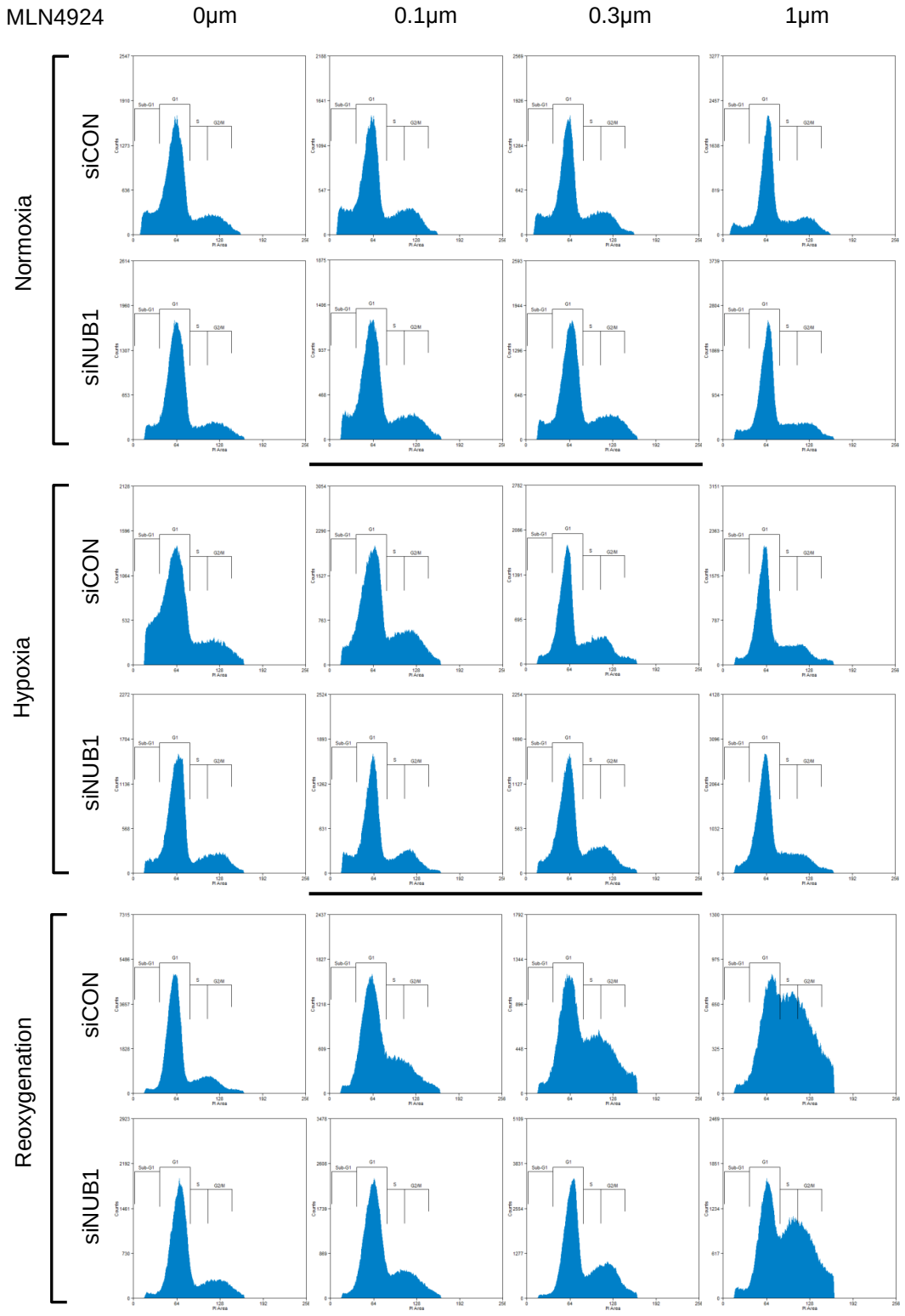


Figure 4. 10 Cell cycle profile of MDA-MB-231. The MDA-MB-231 cells were treated with MLN 4924, a neddylation inhibitor with 24hr in prior. NUB1 gene were transiently knockdown using siRNA and incubated for 48 hours in normoxic and hypoxic environment. For reoxygenation experiment, the cells were further incubated for 12 hours in normoxic environment. Cells were harvested and stained with propidium iodide as proposed. *Abbr*=siCON: control siRNA, siNUB1: NUB1 siRNA.

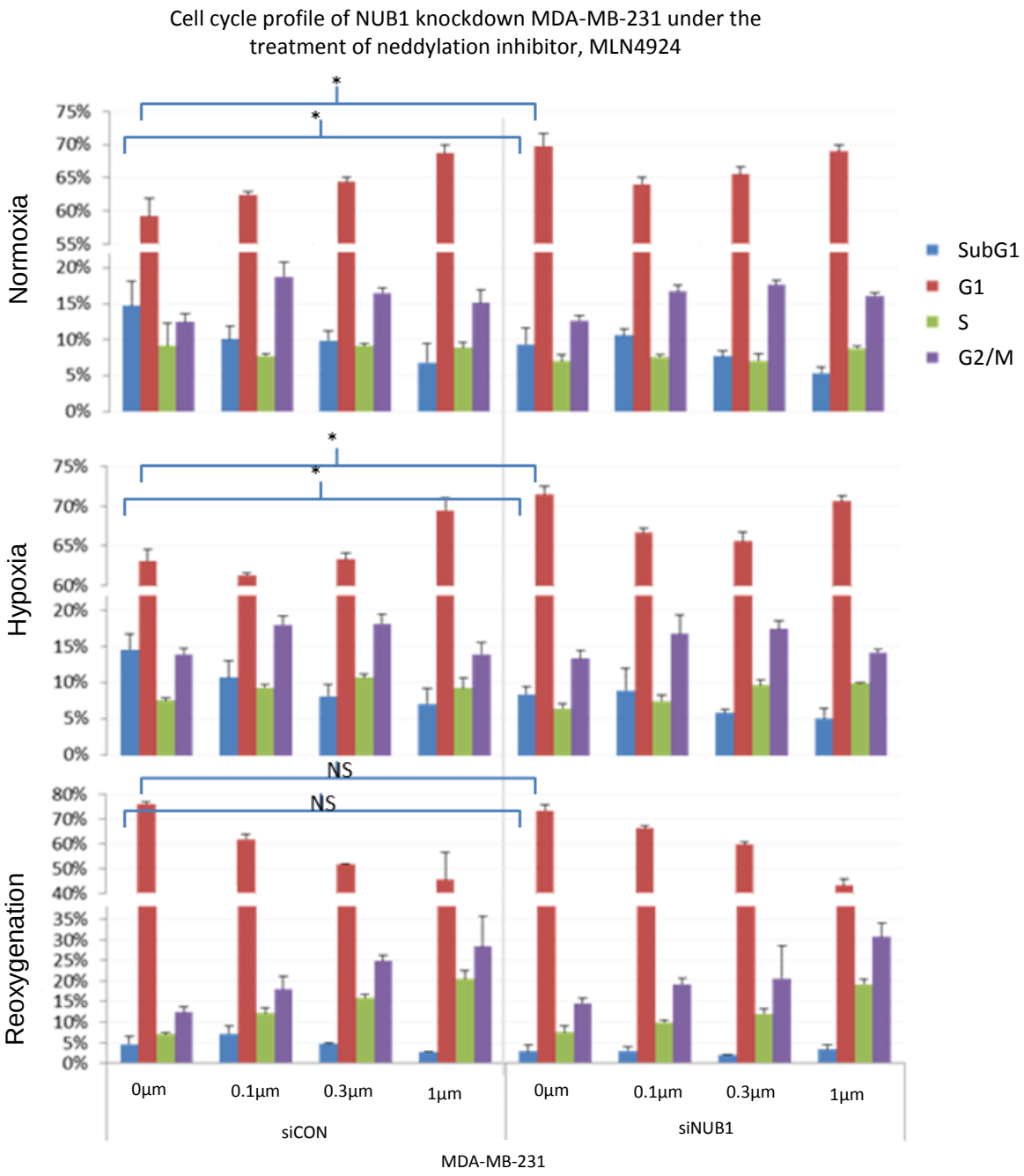


Figure 4. 11 Knockdown of NUB1 and cell cycle analysis. Cell cycle analysis was performed to examine the cell cycle distribution in each group, and quantification. Data represented as mean±s.d; *p<0.05.

4.9 Discussion and Chapter Summary

It was observed that AIPL1 and NUB1 transcripts did not match the protein levels in unstressed condition. This is due to post-transcriptional and/or epigenetic changes which affect the proteins levels. Furthermore, we showed that AIPL1, NUB1 and FAT10 can be located in the cytoplasm and in the nucleus.

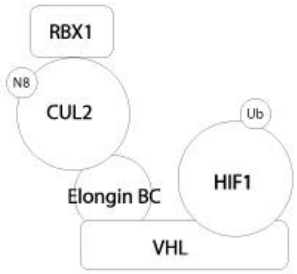
AIPL1 present either as a monomer or dimer, and the proportion between the two forms changes under stresses. Upon hypoxia and reoxygenation, AIPL1 forms dimer and migrated from nucleus to cytoplasm. Reversely, NUB1 localised into the nucleus under the same condition.

In reoxygenation, NUB1 and neddylated CULs were upregulated at protein levels as early as after 5 minutes. They hinted both proteins were responsive to reoxygenation stress. Furthermore, NUB1 knockdown caused MDA-MB-231 cell cycle arrest with lower sub-G1. There was a lack of S-phase transition. The results are consistent with a previous study describing that NUB1 overexpression promotes S-phase transition in A549 renal cells (Hosono *et al.*, 2010). The result also indicated that depleted NUB1 protein increased p27 and p21 through neddylation-dependent CUL1 and subsequent inhibition of ubiquitin-mediated degradation.

Chapter 5
NUB1 protein destabilise p21 and p27 proteins through VHL-dependent CUL2-based E3 ligase

5.1 Rationale of the study

We performed cell cycle analysis on MDA-MB-231 breast cancer cells in last chapter and found that NUB1 silencing decreases the number of cells in subG1, increases the number of cells inn G_0/G_1 and upregulated p27 and p21 in normoxia and hypoxia. Neddylation inhibitor prevents CUL1 neddylation and deactivates the ubiquitin E3 ligase which results in further up-regulation of p27 and p21. This chapter works on the basis that there might be an alternative pathway that confers p21 and p27 up-regulation. A previous study demonstrated that VHL stabilise and increases p21 and p27 levels and protects from apoptosis (Schoenfeld *et al.*, 2000): the authors suggests that one possible mechanism could VHL consumption of NEDD8 and RBX1 proteins which leave them unavailable to facilitate p27 and possibly p21 degradation (Fig 5.2) (Schoenfeld *et al.*, 2000): RBX1 could have this effect trough the CUL2 and Ubiquitin E3 ligases pathway as well. In the ubiquitin E3 ligase, CUL2 assembles with RING protein (RBX1), Elongin B/C proteins as adapter proteins and VHL substrate recognition receptors (Zimmerman *et al.*, 2010; Sarikas *et al.*, 2011).



Scaffold	Adaptor	Receptor	Ring box	Substrates
Cul-1	Skp1	Skp2	Rbx1*	p21, p27, p73, p1 30, Cydin A/ D
Cul-2	Elongin BC	VHL	Rbx1*	HIF1α

Figure 5. 1 Ubiquitin E3 ligases and their substrates. * shared protein as a part of two different complexes.

VHL down-regulates the expression of hypoxia-inducible genes such as vascular endothelial growth factor (VEGF), glucose transporter, GLUT1 and platelet derived growth factor (PDGF) B chain (Iliopoulos *et al.*, 1996), *via* degradation of hypoxia-inducible factor (HIF) alpha subunits (Maxwell *et al.*, 1999; Ohh *et al.*, 2000). The focus of this ongoing study is to examine the activity of NUB1 protein onto the CUL2-based ubiquitin E3 ligase and the cyclin-dependent kinase (CDK) inhibitors, p21 and p27, during hypoxia and reoxygenation. This will provide a rationale on how both AIPL1 and NUB1 work in relation to VHL-mediated cell cycle regulation in cancers, through p21 and p27.

VHL is a known tumor suppressor gene that blocks the development and progression of renal cell carcinogenesis. Individuals with germline mutations in the VHL gene, which lead to its inactivation, are predisposed to VHL disease including renal cell carcinoma (RCC) (Latif *et al.*, 1993; Linehan *et al.*, 1995). Loss of VHL function appears to be an early event in RCC (Lubensky *et al.*, 1996). Furthermore, reintroduction of wild-type VHL expression into VHL-negative renal cells abrogates their cancer causing nature (Iliopoulos *et al.*, 1996; Schoenfeld *et al.*, 1998).

It remains open on how expression of VHL mediates the stabilisation of p27 and p21. VHL protein, which is associated with CUL2-based ubiquitin E3 ligase activities, can block the proteasomal degradation of p21 and p27. VHL protein could sequester ‘sharing’ E3 ligase members such as RBX1 which also facilitate p27 (and perhaps p21) degradation through CUL1-based E3 ligase (Morimoto et al., 2000). Therefore, the stabilisation of these CDK inhibitors may result.

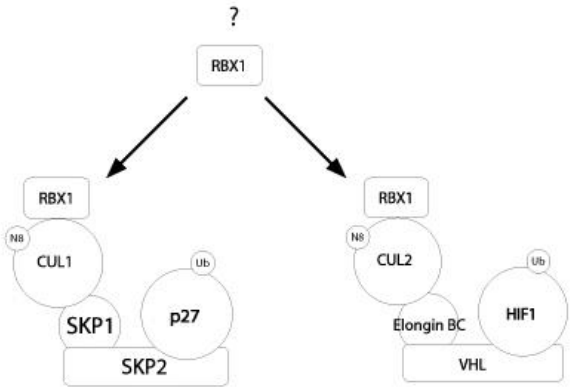


Figure 5. 2 Schoenfeld's first speculation on how VHL regulates p27 and p21.

Secondly, It was also speculated that VHL may increase the half-lives of p21 and p27 mRNAs, perhaps through the degradation of factors that destabilize mRNA, in a manner opposite to HIF1α (Schoenfeld *et al.*, 2000). p21 and p27 stabilisation may therefore occur at the post-transcriptional level. As p21 and p27 cause G_o/G_1 cell cycle arrest, more upregulated p21 and p27 levels in VHL-negative RCC4 might explain why RCC4plusVHL cells differentiate more rapidly.

p21 and p27 belong to the cyclin-dependent kinase (CDK) inhibitors that mediate cell cycle arrest. The roles of the cell cycle inhibitors p21 and p27 are regulated by their cellular localisation. p21 and p27 are tumor suppressors within the nucleus and become oncogenic when localised in the cytoplasm. Therefore, p21 and p27 play a pleomorphic role in cell cycle regulation, its role as an oncogene or a tumour suppressor may be a function of setting.

a. p21 is a tumour suppressor (Katayose *et al.*, 1995; Yang *et al.*, 1995). However, it exerts anti-apoptotic functions when it is localised in the cytoplasm. The binding of p21 to mitogen-activated protein kinase (MAPK) kinase kinase 5 (MAP3K5) in the cytoplasm inhibits the MAPK cascade (Asada *et al.*, 1999; Huang *et al.*, 2003).

Phosphorylation of p21 on T145 by Protein Kinase B (AKT) induces nuclear export of p21 leading to enhanced cell growth (Rossig *et al.*, 2001; Zhou *et al.*, 2001; Li *et al.*, 2002). Cytoplasmic p21 was oncogenic in breast cancer and metastatic *in vivo* (Cheng *et al.*, 2010). Cytoplasmic localisation of p21 is a poor prognostic marker for breast cancer (Winters *et al.*, 2003; Xia *et al.*, 2004), and is involved in mediating resistance to anticancer drugs (Zhang *et al.*, 1995; Ruan *et al.*, 1999; Koster *et al.*, 2010). The cytoplasmic localisation of p21 also resulted in a poor response to tamoxifen (Perez-Tenorio *et al.*, 2006).

b. Cytoplasmic p27 protein is oncogenic as the reduction of cytosolic p27 inhibits cancer cell motility, survival, and tumorigenicity (Wu et al., . T157 phosphorylation by AKT blocks the nuclear import of p27 (Liang *et al.*, 2002; Shin *et al.*, 2002; Viglietto *et al.*, 2002). Whereas S10 phosphorylation induces p27 cytoplasmic localisation and stabilisation (Rodier *et al.*, 2001). The cytoplasmic localisation of p27 is a poor prognostic factor in cancers, including breast (Liang *et al.*, 2002), hepatocellular (Nan *et al.*, 2004), colon (Ogino *et al.*, 2009) and ovarian cancer (Rosen *et al.*, 2005), and Barrett's carcinoma (Singh *et al.*, 1998).

This chapter examines the role of NUB1 in regulating the CUL2-based ubiquitin E3 ligase during hypoxic stress. And the involvement of VHL protein in the cascade with regards to tumour development is examined.

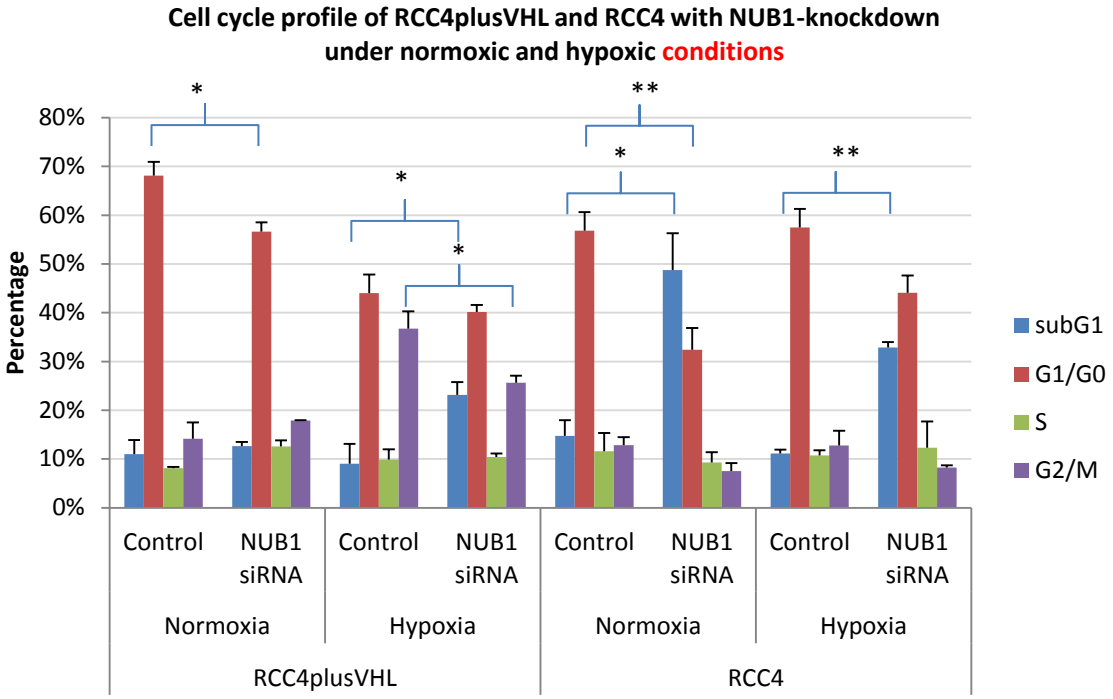
5.2 NUB1 protects cells from hypoxia-mediated cell cycle arrest and apoptosis through VHL

In 2000, Schoenfeld *et al.* found that VHL expression protects UV-treated cells from apoptosis (Schoenfeld *et al.*, 1998). The apoptosis resulted from the perturbation of cell cycle checkpoints in regulating the repair of DNA damage (Schoenfeld *et al.*, 1998). To examine whether chronic severe hypoxia- and reoxygenation-mediated stress exerts the same effect onto these CDK inhibitors (p27 and p21) in renal cancer carcinoma cell line, we explore the effects of NUB1 and VHL protein on the cell cycle regulatory proteins by immunoblot.

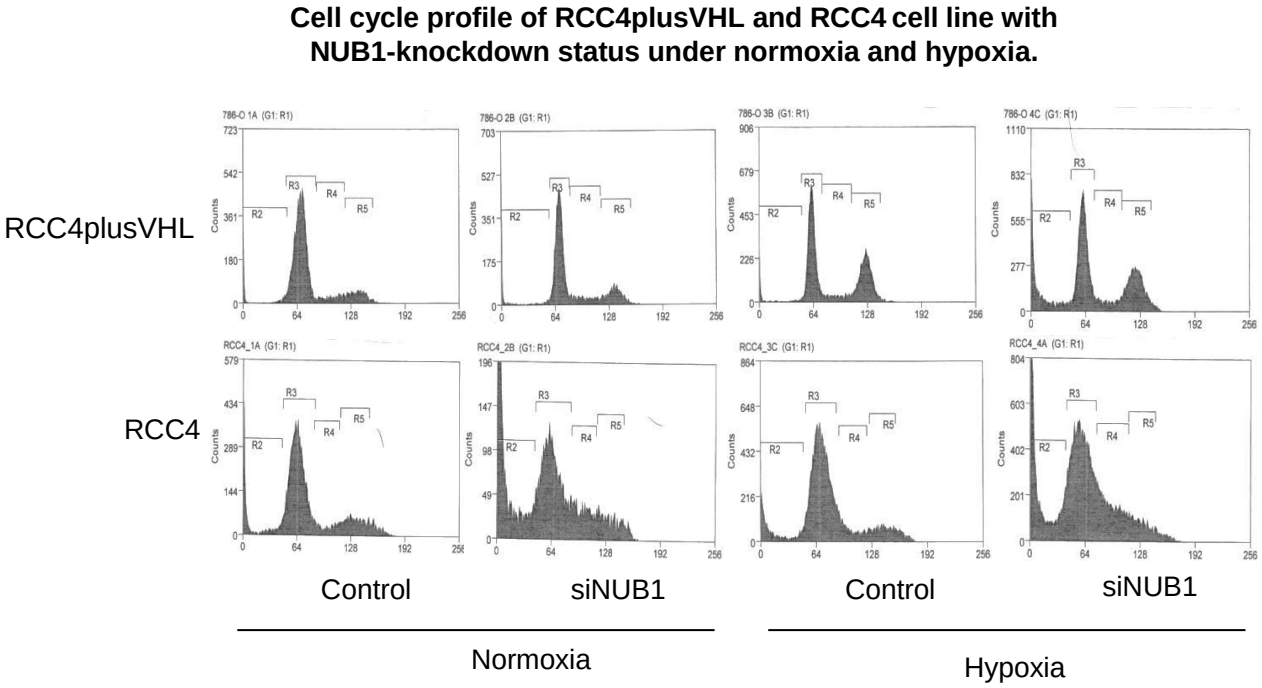
In the RCC4plusVHL cells, NUB1 silencing in hypoxia caused a decrease in G2/M (25.7%±2.5 vs 36.2±3.1; $p<0.001$) and increased sub-G1 (20.2%±0.7 vs. 9.0%±2.16; $p<0.01$) (Fig 5.1a). To differentiate two major type of cell death: apoptotic and necrotic cell death, apoptotic marker, cleaved PARP was observed at hypoxic condition in RCC4plusVHL. Increased sub-G1 with NUB1 knockdown in hypoxia was due to the apoptosis for the presence of cleaved PARP (Fig 5.3). In hypoxia, VHL was reduced (immunoblot) but HIF1α protein was undetected. NUB1 silencing drove the cells toward apoptosis and no apoptosis marker was detected in normoxia. Therefore, NUB1 could protect cells from apoptosis in hypoxia.

In the RCC4 cell cycle, a significantly higher percentage of sub-G1 cells were detected in NUB1 knockdown cells, as compared to non-targeting controls (14.71%±3.21 vs. 48.73%±7.56, $p<0.05$ in normoxia; 11.12%±3.78 vs. 32.89%±2.11, $p<0.05$ in hypoxia). For RCC4plusVHL cells, increased cell death was observed in the hypoxic and NUB1 siRNA treated group. p21 protein in RCCplusVHL remain undetected while increased in NUB1-knockdown in RCC4 cells. This cell cycle analysis underlined a role of NUB1 in protecting cells from cell death under both hypoxia and normoxia. This protective role of NUB1 is independent of VHL.

A.


Cell cycle profile of RCC4plusVHL and RCC4 with NUB1-knockdown under normoxic and hypoxic conditions
Percentage
80%
70%
60%
50%
40%
30%
20%
10%
0%
subG1
G1/G0
S
G2/M
Control
NUB1 siRNA
Normoxia
Hypoxia
RCC4plusVHL
RCC4

B.


Cell cycle profile of RCC4plusVHL and RCC4 cell line with NUB1-knockdown status under normoxia and hypoxia.
RCC4plusVHL
RCC4
Control
siNUB1
Normoxia
Hypoxia

C.

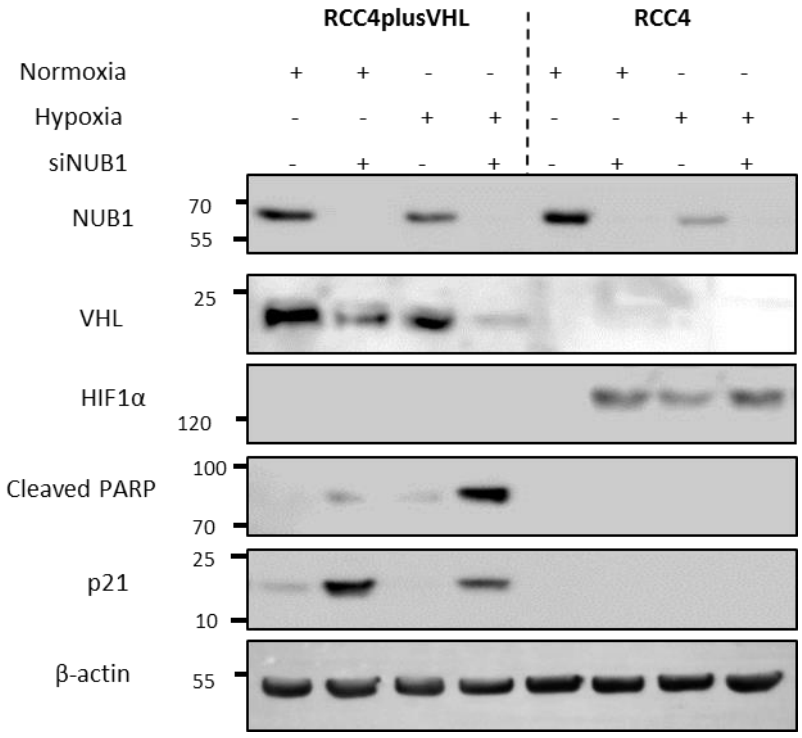
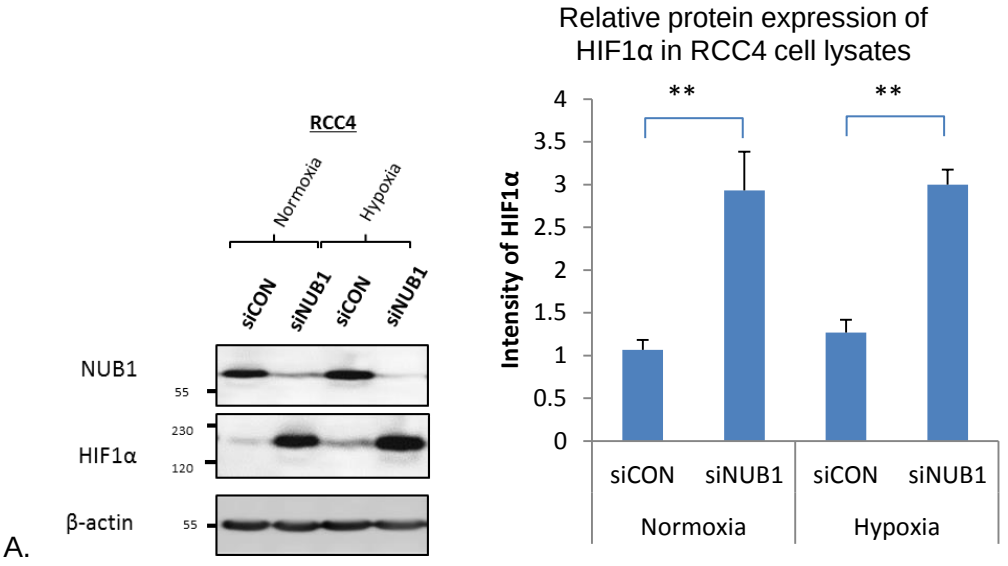


Figure 5. 3 Effect of NUB1 knowckdown on the cell cycle of RCC4plusVHL and control cells under normoxic and hypoxic conditions. Both cell line were transfected with siNUB1 and incubated for 48 hours. A. The cells were harvested and stained with propidium iodide and subjected to FACs analysis. B. Cell cycle profile of each experiment group. Data (A) shown are means of 3 independent experiments with error bars representing standard deviation. C. Immunoblotting of p21 (G1/G0) marker and apoptosis marker, PARP under the different experimental conditons. Each bar represents mean ± SEM for each cell line (n=9). * significant at $p<0.05$; ** significant at $p<0.005$.

5.3 Up-regulation of HIF1α and VHL protein levels due to NUB1 knockdown

CUL2 as part of the ubiquitin E3 ligase regulates ubiquitination and degradation of HIF1α. To test whether NUB1 influences the activity of the CUL2-based complexes, HIF1α and VHL levels were measured in a renal cell carcinoma cell line. The level of HIF1α in normoxia in the NUB1 knockdown RCC4 group was almost 3-fold greater than that found in the control siRNA group (0.73±0.21 vs. 2.1±0.36 fold, P<0.001). The VHL level dropped following NUB1 knockdown in RCC4plusVHL cells (1.06±0.06 vs. 0.32±0.10; p<0.001) (Fig 5.4). Therefore, it was found that stabilised HIF1α in NUB1 knockdown cells is likely due to the down-regulation of VHL and possibly ubiquitin E3 ligase activity.



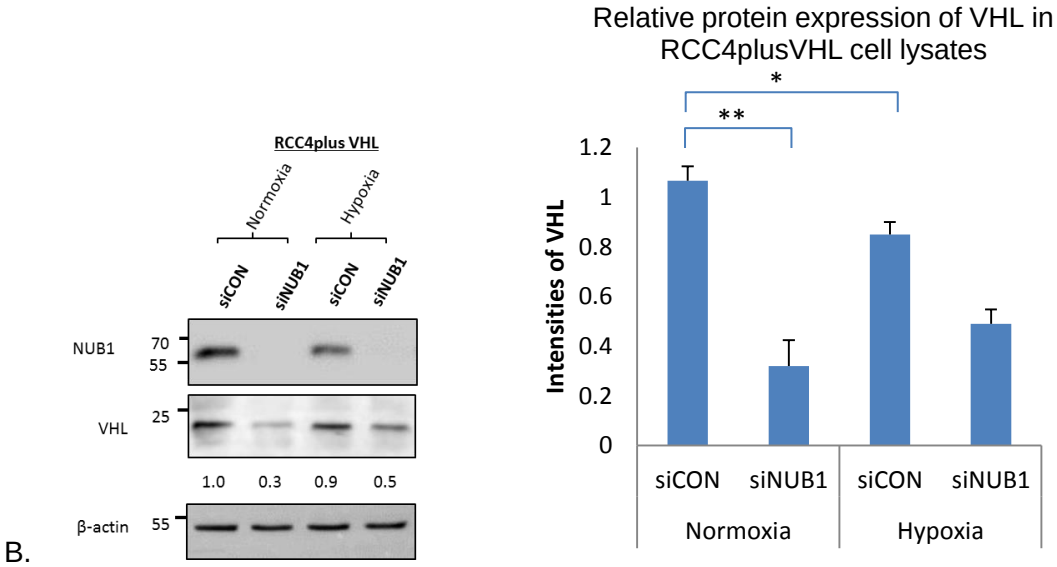


Figure 5. 4 NUB1 knockdown up-regulates HIF1α (A) and down-regulates VHL (B). RCC4plusVHL and RCC4 cells were transfected with 100pmol siRNA as indicated. The amount of HIF-1α was calculated as the difference between siCon and siNUB1 groups. Bars represent the means ± S.D. of 3 independent biological replicates. * significant at $p<0.05$; ** significant at $p<0.005$.

5.4 Cell cycle analysis with NUB1 knockdown status under severe hypoxic conditions.

To examine whether the roles of NUB1 were VHL-dependent, cell cycle profiles of cells exposed to normoxic or hypoxic conditions were examined (Figure 5.5). We use renal cancer cell line, RCC4 in the experiment for they are established cell line with VHL and null-VHL within the cells (Maxwell *et al.*, 1999). Expression of NUB1 was reduced in RCC4 ($VHL^{-/-}$) cells by siRNA, and each treatment was performed in triplicate. In RCC4 cells, a greater percentage of sub-G1 cells were detected in NUB1 siRNA treated samples under hypoxia, as compared to non-targeting controls. Increased cell death was observed in the hypoxic and NUB1 siRNA treated group, suggesting a role for NUB1 in protecting cells from hypoxia induced replication stress. HIF1α was upregulated in NUB1 knockdown cells. This cell cycle analysis has highlighted a potential role for the NUB1 in protecting cells undergoing cell death responses under severe hypoxic conditions.

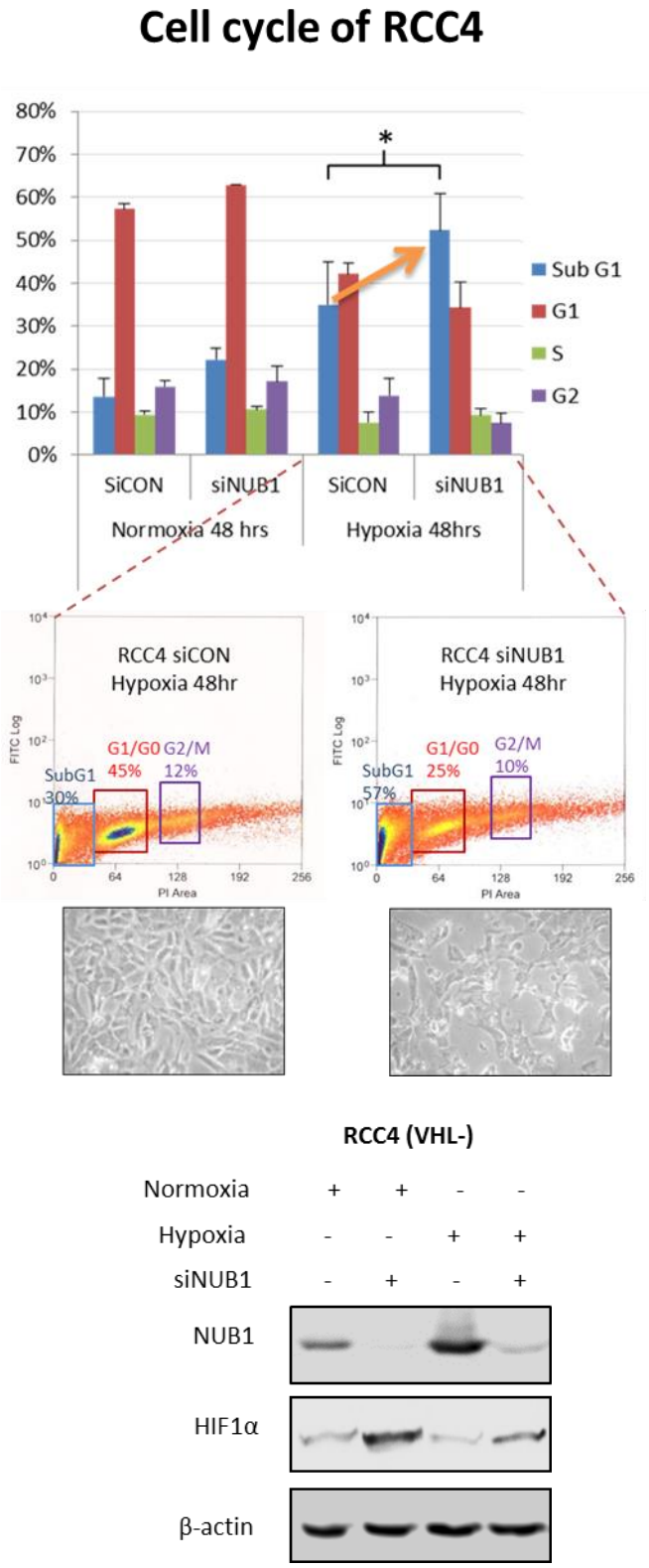


Figure 5. 5 Cell cycle analysis on the NUB1 knowckdown effect in RCC4 cells under normoxic and hypoxic conditions. Cell line were transfected with siNUB1 and incubated for 48 hours. NUB1 knockdown of hypoxic RCC4 showed significant cell death compared to the control. HIF1α was up-regulated in NUB1 knockdown cells. Data shown are means of 3 independent experiments with error bars representing standard deviation. * significant at $p<0.05$; ** significant at $p<0.005$.

5.5 Stabilisation of p27 and HIF1α by NUB1 depletion are independent of VHL

To test Schoenfeld's speculation whether VHL could sequester both RBX1 and SKP1, resulting in reduced engagement of these proteins in CUL1 based degradation complexes, thereby stabilising p21 and p27 (Schoenfeld *et al.*, 2000), we examined both CUL1-based and CUL2-based ubiquitin E3 ligases in RCC4plusVHL and RCC4 cells (Fig. 5.6). It was found that depleted NUB1 upregulates p27 and p21 proteins in RCC4 cells and RCC4plusVHL cells. The cell cycle arrest is NUB1- and VHL-dependent. The amount of p27 was greater in VHL-null cells in normoxia. These data hinted that VHL could occupy the RBX1 which facilitate p27 degradation.

To characterise CUL2 neddylation in the context of NUB1, we examined a representative protein, HIF1α, to test CUL2 activity in normoxia, hypoxia and reoxygenation. We observed that NUB1 knockdown stabilised p27 and p21 protein in both cell line and only HIF1α in RCC4. The result hinted that p27 and p21 stabilisation through NUB1 depletion is independent of RBX1 factor as per suggested by Schoefeld's idea.

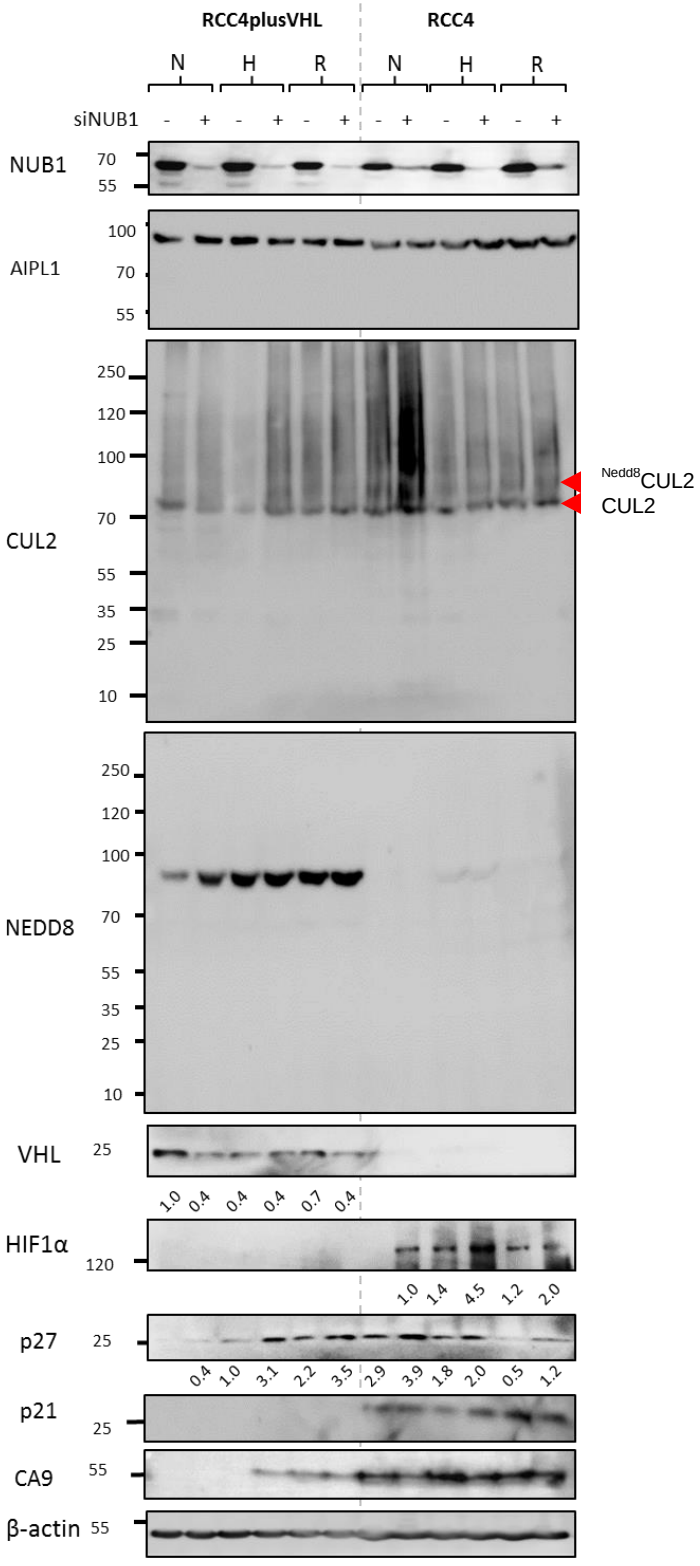


Figure 5. 6 Depletion of NUB1 upregulated HIF1α and p27 proteins. The lysates from RCC4plusVHL and RCC4 cells were transfected with siNUB1 and underwent normoxia, hypoxia for 48 hr and reoxygenated 24 hours. The cell lysates were analysed by Western blotting using antibodies, and by the densitometric analysis. N=normoxia, H: hypoxia, R: reoxygenation. Densitometry was quantified using ImageJ and the figure indicated the relative densities to a band equal to 1.0.

5.6 HIF1α is neddylated and FAT10ylated

We observed up-regulation of HIF1α even when VHL is absent and during NUB1.siRNA treatment. It was thought that HIF1α is stabilised through non-ubiquitin regulated mechanism. To determine whether HIF1α is neddylated, endogenous HIF1α was immunoprecipitated from MDA-MB-231 cell lysate. We checked HIF-1α expression and activity in MDA-MB-231 cells incubated in hypoxia for 48 hours and 1-hr reoxygenation. Endogenous HIF1α was immunoprecipitated from 500μg MDA-MB-231 cell lysate. We found HIF1α was both neddylated and FAT10ylated (Fig 5.7).

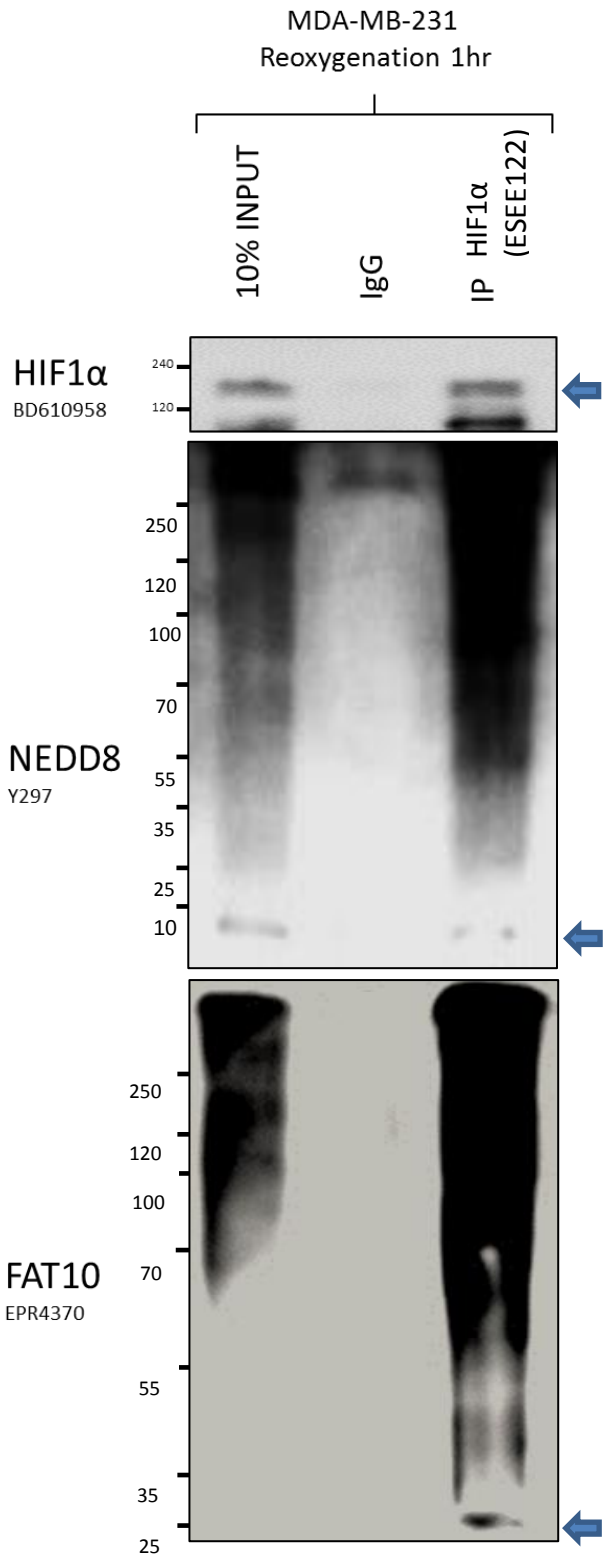


Figure 5. 7 NEDD8 and FAT10 signals detected in endogenous HIF1α. Cells lysate from MDA-MB-231 cells were immunoprecipitated with control IgG or HIF1α antibodies, and subsequently immunoblotted with the indicated antibodies. Input levels of HIF1α protein are as shown.

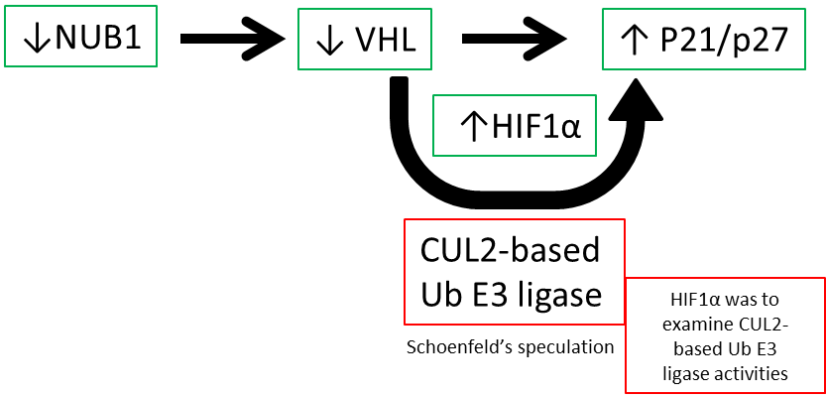
5.7 Discussion and Chapter Summary

As we examine the effect of VHL on RCC4 cells, NUB1 was found to protect RCC4 renal cell carcinoma cells from apoptosis in the presence of VHL especially in chronic severe hypoxia. In absence of VHL, NUB1 is still protecting cells from death through non-apoptotic pathways, as no cleaved-PARP was detected when cell death occurs in absence of NUB1. In the presence of VHL, NUB1 knockdown increased the number of cells in G_0/G_1 in hypoxia. While in absence of VHL, NUB1 silencing caused increase in G_0/G_1 fraction both in hypoxia and normoxia.

It was found that depleted NUB1 down-regulated VHL. In null-VHL RCC4, upregulated HIF1α, p21 and p27 were observed in the same condition. VHL caused a subset of neddylated CUL2 to degrade and increased the levels of total NEDD8. In RCC4plusVHL, the stabilisation of HIF1α did not happen, but p27 and p21 did under hypoxia. In RCC4-null cells, the other mechanism of NUB1 regulating p27/p21 levels remains open.

NUB1 caused a subset of neddylated CUL2 to degrade whilst the other neddylated CUL2-based ubiquitin E3 ligase remain in complex with RBX1. We worked on the hypothesis that CUL2-based ubiquitin E3 ligase competitively bind to RBX1, resulting in less engagement of CUL1-based ubiquitin E3 ligases. This could therefore lead to increased p27 and p21 degradation.

A)



B)

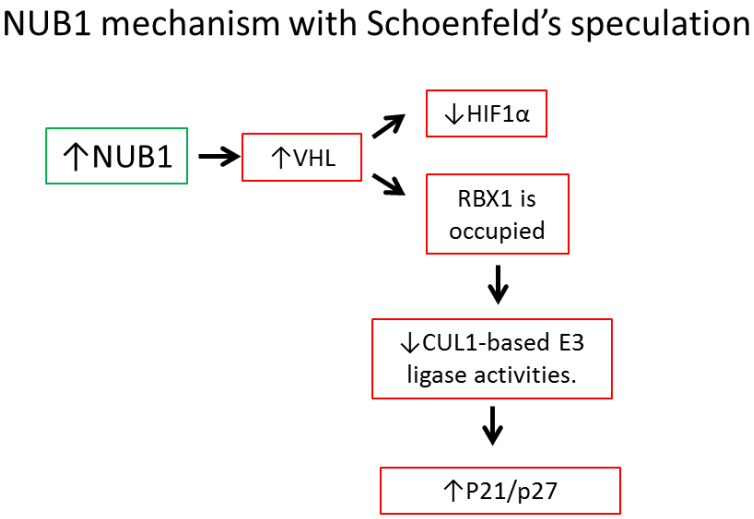


Figure 5. 8 Hypothesis pipeline of the chapter 5. A) The flow chart which explains our observations on reduced VHL would cause stabilisation of HIF1α, p21 and p27. Our finding of depleted NUB1 caused the decreased VHL and upregulated HIF1α. B) NUB1 and VHL may act in the same pathway, VHL caused down-regulation of HIF1α and up-regulation of p21 and p27.

Chapter 6
Tissue microarray analysis of NUB1 in primary Breast Cancer shows cytoplasmic localisation is associated with poorer prognosis

6.1 Rationale of study

The previous chapters have examined the expression and localisation of AIPL1 and NUB1 in ER- subtype breast cancer cell lines. In hypoxia, AIPL1 was found to be predominantly dimerised in the cytoplasm, whereas NUB1 remained mainly in the nucleus. Previous studies have shown that a nuclear localisation signal (NLS) near the C terminus of NUB1 responsible for this nuclear localisation (Kito *et al.*, 2001; van der Spuy *et al.*, 2002; van der Spuy *et al.*, 2003). AIPL1 was found to negatively regulate the nuclear translocation of NUB1.

Subcellular localisation is essential for NUB1 protein to regulate the cell cycle (Kito *et al.*, 2001). The regulation of NUB1 protein trafficking relies on the information that is encoded within its NLS. Subcellular localisation of NUB1 determines the access of proteins to interacting partners and the FAT10 and NEDD8 post-translational modification machinery and enables the conjugated proteins to be modified by the UPS. Generally, aberrantly localised proteins have been linked to human diseases as diverse as Alzheimer's disease, kidney stones and cancer. It is therefore myrationale to examine the mechanisms that regulate subcellular protein localisation implicated in the pathogenesis of human cancer. So we employed immunohistochemistry techniques to compare the subcellular localisation of NUB1 in patients' breast cancer tissue.

Tissue microarray (TMA) is a technique that allows for the immunophenotypical characterisation of hundreds of samples simultaneously (Kononen *et al.*, 1998). More than 1000 different tissue samples can be combined on a single microscope slide to be simultaneously characterised by *in situ* analysis. However, this depends on the needle diameter of the microarray device (Takikita *et al.*, 2007). Virtually all research involving *in situ* tissue studies can be carried out on a TMA format.

In TMA, the specimens with clinical data make the technique a very powerful validation tool to complement the results obtained from the genomic data. The technology reduces the laborious, time-consuming, and expensive conventional immunophenotypical characterisations on single slides. It also diminishes the technical experimental variability in biomarker identification, allowing the analysis of a large number of samples at the same time. TMAs have been constructed from paraffin-embedded tissue cell line or cell blocks representative of the conventional tumour specimens. The breast cancer TMAs has high concordance for common biomarkers as well as reproducible prognostic associations (Kononen *et al.*, 1998). Expression of the TMAs could correspond to the whole section. The protein expression can be analysed retrospectively with the benefit of long-term follow up information.

Besides, the effect of subcellular localisation of NUB1 protein in benign and malignant human cancer has been poorly studied. NUB1 and its splicing variant, NUB1L are found in multiple tissues. Their distributions in cancer cells have been mapped by qPCR techniques, and western blots. However, the expression level of NUB1 has not yet been compared in its relation to cancer progression.

To further elucidate the role of NUB1 in breast cancers, NUB1 expression patterns were correlated with survival outcome and clinico-pathological parameters in a large cohort of primary breast tissues. This study performed immunohistochemistry (IHC) on approximately 125 human primary breast tissues to determine the subcellular localisation of NUB1 in breast cancer and to provide information for future studies on cancer biology.

Classification of breast cancer

There are two main molecular classifications of breast cancer which are of prognostic value. The oldest classify the tumour into Oestrogen Receptor (ER) positive or negative groups. The most update further subdivides these two groups into a total of five subtypes. The ER positive, one within the two groups classification, and the Luminal A within the active group have the best outcome. The joint triple negative (Basal-like and Normal breast like) has the worst outcome within the five groups classification.

Subtypes	Features
Luminal A	ER and PgR positive but Her2 negative; Low proliferation index
Lumina B	ER positive, Her-2 positive, PgR positive or negative; ER positive, Her-2 negative, PgR negative; High proliferation index
Her-2 non luminal	Her-2 positive but ER and PgR (Progesteron Receptor) negative
Basal-like (triple negative)	ER, PgR and Her2 negative; Positive for CK5 and EGFR
Normal breast-like (triple negative)	ER, PgR and Her2 negative; Negative for CK5 and EGFR

Table 3. 9 Classification of breast cancer and the key features of the subtypes (Yersal and Barutca, 2014).

6.2 Validation of NUB1 antibody on cancer cells

Clinical implementation of NUB1 as a biomarker depends on the reliable and validated detection method for the NUB1 protein. As the NUB1 antibody (clone 4H2) was not reported in any previous publication, immunohistochemical validation was performed to examine its binding to the antigen in breast cancer tissue specimens. Two independent pathologist-based evaluations approved the representative staining patterns for antibody in the specimens.

A clear difference of NUB1 immunostaining was observed between the endogenous NUB1 of RCC4plusVHL cells (Fig 6.1) and their corresponding NUB1-knockdown cells. There was no staining in the negative control. To have a technical negative control that helps to avoid false positive, saline was used to replace primary antibody. In another sample, CD34 primary antibody was used as a positive control to make sure the staining protocol was performed correctly.

To ensure the NUB1 protein retains the antigenicity in archival tissues, we stained on aged tonsils. The tonsil was also used as a multi-tissue control block that showed a subset of cells were stained with NUB1 antibody. Although the number of sample in this validation remained small, no systematic loss of antigenicity was observed.

The validation of the antibody for use in western blotting was achieved in a similar way. Targeting the NUB1 by siRNA resulted in the loss of an immunoreactive band at approximately 79 kDa. No other bands were seen on the western blot. Therefore, the 4H2 clone NUB1 antibody is specific towards NUB1 proteins.

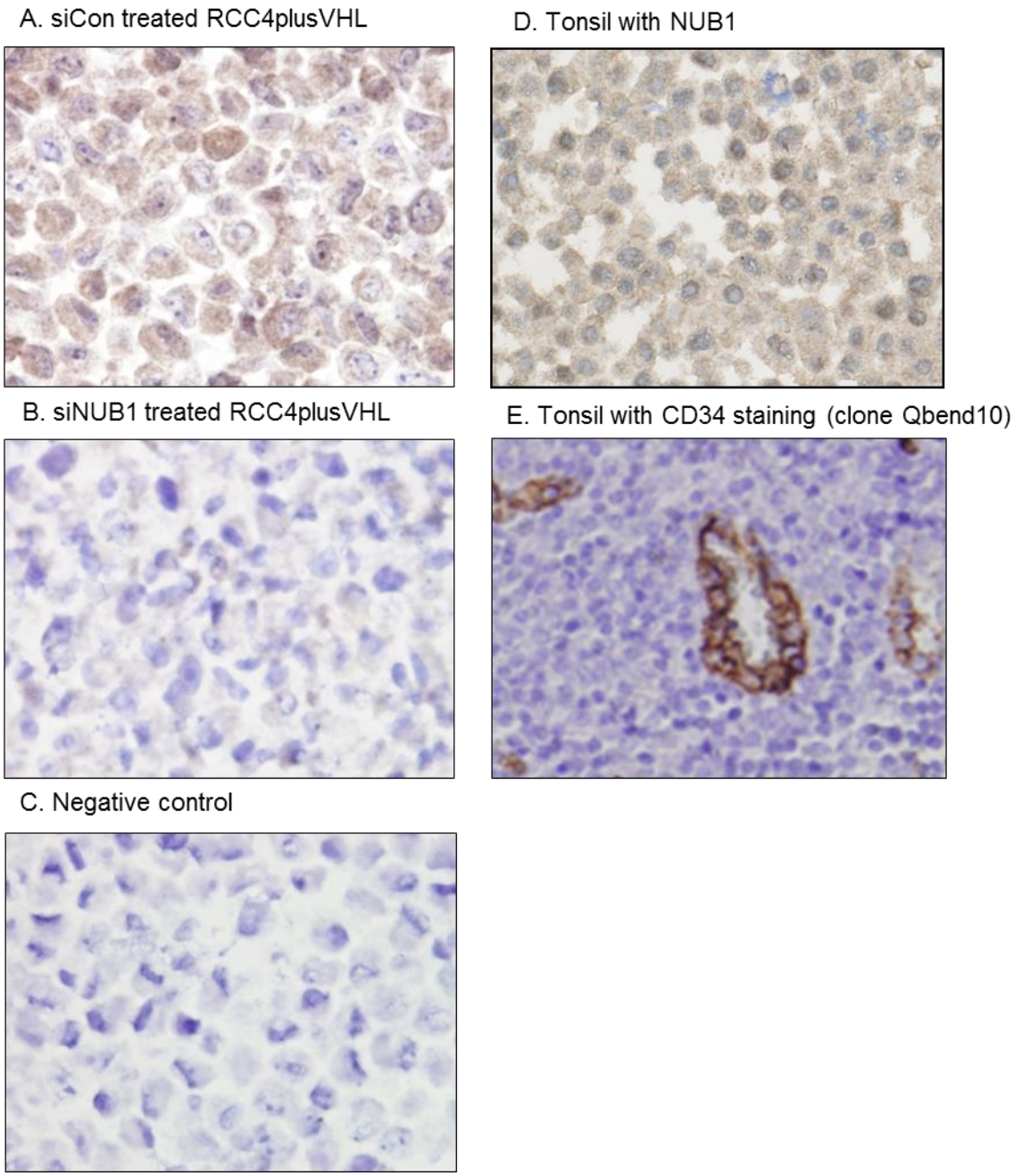


Figure 6. 1 Immunostaining of NUB1 using monoclonal mouse antibody (4H2) (1:20) dilution on RCC4plusVHL cells counterstain with hematoxylin. NUB1 was visualised with DAB (Brown), 40X magnification. A. Endogenous NUB1 treated with siCON. B. RCC4plusVHL treated with siNUB1. C. PBS in replacement of primary antibody was used as technical negative control. D. Tonsil E. Tonsil with CD34 staining serves a positive control. All images were at the magnificantion of 20X.

6.3 NUB1 immunohistochemical staining of primary breast tumour tissue

To have the high-throughput analysis of breast cancer tissue specimens stained for biological markers, we performed TMA on NUB1 staining. Of the 152 primary breast cancer tumours on the tissue microarray, 125 tumour cores (80%) were interpretable for NUB1 staining, all of which had associated survival information. Uninterpretable spots were caused by either loss of tissue on the tissue microarray or no tumour cells in the spot. The immunohistochemical staining of the breast cancer tissue microarray with NUB1 showed cytoplasmic (Fig. 6.2) and/or nuclear localisation. In comparison to ER- (Fig. 6.3), similar distribution pattern but with more 3+ score of NUB1 in ER+ subgroup patients. There were highest frequency of 1+ cytoplasmic staining in ER negative patients whereas highest frequency of 2+ cytoplasmic staining in ER positive subgroup. There were 100 tumours (80%) that were positive for NUB1 cytoplasmic staining and 66 tumours (23.1%) positive for NUB1 nuclear staining. A subset of 99 tumours was positive for both NUB1 cytoplasmic staining and NUB1 nuclear staining (80%).

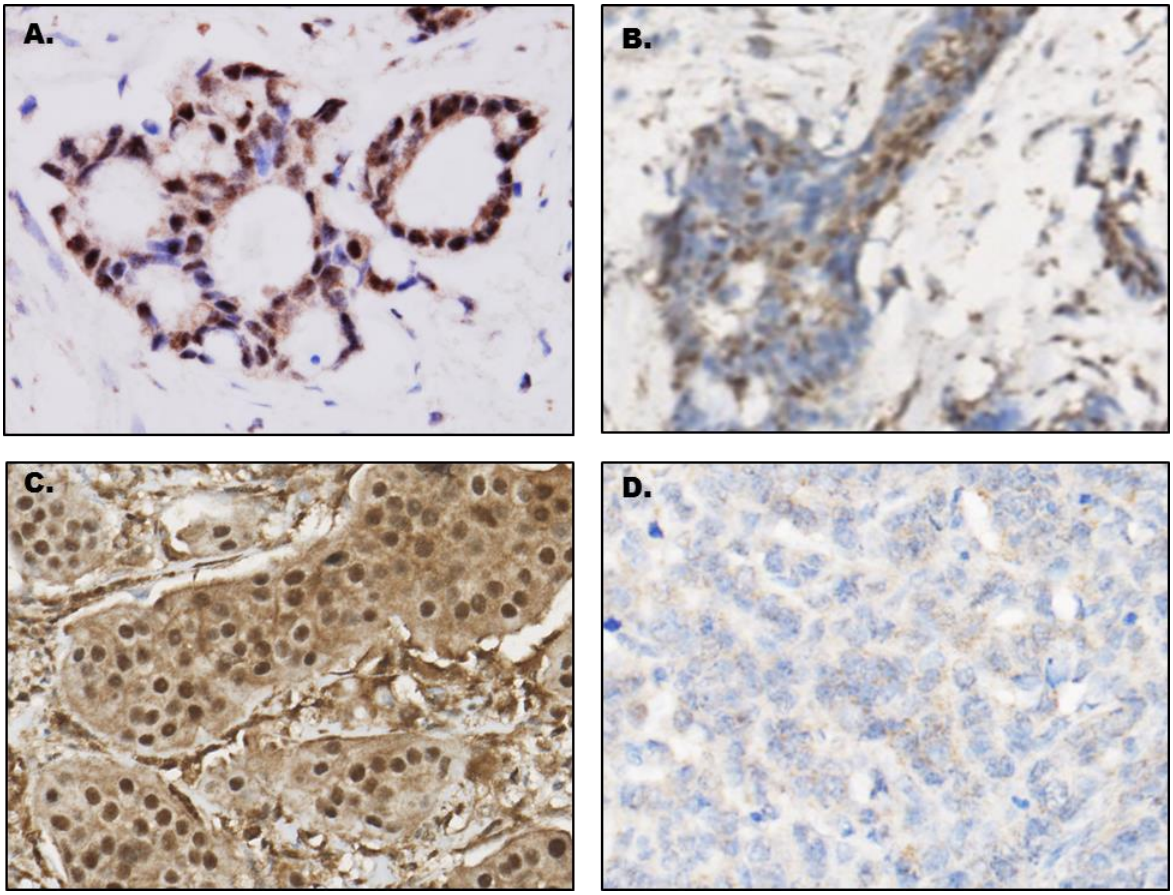


Figure 6. 2 NUB1 expression on representative node negative breast cancer tissue microarray spots. A, normal mammary tissue with glandular cells. B. Heterogenous NUB1 with some mixed cytoplasmic and nuclear staining; C. homogenous strong nuclear NUB1 staining with less cytoplasmic staining; C, Negative NUB1 staining. Figures are at ×100 magnification.

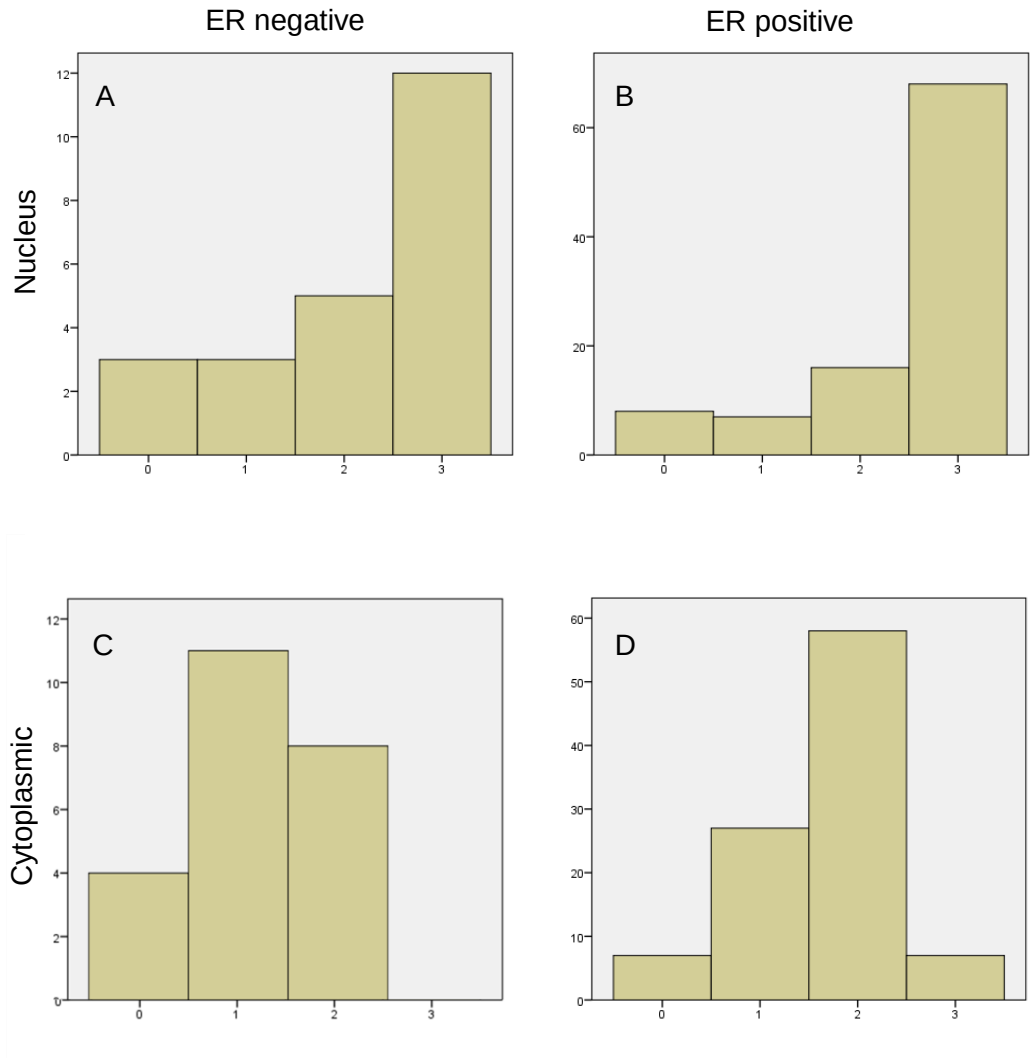


Figure 6. 3 Distribution of NUB1 immunohistochemical staining scores in primary breast cancer. A, NUB1 nuclear staining scores in ER- subgroup; B, NUB1 nuclear staining scores in ER+ subgroup C, NUB1 cytoplasmic staining scores in ER- subgroup; D, NUB1 cytoplasmic staining scores in ER+ subgroup.

6.4 Oestrogen receptor (ER) expression and association with clinicopathological factors

We obtained clinical data and breast cancer characterisation of ER and HER2 staining are from the collaborator, Professor Adrian Harris. ER immunoreactivity was evaluable in 122 (96.1%) cases, and scored positively in 99 (78%) cases (Fig. 6.1) using intensity scores of 2+ and 3+ as indication of ER protein overexpression. Tumours with ER intensity scores of 0 or 1+ were assessed as negative. ER expression was analysed in relation to clinicopathologic criteria (Table 6.1), with a significant association of ER negativity with positive node status (p = 0.009), ER-negative with highest histological grade tumours (p = 0.0001) and ER negative with larger tumour size (p=0.008).

	ER-negative	ER-positive	*p*-value	Overall
Total	23	99		122
c-erbB2 receptor status				
Negative	6	50	0.092	56
Postive	7	17		24
Node status				
Negative	9	16	0.009*	23
Positive	58	38		96
Histologic grade				
Grade I	0	18	0.0001****	18
Grade II	2	50		52
Grade III	15	17		32
Age				
< 50 years	7	19	0.236	28
≥ 50 years	16	80		39
Median (range)	53 (26–90)	59 (34–83)		58 (26–90)
Tumour size				
≤ 2 cm	4	47	0.008**	51
> 2 cm	19	52		71
Median (range)	3.7 (0–8.0)	2.36 (0–7.3)		2.5 (0–8.0)

Table 6. 1 Clinicopathological variables according to ER status. Grade I patients showed significantly more frequent to the rest of the grades in ER positive patients.Positive nodal status was found significantly in ER negative patients. Significantly more patients at > 50 years old were found in ER positive.

6.5 Association of ER status and menopausal status with subcellular localisation of NUB1

To correlate the subcellular distribution to the clinicopathological factors from the patients, we analyse the data statistically. NUB1 expression measured as an IPS was categorised in the nucleus and in the cytoplasm in breast cancer. There was a strong correlation of nuclear NUB1 IPS to the cytoplasmic NUB1 IPS (r=0.76 (0.67-0.83) (Fig. 6.4). Cytoplasmic NUB1 was significantly higher in ER-positive tumours with a mean IPS of 138 (95% CI, 121-155), compared with a mean IPS of 86 (53-120) in ER-negative breast cancers (*P* = 0.017*) (Fig. 6.5). Nuclear NUB1 staining in both ER status groups did not show a significant difference.

These results highlighted that ER-positive tumours showed an increase in both cytoplasmic and nuclear NUB1. The amount of cytoplasmic NUB1 levels is significantly higher in ER-positive compared to ER-negative. This suggests that the link between cytoplasmic NUB1 and ER- positivity.

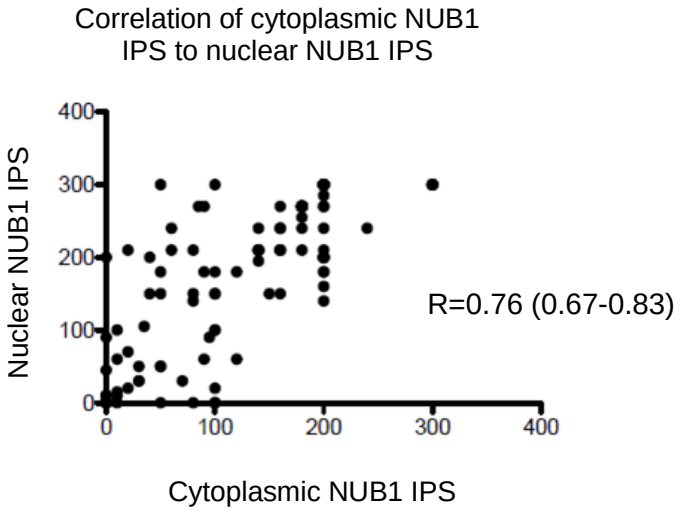


Figure 6. 4 Correlation of NUB1 cytoplasmic IPS with nuclear IPS, r=0.76 (0.67-0.83)

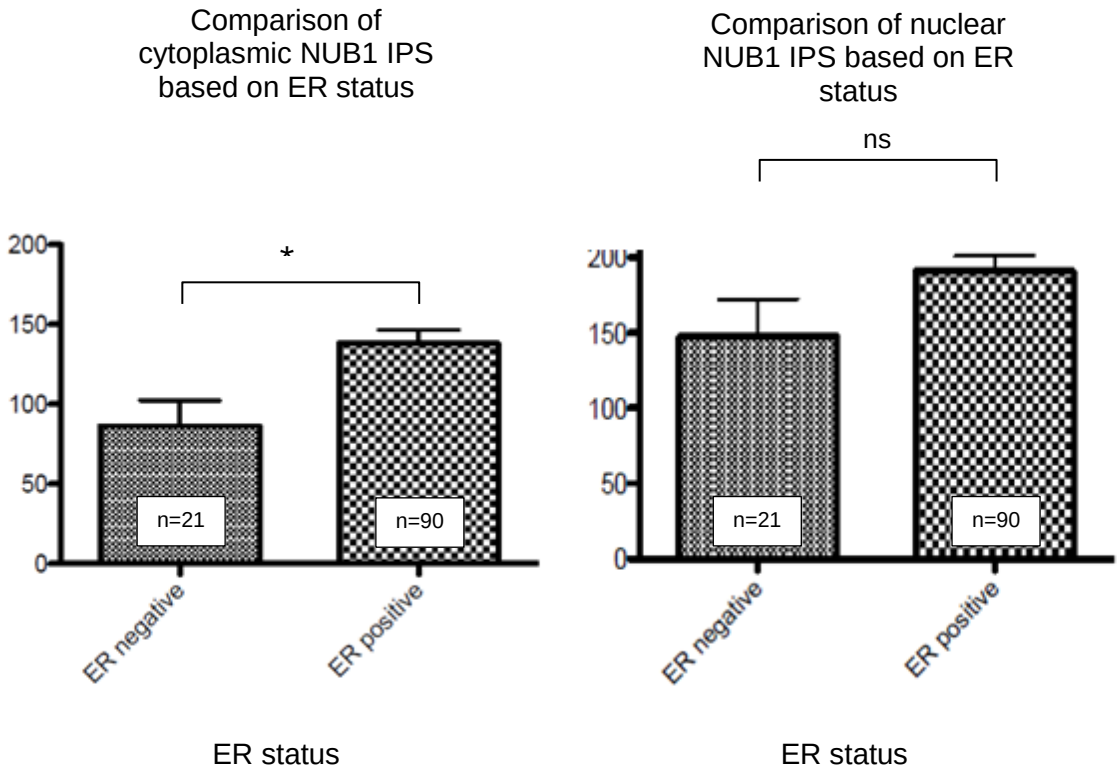


Figure 6. 5 Relationship between ER status and NUB1 localisation. Bar charts according to ER status and the subcellular localisation of NUB1 measured as an IPS. (a)Distribution of cytoplasmic NUB1 IPS and medians according to ER-negative and ER-positive breast cancers, with patient numbers shown. (b) Nuclear NUB1 IPS and medians according to ER status, and numbers of patients. *P* values indicate significance.

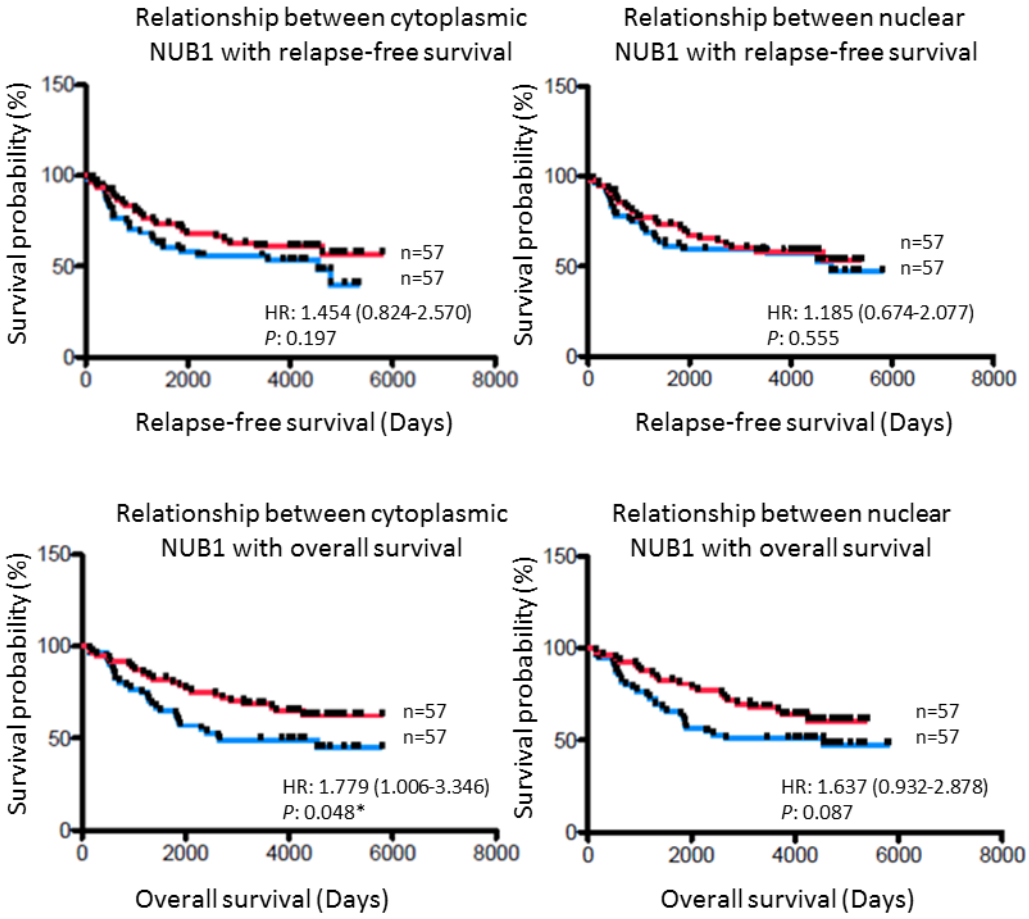
6.6 Survival analyses

The expression of NUB1 evaluated by immunohistochemical staining was correlated with overall survival of the patients with 16-year follow-up times. To determine whether NUB1 expression level is correlated with outcome, Kaplan-Meier survival curves were generated based on the subcellular localisation.

There was no significant difference in overall survival for nuclear NUB1 staining or for ER-negative subgroup (Table 6.3). However, significant survival differences were seen with NUB1 cytoplasmic staining.110 of 128 tumours positive for NUB1 nuclear staining were also positive for NUB1 cytoplasmic staining (88%). It was found that lower NUB1 cytoplasmic staining was significantly correlated with the poorer outcome with 16 years overall survival (p=0.0478; HR=1.779, 95% CI (1.006-3.146) but not with relapse free survival (p=0.1965; HR=1.454, 95% CI, 0.8238-2.568). No significant correlation between nuclear NUB1 staining was seen at 16 years of RFS (p = 0.5545, HR 1.185; 95% CI=0.6755-2.077)) and OS (p= 0.0866, HR=1.637, 95%CI= 0.9315-2.878) respectively.

In the ER status multivariant analysis, lower NUB1 and ER-negative patients showed significantly poorer survival HR=1.854 (0.954-2.124); p: 0.0041 (Fig 6.6). Our result indicated that depleted of both NUB1 and ER would cause significantly poorer survival in the breast cancer patients.

Table 6. 2 Relationship between high/low NUB1 subcellular localisation and overallsurvival/relapse free survival.



	Number of Patients	*Cytoplasmic*			*Nucleus*		
		Hazard ratio	95% confidence interval	*p*	Hazard ratio	95% confidence interval	*p*
Relapse-free survival	114	1.454	0.824-2.570	0.197	1.185	0.674-2.077	0.555
Overall survival	114	1.779	1.006-3.146	0.048*	1.637	0.932-2.878	0.087

Hazard ratios, confidence intervals and P values are given for the results of the univariate analyses. For univariate analyses, the hazard ratio is given for nuclear and cytoplasmic NUB1 in intensity percentage score (IPS), along with the 95% confidence interval. Patients with ductal, lobular or 'mixed' cancer were included where the marker data was available. *Relationship reached significance (P < 0.05). p<0.0001****

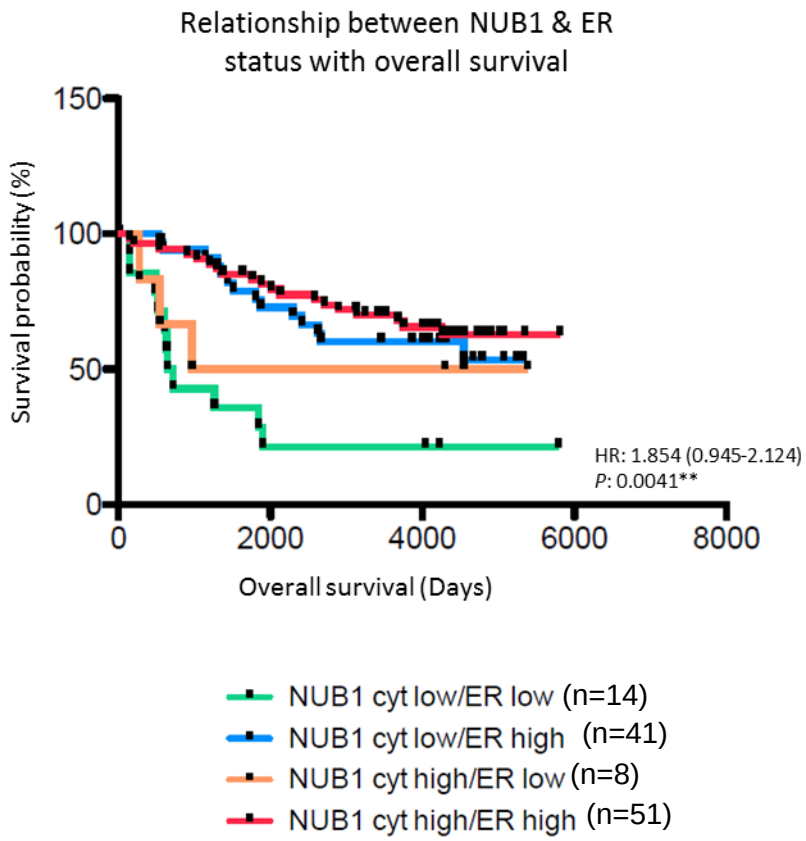


Figure 6. 6 Relationship between ER and prognosis in breast cancer patients using the log-rank test. Overall survival curves according to ER and NUB1 status, classified as negative or positive (b) Relapse-free survival curves according to HER-2 expression. Significant P values are indicated in bold.

6.7 Clinicopathological correlation and analysis

To describe an objective summary and correlation of clinical findings with gross and microscopic findings and with the results of studies performed on the breast cancer tissues, we looked at the clinic pathological characteristics in its relation to IPS (Table 6.3). Significantly lower cytoplasmic IPS was found in the ER-negative subgroup patients as well as pre-menopausal patients. Nuclear NUB1 score was found to be significantly lower in HER2+ and pre-menopausal samples.

Table 6. 3 Summary of overall survival analysis based on the mean IPS.

Variable	Events	Cytoplasmic			nuclear		
		Mean IPS	95% confidence interval	*P*	Mean IPS	95% confidence interval	*P*
Age, yr	116		-0.011, -0.26	0.079[a]		-0.12, 0.25	0.065[a]
Size, cm							
≤2	72	124	105-143		190	157-222	
>2	41	139	114-164	0.371	177	152-201	0.534
Lymph nodes							
Uninvolved	59	137	117-157		190	164-216	
Involved	54	115	92-138	0.172	164	134-194	0.195
Grade							
1	15	143	104-183		206	146-265	
2	51	133	111-155	Ns	180	152-208	ns
3	33	103	74-133	Ns	113	113-189	ns
Histology							
Ductal	94	122	104-183		172	150-194	
Lobular	14	133	111-155	Ns	222	179-265	ns
Other	8	103	74-133	Ns	186	98-274	ns
ER							
Negative	**21**	**86**	**53-120**		147	95-200	
Positive	**90**	**138**	**121-155**	**0.017***	191	170-211	0.166
HER2							
Negative	**52**	132	109-156		**189**	**160-219**	
Positive	**21**	104	64-144	0.300	**138**	**90-187**	**0.043***
Menopausal status							
Pre	**25**	**95**	**58-132**		**138**	**160-183**	
Post	**91**	**135**	**119-151**	**0.022***	**190**	**169-211**	**0.043***
EGFR							
negative	42	130	105-155		183	150-215	
positive	44	145	125-166	0.437	216	192-240	0.143

*Significant p-value, [a] Pearson correlation analysis

6.6 Discussion and Chapter Summary

Tissue microarray provides translational value of the AIPL1 and NUB1 in the breast cancer patients. We first validated a commercialised NUB1 antibody (clone 4H2) in immunoblots and immunohistochemistry.

Normal breast tissue was found positive with NUB1 antibody in the nucleus (Fig. 6.2). The signal was weaker in the cytoplasm. Cancer cells showed varying degree of staining in either nucleus and/or cytoplasm (Fig. 6.2). ER-negative breast cancer cells confer to the presence of nodes and bigger tumour size (Table 6.1). Nuclear NUB1 IPS has strong correlation to cytoplasmic NUB1 IPS (Fig. 6.4). In the survival analyses, the result revealed that depleted of both NUB1 and ER proteins have significantly lower survival rate. This was in full agreement with the mRNA data.

The localisation of AIPL1 and NUB1 could be and indicator of the role exerted onto cancer cells. p21 and p27 protein functions are dependent on their subcellular localisation. We were planning to utilise multiplexed ion beam imaging (MIBI) techniques to compare a panel of in situ proteins expression of high and low cytoplasmic NUB1 protein among ER-negative subgroup primary tumour. The optimised method was showed in Appendix 2.

Chapter 7

Discussion

7.1 Role of of AIPL1 and NUB1 in cancer

In Oncomine®, down-regulated AIPL1 mRNA levels have been demonstrated to associate with cancer growth in several types of cancers. This observation of down-regulated AIPL1 confirmed the meta-analysis on 30 microarrays done by Ramasamy in 2009. Meta-analysis of combined transcriptomic microarray datasets is a powerful method to greatly increase the sensitivity in revealing biomarkers for disease and, potentially, with better specificity with bigger series. In order to identify new biomarkers for (breast) cancer based on survival, we performed meta-analysis which led us to AIPL1 as our candidate of choice.

AIPL1 is required for complex protein folding but the role of AIPL1 has not been studied in any cancer. From the bioinformatics analysis of cancer databases, the AIPL1 fold change was not strongly decreased, marked by less than 0.5 $\log_2$FC difference in between cancer and normal tissue. The opposite role of AIPL1 (down-regulated in cancer) and NUB1 (upregulated) is suggested in causing normal cells to turn into cancer. In a retinal model, AIPL1 protein negatively regulates NUB1 protein trafficking across the nuclear membrane (van der Spuy *et al.*, 2002). Meanwhile, NUB1 showed stronger up-regulation potentials as the $\log_2$FC was frequently more than 0.5 in cancer tissues compared to the normal tissue.

7.2 Pathways involved in AIPL1 and NUB1

Data mining supports the importance of AIPL1 and NUB1 in cancer and give some clues about the possible pathway involved. The Oncomine® evidences support the findings that AIPL1 functions as a tumour suppressor gene in cancer. However, in the present study, NUB1 disagrees with previous work that suggests NUB1 was acting as a tumour suppressor (Hosono *et al.*, 2010). Hosono *et al.* demonstrated that expression levels of cyclin E, p27 and p21 were increased in A498 cells with overexpression of NUB1 as compared to cells expressing an empty vector control (Hosono *et al.*, 2010). However, this thesis presents on *in vitro* study in which we observed the up-regulation of p27 and p21 with NUB1 knockdown in MDA-MB-231, RCC4 and 786-O cells. We believe overexpression of NUB1 does not reflect its physiological state, since NUB1 was aggregated into cytoplasmic inclusion bodies and localised poorly to the nucleus (Tanji *et al.*, 2006).

We analysed NUB1 mRNA coexpression of four dataset from breast cancer samples and identified 28 genes of interests. CUL1 was frequently observed in the search, highlighting the robustness of the observed pattern. This bioinformatics approach provides the *in vivo* system-level understanding of the behaviours of AIPL1 and NUB1 in cancer. Furthermore, both NUB1 and CUL1 were enriched in common biological processes including TCR signaling, signaling by interferon, interleukin *etc.* This is in agreement with the fact that NUB1 is known to be involved in the immunity pathway and is inducible by interferon β (Hosono *et al.*, 2010).

The prognostic role of the mRNA levels further supported the hypothesis that both of the gene products are relevant to cancer. METABRIC data on survival curves showed lower NUB1 mRNA levels corresponded to poorer overall survival in ER-negative and triple negative subgroup patients. The subgroups are considered an aggressive disease and are often associated with poor survival. Our results have shed new light on the intrinsic

heterogeneity within this ER-negative and triple negative subtype and strengthen the importance of genomic studies within tumour subpopulations. The selection of gene expression subtypes for a single cancer is challenging in the clinics (Chen *et al.*, 2012). In clinical practice, the staining of a tumour biopsy for NUB1 may be useful for cancer prognosis assessment and/or for disease progression monitoring.

NUB1 is known to act as the degrading enzyme of NEDD8 and FAT10 and their conjugates. In comparison to NEDD8, FAT10 showed more cancer promoting capabilities in cancers especially in lymphoma, lung cancer, liver and brain cancer via the Oncomine® database. NUB1 recruits both NEDD8 and FAT10 and their conjugates for further proteasomal degradation. In comparison to the ER+/HER2+ patients subgroup, NEDD8 was found to be significantly lower in the ER-/HER2+ subgroup. In the METABRIC dataset, low FAT10 expression significantly stratifies patients in ER-, triple negative and basal subgroups (Fig 3.8). Moreover, FAT10 mRNA is upregulated in all subgroups, suggesting it could be a good anti-cancer target.

In vitro, we reported the presence of folded and unfolded AIPL1 monomer as well as the dimer forms (Fig 4.1). Most of the tested unstressed cancer cell line showed unfolded monomer while the positive control, Y79, exhibited both folded protein and unfolded forms of AIPL1 (Fig 4.1). This intriguing observation leads to the question of whether the folded could be a more active form of AIPL1. For instance, the chaperones protein, calreticulin interacts better in its folded form than its native form with certain peptides (Kim *et al.*, 2013). In a similar fashion, the folded AIPL1 protein would result in a higher affinity for its client proteins and peptides. In neutral pH, Histone-like nucleoid structuring-dependent expression A (HdeA) is a folded, but chaperones-inactive dimer in the native state (Hori *et al.*, 1999). HdeA adopts different conformations when bound to different substrates (Salon *et al.*, 2007).

7.3 Hypoxia and reoxygenation stress

AIPL1 and NUB1 responded to hypoxia and reoxygenation. In reoxygenated conditions, the AIPL1 proteins existed in dimer, trimer and multimer forms (Fig 4.4). The oligomers break down into dimer and monomers as the lysates were treated with reducing agent, DTT. This phenomenon suggests there is more than one type of cysteine-cysteine disulphide bond in between AIPL1 molecules. However, it is too premature at this early stage to infer the different forms of AIPL1 (folded and unfolded). These examples mark the dynamicity of AIPL1 protein to translocate NUB1 into the nucleus, giving us a true physiological picture.

Varying expression levels of NUB1 were observed among the unstressed cancer cell line panels, with the lowest expression observed in U2OS and SKBR3 cells. This observation is in concordance with Hosono *et al., 2002.* Examining the global neddylation in cells indicated varying degrees of neddylated CULs and some NEDD8 monomers in cell lines such as HCT116, U2OS, HCC1806 and MDA-MB-231. Meanwhile, when examining global Fat10-ylation, most of the FAT10-conjugated proteins remain unknown and FAT10 monomer was not found in unstressed cells. Very low levels of AIPL1 mRNA transcripts were observed in the cells, which did not match the abundance of its protein, suggesting the proteins are stable with a long half-life. It is also speculated that AIPL1 mRNA could be induced under stress condition including hypoxia and reoxygenation.

In the reoxygenation of MDA-MB-231 cells, NUB1 and neddylated CUL proteins were upregulated in a timely manner. NUB1 levels were responsive to hypoxia and reoxygenation as hypothesised, since NUB1 mRNA coexpressed with FAS and ATM, two proteins from signaling pathway which are frequently upregulated upon reoxygenation (Olcina *et al.*, 2010).

Through pathway analysis, both NUB1 and CUL1 are enriched in the cell cycle regulation pathway. In 2012, Hosono *et al.* demonstrated that overexpressed NUB1 causes up-regulation of p21 and p27 in renal cell carcinoma (RCC4) cells. In contrast, we observed that reducing NUB1 levels by transient expression of siRNA causes G_0/G_1 cell cycle arrest in MDA-MB-231 (Fig. 4.6) cells, confirmed with three independent biological replicates. We did not perform overexpression experiment for NUB1, since it forms aggregates in cells which are functionally redundant (van der Spuy and Cheetham, 2004). HSP70 and ubiquitin were recruited to these inclusions, suggesting that they may be targeted for proteasomal degradation (van der Spuy and Cheetham, 2004), and AIPL1 was able to suppress the formation of the inclusion bodies(van der Spuy and Cheetham, 2004).

Although there were no significant changes under normoxic conditions, both MDA-MB-231 (ER-) and T-47D (ER+) cells significantly grew slower after NUB1 knockdown in hypoxia. We speculated the altered subcellular distribution of NUB1 protein in hypoxia to the nucleus could determine the cell fate decision making of cancer cells (van der Spuy and Cheetham, 2004). In our study, NUB1 is essential to regulate the cell cycle during limited oxygen supply; its depletion abrogates the G_1 to S phase transition and dampens the growth rate of cancer cells (Fig 4.7).

In the subcellular fractionation experiment (Fig 4.8), AIPL1 migrated into the cytoplasm and formed multimers upon hypoxia and reoxygenation. We observed an interesting interplay. The unfolded AIPL1 monomer was retained in the nucleus whereas the folded AIPL1 protein was observed in the cytoplasm. Folded AIPL1 might suggest its active chaperoning of NUB1 then cause the NUB1 translocation into the nucleus. Opposite to that of AIPL1, NUB1 protein migrated into the nucleus upon hypoxia and reoxygenation in a timely manner. These opposite phenomena mark the oxygen sensing capability of NUB1 and AIPL1 affecting the shuttling of the proteins across the nuclear membrane.

To date, there is no information on how NUB1 regulates neddylated CULs. CULs are the only established neddylation substrates describe this far because overexpression of NEDD8 results in unphysiological false positives that require re-evaluation (Enchev *et al.*, 2015). Neddylated CUL1 was known to be more strongly engaged in the ubiquitin E3 ligase, which causes the degradation of p21 and p27 (Wu *et al.*, 2000). NUB1 depletion reduced the neddylated CUL1 (Fig 7.2). This was thought to be caused by NUB1 knockdown down-regulating the NEDD8 levels (Hosono *et al.*, 2010). NUB1 silencing upregulated the p27 and p21 protein levels in cells. This is in concordance with treatment of cells with the small molecule MLN4724, a neddylation inhibitor, which upregulated p21 and p27 further. This observation is in concordance with a previous study that the demonstrated upregulated p21 and p27 levels in the cells with reduced neddylated CUL1 levels (Wu *et al.*, 2015).

Free CUL1 proteins could act as a reservoir, that when neddylated can engage with the ubiquitin E3 ligase enhancing the degradation of p27 and p21. In the presence of NUB1, we observed the accumulation of the p21 and p27 proteins upon treatment of cells with an increasing concentration of neddylation inhibitor. This correlated with the delay in G1 cell cycle arrest. NUB1 silencing abolished the titrating effect of neddylation inhibitor and caused the accumulation of p27. We observed CUL1 level was down-regulated with titrated MLN4924, without siNUB1. We observed the accumulation of p27 when the cells were treated with neddylation inhibitor and NUB1 knockdown. Based on these, we speculated that NUB1 might cause the degradation of neddylated CUL1.

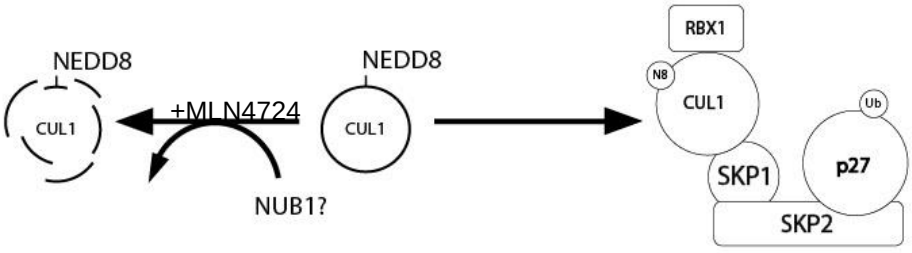


Figure 7. 1 Central dogma of NUB1-mediated cell cycle regulation via p27 and p21. Neddylated CUL1 locks the SCF complex with phosphrylated p27 and cyclin E as suggested by Bornstein et al., 2006 and Tanaka et al., 2012. NUB1 recruits neddylated CUL1 for proteasomal degradation.

7.4 Relationship with VHL

In RCC4plusVHL cells, NUB1 knockdown caused the down-regulation of VHL. Similar findings were also observed when we tried different siRNA sequences (Data not shown). This ruled out any off target effects. We observed more p21 (in normoxia) and more apoptotic cell death (in hypoxia) under NUB1 siRNA treatment as compared to the control condition. NUB1 is essential to foster cell cycle progression in hypoxia, and it also protects cells from cell cycle arrest/ entering senescence. Meanwhile in VHL-null RCC4 cells, NUB1 knockdown caused cell death in normoxic and hypoxic condition, suggesting a necrotic cell death was occurring as there is no cleaved-PARP and no G_o/G_1 cell cycle arrest markers observed. VHL is therefore important for orchestrating the cell fate decision (apoptotic or necrotic) upon NUB1 depletion. In the depleted NUB1 condition, the presence of VHL drives the cells towards apoptosis, while the absence of VHL drives the cells towards non-apoptotic cell death (significant percentage portion of cell death). The number of dead cells were significantly increased in hypoxic cells, suggesting a contribution of NUB1 migrating to the nucleus in hypoxia. We also observed that null-VHL RCC4 cells further upregulated HIF1α, especially in both normoxia and hypoxia in a VHL-independent manner.

NUB1 was examined in the Schoenfeld's idea (Fig 5.2) on how VHL upregulates p21 and p27 using RCC4 and RCC4plusVHL cells. According to Schoenfeld, VHL, a member protein of CUL2-based ubiquitin E3 ligase, is hypothesised to competitively occupy RBX1 and indirectly deactivates CUL1-based ubiquitin E3 ligase. As a result, the p21 and p27 proteins were stabilised within the cells. Therefore, HIF1α levels were examined to assess as the activity of CUL2-based ubiquitin E3 ligase.

In RCC4plusVHL cells, there was low HIF1α levels but upregulated p27, as detected by immunoblot signifying CUL2-based ubiquitin E3 ligase was more active than the CUL1-based one. NUB1 knockdown further stabilised p27 levels. In VHL-null RCC4 cells, increased p21 and p27 levels were observed, hinting that RBX1 is not bound to CUL1 based ubiquitin E3 ligase upon stress. HIF1α levels were stabilised further with NUB1 silencing.

When examining CUL2 protein levels we observed a possible polyubiquitination with multiple higher molecular weight forms. Although there is no report of polyubiquitinated CUL2, CUL1 polyubiquitination was reported *in vivo* and alters the ability of CUL1 to bind to S5a without affecting the stability of CUL1 (Bloom *et al.*, 2006). CUL1 ubiquitination promotes binding to the proteasome, but not degradation (Bloom *et al.*, 2006). In normoxia, NUB1 knockdown increase the polyubiquitination of CUL2 (Bloom *et al.*, 2006), though the functional consequences of this polyubiquitination remain unexplored.

In an attempt to unravel how HIF1α is stabilised in a VHL-independent manner, we examine whether HIF1α is a neddylation and FAT10ylation substrate. HIF-1α was identified to be covalently modified by NEDD8 and FAT10 (Fig. 5.7). Endogenous neddylated HIF1α is a reliable detection compared to transient NEDD8 overexpression. Neddylated HIF1α was reported previously (Ryu *et al.*, 2011). In this study, NEDD8 stabilised HIF-1α even in normoxia and further increased its level in hypoxia. Neddylated HIF1α was observed in VHL-null cell line (Ryu *et al.*, 2011).

The mechanism of how HIF1α degraded by VHL and CUL2 is long standing. The oxygen-dependent degradation of HIF-1α is initiated by the hydroxylation of proline 402 and 564. VHL targets the hydroxylated HIF1α and recruits ElonginB/C, CUL2, and RBX1, which forms the CUL2-based ubiquitin E3 ligase complex to ubiquitinate HIF-1α (Ivan *et al.*, 2001). VHL and CUL2 have been identified to be covalently conjugated by NEDD8. Neddylated VHL preferentially interacts with fibronectin (Russell and Ohh, 2008) and negatively regulate the ubiquitination of HIF1α. On the contrary, CUL2 is neddylated after its recruitment by VHL, and the neddylated CUL2 facilitates the polyubiquitination of HIF1α (Liakopoulos *et al.*, 1999; Sufan and Ohh, 2006; Miyauchi *et al.*, 2008). The net effect of neddylation on HIF-1α stability is obscure. Nonetheless, Ohh et al. suggested that the neddylation process is required for the ubiquitination and subsequent degradation of HIF1α (Ohh *et al.*, 2002). The effects of NEDD8 on HIF1α are linked with VHL-mediated HIF-1α ubiquitination. HIF1α expression and activity were both still regulated by NEDD8 in VHL-defective cells. Therefore, the direct neddylation of HIF1α may overcome the HIF1α-destructive effect of neddylated CUL2. The reciprocal regulations of HIF1α by neddylation remain to be investigated.

To our knowledge, this is the first study investigating the impact of NUB1 in breast cancer patients. NUB1 antibody (Clone 4H2) is an internally validated commercial antibody for both immunoblot and immunohistochemistry. We found a prognostic value of both nuclear and cytoplasmic NUB1 expression in breast cancer. A high expression of cytoplasmic NUB1 tended to be correlated to a better overall survival (Table 6.2). Low expression of NUB1 had a poorer overall survival (but not relapse-free survival) caused by metastasis-induced death. NUB1 mRNA transcript was found to be elevated in several cancers via bioinformatics analysis. Although high NUB1 expression was associated in cancer formation, the distant metastatic clone should be of a very different clone than which a cancer forms. It can be explained by tumour evolution (Fig. 7.1).

The nuclear import of NUB1 is dependent on the AIPL1 protein trafficking machinery (van der Spuy *et al.*, 2002). This report managed to associate NUB1 with initial tumourigenesis and cancer progression. We also explored the role of NUB1 entry to the cancer cell nucleus and reduced the tumour suppressor p21 and p27 levels.

7.5 Translational perspectives

High NUB1 protein expression can be a good prognostic marker to poor overall survival which further stratifies the patient survival in ER-negative patient's subgroup upon tumour initiation and progression. Reduced NUB1 levels may result in reduced nuclear availability to overcome different assaults including hypoxia, DNA damage repair and driver mutations which may potentially cause a failure of the DNA damage signaling cascade and consequently less activation of the downstream apoptotic cell death pathway. Due to the lack of cell death pathway activation, the tumor may continue to proliferate, resulting in distant metastasis.

Alteration of NUB1-mediated tumor-suppressor functions of the p21 and p27 proteins by decreased NUB1-expression could explain this tumour progression. Low NUB1 levels have been demonstrated to upregulate p21 and p27 proteins with tumor-suppressive as well as cancer promoting properties. The roles of p21 and p27 are explained in chaper 6.1, and their functions are localisation dependent . Implementing NUB1 immunostaining for ER-negative subtyped patients could inform the clinical specialists about the prognosis of patients.

The evidences suggested that NUB1 is cancer causing because of its inhibitory effect on apoptosis. However, we found its expression associated with better outcome. For instance, the BCL2 noted as oncogene, acts in the similar way (Pezzella *et al.*, 1993). While some very aggressive tumour, e.g. Burkitt's lymphma, *etc*. which are characterised by BCL2 negativity, showed high levels of apoptosis with high proliferation. It is plausible that both NUB1 and BCL2 are oncogenic but are associated with less aggressive cancer pathways. This suggests that NUB1 positive and negative tumours are different in their biologies.

Targeting strategies for NUB1 have been of interest for treatment of Huntington's disease (Lu *et al.*, 2013). Unfortunately, NUB1 may not be a druggable target for it does not have a receptor or enzymatic function that can be targeted by small molecule inhibitor. Moreover, its major function is achieved *via* interaction with other proteins.

One potential approach to elevate NUB1 expression is through IFNβ (Tanji *et al.*, 2005), a US Food and Drug Administration-approved drug for treating multiple sclerosis (Meyer *et al.*, 2012). Combinational IFNβ treatment in the *in vivo* animal models is a good concept of potential NUB1 therapy.

A potential therapeutics strategy to enhance NUB1 functions could work on the adaptor function of NUB1 and synergise its interaction with neddylated CULs in the pathway. This could be achieved by low-molecular-weight-compound screening using bioluminescence resonance energy transfer technology (Boute *et al.*, 2002). This technology successfully applied to identify Tau–Fyn SH3 interaction inhibitors for Alzheimer's disease (Cochran *et al.*, 2014).

Chapter 8

Concluding Statement

The aim of this study was to evaluate the prognostic influence of NUB1 expression in breast cancer of different stages surveying relapse free survival and overall-survival.

The combination of low nuclear and low cytoplasmic expression was significantly associated with an adverse prognosis in breast cancer, ER-negative cohorts. Interestingly, in the overall survival and tumor specific-survival analysis both the low nuclear/low cytoplasmic NUB1 tended to have an adverse prognosis. This leads to the possible assumption that rather the alteration per se irrespective of the direction of alteration may be relevant in distant metastasis. It remains open if any aberration in NUB1 expression may contribute to resistance.

Data from my work show that they are, as NUB1, which is regulated by AIPL1, affects cell cycle and apoptosis regulation trough NEDD8 and Cullin 1, p21 and p27. Data support the hypothesis that by down regulating p21 and p72, NUB1 has an cancer promoting effect mostly by protecting form apoptosis. In breast cancer NUB1 is associated with a group of less aggressive tumours, in a fashion similar to Bcl2, the prototype of cancer promoting by inhibition of apoptosis.

These results demonstrate that the cytoplasmic and nuclear localisations of proteins might be underestimated. NUB1-expression may be a prognostic marker in breast cancer. In multivariate analysis of prognostic clinicopathologic parameters only NUB1 was an independent significant predictive variable concerning overall survival. Further studies will be needed to estimate whether NUB1 expression is useful as a supplement to conventional clinicopathologic risk factors.

Appendix 1

28 common elements in "Metabric Nat", "TCGA Prov", "TCGA Nat 2012" and "TCGA Cell 2015":

1.	ACAP1,
2.	APOBEC3G,
3.	APOBEC3H,
4.	ARHGAP30,
5.	ARHGAP9,
6.	BTN3A1,
7.	CD4
8.	CORO1A
9.	CUL1
10.	HLA-F
11.	IL10RA
12.	IRF1
13.	MAP4K1
14.	MKRN1
15.	NLRC5
16.	PARP12
17.	PARP14
18.	PRF1
19.	PTPN7
20.	RAC2
21.	SAMD3
22.	SASH3
23.	SEMA4D
24.	SLA2
25.	TAP1
26.	TMEM140
27.	TNFRSF1B
28.	UBASH3A

List of Awards, Presentations and Publications

1. Poster presentation at FASEB SRC on ubiquitin and cellular regulation with poster presentation (June 12-17 2016) in United States.
2. Poster presentation and travel award at 24th Congress of the European Association for cancer research (July 9-11 2016) in Manchester, UK
3. Oral presentation and bursary award for Summer School (24-28 October 2016) in Albufeira, Portugal
4. Paper entitled 'Inhibition of NEDD8- and FAT10-ligase activities through degrading enzyme NUB1- A potential anticancer approach' in Oncology Letter. IF=1.5.

References

Aguila, M., Bevilacqua, D., McCulley, C., Schwarz, N., Athanasiou, D., Kanuga, N., Novoselov, S. S., Lange, C. A., Ali, R. R., Bainbridge, J. W., Gias, C., Coffey, P. J., Garriga, P. & Cheetham, M. E. (2014). Hsp90 inhibition protects against inherited retinal degeneration. *Hum Mol Genet,* **23(8),** 2164-75.

Aichem, A., Kalveram, B., Spinnenhirn, V., Kluge, K., Catone, N., Johansen, T. & Groettrup, M. (2012). The proteomic analysis of endogenous FAT10 substrates identifies p62/SQSTM1 as a substrate of FAT10ylation. *J Cell Sci,* **125(Pt 19),** 4576-85.

Aichem, A., Pelzer, C., Lukasiak, S., Kalveram, B., Sheppard, P. W., Rani, N., Schmidtke, G. & Groettrup, M. (2010). USE1 is a bispecific conjugating enzyme for ubiquitin and FAT10, which FAT10ylates itself in cis. *Nat Commun,* **1,** 13.

Akey, D. T., Zhu, X., Dyer, M., Li, A., Sorensen, A., Blackshaw, S., Fukuda-Kamitani, T., Daiger, S. P., Craft, C. M., Kamitani, T. & Sohocki, M. M. (2002). The inherited blindness associated protein AIPL1 interacts with the cell cycle regulator protein NUB1. *Hum Mol Genet,* **11(22),** 2723-33.

Ali, M. M., Roe, S. M., Vaughan, C. K., Meyer, P., Panaretou, B., Piper, P. W., Prodromou, C. & Pearl, L. H. (2006). Crystal structure of an Hsp90-nucleotide-p23/Sba1 closed chaperone complex. *Nature,* **440(7087),** 1013-7.

Anfinsen, C. B. (1973). Principles that govern the folding of protein chains. *Science,* **181(4096),** 223-30.

Asada, M., Yamada, T., Ichijo, H., Delia, D., Miyazono, K., Fukumuro, K. & Mizutani, S. (1999). Apoptosis inhibitory activity of cytoplasmic p21(Cip1/WAF1) in monocytic differentiation. *EMBO J,* **18(5),** 1223-34.

Aveic, S., Pigazzi, M. & Basso, G. (2011). BAG1: the guardian of anti-apoptotic proteins in acute myeloid leukemia. *PLoS One,* **6(10),** e26097.

Bae, M. K., Jeong, J. W., Kim, S. H., Kim, S. Y., Kang, H. J., Kim, D. M., Bae, S. K., Yun, I., Trentin, G. A., Rozakis-Adcock, M. & Kim, K. W. (2005). Tid-1 interacts with the von Hippel-Lindau protein and modulates angiogenesis by destabilization of HIF-1alpha. *Cancer Res,* **65(7),** 2520-5.

Balch, W. E., Morimoto, R. I., Dillin, A. & Kelly, J. W. (2008). Adapting proteostasis for disease intervention. *Science,* **319(5865),** 916-9.

Barraclough, R. & Ellis, R. J. (1980). Protein synthesis in chloroplasts. IX. Assembly of newly-synthesized large subunits into ribulose bisphosphate carboxylase in isolated intact pea chloroplasts. *Biochim Biophys Acta,* **608(1),** 19-31.

Bawa-Khalfe, T. & Yeh, E. T. (2010). SUMO Losing Balance: SUMO Proteases Disrupt SUMO Homeostasis to Facilitate Cancer Development and Progression. *Genes Cancer,* **1(7),** 748-752.

Berg, P. & Pongratz, I. (2002). Two parallel pathways mediate cytoplasmic localization of the dioxin (aryl hydrocarbon) receptor. *J Biol Chem,* **277(35),** 32310-9.

Blagosklonny, M. V., Toretsky, J., Bohen, S. & Neckers, L. (1996). Mutant conformation of p53 translated in vitro or in vivo requires functional HSP90. *Proc Natl Acad Sci U S A,* **93(16),** 8379-83.

Bloom, J., Peschiaroli, A., Demartino, G. & Pagano, M. (2006). Modification of Cul1 regulates its association with proteasomal subunits. *Cell Div,* **1,** 5.

Bornstein, G., Ganoth, D. & Hershko, A. (2006). Regulation of neddylation and deneddylation of cullin1 in SCFSkp2 ubiquitin ligase by F-box protein and substrate. *Proc Natl Acad Sci U S A,* **103(31),** 11515-20.

Boute, N., Jockers, R. & Issad, T. (2002). The use of resonance energy transfer in high-throughput screening: BRET versus FRET. *Trends Pharmacol Sci,* **23(8),** 351-4.

Braig, K., Otwinowski, Z., Hegde, R., Boisvert, D. C., Joachimiak, A., Horwich, A. L. & Sigler, P. B. (1994). The crystal structure of the bacterial chaperonin GroEL at 2.8 A. *Nature,* **371(6498),** 578-86.

Brizel, D. M., Scully, S. P., Harrelson, J. M., Layfield, L. J., Bean, J. M., Prosnitz, L. R. & Dewhirst, M. W. (1996). Tumor oxygenation predicts for the likelihood of distant metastases in human soft tissue sarcoma. *Cancer Res,* **56(5),** 941-3.

Bukau, B. & Horwich, A. L. (1998). The Hsp70 and Hsp60 chaperone machines. *Cell,* **92(3),** 351-66.

Calderwood, S. K. (2013). Molecular cochaperones: tumor growth and cancer treatment. *Scientifica (Cairo),* **2013,** 217513.

Calderwood, S. K., Khaleque, M. A., Sawyer, D. B. & Ciocca, D. R. (2006). Heat shock proteins in cancer: chaperones of tumorigenesis. *Trends Biochem Sci,* **31(3),** 164-72.

Calderwood, S. K., Theriault, J. R. & Gong, J. (2005). Message in a bottle: role of the 70-kDa heat shock protein family in anti-tumor immunity. *Eur J Immunol,* **35(9),** 2518-27.

Calderwood, S. K., Xie, Y., Wang, X., Khaleque, M. A., Chou, S. D., Murshid, A., Prince, T. & Zhang, Y. (2010). Signal Transduction Pathways Leading to Heat Shock Transcription. *Sign Transduct Insights,* **2,** 13-24.

Cappello, F., Conway de Macario, E., Di Felice, V., Zummo, G. & Macario, A. J. (2009). Chlamydia trachomatis infection and anti-Hsp60 immunity: the two sides of the coin. *PLoS Pathog,* **5(8),** e1000552.

Carver, L. A., LaPres, J. J., Jain, S., Dunham, E. E. & Bradfield, C. A. (1998). Characterization of the Ah receptor-associated protein, ARA9. *J Biol Chem,* **273(50),** 33580-7.

Cazabat, L., Bouligand, J. & Chanson, P. (2011). AIP mutation in pituitary adenomas. *N Engl J Med,* **364(20),** 1973-4; author reply 1974-5.

Chadli, A., Felts, S. J., Wang, Q., Sullivan, W. P., Botuyan, M. V., Fauq, A., Ramirez-Alvarado, M. & Mer, G. (2010). Celastrol inhibits Hsp90 chaperoning of steroid receptors by inducing fibrillization of the Co-chaperone p23. *J Biol Chem,* **285(6),** 4224-31.

Chan, Y., Yoon, J., Wu, J. T., Kim, H. J., Pan, K. T., Yim, J. & Chien, C. T. (2008). DEN1 deneddylates non-cullin proteins in vivo. *J Cell Sci,* **121(Pt 19),** 3218-23.

Chapple, J. P., Grayson, C., Hardcastle, A. J., Saliba, R. S., van der Spuy, J. & Cheetham, M. E. (2001). Unfolding retinal dystrophies: a role for molecular chaperones? *Trends in molecular medicine,* **7(9),** 414-421.

Chen, B., Zhong, D. & Monteiro, A. (2006). Comparative genomics and evolution of the HSP90 family of genes across all kingdoms of organisms. *BMC Genomics,* **7,** 156.

Chen, C. F., Chen, Y., Dai, K., Chen, P. L., Riley, D. J. & Lee, W. H. (1996). A new member of the hsp90 family of molecular chaperones interacts with the retinoblastoma protein during mitosis and after heat shock. *Mol Cell Biol,* **16(9),** 4691-9.

Chen, S. & Smith, D. F. (1998). Hop as an adaptor in the heat shock protein 70 (Hsp70) and hsp90 chaperone machinery. *J Biol Chem,* **273(52),** 35194-200.

Chen, S., Sullivan, W. P., Toft, D. O. & Smith, D. F. (1998). Differential interactions of p23 and the TPR-containing proteins Hop, Cyp40, FKBP52 and FKBP51 with Hsp90 mutants. *Cell Stress Chaperones,* **3(2),** 118-29.

Chen, X., Li, J., Gray, W. H., Lehmann, B. D., Bauer, J. A., Shyr, Y. & Pietenpol, J. A. (2012). TNBCtype: A Subtyping Tool for Triple-Negative Breast Cancer. *Cancer Inform,* **11,** 147-56.

Cheng, X., Xia, W., Yang, J. Y., Hsu, J. L., Chou, C. K., Sun, H. L., Wyszomierski, S. L., Mills, G. B., Muller, W. J., Yu, D. & Hung, M. C. (2010). Activation of p21(CIP1/WAF1) in mammary epithelium accelerates mammary tumorigenesis and promotes lung metastasis. *Biochem Biophys Res Commun,* **403(1),** 103-7.

Chinkers, M. (1994). Targeting of a distinctive protein-serine phosphatase to the protein kinase-like domain of the atrial natriuretic peptide receptor. *Proc Natl Acad Sci U S A,* **91(23),** 11075-9.

Chiu, Y. H., Sun, Q. & Chen, Z. J. (2007). E1-L2 activates both ubiquitin and FAT10. *Mol Cell,* **27(6),** 1014-23.

Ciechanover, A. (1998). The ubiquitin-proteasome pathway: on protein death and cell life. *EMBO J,* **17(24),** 7151-60.

Ciechanover, A. & Schwartz, A. L. (1998). The ubiquitin-proteasome pathway: the complexity and myriad functions of proteins death. *Proc Natl Acad Sci U S A,* **95(6),** 2727-30.

Ciocca, D. R., Arrigo, A. P. & Calderwood, S. K. (2013). Heat shock proteins and heat shock factor 1 in carcinogenesis and tumor development: an update. *Arch Toxicol,* **87(1),** 19-48.

Cochran, J. N., Diggs, P. V., Nebane, N. M., Rasmussen, L., White, E. L., Bostwick, R., Maddry, J. A., Suto, M. J. & Roberson, E. D. (2014). AlphaScreen HTS and live-cell bioluminescence resonance energy transfer (BRET) assays for identification of Tau-Fyn SH3 interaction inhibitors for Alzheimer disease. *J Biomol Screen,* **19(10),** 1338-49.

Couvelard, A., O'Toole, D., Leek, R., Turley, H., Sauvanet, A., Degott, C., Ruszniewski, P., Belghiti, J., Harris, A. L., Gatter, K. & Pezzella, F. (2005). Expression of hypoxia-inducible factors is correlated with the presence of a fibrotic focus and angiogenesis in pancreatic ductal adenocarcinomas. *Histopathology,* **46(6),** 668-76.

Cowen, L. E. & Lindquist, S. (2005). Hsp90 potentiates the rapid evolution of new traits: drug resistance in diverse fungi. *Science,* **309(5744),** 2185-9.

Cox, M. B., Riggs, D. L., Hessling, M., Schumacher, F., Buchner, J. & Smith, D. F. (2007). FK506-binding protein 52 phosphorylation: a potential mechanism for regulating steroid hormone receptor activity. *Mol Endocrinol,* **21(12),** 2956-67.

Craig, E. A. (1985). The heat shock response. *CRC Crit Rev Biochem,* **18(3),** 239-80.

Csermely, P., Schnaider, T., Soti, C., Prohaszka, Z. & Nardai, G. (1998). The 90-kDa molecular chaperone family: structure, function, and clinical applications. A comprehensive review. *Pharmacol Ther,* **79(2),** 129-68.

Czarnecka, A. M., Campanella, C., Zummo, G. & Cappello, F. (2006). Mitochondrial chaperones in cancer: from molecular biology to clinical diagnostics. *Cancer Biol Ther,* **5(7),** 714-20.

Davies, L., Paraskevopoulou, E., Sadeq, M., Symeou, C., Pantelidou, C., Demonacos, C. & Krstic-Demonacos, M. (2011). Regulation of glucocorticoid receptor activity by a stress responsive transcriptional cofactor. *Mol Endocrinol,* **25(1),** 58-71.

Denny, W. B., Valentine, D. L., Reynolds, P. D., Smith, D. F. & Scammell, J. G. (2000). Squirrel Monkey Immunophilin FKBP51 Is a Potent Inhibitor of Glucocorticoid Receptor Binding* * This work was supported by Grants 13200 and 01254 from the National Center for Research Resources (to J.G.S.) and NIH Grant DK48218 (to D.F.S.). *Endocrinology,* **141(11),** 4107-4113.

Dobson, C. M. & Karplus, M. (1999). The fundamentals of protein folding: bringing together theory and experiment. *Curr Opin Struct Biol,* **9(1),** 92-101.

Doyle, S. M., Genest, O. & Wickner, S. (2013). Protein rescue from aggregates by powerful molecular chaperone machines. *Nat Rev Mol Cell Biol,* **14(10),** 617-29.

Duda, D. M., Borg, L. A., Scott, D. C., Hunt, H. W., Hammel, M. & Schulman, B. A. (2008). Structural insights into NEDD8 activation of cullin-RING ligases: conformational control of conjugation. *Cell,* **134(6),** 995-1006.

Ekman, S., Bergqvist, M., Tell, R., Bergstrom, S. & Lennartsson, J. (2010). Hsp90 as a therapeutic target in patients with oesophageal carcinoma. *Expert Opin Ther Targets,* **14(3),** 317-28.

Ellis, J. (1987). Proteins as molecular chaperones. *Nature,* **328(6129),** 378-9.

Ellis, R. J. (1990). Molecular chaperones: the plant connection. *Science,* **250(4983),** 954-9.

Ellis, R. J. (2006). Molecular chaperones: assisting assembly in addition to folding. *Trends Biochem Sci,* **31(7),** 395-401.

Ellis, R. J. (2007). Protein misassembly: macromolecular crowding and molecular chaperones. *Adv Exp Med Biol,* **594,** 1-13.

Ellis, R. J. (2013). Assembly chaperones: a perspective. *Philos Trans R Soc Lond B Biol Sci,* **368(1617),** 20110398.

Enchev, R. I., Schulman, B. A. & Peter, M. (2015). Protein neddylation: beyond cullin-RING ligases. *Nat Rev Mol Cell Biol,* **16(1),** 30-44.

Erler, J. T., Bennewith, K. L., Nicolau, M., Dornhofer, N., Kong, C., Le, Q. T., Chi, J. T., Jeffrey, S. S. & Giaccia, A. J. (2006). Lysyl oxidase is essential for hypoxia-induced metastasis. *Nature,* **440(7088),** 1222-6.

Gao, Y., Theng, S. S., Zhuo, J., Teo, W. B., Ren, J. & Lee, C. G. (2014). FAT10, an ubiquitin-like protein, confers malignant properties in non-tumorigenic and tumorigenic cells. *Carcinogenesis,* **35(4),** 923-34.

Ghosh, J. C., Dohi, T., Kang, B. H. & Altieri, D. C. (2008). Hsp60 regulation of tumor cell apoptosis. *J Biol Chem,* **283(8),** 5188-94.

Goldenberg, S. J., Cascio, T. C., Shumway, S. D., Garbutt, K. C., Liu, J., Xiong, Y. & Zheng, N. (2004). Structure of the Cand1-Cul1-Roc1 complex reveals regulatory mechanisms for the assembly of the multisubunit cullin-dependent ubiquitin ligases. *Cell,* **119(4),** 517-28.

Goloubinoff, P., Christeller, J. T., Gatenby, A. A. & Lorimer, G. H. (1989). Reconstitution of active dimeric ribulose bisphosphate carboxylase from an unfoleded state depends on two chaperonin proteins and Mg-ATP. *Nature,* **342(6252),** 884-9.

Gong, N., Li, X. Y., Xiao, Q. & Wang, Y. X. (2014). Identification of a novel spinal dorsal horn astroglial D-amino acid oxidase-hydrogen peroxide pathway involved in morphine antinociceptive tolerance. *Anesthesiology,* **120(4),** 962-75.

Groettrup, M., Pelzer, C., Schmidtke, G. & Hofmann, K. (2008). Activating the ubiquitin family: UBA6 challenges the field. *Trends Biochem Sci,* **33(5),** 230-7.

Haas, A. L., Ahrens, P., Bright, P. M. & Ankel, H. (1987). Interferon induces a 15-kilodalton protein exhibiting marked homology to ubiquitin. *J Biol Chem,* **262(23),** 11315-23.

Hammond, E. M., Dorie, M. J. & Giaccia, A. J. (2003). ATR/ATM targets are phosphorylated by ATR in response to hypoxia and ATM in response to reoxygenation. *J Biol Chem,* **278(14),** 12207-13.

Hartl, F. U. (1996). Molecular chaperones in cellular protein folding. *Nature,* **381(6583),** 571-9.

Hartl, F. U. & Hayer-Hartl, M. (2002). Molecular chaperones in the cytosol: from nascent chain to folded protein. *Science,* **295(5561),** 1852-8.

Hatakeyama, S., Kitagawa, M., Nakayama, K., Shirane, M., Matsumoto, M., Hattori, K., Higashi, H., Nakano, H., Okumura, K., Onoe, K., Good, R. A. & Nakayama, K. (1999). Ubiquitin-dependent degradation of IkappaBalpha is mediated by a ubiquitin ligase Skp1/Cul 1/F-box protein FWD1. *Proc Natl Acad Sci U S A,* **96(7),** 3859-63.

Hemmingsen, S. M., Woolford, C., van der Vies, S. M., Tilly, K., Dennis, D. T., Georgopoulos, C. P., Hendrix, R. W. & Ellis, R. J. (1988). Homologous plant and bacterial proteins chaperone oligomeric protein assembly. *Nature,* **333(6171),** 330-4.

Hershko, A. (2005). The ubiquitin system for protein degradation and some of its roles in the control of the cell division cycle. *Cell Death Differ,* **12(9),** 1191-7.

Hershko, A. & Ciechanover, A. (1998). The ubiquitin system. *Annu Rev Biochem,* **67,** 425-79.

Hidalgo-de-Quintana, J., Evans, R. J., Cheetham, M. E. & van der Spuy, J. (2008). The Leber congenital amaurosis protein AIPL1 functions as part of a chaperone heterocomplex. *Invest Ophthalmol Vis Sci,* **49(7),** 2878-87.

Hieronymus, H., Lamb, J., Ross, K. N., Peng, X. P., Clement, C., Rodina, A., Nieto, M., Du, J., Stegmaier, K., Raj, S. M., Maloney, K. N., Clardy, J., Hahn, W. C., Chiosis, G. & Golub, T. R. (2006). Gene expression signature-based chemical genomic prediction identifies a novel class of HSP90 pathway modulators. *Cancer Cell,* **10(4),** 321-30.

Hipp, M. S., Kalveram, B., Raasi, S., Groettrup, M. & Schmidtke, G. (2005). FAT10, a ubiquitin-independent signal for proteasomal degradation. *Mol Cell Biol,* **25(9),** 3483-91.

Hipp, M. S., Raasi, S., Groettrup, M. & Schmidtke, G. (2004). NEDD8 ultimate buster-1L interacts with the ubiquitin-like protein FAT10 and accelerates its degradation. *J Biol Chem,* **279(16),** 16503-10.

Hjerpe, R., Thomas, Y., Chen, J., Zemla, A., Curran, S., Shpiro, N., Dick, L. R. & Kurz, T. (2012). Changes in the ratio of free NEDD8 to ubiquitin triggers NEDDylation by ubiquitin enzymes. *Biochem J,* **441(3),** 927-36.

Hori, T., Osaka, F., Chiba, T., Miyamoto, C., Okabayashi, K., Shimbara, N., Kato, S. & Tanaka, K. (1999). Covalent modification of all members of human cullin family proteins by NEDD8. *Oncogene,* **18(48),** 6829-34.

Hosono, T., Tanaka, T., Tanji, K., Nakatani, T. & Kamitani, T. (2010). NUB1, an interferon-inducible protein, mediates anti-proliferative actions and apoptosis in renal cell carcinoma cells through cell-cycle regulation. *Br J Cancer,* **102(5),** 873-82.

Hu, J., Bianchi, F., Ferguson, M., Cesario, A., Margaritora, S., Granone, P., Goldstraw, P., Tetlow, M., Ratcliffe, C., Nicholson, A. G., Harris, A., Gatter, K. & Pezzella, F. (2005). Gene expression signature for angiogenic and nonangiogenic non-small-cell lung cancer. *Oncogene,* **24(7),** 1212-9.

Huang, D. T., Ayrault, O., Hunt, H. W., Taherbhoy, A. M., Duda, D. M., Scott, D. C., Borg, L. A., Neale, G., Murray, P. J., Roussel, M. F. & Schulman, B. A. (2009). E2-RING expansion of the NEDD8 cascade confers specificity to cullin modification. *Mol Cell,* **33(4),** 483-95.

Huang, D. T., Hunt, H. W., Zhuang, M., Ohi, M. D., Holton, J. M. & Schulman, B. A. (2007). Basis for a ubiquitin-like protein thioester switch toggling E1-E2 affinity. *Nature,* **445(7126),** 394-8.

Huang, J. & Manning, B. D. (2008). The TSC1-TSC2 complex: a molecular switchboard controlling cell growth. *Biochem J,* **412(2),** 179-90.

Huang, S., Shu, L., Dilling, M. B., Easton, J., Harwood, F. C., Ichijo, H. & Houghton, P. J. (2003). Sustained activation of the JNK cascade and rapamycin-induced apoptosis are suppressed by p53/p21(Cip1). *Mol Cell,* **11(6),** 1491-501.

Ichimura, Y., Kirisako, T., Takao, T., Satomi, Y., Shimonishi, Y., Ishihara, N., Mizushima, N., Tanida, I., Kominami, E., Ohsumi, M., Noda, T. & Ohsumi, Y. (2000). A ubiquitin-like system mediates protein lipidation. *Nature,* **408(6811),** 488-92.

Iliopoulos, O., Levy, A. P., Jiang, C., Kaelin, W. G., Jr. & Goldberg, M. A. (1996). Negative regulation of hypoxia-inducible genes by the von Hippel-Lindau protein. *Proc Natl Acad Sci U S A,* **93(20),** 10595-9.

Isomoto, H., Oka, M., Yano, Y., Kanazawa, Y., Soda, H., Terada, R., Yasutake, T., Nakayama, T., Shikuwa, S., Takeshima, F., Udono, H., Murata, I., Ohtsuka, K. & Kohno, S. (2003). Expression of heat shock protein (Hsp) 70 and Hsp 40 in gastric cancer. *Cancer Lett,* **198(2),** 219-28.

Ivan, M., Kondo, K., Yang, H., Kim, W., Valiando, J., Ohh, M., Salic, A., Asara, J. M., Lane, W. S. & Kaelin, W. G., Jr. (2001). HIFalpha targeted for VHL-mediated destruction by proline hydroxylation: implications for O2 sensing. *Science,* **292(5516),** 464-8.

Jaattela, M. (1999a). Escaping cell death: survival proteins in cancer. *Exp Cell Res,* **248(1),** 30-43.

Jaattela, M. (1999b). Heat shock proteins as cellular lifeguards. *Ann Med,* **31(4),** 261-71.

Jiang, J., Prasad, K., Lafer, E. M. & Sousa, R. (2005). Structural basis of interdomain communication in the Hsc70 chaperone. *Mol Cell,* **20(4),** 513-24.

Jin, J., Li, X., Gygi, S. P. & Harper, J. W. (2007). Dual E1 activation systems for ubiquitin differentially regulate E2 enzyme charging. *Nature,* **447(7148),** 1135-8.

Johnson, J. L. (2012). Evolution and function of diverse Hsp90 homologs and cochaperone proteins. *Biochim Biophys Acta,* **1823(3),** 607-13.

Johnson, J. L., Beito, T. G., Krco, C. J. & Toft, D. O. (1994). Characterization of a novel 23-kilodalton protein of unactive progesterone receptor complexes. *Mol Cell Biol,* **14(3),** 1956-63.

Kamitani, T., Kito, K., Fukuda-Kamitani, T. & Yeh, E. T. (2001). Targeting of NEDD8 and its conjugates for proteasomal degradation by NUB1. *J Biol Chem,* **276(49),** 46655-60.

Kamitani, T., Kito, K., Nguyen, H. P. & Yeh, E. T. (1997). Characterization of NEDD8, a developmentally down-regulated ubiquitin-like protein. *J Biol Chem,* **272(45),** 28557-62.

Kampinga, H. H., Hageman, J., Vos, M. J., Kubota, H., Tanguay, R. M., Bruford, E. A., Cheetham, M. E., Chen, B. & Hightower, L. E. (2009). Guidelines for the nomenclature of the human heat shock proteins. *Cell Stress Chaperones,* **14(1),** 105-11.

Kamura, T., Conrad, M. N., Yan, Q., Conaway, R. C. & Conaway, J. W. (1999). The Rbx1 subunit of SCF and VHL E3 ubiquitin ligase activates Rub1 modification of cullins Cdc53 and Cul2. *Genes Dev,* **13(22),** 2928-33.

Kamura, T., Sato, S., Iwai, K., Czyzyk-Krzeska, M., Conaway, R. C. & Conaway, J. W. (2000). Activation of HIF1alpha ubiquitination by a reconstituted von Hippel-Lindau (VHL) tumor suppressor complex. *Proc Natl Acad Sci U S A,* **97(19),** 10430-5.

Kanaya, K., Sohocki, M. M. & Kamitani, T. (2004). Abolished interaction of NUB1 with mutant AIPL1 involved in Leber congenital amaurosis. *Biochem Biophys Res Commun,* **317(3),** 768-73.

Kane, R. C., Dagher, R., Farrell, A., Ko, C. W., Sridhara, R., Justice, R. & Pazdur, R. (2007). Bortezomib for the treatment of mantle cell lymphoma. *Clin Cancer Res,* **13(18 Pt 1),** 5291-4.

Katayose, D., Wersto, R., Cowan, K. H. & Seth, P. (1995). Effects of a recombinant adenovirus expressing WAF1/Cip1 on cell growth, cell cycle, and apoptosis. *Cell Growth Differ,* **6(10),** 1207-12.

Kato, I., Maita, H., Takahashi-Niki, K., Saito, Y., Noguchi, N., Iguchi-Ariga, S. M. & Ariga, H. (2013). Oxidized DJ-1 inhibits p53 by sequestering p53 from promoters in a DNA-binding affinity-dependent manner. *Mol Cell Biol,* **33(2),** 340-59.

Kazlauskas, A., Poellinger, L. & Pongratz, I. (2000). The immunophilin-like protein XAP2 regulates ubiquitination and subcellular localization of the dioxin receptor. *J Biol Chem,* **275(52),** 41317-24.

Kennaway, C. K., Benesch, J. L., Gohlke, U., Wang, L., Robinson, C. V., Orlova, E. V., Saibil, H. R. & Keep, N. H. (2005). Dodecameric structure of the small heat shock protein Acr1 from Mycobacterium tuberculosis. *J Biol Chem,* **280(39),** 33419-25.

Kim, D. Y., Kwon, E., Hartley, P. D., Crosby, D. C., Mann, S., Krogan, N. J. & Gross, J. D. (2013). CBFbeta stabilizes HIV Vif to counteract APOBEC3 at the expense of RUNX1 target gene expression. *Mol Cell,* **49(4),** 632-44.

Kitagawa, M., Hatakeyama, S., Shirane, M., Matsumoto, M., Ishida, N., Hattori, K., Nakamichi, I., Kikuchi, A., Nakayama, K. & Nakayama, K. (1999). An F-box protein, FWD1, mediates ubiquitin-dependent proteolysis of beta-catenin. *EMBO J,* **18(9),** 2401-10.

Kito, K., Yeh, E. T. & Kamitani, T. (2001). NUB1, a NEDD8-interacting protein, is induced by interferon and down-regulates the NEDD8 expression. *J Biol Chem,* **276(23),** 20603-9.

Kononen, J., Bubendorf, L., Kallioniemi, A., Barlund, M., Schraml, P., Leighton, S., Torhorst, J., Mihatsch, M. J., Sauter, G. & Kallioniemi, O. P. (1998). Tissue microarrays for high-throughput molecular profiling of tumor specimens. *Nat Med,* **4(7),** 844-7.

Koster, R., di Pietro, A., Timmer-Bosscha, H., Gibcus, J. H., van den Berg, A., Suurmeijer, A. J., Bischoff, R., Gietema, J. A. & de Jong, S. (2010). Cytoplasmic p21 expression levels determine cisplatin resistance in human testicular cancer. *J Clin Invest,* **120(10),** 3594-605.

Kubota, H., Yamamoto, S., Itoh, E., Abe, Y., Nakamura, A., Izumi, Y., Okada, H., Iida, M., Nanjo, H., Itoh, H. & Yamamoto, Y. (2010). Increased expression of co-chaperone HOP with HSP90 and HSC70 and complex formation in human colonic carcinoma. *Cell Stress Chaperones,* **15(6),** 1003-11.

Kuzhandaivelu, N., Cong, Y. S., Inouye, C., Yang, W. M. & Seto, E. (1996). XAP2, a novel hepatitis B virus X-associated protein that inhibits X transactivation. *Nucleic Acids Res,* **24(23),** 4741-50.

LaPres, J. J., Glover, E., Dunham, E. E., Bunger, M. K. & Bradfield, C. A. (2000). ARA9 modifies agonist signaling through an increase in cytosolic aryl hydrocarbon receptor. *J Biol Chem,* **275(9),** 6153-9.

Laskey, R. A., Honda, B. M., Mills, A. D. & Finch, J. T. (1978). Nucleosomes are assembled by an acidic protein which binds histones and transfers them to DNA. *Nature,* **275(5679),** 416-20.

Latif, F., Tory, K., Gnarra, J., Yao, M., Duh, F. M., Orcutt, M. L., Stackhouse, T., Kuzmin, I., Modi, W., Geil, L. & et al. (1993). Identification of the von Hippel-Lindau disease tumor suppressor gene. *Science,* **260(5112),** 1317-20.

Laufen, T., Mayer, M. P., Beisel, C., Klostermeier, D., Mogk, A., Reinstein, J. & Bukau, B. (1999). Mechanism of regulation of hsp70 chaperones by DnaJ cochaperones. *Proc Natl Acad Sci U S A,* **96(10),** 5452-7.

Le, Q. T., Denko, N. C. & Giaccia, A. J. (2004). Hypoxic gene expression and metastasis. *Cancer Metastasis Rev,* **23(3-4),** 293-310.

Lee, C. G., Ren, J., Cheong, I. S., Ban, K. H., Ooi, L. L., Yong Tan, S., Kan, A., Nuchprayoon, I., Jin, R., Lee, K. H., Choti, M. & Lee, L. A. (2003). Expression of the FAT10 gene is highly upregulated in hepatocellular carcinoma and other gastrointestinal and gynecological cancers. *Oncogene,* **22(17),** 2592-603.

Lees, M. J., Peet, D. J. & Whitelaw, M. L. (2003). Defining the role for XAP2 in stabilization of the dioxin receptor. *J Biol Chem,* **278(38),** 35878-88.

Lees, M. J. & Whitelaw, M. L. (2002). Effect of ARA9 on dioxin receptor mediated transcription. *Toxicology,* **181-182,** 143-6.

Lemieux, P., Oesterreich, S., Lawrence, J. A., Steeg, P. S., Hilsenbeck, S. G., Harvey, J. M. & Fuqua, S. A. (1997). The small heat shock protein hsp27 increases invasiveness but decreases motility of breast cancer cells. *Invasion Metastasis,* **17(3),** 113-23.

Li, B., Smith, C. C., Laing, J. M., Gober, M. D., Liu, L. & Aurelian, L. (2007). Overload of the heat-shock protein H11/HspB8 triggers melanoma cell apoptosis through activation of transforming growth factor-beta-activated kinase 1. *Oncogene,* **26(24),** 3521-31.

Li, J., Richter, K., Reinstein, J. & Buchner, J. (2013a). Integration of the accelerator Aha1 in the Hsp90 co-chaperone cycle. *Nat Struct Mol Biol,* **20(3),** 326-31.

Li, J., Soroka, J. & Buchner, J. (2012). The Hsp90 chaperone machinery: conformational dynamics and regulation by co-chaperones. *Biochim Biophys Acta,* **1823(3),** 624-35.

Li, J., Zoldak, G., Kriehuber, T., Soroka, J., Schmid, F. X., Richter, K. & Buchner, J. (2013b). Unique proline-rich domain regulates the chaperone function of AIPL1. *Biochemistry,* **52(12),** 2089-96.

Li, Y., Dowbenko, D. & Lasky, L. A. (2002). AKT/PKB phosphorylation of p21Cip/WAF1 enhances protein stability of p21Cip/WAF1 and promotes cell survival. *J Biol Chem,* **277(13),** 11352-61.

Liakopoulos, D., Busgen, T., Brychzy, A., Jentsch, S. & Pause, A. (1999). Conjugation of the ubiquitin-like protein NEDD8 to cullin-2 is linked to von Hippel-Lindau tumor suppressor function. *Proc Natl Acad Sci U S A,* **96(10),** 5510-5.

Liang, J., Zubovitz, J., Petrocelli, T., Kotchetkov, R., Connor, M. K., Han, K., Lee, J. H., Ciarallo, S., Catzavelos, C., Beniston, R., Franssen, E. & Slingerland, J. M. (2002). PKB/Akt phosphorylates p27, impairs nuclear import of p27 and opposes p27-mediated G1 arrest. *Nat Med,* **8(10),** 1153-60.

Lindquist, S. & Craig, E. A. (1988). The heat-shock proteins. *Annu Rev Genet,* **22,** 631-77.

Linehan, W. M., Lerman, M. I. & Zbar, B. (1995). Identification of the von Hippel-Lindau (VHL) gene. Its role in renal cancer. *JAMA,* **273(7),** 564-70.

Liu, J., Furukawa, M., Matsumoto, T. & Xiong, Y. (2002). NEDD8 modification of CUL1 dissociates p120(CAND1), an inhibitor of CUL1-SKP1 binding and SCF ligases. *Mol Cell,* **10(6),** 1511-8.

Liu, Y. C., Pan, J., Zhang, C., Fan, W., Collinge, M., Bender, J. R. & Weissman, S. M. (1999). A MHC-encoded ubiquitin-like protein (FAT10) binds noncovalently to the spindle assembly checkpoint protein MAD2. *Proc Natl Acad Sci U S A,* **96(8),** 4313-8.

Lu, B., Al-Ramahi, I., Valencia, A., Wang, Q., Berenshteyn, F., Yang, H., Gallego-Flores, T., Ichcho, S., Lacoste, A., Hild, M., Difiglia, M., Botas, J. & Palacino, J. (2013). Identification of NUB1 as a suppressor of mutant Huntington toxicity via enhanced protein clearance. *Nat Neurosci,* **16(5),** 562-70.

Lubensky, I. A., Gnarra, J. R., Bertheau, P., Walther, M. M., Linehan, W. M. & Zhuang, Z. (1996). Allelic deletions of the VHL gene detected in multiple microscopic clear cell renal lesions in von Hippel-Lindau disease patients. *Am J Pathol,* **149(6),** 2089-94.

Lukasiak, S., Schiller, C., Oehlschlaeger, P., Schmidtke, G., Krause, P., Legler, D. F., Autschbach, F., Schirmacher, P., Breuhahn, K. & Groettrup, M. (2008). Proinflammatory cytokines cause FAT10 upregulation in cancers of liver and colon. *Oncogene,* **27(46),** 6068-74.

Lyapina, S., Cope, G., Shevchenko, A., Serino, G., Tsuge, T., Zhou, C., Wolf, D. A., Wei, N., Shevchenko, A. & Deshaies, R. J. (2001). Promotion of NEDD-CUL1 conjugate cleavage by COP9 signalosome. *Science,* **292(5520),** 1382-5.

Ma, Q. & Whitlock, J. P., Jr. (1997). A novel cytoplasmic protein that interacts with the Ah receptor, contains tetratricopeptide repeat motifs, and augments the transcriptional response to 2,3,7,8-tetrachlorodibenzo-p-dioxin. *J Biol Chem,* **272(14),** 8878-84.

Macario, A. J. & Conway de Macario, E. (2007). Chaperonopathies by defect, excess, or mistake. *Ann N Y Acad Sci,* **1113,** 178-91.

Maxwell, P. H., Wiesener, M. S., Chang, G. W., Clifford, S. C., Vaux, E. C., Cockman, M. E., Wykoff, C. C., Pugh, C. W., Maher, E. R. & Ratcliffe, P. J. (1999). The tumour suppressor protein VHL targets hypoxia-inducible factors for oxygen-dependent proteolysis. *Nature,* **399(6733),** 271-5.

Mayer, M. P., Brehmer, D., Gassler, C. S. & Bukau, B. (2001). Hsp70 chaperone machines. *Adv Protein Chem,* **59,** 1-44.

Mayer, M. P. & Bukau, B. (2005). Hsp70 chaperones: cellular functions and molecular mechanism. *Cell Mol Life Sci,* **62(6),** 670-84.

Mazumdar, A., Wang, R. A., Mishra, S. K., Adam, L., Bagheri-Yarmand, R., Mandal, M., Vadlamudi, R. K. & Kumar, R. (2001). Transcriptional repression of oestrogen receptor by metastasis-associated protein 1 corepressor. *Nat Cell Biol,* **3(1),** 30-7.

McKeen, H. D., Brennan, D. J., Hegarty, S., Lanigan, F., Jirstrom, K., Byrne, C., Yakkundi, A., McCarthy, H. O., Gallagher, W. M. & Robson, T. (2011). The emerging role of FK506-binding proteins as cancer biomarkers: a focus on FKBPL. *Biochem Soc Trans,* **39(2),** 663-8.

Mendoza, H. M., Shen, L. N., Botting, C., Lewis, A., Chen, J., Ink, B. & Hay, R. T. (2003). NEDP1, a highly conserved cysteine protease that deNEDDylates Cullins. *J Biol Chem,* **278(28),** 25637-43.

Meyer, B. K. & Perdew, G. H. (1999). Characterization of the AhR-hsp90-XAP2 core complex and the role of the immunophilin-related protein XAP2 in AhR stabilization. *Biochemistry,* **38(28),** 8907-17.

Meyer, B. K., Petrulis, J. R. & Perdew, G. H. (2000). Aryl hydrocarbon (Ah) receptor levels are selectively modulated by hsp90-associated immunophilin homolog XAP2. *Cell Stress Chaperones,* **5(3),** 243-54.

Meyer, B. K., Pray-Grant, M. G., Vanden Heuvel, J. P. & Perdew, G. H. (1998). Hepatitis B virus X-associated protein 2 is a subunit of the unliganded aryl hydrocarbon receptor core complex and exhibits transcriptional enhancer activity. *Mol Cell Biol,* **18(2),** 978-88.

Meyer, H., Bug, M. & Bremer, S. (2012). Emerging functions of the VCP/p97 AAA-ATPase in the ubiquitin system. *Nat Cell Biol,* **14(2),** 117-23.

Michel, L., Diaz-Rodriguez, E., Narayan, G., Hernando, E., Murty, V. V. & Benezra, R. (2004). Complete loss of the tumor suppressor MAD2 causes premature cyclin B degradation and mitotic failure in human somatic cells. *Proc Natl Acad Sci U S A,* **101(13),** 4459-64.

Miyata, Y., Nakamoto, H. & Neckers, L. (2013). The therapeutic target Hsp90 and cancer hallmarks. *Curr Pharm Des,* **19(3),** 347-65.

Miyauchi, Y., Kato, M., Tokunaga, F. & Iwai, K. (2008). The COP9/signalosome increases the efficiency of von Hippel-Lindau protein ubiquitin ligase-mediated hypoxia-inducible factor-alpha ubiquitination. *J Biol Chem,* **283(24),** 16622-31.

Morimoto, M., Nishida, T., Honda, R. & Yasuda, H. (2000). Modification of cullin-1 by ubiquitin-like protein Nedd8 enhances the activity of SCF(skp2) toward p27(kip1). *Biochem Biophys Res Commun,* **270(3),** 1093-6.

Morimoto, M., Nishida, T., Nagayama, Y. & Yasuda, H. (2003). Nedd8-modification of Cul1 is promoted by Roc1 as a Nedd8-E3 ligase and regulates its stability. *Biochem Biophys Res Commun,* **301(2),** 392-8.

Muller, L., Schaupp, A., Walerych, D., Wegele, H. & Buchner, J. (2004). Hsp90 regulates the activity of wild type p53 under physiological and elevated temperatures. *J Biol Chem,* **279(47),** 48846-54.

Muthukumaran, S., Umashankar, V. & Valliappan, M. R. (2012). Structural studies on AIPL1 and its functional interactions with NUB1 to identify key interacting residues in LCA4. *J Ocul Biol Dis Infor,* **5(3-4),** 54-60.

Nan, K. J., Jing, Z. & Gong, L. (2004). Expression and altered subcellular localization of the cyclin-dependent kinase inhibitor p27Kip1 in hepatocellular carcinoma. *World J Gastroenterol,* **10(10),** 1425-30.

Ogino, S., Shima, K., Nosho, K., Irahara, N., Baba, Y., Wolpin, B. M., Giovannucci, E. L., Meyerhardt, J. A. & Fuchs, C. S. (2009). A cohort study of p27 localization in colon cancer, body mass index, and patient survival. *Cancer Epidemiol Biomarkers Prev,* **18(6),** 1849-58.

Ohh, M., Kim, W. Y., Moslehi, J. J., Chen, Y., Chau, V., Read, M. A. & Kaelin, W. G., Jr. (2002). An intact NEDD8 pathway is required for Cullin-dependent ubiquitylation in mammalian cells. *EMBO Rep,* **3(2),** 177-82.

Ohh, M., Park, C. W., Ivan, M., Hoffman, M. A., Kim, T. Y., Huang, L. E., Pavletich, N., Chau, V. & Kaelin, W. G. (2000). Ubiquitination of hypoxia-inducible factor requires direct binding to the beta-domain of the von Hippel-Lindau protein. *Nat Cell Biol,* **2(7),** 423-7.

Olcina, M., Lecane, P. S. & Hammond, E. M. (2010). Targeting hypoxic cells through the DNA damage response. *Clin Cancer Res,* **16(23),** 5624-9.

Olsen, S. K., Capili, A. D., Lu, X., Tan, D. S. & Lima, C. D. (2010). Active site remodelling accompanies thioester bond formation in the SUMO E1. *Nature,* **463(7283),** 906-12.

Osaka, F., Kawasaki, H., Aida, N., Saeki, M., Chiba, T., Kawashima, S., Tanaka, K. & Kato, S. (1998). A new NEDD8-ligating system for cullin-4A. *Genes Dev,* **12(15),** 2263-8.

Ozfirat, Z. & Korbonits, M. (2010). AIP gene and familial isolated pituitary adenomas. *Mol Cell Endocrinol,* **326(1-2),** 71-9.

Pauling, L., Corey, R. B. & Branson, H. R. (1951). The structure of proteins; two hydrogen-bonded helical configurations of the polypeptide chain. *Proc Natl Acad Sci U S A,* **37(4),** 205-11.

Pearl, L. H. & Prodromou, C. (2006). Structure and mechanism of the Hsp90 molecular chaperone machinery. *Annu Rev Biochem,* **75,** 271-94.

Pelzer, C., Kassner, I., Matentzoglu, K., Singh, R. K., Wollscheid, H. P., Scheffner, M., Schmidtke, G. & Groettrup, M. (2007). UBE1L2, a novel E1 enzyme specific for ubiquitin. *J Biol Chem,* **282(32),** 23010-4.

Perez-Tenorio, G., Berglund, F., Esguerra Merca, A., Nordenskjold, B., Rutqvist, L. E., Skoog, L. & Stal, O. (2006). Cytoplasmic p21WAF1/CIP1 correlates with Akt activation and poor response to tamoxifen in breast cancer. *Int J Oncol,* **28(5),** 1031-42.

Petrulis, J. R., Hord, N. G. & Perdew, G. H. (2000). Subcellular localization of the aryl hydrocarbon receptor is modulated by the immunophilin homolog hepatitis B virus X-associated protein 2. *J Biol Chem,* **275(48),** 37448-53.

Petrulis, J. R., Kusnadi, A., Ramadoss, P., Hollingshead, B. & Perdew, G. H. (2003). The hsp90 Co-chaperone XAP2 alters importin beta recognition of the bipartite nuclear localization signal of the Ah receptor and represses transcriptional activity. *J Biol Chem,* **278(4),** 2677-85.

Pezzella , F., Turley , H., Kuzu , I., Tungekar , M. F., Dunnill , M. S., Pierce , C. B., Harris , A., Gatter , K. C. & Mason , D. Y. (1993). bcl-2 Protein in Non-Small-Cell Lung Carcinoma. *New England Journal of Medicine,* **329(10),** 690-694.

Picard, D. (2002). Heat-shock protein 90, a chaperone for folding and regulation. *Cell Mol Life Sci,* **59(10),** 1640-8.

Pirkl, F., Fischer, E., Modrow, S. & Buchner, J. (2001). Localization of the chaperone domain of FKBP52. *J Biol Chem,* **276(40),** 37034-41.

Podust, V. N., Brownell, J. E., Gladysheva, T. B., Luo, R. S., Wang, C., Coggins, M. B., Pierce, J. W., Lightcap, E. S. & Chau, V. (2000). A Nedd8 conjugation pathway is essential for proteolytic targeting of p27Kip1 by ubiquitination. *Proc Natl Acad Sci U S A,* **97(9),** 4579-84.

Poetsch, M., Dittberner, T., Cowell, J. K. & Woenckhaus, C. (2000). TTC4, a novel candidate tumor suppressor gene at 1p31 is often mutated in malignant melanoma of the skin. *Oncogene,* **19(50),** 5817-20.

Pratt, W. B. & Toft, D. O. (1997). Steroid receptor interactions with heat shock protein and immunophilin chaperones. *Endocr Rev,* **18(3),** 306-60.

Pratt, W. B. & Toft, D. O. (2003). Regulation of signaling protein function and trafficking by the hsp90/hsp70-based chaperone machinery. *Exp Biol Med (Maywood),* **228(2),** 111-33.

Qian, Y. Q., Patel, D., Hartl, F. U. & McColl, D. J. (1996). Nuclear magnetic resonance solution structure of the human Hsp40 (HDJ-1) J-domain. *J Mol Biol,* **260(2),** 224-35.

Qin, H., Shi, J., Noberini, R., Pasquale, E. B. & Song, J. (2008). Crystal structure and NMR binding reveal that two small molecule antagonists target the high affinity ephrin-binding channel of the EphA4 receptor. *J Biol Chem,* **283(43),** 29473-84.

Rabut, G. & Peter, M. (2008). Function and regulation of protein neddylation. 'Protein modifications: beyond the usual suspects' review series. *EMBO Rep,* **9(10),** 969-76.

Ramasamy, A. (2009). DPhil Thesis: Increasing statistical power and generalizability in genomic microarray research. Department of Statistics, University of Oxford.

Rampelt, H., Mayer, M. P. & Bukau, B. (2011). Nucleotide exchange factors for Hsp70 chaperones. *Methods Mol Biol,* **787,** 83-91.

Read, M. A., Brownell, J. E., Gladysheva, T. B., Hottelet, M., Parent, L. A., Coggins, M. B., Pierce, J. W., Podust, V. N., Luo, R. S., Chau, V. & Palombella, V. J. (2000). Nedd8 modification of cul-1 activates SCF(beta(TrCP))-dependent ubiquitination of IkappaBalpha. *Mol Cell Biol,* **20(7),** 2326-33.

Reebye, V., Querol Cano, L., Lavery, D. N., Brooke, G. N., Powell, S. M., Chotai, D., Walker, M. M., Whitaker, H. C., Wait, R., Hurst, H. C. & Bevan, C. L. (2012). Role of the HSP90-associated cochaperone p23 in enhancing activity of the androgen receptor and significance for prostate cancer. *Mol Endocrinol,* **26(10),** 1694-706.

Ritossa, F. (1962). A new puffing pattern induced by temperature shock and DNP in drosophila. *Experientia,* **18(12),** 571-573.

Ritossa, F. M. (1964). Experimental activation of specific loci in polytene chromosomes of Drosophila. *Experimental Cell Research,* **35(3),** 601-607.

Rodier, G., Montagnoli, A., Di Marcotullio, L., Coulombe, P., Draetta, G. F., Pagano, M. & Meloche, S. (2001). p27 cytoplasmic localization is regulated by phosphorylation on Ser10 and is not a prerequisite for its proteolysis. *EMBO J,* **20(23),** 6672-82.

Rosen, D. G., Yang, G., Cai, K. Q., Bast, R. C., Jr., Gershenson, D. M., Silva, E. G. & Liu, J. (2005). Subcellular localization of p27kip1 expression predicts poor prognosis in human ovarian cancer. *Clin Cancer Res,* **11(2 Pt 1),** 632-7.

Rosser, M. F. N. & Cyr, D. M. (2007). Do Hsp40s Act as Chaperones or Co-Chaperones? In, *Networking of Chaperones by Co-Chaperones*. New York, NY: Springer New York, pp 38-51.

Rossig, L., Jadidi, A. S., Urbich, C., Badorff, C., Zeiher, A. M. & Dimmeler, S. (2001). Akt-dependent phosphorylation of p21(Cip1) regulates PCNA binding and proliferation of endothelial cells. *Mol Cell Biol,* **21(16),** 5644-57.

Ruan, S., Okcu, M. F., Pong, R. C., Andreeff, M., Levin, V., Hsieh, J. T. & Zhang, W. (1999). Attenuation of WAF1/Cip1 expression by an antisense adenovirus expression vector sensitizes glioblastoma cells to apoptosis induced by chemotherapeutic agents 1,3-bis(2-chloroethyl)-1-nitrosourea and cisplatin. *Clin Cancer Res,* **5(1),** 197-202.

Ruaro, E. M., Collavin, L., Del Sal, G., Haffner, R., Oren, M., Levine, A. J. & Schneider, C. (1997). A proline-rich motif in p53 is required for transactivation-independent growth arrest as induced by Gas1. *Proc Natl Acad Sci U S A,* **94(9),** 4675-80.

Russell, R. C. & Ohh, M. (2008). NEDD8 acts as a 'molecular switch' defining the functional selectivity of VHL. *EMBO Rep,* **9(5),** 486-91.

Ryu, J. H., Li, S. H., Park, H. S., Park, J. W., Lee, B. & Chun, Y. S. (2011). Hypoxia-inducible factor alpha subunit stabilization by NEDD8 conjugation is reactive oxygen species-dependent. *J Biol Chem,* **286(9),** 6963-70.

Saha, A. & Deshaies, R. J. (2008). Multimodal activation of the ubiquitin ligase SCF by Nedd8 conjugation. *Mol Cell,* **32(1),** 21-31.

Salon, C., Brambilla, E., Brambilla, C., Lantuejoul, S., Gazzeri, S. & Eymin, B. (2007). Altered pattern of Cul-1 protein expression and neddylation in human lung tumours: relationships with CAND1 and cyclin E protein levels. *J Pathol,* **213(3),** 303-10.

Sanderson, S., Valenti, M., Gowan, S., Patterson, L., Ahmad, Z., Workman, P. & Eccles, S. A. (2006). Benzoquinone ansamycin heat shock protein 90 inhibitors modulate multiple functions required for tumor angiogenesis. *Mol Cancer Ther,* **5(3),** 522-32.

Sarikas, A., Hartmann, T. & Pan, Z. Q. (2011). The cullin protein family. *Genome Biol,* **12(4),** 220.

Scheufler, C., Brinker, A., Bourenkov, G., Pegoraro, S., Moroder, L., Bartunik, H., Hartl, F. U. & Moarefi, I. (2000). Structure of TPR domain-peptide complexes: critical elements in the assembly of the Hsp70-Hsp90 multichaperone machine. *Cell,* **101(2),** 199-210.

Schmid, A. B., Lagleder, S., Grawert, M. A., Rohl, A., Hagn, F., Wandinger, S. K., Cox, M. B., Demmer, O., Richter, K., Groll, M., Kessler, H. & Buchner, J. (2012). The architecture of functional modules in the Hsp90 co-chaperone Sti1/Hop. *EMBO J,* **31(6),** 1506-17.

Schoenfeld, A., Davidowitz, E. J. & Burk, R. D. (1998). A second major native von Hippel-Lindau gene product, initiated from an internal translation start site, functions as a tumor suppressor. *Proc Natl Acad Sci U S A,* **95(15),** 8817-22.

Schoenfeld, A. R., Parris, T., Eisenberger, A., Davidowitz, E. J., De Leon, M., Talasazan, F., Devarajan, P. & Burk, R. D. (2000). The von Hippel-Lindau tumor suppressor gene protects cells from UV-mediated apoptosis. *Oncogene,* **19(51),** 5851-7.

Schrag, J. D., Bergeron, J. J., Li, Y., Borisova, S., Hahn, M., Thomas, D. Y. & Cygler, M. (2001). The Structure of calnexin, an ER chaperone involved in quality control of protein folding. *Mol Cell,* **8(3),** 633-44.

Schulke, J. P., Wochnik, G. M., Lang-Rollin, I., Gassen, N. C., Knapp, R. T., Berning, B., Yassouridis, A. & Rein, T. (2010). Differential impact of tetratricopeptide repeat proteins on the steroid hormone receptors. *PLoS One,* **5(7),** e11717.

Schwartz, M. L., Hurley, J. B. & Ramamurthy, V. (2006). Biochemical function of the LCA linked protein, aryl hydrocarbon receptor interacting protein like-1 (AIPL1). Role of AIPL1 in retina. *Adv Exp Med Biol,* **572,** 89-94.

Schwechheimer, C., Serino, G., Callis, J., Crosby, W. L., Lyapina, S., Deshaies, R. J., Gray, W. M., Estelle, M. & Deng, X. W. (2001). Interactions of the COP9 signalosome with the E3 ubiquitin ligase SCFTIRI in mediating auxin response. *Science,* **292(5520),** 1379-82.

Seo, J. S., Park, Y. M., Kim, J. I., Shim, E. H., Kim, C. W., Jang, J. J., Kim, S. H. & Lee, W. H. (1996). T cell lymphoma in transgenic mice expressing the human Hsp70 gene. *Biochem Biophys Res Commun,* **218(2),** 582-7.

Shin, I., Yakes, F. M., Rojo, F., Shin, N. Y., Bakin, A. V., Baselga, J. & Arteaga, C. L. (2002). PKB/Akt mediates cell-cycle progression by phosphorylation of p27(Kip1) at threonine 157 and modulation of its cellular localization. *Nat Med,* **8(10),** 1145-52.

Siegert, R., Leroux, M. R., Scheufler, C., Hartl, F. U. & Moarefi, I. (2000). Structure of the molecular chaperone prefoldin: unique interaction of multiple coiled coil tentacles with unfolded proteins. *Cell,* **103(4),** 621-32.

Singer, J. D., Gurian-West, M., Clurman, B. & Roberts, J. M. (1999). Cullin-3 targets cyclin E for ubiquitination and controls S phase in mammalian cells. *Genes Dev,* **13(18),** 2375-87.

Singh, S. P., Lipman, J., Goldman, H., Ellis, F. H., Jr., Aizenman, L., Cangi, M. G., Signoretti, S., Chiaur, D. S., Pagano, M. & Loda, M. (1998). Loss or altered subcellular localization of p27 in Barrett's associated adenocarcinoma. *Cancer Res,* **58(8),** 1730-5.

Sohocki, M. M., Bowne, S. J., Sullivan, L. S., Blackshaw, S., Cepko, C. L., Payne, A. M., Bhattacharya, S. S., Khaliq, S., Qasim Mehdi, S., Birch, D. G., Harrison, W. R., Elder, F. F., Heckenlively, J. R. & Daiger, S. P. (2000). Mutations in a new photoreceptor-pineal gene on 17p cause Leber congenital amaurosis. *Nat Genet,* **24(1),** 79-83.

Spolar, R. S., Ha, J. H. & Record, M. T., Jr. (1989). Hydrophobic effect in protein folding and other noncovalent processes involving proteins. Proc Natl Acad Sci U S A, 86(21), 8382-5.

Souza, A. P., Albuquerque, C., Torronteguy, C., Frasson, A., Maito, F., Pereira, L., Duval da Silva, V., Zerwes, F., Raynes, D., Guerriero, V. & Bonorino, C. (2009). HspBP1 levels are elevated in breast tumor tissue and inversely related to tumor aggressiveness. *Cell Stress Chaperones,* **14(3),** 301-10.

Stepanova, L., Finegold, M., DeMayo, F., Schmidt, E. V. & Harper, J. W. (2000). The oncoprotein kinase chaperone CDC37 functions as an oncogene in mice and collaborates with both c-myc and cyclin D1 in transformation of multiple tissues. *Mol Cell Biol,* **20(12),** 4462-73.

Stuart, J. K., Myszka, D. G., Joss, L., Mitchell, R. S., McDonald, S. M., Xie, Z., Takayama, S., Reed, J. C. & Ely, K. R. (1998). Characterization of interactions between the anti-apoptotic protein BAG-1 and Hsc70 molecular chaperones. *J Biol Chem,* **273(35),** 22506-14.

Sufan, R. I. & Ohh, M. (2006). Role of the NEDD8 modification of Cul2 in the sequential activation of ECV complex. *Neoplasia,* **8(11),** 956-63.

Suzuki, H., Chiba, T., Kobayashi, M., Takeuchi, M., Suzuki, T., Ichiyama, A., Ikenoue, T., Omata, M., Furuichi, K. & Tanaka, K. (1999). IkappaBalpha ubiquitination is catalyzed by an SCF-like complex containing Skp1, cullin-1, and two F-box/WD40-repeat proteins, betaTrCP1 and betaTrCP2. *Biochem Biophys Res Commun,* **256(1),** 127-32.

Tai, P. K., Chang, H., Albers, M. W., Schreiber, S. L., Toft, D. O. & Faber, L. E. (1993). P59 (FK506 binding protein 59) interaction with heat shock proteins is highly conserved and may involve proteins other than steroid receptors. *Biochemistry,* **32(34),** 8842-7.

Takikita, M., Chung, J. Y. & Hewitt, S. M. (2007). Tissue microarrays enabling high-throughput molecular pathology. *Curr Opin Biotechnol,* **18(4),** 318-25.

Tanaka, T., Kawashima, H., Yeh, E. T. & Kamitani, T. (2003). Regulation of the NEDD8 conjugation system by a splicing variant, NUB1L. *J Biol Chem,* **278(35),** 32905-13.

Tanaka, T., Nakatani, T. & Kamitani, T. (2012). Inhibition of NEDD8-conjugation pathway by novel molecules: potential approaches to anticancer therapy. *Mol Oncol,* **6(3),** 267-75.

Tanaka, T., Nakatani, T. & Kamitani, T. (2013). Negative regulation of NEDD8 conjugation pathway by novel molecules and agents for anticancer therapy. *Curr Pharm Des,* **19(22),** 4131-9.

Tang, D., Khaleque, M. A., Jones, E. L., Theriault, J. R., Li, C., Wong, W. H., Stevenson, M. A. & Calderwood, S. K. (2005). Expression of heat shock proteins and heat shock protein messenger ribonucleic acid in human prostate carcinoma in vitro and in tumors in vivo. *Cell Stress Chaperones,* **10(1),** 46-58.

Tanji, K., Tanaka, T. & Kamitani, T. (2005). Interaction of NUB1 with the proteasome subunit S5a. *Biochem Biophys Res Commun,* **337(1),** 116-20.

Tanji, K., Tanaka, T., Mori, F., Kito, K., Takahashi, H., Wakabayashi, K. & Kamitani, T. (2006). NUB1 suppresses the formation of Lewy body-like inclusions by proteasomal degradation of synphilin-1. *Am J Pathol,* **169(2),** 553-65.

Tapia, C., Kutzner, H., Mentzel, T., Savic, S., Baumhoer, D. & Glatz, K. (2006). Two mitosis-specific antibodies, MPM-2 and phospho-histone H3 (Ser28), allow rapid and precise determination of mitotic activity. *Am J Surg Pathol,* **30(1),** 83-9.

Theng, S. S., Wang, W., Mah, W. C., Chan, C., Zhuo, J., Gao, Y., Qin, H., Lim, L., Chong, S. S., Song, J. & Lee, C. G. (2014). Disruption of FAT10-MAD2 binding inhibits tumor progression. *Proc Natl Acad Sci U S A,* **111(49),** E5282-91.

Thomlinson, R. H. & Gray, L. H. (1955). The histological structure of some human lung cancers and the possible implications for radiotherapy. *Br J Cancer,* **9(4),** 539-49.

van der Spuy, J., Chapple, J. P., Clark, B. J., Luthert, P. J., Sethi, C. S. & Cheetham, M. E. (2002). The Leber congenital amaurosis gene product AIPL1 is localized exclusively in rod photoreceptors of the adult human retina. *Hum Mol Genet,* **11(7),** 823-31.

van der Spuy, J. & Cheetham, M. E. (2004). Role of AIP and its homologue the blindness-associated protein AIPL1 in regulating client protein nuclear translocation. *Biochem Soc Trans,* **32(Pt 4),** 643-5.

van der Spuy, J., Kim, J. H., Yu, Y. S., Szel, A., Luthert, P. J., Clark, B. J. & Cheetham, M. E. (2003). The expression of the Leber congenital amaurosis protein AIPL1 coincides with rod and cone photoreceptor development. *Invest Ophthalmol Vis Sci,* **44(12),** 5396-403.

Viglietto, G., Motti, M. L., Bruni, P., Melillo, R. M., D'Alessio, A., Califano, D., Vinci, F., Chiappetta, G., Tsichlis, P., Bellacosa, A., Fusco, A. & Santoro, M. (2002). Cytoplasmic relocalization and inhibition of the cyclin-dependent kinase inhibitor p27(Kip1) by PKB/Akt-mediated phosphorylation in breast cancer. *Nat Med,* **8(10),** 1136-44.

Voisine, C., Pedersen, J. S. & Morimoto, R. I. (2010). Chaperone networks: tipping the balance in protein folding diseases. *Neurobiol Dis,* **40(1),** 12-20.

Volloch, V. Z. & Sherman, M. Y. (1999). Oncogenic potential of Hsp72. *Oncogene,* **18(24),** 3648-51.

Wada, H., Yeh, E. T. & Kamitani, T. (1999). Identification of NEDD8-conjugation site in human cullin-2. *Biochem Biophys Res Commun,* **257(1),** 100-5.

Wagenaar-Miller, R. A., Gorden, L. & Matrisian, L. M. (2004). Matrix metalloproteinases in colorectal cancer: is it worth talking about? *Cancer Metastasis Rev,* **23(1-2),** 119-35.

Waha, A., Koch, A., Hartmann, W., Milde, U., Felsberg, J., Hubner, A., Mikeska, T., Goodyer, C. G., Sorensen, N., Lindberg, I., Wiestler, O. D., Pietsch, T. & Waha, A. (2007). SGNE1/7B2 is epigenetically altered and transcriptionally down-regulated in human medulloblastomas. *Oncogene,* **26(38),** 5662-8.

Walden, H., Podgorski, M. S., Huang, D. T., Miller, D. W., Howard, R. J., Minor, D. L., Jr., Holton, J. M. & Schulman, B. A. (2003). The structure of the APPBP1-UBA3-NEDD8-ATP complex reveals the basis for selective ubiquitin-like protein activation by an E1. *Mol Cell,* **12(6),** 1427-37.

Walsh, N., Larkin, A., Swan, N., Conlon, K., Dowling, P., McDermott, R. & Clynes, M. (2011). RNAi knockdown of Hop (Hsp70/Hsp90 organising protein) decreases invasion via MMP-2 down regulation. *Cancer Lett,* **306(2),** 180-9.

Wandinger, S. K., Richter, K. & Buchner, J. (2008). The Hsp90 chaperone machinery. *J Biol Chem,* **283(27),** 18473-7.

Watanabe, K., Ozaki, T., Nakagawa, T., Miyazaki, K., Takahashi, M., Hosoda, M., Hayashi, S., Todo, S. & Nakagawara, A. (2002). Physical interaction of p73 with c-Myc and MM1, a c-Myc-binding protein, and modulation of the p73 function. *J Biol Chem,* **277(17),** 15113-23.

Wayne, N. & Bolon, D. N. (2010). Charge-rich regions modulate the anti-aggregation activity of Hsp90. *J Mol Biol,* **401(5),** 931-9.

Winters, Z. E., Leek, R. D., Bradburn, M. J., Norbury, C. J. & Harris, A. L. (2003). Cytoplasmic p21WAF1/CIP1 expression is correlated with HER-2/ neu in breast cancer and is an independent predictor of prognosis. *Breast Cancer Res,* **5(6),** R242-9.

Workman, P. (2002). Pharmacogenomics in cancer drug discovery and development: inhibitors of the Hsp90 molecular chaperone. *Cancer Detect Prev,* **26(6),** 405-10.

Wu, J., Zhao, X., Lin, Z. & Shao, Z. (2015). A system level analysis of gastric cancer across tumor stages with RNA-seq data. *Mol Biosyst,* **11(7),** 1925-32.

Wu, K., Chen, A. & Pan, Z. Q. (2000). Conjugation of Nedd8 to CUL1 enhances the ability of the ROC1-CUL1 complex to promote ubiquitin polymerization. *J Biol Chem,* **275(41),** 32317-24.

Xia, W., Chen, J. S., Zhou, X., Sun, P. R., Lee, D. F., Liao, Y., Zhou, B. P. & Hung, M. C. (2004). Phosphorylation/cytoplasmic localization of p21Cip1/WAF1 is associated with HER2/neu overexpression and provides a novel combination predictor for poor prognosis in breast cancer patients. *Clin Cancer Res,* **10(11),** 3815-24.

Xiang, S. L., Kumano, T., Iwasaki, S. I., Sun, X., Yoshioka, K. & Yamamoto, K. C. (2001). The J domain of Tpr2 regulates its interaction with the proapoptotic and cell-cycle checkpoint protein, Rad9. *Biochem Biophys Res Commun,* **287(4),** 932-40.

Yang, Z. Y., Perkins, N. D., Ohno, T., Nabel, E. G. & Nabel, G. J. (1995). The p21 cyclin-dependent kinase inhibitor suppresses tumorigenicity in vivo. *Nat Med,* **1(10),** 1052-6.

Yeh, E. T., Gong, L. & Kamitani, T. (2000). Ubiquitin-like proteins: new wines in new bottles. *Gene,* **248(1-2),** 1-14.

Yersal, O. & Barutca, S. (2014). Biological subtypes of breast cancer: Prognostic and therapeutic implications. *World J Clin Oncol,* **5(3),** 412-24.

Young, J. C., Agashe, V. R., Siegers, K. & Hartl, F. U. (2004). Pathways of chaperone-mediated protein folding in the cytosol. *Nat Rev Mol Cell Biol,* **5(10),** 781-91.

Young, J. C., Barral, J. M. & Ulrich Hartl, F. (2003). More than folding: localized functions of cytosolic chaperones. *Trends Biochem Sci,* **28(10),** 541-7.

Young, J. C., Obermann, W. M. & Hartl, F. U. (1998). Specific binding of tetratricopeptide repeat proteins to the C-terminal 12-kDa domain of hsp90. *J Biol Chem,* **273(29),** 18007-10.

Yu, Z. K., Gervais, J. L. & Zhang, H. (1998). Human CUL-1 associates with the SKP1/SKP2 complex and regulates p21(CIP1/WAF1) and cyclin D proteins. *Proc Natl Acad Sci U S A,* **95(19),** 11324-9.

Zabka, M., Lesniak, W., Prus, W., Kuznicki, J. & Filipek, A. (2008). Sgt1 has co-chaperone properties and is up-regulated by heat shock. *Biochem Biophys Res Commun,* **370(1),** 179-83.

Zhang, W., Kornblau, S. M., Kobayashi, T., Gambel, A., Claxton, D. & Deisseroth, A. B. (1995). High levels of constitutive WAF1/Cip1 protein are associated with chemoresistance in acute myelogenous leukemia. *Clin Cancer Res,* **1(9),** 1051-7.

Zhao, L., Liu, L., Wang, S., Zhang, Y. F., Yu, L. & Ding, Y. Q. (2007). Differential proteomic analysis of human colorectal carcinoma cell lines metastasis-associated proteins. *J Cancer Res Clin Oncol,* **133(10),** 771-82.

Zheng, H., You, H., Zhou, X. Z., Murray, S. A., Uchida, T., Wulf, G., Gu, L., Tang, X., Lu, K. P. & Xiao, Z. X. (2002a). The prolyl isomerase Pin1 is a regulator of p53 in genotoxic response. *Nature,* **419(6909),** 849-53.

Zheng, N., Schulman, B. A., Song, L., Miller, J. J., Jeffrey, P. D., Wang, P., Chu, C., Koepp, D. M., Elledge, S. J., Pagano, M., Conaway, R. C., Conaway, J. W., Harper, J. W. & Pavletich, N. P.

(2002b). Structure of the Cul1-Rbx1-Skp1-F boxSkp2 SCF ubiquitin ligase complex. *Nature,* **416(6882),** 703-9.

Zhou, B. P., Liao, Y., Xia, W., Spohn, B., Lee, M. H. & Hung, M. C. (2001). Cytoplasmic localization of p21Cip1/WAF1 by Akt-induced phosphorylation in HER-2/neu-overexpressing cells. *Nat Cell Biol,* **3(3),** 245-52.

Zimmerman, E. S., Schulman, B. A. & Zheng, N. (2010). Structural assembly of cullin-RING ubiquitin ligase complexes. *Curr Opin Struct Biol,* **20(6),** 714-21.

Zou, Z., Cao, L., Zhou, P., Su, Y., Sun, Y. & Li, W. (2008). Hyper-acidic protein fusion partners improve solubility and assist correct folding of recombinant proteins expressed in Escherichia coli. *J Biotechnol,* **135(4),** 333-9.